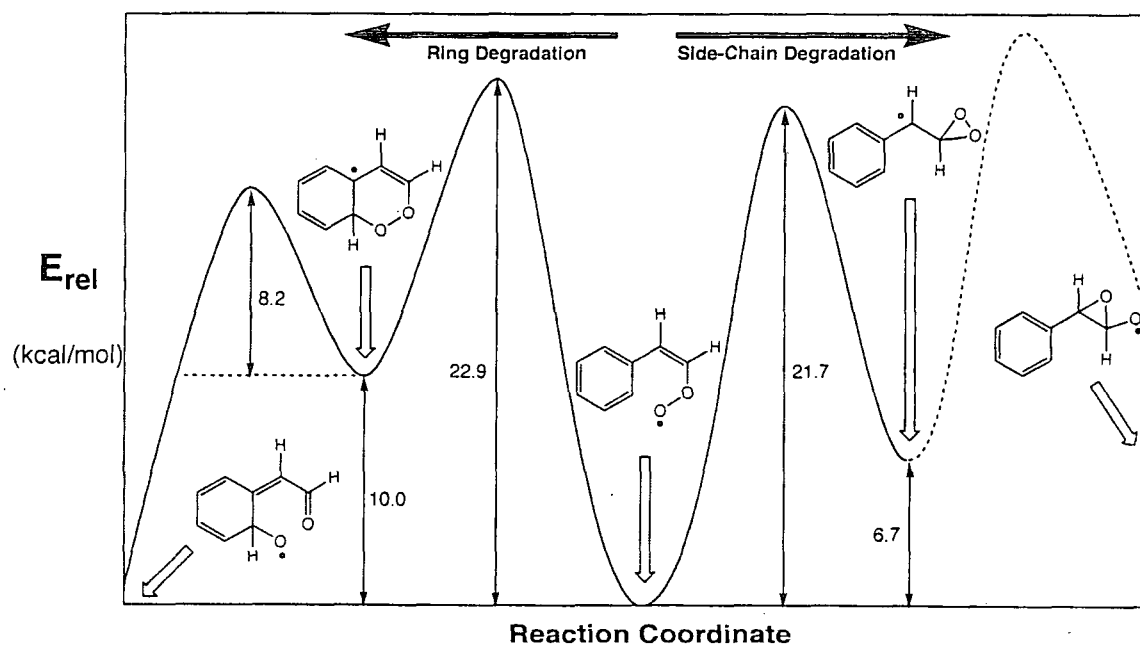


23rd Annual Combustion Research Conference

U.S. Department of Energy
Office of Basic Energy Sciences



Airlie Conference Center
Warrenton, Virginia
May 28 – May 31, 2002

Cover Figure: UB3LYP/6-31G(d) energies for the oxidative degradation of the Z-styrylperoxy radical. Figures are ZPE-corrected potential energies. (*Independent Generation and Study of Key Radicals in Hydrocarbon Combustion*, Barry K. Carpenter, p 33)

FOREWORD

The achievement of National goals for energy conservation and environmental protection will rely on technology more advanced than we have at our disposal today. Combustion at present accounts for 85% of the energy generated and used in the U.S. and is likely to remain a dominant source of energy for the coming decades. Achieving energy conservation while minimizing unwanted emissions from combustion processes could be greatly accelerated if accurate and reliable means were at hand for quantitatively predicting process performance.

The reports appearing in this volume present work in progress in basic research contributing to the development of a predictive capability for combustion processes. The work reported herein is supported by the Department of Energy's Office of Basic Energy Sciences (BES) and in large measure by the chemical physics program. The long-term objective of this effort is the provision of theories, data, and procedures to enable the development of reliable computational models of combustion processes, systems, and devices.

The development of reliable models for combustion requires the accurate knowledge of chemistry, turbulent flow, and the interaction between the two at temperatures and pressures characteristic of the combustion environment. In providing this knowledge, the research supported by BES addresses a wide range of continuing scientific issues of long standing.

- For even the simplest fuels, the chemistry of combustion consists of hundreds of reactions. Key reaction mechanisms, the means for developing and testing these mechanisms and the means for determining which of the constituent reaction rates are critical for accurate characterization are all required.
- For reactions known to be important, accurate rates over wide ranges of temperature, pressure and composition are required. To assess the accuracy of measured reaction rates or predict rates that would be too difficult to measure, theories of reaction rates and means for calculating their values are needed. Of particular importance are reactions involving open shell systems such as radicals and excited electronic states.
- To assess the accuracy of methods for predicting chemical reaction rates, the detailed, state-specific dynamics of prototypical reactions must be characterized.
- Methods for observing key reaction species in combustion environments, for interpreting these observations in terms of species concentrations, and for determining which species are key are all required
- Energy flow and accounting must be accurately characterized and predicted.
- Methods for reducing the mathematical complexity inherent in hundreds of reactions, without sacrificing accuracy and reliability are required. Methods for reducing the computational complexity of computer models that attempt to address turbulence, chemistry, and their interdependence and also needed.

Although the emphasis in this list is on the development of mathematical models for simulating the gas phase reactions characteristic of combustion, *such models, from the chemical dynamics of a single molecule to the performance of a combustion device,*

have value only when confirmed by experiment. Hence, the DOE program represented by reports in this volume supports the development and application of new experimental tools in chemical dynamics, kinetics, and spectroscopy.

The success of this research effort will be measured by the quality of the research performed, the profundity of the knowledge gained, as well as the degree to which it contributes to goals of resource conservation and environmental stewardship. In fact, without research of the highest quality, the application of the knowledge gained to practical problems will not be possible.

The emphasis on modeling and simulation as a basis for defining the objectives of this basic research program has a secondary but important benefit. Computational models of physical processes provide the most efficient means for ensuring the usefulness and use of basic theories and data. The importance of modeling and simulation remains well recognized in the Department of Energy and is receiving support through the Scientific Discovery through Advanced Computing (SciDAC) initiative; several work-in-progress reports funded through SciDAC are included in this volume.

During the past year, the Chemical Physics program has continued to benefit from the involvement of Dr. William Kirchhoff, acting director of the Chemical Sciences, Geosciences, and Biosciences Division in the Office of Basic Energy Sciences, Dr. Eric Rohlfing, program manager for the Atomic, Molecular and Optical Physics program, Dr. Allan Laufer, team leader for the Fundamental Interactions programs, and Dr. Walter Stevens, program manager for Biophysics. The efforts of Polly Blackburn, Kellye Sliger, Rachel Smith, and Andreene Witt of the Oak Ridge Institute for Science Education and Karen Talamini of the Division of Chemical Sciences, Geosciences, and Biosciences, Office of Basic Energy Sciences in the arrangements for the meeting are also much appreciated.

Frank P. Tully, SC-14
Division of Chemical Sciences, Geosciences, and Biosciences
Office of Basic Energy Sciences

May 28, 2002

Wednesday, May 29, 2002
Evening Session

Larry Rahn, Chair

6:15 pm	<i>"Investigation of Non-Premixed Turbulent Combustion,"</i> Stephen B. Pope.....	265
6:45 pm	<i>"Analysis of Turbulent Reacting Flow,"</i> William T. Ashurst.....	1
7:15 pm	<i>"Reacting Flow Modeling with Detailed Chemical Kinetics,"</i> Habib N. Najm.....	242
7:45 pm	Break	
8:00 pm	<i>"Computational and Experimental Study of Laminar Flames,"</i> Mitchell Smooke.....	297
8:30 pm	<i>"Nonlinear Diagnostic Techniques and Strategies,"</i> Thomas B. Settersten.....	289
9:00 pm	<i>"Investigation of Polarization Spectroscopy and Degenerate Four-Wave Mixing for Quantitative Concentration Measurements,"</i> Robert P. Lucht.....	203
9:30 pm	Social	

Thursday, May 30, 2002
Morning Session

Trevor Sears, Chair

8:00 am	<i>"Intermolecular Interactions of Hydroxyl Radicals on Reactive Potential Energy Surfaces,"</i> Marsha I. Lester.....	187
8:30 am	<i>"The Effect of Large Amplitude Motion on the Vibrational Level Structure and Dynamics of Internal Rotor Molecules,"</i> David S. Perry.....	257
9:00 am	<i>"Multiresonant Spectroscopy and the High-Resolution Threshold Photoionization of Combustion Free Radicals,"</i> Edward R. Grant.....	120

9:30 am	<i>"Laser Studies of the Chemistry and Spectroscopy of Excited State Hydrocarbons,"</i> Timothy S. Zwiier.....	351
10:00 am	Break	
10:30 am	<i>"Combustion Chemistry,"</i> Nancy J. Brown.....	25
11:00 am	<i>"Kinetic Modeling of Combustion Chemistry,"</i> Charles K. Westbrook..	331
11:30 am	<i>"Multiple-time-scale-kinetics,"</i> Michael Davis.....	75
12:15 pm	Lunch	

Thursday, May 30, 2002
Afternoon and Evening Session

John Kiefer, Chair

4:00 pm	<i>"Low-Energy Ion-Molecule Reactions: Gases and Interfaces,"</i> James M. Farrar.....	92
4:30 pm	<i>"Infrared Absorption Spectroscopy and Chemical Kinetics of Free Radicals,"</i> Robert F. Curl and Graham P. Glass.....	64
5:00 pm	<i>"Time-Resolved Infrared Absorption Studies of the Dynamics of Radical Reactions,"</i> R. Glen MacDonald.....	207
5:30 pm	Break	
5:45 pm	<i>"Kinetics and Dynamics of Combustion Chemistry,"</i> David L. Osborn.....	253
6:15 pm	<i>"Studies of Combustion Kinetics and Mechanisms,"</i> Irene Slagle.....	301
6:45 pm	<i>"Gas-Phase Molecular Dynamics: Kinetics of Radical-Radical Reactions,"</i> Christopher Fockenberg.....	108
7:30 pm	Cash Bar	
8:00 pm	Dinner	

Friday, May 31, 2002
Morning Session

H. Floyd Davis, Chair

8:00 am	<i>"Gas-Phase Molecular Dynamics: Theoretical Studies of Reaction Dynamics and Spectroscopy," James Muckerman.....</i>	<i>238</i>
8:30 am	<i>"Reaction of Phenyl Radical with Propyne," Henry F. Schaefer.....</i>	<i>285</i>
9:00 am	<i>"Theoretical Studies of the Reactions and Spectroscopy of Radical Species Relevant to Combustion Reactions and Diagnostics," David R. Yarkony.....</i>	<i>346</i>
9:30 am	<i>Break</i>	
9:45 am	<i>"Molecular Beam Studies of Radical Combustion Intermediates," Laurie J. Butler.....</i>	<i>29</i>
10:15 am	<i>"Radical Chemistry and Photochemistry," Daniel M. Neumark.....</i>	<i>246</i>
10:45 am	<i>"Small Molecular Systems," Curt Wittig.....</i>	<i>342</i>
11:15 am	<i>Closing Remarks</i>	

Table of Contents

<p>William T. Ashurst and Allan R. Kerstein <i>Analysis of Turbulent Reacting Flow</i> 1</p> <p>Tomas Baer <i>Photoelectron Photoion Coincidence Studies: Heats of Formation of Ions, Molecules, and Free Radicals</i> 5</p> <p>Robert S. Barlow <i>Turbulence-Chemistry Interactions in Reacting Flows</i> 9</p> <p>Richard Bersohn <i>Energy Partitioning in Elementary Chemical Reactions</i> 13</p> <p>Joel M. Bowman <i>Theoretical Studies of Combustion Dynamics</i> 17</p> <p>Kenneth Brezinsky <i>Very High Pressure Single Pulse Shock Tube Studies of Aromatic Species</i> 21</p> <p>Nancy J. Brown <i>Combustion Chemistry</i> 25</p> <p>Laurie J. Butler <i>Molecular Beam Studies of Radical Combustion Intermediates</i> 29</p> <p>Barry K. Carpenter <i>Independent Generation and Study of Key Radicals in Hydrocarbon Combustion</i> 33</p> <p>David W. Chandler <i>Molecular-Beam Ion Imaging Experiments</i> 37</p> <p>Jacqueline H. Chen, Tarek Echehki, and Scott Mason <i>Direct Numerical Simulation of Turbulent Combustion with Detailed Chemistry</i> 41</p> <p>Robert K. Cheng and Lawrence Talbot <i>Turbulent Combustion</i> 45</p> <p>J. Cioslowski and D. Moncrieff <i>Electronic Structure Studies of Geochemical and Pyrolytic Formation of Heterocyclic Compounds in Fossil Fuels</i> 49</p> <p>Robert E. Continetti <i>Half-Collision Dynamics of Elementary Combustion Reactions</i> 53</p> <p>Terrill A. Cool <i>Flame Sampling Photoionization Mass Spectrometry</i> 57</p> <p>F. F. Crim <i>State-Controlled Photodissociation of Vibrationally Excited Molecules and Hydrogen Bonded Dimers</i> 61</p> <p>Robert F. Curl and Graham P. Glass <i>Infrared Absorption Spectroscopy and Chemical Kinetics of Free Radicals</i> 64</p> <p>Hai-Lung Dai <i>Vibrational Spectroscopy and Reactions of Highly Excited Transient Radicals</i> 68</p> <p>H. Floyd Davis <i>Bimolecular Dynamics of Combustion Reactions</i> 72</p> <p>Michael J. Davis <i>Multiple-time-scale kinetics</i> 75</p>	<p>Frederick L. Dryer <i>Comprehensive Mechanisms for Combustion Chemistry: Experiment, Modeling, and Sensitivity Analysis</i> 79</p> <p>G. Barney Ellison <i>Laser Photoelectron Spectroscopy of Ions</i> 83</p> <p>Kent M. Ervin <i>Thermochemistry of Hydrocarbon Radicals: Guided Ion Beam Studies</i> 88</p> <p>James M. Farrar <i>Low Energy Ion-Molecule Reactions: Gases and Interfaces</i> 92</p> <p>Peter M. Felker <i>Nonlinear Raman spectroscopy of jet-cooled organic radicals and radical complexes</i> 96</p> <p>Robert W. Field and Robert J. Silbey <i>Spectroscopic and Dynamical Studies of Highly Energized Small Polyatomic Molecules</i> 100</p> <p>George Flynn <i>Laser Studies of Chemical Reaction and Collision Processes</i> 104</p> <p>Christopher Fockenberg and Jack M. Preses <i>Gas-Phase Molecular Dynamics: Kinetics of Radical-Radical Reactions</i> 108</p> <p>Jonathan H. Frank <i>Quantitative Imaging Diagnostics for Reacting Flows</i> 112</p> <p>Michael Frenklach <i>Mechanism and Detailed Modeling of Soot Formation</i> 116</p> <p>Edward R. Grant <i>Multiresonant Spectroscopy and the High-Resolution Threshold Photoionization of Combustion Free Radicals</i> 120</p> <p>Stephen K. Gray <i>Chemical Dynamics in the Gas Phase: Quantum Mechanics of Chemical Reactions</i> 124</p> <p>William H. Green, Jr. <i>Computer-Aided Construction of Chemical Kinetic Models</i> 128</p> <p>Gregory E. Hall, Trevor J. Sears, and Arthur Suits <i>Spectroscopy and Dynamics of Molecular Free Radicals</i> 132</p> <p>Ronald K. Hanson and Craig T. Bowman <i>Spectroscopy and Kinetics of Combustion Gases at High Temperatures</i> 136</p> <p>Lawrence B. Harding <i>Theoretical Studies of Potential Energy Surfaces</i> 140</p> <p>Carl Hayden <i>Femtosecond Laser Studies of Ultrafast Intramolecular Processes</i> 144</p> <p>Martin Head-Gordon <i>Chemical Accuracy from Ab Initio Molecular Orbital Calculations</i> 148</p>
---	---

John F. Hershberger		C. Bradley Moore	
<i>Laser Studies of the Combustion Chemistry of Nitrogen</i>	152	<i>Unimolecular Reaction Dynamics of Free Radicals</i>	235
Jan P. Hessler		James T. Muckerman	
<i>Small-Angle X-Ray Scattering Studies of Soot Inception and Growth</i>	156	<i>Gas-Phase Molecular Dynamics: Theoretical Studies of Reaction Dynamics and Spectroscopy</i>	238
P. L. Houston		Habib N. Najm	
<i>Product Imaging of Combustion Dynamics</i>	160	<i>Reacting Flow Modeling with Detailed Chemical Kinetics</i>	242
J. B. Howard and H. Richter		Daniel M. Neumark	
<i>Aromatics Oxidation and Soot Formation in Flames</i>	164	<i>Radical Chemistry and Photochemistry</i>	246
Philip M. Johnson		C. Y. Ng	
<i>Ionization Probes of Molecular Structure and Chemistry</i>	168	<i>High-Resolution Photoionization and Photoelectron Studies: Determination of Accurate Energetic Database for Combustion Chemistry</i>	250
Michael E. Kellman		David L. Osborn	
<i>Dynamical Analysis of Highly Excited Molecular Spectra</i>	171	<i>Kinetics and Dynamics of Combustion Chemistry</i>	253
J. H. Kiefer and R. S. Tranter		David S. Perry	
<i>Kinetics of Combustion-Related Processes at High Temperatures</i>	175	<i>The Effect of Large Amplitude Motion on the Vibrational Level Structure and Dynamics of Internal Rotor Molecules</i>	257
Stephen J. Klippenstein		Robert W. Pitz, Michael C. Drake, Todd D. Fansler, and Volker Sick	
<i>Theoretical Chemical Kinetics</i>	179	<i>Partially-Premixed Flames in Internal Combustion Engines</i>	261
Stephen R. Leone		Stephen B. Pope	
<i>Time-Resolved FTIR Emission Studies of Laser Photofragmentation and Radical Reactions</i>	183	<i>Investigation of Non-Premixed Turbulent Combustion</i>	265
Marsha I. Lester		S. T. Pratt	
<i>Intermolecular Interactions of Hydroxyl Radicals on Reactive Potential Energy Surfaces</i>	187	<i>Optical Probes of Atomic and Molecular Decay Processes</i>	269
William A. Lester, Jr.		Herschel Rabitz and Tak-San Ho	
<i>Theoretical Studies of Molecular Systems</i>	191	<i>Studies in Chemical Dynamics</i>	273
John C. Light		Hanna Reisler	
<i>Quantum Dynamics of Fast Chemical Reactions</i>	195	<i>Reactions of Atoms and Radicals in Pulsed Molecular Beams</i>	277
M. C. Lin		Branko Ruscic	
<i>Kinetics of Elementary Processes Relevant to Incipient Soot Formation</i>	199	<i>Photoionization Studies of Transient and Metastable Species</i>	281
Robert P. Lucht		Henry F. Schaefer III	
<i>Investigation of Polarization Spectroscopy and Degenerate Four-Wave Mixing for Quantitative Concentration Measurements</i>	203	<i>Reaction of Phenyl Radical with Propyne</i>	285
R. G. Macdonald		T.B. Settersten	
<i>Time-Resolved Infrared Absorption Studies of the Dynamics of Radical Reactions</i>	207	<i>Nonlinear Diagnostic Techniques and Strategies</i>	289
Andrew McLroy		Ron Shepard	
<i>Flame Chemistry and Diagnostics</i>	211	<i>Theoretical Studies of Potential Energy Surfaces and Computational Methods</i>	293
Joe V. Michael		M. D. Smooke and M. B. Long	
<i>Flash Photolysis-Shock Tube Studies</i>	215	<i>Computational and Experimental Study of Laminar Flames</i>	297
H. A. Michelsen		Irene R. Slagle	
<i>Particle Diagnostics Development</i>	219	<i>Studies of Combustion Kinetics and Mechanisms</i>	301
James A. Miller		Craig A. Taatjes	
<i>Chemical Kinetics and Combustion Modeling</i>	223	<i>Elementary Reaction Kinetics of Combustion Species</i>	305
Terry A. Miller		H.S. Taylor	
<i>Detection and Characterization of Free Radicals Relevant to Combustion Processes</i>	227	<i>The Extraction of Underlying Molecular Vibrational Dynamics from Complex Spectral Regions</i>	309
William H. Miller			
<i>Reaction Dynamics in Polyatomic Molecular Systems</i>	231		

Arnaud Trouve, Jacqueline Chen, Hong G. Im, Christopher J. Rutland, Raghurama Reddy, and Sergiu Sanielevici <i>Terascale High-Fidelity Simulations of Turbulent Combustion with Detailed Chemistry</i>	312
Donald G. Truhlar <i>Variational Transition State Theory</i>	315
Wing Tsang <i>Kinetic Database For Combustion Modeling</i>	319
James J. Valentini <i>Single-Collision Studies of Energy Transfer and Chemical Reaction</i>	323
Albert F. Wagner <i>Theoretical Studies of the Dynamics of Chemical Reactions</i>	327
Charles K. Westbrook and William J. Pitz <i>Kinetic Modeling of Combustion Chemistry</i>	331
Phillip R. Westmoreland <i>Probing Flame Chemistry with MBMS, Theory, and Modeling</i>	336
M. G. White and R. J. Beuhler <i>Photoinduced Molecular Dynamics in the Gas and Condensed Phases</i>	339
Curt Wittig, Joelle Underwood, Delphine Chastaing, and Sun Lee <i>Small Molecular Systems</i>	342
David R. Yarkony <i>Theoretical Studies of the Reactions and Spectroscopy of Radical Species Relevant to Combustion Reactions and Diagnostics</i>	346
Timothy S. Zwier <i>Laser Studies of the Chemistry and Spectroscopy of Excited State Hydrocarbons</i>	351
Participants	355
Author Index	360

Analysis of Turbulent Reacting Flow

William T. Ashurst and Alan R. Kerstein
Combustion Research Facility
Sandia National Laboratories
Livermore, CA 94551-0969
Email: arkerst@sandia.gov

PROGRAM SCOPE

Ongoing work during this project has employed various numerical modeling approaches - atomistic, continuum, and stochastic - to study the interactions between fluid flow and fine-scale physical and chemical processes in turbulent combustion environments. A central focus of recent and planned future work is the role of density variations resulting from either the mixing of dissimilar fluids or from density changes, possibly accompanied by phase change, caused by thermodynamic transients. Combustion-related processes that are considered in this context include (i) dilatation caused by exothermic chemical reactions, (ii) cavitation, atomization, spray development, and vaporization during and following fuel injection, (iii) transport of a dense dispersed phase in turbulent flow, as in spray or particulate combustion, (iv) density variations due to compressibility effects in high speed flow, and (v) buoyancy effects resulting from density stratification.

Much of the ongoing effort has been devoted to the development of a new modeling approach applicable to the aforementioned problems, and more broadly, to the prediction of turbulent flow phenomena and turbulence-microscale interactions. The new approach was originally motivated by recognition of the inability of existing approaches to capture advective-diffusive-reactive couplings in the fundamentally sound manner that would be required for predictive modeling of turbulent combustion. The need for a fundamental rethinking of this issue led to an approach that has been shown, through the work performed during this project, to provide significant new modeling capabilities applicable to a wide range of multiphysics turbulent flow processes, including turbulent combustion.

The modeling strategy that is adopted is motivated by two existing approaches that reflect two distinct attributes of turbulent flow. One approach is the use of mixing-length theory to achieve closure of the ensemble-averaged momentum equation through phenomenological estimation of the eddy viscosity, which represents the contribution of turbulent flow fluctuations to mean transport. The other is stochastic modeling of the instantaneous spatial structure of turbulent flow fields by applying a random sequence of additive or multiplicative operations that is designed to emulate the wide range of spatial scales of turbulent flow fluctuations. The first approach captures the effects of initial conditions, boundary conditions, and forcings (shear, buoyancy, dilatation, etc.) on the mean flow structure, and includes partial representation of fluctuation effects. The second approach represents fluctuation effects in detail, and in fact is designed specifically for the study of these fluctuations. However, it contains no representation of the physical processes that drive these fluctuations, so it is useful primarily for studying the generic (universal) properties of turbulent fluctuations rather than flow-specific effects.

Both of these approaches have been applied in one spatial dimension (1D). In particular, the 1D boundary-layer approximation is a convenient framework for mixing-length theory. The present goal is to develop and use an economical 1D representation with broad predictive capabilities.

The new modeling strategy, denoted One-Dimensional Turbulence (ODT), involves a synthesis of the two approaches, achieved by treating the 1D boundary-layer equations for the mean flow as instantaneous equations. Instead of representing turbulent transport by an eddy viscosity, turbulence effects are incorporated by performing a random sequence of operations somewhat analogous to the stochastic approach. Each operation is the model analog of an individual turbulent eddy. The resulting formulation captures both turbulent cascade properties, as in previous stochastic models, and the coupling of cascade dynamics to the initial and boundary conditions and forcings corresponding to various inhomogeneous turbulent flows of practical interest. Numerous demonstrations of the novel predictive capabilities of this approach have been performed, including several recent demonstrations that are described below.

Turbulent flows with large density variations are subject to several forcing mechanisms that are absent from constant-property flows, such as buoyancy and (in multiphase flows) surface tension and inter-phase momentum transfer. A robust model of variable-density flows must capture these mechanisms as well as the variable-density dynamics of the single-phase buoyancy-free momentum equation. Recent and planned future extensions of ODT incorporate these phenomena into the model.

RECENT PROGRESS

ODT has been generalized to incorporate the full variable-density dynamics of the momentum equation. The most detailed experimental investigations of these dynamics involves spatially developing flows, so ODT has also been generalized to reflect the conservation properties of this class of flows.

In planar mixing layers, the growth rate of the turbulent zone is found experimentally to increase monotonically with the ratio of the density of the slow inlet stream to the density of the fast inlet stream. ODT reproduces this trend over the experimentally observed range of conditions and reproduces many details of measured flow structure with a degree of accuracy that is unprecedented for this flow. In addition, ODT indicates a reversal of the apparent monotonic trend at density ratios beyond the range studied experimentally. Examination of computed results indicates that high density contrast induces an inertia barrier to fluid entrainment analogous to the gravitational potential energy barrier that inhibits turbulent entrainment of heavy fluid across stably stratified fluid interfaces. This fundamental insight may aid in the interpretation of more complex entrainment processes subject to multiple inhibition mechanisms.

ODT has also been used to simulate the flow between two horizontal plates, driven by gravitational instability due to an imposed temperature difference between the plates. The governing parameters are the Rayleigh number Ra , which represents the buoyant forcing scaled by molecular dissipation, and the Prandtl number Pr , a fluid property (viscosity scaled by thermal diffusivity). Key observables are the Nusselt number Nu (mean heat flux scaled by the heat flux through motionless fluid) and temperature fluctuation statistics.

If the flow near each wall is unaffected by the other wall, then dimensional considerations give $Nu \sim Ra^{1/3}$. Measurements indicate that the exponent depends on Ra and Pr , implying wall interactions. Adjustment of two model parameters reproduces these dependencies as well as the prefactor of the Nu scaling to good accuracy over a wide range of parameter space. With no further adjustment, measured temperature fluctuation statistics are predicted with good accuracy, demonstrating a first-of-a-kind capability in this regard. Collectively, the model results suggest a novel interpretation of the mean behaviors and fluctuation properties based on the competition

between two mechanisms that generate temperature fluctuations in the central region of the flow.

A variety of other topics have also been studied recently. ODT was used to investigate extinction and reignition mechanisms in nonpremixed turbulent combustion, leading to the identification of an unexpected slow time scale controlling the evolution of these processes [1]. Turbulent premixed flame structure and burning velocity regimes were analyzed as a function of Pr in order to identify connections between gas-phase combustion (Pr near unity), liquid-phase turbulent-flame analogs (high Pr), and premixed nuclear combustion in exploding stars (low Pr) [2]. A phenomenological model explaining measured manifestations of small-scale anisotropy in turbulence was developed [3].

FUTURE PLANS

ODT as presently formulated does not incorporate effects of fluid compressibility that are relevant to supersonic propulsion, engine knock, and other phenomena associated with combustion processes. For many compressible-flow applications, the governing equations of fully compressible laminar flow are reduced to a 1D form that provides a convenient starting point for compressible ODT. The basic strategy is to introduce eddy events that interact with evolving property profiles much as in the incompressible formulation. Complications arise because eddy-induced fluid displacements should be isentropic, so the couplings among the equation of state, the pressure field, and the gravitational field (if any) may require concurrent fluid-element dilatations. These couplings imply exchanges among four forms of energy that would be distinguishable in compressible ODT: vortical kinetic energy, dilatational kinetic energy, internal energy, and gravitational potential energy. A physically based procedure for implementing these exchanges has been formulated. Estimates indicate that this approach will capture the leading-order behavior of various compressible-flow regimes of interest.

ODT will be used to support line Raman experiments performed in the Turbulent Combustion Laboratory in the Sandia Combustion Research Facility. ODT simulations incorporating representations of diagnostic performance (space and time resolution, noise and bias characteristics, etc.) will be used to optimize experimental conditions and estimate measurement precision. Fully resolved measurements are not needed because instrument coarse-graining effects can be applied to simulated profiles, so that the model output is directly analogous to the experimental data. ODT is unique among available models in this regard.

The primary breakup of a liquid fuel column injected into an engine cylinder has an important influence on spray development, fuel-air mixing, and combustion in the chamber. Existing models do not capture the relevant microphysical processes in a sufficiently fundamental manner to provide the robust predictive capability needed for engine design studies.

An adaptation of the ODT approach will be developed to model liquid-jet breakup. For this application, the ODT domain represents a line normal to the axis of the liquid column. A potential energy per unit area arising from surface tension is associated with each liquid-gas interface along the 1D domain. Each eddy operation within the simulation triples the number of interfaces contained within the eddy. The energy stored in the newly formed interfaces is subtracted from the energy available to drive the eddy, and accordingly, reduces the likelihood of eddy occurrence. This formulation emulates the inhibition of jet breakup by surface tension.

An advantage of ODT for the liquid-breakup problem is that the model resolves the range of scales required in order to capture the broad size distribution of the evolved droplets. Spectral-

type models that reflect the range of scales, but not the spatial variation of structure, do not readily capture important factors such as the difference between liquid interior flow, whose internal turbulence can promote breakup, and near-surface shear across the liquid-gas interface that contributes to breakup. The ODT approach captures both the range of scales and the spatial variation of structure, thus offering the possibility of higher-fidelity simulation of this process.

ODT simulations of turbulent diffusion flames will be performed to address the unresolved fundamental question of whether flame structure becomes independent of turbulence intensity at very high intensities. This study has bearing on the feasibility of developing sub-grid scale combustion models for turbulent flow simulations, which are predicated on universal small-scale dynamics. In addition, turbulent autoignition processes will be simulated in coordination with ongoing investigation of this topic at the Combustion Research Facility using direct numerical simulation.

REFERENCES

- [1] J. C. Hewson and A. R. Kerstein, *Combust. Sci. Tech.*, in press (2002).
- [2] A. R. Kerstein, *Phys. Rev. E* **64**, 066306 (2001).
- [3] A. R. Kerstein, *Phys. Rev. E* **64**, 036306 (2001).

PUBLICATIONS SINCE 2000

1. Wm. T. Ashurst, "Flow Frequency Effect upon Huygens Front Propagation," *Combust. Theor. Model.* **4**, 99 (2000).
2. Wm. T. Ashurst, H. N. Najm and P. H. Paul, "Chemical Reaction and Diffusion: a Comparison of Molecular Dynamics Simulations with Continuum Solutions," *Combust. Theor. Model.* **4**, 139 (2000).
3. T. D. Dreeben and A. R. Kerstein, "Simulation of Vertical Slot Convection Using One-Dimensional Turbulence," *Int. J. Heat Mass Transf.* **43**, 3823 (2000).
4. A. R. Kerstein and T. D. Dreeben, "Prediction of Turbulent Free Shear Flow Statistics Using a Simple Stochastic Model," *Phys. Fluids* **12**, 418 (2000).
5. A. M. Lisewski, W. Hillebrandt, S. E. Woosley, J. C. Niemeyer, and A. R. Kerstein, "Distributed Burning in Thermonuclear Supernovae of Type IA," *Astrophys. J.* **537**, 405 (2000).
6. S. Wunsch and A. R. Kerstein, "A Model for Layer Formation in Stably Stratified Turbulence," *Phys. Fluids* **13**, 702 (2001).
7. T. Echekki, A. R. Kerstein, J.-Y. Chen, and T. D. Dreeben, "One-Dimensional Turbulence Simulation of Turbulent Jet Diffusion Flames: Model Formulation and Illustrative Applications," *Combust. Flame* **125**, 1083 (2001).
8. A. R. Kerstein, Wm. T. Ashurst, S. Wunsch, and V. Nilsen, "One-Dimensional Turbulence: Vector Formulation and Application to Free Shear Flows," *J. Fluid Mech.* **447**, 85 (2001).
9. A. R. Kerstein, "Kinematics of Small Scale Anisotropy in Turbulence," *Phys. Rev. E* **64**, 036306 (2001).
10. A. R. Kerstein, "Prandtl-Number Dependence of Turbulent Flame Propagation," *Phys. Rev. E* **64**, 066306 (2001).
11. J. C. Hewson and A. R. Kerstein, "Stochastic Simulation of Transport and Chemical Kinetics in Turbulent CO/H₂/N₂ Flames," *Combust. Theor. Model.* **5**, 669 (2001).
12. J. C. Hewson and A. R. Kerstein, "Local Extinction and Reignition in Nonpremixed Turbulent CO/H₂/N₂ Jet Flames," *Combust. Sci. Tech.*, in press (2002).

Photoelectron Photoion Coincidence Studies: Heats of Formation of Ions, Molecules, and Free Radicals

Tomas Baer (baer@unc.edu)
Department of Chemistry
University of North Carolina
Chapel Hill, NC 27599-3290
DOE Grant DE-FG02-97ER14776

Program Scope

The photoelectron photoion coincidence (PEPICO) technique is utilized to investigate the dissociation dynamics and thermochemistry of energy selected medium to large organic molecular ions. Extensive modeling of the dissociation rate constant using the RRKM theory or variational transition state theory (VTST) is used in order to determine the dissociation limits of energy selected ions. These studies are carried out with the aid of molecular orbital calculations of both ions and the transition states connecting the ion structure to their products. The results of these investigations yield accurate heats of formation of ions and free radicals. In addition, they provide information about the potential energy surface that governs the dissociation process. Isomerization reactions prior to dissociation are readily inferred from the PEPICO data.

The PEPICO Experiment

Although the PEPICO experiment is now about 30 years old, we have managed to make some major improvements in its execution by the application of velocity focusing optics. The photoelectron photoion coincidence (PEPICO) experiment in Chapel Hill is carried out with a laboratory H₂ discharge light source. Threshold electrons are collected by passing them through a set of small holes that discriminate against electrons with perpendicular velocity components. The electrons provide the start signal for measuring the ion time of flight distribution. When ions dissociate in the microsecond time scale, their TOF distributions are asymmetric. The dissociation rate constant can be extracted by modeling the asymmetric TOF distribution. A high-resolution version of this experiment is carried out at the Chemical Dynamics Beamline of the ALS, in which pulsed field ionization is used to detect the electrons with a resolution of 1 meV. When combined with coincidence ion detection, the results permit the measurement of ion dissociation limits to within 1 meV or 0.1 kJ/mol.

Recent Results

Threshold Photoelectron Spectroscopy with Velocity Focusing: An Ideal Match for Coincidence Studies

Velocity focusing of low energy electrons has been used to collect threshold photoelectron spectra with a continuous tunable vacuum UV light source. Velocity focusing permits focusing the photoionization image from 5 x 8 mm to 1x1 mm, and thus to collect threshold electrons (less than 10 meV) with a collection efficiency close to 50%. The overall resolution for Xe⁺ of 13 meV is limited primarily by the 12 meV band pass of the photon monochromator. The collection efficiency for energetic electrons of 1 eV is reduced 0.07 %. This method of detecting threshold electrons has improved the resolution by a factor of four and increased the signal by a factor of ten. It is an ideal approach for photoelectron photoion coincidence studies because it permits the collection of electrons and ions with relatively high electric fields of 20 V/cm, which are necessary to have narrow time of flight peaks for the

coincident ion signals. Not only is the performance of this detector much improved, it is a far simpler design than previously used set-ups.

Threshold Photoelectron-Photoion Coincidence Spectroscopy: Dissociation of the 1-Chloroadamantane Ion (the Heat of Formation of the 1-Adamantyl Cation)

Threshold photoelectron-photoion coincidence spectroscopy (TPEPICO) was used to investigate the dissociation of the 1-chloroadamantane ion ($C_{10}H_{15}Cl^+$). The product of Cl loss reaction, $1-C_{10}H_{15}^+$, was the only fragment ion at experimental photon energies (below 13.0 eV). Through the simulation of the metastable TOF distributions of the $1-C_{10}H_{15}^+$ ion and the breakdown diagram, the 0 K appearance energy of $1-C_{10}H_{15}^+$ was determined to be 10.10 ± 0.02 eV. Using this result and the IE value of $1-C_{10}H_{15}Cl$, 9.61 ± 0.02 eV, the dissociation energy of the Cl loss reaction was determined to be 0.49 ± 0.03 eV. Using the known heats of formation of $C_{10}H_{15}Cl$ and Cl, the 298 K and 0 K heats of formation of the $1-C_{10}H_{15}^+$ ion were obtained to be 679.2 ± 3.2 and 731.9 ± 3.2 kJ/mol, respectively. This study has provided us with the first accurate heat of formation of the adamantyl free radical, which we obtain by combining the IE value of $1-C_{10}H_{15}$, with our measured ion heat of formation. The derived 298 K and 0 K heats of formation of $1-C_{10}H_{15}$ are 79.5 ± 4.3 and 132.7 ± 4.3 kJ/mol, respectively.

The Dissociation Dynamics and Thermochemistry of the Acrolein Ion Studied by Threshold Photoelectron-Photoion Coincidence Spectroscopy

Threshold photoelectron-photoion coincidence spectroscopy has been used to investigate the dissociation dynamics of the acrolein ion (CH_2CHCHO^+). The two lowest energy dissociation channels to $C_2H_4^+ + CO$ and $C_3H_3O^+ + H$ are observed at photon energies between 10.0 and 12.0 eV. The $C_2H_4^+$ ion time-of-flight distributions exhibit characteristics of a two-component reaction rate. A three-well-two-channel model is proposed to explain the multi-component dissociation rate. The simulation that fits both the time-of-flight distributions and the breakdown diagram shows that the slow component of the reaction rate for $C_2H_4^+$ production is dominantly caused by tunneling through the isomerization barrier connecting the acrolein ion (A) and the distonic ion, $CH_2CH_2CO^+$ (B). After being produced, only small amounts of B isomerize to the lowest energy conformer, the methylketene ion (C). The energy barrier heights of the isomerization from A to B and the $C_3H_3O^+$ ion production are 0.87 ± 0.02 and 0.92 ± 0.02 eV, respectively. The 0 K appearance energy of the $C_3H_3O^+$ ion is determined to be 11.03 ± 0.02 eV. Using the acrolein heat of formation of -69 ± 10 kJ/mol, the 298 K heat of formation of the CH_2CHCHO^+ ion is determined to be 783 ± 10 kJ/mol.

Exclusive Production of Excited State Sulfur (¹D) atoms from 193 nm Photolysis of Thietane

Tunable synchrotron radiation has been used to probe the dissociation dynamics of thietane (C_3H_6S) at 193 nm, providing selective determination of the translational energy distribution of both excited (¹D) and ground-state (³P) sulfur atoms, with momentum-matching to the C_3H_6 co-fragment. The results suggest that the sulfur atom is produced almost exclusively in its excited (¹D) state, with ground-state (³P) production less than 5%. The first single-photon ionization efficiency (PIE) spectrum for the $S(^1D)$ state with a resolution of 0.2 eV is reported.

One Year as Director of the Chemical Dynamics Beamline at the ALS

Between July 1, 2000 and June 30, 2001, the PI assumed the directorship of the Chemical Dynamics Beamline at the ALS. He has continued this role, but from Chapel Hill. During this

time, the beamline underwent a number of changes including the initiation of two new experiments; the flame diagnostics experiment in which the products and intermediates generated in flames will be detected by photoionization, and the liquid He droplet experiment in which super-cold molecules dissolved in liquid He are photoionized. The first results of the latter experiment have been collected. Both of these experiments are located at the high flux 3m monochromator, which was finally brought on line with a new grating.

Future Plans

The dissociation dynamics of large ions generally involve slow dissociations. In addition, it is often difficult to produce cold beams using cw beam technology. As a result, the high resolution PFI-PEPICO approach may not be the most suitable. The remarkable success of the velocity focusing optics for detection of zero energy electrons will provide an avenue to do TPEPICO experiments with continuous synchrotron radiation without hot electrons. The plan is to use an imaging detector to collect both the zero energy electrons (plus hot electrons) which will be collected in a small spot on the center of the plate, and then to subtract from this signal the hot electron signal that is detected in a ring around the central spot. This approach is currently being tried in the Chapel Hill apparatus. The beauty of this approach is that resolution and flux can be traded off, the ions can be extracted with high electric fields DC (i.e. 20 V/cm) that will result in narrow TOF distributions. This is currently not possible with PFI-PEPICO and greatly limits its application to larger molecules or to free radicals that are not sufficiently cold to product sharp spectra. This project at the ALS is currently being undertaken by the PI, Musa Ahmed (ALS) and a post doc at the ALS. This experiment will be useful not only for TPEPICO studies but also for TPES studies of free radicals. A 1000 Hz excimer laser along with a 1000 Hz pulsed valve will be used to generate these free radicals for ionization with the continuous synchrotron radiation. Among the molecules to be investigated are the 2,3-pentanedione which produces $\text{CH}_3\text{CO}^+ + \text{CH}_3\text{CH}_2\text{CO}^\bullet$ and $\text{CH}_3\text{CO}^\bullet + \text{CH}_3\text{CH}_2\text{CO}^+$, and butanone, which produces $\text{CH}_2\text{COCH}_3^+ + \text{CH}_3^\bullet$ as well as $\text{CH}_3\text{CO}^+ + \text{C}_2\text{H}_5^\bullet$. The dissociative ionization onsets can then be combined with the direct measurement of the corresponding free radical ionization energies to determine free radical heats of formation and thus neutral bond energies. TPEPICO data will initially be collected in the Chapel Hill experiment so that the overall features can be worked out, thereby greatly improving the efficiency of the synchrotron based experiments.

Research Publications Resulting from DOE grant 2000-2002

T. Baer, Y.Song, C.Y. Ng, J.Liu, and W. Chen, "The heat of formation of $2\text{-C}_3\text{H}_7^+$ and proton affinity of C_3H_6 determined by pulsed field ionization - photoelectron photoion coincidence spectroscopy" *J.Phys.Chem.-A*, **104**, 1959-1964 (2000)

R.D. Lafleur, B. Sztaray, and T. Baer "A photoelectron-photoion coincidence study of the ICH_2CN ion dissociation: The Thermochemistry of $^\bullet\text{CH}_2\text{CN}$, $^+\text{CH}_2\text{CN}$, and ICH_2CN " *J. Phys.Chem. A* **104**, 1450-1455 (2000)

Baer, Y.Song, J.Liu, W. Chen, and C.Y. Ng, "Pulsed field ionization - photoelectron photoion coincidence spectroscopy with synchrotron radiation: The heat of formation of the C_2H_5^+ ion" *Disc. Faraday Soc.* # **115** 137-145 (2000)

- B. Sztaray and T. Baer, "The dissociation dynamics and thermochemistry of energy selected $\text{CpCo}(\text{CO})_2^+$ ions" *J. Am. Chem. Soc.* **122**, 9219-9226 (2000)
- T. Baer "Ion dissociation dynamics and thermochemistry by photoelectron photoion coincidence (PEPICO) spectroscopy", *In. J. Mass Spectrom.* **200** 443-457(2000)
- Y. Li, B. Sztaray, and T. Baer, "The dissociation kinetics of energy selected $\text{CpMn}(\text{CO})_3^+$ ions studied by threshold photoelectron photoion coincidence spectroscopy", *J. Am. Chem. Soc.* **123** 9388-9396 (2001)
- K.-M. Weitzel, G. Jarvis, M. Malow, Y. T. Baer, Song, and C. Y. Ng, "Observation of Accurate Ion Dissociation Thresholds in Pulsed Field Ionization Photoelectron Studies", *Phys. Rev. Lett.*, **86** 3526-3529 (2001)
- Y. Li and T. Baer, Threshold photoelectron-photoion coincidence spectroscopy: Dissociation of the 1-chloroadamantane ion and the heat of formation of the 1-adamantyl cation, *J. Phys. Chem. A*, **106** 272-278 (2002)
- F. Qi, L. Sheng, M. Ahmed, D.S. Peterka, and T. Baer, Exclusive production of excited state sulfur (^1D) from 193 nm photolysis of thietane, *Chem. Phys. Lett.* (2001) in press
- Y. Li, J.E. McGrady, and T. Baer, Metal-benzene and metal-CO bond energies in neutral and ionic $\text{C}_6\text{H}_6\text{Cr}(\text{CO})_3$ studied by threshold photoelectron photoion coincidence spectroscopy and DFT theory, *J. Am. Chem. Soc.*, (2002) in press
- Y. Li and T. Baer, Neutral and ionic bond energies in $(\text{C}_6\text{H}_6)_2\text{Cr}$ studied by threshold photoelectron photoion coincidence spectroscopy, *J. Am. Chem. Soc.* (2002) submitted
- T. Baer and Y. Li, Threshold photoelectron spectroscopy with velocity focusing: An ideal match for coincidence studies, *Int. J. Mass Spectrom.* (2002) in press
- Y. Li, B. Sztaray, and T. Baer, The dissociation kinetics of energy selected Cp_2Mn^+ ions studied by threshold photoelectron photoion coincidence spectroscopy, *J. Am. Chem. Soc.* (2002) in press
- B. Sztáray, L. Szepes, and T. Baer, Neutral Cobalt-Carbonyl Bond Energy By Combining Threshold Photoelectron Photoion Coincidence Spectroscopy with He(I) Photoelectron Spectroscopy, *J. Am. Chem. Soc.* (2002) submitted
- Y. Li and T. Baer, Theoretical studies on the isomerization and dissociation of the acrolein ions, *Int. J. Mass Spectrom.* (2002) submitted
- Y. Li and T. Baer, The Dissociation Dynamics and Thermochemistry of the Acrolein Ion Studied by Threshold Photoelectron-Photoion Coincidence Spectroscopy, *Int. J. Mass Spectrom.* (2002) submitted

Turbulence-Chemistry Interactions in Reacting Flows

Robert S. Barlow
Combustion Research Facility
Sandia National Laboratories, MS 9051
Livermore, California 94551
barlow@ca.sandia.gov

Program Scope

This experimental program is directed toward achieving a more complete understanding of the coupling between turbulence and chemistry in both nonpremixed and premixed reacting flows. Spontaneous Raman scattering, Rayleigh scattering, and laser-induced fluorescence are applied simultaneously to obtain spatially and temporally resolved measurements of temperature, multiple species (N_2 , O_2 , H_2 , H_2O , CH_4 , CO_2 , CO , OH , and NO), and other derived scalar quantities, such as the mixture fraction or local equivalence ratio. These detailed measurements of instantaneous thermochemical states in turbulent flames provide insights into the fundamental nature of turbulence-chemistry interactions.

Experiments are conducted in two laboratories and frequently involve visiting scientists, primarily from universities. The Turbulent Diffusion Flame laboratory is equipped for multiscale point measurements and has been productive for many years. The Turbulent Combustion Laboratory is relatively new and includes unique capabilities for single-shot, line-imaging measurements of multiple scalars, as well as state-of-the-art diagnostics for velocity measurements and combined velocity/scalar imaging. This new laboratory allows quantitative investigations of the spatial structure of turbulent flames that are being used to investigate fundamental aspects of emerging combustion technologies and to evaluate turbulent combustion models.

In addition to our experimental work, this program has the leading role in organizing the International Workshop on Measurement and Computation of Turbulent Nonpremixed Flames (TNF), which facilitates collaboration among experimental and computational researchers, who are working on fundamental issues of turbulence-chemistry interactions. A central theme of the TNF Workshop series is to contribute to the development and validation of advanced, predictive models for turbulent combustion. Most of our visiting experiments and external collaborations are carried out in the context of the TNF Workshop, and this arrangement gains significant leverage for the BES Combustion Program.

Recent Progress

We completed our first experiments on scalar dissipation in the Turbulent Combustion Laboratory. The main experiments were conducted in a partially premixed, piloted, CH_4 /air jet flame (Sandia flame D), which is already established as a benchmark for testing of turbulent combustion models. Scalar dissipation is defined as $\chi = 2D_\xi (\nabla \xi \cdot \nabla \xi)$, where ξ is the mixture fraction and D_ξ is its diffusivity. Submodels for scalar dissipation in turbulent flames are central to many modeling approaches, yet they are largely unproven because accurate measurements of scalar dissipation are difficult to achieve, particularly in hydrocarbon flames.

The optical configuration for these scalar dissipation measurements (Fig. 1) combines line imaging of Rayleigh scattering, spontaneous Raman scattering, and CO-LIF. The Raman

imaging system uses a Sandia-developed rotating mechanical shutter (9 μ s gate) in combination with an imaging spectrograph and an unintensified, back-illuminated, cryogenically cooled CCD array detector. The high collection efficiency, wide dynamic range, and low noise achieved with this system are critical for the measurement of scalar dissipation, χ , which is determined from the square of the spatial derivative of the mixture fraction, ξ .

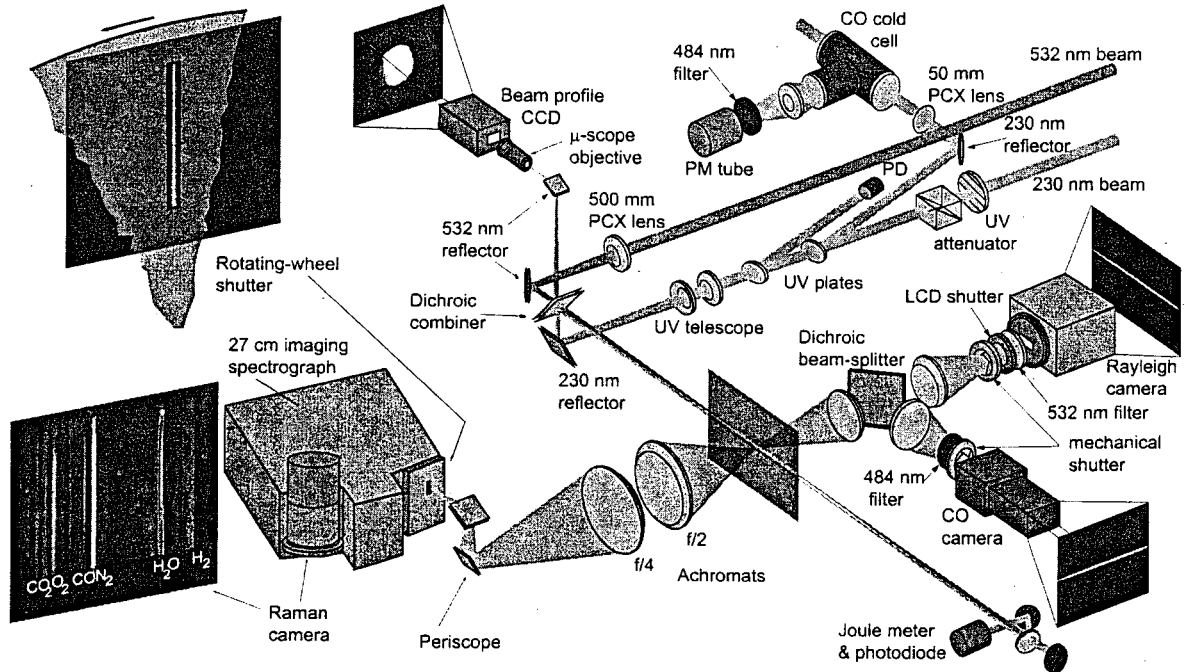


Fig. 1. Experimental system for simultaneous line-imaging of Raman scattering, Rayleigh scattering, and CO LIF.

Results for the radial component of scalar dissipation at three streamwise locations in turbulent flame D are presented in Fig. 2 as two-dimensional density plots. These plots are constructed from one-dimensional probability density functions (*pdf*'s) of scalar dissipation conditioned upon the mixture fraction, such that each represented value of ξ (each vertical slice) has equal probability. Scalar dissipation is examined in logarithmic space, hence the presentation of $pdf(\ln \chi | \xi)$. The darker areas correspond to higher probability. The solid line in each density plot represents the average value of scalar dissipation conditioned upon the mixture fraction, $(\ln \langle \chi | \xi \rangle)$.

Scalar dissipation is broadly distributed at all measured positions in the flame except on the fuel-lean side close to the exit ($x/d=7.5$), where the flow field is not fully turbulent. There is a clear trend towards smaller values of χ with increasing downstream distance, manifested both in the density plots and the average values. The streamwise decay in ξ , manifested in the progressive erosion of very rich samples, is also evident. The double-peak structure noted in the laminar jet flame persists in the turbulent flame. A local minimum in χ can be seen near the stoichiometric value (marked by a dotted line in Fig. 2 at all three streamwise locations). The local maxima in χ are higher on the fuel-rich side of the flame.

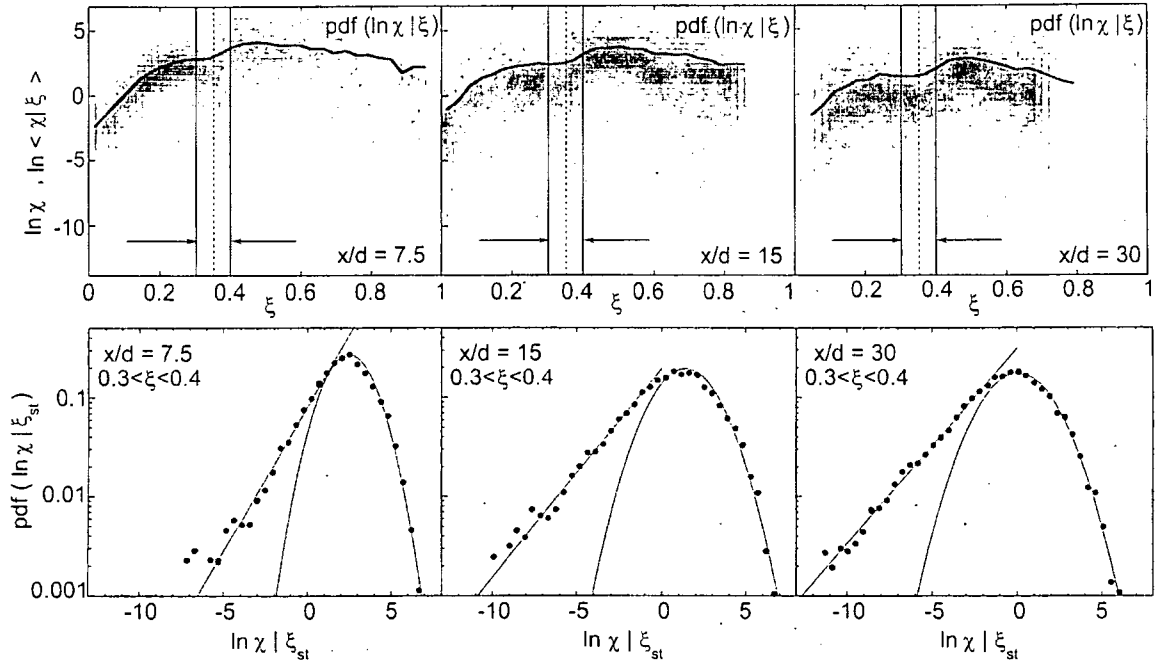


Fig. 2. Top row: density plots of scalar dissipation for the three axial positions ($x/d = 7.5, 15, \text{ and } 30$) in flame D. Darker areas correspond to higher density in the $pdf(\ln \chi | \xi)$. The average conditional scalar dissipation ($\ln \langle \chi | \xi \rangle$) is plotted as a solid line. Bottom row: 1D pdf of scalar dissipation conditioned upon the mixture fraction around the stoichiometric value ($pdf(\ln \chi | \xi_{st})$). Data within the range $0.3 \leq \xi \leq 0.4$ were used to form the 1D $pdfs$. Solid lines represent exponential and log-normal fits to the left and right tails of the pdf , respectively.

Future Plans

Future work will push the line measurements to better spatial resolution, particularly for the Rayleigh imaging system. Diagnostic systems for planar laser-induced fluorescence imaging of OH in two planes that intersect the Raman/Rayleigh/LIF line will be added. This will allow for determination of the instantaneous flame normal direction and flame curvature at the point of intersection with the multiscalar line, so that the joint conditional statistics of various scalars (species mass fractions, mixture fraction, scalar dissipation, the differential diffusion parameter, etc.) and flame structure parameters may be quantified. The investigation of piloted flames will be expanded to include the other flames in this series, which have significant localized extinction and re-ignition, and will include larger statistical samples and measurements of the tangential component of scalar dissipation, as well as the radial component.

BES Supported Publications (2000 - present)

- R. S. Barlow and P. C. Miles, "A Shutter-Based Line-Imaging System for Single-Shot Raman Scattering Measurements of Gradients in Mixture Fraction," *Prog. Comb. Inst.* **28**:269 (2000).
- R. S. Barlow, G. J. Fiechtner, C. D. Carter, and J.-Y. Chen, "Experiments on the Structure of Turbulent CO/H₂/N₂ Jet Flames," *Combust. Flame* **120**:549 (2000).
- R. S. Barlow, A. N. Karpetis, J. H. Frank, and J.-Y. Chen, "Scalar Profiles and NO Formation in Laminar Opposed-Flow Partially-Premixed Methane/Air Flames," *Combust. Flame* **127**:2102 (2001).
- R. S. Barlow, C. D. Carter, R. W. Pitz, "Multiscalar Diagnostics in Turbulent Flames," in *Applied Combustion Diagnostics*, J. B. Jeffries and K. Kohse-Hoeinghaus, eds., Taylor & Francis (in press).
- R. Cabra, T. Myhrvold, J.-Y. Chen, R. W. Dibble, A. N. Karpetis, and R. S. Barlow, "Simultaneous Laser Raman-Rayleigh-LIF Measurements and Numerical Modeling Results of a Lifted Turbulent H₂/N₂ Jet Flame in a Vitiated Coflow," *29th International Combustion Symposium* (accepted).
- B. B. Dally, A. N. Karpetis, and R. S. Barlow, "Structure of Turbulent Nonpremixed Jet Flames in a Dilute Hot Coflow," *29th International Combustion Symposium* (accepted).
- J. H. Frank, R. S. Barlow, and C. Lundquist, "Radiation and Nitric Oxide Formation in Turbulent Nonpremixed Jet Flames," *Prog. Comb. Inst.* **28**:447 (2000).
- P. A. M. Kalt, Y. M. Al-Abdeli, A. R. Masri, and R. S. Barlow, "Swirling Turbulent Nonpremixed Flames of Methane: Flowfield and Compositional Structure," *29th International Combustion Symposium* (accepted).
- W. Meier, R. S. Barlow, Y.-L. Chen, and J.-Y. Chen, "Raman/Rayleigh/LIF Measurements in a Turbulent CH₄/H₂/N₂ Jet Diffusion Flame: Experimental Techniques and Turbulence-Chemistry Interactions," *Combust. Flame* **123**:326 (2000).
- P. C. Miles and R. S. Barlow, "Fast Mechanical Shutter for Spectroscopic Applications," *Meas. Sci. Technol.* **11**:392 (2000).
- P. A. Nooren, M. Versuijs, T. H. van der Meer, R. S. Barlow, and J. H. Frank, "Raman-Rayleigh-LIF Measurements of Temperature and Species Concentrations in the Delft Piloted Turbulent Jet Diffusion Flame," *Appl. Phys. B*, **71**:95 (2000).
- X. L. Zhu, J. P. Gore, A. N. Karpetis, and R. S. Barlow, "The Effects of Self-Absorption of Radiation on an Opposed Flow Partially Premixed Flame," *Combust. Flame* (in press).

Web-Based Information

<http://www.ca.sandia.gov/CRF/staff/barlow.html>
<http://www.ca.sandia.gov/tdf/Workshop>

Research Page
TNF Workshop

Energy Partitioning in Elementary Chemical Reactions

Richard Bersohn
Department of Chemistry
Columbia University
New York, NY 10027
E-mail rb18@columbia.edu

The goals of this research are 1) to measure the yields of all the important channels of the reactions of O(³P) with unsaturated hydrocarbons and radicals and 2) by measurement of state distributions to understand the detailed mechanism. i.e. the trajectories of the atoms during the reactive collision.

1. Mechanisms of Formation of Vinyoxy Radicals

The position of O atom substitution in propene which leads to the vinyoxy + methyl channel can be deduced, as will be shown, from an identification of partially deuterated vinyoxys. These, in turn, are generated from partially deuterated propenes. An examination of the emission spectrum and the hot band LIF excitation spectrum of vinyoxy shows that the 4₁⁰ band head is particularly strong and resolved.¹ While ν_4 is nominally the C-O stretch its frequency is nevertheless sensitive to deuterium substitution at either carbon atom. Table 1 shows the effect of deuterium substitution at C-1, the aldehyde carbon and C-2, the methylene carbon.

Table 1 Frequency shifts of 4₁⁰ relative to that in CH₂CHO

isotopomer	frequency shift (cm ⁻¹)	isotopomer	frequency shift (cm ⁻¹)
CH ₂ CHO	0	CHDCHO	14(18)
CD ₂ CHO	37	CHDCDO	50(58)
CH ₂ CDO	40		
CD ₂ CDO	81 (77)		

Numbers in parentheses are calculated from the first three numbers in column 1..

An assumption which was previously shown to hold for similar transitions in formaldehyde and acetaldehyde is that the D atom isotope shifts are additive and independent. That is 77 is close to 81. Let us assume that the frequency shift on substitution of a D at C-1 is 40 cm⁻¹ and at C-2 37/2 ≈ 18, the shifts of the isotopomers in the third column of Table 1 given in parentheses are in rough agreement with the observed frequencies. There is a difficulty with the observed frequencies in that CHDCHO and CHDCDO exist as *cis* and *trans* isomers between which there is an unknown splitting.

Fig. 2A shows the LIF excitation spectrum of the vinoxy resulting from the reaction of $O(^3P)$ with $CH_3CH=CD_2$. Attack at C-1 produces $CHDCDO$ and attack at C-2 produces CD_2CHO . There are two band heads of comparable intensity and 13 cm^{-1} apart. The higher frequency band must be due to $CHDCDO$ whereas the other is assigned to CD_2CHO . Our interpretation is that vinoxy results from attacks at C-1 and C-2 in comparable yields. Fig. 2B shows the LIF excitation spectrum of the vinoxys resulting from the reaction of $O(^3P)$ with $CH_3CD=CH_2$. Attack at C-1 produces $CHDCHO$ whereas attack at C-2 produces CH_2CDO . The first sharp 4_1^0 band is 40 cm^{-1} higher than that of vinoxy and is therefore assigned to CH_2CDO . The overall shape of the band is very different from the flat topped bands shown in Fig. 1. It rises with increasing wave length, suggesting that it is a superposition of two vinoxy isotopomers in roughly equal amounts. The conclusion again is that vinoxy radicals are derived roughly equally from attacks at C-1 and C-2. This does *not* mean that reactions at C-1 and C-2 have the same probability. Attack at C-1 yields several different product channels with the major one being the molecular product channel of formaldehyde and ethylene. Attack at C-2 yields almost exclusively methyl and vinoxy radicals.

When ethylene reacts with oxygen atoms, vinoxy can be formed by attack at one carbon atom and loss of a hydrogen atom from that same carbon atom. The alternative path involves the migration of an H atom from the attacked carbon atom to the other carbon atom to form a hot acetaldehyde with subsequent release of one of the three methyl H atoms. Reaction of O atoms with $CH_2=CD_2$ produces a mixture of CH_2CDO and CD_2CHO with only a small band head due to $CHDCDO$. Evidently the channel of direct release of a hydrogen atom is preferred over the channel of indirect release via a hot acetaldehyde. In other words, the hot acetaldehyde preferentially decomposes to break its C-C bond forming HCO and CH_3 rather than to break a methyl C-H bond. The weaker bond is more likely to break.

2. Generation of ketyl, HCCO

The usual method of generating ketyl radical, HCCO is by photodissociating ketene at 193 nm. The method has two drawbacks. First the unstable ketene must be synthesized. Second, ketene has only a very weak absorption at 193 nm. Ethynyl ethyl ether, commercially available is an attractive starting point. It has a strong absorption at 193 nm and is therefore a more convenient source of HCCO. Unlike, vinoxy, ethynyl does not display a rich hot band $B\leftarrow X$ LIF excitation spectrum. Appreciable fluorescence was detected by exciting the nascent HCCO at the band origin but not at lower energies.²

Fig. 1 Partial hot band spectra of CH_2CO , CD_2CHO and CD_2CDO . The relatively large isotope shifts of the 4_1^0 band head allow identification of vinyloxy isotopomers. The X-State energy on the upper axis is relative to the lowest ground state level.

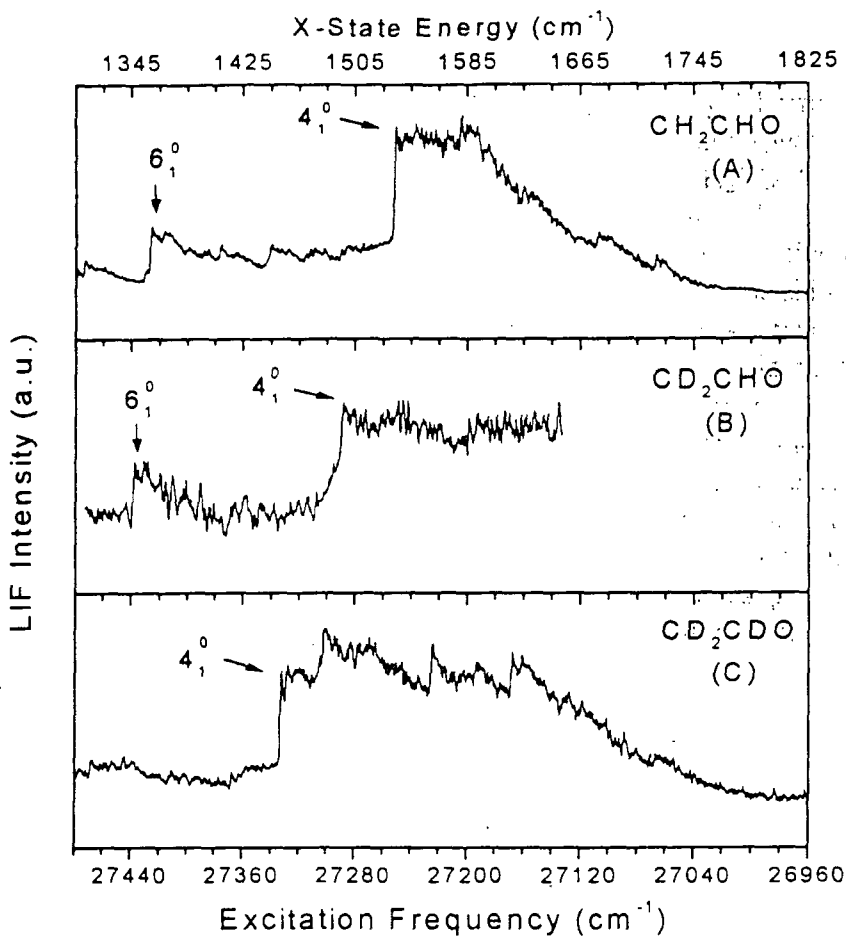
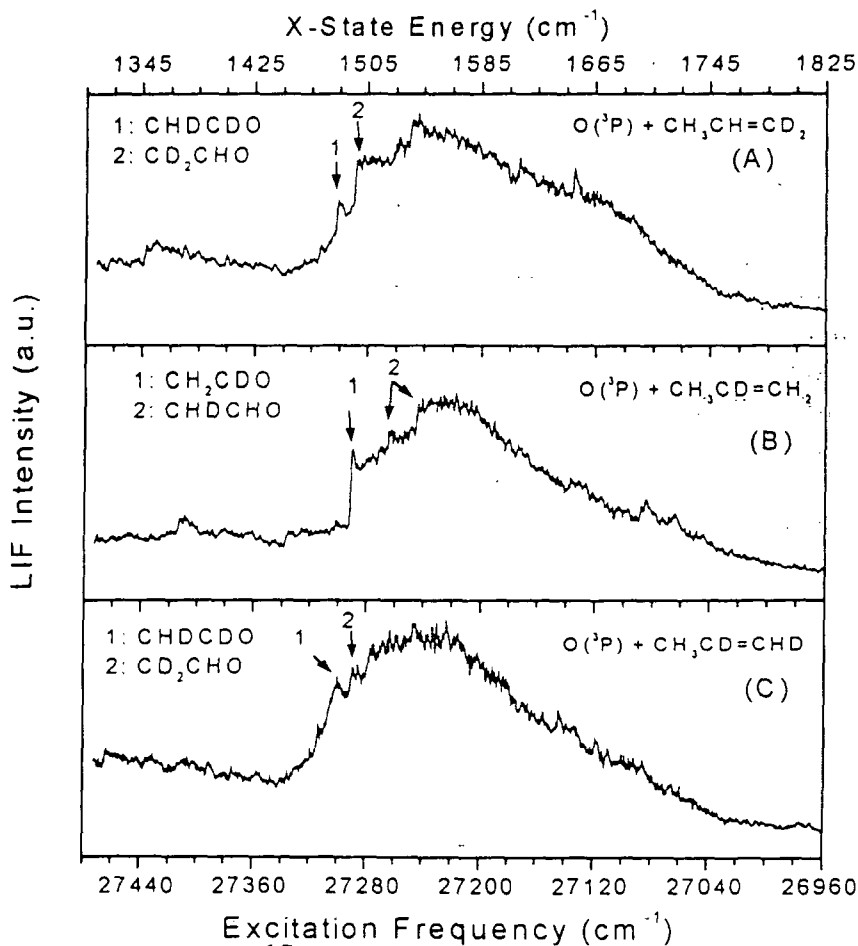


Fig. 2 Partial hot band spectra of the mixture of vinyloxy isotopomers produced by the reaction of $\text{O}({}^3\text{P})$ with CH_3CHCD_2 , CH_3CDCH_3 and CH_3CDCHD .



Future experiments

Final tests are being carried out on a newly built minimolecular beam machine in which two oppositely directed valves will open for 10 μ s and release hydrocarbon molecules and N₂O molecules respectively. The N₂O will pass through a short very hot zirconia tube forming oxygen atoms.³ The reacting gases collide above the repeller plate of a TOF mass spectrometer. Synchronized pulses of vuv light will ionize the radical products. This is a new version of an experiment of D.Gutman and coworkers,⁴ which will be closer to the ideal limit of single collisions. The apparatus will not measure angular distributions but will, it is hoped measure relative product yields of radicals quantitatively.

References

1. L.R.Brock and E.A.Rohlfing, J.Chem.Phys. **106**,10048(1997)
2. L.R.Brock, E.Mischler, E.A.Rohlfing, J.Chem.Phys. **110**,6773(1999)
3. D.W.Kohn, H.Clauberg, P.Chen, Rev.Sci.Inst. **63**,4003(1992)
- 4.J.R.Kanofsky,D.Lucas,F.Pruss and D.Gutman, J.Phys.Chem.**78**,311(1973)

Publications in years 2000, 2001 and 2002

1. Reaction of O(³P) with Alkenes: Side Chain vs. Double Bond Attack, Zhiyuan Min, Teh-Hwa Wong, Hongmei Su and Richard Bersohn, J.Phys.Chem.A **104**,9941(2000)
- 2.Photodissociation of acetaldehyde: the CO + CH₄ Channel Benjamin Gherman, Richard Friesner, Teh-Hwa Wong, Zhiyuan Min, J.Chem.Phys. **114**,6128(2001)
3. Vibrational Distribution and Relaxation of Vinyloxy Radicals, Hongmei Su and Richard Bersohn, J.Chem.Phys. **115**,217(2001)
4. Mechanism of Formation of Vinyloxy Radicals in the Reaction of O(³P) with Terminal Alkenes, Hongmei Su and Richard Bersohn, J.Phys. Chem. **105**,9178(2001)
5. Chemical Physics, Richard Bersohn and Bruce Berne, chapter in *Encyclopedia of Science & Technology*, Vol2 3rd Ed.Academic Prsss, New York, 2002

Theoretical Studies of Combustion Dynamics

Joel M. Bowman
Cherry L. Emerson Center for Scientific Computation and
Department of Chemistry, Emory University
Atlanta, GA 30322,
bowman@euch4e.chem.emory.edu

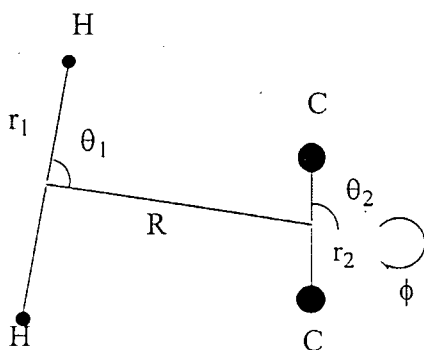
Program Scope

We develop and apply *ab initio* and quantum dynamical approaches to chemical processes of importance in gas-phase combustion. Recent work has focused on two important and challenging problems: acetylene/vinylidene isomerization and the role of van der Waals wells in chemical reactions, as exemplified by the $O(^3P)+HCl$ reaction. The highlights of this work are described below.

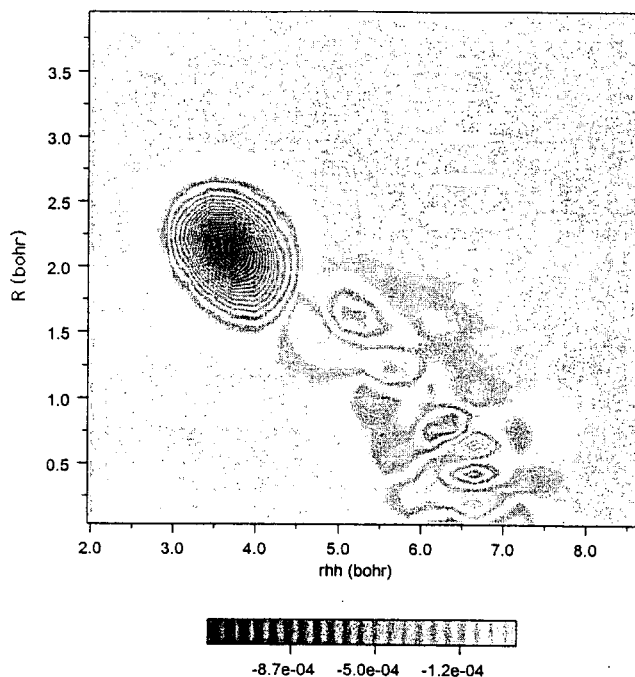
Recent Progress

Acetylene/vinylidene isomerization

The existence of a metastable vinylidene isomer among a sea of highly excited acetylenic eigenstates has been of intense interest to both experimentalists and theorists for more than a decade.¹⁻⁸ A full-dimensionality quantum approach remains out of reach (although on the horizon, I believe), and so we have opted to consider a reduced dimensionality approach. This has been successful and some of the highlights are as follows. First, in order to carry out a reduced dimensionality approach, active degrees of freedom need to be selected. The diatom-diatom Jacobi coordinates shown below satisfy this very well. As can be easily imagined the acetylene minimum corresponds to $R = 0$ and both θ_1 and θ_2 equal to 90 degrees. Isomerization to the vinylidene minimum can be described by three active degrees of freedom R , r_1 and θ_2 . Clearly these three variables must undergo large amplitude motion in order to describe isomerization of linear acetylene to the C_{2v} minimum structure of vinylidene. Our strategy to obtain eigenstates began with a reduced



dimensionality Hamiltonian in the two degrees of freedom R and θ_2 , where the potential is relaxed in the remaining four degrees of freedom. Then, successively, eigenstate calculations were done in 3 and 4 degree-of-freedom calculations by adding the HH-stretch (r_1) and the spectator CC-stretch (r_2) as active degrees of freedom. At all of these levels of reduced dimensionality molecular eigenstates with characteristics (i.e., expectation values) of a vinylidene-like state were found. A contour plot in R and r_1 of the lowest energy vinylidene-like state obtained from the 4 degree-of-freedom

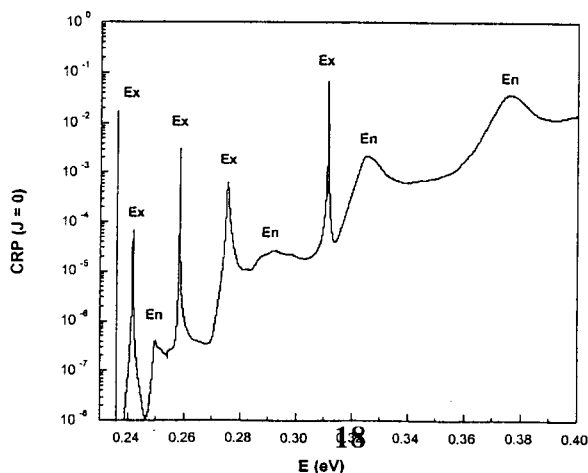


calculations is shown below. As seen, the wavefunction is highly concentrated in the vicinity of the vinylidene minimum

($R = 2.25$ bohr, $r_{\text{HH}} = 3.54$ bohr) but wisps of the large amplitude motion down to the acetylene minimum are clearly seen as well. This is the first calculation of a vinylidene-like molecular eigenstate.

$O(^3P)+HCl$

The $O(^3P)+HCl$ reaction has played an important role in quantum reactive scattering,¹⁰⁻¹⁶ with most calculations done on a potential energy surface missing van der Waals (vdW) wells in the entrance and exit channels.¹⁰ Quantum dynamics calculations on a new potential,¹⁴ which does contain these wells, were done in collaboration with Stephen Gray (ANL) and revealed intriguing resonance structures in the deep tunneling region of the reaction.¹⁵ In a more recent collaboration with David Manolopoulos (Oxford)¹⁶ we verified that these structures are due to quasibound states of the vdW wells.¹⁶ We were able to assign each resonance to a quasibound state of a given well, as shown below in the plot of the cumulative reaction probability for zero total angular



momentum versus the total energy ("Ex" and "En" indicate the vdW in the entrance or exit channel, respectively, and the barrier height is 0.424 eV.)

Future Plans

We are setting up to do full dimensionality calculations of the acetylene/vinylidene isomerization, with the goal of obtaining realistic results that will, however, almost certainly fall short of "spectroscopic" accuracy. The coding to do this, which is underway, will require a proper coupling of the two internal rotational degrees of freedom. We also plan to do further calculations of the rate constant of the $O(^3P)+HCl$ and will consider the importance of the A' surface at high temperatures.

References

1. K. M. Ervin, J. Ho, and W. C. Lineberger, *J. Chem. Phys.* **91**, 5974 (1989).
2. (a) M. P. Jacobson, J. P. O'Brian, R. J. Silbey, and R. W. Field, *J. Chem. Phys.* **109**, 121 (1998); (b) M. P. Jacobson and R. W. Field, *J. Phys. Chem. A*, **104**, 3073 (2000), and references therein.
3. J. Levin, H. Feldman, A. Baer, D. Ben-Hamu, O. Heber, D. Zajfman, and Z. Vager, *Phys. Rev. Lett.* **81**, 3347 (1998).
4. T. Carrington Jr., L. M. Hubbard, H. F. Schaefer, III, and W. H. Miller, *J. Chem. Phys.* **80**, 4347 (1984).
5. J. F. Stanton and J. Gauss, *J. Chem. Phys.* **110**, 6079 (1999) and private communication.
6. T. Germann and W. H. Miller, *J. Chem. Phys.* **109**, 94 (1998).
7. (a) R. Schork and H. Köppel, *J. Chem. Phys.* **115**, 7907 (2001); (b) R. Schork and H. Köppel, *Phys. Chem. Chem. Phys.* **3**, 891 (2001).
8. R. L. Hayes, E. Fattal, N. Govind, and E. A. Carter, *J. Amer. Chem. Soc.* **123**, 641 (2001).
9. S.-L. Zou and J. M. Bowman, *J. Chem. Phys.* **116**, 6667 (2002).
10. H. Koizumi, G. C. Schatz, and M. S. Gordon, *J. Chem. Phys.* **85**, 6421 (1991).
11. W. H. Thompson and W. H. Miller, *J. Chem. Phys.*, **106**, 142 (1996).
12. K. Nobusada and H. Nakamura, *J. Phys. Chem. A*, **103**, 6715 (1999).
13. F. Matzkies and U. Manthe, *J. Chem. Phys.* **112**, 130 (2000).
14. B. Ramachandran, E. A. Schrader, III; J. Senekowitsch, and R. E. Wyatt, *J. Chem. Phys.* **111**, 3862 (1999).
15. (a) S. Skokov, T. Tsuchida, S. Nanbu, J. M. Bowman, and S. K. Gray, *J. Chem. Phys.* **113**, 227 (2000); (b) K. Nobusada, H. Nakamura, Y. Lin, B. Ramachandran, *J. Chem. Phys.* **113**, 1018 (2000).
16. T. Xie, D. Wang, J. M. Bowman, and D. E. Manolopoulos, *J. Chem. Phys.* **116** xxxx (2002).

PUBLICATIONS SUPPORTED BY THE DOE (2000-present)

Wavepacket propagation for reactive scattering using real L^2 eigenfunctions with damping, S. Skokov and J.M. Bowman, *Phys. Chem. Chem. Phys.* **2**, 495 (2000)

Approximate time independent methods for polyatomic reactions, J. M. Bowman, in *Reaction and Molecular Dynamics (Proceedings of the European School on Computational Chemistry, Perugia, Italy, July (1999))* Lagana, A., Riganelli, A., (Eds.) (Springer, 2000)

Quantum dynamics and rate constant for the $O(^3P)+HCl$ reaction, S. Skokov, T. Tsuchida, S. Nambu, J. M. Bowman, and S. Gray, *J. Chem. Phys.* **113**, 227 (2000).

- A reduced dimensionality quantum calculation of the reaction of H₂ with diamond (111) surface, S. Skokov and J. M. Bowman, *J. Chem. Phys.* **113**, 779 (2000)
- A wavepacket calculation of the effect of reactant rotation and alignment on product branching in the O(¹D)+HCl → ClO+H, OH+Cl reaction, M. Bittererova and J. M. Bowman, *J. Chem. Phys.* **113**, 1 (2000).
- Quantum scattering calculations of the O(¹D)+HCl reaction using a new *ab initio* potential and extensions of J-shifting, M. Bittererova, J. M. Bowman, and K. Peterson, *J. Chem. Phys.* **113**, 6186 (2000).
- Quantum calculations of the effect of bend excitation in methane on the HCl rotational distribution in the reaction CH₄ + Cl → CH₃ + HCl, S. Skokov and J. M. Bowman, *J. Chem. Phys.* **113**, 4495 (2000).
- Thermal and state-selected rate coefficients for the O(³P) + HCl reaction and new calculations of the barrier height and width, S. Skokov, S. Zou, J. M. Bowman, T. C. Allison, D. G. Truhlar, Y. Lin, B. Ramachandran, B. C. Garrett, and B. J. Lynch, *J. Phys. Chem.* **105** 2298 (2001).
- State-to state reactive scattering via real L² wave packet propagation for reduced dimensionality AB + CD reactions, S. Skokov and J. M. Bowman, *J. Phys. Chem. A* **105**, 2502 (2001).
- Ab initio* calculation of resonance energies and widths of HOCl(7v_{OH}) and (8v_{OH}) and comparison with experiment, S. L. Zou, S. Skokov, and J. M. Bowman, *Chem. Phys. Lett.* **339**, 290 (2001)
- A reduced dimensionality, six-degree-of-freedom, quantum calculation of the H+CH₄ H₂+CH₃, D. Wang and J. M. Bowman, *J. Chem. Phys.* **115**, 2055 (2001).
- The importance of an accurate CH₄ vibrational partition function in full dimensionality calculations of the H + CH₄ → H₂ + CH₃ reaction, J. M. Bowman, D. Wang, X. Huang, F. Huarte-Larrañaga and U. Manthe, *J. Chem. Phys.* **114**, 9683 (2001).
- The unimolecular dissociation of the OH stretching states of HOCl: Comparison with experimental data, J. Weiss, J. Hauschildt, R. Schinke, O. Haan, S. Skokov, J. M. Bowman, V. A. Mandelshtam, and K. A. Peterson, *J. Chem. Phys.* **115**, 8880 (2001).
- The challenge of high resolution dynamics: Rotationally mediated unimolecular dissociation of HOCl, J. M. Bowman, in Accurate Description of Low-Lying Electronic States, edited by M. Hoffman (ACS, Washington, DC, 2002).
- A quasiclassical trajectory study of O(¹D)+HCl reactive scattering on an improved *ab initio* surface, K. M. Christoffel and J. M. Bowman, *J. Chem. Phys.* **116**, 4842 (2002).
- Reduced dimensionality quantum calculations of acetylene vinylidene isomerization, S.-L. Zou and J. M. Bowman, *J. Chem. Phys.* **116**, 6667 (2002).
- Resonances in the O(³P)+HCl reaction due to Van der Waals minima, T. Xie, D. Wang, J. M. Bowman, and D. E. Manolopoulos, *J. Chem. Phys.* **116** xxxx (2002).

Very High Pressure Single Pulse Shock Tube Studies of Aromatic Species
Kenneth Brezinsky
Department of Chemical Engineering (M/C 110)
University of Illinois at Chicago
810 S. Clinton St.
Chicago, IL 60661
Kenbrez@uic.edu

PROGRAM SCOPE AND FOCUS

The research in this program focuses on oxidation and pyrolysis experiments of benzene, toluene and the related species, phenol and cyclopentadiene, in a very high pressure single pulse shock tube in order to obtain data at extremes of pressure and temperature. With these data, existing models can be validated at extreme conditions permitting the development of a comprehensive benzene/toluene oxidation model potentially applicable to the reduction and prevention of pollution.

In addition, individual unimolecular and bimolecular reactions that have already been identified in the literature as needing further examination will be probed. Probing can be accomplished in the shock tube by variation in a) temperature b) pressure c) time d) initial reactant concentrations, and/or by e) the addition of radical or precursor species. Changing the reaction conditions or doping the system with additives will lead to changes in detected species that will be elucidated with complementary modeling.

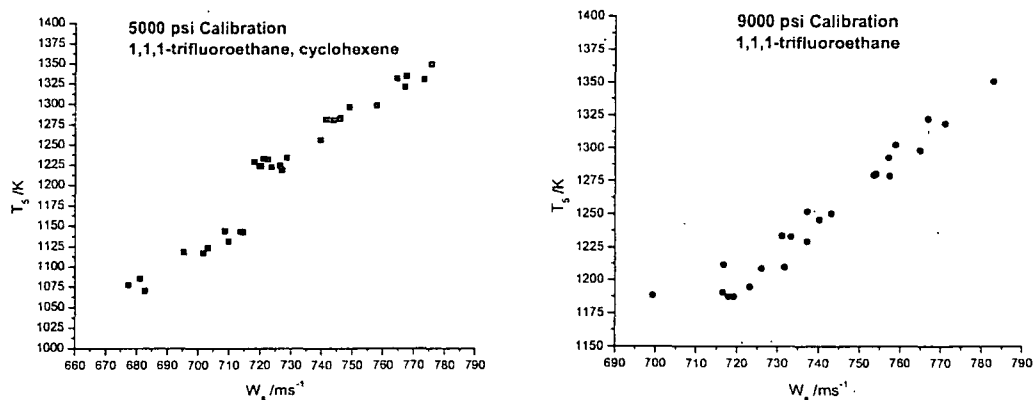
RECENT PROGRESS

Shock Tube Performance

Design, construction and testing of the single pulse shock tube to achieve extremely high pressures and temperatures to facilitate gas-phase chemical kinetic studies have been completed. The shock tube has been designed and demonstrated to operate at pressures up to 1000 atmospheres. Reaction times in the shock tube have been varied from 0.5 ms to 2.5 ms by using variable driven section lengths. For any particular reaction time, stable gas-phase reactant and product samples are withdrawn from the shock tube through an automated sampling apparatus. Samples have been subsequently analyzed using state of the art GC, GC/MS apparatus. The details of the design, construction and testing that have permitted very high shock pressures to be achieved are described in a recent publication¹.

The temperature is a very important parameter in the shock tube. Real gas effects² at the high pressures in the shock tube give incorrect estimates if the ideal shock wave relations are used to calculate the reaction temperatures. An external chemical thermometer method has been developed to calculate the temperature in the high-pressure shock tube³. Two chemical thermometers, 1,1,1-trifluoroethane and cyclohexene, have been used to calibrate the temperatures behind reflected shock waves, T_{5real} , as a function of end wall shock velocity. Experiments with 1,1,1-trifluoroethane were performed at post-shock pressures of 5000 psi and 9000 psi and T_{5real} was calculated from the extent of reaction and literature values for k_{∞} . At each pressure the two methods of calculating

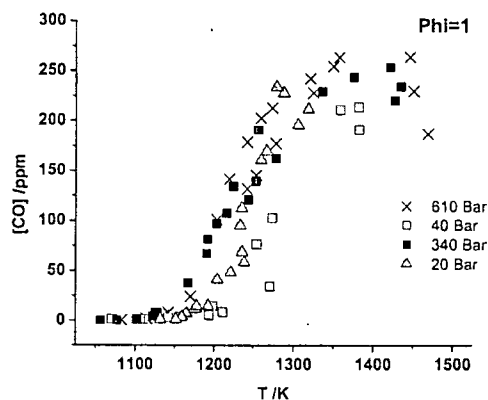
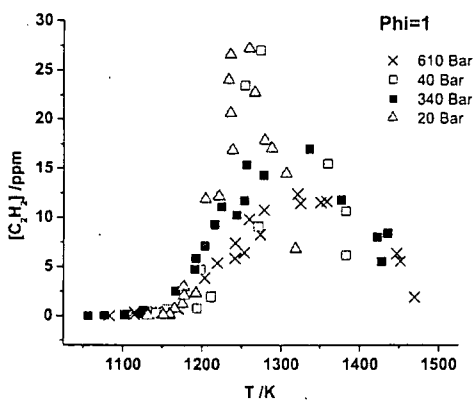
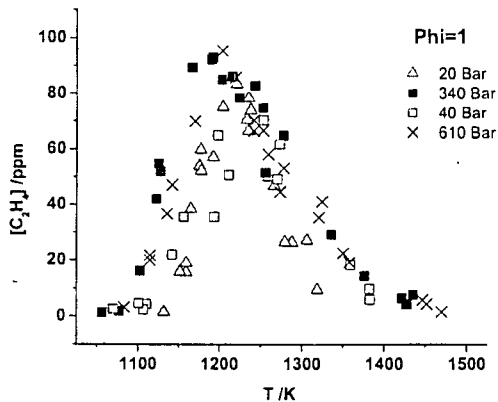
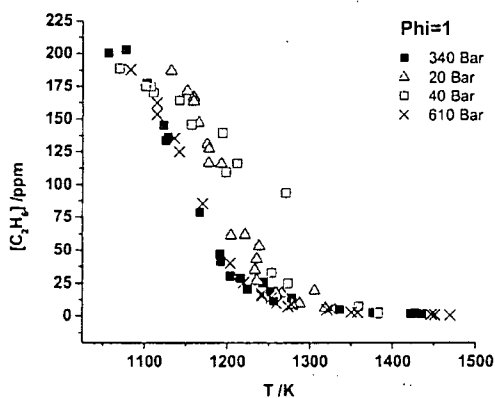
$T_{5\text{real}}$ are in excellent agreement. The values for $T_{5\text{real}}$ obtained from the cyclohexene experiments are in good agreement with those from 1,1,1-trifluoroethane. The range of the temperature calibration is 1050-1350 K. No discernible pressure dependence between the two sets of experiments was observed for the calculated values of $T_{5\text{real}}$. The effect of a 10% rise in pressure during the residence time on the calculated temperatures was also examined and found to give rise to only small errors in $T_{5\text{real}}$. Representative calibration curves used to calculate the temperature in the high pressure shock tube are shown below.



Ethane Oxidation and Pyrolysis Studies Over Very Wide Pressure Ranges:

The high pressure shock tube has been used to obtain the first experimental data for ethane oxidation and pyrolysis at very high pressures and temperatures. Experiments were performed at two nominal reaction pressures of 340 bar and 610 bar in the temperature range 1050 K to 1400 K⁴. The major stable species were identified and their concentrations determined using gas chromatography. Several minor species, with up to six carbon atoms and including oxygenates, were also observed in the oxidation studies. Three models based on literature mechanisms for hydrocarbon oxidation were used to simulate the experimental data. All of the models simulate the pyrolysis data well although only one of the models was capable of accurately describing the oxidation data.

Ethane oxidation was also studied at reaction pressures of 5, 20, 40 and 1000 bar and at temperatures between 1000 and 1400 K. Oxidation was studied with stoichiometric ratios of $\Phi = 1$ and $\Phi = 5$ ⁵. As with the high pressure oxidation, gas chromatography was used to quantify the major stable species formed in the reactions. The experimental data were simulated using two models for ethane combustion that had previously been tested against very high pressure (300-600 bar) oxidation and pyrolysis experimental data obtained in the same apparatus. Good agreement with stoichiometry of $\Phi = 1$ was obtained, however neither model was capable of simulating the $\Phi = 5$ data. Several modifications to one of the models were made and these modifications are discussed. The final version of the model provides much more accurate predictions of the experimental data and forms the first step in developing a comprehensive model for ethane oxidation that has been tested against experimental data covering a pressure range from 1 bar to 1000 bar.



The plots shown above represent the experimental data that have been obtained for ethane oxidation with $\Phi = 1$ over a very wide range of pressures from around 20-610 bar covering the temperature range from 1050-1400 K. Note the reaction times for the above data span 1.3 to 1.8 msec.

FUTURE WORK

Toluene oxidation experiments have been initiated. Some experimental difficulties handling toluene have been resolved so that subsequent experiments focusing on the 9000 psi (610 bar) pressure regime can commence. At this high pressure, species concentrations as a function of temperature and stoichiometry will be obtained. Additional experiments at different temperatures and reaction times are also planned.

REFERENCES

1. Tranter R.S., Fulle D. and Brezinsky K., *Rev. Sci. Inst.*, 72, 3046 (2001).
2. Davidson D.F., Hanson R.K., *Israel J. Chem.*, 36, 321 (1996).
3. Tranter R.S., Sivaramakrishnan R., Srinivasan N. and Brezinsky K., *Int. J. Chem. Kin.*, 33, 722 (2001).
4. Tranter R.S., Sivaramakrishnan R., Brezinsky K. and Allendorf M.D., *Phys. Chem., Chem. Phys.*, In Press.
5. Tranter R.S., Ramamoorthy H., Raman A., Brezinsky K., Allendorf M.D., Paper accepted for presentation at 29th International Symposium on Combustion.

Publications based on the DOE supported work:

Tranter R.S., Fulle D. and Brezinsky K., "Design of a High Pressure Single Pulse Shock Tube for Chemical Kinetic Investigations", *Rev. Sci. Inst.*, 72, 3046 (2001).

Tranter R.S., Sivaramakrishnan R., Srinivasan N. and Brezinsky K., "Calibration of Reaction Temperatures in a Very High Pressure Shock Tube Using Chemical Thermometers", *Int. J. Chem. Kin.*, 33, 722 (2001).

Tranter R.S., Sivaramakrishnan R., Brezinsky K. and Allendorf M.D., "High Pressure, High Temperature Shock Tube Studies of Ethane Pyrolysis and Oxidation", *Phys. Chem., Chem. Phys.*, In Press.

Tranter R.S., Ramamoorthy H., Raman A., Brezinsky K., Allendorf M.D., "High Pressure Single Pulse Shock Tube Investigation of Rich and Stoichiometric Ethane Oxidation", Paper accepted for presentation at 29th International Symposium on Combustion.

Tranter R.S., Ramamoorthy H., Raman A., Sivaramakrishnan, R. and Brezinsky K., "Shock Tube Investigations of Hydrocarbon Oxidation and Pyrolysis Over Very Wide Pressure Ranges", *Proceedings of the 2002 Technical Meeting of the Central States Section of the Combustion Institute.*

COMBUSTION CHEMISTRY

Principal Investigator: Nancy J. Brown

Environmental Energy Technologies Division

Lawrence Berkeley National Laboratory

Berkeley, California, 94720

510-486-4241

NJBrown@lbl.gov

PROJECT SCOPE

Combustion processes are governed by chemical kinetics, energy transfer, transport, fluid mechanics, and their complex interactions. Understanding the fundamental chemical processes offers the possibility of optimizing combustion processes. The objective of our research is to address fundamental issues of chemical reactivity and molecular transport in combustion systems. Our long-term research objective is to contribute to the development of reliable combustion models that can be used to understand and characterize the formation and destruction of combustion-generated pollutants. We emphasize studying chemistry at both the microscopic and macroscopic levels. To contribute to the achievement of this goal, our current activities are concerned with three tasks: Task 1) developing models for representing combustion chemistry at varying levels of complexity to use with models for laminar and turbulent flow fields to describe combustion processes; Task 2) developing tools to facilitate building and validating chemical mechanisms; and Task 3) modeling combustion in multi-dimensional flow fields. A theme of our research is to bring new advances in computing and, in particular, parallel computing to the study of important and computationally intensive combustion problems.

RECENT PROGRESS

Task 1: Developing models for representing combustion chemistry at varying levels of complexity to use with models for laminar and turbulent flow fields to describe combustion processes (with Shaheen R. Tonse, Michael Frenklach, and Nigel W. Moriarty): Most practical combustion systems are turbulent, and the dominant computational cost in modeling turbulent combustion phenomena numerically with high fidelity chemical mechanisms is the time required to solve the ordinary differential equations associated with the chemical kinetics. To develop models that describe pollutant formation in practical fuels, the computational burden attributable to chemistry must be reduced. We have pursued an approach that can contribute to this problem, PRISM (Piecewise Reusable Implementation of Solution Mapping). PRISM has been developed as an economical strategy for implementing complex kinetics into high fidelity fluids codes. This approach to mechanism reduction draws upon factorial design, statistics and numerics, caching strategies, data structures, and long term reuse of chemical kinetic calculations. A solution-mapping procedure is applied to parameterize the solution of the initial-value ordinary differential equation system as a set of algebraic polynomial equations. In a previous PRISM study we simulated laminar premixed and turbulent non-premixed H₂+air combustion and gained considerable speedup (for chemistry alone). Mean reuse rates of several thousand per hypercube were observed, ample to recover costs, since cost-effectiveness is achieved at reuse of ~250 for the H₂+air case. Although the reuse distribution has a mean of ~2500, it is skewed with a large number of hypercubes having very low reuse (less than 10). The mean usage is raised by a small number of very highly reused hypercubes. Consequently, an *a priori* calculation of the number of expected reuses would help to identify hypercubes with insufficient reuse because we could call the ODE solver rather than construct polynomials for these hypercube.

We completed work on a method that estimated how many steps a trajectory would take in moving through a hypercube by calculating a trajectory “velocity” using either solely chemical rate information, or including the displacement of the chemical composition vector from CFD effects such as diffusion and convection. The trajectory velocity is then combined with an estimated trajectory length to determine the number of expected reuses. Although the results were encouraging, hypercubes are used by multiple CFD cells during a simulation. This confuses our prediction, adding a dependence on simulation domain size, and making it difficult to specify *a priori* a trajectory-velocity threshold beyond which hypercube construction is deemed uneconomical.

Another method developed to increase economy was Deferred Polynomial Construction (DPC), which takes advantage of the shape of the distribution to defer polynomial construction for a hypercube until a certain number of reuses have occurred. Until then the ODE solver is called. Four cases were studied:

1. a 1D laminar premixed H₂+air flame,
2. a 2D premixed H₂+air turbulent jet,
3. a 2D non-premixed H₂+air turbulent jet,
4. a 1D laminar premixed CH₄+air flame.

DPC lowers the CPU time used in PRISM’s hypercube construction for all three H₂+air cases by a factor ranging from 1.5 for the premixed turbulent flame to 2.5 for the non-premixed flame. In summary, DPC is an effective way of increasing PRISM’s efficiency by approximately a factor 2 for H₂+air, through elimination of unnecessary polynomial construction. Although it seems that advance knowledge of the reuse distribution is needed, in practice all the distributions we have encountered are well suited to DPC i.e. skewed toward low reuse, with mean reuse raised by a relatively small number of hypercubes. For CH₄+air, DPC gives us only about a factor of 2 improvement over the ODE. This is not a problem of DPC but of PRISM itself, as the high dimensionality of the system lowers the hypercube reuse. Application of DPC alleviates this somewhat but not to the extent that it becomes practical to use. However, if a dimensional reduction method we are developing succeeds, then DPC can be applied with it and should provide an additional gain.

Extension of PRISM to more complex systems: We previously extended PRISM to CH₄ + Air combustion, by developing new orthogonal factorial designs of type 2_v^{22-13} . The 22-d design gave accurate results, however the economy was not good because the number of ODE calls was high and the hypercube reuse insufficient to recover construction costs. Factorial designs produced by the GOSSET program (<http://www.research.att.com/~njas/gosset/>) provide similar accuracy to an orthogonal fractional design, while requiring only about half the number of design points, i.e. ODE calls. To achieve further improvements in economy, we are developing an approach called Dynamic Dimensional Reduction that is based on identifying and isolating chemical species that have both fast time-scales and low concentration. The idea is motivated by the Steady-State approximation and Intrinsic Low Dimensional Manifold (ILDM) concepts in which concentrations of fast species follow those of slow species. For a 32-species GRI-Mech 1.2 reaction set, preliminary results show the number of reduced dimensions for time steps of 10⁻⁷s, 10⁻⁶s and 10⁻⁵s are approximately 28, 15 and 11, respectively.

Task 2: Developing tools for to facilitate building and validating chemical mechanisms (with Kenneth Revzan): We evaluated the dipole reduced formalism (DRFM) for determining transport properties of gas-phase mixtures, developed by Paul and Paul and Warnatz as a replacement for the old TRANLIB that is part of the CHEMKIN package. This was accomplished by modifying PREMIX, the CHEMKIN premixed flame application, to incorporate the new method. We began with a previously-developed version of PREMIX, in which the species binary diffusion coefficients, thermal diffusion factors, and thermal conductivities were calculated directly, rather than indirectly from polynomial fits. This allowed for the determination of both first- and second-order sensitivities of flame speed, species

mass fractions, and temperature to transport parameters. The sensitivities were calculated analytically through the use of automatic differentiation. The DRFM method was added to PREMIX by encoding the DRFM formalism and adding the necessary changes to the user interface to allow for a choice of the method for determining the transport parameters: DRFM with mixture-averaged coefficients or TRANLIB with either mixture-averaged or multicomponent coefficients. Using Paul's chemical mechanism, we determined transport properties for an H_2 -CO- O_2 - N_2 flame and compared them with his published plots. Although differences in many parameters are relatively small, there are compensating errors attributable to the numerics, levels of approximations, and the potential parameters used. We found sensitivities to the transport parameters to be similar using the old and new formalism. Using DRFM, we found the most important first-order flame speed sensitivities to be those to the Lennard-Jones collision diameter and its counterpart in the exponential repulsive potential, the length scaling parameter. We also found second-order sensitivities to be small.

Task 3: Modeling combustion in multi-dimensional flow fields (with Shaheen R. Tonse): We have continued our efforts concerned with finding the dimensionality of chemical composition space. Chemical concentrations of a spatially extended chemical reaction plotted on a multi-dimensional chemical composition space C form a continuous multi-dimensional manifold M embedded in C . A manifold constructed in this manner is a dense set of discrete points. However, if this is not viewed at too fine a resolution, we can make a continuum approximation and determine its dimensionality. In the limit of infinitely small length-scales, the dimensionality \underline{d} of M is upper bounded to that of the physical space, but at larger length-scales it may appear to have a higher dimension than the theoretical bounds, provided that M is sufficiently convoluted. PRISM's accuracy increases as partition size decreases, but this requires construction of more partitions in a way that depends exponentially on \underline{d} . Therefore determination of \underline{d} is of importance in the design and development of PRISM and similar chemical mechanism reduction methods. We calculate \underline{d} by three independent methods:

1. by repeatedly reducing the partition size and measuring the increase in number of partitions required to cover M . In general the number of partitions used should rise by $2^{\underline{d}}$.
2. Principal Component Analysis (PCA) is an eigenvalue approach used to determine the most significant variables (or linear combinations of variables) in a multi-variate data set, and in our case, returns an estimate of the dimensionality. It is applied independently to the manifold of each partition. Tests on Monte Carlo'd manifolds of known dimensionality show it to be very accurate provided the shape of the manifold is determined from mostly linear polynomials.
3. Grassberger and Procaccia's method to measure the dimensionalities of strange attractors extracts \underline{d} by looking at the number, $C(r)$ of manifold points, contained within a hypersphere of radius r . As r is increased, the number of points should increase as $C(r) \sim r^{\underline{d}}$. This method has the advantage of being able to view the length scale-dependence of dimensionality.

Results from the first two methods have been reported. Preliminary results from the third method indicate that the manifolds produced in turbulent CH_4 combustion simulations with domains of 2 and 3 spatial dimensions have values of \underline{d} between 1.5 and 4.0, depending on the degree of turbulence.

PUBLICATIONS

Bell, J.B., Brown, N.J., Day, M.S., Frenklach, M., Grcar, J.F., Propp, R.M., and Tonse, S.R., "Scaling and Efficiency of PRISM in Adaptive Simulations of Turbulent Premixed Flames," (2000) Proceedings of the Combustion Institute 28, 107-113. Also Lawrence Berkeley National Laboratory Report No. LBNL-44732

Bell, J.B., Brown, N.J., Day, M.S., Frenklach, M., Grcar, J.F., and Tonse, S.R., "Effect of Stoichiometry on Vortex-Flame Interactions," (2000) Proceedings of the Combustion Institute 28, 1933-1939. Also Lawrence Berkeley National Laboratory Report No. LBNL-44730

Tonse, Shaheen R. and Brown, N.J., "Emulation of Chemical ODE System by Response Surfaces in CH₄ Combustion," Division of Fluid Dynamics, American Physical Society, Washington DC, November 2000

Tonse, Shaheen R., Bell, J.B., Brown, N.J., and Day, M.S., "The Dimensionality of a Chemical Manifold through a Progressing Reaction, 2nd Joint Symposium of the Combustion Institute at Oakland, CA, March 2001

Tonse, Shaheen R. and Brown, N.J., "Improving the Efficiency of PRISM through Deferred Polynomial Construction." Fall Meeting of Western States Section of The Combustion Institute, Salt Lake City, UT. Oct 2001.

Tonse, S.R., Moriarty, N. L., Brown, N. J., Frenklach, M., (1999), "PRISM: Piecewise Reusable Implementation of Solution Mapping. An Economical Strategy for Chemical Kinetics," Israel Journal of Chemistry **39**, pp 97-106. Invited paper for a special issue on Combustion Chemistry to commemorate the 70th birthday of Professor Assa Lifshitz. Also Lawrence Berkeley National Laboratory Report No. LBNL-42576

Moriarty, N. W., Brown, N.J., and Frenklach, Michael, (1999), "Hydrogen Migration in the Phenylethene-2-yl Radical," J.Phys. Chem. **103**, pp 7127-7135. Also Lawrence Berkeley National Laboratory Report No. LBNL-43163

A co-author of the National Research Council Report of the Committee on Ozone-Forming Potential of Reformulated Gasoline, National Academy Press, (1999) Committee members: W.L. Chameides, C.A. Amann, R. Atkinson, N.J. Brown, J.G. Calvert, F.C. Fehsenfeld, J.P. Longwell, M.J., Molina, S.T. Rao, A.G. Russell, S.L. Saricks.

Molecular Beam Studies of Radical Combustion Intermediates

Laurie J. Butler

The University of Chicago, The James Franck Institute
5640 South Ellis Avenue, Chicago, IL 60637
LJB4@midway.uchicago.edu

I. Program Scope

Polyatomic radical intermediates play a key role in a wide range of combustion processes. The DOE-supported experiments in my lab pursue three avenues of research on the reaction dynamics of radicals. The first two extend our previous work by 1) investigating competing product channels in photodissociation processes used to generate radical intermediates important in combustion and 2) generalizing a method for determining absolute branching ratios for competing radical and molecular product channels in ground state bimolecular reactions in mass spectrometric experiments. The third avenue of research is new, the methodology growing from work we initiated two years ago on the competing dissociation channels of high-energy hydrocarbon radical isomers. The work seeks to probe dynamics on key portions of the potential energy surface for $O + \text{hydrocarbon radical}$ reactions by generating a highly internally excited radical intermediate, such as CH_3O , and investigating the branching between the ensuing product channels of the energized radical under collisionless conditions. Our technique disperses the radical intermediates by velocity and thus by internal energy, and then measures the velocity of the reaction products, allowing us to identify the product branching as a function of internal energy in the radical intermediate for energies that span the lowest energy product channels. Most of our experimental studies use a combination of techniques including analysis of product velocity and angular distributions in a crossed laser-molecular beam apparatus, emission spectroscopy of dissociating molecules, and high- n Rydberg H atom time-of-flight spectroscopy (HRTOF). Much of the work also serves to test and develop our fundamental understanding of chemical reaction dynamics. We focus on testing the range of applicability of two fundamental assumptions used in calculating reaction cross sections and the branching between energetically-allowed product channels: the assumption of complete intramolecular vibrational energy redistribution often used in transition state theories and the assumption of electronic adiabaticity used in defining the reaction coordinate in transition state theories and the multidimensional potential energy surface in quantum scattering calculations. The influence of angular momentum on product branching is also of increasing interest.

II. Recent Progress

Our work in the last year included: 1) completing experiments (Publication 6) that generated highly rotationally excited allyl radicals and allowed us to investigate centrifugal effects in the dissociation to $H + \text{allene}$ and the proposed isomerization pathway to 2-propenyl radical; 2) finishing (Pub. 4) a manuscript on our crossed laser-molecular beam photofragment scattering experiments on the primary and secondary reactions in the photodissociation of allyl chloride, including the secondary unimolecular dissociation of the allyl radical from primary C-Cl fission and of the C_3H_4 product (to propargyl + H) from primary HCl elimination; 3) completing (Pub. 5) our theoretical investigation of the transition states for HCl elimination in 2-chloropropene; and 4) initiating crossed-laser molecular beam experiments on the photodissociation of ethyl ethynyl ether, a potential photolytic precursor, suggested by R. Bersohn, of the HCCO radical. In collaboration with Prof. F. Blase at Haverford we also set up a synthetic apparatus for CH_3OCl , the photolytic precursor for highly rotationally excited CH_3O radicals required for the work in the Future Plans section. Much of the data in the work

described in A and B below was taken in collaboration with Dr. Fei Qi at the Chemical Dynamics Beamline at the Advanced Light Source (ALS) in Berkeley.

A. Centrifugal Effects in the Unimolecular Dissociation of the Allyl Radical and Comparison with Product Branching in the Noncyclic C₃H₅ Radical Isomers

Radical intermediates typically have many energetically accessible isomeric forms; unraveling the competing isomerization and dissociation reactions of these radicals is important in many combustion mechanisms. Of the three non-cyclic C₃H₅ radicals, only the allyl radical has been extensively studied under collisionless conditions, and these studies have primarily been on allyl radicals energized with the absorption of a UV photon, so they produce the radicals at energies well above the barriers to the isomerization to 2-propenyl and to 1-propenyl and the barriers to dissociation of each isomer. Branching to product channels at such high excess energies is more sensitive to ratios of A factors than relative barrier heights. As a result, a discrepancy of about 15 kcal/mole between the experimentally determined versus the theoretically predicted allyl→2-propenyl radical isomerization barrier has persisted, and the relative energetics of many of the other isomerization and C-H and C-C fission barriers of these isomers have eluded reliable determination. It has also not been possible to probe the dissociation dynamics of highly rotationally excited allyl radicals under collisionless conditions. Initiated in March 2000 with NSF support but continued in most of 2000 and 2001 with DOE support, our molecular beam scattering method allowed us to resolve the branching between the competing C-H (and C-C, for 1-propenyl) bond fission channels of each of the three non-cyclic C₃H₅ radical isomers as a function of internal energy in the selected radical at energies that span the lowest dissociation and isomerization barriers. The data on product branching is sensitive to the relative barrier heights of the competing dissociation channels to within less than a couple kcal/mol.

The work reported in Pub. 6 used photofragment translational spectroscopy and H atom Rydberg time-of-flight (HRTOF) spectroscopy to study the photolytic generation at 193 nm of the allyl radical from allyl iodide and the ensuing dissociation of the nascent allyl radicals as a function of their internal energy. Two C-I bond fission channels in the precursor produce the allyl radical, one channel forming I (²P_{3/2}) and the other forming I (²P_{1/2}) cofragments. The nascent allyl radicals are dispersed as a function of the translational energy imparted from the photolysis, and therefore by their internal energy. Although all of the I (²P_{3/2}) and a portion of the I (²P_{1/2}) channel allyl radical products have enough internal energy to overcome the 60 kcal/mol barrier to form allene + H, the data showed that a substantial fraction of the allyl radicals from the I (²P_{1/2}) channel formed with internal energies as high as 15 kcal/mol above the 60 kcal/mol barrier were stable to H atom loss. The stability is due to centrifugal effects caused by significant rotational energy imparted to the allyl radical during the precursor photolysis and the small impact parameter and reduced mass characterizing the loss of an H atom from an allyl radical to form allene + H. Concomitantly large H atom recoil energies were detected via HRTOF. A photoionization efficiency (PIE) curve identified the major C₃H₄ secondary dissociation products as allene. Comparison of the mass 40 signal in the TOF spectra at two photoionization energies showed that branching to H + propyne doesn't occur at near threshold internal energies, indicating the experimentally determined allyl → 2-propenyl radical isomerization barrier, which is lower than recent ab initio calculations of the barrier by ~15 kcal/mol, is far too low.

B. C-Cl Bond Fission, HCl Elimination, and Secondary Radical Decomposition in the 193 nm Photodissociation of Allyl Chloride

This study, completed in 2001 (Pub. 4) elucidates the competing HCl elimination channels and C-Cl bond fission channels of allyl chloride photodissociated at 193 nm as well as the

secondary dissociation of both the allyl radical produced from C-Cl fission and the C_3H_4 product from HCl elimination. Prior work showed that C-Cl fission and HCl elimination occur upon $\pi\pi^*$ excitation of allyl chloride, but did not elucidate the mechanisms for the two HCl elimination processes. Tunable VUV photoionization detection of the HCl and its momentum-matched C_3H_4 product in the present work allows us to gain both a crude measure of the level of HCl vibrational excitation as well as a probe of the secondary dissociation of some of the C_3H_4 products to propargyl + H. It also detected a previously undetected low kinetic energy C-Cl bond fission channel, the channel that forms allyl radicals which undergo secondary dissociation. The measured branching of these primary reaction channels of [all C-Cl] : [fast C-Cl] : [slow C-Cl] : [fast HCl] : [slow HCl] : [all HCl] is 1.0: 0.97: 0.03: 0.29: 0.17: 0.46 (where fast refers to the high recoil kinetic energy channels.). Interestingly, the photoionization detection of HCl from allyl chloride showed the HCl to have considerably less internal vibrational energy than the HCl elimination product from 2-chloropropene. Since HCl elimination from 2-chloropropene can only proceed via four-center elimination transition states that have a long H-Cl distance compared to R_e of the HCl product, 1.8 angstroms at the transition state, one is tempted to conclude that a significant contributor to HCl elimination in allyl chloride is a three-center, 1,1, elimination of HCl with a smaller H-Cl distance at the transition state, not a 4-center process. This sheds some light on the elusive mechanism for HCl elimination at 193 nm from vinyl chloride, for which a three-center mechanism with synchronous isomerization for the HCl elimination was proposed. We find that the onset of the photoionization spectrum of the HCl product measured for vinyl chloride indicates that a significant fraction of the products is much more vibrationally excited than the HCl product from allyl chloride. Indeed, the onset of the photoionization efficiency curve for HCl from vinyl chloride is nearly identical to that of the HCl product from 2-chloropropene, indicating that a major HCl elimination pathway in vinyl chloride is via a four-center mechanism.

C. Theoretical Investigation of the Transition States Leading to HCl Elimination in 2-Chloropropene

This paper (Pub. 5) presents *ab initio* electronic structure calculations on the planar transition states of 2-chloropropene leading to HCl elimination on the ground electronic state to form either propyne or allene as the cofragment. They were undertaken to better understand potential mechanisms for HCl elimination in 2-chloropropene studied in my group and the bearing on the HCl elimination channels of vinyl chloride, which has been pursued by several experimental groups and for which K. Morokuma has calculated *ab initio* transition state structures and energies. Our calculations on 2-chloropropene provide optimized geometries of the HCl elimination transition states as well as vibrational frequencies, barrier heights, and reaction endothermicities. The calculated barrier heights for the two distinct four-center HCl elimination transition states, one leading to HCl and propyne and the other leading to HCl and allene, are 72.5 kcal/mol (77.8 kcal/mol without zero point correction) and 73.2 kcal/mol (78.7 kcal/mol) at the MP2/6-311G(d,p) level, 71.0 kcal/mol (76.3 kcal/mol) and 70.5 kcal/mol (76.0 kcal/mol) at the QCISD(T)/6-311+G(d,p)//MP2/6-311G(d,p) level, and 66.9 kcal/mol (71.7 kcal/mol) and 67.3 kcal/mol (72.1 kcal/mol) at the G3//B3LYP level of theory. Calculated harmonic vibrational frequencies at the B3LYP/6-31G(d) level along with transition state barrier heights from the G3//B3LYP level of theory are used to obtain RRKM reaction rate constants for each transition state, which determine the branching ratio between the two HCl elimination channels. Even at internal energies well above both HCl elimination barriers, the HCl elimination leading to propyne is strongly favored. The smaller rate constant for the HCl elimination leading to allene can be attributed to the freezing of the methyl rotor at the corresponding transition state.

D. Photofragmentation Experiments on Ethyl Ethynyl Ether, an HCCO Radical Precursor

Motivated by R. Bersohn, we initiated this year molecular beam photofragmentation experiments to investigate the generation of the HCCO radical from the 193 nm photodissociation of ethyl ethynyl ether. The reaction of HCCO with NO has been shown to be the major NO removal pathway in the reburning of hydrocarbon fuels at low temperature, yet there is currently no clean photolytic source of the HCCO radical for kinetic studies trying to measure the product branching. Our studies on ethyl ethynyl ether seek to assess its utility as a photolytic precursor for HCCO, detecting all the possible bond fission and molecular elimination pathways. The preliminary data obtained thus far indicate that C-O bond fission to form HCCO + C₂H₅ dominates the product branching, no significant branching to cleavage of the other C-O bond or ethylene elimination is observed. The quantum yield of the HCCO radical is thus near unity, but the measured recoil kinetic energy distribution for the HCCO + C₂H₅ product channel is very broad (extending from 0 to 60 kcal/mol), reflecting a broad internal energy distribution of the nascent HCCO product. This is likely the result of at least two different dissociation pathways for C-O fission to make HCCO + CH₂CH₃.

III. Future Plans

In parallel with the work on ethyl ethynyl ether, we plan to investigate the product branching from a radical intermediate of the O(³P) + CH₃ bimolecular reaction. The studies measure the unimolecular dissociation of CH₃O to the two competing product channels H + H₂CO and H₂ + HCO (the HCO unimolecularly dissociates to H + CO in the bimolecular reaction) as a function of internal energy in the radical. Since significant branching to the H₂ + HCO is only predicted for high J in the bimolecular reaction, our experimental approach generates rotationally hot unstable CH₃O radicals in a scattering apparatus dispersed by internal energy. This experiment provides the first collision-free data on the dissociation of rotationally hot CH₃O radicals as a function of internal energy in the radical, so provide a critical test of the most important regions of the *ab initio* potential energy surface used to obtain predictive ability for the O + CH₃ bimolecular reaction. The methodology can be generalized to study a wide range of reactions with unstable radical intermediates.

IV. Publications Acknowledging DE-FG02-92ER14305 (2000 or later)

1. A Combined Experimental and Theoretical Study of Resonance Emission Spectra of SO₂ (\tilde{C}^1B_2), B. Parsons, L.J. Butler, D. Xie, and H. Guo, Chem. Phys. Lett. **320**, 499-506 (2000).
2. Characterization of Nitrogen-Containing Radical Products from the Photodissociation of Trimethylamine at 193 nm using Photoionization Detection, N. R. Forde, L. J. Butler, B. Ruscic, O. Sorkabi, F. Qi and A. Suits, J. Chem. Phys. **113**, 3088-97 (2000).
3. Photodissociating Methyl Vinyl Ether to Calibrate O + Ethylene Product Branching and to Test Propensity Rules for Product Channel Electronic Accessibility, M. L. Morton, D. E. Szpunar, and L. J. Butler, J. Chem. Phys. **115**, 204-16 (2001).
4. C-Cl Bond Fission, HCl Elimination, and Secondary Radical Decomposition in the 193 nm Photodissociation of Allyl Chloride, M. L. Morton, L. J. Butler, T. A. Stephenson, and F. Qi, J. Chem. Phys. **116**, 2763-75 (2002).
5. Theoretical Investigation of the Transition States Leading to HCl Elimination in 2-Chloropropene, B. F. Parsons, L. J. Butler, and B. Ruscic, Molecular Physics **100**, 865-74 (2002).
6. Primary and Secondary Dissociation of Allyl Iodide Excited at 193 nm: Centrifugal Effects in the Unimolecular Dissociation of the Allyl Radical, D. E. Szpunar, M. L. Morton, L. J. Butler, and P. M. Regan, submitted to J. Phys. Chem. A. (2002).

Independent Generation and Study of Key Radicals in Hydrocarbon Combustion (DE-FG02-98ER14857).

Barry K. Carpenter

Department of Chemistry and Chemical Biology

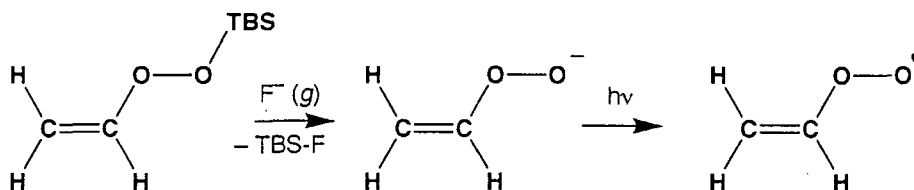
Cornell University

Ithaca, NY 14853-1301

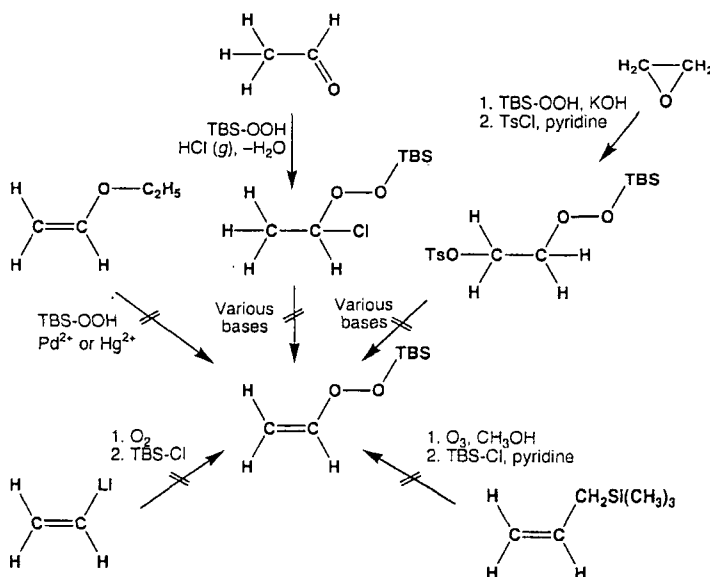
E-mail: bkc1@cornell.edu

1. Preparation of Precursors Vinylperoxy and Phenylperoxy Radicals.

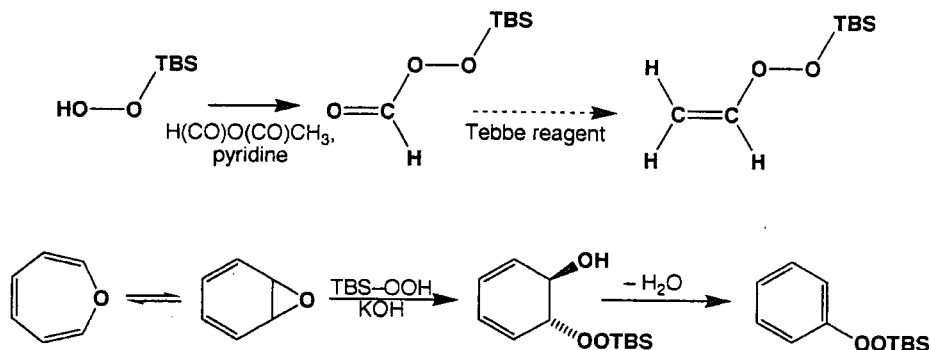
The importance of the vinylperoxy and phenylperoxy radicals in combustion mechanisms is well known. Nevertheless, the generation of these species under conditions that can allow complete determination of their physical and chemical properties has not yet been accomplished. We have devoted considerable experimental effort to the preparation of precursors that would make such studies possible. Specifically, we have been working on the syntheses of two trialkylsilyl derivatives, in the expectation that gas-phase removal of the silyl groups should be possible with F^- , and that laser photodetachment of the resulting peroxyanions would allow generation of the radicals, and would also provide important information that could lead to experimental determination of their heats of formation. The approach is illustrated for the vinylperoxy radical in the diagram below (TBS = $Si(CH_3)_2C(CH_3)_3$):



Despite the simplicity of structure of the precursor, its synthesis has proven extremely challenging. Some of the unsuccessful attempts are summarized in the following scheme:



A similar number of approaches have been tried for the preparation of Ph-O-O-TBS, also without success to date. At present, we are exploring the following synthetic procedures:



The Tebbe reagent, employed in the synthesis of the vinyl peroxide is $\text{Cp}_2\text{Ti}-\mu\text{-Cl}-\mu\text{-CH}_2\text{-Al}(\text{CH}_3)_2$, which is known to convert formate esters to vinyl ethers.¹

The route to the phenyl peroxide looks particularly promising since the addition of H_2O_2 to oxepine is already known.² However, oxepine is not commercially available. Its synthesis is in progress at the time of writing.

2. Oxygen Interception of Radicals Involved in Soot Formation.

2.1 Introduction.

The process of hydrocarbon oxidation under conditions of combustion involves, in general terms, a series of steps that take hydrocarbon fuels of medium-to-high molecular mass through intermediates of ever decreasing molecular mass to the final products CO_2 and H_2O . Under the right conditions there can also be a parallel series of reactions that occur via intermediates of ever *increasing* molecular mass, leading eventually to soot. In most prior studies these degradation (oxidation) and aggregation (soot-forming) reactions have been viewed largely independently, although it has certainly been recognized that they must be coupled.³ The intermediates in one set of reactions must be candidates for inclusion in the other. We have begun to look at key radicals believed to be involved in the early stages of soot formation and to ask what their reactions with oxygen might be. Of special interest are the rates of formation, identity, and subsequent reactions of the products formed by oxygen interception. Although the larger radicals involved in the later stages of soot formation will also presumably be susceptible to oxidation, we have chosen to focus on the early-stage species because their interception would have the greatest kinetic consequence on the overall soot-formation process.

We believe it is useful to define three general classes of reaction that can occur from the peroxy radicals generated by the initial O_2 interception. These are:

- 1) Reversion: i.e. regeneration of O_2 and the original radical. If this were the most favorable reaction of the peroxy radical, the oxygen interception would have little impact on soot formation. Benzyl radical appears to be one potential soot-forming intermediate whose O_2 adduct falls in this class.
- 2) Oxidative degradation to regenerate radicals that occur earlier in the soot-forming chain. Reactions of this class would have some impact on the overall rate of soot formation, but not as great an impact as those in class (3).

3) Oxidative degradation to generate radicals that are not significant intermediates in soot formation. Reactions of this kind would be the most important because they would constitute major pathways for inhibiting soot formation.

2.2 Computational and Experimental Studies Related to Styrylperoxy Radicals.

The β -styryl radical is one of the key intermediates in the so-called HACA mechanism of PAH formation.⁴ While its role in the aggregation reactions leading to soot formation seems well established, little seems to be known about its competitive degradative reactions with oxygen. We have undertaken computational and experimental studies of that problem.

Interception of the β -styryl radical undoubtedly generates *E* and *Z* stereoisomeric styrylperoxy radicals. The *E* stereoisomer in all probability undergoes reactions analogous to the oxidative degradation of vinyl, leading eventually to benzaldehyde and the formyl radical. Benzaldehyde easily loses the aldehyde hydrogen to generate the benzoyl radical, which decarbonylates to give phenyl.⁵ Since phenyl is the immediate precursor to the β -styryl radical, this whole sequence merely sets the soot-forming reactions back a step, but does not remove the aromatic fragment completely from the game. In other words, this sequence would be of class (2) in the classification that we have proposed.

The situation is potentially different for the *Z* stereoisomer. It has open to it the analogous side-chain oxidation reactions, but it also has the potential for intramolecular attacks on the aromatic ring. We have investigated the feasibility of these reactions with some preliminary UB3LYP/6-31G(d) calculations. The results for one of them are summarized in the figure below:

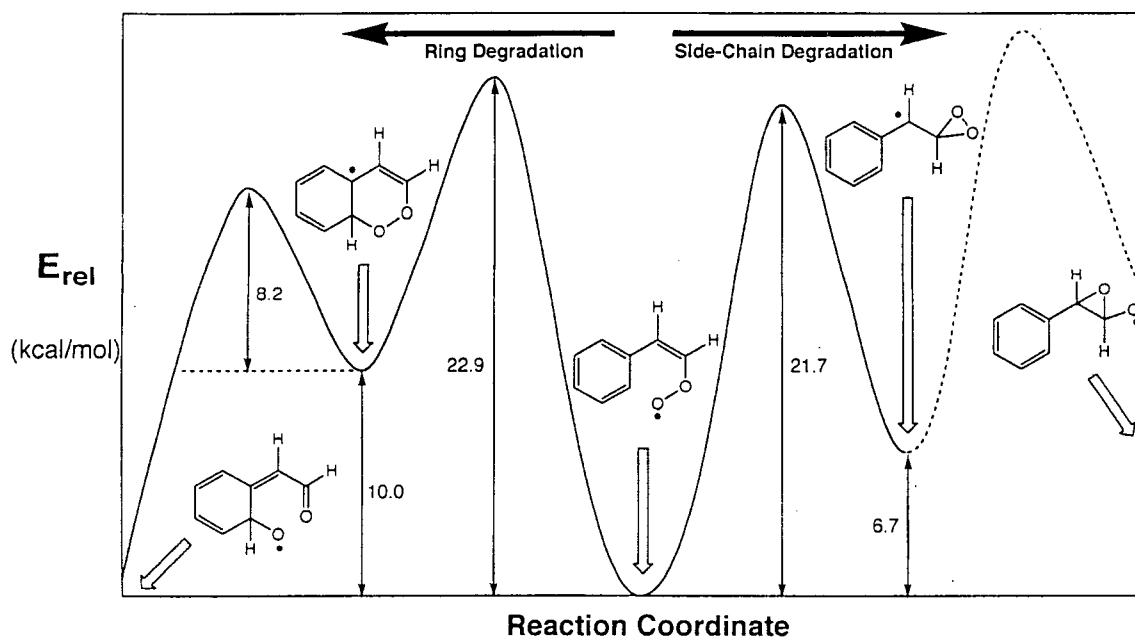


Figure 1 UB3LYP/6-31G(d) energies for the oxidative degradation of the *Z*-styrylperoxy radical. Figures are ZPE-corrected potential energies.

One sees that the barriers to initial ring closing are found to be only 1.2 kcal/mol apart – well within the likely uncertainty of the calculations. The UB3LYP energy profile for rearrangement of the dioxiranylbenzyl radical is shown as a dashed curve in Figure 1 because we have reason to doubt its validity. We have recently shown that the analogous rearrangement of dioxiranylmethyl radical requires a large-active-space CASPT2 calculation for accurate description,⁶ and it is likely to be the case here too. The problem is that calculations of this kind are not feasible for the phenyl derivative, and so we are exploring more tractable alternatives. The issue is crucial to the problem at hand because the UB3LYP barrier suggests that the dioxiranylbenzyl rearrangement would actually be the rate-determining step of the side-chain-oxidation branch, making the ring-degradation branch more favorable. This would be of significance if correct, because once an oxygen has been attached to the erstwhile aromatic ring, a number of facile ring-opening reactions can follow. In other words, this branch of the process would be of class (3).

Experimentally we are investigating the reaction of the β -styryl radical with O₂ in order to find out what the products really are. There is one report of such a study already in the literature.⁷ Only sidechain oxidation products were identified in that work. However, only 60% of the products were characterized and so it is difficult to know whether ring degradation occurred or not. We are beginning our study by repeating the earlier work with a more thorough identification of all of the products. If both sidechain and ring oxidation products are found, we will look at the temperature dependence of the branching ratio and compare it with that predicted from our calculations.

Literature Citations

- (1) Pine, S. H. *Org. React.* **1993**, *43*, 1.
- (2) Jeffrey, A. M.; Yeh, H. J. C.; Jerina, D. M.; DeMarinis, R. M.; Foster, C. H.; Piccolo, D. E.; Berchtold, G.A. *J. Am. Chem. Soc.* **1974**, *96*, 6929.
- (3) Marinov, N. M.; Pitz, W. J.; Westbrook, C. K.; Castaldi, M. J.; Senkan, S. M. *Combust. Sci. Technol.* **1996**, *116-117*, 211.
- (4) (a) Frenklach, M.; Warnatz, J. *Combust. Sci. Technol.* **1987**, *51*, 265. (b) Moriarty, N.W.; Brown, N.J.; Frenklach, M. *J. Phys. Chem. A* **1999**, *103*, 7127.
- (5) Nam, G.-J.; Xia, W.; Park, J.; Lin, M.C. *J. Phys. Chem. A* **2000**, *104*, 1233.
- (6) Carpenter, B.K. *J. Phys. Chem. A* **2001**, *105*, 4585.
- (7) Tokumaru, K. *Chem. Ind. (London)* **1969**, 297.

Publications from 2000 on citing DOE support

- (1) "Computational Studies on the Ring Openings of Cyclopropyl Radical and Cation," Arnold, P.A.; Carpenter, B.K. *Chem. Phys. Lett.* **2000**, *328*, 90.
- (2) "Evidence of a Double Surface Crossing Between Open- and Closed-Shell Surfaces in the Photodissociation of Cyclopropyl Iodide," Arnold, P.A.; Cosofret, B.R.; Dylewski, S.M.; Houston, P.L.; Carpenter, B.K. *J. Phys. Chem. A* **2001**, *105*, 1693.
- (3) "The Ring Opening of Dioxiranylmethyl Radical: A Caution on the Use of G2-Type Ab Initio MO Models for Mechanistic Analysis," Carpenter, B.K. *J. Phys. Chem. A* **2001**, *105*, 4585.
- (4) "Polarized Infrared Absorption Spectrum of Matrix-Isolated Allyl Radicals," Nandi, S.; Arnold, P.A.; Carpenter, B.K.; Nimlos, M.R.; Dayton, D.R.; Ellison, G.B. *J. Phys. Chem. A* **2001**, *105*, 7514.

Molecular-Beam Ion Imaging Experiments

David W. Chandler

Combustion Research Facility, MS 9054, Sandia National Laboratory,
chandler@ca.sandia.gov

Scope of Program:

My research has focused on developing and using two-dimensional imaging techniques to study chemical dynamics. These techniques allow one to measure the velocity of state-selectively photoionized products of unimolecular and bimolecular interactions. This information is quite useful in understanding the details of chemical processes. In the last two years we have made significant improvements in these techniques with the further development of the velocity mapping technique and the utilization of a crossed molecular beam apparatus for the study of bimolecular collisions. A major effort has been to develop methods for extracting quantitative differential cross sections and alignment parameters and measurement of orientation from crossed-molecular-beam ion imaging experiments. Crossed molecular beam experiments have provided a wealth of detailed information on inelastic and reactive bimolecular collisions. Scalar quantities measured in such experiments include chemical reaction probabilities and energy partitioning among the various product states. Measurements of vector quantities reveal the spatial angular correlations among the directional properties of the reactant and product trajectories. In the last year we have focused on measurement of these vector quantities. This work was done in collaboration with Prof. Joe Cline (University of Nevada at Reno) and his students as well as with postdocs Thomas Lorenz, Elisabeth Wade, Mike Elioff and Bradley Parsons.

Recent Progress:

Rotational state-resolved and alignment-corrected differential cross sections (DCS) for the j -changing collisions of NO by Ar have been measured. This has been done for both spin-orbit conserving and spin-orbit changing collisions. These measured differential cross sections have been compared to theory. We have calculated the DCS and alignment moments directly from the scattering matrix obtained in full close-coupled quantum calculations using two recent *ab initio* NO-Ar potentials of Alexander and the Hybridon scattering package. Calculated and experimentally measured differential cross sections for scattering are remarkably well reproduced in the calculations for both spin-orbit conserving and changing collisions. In figure 1 is shown ion images for the inelastic scattering of $\text{NO}(^2\Pi_{1/2}, j=0.5) + \text{Ar} \rightarrow \text{NO}(^2\Pi_{3/2}, j') + \text{Ar}$, $j'=3.5-6.5$, at a collision energy of 477 cm^{-1} . The experimentally observed images were collected using the $Q_{22}+R_{12}$ transition for $j'=3.5$, and 5.5 ; the $R_{22}(4.5)$ transition; and the $P_{22}+Q_{12}$ transition for $j'=6.5$. The integration time for each of these images was approximately two hours and the highest intensity represents approximately 7000 ion counts. Lower intensities are represented by darker shading, higher intensities by lighter shading.

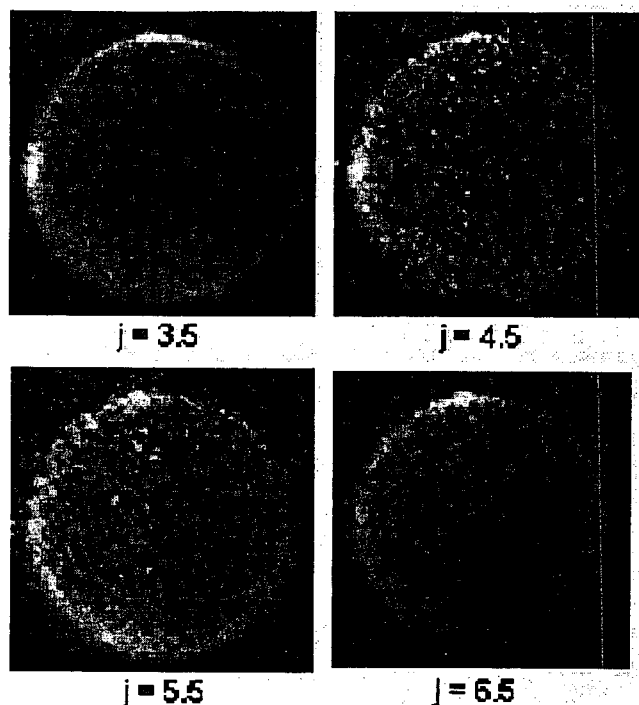


Figure 1: Ion Images of $\text{NO}(^2\Pi_{3/2}, j')$ $j'=3.5-6.5$ from $\text{NO}(^2\Pi_{1/2}, j=0.5) + \text{Ar}$ collisions.

Other crossed-beam experiments have examined the alignment and orientation of the rotational angular momentum of scattered NO from rotationally inelastic collisions with Ar at nominally 500 cm^{-1} collision energy. The NO product is probed by polarized (linearly in the case of alignment and circularly in the case of orientation), two-color $1+1'$ REMPI through the NO $A^2\Sigma$ state. By using very low probe laser power, we avoid saturation of the resonant transition. Rotational alignment is obtained from comparison of images obtained with different polarization geometries of linearly polarized probe light. Analysis of the normalized difference images shows that the alignment is well described by the kinetic apse model proposed by Dr. Koury that assumes sudden collisions and no addition of angular momentum along the impact direction.

Orientation is determined in a similar manner using circularly polarized light to detect the scattering spheres. Analysis of the normalized difference images $(\text{Right-Left})/(\text{Right} + \text{Left})$ show a changing pattern of clockwise and counterclockwise spinning molecules. Fig.2 compares the calculated oscillation pattern in the NO rotational orientation of two similar Ar-NO potential energy surfaces. The two PES's predict similar NO product rotational distributions, DCS's, and alignments. In our experiments at high j' the two PES's predict virtually identical rotational orientations. However, there are significant differences at low j' , and the most recent potential better predicts the measured oscillatory pattern of rotational orientation. This demonstrates the unusual sensitivity of the θ -dependent pattern of product rotational orientation to the PES. We note that both PES's predict a larger overall magnitude of orientation than is observed experimentally. The origin of this difference in magnitude remains unclear. The similarity of the three predictions of rotational orientation at high j' suggests the dynamics in these cases is dominated by relatively simple repulsive kinematics and the details of the PES are relatively unimportant.

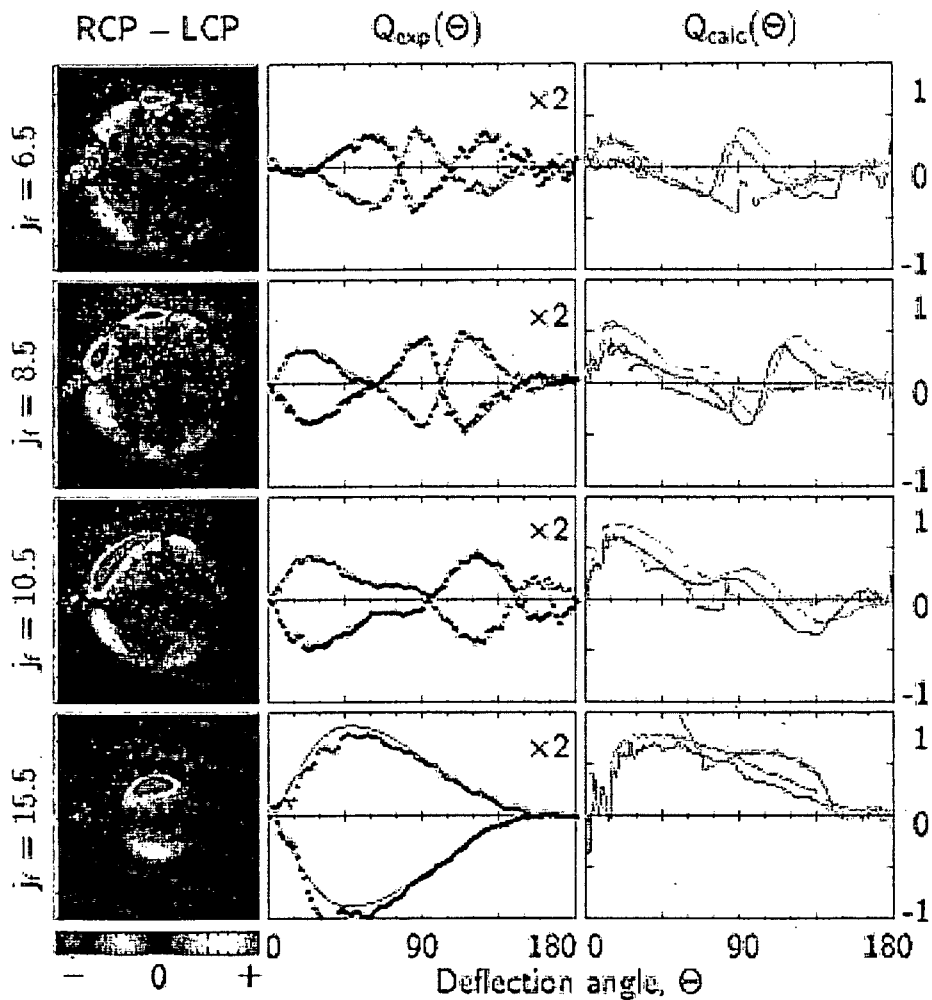


Figure 2: Normalized difference images showing NO orientation along with extracted angle dependent orientation and calculated angle dependent orientation for several J states.

We have also studied the unimolecular dissociation of the NO dimer. NO dimers were formed in a molecular expansion of Ar and He. Ultraviolet light was used to excite the dimer at the threshold for forming an NO (A) state and an NO (X) state molecule. The NO(A) state molecules absorb a second photon non-resonantly and ionize. At threshold there is no kinetic energy for the fragments and they appear as a spot on our imaging detector. With this technique we were able to determine the dissociation energy of the dimer to be $697 \pm 4 \text{ cm}^{-1}$.

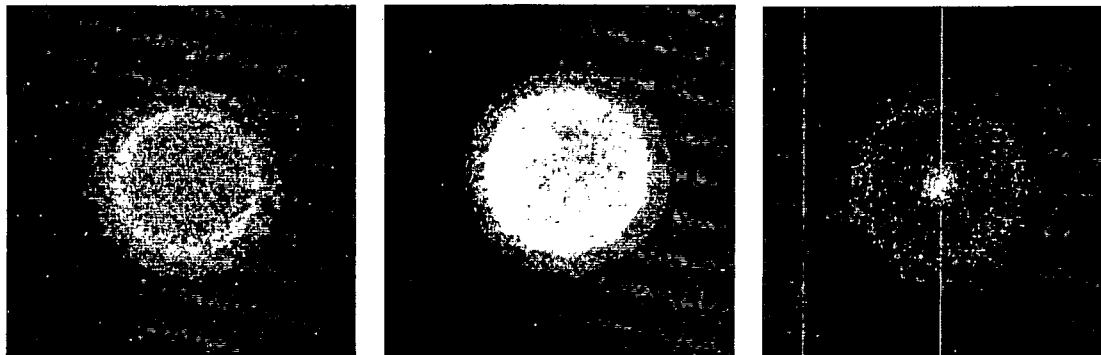


Figure 3: Images of NO near the threshold of the $(\text{NO})_2 \rightarrow \text{NO(A)} + \text{NO(X)}$ process.

Future Directions:

We will continue to develop techniques for the study of unimolecular photochemistry and bimolecular interactions using photofragment imaging and velocity mapped crossed-molecular-beam ion imaging techniques. The study of rotationally inelastic collisions between diatomic molecules gives the opportunity to measure correlated energy transfer. The NO/N₂ system is promising because the signal to noise is adequate to obtain correlated information. NO images of single J states will be taken. The image consists of a set of concentric rings each ring associated with production of a multiple rotational state of the sibling N₂ product. Due to the velocity spreads in the molecular beams the rings are not isolated and resolved. We are improving the data and developing techniques for the extraction of the N₂ rotational distribution associated with each NO rotational state from the data. We hope to extend this type study to the NO + Pyrazine system. We would also like to study reactive systems such as Cl (²P_{1/2} and ²P_{3/2}) + H₂. This reaction is a particularly important and timely one to study because it has recently been reported that the excited state reaction of the Cl(²P_{1/2}) is more reactive than the ground state Cl(²P_{3/2}) reaction.

Publications:

- 1) K. T. Lorenz, M. S. Westley, D. W. Chandler, "Rotational state-to-State differential Cross sections of the HCl-Ar Collision system using velocity Mapped Ion imaging" *Phys. Chem. Chem. Phys.* **2**, 481 (2000).
- 2) J. M. Teule, G. C. Groenenboom, D. W. Neyer, D. W. Chandler and M. H. M. Janssen, "State-to-state photodynamics of nitrous oxide and the effect of long-range interaction on the alignment of O(1D2)" *Chem. Phys. Lett.*, Volume: 320, Issue: 1-2, 177 (2000)
- 3) J. A. Davies, R. E. Continetti, D. W. Chandler, and C. C. Hayden "Femtosecond Time-Resolved Photoelectron Angular Distributions Probed during Photodissociation of NO₂" *Phys. Rev. Lett.* **84**, 5983 (2000).
- 4) D. W. Chandler, J. R. Barker, A. J. R. Heck, M. H. M. Janssen, K. T. Lorenz, D. W. Neyer, W. Roeterdink., S. Stolte and L. M. Yoder "Ion Imaging Studies of Chemical Dynamics" *Atomic and Molecular Beams: the state of the art 2000* edited by R. Campargue, Springer publishing 2000 page 519.
- 5) M. S. Westley, K. T. Lorenz and D. W. Chandler and P. L. Houston "Differential cross sections for rotationally inelastic scattering of NO from He and D₂" *Chem. Phys.* **114**, 2669 (2001).
- 6) L. M. Yoder, J. R. Barker, K. T. Lorenz and D. W. Chandler "Recoil Energy Distributions in van der Waals Cluster Vibrational Predissociation" In *Imaging in Chemical Dynamics* ed Arthur Suits and Robert Continetti, ACS symposium series, page 151 (2001).
- 7) K. T. Lorenz, M. S. Westley and D. W. Chandler "Extracting Rotational State-to-State Differential Cross-Sections from Velocity-Mapped Ion Imaging Data" In *Imaging in Chemical Dynamics* ed Arthur Suits and Robert Continetti, ACS symposium series, page 197 (2001)
- 8) V. K. Nesterov, R. Hinchliffe, R. Uberna, J. I. Cline, K. T. Lorenz and D. W. Chandler "Measurement of bipolar moments for photofragment angular correlations in ion imaging experiments". *J. Chem. Phys.* **115**(17), 7881 (2001).
- 9) J. I. Cline, K. T. Lorenz, W. A. Wade, J. W. Barr and D. W. Chandler "Ion Imaging Measurement of Collision-Induced Rotational Alignment in Ar-NO Scattering" *J. Chem. Phys.* **115** (14), 6277 (2001).
- 10) K. T. Lorenz, D. W. Chandler, J. M., Barr, Chen W. W., Barnes G. L. and J. I. Cline Direct Measurement of the Preferred Sense of NO Rotation after Collision with Argon, *Science* **293** vol. 5537, 2063 (2001).
- 11) P. L. Houston, B. R. Cosofret, A., S. M Dixit, Dylewski, J. D. Geiser, J. A Mueller, R. J. Wilsomn., P. J. Pisano, M. S. Westley, K. T. Lorenz and D. W. Chandler, *Product Imaging Studies of Photodissociation and Bimolecular Reaction Dynamics*, *J Chinese Chem. Soc.* **48**, 309 (2001).
- 12) Chandler D.W. and Hayden C.C., *Ion Imaging Techniques for the Measurement of Ion Velocities*, *Encyclopedia of Mass spectroscopy*. Editor Peter Armentrout. (2002).
- 13) E. A. Wade, J. I. Cline, Lorenz K. T., Hayden C. C., and Chandler D. W. Direct Measurement of the Binding Energy of the NO dimer, *JCP* **116**, 4755 (2002).
- 14) Lorenz K. T., Chandler D. W., McBane G. C., State-to-State Differential Cross Sections by Velocity Mapping for Rotational Excitation of CO by Ne, *J. Phys. Chem. A* **106**(7); 1144-115(2002).

Direct Numerical Simulation of Turbulent Combustion with Detailed Chemistry

Jacqueline Chen, Tarek Echehki and Scott Mason
Sandia National Laboratories, Mail Stop 9051
Livermore, California 94551-0969
phone: (925) 294-2586
email: jhchen@ca.sandia.gov

BACKGROUND

The goal of this research program is to gain fundamental insight into unsteady flow/chemistry interactions that occur in turbulent combustion, and to develop and validate combustion models required in various engineering CFD approaches including Reynolds Averaged Navier-Stokes (RANS) and Large-eddy simulation (LES). A high-fidelity numerical approach known as direct numerical simulation (DNS) has been coupled with detailed chemistry and transport models. Using high-order numerical methods, this approach permits the efficient investigation of fine-grained physical phenomena associated with interactions between convective and diffusive transport with detailed chemistry in the combustion of hydrocarbon fuels. Together with experiments and zero- and one-dimensional simulations, DNS is used to understand a particular aspect of an unsteady flow/chemistry interaction occurring in the autoignition and high-temperature turbulent combustion of hydrogen and hydrocarbon fuels.

A major new thrust in the past couple of years has been the extension of the DNS capability to study the influence of turbulent mixing on the autoignition of inhomogeneous hydrogen/air and hydrocarbon/air mixtures, and to identify the subsequent high-temperature combustion modes. In the following, we review some of these accomplishments.

RESEARCH ACCOMPLISHMENTS

DNS of Autoignition in Non-homogeneous Hydrogen/Air Mixtures¹

The objective of the present study is to understand the competition between scalar dissipation and chemistry in the high-temperature autoignition of spatially non-homogeneous hydrogen-air mixtures with detailed chemistry. This competition may be present during autoignition in a turbulent diesel jet as a cold fuel jet mixes with a coflowing heated oxidizer stream. The present study is concerned with only one aspect of turbulence, which is molecular mixing effects on autoignition in a non-uniform mixture. This is the first numerical study that documents the transient evolution of autoignition that spans a wide range of mixtures and pressures, and that accounts for both thermal energy and radical loss. The present study also documents the transient events that occur during the induction phase of autoignition through thermal runaway, prior to the establishment of a propagating front.

The simulations show that autoignition is initiated in discrete kernels by radical build-up in high-temperature, lean mixtures, and at relatively low dissipation rates. These observations are consistent with simple chemistry DNS [2]. However, the subsequent evolution of these kernels is characterized by a strong coupling between the dominant chemistry responsible for the growth of the radical pool and the competitive process of thermal and radical species dissipation at the kernels' cores. This coupling can lead to significant differences in ignition delay by as much as three times over the corresponding homogeneous delay.

Detailed analysis of the dominant chemistry and the relative roles of reaction and diffusion is implemented by tracking the evolution of four representative kernels. The first kernel is characterized by a relatively low rate of dissipation at its core throughout the induction time. It evolves similar to its corresponding homogeneous mixture, albeit at a different reference mixture due to differential diffusion effects. The second and third kernels undergo significant radical and heat loss by dissipation, resulting in increased delay time and a shift in the relative roles of dominant reactions that contribute to radical production and consumption during the induction phase. The shift is characterized by an increased role of termination reactions during the intermediate stages of the induction period. The termination reaction, $H + O_2 + M = HO_2 + M$, helps to promote the build-up of hydroperoxy, a key radical storage species, and to promote an increase in temperature at the kernel, which in turn, leads to a shift in chemistry favoring chain-branching reactions. The branching reaction $HO_2 + H = OH + OH$ further converts the chain terminating reaction $H + O_2 + M = HO_2 + M$ into a chain propagating pathway, thereby leading to a suspended radical level at the kernel core until the temperature increase is sufficient to promote active chain-branching.

The same shift towards chain termination is responsible for extinction in the fourth kernel that is promoted by high rates of heat and radical dissipation and a moderate heat release during induction. We find that the fate of the different kernels is associated with 1) the dissipation of heat that contributes to a slow down in chemical reactions and a shift in balance between chain-branching and chain-termination reactions, and 2) the dissipation of mass that keeps the radical pool growth in check, and that is promoted by slower reaction rates.

We further find that a single measure of the competition between chemistry and transport may be insufficient to describe autoignition. The disparate scales of the radical and thermal layers during autoignition brings to question whether a definition of the scalar dissipation rate based on a major species or temperature is adequate. This is particularly important at temperature ranges in the vicinity of the cross-over temperature where chain branching/chain termination reactions are most sensitive to temperature. Damköhler numbers for the different species and energy equation, that are associated with the relative balance of diffusive transport and chemistry, diverge significantly during the transient evolution of the kernels. Here, we propose an additional Damköhler number that tracks the evolution of a representative radical in addition to the Damköhler number associated with thermal loss.

Effects of Unsteady Scalar Dissipation Rate on Ignition of Non-Premixed Hydrogen/Air Mixtures in Counterflow³

In the DNS study above, the turbulent mixing conditions are such that the characteristic ignition delay is comparable to mixing time scales. As a result, many kernels experience a single impulsive strain event during their evolution, as opposed to several repetitive strain events. To reproduce similar turbulent mixing conditions under a simpler configuration, the effects of radical dissipation on the ignition delay and kernel evolution are examined by impulsively changing the scalar dissipation rate via the counterflow freestream velocities. In particular, the impulse is applied at different times during the induction period to assess the radical evolution dependence on the kernel mixing history.

The one-dimensional counterflow study is performed in the high-temperature ignition limit and then extended to the low-temperature ignition limit, which is relevant to many practical combustion devices including

diesel and homogeneous charge compression ignition (HCCI) engines. The sensitivity of the kernel growth is quantified by examining the time evolution of key radical species as well as their reaction and flow flux balances over a range of impulse amplitudes and times.

We find that transient ignition in both high- and low-temperature ignition limits is sensitive to changes in scalar dissipation rate. Increases in ignition delay of as much as five times are observed, depending upon the impulsive forcing amplitude and timing. For a given impulse amplitude, kernels that accumulate more radicals by a given time during induction are found to ignite much sooner, indicating that the time history of the kernel radical pool relative to the impulse time is important. Furthermore, kernels are found to be able to survive excursions in the scalar dissipation rate to values that far exceed the steady ignition state. The increase in ignition delay in both limits is attributed to a shorter residence time of radicals in the kernel as measured by an instantaneous Damköhler number. A new ignition criterion based on the instantaneous Damköhler is found to be an accurate measure of predicting the ignitability under highly transient conditions.

DNS of High-Temperature Combustion in Nonhomogeneous Hydrogen/Air Mixtures⁴

Following the accumulation of a radical pool by chemical chain branching during the induction phase, thermal runaway occurs during which isolated ignition kernels form premixed fronts that propagate from the ignition sites. The fronts subsequently propagate into inhomogeneous thermal and reactant composition fields, converting reactants into intermediates and products in their wake. We continued the ignition DNS simulations past thermal runaway into the high-temperature combustion and burnout stages. Our primary motivation in this follow-on study is to identify the effects of a nonhomogeneous mixture fraction field on the high-temperature combustion modes and the relative contributions of these modes to heat release and pollutant formation. A secondary objective is to investigate the presence and potential roles played by triple flames. Previous studies have shown that these structures may play a key role in the propagation of ignition along stoichiometric contours. Initially combustion is initiated in lean premixed flames that subsequently propagate into richer mixtures. As these fronts cross the stoichiometric mixture fraction, rich premixed flames are formed. Because of gas expansion and premixed flame propagation, these diffusion flames evolve from intensely burning diffusion flames that are attached to rich premixed fronts, to detached, slowly quenched diffusion flames that scavenge radicals behind the front. We find that mixture stratifications play a vital role in the detachment rate of these flames, such that mixtures with higher dissipation rates and faster variations in the mixture fraction promote flame detachment.

In addition to premixed and diffusion flame fronts, triple flames and diffusive, distributed reaction zones also develop. Triple flames are formed during the transition along an autoignition kernel from lean to rich premixed flames and during the propagation of these rich premixed flames into quenched fuel-lean mixtures. At the intersection of lean and rich premixed flames and stoichiometric lines, the so-called triple point, burning is more intense. However, the overall contribution of triple flames to the ignition and burning rate of detached diffusion flames remains insignificant.

The contribution of combustion in premixed and diffusion flame modes to heat release rate is found to be strongly affected by the mixture field. An increased and sustained contribution of diffusion flames to heat release is found for low dissipation, slowly varying mixture fraction fields. Finally, the dominant contribution to NO

formation, as estimated using a simple Zeldovich formulation, may be attributed primarily to diffusion flames for the mixture conditions considered.

FUTURE RESEARCH

In the next couple of years we plan to extend ongoing research in the areas of autoignition and high-temperature partially-premixed turbulent combustion. In particular, we plan to study the effect of turbulent mixing on the ignition delay of single and multi-stage ignition hydrocarbon fuels over a range of pressure and mixing conditions. We further plan to extend current models of autoignition and flame propagation in RANS and LES approaches. The statistical data obtained from DNS will be used to characterize the evolution of the scalar dissipation rate and mixture integral scales required to develop models of high-temperature partially-premixed combustion.

REFERENCES

- [1] T. Echekki and J. H. Chen, "Direct Numerical Simulation of Autoignition in Non-homogeneous Hydrogen-Air Mixtures," *Combust. Flame*, submitted, (2001).
- [2] Mastorakos, E., Baritaud, T. A., and Poinso, T., *Combust. Flame* 109: 198-223 (1997).
- [3] S. D. Mason, J. H. Chen, H.G. Im, "Effects of Unsteady Scalar Dissipation Rate on Ignition of Non-premixed Hydrogen/Air Mixtures in Counterflow," *Twenty-Ninth Symposium (International) on Combustion*, (Sapporo, Japan, July 21-July 26, 2002) submitted.
- [4] T. Echekki and J. H. Chen, "High-Temperature Combustion in Autoigniting Non-Homogeneous Hydrogen-Air Mixtures", *Twenty-Ninth Symposium (International) on Combustion*, (Sapporo, Japan, July 21-July 26, 2002) accepted.

PUBLICATIONS (2000-2002)

- [1] J. H. Chen and H. G. Im, "Stretch Effects on the Burning Velocity of Turbulent Premixed Hydrogen-Air Flames," *Twenty-Eighth Symposium (International) on Combustion*, (Edinburgh, Scotland, July 30-August 4, 2000), pp. 211-218.
- [2] H. G. Im and J. H. Chen, "Effects of Flow Transients on the Burning Velocity of Hydrogen-Air Premixed Flames," *Twenty-Eighth Symposium (International) on Combustion*, (Edinburgh, Scotland, July 30-August 4, 2000), pp. 1833-1840.
- [3] H. G. Im and J. H. Chen, "Effects of Flow Strain on Triple Flame Propagation", *Combust. Flame*, **126**:1384-1392, 2001.
- [4] W. Kollmann, J. H. Chen, and H. G. Im, "A Geometric Criterion for Non-equilibrium and Triple Flame Domains," *Advances in Turbulence VIII, Proceedings of the Eighth European Turbulence Conference*, C. Dopazo (Eds.), Barcelona, 2000.
- [5] J. H. Chen, "Burning Velocity Statistics in the Flamelet and Thin-Reaction Zone Regimes, " 2nd Joint Meeting of the U.S. Sections of the Combustion Institute, Oakland, CA, (2001).
- [6] H. G. Im, J. H. Chen, R. Subramanya and R. Reddy, "Direct Numerical Simulations of Turbulent Premixed Flame Interaction using Parallel Computing, " *1st MIT Conference on Applied Mechanics and Fluid Mechanics*, Elsevier Science, June, 2001.
- [7] T. Echekki and J. H. Chen, "Direct Numerical Simulation of Autoignition in Non-homogeneous Hydrogen-Air Mixtures," *Combust. Flame*, in press, (2001).
- [8] H. G. Im and J. H. Chen, "Direct Numerical Simulation of Turbulent Premixed Flame Interaction," *Combust. Flame*, in press, (2002).
- [9] S. D. Mason, J. H. Chen, H.G. Im, "Effects of Unsteady Scalar Dissipation Rate on Ignition of Non-premixed Hydrogen/Air Mixtures in Counterflow," *Twenty-Ninth Symposium (International) on Combustion*, (Sapporo, Japan, July 21-July 26, 2002) submitted.
- [10] T. Echekki and J. H. Chen, "High-Temperature Combustion in Autoigniting Non-Homogeneous Hydrogen-Air Mixtures", *Twenty-Ninth Symposium (International) on Combustion*, (Sapporo, Japan, July 21-July 26, 2002) accepted.

Turbulent Combustion

Robert K. Cheng
Environmental Energy Technologies Division
Lawrence Berkeley National Laboratory
70-108B, 1 Cyclotron Rd.
Berkeley, CA 94720

E-mail: rkcheng@lbl.gov

Lawrence Talbot
Department of Mechanical Engineering
University of California at Berkeley
6173 Etcheverry Hall, MC 1740
Berkeley, CA 94720-1740

E-mail: talbot@cmsa.berkeley.edu

Scope

This research program focuses on lean premixed combustion which is an emerging low emission energy technology being deployed in advanced heat and power generation systems. Our objective is to investigate experimentally the fluid mechanic processes that control combustion intensity, flame stabilization, extinction and pollutant formation. The goal is to provide the scientific underpinnings which can then be incorporated into models that will become more accurate and reliable tools for predicting combustion process performance. This effort is responsive to DOE's mission to "foster a secure and reliable energy system that is environmentally and economically sustainable." Combustion processes of practical interest are turbulent and are not yet sufficiently well characterized or understood to guide the refinement of turbulent combustion theories and to support the development of robust numerical models. Our approach follows a theoretical concept of classifying premixed flames based on the initial turbulence conditions and chemistry. To conduct a systematic exploration of the evolving flame structures at different turbulence intensities and scales, we use laser diagnostics and laboratory burners capable of operating over a wide range of fuel/air ratios and turbulence conditions. In the past, our laboratory experiments have concentrated on flames at standard temperature and pressure (i.e., typical furnace and boiler conditions). With the development of new experimental facilities, the experimental conditions will be extended to higher flow velocities (i.e., a closer simulation of conditions in large burners) and higher pressures and temperatures (i.e., a closer simulation of gas turbine conditions).

Recent Progress

Our low-swirl burner (LSB) has been very useful for investigating the evolution of flame front structures with increasing turbulence. Fitted with a special turbulence generator, it has enabled the study of flames with high intensity, near-isotropic turbulence up to 4 m/s RMS velocity. Previous investigations have supported the concept of a new 'thin reaction zone' regime ($1 < Ka < 10$) proposed by Peters. Here, the smallest turbulent eddy is smaller than the flame front thickness, d_L (about 1 mm for most atmospheric hydrocarbon flames), but is still an order of magnitude larger than the reaction zone (about 0.1 mm). The significant change in flame structure between the wrinkled flame regime and the thin reaction zone regime is the broadening of the preheat zone due to disturbance by turbulence. The main implication for modeling is that turbulent transport becomes significant within the preheat zone. To what extent this will influence the local reaction rate remains unknown. To better characterize preheat zone broadening, we studied six methane/air flames of equivalence ratio 0.7, $Ka = 1-17$ by Rayleigh laser sheet measurements of the gas density. Within the preheat zone (approximately 400-

1000 K) a new approach to analyzing flame front broadening has been developed to address issues of flame three dimensionality.

Instantaneous progress variable, c , contour sets, extracted from the 2D Rayleigh images, constitute the basic data set. A statistical analysis of three aspects of this data has been developed and performed: a) c contour spacing, b) flame front curvature, and c) flame surface density. A detailed investigation revealed little change in these parameters with turbulence, even at the highest Ka numbers; the contour spacings were similar to those derived from numerical laminar simulations and neither the flame front curvature nor the flame surface density varied significantly with c . Geometric effects of turbulence on flame front structure still predominate at these turbulence levels. The primary effect of higher turbulence is increasingly to convolute the flame front, raise the flame surface density, reduce the scalar length scales and so increase the burning rate. This finding is also reflected in a significant broadening of the flame front curvature distributions with increasing u'/S_L . These results indicate that the diagrams often used to delimit the various regimes of premixed turbulent combustion and hence guide modeling are based on parameters which need to be carefully investigated to determine their appropriateness. This argues for an interpretation of combustion/turbulence interactions which sees the reaction zone thickness as the significant scalar length scale.

Our basic research on turbulent combustion has spun-off applied work for developing our LSBs into economical low emission combustion products. They are being commercialized by a U.S. burner manufacturer and will be introduced in 2003 for industrial process heating of up to 3 MW (10 MMBtu/hr). Experience gained from scaling the burner to large sizes for industrial application has provided interesting insight into premixed turbulent flame properties. Typical operating velocities of practical LSBs are from 10 to 90 m/s. The fact that the LSB operates over such a large velocity range implies a linear relationship between the displacement flame speed and turbulence intensity. This is in direct contrast with current theoretical consensus on a "bending effect" where the displacement flame speed correlation ceases to increase with increasing turbulence. To obtain a fundamental understanding of this interesting flame phenomenon, we have built a half-scale LSB (2.5 cm ID) that operates up to 50 m/s. Preliminary tests are complete and Rayleigh scattering and OH-Planar Laser Induced Fluorescence (OH-PLIF) are being applied to study the wrinkled flame structures. Particle Image Velocimetry (PIV) measurements will commence once the new diagnostics are fully commissioned.

The development of PIV is a significant enhancement of our capability to study the flowfields of turbulent premixed flames in high velocities. In the past, we have depended on two-component laser Doppler anemometry (LDA) to measure velocity statistics. Although LDA is a robust method, it produces velocity information only at one point in the flowfield at a time. Scanning a very large flame is therefore quite time consuming. The long run time necessary to scan flames requiring high air and fuel flowrates are difficult to accommodate. They burden laboratory resources and put stringent demands on safety monitoring and control. PIV captures the velocity within a spatial domain that covers most of the laboratory flame zones. Instantaneous velocities in 2D are rendered by analyzing the displacement of particle positions between two images obtained by short successive laser pulses. Flow direction is readily resolved on the 2D image plane. It provides a much faster means of obtaining flowfield information and also information such as instantaneous velocity gradients, unavailable from LDV. This method is relatively mature and commercial units are available. The system we have developed is cost-shared with the

NASA Microgravity Combustion Program. It consists of a dual, synchronized YAG laser system interfaced with a PC-controlled frame grabber and a 2K by 2K digital camera. Data acquisition and analysis software is provided by Mark Wernet of NASA Glenn Research Center. This system is being calibrated by mapping the flowfield of a 50 mm diameter LSB. The data will provide the baseline data for comparison with the results to be obtained in the smaller burner at higher velocities.

We also continue the development of an experimental facility to study lean premixed turbulent flames at high initial pressures and temperatures. It is designed to simulate idle and mid-load conditions of a small gas turbine combustor (15 atm and 200° C inlet temperature). The centerpiece is an optically accessible stainless steel combustion chamber that is mounted on top of a premixed burner. This facility has computer-controlled provision to set the fuel/air ratio, monitor chamber pressure and surface temperatures, and to analyze combustion products. After extensive overhaul of our original flow control system to provide better operational stability at moderate pressures, the commissioning process of the facility is near completion. Conditions tested thus far include conical flames with mean flow velocity of 3m/s at 2 atm.

In addition to our experimental effort, we are also pursuing a modest numerical study of the simulation of turbulent open v-flames. This 2D method is particularly well-suited for investigating the dynamics of turbulent flow and its effects on flame wrinkling. Though other more elaborate numerical approaches have been developed for premixed turbulent flames, the discrete vortex method focuses on the fluid mechanical processes and provides a better tool to resolve the dynamic flame/turbulence interactions that control the development of the turbulent flame brush. A rod-stabilized v-flame was chosen for simulation because of the wealth of experimental data on the turbulent flowfield and flame wrinkle structures that have been collected in our experimental database, and are available for direct comparison with numerical results.

Our collaborator on the numerical simulation is Prof. C.K. Chan of the Hong Kong Polytechnic University. The achievements in the past year include improvement in the simulation of the complex flame fronts by a novel numerical technique called Contour Advection with Surgery (CAS). Having been used in geophysical research for more than a decade, CAS is a new numerical scheme for studying flame front propagation. By continuously redistributing marker nodes at a desired density, CAS is able to avoid the numerical instability caused by the clustering of marker nodes in regions of high curvature. Furthermore, the novel Contour Surgery (CS) accompanying CAS allows topological changes of the flame front while it evolves without causing any difficulty. To test the robustness and accuracy of CAS, we have performed two numerical experiments with carefully selected parameters. The first experiment had a moderate turbulence intensity of 7%, and the computed velocity statistics, as well as flame surface density show a good agreement with laboratory measurements. The second experiment has a higher turbulence intensity of 14%. In this case, CS is found to play an active role in treating the frequent topological changes of the convoluted flame front which results in the formation of small flame islands. In principle, CAS can be extended to other combustion geometries, such as stagnation flame, when the reaction sheet model is employed.

Summary of Planned Research

For our study of open high speed flames at atmospheric conditions, the use of PIV will determine the displacement flame speed and provide an explanation of why the low-swirl flame stabilization method does not exhibit non-linearity in its flame speed correlation. OH-PLIF and Rayleigh techniques (point or 2D) will be used to study the local and mean burning rates and to investigate if wrinkled flame structures still exist at high flow rates.

For our study of premixed turbulent flames at high pressures, the initial effort will be focused on an extensive survey of the effects of high pressure on overall flame features using imaging methods. Changes in flame size with pressures will provide qualitative information on the mean combustion intensity and the mean burning rate. The laminar flame thickness decreases with increasing pressure indicating that the wrinkle flame model will still be valid. The validation of thin flame structures under high pressures requires detailed measurement of turbulence flowfield and flame structure. Adapting OH-PLIF and Rayleigh scattering techniques to high pressures will be one of the major efforts.

If funding is available, we plan to use the improved discrete vortex model and extend the computations to high turbulence intensities and possible predictions of local extinction. Another extension would be to treat the problem of flame stabilization by a recirculation region behind a finite size flameholder. The model would include the effects of shear turbulence produced by the flame stabilizer and its role in the recirculation zone within the products. Formulation and exploitation of the model for the stagnation point flame configuration will also be explored. These new numerical simulation developments would represent a significant and practically important advance in the prediction of premixed flame behavior by means of vortex dynamics, but the numerical problems which would have to be overcome are far from trivial. Additional experiments designed to validate numerical predictions will also be formulated.

We also plan to organize our prior measurements into a database accessible to collaborators. We routinely receive requests to provide data to support theoretical and numerical development.

Publications

1. Shepherd, I.G. and Cheng, R.K., "The Burning Rate of Premixed Flames in Moderate and Intense Turbulence," *Combustion and Flame*, 127:2066-2075 (2001).
2. Cheng, R.K., Bedat, B., Shepherd I.G. and Talbot, L., "Premixed Turbulent Flame Structures in Moderate and Intense Isotropic Turbulence," *Combustion Science and Technology*, 174(1):29-59, 2002.
3. Shepherd, I.G. and Cheng, R.K., "Premixed Flame Front Structure in Intense Turbulence," to appear in *Proceedings of the Combustion Institute*, 39 (2002).
4. Lam, J.S.L., Chan, C.K., Talbot, L. and Shepherd, I.G., "On the High-Resolution Modeling of Turbulent Premixed Open V-flame," submitted to *Combustion Theory and Modeling*, (2002).

*Electronic Structure Studies of Geochemical
and Pyrolytic Formation of Heterocyclic
Compounds in Fossil Fuels*

DOE Chemical Science Grant # DE-FG02-97ER14758

J. Cioslowski

Department of Chemistry & Biochemistry and
School of Computational Science & Information Technology
Florida State University
Tallahassee, FL 32306.

jerzy@csit.fsu.edu
(850) 644-8274

and

D. Moncrieff

School of Computational Science & Information Technology
Florida State University
Tallahassee, FL 32306.

moncrieff@csit.fsu.edu
(850) 644-4885

Program Scope

This research program has as its objective uncovering of the reaction mechanisms responsible for the formation of various heteroatom-containing combustion emittants. As such, it holds the promise of guiding the practitioners of applied science and engineering in their efforts to significantly reduce the pyrolytic production of carcinogens and other hazardous substances. At the same time, it is slated to test practical limits of the predictive power of modern quantum-chemical methods and shed light on mechanisms of many reactions that are commonly employed in organic syntheses.

Our research targets a large number of reaction pathways of relevance to pyrolytic processes involving heterocyclic compounds that occur during genesis, acquisition, and combustion of fossil fuels. A broad spectrum of theoretical approaches, ranging from very accurate interpolative schemes such as G3 to the methods of density functional theory, is invoked. As the result, reliable values of thermodynamic properties become available for molecules that are not readily amenable to experimental measurements. New mechanisms of important reactions are revealed and the rules governing thermal fates of heterocyclic species are discovered.

Recent Progress

A number of research projects were completed in 2001. These projects, which yielded data of much interest to both experimental and theoretical chemists, required very substantial computer resources.

According to both UB3LYP/6-311G* and UMP2/6-311G* calculations, the lowest-energy conformer of the S_8^+ radical cation possesses C_s symmetry [10]. However, there are three other structures with low relative energies that do not exceed 6.5 [kcal/mol]. These conformers, which are found to be very prone to pseudorotation, are predicted to interconvert readily. The fluxional nature of S_8^+ is expected to facilitate its reactions with organic species where a specific conformation is demanded by steric constraints, which may explain its high reactivity towards PAHs with crowded hydrogen atoms.

Utilizing UB3LYP/6-311G* and UMP2/6-311G* calculations, the S_5^+ homocyclic radical cation exists in only one conformer of C_s symmetry that undergoes a facile pseudorotation through a C_2 transition state [11]. A structure with D_{3d} symmetry is predicted to be the global minimum for the S_6^+ species. This study

uncovers the gradual transition from the conformational simplicity of smaller homocyclic sulfur cations, for which the rigidity of the rings apparently translates into a relatively weak influence of electron correlation effects on their relative energetics and geometries, to the conformational complexity of larger species, for which significant discrepancies between the predictions of different electronic structure methods are observed.

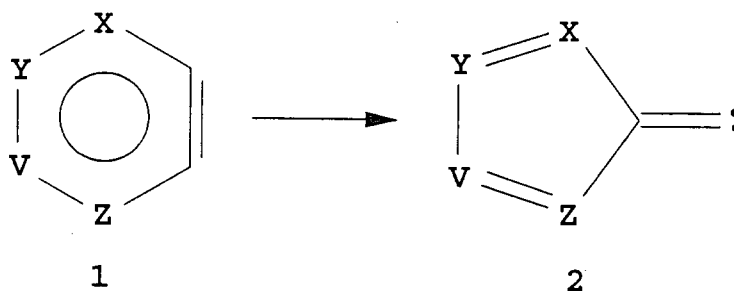
When calibrated against the available experimental data for didehydrobenzenes, RB3LYP/cc-pVTZ, QCISD/cc-pVTZ, CCSD(T)/cc-pVTZ, and G3 electronic structure calculations provide reliable predictions of standard enthalpies and singlet-triplet splittings in all possible isomers of didehydroazines, which (with a possible exception of 2,6-didehydropyridine) possess singlet ground states [12]. Singlet didehydroazines with larger numbers of nitrogen atoms turn out to be more prone to ring opening, as indicated by the fact that out of the 6, 11, 6, and 3 possible didehydropyridines, didehydrodiazines, didehydrotriazines, and didehydrotetrazines, respectively, 5, 7, 2, and none are actually found. Immediate proximity of the nitrogen atom to the formally triple carbon-carbon bond confers decreased thermodynamic stabilities and smaller singlet-triplet splittings on the species of the 1,2-didehydro type. Some of the aza-analogs of singlet 1,3-didehydrobenzene were as stable as their 1,2-didehydro counterparts. The only existing aza-analog of singlet 1,4-didehydrobenzene is 2,5-didehydropyrazine, which is particularly stable and possesses a large singlet-triplet splitting, making it a feasible synthetic target. The calculations also indicate that the experimental standard enthalpies of formation of pyrimidine and pyrazine are in error.

Standard enthalpies of formation, ionization potentials, electron affinities, and band gaps of finite-length [5,5] armchair and [9,0] zigzag single-walled carbon nanotubes (SWNTs) capped with C₃₀ hemispheres obtained by halving the C₆₀ fullerene were computed at the B3LYP/6-311G* level of theory [13]. Properties of SWNTs were found to depend strongly on the tube length and, in the case of the [9,0] zigzag species, on the relative orientation of the caps. The metallic character of an uncapped infinite-length [5,5] armchair SWNT manifests itself in the oscillatory dependence of the properties of capped finite-length tubes on their size. An infinite-length [9,0] zigzag SWNT is predicted to be a semiconductor rather than a metal irrespective of the presence of caps. The results underscore the slow convergence of SWNT properties with respect to the tube length and uncover small but significant radial distortions along the long axes of SWNTs.

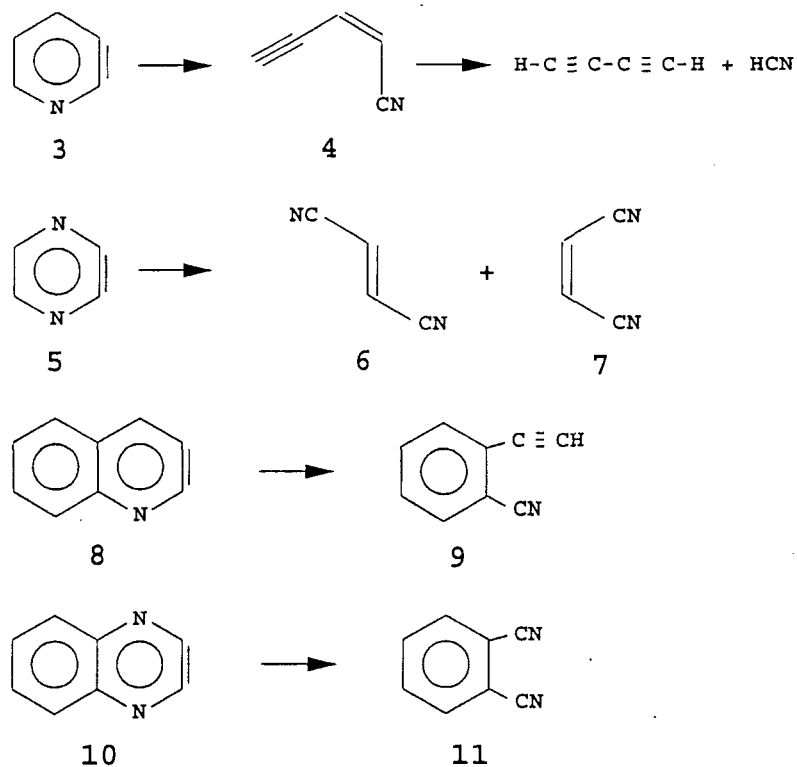
Future Plans

In the coming year, our research will focus on the elucidation of the formation of five- and six-membered heterocycles in pyrolytic reactions. To achieve this end, we are planning to complete the following projects:

The rearrangement of benzyne (**1**, X=Y=V=Z=CH) to cyclopentadienylidencarbene (**2**, X=Y=V=Z=CH) constitutes the key step in the reaction pathway that connects polycyclic aromatic hydrocarbons with their cyclopenta-analogs.



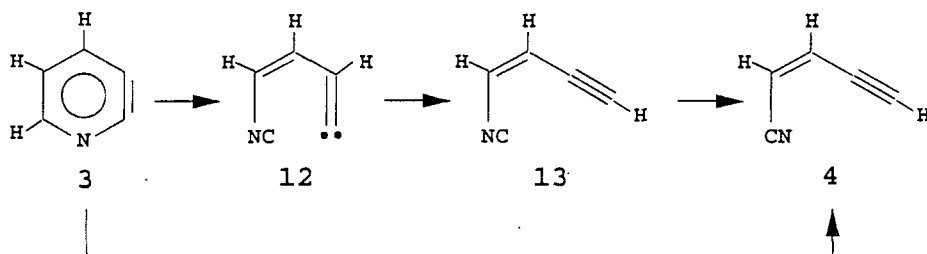
This transformation is ca. 30 [kcal/mol] endothermic and proceeds through a very late transition state. Activation and reaction energies of the rearrangements that lead to annelated cyclopentadienylidencarbenes can be easily predicted from simple considerations that take into account the disruption of aromatic conjugation caused by the bond fixation in the five-membered rings of the reaction products. Interestingly, although such rearrangements have been postulated for many reactions, none of them appears to involve an azine ring. The possible explanation of this fact may lie in the lability of azynes, several of which are known to undergo spontaneous ring fissions. Thus, **3** obtained by pyrolysis of pyridine-2,3-dicarboxylic anhydride at 600 [°C], opens to form the unsaturated nitrile **4**, which rapidly decomposes to HC≡C-C≡CH



and HCN. In a similar reaction, 5 yields a 1:1 mixture of nitriles 6 and 7. These fragmentations occur even at low temperatures, as exemplified by the formation of 4 in matrix photolysis experiments expected to produce 3. Annulated azynes, such as 8 and 10, also undergo ring fissions that yield, respectively, *o*-cyanophenylacetylene (9) and phthalonitrile (11). On the other hand, 3,4-didehydropyridine appears to be somewhat more stable with respect to fragmentation, not only decomposing unimolecularly to $\text{C}_2\text{H}_2 + \text{HC}\equiv\text{C-CN}$ and $\text{HCN} + \text{HC}\equiv\text{C-C}\equiv\text{CH}$ but also dimerizing to diazabiphenylene in the gas phase. In Ar or N_2 matrices, 3,4-didehydropyridine is persistent enough to have a measurable infrared spectrum.

The aforescribed experimental observations call for the following theoretical research:

1. *Thermochemistry and kinetics of rearrangements of azynes to aza analogs of cyclopentadienylidenecarbene.* The electronic factors affecting the barriers and energetics of the 1 \rightarrow 2 rearrangement will be investigated by analyzing the data produced by G3 and CCSD(T) calculations on didehydropyridines and the respective carbene isomers. Stabilities of the latter species with respect to fragmentation will be investigated.



2. *Mechanisms and patterns of ring fissions in azynes.* Two mechanisms have been proposed for the ring fission in azynes. The first alternative involves a scission of the triple bond and the formation of a carbene (12), which undergoes a 1,2-hydrogen shift to isonitrile (13) that in turn thermally rearranges to the reaction product. This mechanism appears to be unlikely in light of the large $\text{C}\equiv\text{C}$ bond dissociation energy and the observed production of the nitrile 4 even at low temperatures. Another possibility is offered by a concerted process. However, such a process does not seem feasible in the case of annulated azynes 8

and **10** that afford ring fission products in high yields. In order to resolve these inconsistencies and possibly uncover a different viable reaction mechanism, detailed high-level electronic structure calculations will be performed for various bond scissions and rearrangements in **3** and its ring fission products. The feasibility of the reaction pathways emerging from the sequences of these elementary processes will be assessed from both thermodynamic and kinetic points of view. Subsequently, analogous studies of fragmentation patterns of didehydroazines will be carried out. Factors that determine stabilities of individual azynes with respect to ring fission and/or fragmentation will be deduced from the resulting data. Ring openings in annelated azynes such as **8** and **10** will also be investigated, albeit at lower levels of theory.

Publications Resulting from the DOE Sponsored Research (2000–2002)

1. J. Cioslowski, G. Liu and D. Moncrieff: **Chemical Physics Letters** **316** (2000) **536**. The Concerted Trimerization of Ethyne to Benzene Revisited.
2. J. Cioslowski, M. Schimeczek, G. Liu and V. Stoyanov: **Journal of Chemical Physics** **113** (2000) **9377**. A Set of Standard Enthalpies of Formation for Benchmarking, Calibration, and Parameterization of Electronic Structure Methods.
3. J. Cioslowski, N. Rao and D. Moncrieff: **Journal of the American Chemical Society** **122** (2000) **8265**. Standard Enthalpies of Formation of IPR Fullerenes and Their Analysis in Terms of Structural Motifs.
4. D.R. Armstrong, N. Feeder, A.D. Hopkins, M.J. Mays, D. Moncrieff, J.A. Wood, A.D. Woods and D.S. Wright: **Journal of Chemical Society Chemical Communications** (2000) **2483**. Electrophilic Ring-Opening of $[(RP)_nAs]^-$ Anions, A Simple Route to Funtionalised Neutral Phosphines of the Type $[(Bu^tP)(Bu^tRP)_2]$.
5. J. Cioslowski, A. Szarecka and D. Moncrieff: **Journal of Physical Chemistry A** **105** (2001) **501**. Conformations and Thermodynamic Properties of Sulfur Homocycles: I. The S_5 , S_6 , S_7 , and S_8 Molecules.
6. J. Cioslowski, N. Rao, A. Szarecka, and K. Pernal: **Molecular Physics** **99** (2001) **1229**. Theoretical Thermochemistry of the $C_{60}F_{18}$, $C_{60}F_{36}$, and $C_{60}F_{48}$, Fluorofullerenes.
7. J. Cioslowski and A. Szarecka: **Journal of Computational Chemistry** **22** (2001) **1279**. First-Principles Conformational Analysis of the $C_{36}H_{36}$ Spheriphane, a Prototype Hydrocarbon Host Cage.
8. Z. Chen, J. Cioslowski, N. Rao, D. Moncrieff, M. Buhl, A. Hirsch, and W. Thiel: **Theoretical Chemistry Accounts** **106** (2001) **364**. Endohedral Chemical Shifts in Higher Fullerenes with 72-86 Carbon Atoms.
9. D.R. Armstrong, F. Benevelli, A.D. Bond, N. Feeder, E.A. Harron, A.D. Hopkins, M. McPartlin, D. Moncrieff, D. Saez, E.A. Quadrelli, A.D. Woods and D.S. Wright: **Inorganic Chemistry** (in press). Formation of Double-cubanes $[Sn_7(NR)_8]$ in the Reactions of Pyridyl and Pyrimidinyl Amines with $Sn(NMe_2)_2$; a Synthetic and Theoretical Study.
10. J. Cioslowski, A. Szarecka, and D. Moncrieff: **Molecular Physics A** (in press). Conformations and Thermodynamic Properties of Sulfur Homocycles: II. The Fluxional S_8^+ Radical Cation.
11. J. Cioslowski, A. Szarecka, and D. Moncrieff: **International Journal of Quantum Chemistry** (submitted). Conformations of the S_5^+ and S_6^+ Homocyclic Radical Cations.
12. J. Cioslowski, A. Szarecka, and D. Moncrieff: **Journal of Physical Chemistry A** (submitted). Energetics, Electronic Structures, and Geometries of Didehydroazines.
13. J. Cioslowski, N. Rao, and D. Moncrieff: **Journal of the American Chemical Society** (submitted). Electronic Structures and Energetics of [5,5] and [9,0] Single-Walled Carbon Nanotubes.

Half-Collision Dynamics of Elementary Combustion Reactions
Grant DE-FG03-908ER14879

Robert E. Continetti
Department of Chemistry and Biochemistry
University of California San Diego
9500 Gilman Drive
La Jolla, CA 92093-0340
rcontinetti@ucsd.edu
April 12, 2002

Program Scope

This research program has continued to focus on studies of the dynamics of hydroxyl radical reactions and in the last year has been extended to the study of radical species, in particular the alkynoxy radicals. The dynamics of hydroxyl radical reactions have been studied using negative-ion photodetachment techniques to prepare energy-selected neutral complexes in configurations near the transition-state for the corresponding bimolecular reactions. The products and dissociation dynamics of the nascent neutral complexes are then measured using translational spectroscopy. We previously applied this technique to both the $\text{OH} + \text{H}_2\text{O}$ and $\text{OH} + \text{OH}$ reactions and have now extended these experiments to the HCO_2 radical and the $\text{OH} + \text{CO} \rightarrow \text{HOCO} \rightarrow \text{H} + \text{CO}_2$ reaction. The central goal is to study the reaction dynamics of these species, providing experimental benchmarks for the evaluation of potential energy surfaces and dynamics calculations on these important systems. In studies of the energetics and dynamics of combustion-relevant free-radical species our interests lie in quantification of the anion and neutral energetics of these species. To support these experimental efforts we have carried out a number of *ab initio* and dynamics calculations, and have also established a collaboration with Professor Joseph Francisco of Purdue University.

Recent Progress

1. Dynamics of Elementary Combustion Reactions

Probing the HOCO potential energy surface by photodetachment of HOCO^-

The most exciting recent development in our studies of the half-collision dynamics of elementary combustion reactions has been our success at production of the HOCO^- anion and our study of the dissociative photodetachment (DPD) of this species. Formed in a pulsed-discharge ion source containing $\text{N}_2\text{O}/\text{CH}_4$ and CO , this anion has a photoelectron spectrum vastly different from the previously studied formate anion, HCO_2^- , discussed below. The most interesting aspect of this anion, however, is the observation that upon photodetachment this species yields stable radicals and both combustion-relevant product channels, $\text{H} + \text{CO}_2 + \text{e}^-$ and $\text{OH} + \text{CO} + \text{e}^-$.

The broad photoelectron spectrum observed for the HOCO^- anion indicates a vertical detachment energy (VDE) of 2.18 eV. Since the anion has not been previously characterized, we contacted Prof. Francisco of Purdue University, who carried out high-level (CCSD(T) // 6-311++G(3df,3pd)) *ab initio* calculations of the anion and neutral equilibrium geometries and energetics. Franck-Condon simulations of the observed spectra are most consistent with the

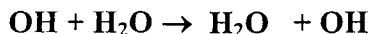
presence of the trans-HOCO⁻ anion in the source, however, the calculations show that the trans- and cis-HOCO⁻ anions are nearly isoenergetic so it is likely that a mixture of these species are present. The energetics determined from the calculations are in excellent accord with the experimental data, and indicate an electron affinity (EA) for trans-HOCO of 1.29 eV, and a bond dissociation energy for HOCO⁻ → OH⁻ + CO of 0.8 eV. Comparison of the expected Franck-Condon region in terms of the calculated cis- and trans-anion geometries to the neutral HOCO potential energy surface of Muckerman and co-workers¹ shows that these experiments access the ground state potential on the repulsive wall of the HOCO radical well.

In addition to production of stable HOCO radicals upon photodetachment, both OH + CO and H + CO₂ products were observed. The OH + CO channel shows evidence for two distinct dissociation pathways – one characterized by high-energy photoelectrons and a product translational energy distribution peaked near 0 eV, and the other channel characterized by a very broad photoelectron spectrum in coincidence with a large OH + CO product translational energy release (peaking at 1.6 eV). The latter channel can be understood in terms of excitation from HOCO⁻ to a repulsive OH + CO curve, consistent with calculations by Li and Francisco on the excited states of HOCO.² The low-energy channel (peaking at E_T near 0 eV) OH + CO products are consistent with unimolecular decomposition on the ground HOCO surface after Franck-Condon excitation into the region of the HOCO well. Similarly, in the H + CO₂ product channel a peak translational energy release of 0.53 eV is observed, consistent with unimolecular decomposition of HOCO. This channel peaks considerably away from 0 eV due to the 1.3 eV barrier from the H + CO₂ exit channel transition state to the asymptotic H + CO₂ products.

This work is nearly ready for submission for publication, and marks the first characterization of the HOCO⁻ molecular anion, and more importantly provides new insights into the dynamics on both ground and electronically excited state HOCO surfaces. Given the attention focused on the neutral potential energy surface for this system, future dynamics calculations for comparison with these results should be possible and will be of great interest.



Prior to our studies of the HOCO⁻ molecular anion, we studied the DPD of the formate anions HCO₂⁻ and DCO₂⁻ at 258 nm. In these experiments, we observed photoelectron spectra consistent with those obtained by Neumark and co-workers,³ and we found that all of the nascent formyloxyl (HCO₂) radicals dissociated to H + CO₂ products. State-resolved translational energy distributions were observed correlated with bending excitation in the CO₂ product, indicating very low rotational excitation in the products consistent with predissociation of a C_{2v} HCO₂ molecule. No evidence was found for dissociation into OH + CO. All three low-lying electronic states (²A₁, ²B₂ and ²A₂) were found to dissociate, but resolved progressions were only observed from photodetachment to the ²A₁ and ²B₂ states. Photoelectron-photofragment coincidence spectra for DCO₂⁻ show resolved vertical bands and indicate that multiple CO₂ vibrational states are accessible from each vibrational level in the predissociating DCO₂ molecule. The resolved structure is assigned to vibrational predissociation sequence bands, observable in this DPD process owing to the dissociation dynamics and the near degeneracy of the vibrational levels in the ²A₁ and ²B₂ states of HCO₂ and the bending mode of the CO₂ products. These results are described in our publication 9 published in September, 2001.



Our previous experimental studies of the OH + OH and OH + H₂O reactions (publications 1 and 8 below) were in both cases supported by *ab initio* calculations of relevant regions of the potential energy surfaces for both the anionic precursor and the neutral products. The most extensive work we carried out on the simpler OH + H₂O → H₂O + OH reaction. The initial goal in these studies was to calculate the electronic structures of the stationary points in the anion and neutral consistently and find a method accurate enough for calculation of the potential energy surface for both the anion and the neutral. To complete these calculations in a reasonable time, calculations were carried out at the (U)QCISD level of theory with the 6-311++G(d,p) basis set. The most extensive work was done on the neutral potential energy surface. The energy of the system was calculated at 60 points (120 by symmetry) for the anion and 120 points (240 by symmetry) for the neutral, varying the bond distances between the shared H atom and the O atoms in a collinear O-H-O geometry with overall C_{2h} symmetry in the H-O-H-O-H complex. The points on both surfaces were fit with an analytic function, allowing two-dimensional time-dependent wavepacket dynamics simulations of the observed photoelectron spectra, extending the previous one-dimensional calculations of Arnold, *et al.*⁴ The simulations showed that use of the *ab initio* surfaces for the anion and neutral lead to a significant broadening of the simulated photoelectron spectra, more consistent with the experimental result, and also providing a measure of the sensitivity of these data to the true potential energy surface governing hydroxyl radical reactions. This work is nearly ready for submission, and we hope that our theoretical efforts and observations will encourage further high-level theoretical structure and dynamics calculations in a larger number of degrees of freedom for this benchmark reaction of hydroxyl radicals.

2. Energetics of Free Radicals: Photoelectron Spectroscopy and Photodetachment Imaging of Alkynoxides.

In our efforts to characterize relevant combustion intermediates, we turned our attention in the last year to the alkynoxy radicals. Propargyl alcohol, HOCH₂CCH₃, is the simplest alkynol and is an energetic species owing to the presence of the acetylenic triple bond. To the best of our knowledge, however, there have been no prior studies of the energetics and dynamics of the related alkynoxy radicals. In the current study, the ground and low-lying excited states of the alkynoxy radicals were measured. Photoelectron images and spectra of 2-propyn-1-oxide, 2-butyn-1-oxide and 3-butyn-1-oxide have been obtained at various wavelengths. Photodetachment to the ground and low-lying excited states of the corresponding neutral radicals was observed. These experiments constitute the first spectroscopic measurements of energetics and angular distributions of alkynoxy species. The photoelectron images and spectra provide information about the structures and stabilities that has been corroborated by high level *ab initio* and Franck-Condon factor calculations. The CC triple bond interaction with the oxygen lone pairs in 2-propyn-1-oxide is shown to give rise to only a small splitting of the lowest A' and A'' states of the radical that are produced by photodetachment from the O lone pairs in the anion. However, a low-lying excited state has been found for these species that originates from photodetachment out of the carbon-carbon triple bond, and the effects of methylene insertion and methyl termination in 3-butyn-1-oxide are discussed. The adiabatic electron affinity of propynoxy radical is found to be 2.15 eV, and the carbon-carbon triple bond excited state is 1.05 eV higher in energy.

Future Plans

In the coming year we plan to begin PPC experiments on the OH+F,Cl and OH+H₂ reactions. These systems are simpler than those we have studied to date, and should permit a more direct comparison with detailed dynamics calculations. We are also currently developing a VUV light source so we can expand our studies of the energetics and dynamics of combustion radicals (including vinylidene, allyl and cyclopentadienyl radicals) by implementing VUV photodetachment methods to reach higher excited states of these species. We hope to establish new collaborations with groups involved in dynamics calculations and possibly further develop our own expertise in modeling the transition-state dynamics studied in these dissociative photodetachment experiments.

Publications: 2000 - Present

1. H.-J. Deyerl, A.K. Luong, T.G. Clements and R.E. Continetti, "Transition State Dynamics of the OH + H₂O Hydrogen Exchange Reaction Studied by Dissociative Photodetachment of H₃O⁺", *Faraday Discussion* **115**, 147-160 (2000).
2. L.S. Andrews, A. Rohrbacher, C.M. Laperle and R.E. Continetti, "Laser Desorption - Ionization of Transition Metal Atoms and Oxides from Solid Argon.", *J. Phys. Chem. A* **104**, 8173-8177 (2000).
3. R.E. Continetti, "Dissociative Photodetachment Studies of Transient Molecules by Coincidence Techniques.", in Advanced Series in Physical Chemistry: Photoionization and Photodetachment Vol. II, ed. C.Y. Ng, World Scientific, Singapore (2000), pp. 748-808 .
4. A.G. Suits and R.E. Continetti, "Imaging in Chemical Dynamics - the State of the Art.", ACS Symposium Series Vol. 770, Imaging in Chemical Dynamics, eds. A.G. Suits and R.E. Continetti, ACS , Washington DC (2000), pp. 1-18.
5. H.-J. Deyerl, L.S. Alconcel and R.E. Continetti, "Photodetachment Imaging Studies of the Electron Affinity of CF₃.", *J. Phys. Chem. A* **105**, 552-557 (2001).
6. A. Rohrbacher and R.E. Continetti, "A Multiple-Ion-Beam Time-of-Flight Mass Spectrometer.", *Rev. Sci. Instrum.* **72**, 3386-3389 (2001).
7. R.E. Continetti, "Coincidence Spectroscopy.", *Annual Reviews of Physical Chemistry*, Vol. 52, (2001), pp. 165-192.
8. H.-J. Deyerl, T.G. Clements, A.K. Luong and R.E. Continetti, "Transition state dynamics of the OH + OH → O + H₂O reaction studied by dissociative photodetachment of H₂O⁺.", *J. Chem. Phys.* **115**, 6931-6939 (2001).
9. T.G. Clements and R.E. Continetti, "Predissociation Dynamics of HCO₂/DCO₂ studied by the Dissociative Photodetachment of HCO₂⁺/DCO₂⁺ + hv → H/D + CO₂ + e⁻.", *J. Chem. Phys.* **115**, 5345-5348 (2001).

Literature Cited

1. H.-G. Yu, J. T. Muckerman, and T. J. Sears, *Chemical Physics Letters* **349**, 547-554 (2001).
2. Y. Li and J. S. Francisco, *Journal of Chemical Physics* **113**, 7963-70 (2000).
3. E. H. Kim, S. E. Bradforth, D. W. Arnold, R. B. Metz, and D. M. Neumark, *Journal of Chemical Physics* **103**, 7801-14 (1995).
4. D. W. Arnold, C. Xu and D. M. Neumark, *Journal of Chemical Physics* **102**, 6098 (1995).

Flame Sampling Photoionization Mass Spectrometry

Terrill A. Cool
School of Applied and Engineering Physics
Cornell University, Ithaca, New York 14853
tac13@cornell.edu

Project Scope

Photoionization mass spectrometry (PIMS), recently applied to the detection of key reaction intermediates in laboratory flames[1-6], offers significant advantages over the use of conventional electron-impact mass spectrometry for the development of kinetic models of combustion. To date flame sampling PIMS experiments have been limited by the range of photon energies (8.2 to 10.5 eV) that are easily accessible with tunable VUV laser sources. Because many chemically interesting flame species have ionization potentials above 10.5 eV, full implementation of flame sampling PIMS will require higher photon energies. Synchrotron radiation, tunable over the entire range of photon energies (7 to 16 eV) required for the detection of virtually any species of combustion interest, with 10 meV energy resolution and average photon fluxes 100 times larger than those produced by tunable VUV laser sources, is currently available at the Advanced Light Source (ALS) of the Lawrence Berkeley Laboratory.

For these reasons a collaborative flame sampling PIMS experimental facility has been designed, fabricated, and recently tested on the Chemical Sciences Beamline at the ALS. The principal project goals are:

- Use synchrotron radiation PIMS to selectively monitor wide classes of combustion intermediates in hydrocarbon chemistry. Studies of interest include: the chemistry of alternatives to conventional diesel fuels, of hydrocarbon flames under near-sooting conditions, and studies of ethylene/oxygen flames to refine existing models of C₁ and C₂ hydrocarbon chemistry.
- Secondly, to develop a one-of-a-kind collaborative research facility for measurements of flame species concentration profiles needed in combustion modeling, and for precise measurements of photoionization cross sections and photoionization thresholds for combustion radicals and intermediates.

The Flame Facility

The ALS flame-sampling PIMS system incorporates the geometry of the burner, sampling cone, and skimmer that has been used in the VUV laser PIMS laboratories at Cornell University and the Sandia Combustion Research Facility during the past few years. Figure 1 illustrates principal features of the system.

A pulsed ion extraction approach is used to repetitively sweep ions from the ionization region at the intersection between the synchrotron light beam and the molecular beam containing continuously sampled flame species.

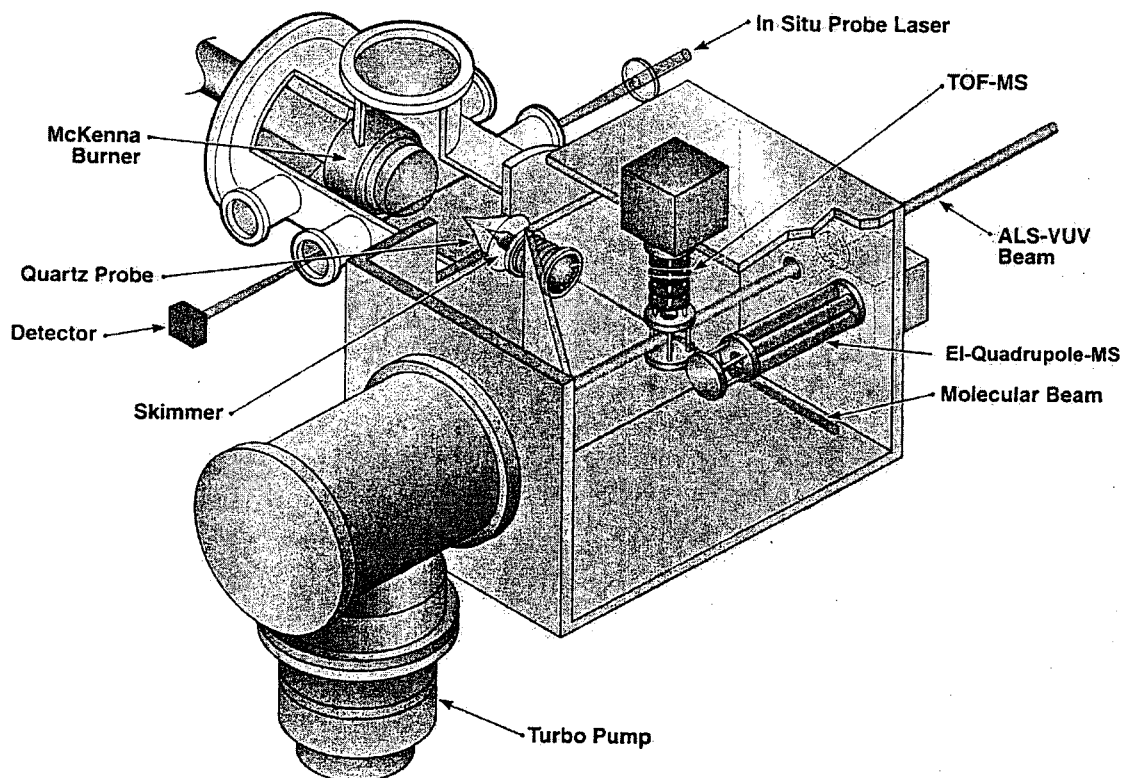


Figure 1: The flame-sampling VUV photoionization mass spectrometer facility. The flat flame burner (McKenna) may be translated along the molecular beam axis to sample flame species at various distances from the burner face. Typical flame pressures are 25 to 50 Torr. The flame sample passes through the 200 μ dia. orifice of the quartz probe and expands supersonically, to free molecule flow conditions at a pressures of 10^{-4} to 10^{-5} Torr, before reaching the 2 mm dia. aperture of the molecular beam skimmer. This first stage expansion is maintained with a 2000 liter/s turbo pump. Additional turbo pumps (not shown) keep the pressure in the main chamber, downstream of the skimmer, at pressures below 10^{-6} Torr. A vertically aligned TOFMS flight tube (not shown) provides a flight path of 1.2 m between the ionization region and a multichannel plate (MCP) detector. (Figure courtesy of Dr. Andy McIlroy, Sandia Combustion Research Facility)

Recent Progress

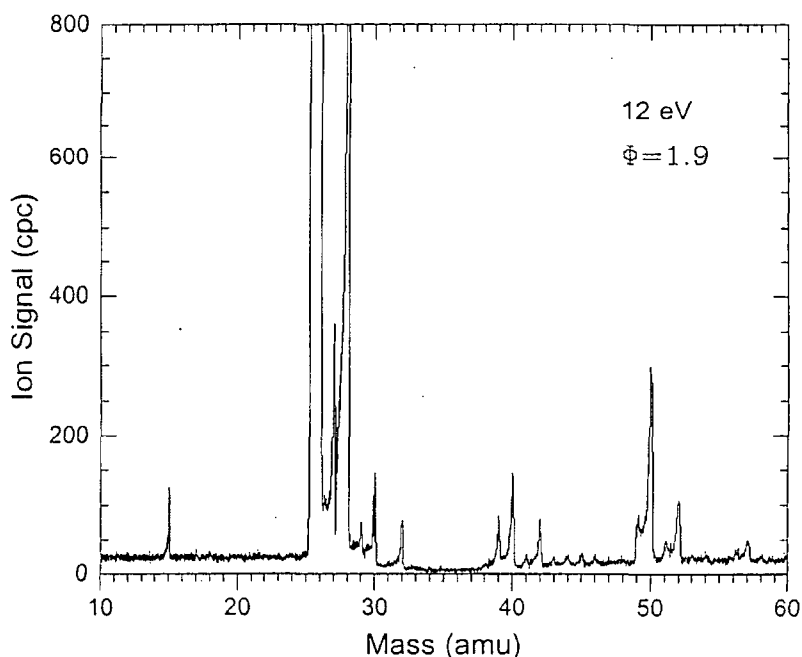
Low-pressure ethylene/oxygen flames are well suited for initial PIMS studies at the ALS for kinetic model development. Such flames offer reaction mechanisms of moderate complexity linking a rich assortment of stable and radical intermediate species. Kinetic models of the combustion of compounds

containing two carbon atoms are at the state-of-the-art in flame chemistry. Although the basic mechanisms in these models are well established, many of the chemical reaction rates are of uncertain accuracy and relatively little experimental data are available for comparison.

Recently, Bhargava and Westmoreland [7,8] have measured mole fraction profiles for numerous stable and radical species for well-documented fuel-rich and fuel-lean ethylene/oxygen flames using conventional electron-impact mass spectrometry (EIMS). These measurements present an ideal opportunity for a direct comparison of the relative merits of PIMS and EIMS.

We have just completed PIMS measurements on 25 Torr $C_2H_4/O_2/Ar$ flames operated with fuel/air equivalence ratios in the range $0.75 < \Phi < 1.9$ to test our apparatus and evaluate the performance capabilities of this approach to PIMS of flame species. End station 3 of the Chemical Dynamics Beamline provides a quasi-continuous photon flux of about 5×10^{13} photons/second with an energy resolution of about 0.01 eV over the range of energies (10, 11, 12, 13, and 15 eV) of these preliminary tests.

The figure below displays a mass spectrum recorded for the middle of the luminous zone for a fuel rich $\Phi=1.9$ flame at a photon energy of 12 eV. These data are preliminary and data acquisition and TOFMS parameters need to be better optimized. The two strongest mass peaks with peak ion counts of 8.5×10^4 and 5×10^3 for $m/z=26$ (C_2H_2) and $m/z=28$ (C_2H_4) are off-scale. Other values of m/z include 15 (CH_3), 27 (C_2H_3), 29 (HCO and/or C_2H_5), 30 (H_2CO and/or C_2H_6), 32 (O_2), 39 (C_3H_3), 40 (C_3H_4), 42 (H_2CCO and/or C_3H_6), 50 (C_4H_2), and 52 (C_4H_4).



Future Plans

Many questions remain to be investigated in the near future. Two of the most important are:

1. Will it be possible to obtain reproducible spatial species profiles throughout the preheat, flame, and post flame zones for both stable and radical intermediates at mole fractions as low as 10^{-5} to 10^{-6} ?
2. Can reliable, high S/N, near-threshold photoionization efficiency curves be generated with photon beam energies scanned over a 1-2 eV range for reasonable data acquisition times?

These cannot be definitively answered at present, but our preliminary data offer some encouragement that these issues may be favorably resolved during our June-July campaign at the ALS.

Ultimately we plan to study the chemistry of a variety of hydrocarbon flames chosen to assist in the development of useful kinetic models. We also hope to explore the potential of the new facility for precise measurements of photoionization cross sections and photoionization thresholds for combustion radicals and intermediates.

References

1. J. H. Werner and T. A. Cool, "A Kinetic Model for the Decomposition of DMMP in a Hydrogen/Oxygen Flame", *Combustion and Flame*, **117**, 78 (1999).
2. J. H. Werner and T. A. Cool, "The Combustion of Trichloroethylene Studied with VUV Photoionization Mass Spectrometry", *Twenty-Seventh Symposium (International) on Combustion*, The Combustion Institute (1998), pp. 413-423.
3. J. H. Werner and T. A. Cool, "The Kinetics of the Combustion of Trichloroethylene for Low Cl/H Ratios", *Combustion and Flame*, **120**, 125-142 (2000).
4. A. McIlroy, T. D. Hain, H. A. Michelsen, and T. A. Cool, "A Laser and Molecular Beam Mass Spectrometer Study of Low-Pressure Dimethyl Ether Flames", *Twenty-Eighth Symposium (International) on Combustion*, The Combustion Institute (2000), 1647-1653.
5. J. H. Werner and T. A. Cool, "Flame Sampling Photoionization Mass Spectrometry of CH_3PO_2 and CH_3OPO_2 ", *Chem. Phys. Lett.*, **275**, 278 (1997).
6. J. H. Werner and T. A. Cool, "Flame Sampling Photoionization Mass Spectrometry of Dichloroethanol", *Chem. Phys. Lett.*, **290**, 81 (1998).
7. A. Bhargava and P. R. Westmoreland, "Measured Flame Structure and Kinetics in a Fuel-Rich Ethylene Flame", *Combustion and Flame*, **113**, 333-347 (1998).
8. A. Bhargava and P. R. Westmoreland, "MBMS Analysis of a Fuel-Lean Ethylene Flame", *Combustion and Flame*, **115**, 456-467 (1998).

STATE CONTROLLED PHOTODISSOCIATION OF VIBRATIONALLY EXCITED MOLECULES AND HYDROGEN BONDED DIMERS

F.F. Crim
Department of Chemistry
University of Wisconsin-Madison
Madison, Wisconsin 53706
fcrim@chem.wisc.edu

Our research investigates the chemistry of vibrationally excited molecules. The properties and reactivity of vibrationally energized molecules are central to processes occurring in environments as diverse as combustion, atmospheric reactions, and plasmas and are at the heart of many chemical reactions. The goal of our work is to unravel the behavior of vibrationally excited molecules and to exploit the resulting understanding to determine molecular properties and to control chemical processes. A unifying theme is the preparation of a molecule in a specific vibrational state using one of several excitation techniques and the subsequent photodissociation of that prepared molecule. Because the initial vibrational excitation often alters the photodissociation process, we refer to our double resonance photodissociation scheme as *vibrationally mediated photodissociation*. In the first step, fundamental or overtone excitation or stimulated Raman scattering prepares a vibrationally excited molecule and a second photon, the photolysis photon, excites the molecule to an electronically excited state. Vibrationally mediated photodissociation provides new vibrational spectroscopy, measures bond strengths with high accuracy, alters dissociation dynamics, and reveals the properties of and couplings among electronically excited states.

Several recent measurements illustrate the scope of the approach and point to new directions. We have completed an extensive study of the ground and electronically excited state spectroscopy of isocyanic acid (HNCO), are in the midst of a new study of the spectroscopy and non-adiabatic dissociation dynamics of ammonia (NH₃), and have new results on the vibrationally mediated photodissociation of methanol (CH₃OH). In each case, the goals are understanding and exploiting vibrations in the ground electronic state, studying the vibrational structure of the electronically excited molecule, and probing and controlling the dissociation dynamics of the excited state.

Isocyanic Acid (HNCO)

The three photodissociation pathways of HNCO to produce H + NCO, ³NH+CO, and ¹NH+CO provide a rich structure to explore with vibrationally mediated photodissociation. We have now completed a study, involving collaborations with other experimentalists and with theorists, of the vibrational spectroscopy and photodissociation dynamics. We have identified couplings in the ground vibrational state in the region of three, four, and five quanta of the N-H stretching vibrations using vibrationally mediated photodissociation to obtain action spectra of molecules cooled in a supersonic expansion. We have also explored the vibrational structure of the electronically excited state, obtaining a new measure of the electronic origin, determining the threshold for dissociation in both spin-allowed channels (producing either H+NCO or ¹NH+CO), and measuring previously unavailable excited state vibrational frequencies. A collaboration with Professor Reisler provided a detailed picture of the excited state spectroscopy and allowed the identification of the modes that promote internal conversion in the electronically excited molecule. These new measurements of dissociation thresholds and vibrational frequencies were particularly useful points of comparison with theoretical calculations of several groups.

Ammonia (NH₃)

Ammonia is a famously well-studied molecule that holds interesting opportunities for vibrationally mediated photodissociation experiments because it has both an adiabatic dissociation to yield ground state NH₂ + H and a nonadiabatic dissociation to form excited state NH₂* + H. We have used vibrationally mediated photodissociation spectroscopy to observe the symmetric N-H stretching vibration (ν_1), the antisymmetric N-H stretching vibration (ν_3), and the first overtone of the bending vibration ($2\nu_4$), obtaining simplified spectra originating the lowest few rotational states. In addition, we have observed combination bands with the umbrella vibration (ν_2) for each of these states, ($\nu_1+\nu_2$), ($\nu_2+\nu_3$), and ($\nu_2+2\nu_4$). The action spectra come from observing the production of the excited state NH₂* from photolysis well above the threshold energy for its formation. (The production of vibrational excitation wavelengths in the fundamental region is a new experimental capability in our laboratory.) We observe the first hint of the effect of vibrational excitation on the dissociation dynamics in these experiments, finding that the relative yield of excited products is *lower* for photodissociation of molecules containing a quantum of the symmetric stretching vibration in the ground state compared to those with antisymmetric stretching or bending excitation. This differential dissociation disappears completely upon addition of a quantum of the umbrella vibration in the ground state.

The electronic spectroscopy available through vibrationally mediated photodissociation is particularly informative. Because the initial vibrational excitation of NH₃ molecules cooled in a supersonic expansion selects single rotational states of vibrationally excited molecules, both the Franck-Condon factors and positions of the transitions change from the one-photon spectra. By using this extra dimension, we are able for the first time to identify unambiguously the progression in the excited state bending vibration (ν_4'), the combination bands between the bending and excited state umbrella vibration ($\nu_2'+\nu_4'$), and the origin of the excited state symmetric stretch vibration (ν_1'). The resulting new harmonic frequencies and anharmonicities are $\omega_2^0 = 881 \pm 12$ cm⁻¹, $x_{22} = 6 \pm 2$ cm⁻¹, $\omega_4^0 = 910 \pm 23$ cm⁻¹, $x_{44} = 9 \pm 6$ cm⁻¹, $g_{44} = 16 \pm 7$ cm⁻¹, and $x_{24} = 56 \pm 13$ cm⁻¹. The values for the umbrella vibration (ν_2') agree well with those previously determined by Vaida, and the large off-diagonal anharmonicity between the umbrella and bending vibrations is consistent with their near degeneracy, which prevented the direct observation of ν_4' in the past. Our necessarily less precise estimate of the origin of the broad excited state symmetric stretch vibration (ν_1') is $\omega_1^0 \approx 2360$ cm⁻¹.

Information about the excited state structure makes it possible to investigate the dynamics of the dissociation of the different excited states using resonant enhanced multiphoton ionization to perform Doppler spectroscopy on the H atom fragment. In agreement with previous measurements, we observe both slow and fast components in the distribution of recoil velocities upon excitation of different excited state umbrella vibrations. The excited state bending vibrations behave similarly with a slightly larger fraction of fast hydrogen atoms. The dramatic different is in the stretching vibrations, which we can excite unambiguously for the first time. Dissociation from the state containing one quantum of symmetric stretch (ν_1') produces a distribution with both fast and slow components that are similar to that for the origin. Dissociation from the antisymmetric N-H stretch state (ν_3'), however, produces dramatically different results. It forms *only* slow hydrogen atoms, perhaps reflecting preferential decomposition to make solely the excited state product, a proposition we plan to test with Rydberg tagging of the hydrogen atoms.

Methanol (CH₃OH)

Our first explorations of the vibrationally mediated photodissociation of methanol allowed us to obtain vibrational overtone spectra of the second and third overtone of the O-H stretching vibration in the cooled molecules that agreed well with other measurements. We have also obtained similar spectra in the fundamental region and made the first measurements of the vibrationally mediated photodissociation dynamics detecting the H-atom product in order to obtain the ultraviolet spectra of the vibrationally excited molecules.

FUTURE DIRECTIONS

The two near term goals of the project are to complete the vibrationally mediated photodissociation studies of ammonia, determining the details of the influence of vibrations on the nonadiabatic pathways, and to perform a complete study of the dissociation of vibrationally excited methanol. Both studies are likely to involve Rydberg atom time-of-flight techniques along with our existing capabilities for laser induced fluorescence and resonant multiphoton ionization detection. The next step is to investigate the dimers of the same systems to determine how simple complexation influences these well-understood dissociation dynamics.

PUBLICATIONS SINCE 2000 ACKNOWLEDGING DOE SUPPORT

The Electronic Origin and Vibrational Levels of the First Excited Singlet State of Isocyanic Acid (HNCO). H. Laine Berghout, F. Fleming Crim, Mikhail Zyrianov, and Hanna Reisler, *J. Chem. Phys.* **112**, 6678 (2000).

Controlling the Bimolecular Reaction and Photodissociation of HNCO through Selective Excitation of Perturbed Vibrational States. Ephraim Woods III, H. Laine Berghout, Christopher M. Cheatum, and F. Fleming Crim, *J. Phys. Chem. A* **104**, 10356 (2000).

Relative Product Yields in the One-Photon and Vibrationally Mediated Photolysis of Isocyanic Acid (HNCO). H. Laine Berghout, Shizuka Hsieh, and F. Fleming Crim, *J. Chem. Phys.* **114**, 10832 (2001).

Vibrational Spectroscopy and Photodissociation of Jet-Cooled Ammonia. Andreas Bach, J. Matthew Hutchison, Robert J. Holiday, and F. Fleming Crim, *J. Chem. Phys.* **116**, 4955 (2002).

Vibronic Structure and Photodissociation Dynamics of the A State of Jet-cooled Ammonia. Andreas Bach, J. Matthew Hutchison, Robert J. Holiday, and F. Fleming Crim, *J. Chem. Phys.* (2002) (*in press*).

INFRARED ABSORPTION SPECTROSCOPY AND CHEMICAL KINETICS OF FREE RADICALS

Robert F. Curl and Graham P. Glass
Department of Chemistry and Rice Quantum Institute
Rice University, Houston, TX 77251
(713)348-4816 (713)348-3285
rfcurl@rice.edu gglass@rice.edu

PROGRAM SCOPE

This research is directed at the detection, monitoring, and study of the chemical kinetic behavior by infrared absorption spectroscopy of small free radical species thought to be important intermediates in combustion. In the last year, work on the jet-cooled infrared CH stretching fundamentals ν_2 , ν_3 , and ν_{14} of allyl radical has been completed and work on the reactions of O(¹D) with acetaldehyde is progressing.

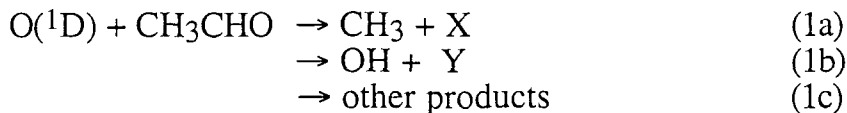
JET-COOLED CH STRETCHING FUNDAMENTALS OF ALLYL RADICAL

In previous work on the infrared spectrum of allyl radical, we found a very complex and congested spectrum because many rotational levels of this species are populated even at 195 K. Supersonic expansion cooling is the way to get more easily analyzable spectra. To this end, we have acquired the high-resolution infrared spectrum of jet-cooled allyl radical (CH₂-CH-CH₂) in the region 3010-3045 cm⁻¹ in a pulsed slit jet expansion. The radicals were produced by both modulated electrical discharge and excimer laser flash photolysis. We find that the S/N is similar for both approaches with flash photolysis producing perhaps a factor of 3 higher radical concentration and the modulated electrical discharge being capable of detecting about a factor of three lower probe laser absorption. The spectra qualitatively look better observed by flash photolysis because the spectrum obtained by this method has smaller and less numerous baseline fluctuations with about the same width as absorption lines, as can be seen in Fig. 1 below.

Over 400 transitions were observed and assigned to the ν_2 , ν_3 , and ν_{14} C-H stretch vibrations. The band origins have been determined to be 3033.8745(6), 3023.4605(6), and 3020.32(1) cm⁻¹, respectively. Spectral analysis indicates that all three upper states are perturbed with the perturbations in the ν_{14} upper state so pervasive as to make least squares analysis difficult. The gas phase frequencies reveal a somewhat unusual, in comparison with the other bands, matrix shift to the blue for ν_2 of 18 cm⁻¹.

O(¹D) REACTION WITH ACETALDEHYDE

Last year we reported that the rate of the reaction between O(¹D) and CH₃CHO has been determined by competition. N₂O was photolyzed at 193 nm to produce O(¹D) which then reacts with or is quenched by N₂O and CH₃CHO. Methyl radical is produced by one channel of the reaction with CH₃CHO and was quantitatively measured by observation of the CH stretch of CH₃. The reaction scheme can be written



We determined both the overall rate of reaction 1 and the branching ratio into (1a). Channel (1b) is the H atom abstraction channel producing OH and either vinyloxy or acetoxy radical. OH production is observed, but it is difficult to make a quantitative estimate of the branching ratio into this channel, because in the presence of adequate amounts of N₂O to give good signals large concentrations of acetaldehyde must be used to compete with N₂O for O(¹D). In the presence of high acetaldehyde concentrations, the reaction between OH and acetaldehyde takes place too rapidly to determine the concentration of OH produced by reaction 1. We have solved this problem by using ozone photolyzed at 248 nm. The high absorption cross-section of O₃ at 248 nm allows us to use ozone concentrations as low as 3x10¹⁴ cm⁻³ with a consequent reduction in the acetaldehyde pressure. Figure 2 illustrates the problem and its solution by comparing the longest OH decay that we were able to obtain using N₂O as the O(¹D) source with a good S/N OH decay obtained using O₃ as the source of O(¹D). In order to determine the branching ratio k_{1b}/k₁, it is necessary to extrapolate the OH signal back to time 0. Fig. 2 demonstrates that this is possible in the ozone system. In the N₂O system, the OH signal clearly starts disappearing long before it has completed its rise.

After the initial investment of effort in learning how to handle and dispose of ozone safely, control its flow, and measure its concentration in the photolysis cell, this work is advancing rapidly. We expect to have a reliable value for the branching into reaction channel (1b) within the near future.

FUTURE PLANS

Electronically excited O(¹D) is an extremely reactive reagent that can be used to abstract H from almost any species containing hydrogen. In this regard, it has the advantages of fluorine atoms, but unlike F atoms it has other addition reaction channels providing access to additional species. Furthermore, under our typical conditions, it disappears from the system either by reaction or quenching to O(³P) within a few microseconds. Thus it should be a powerful, flexible reagent for the production of a number of small free radicals. As examples, it is quite possible its reaction with NH₃ may produce NH₂O + H in addition to NH₂ and OH, and its reaction with ethylene may produce CH₂CHO (vinyloxy) and H in addition to OH + C₂H₃ (vinyl). In the case of this last example, we are interested in attempting to determine product branching ratios. We also plan to examine and measure product branching ratios for the reactions of O(¹D) with formaldehyde and acetylene.

Publications

1. "Kinetics of the Reaction of Propargyl Radical with Nitric Oxide," J. D. DeSain, P.Y. Hung, R. I. Thompson, G. P. Glass, G. Scuseria and R. F. Curl, *J. Phys. Chem. A* **104**, 3356-3363 (2000).
2. "Photolysis of ketene at 193 nm and the rate constant for H+HCCO at 297 K," G.P. Glass, S.S. Kumaran, and J.V. Michael, *J. Phys. Chem. A* **104**, 8360-8367 (2000).
3. "The Photolysis of NO₂ at 193 nm," F. Sun, G. P. Glass, and R. F. Curl, *Chem. Phys. Lett.* **337**, 72-78 (2001).
4. "The reaction of NH₂ with NO₂: the reaction of OH with NH₂O," F. Sun, J. D. DeSain, Graham Scott, P.Y. Hung, R. I. Thompson, G. P. Glass, and R. F. Curl, *J. Phys. Chem. A* **105**, 6121-6128 (2001).
5. "High-resolution infrared spectra of jet-cooled allyl radical (CH₂-CH-CH₂): ν_2 , ν_3 , and ν_{14} C-H stretch vibrations," J-X. Han, Yu. Utkin, H-B. Chen, N. T. Hunt, and R. F. Curl, *J. Chem. Phys.* **116**, 6505-6512 (2002).

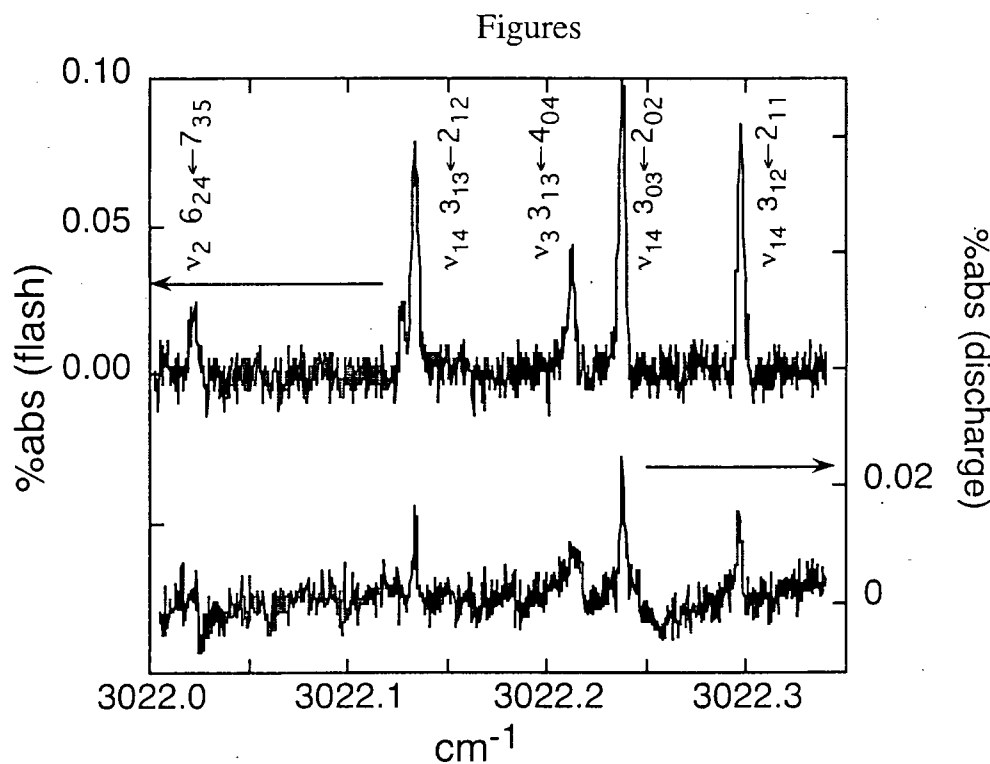


Fig. 1 Allyl CH stretching spectra in a slit jet. Upper trace flash photolysis of 1,5 hexadiene. Lower trace electric discharge modulated at 9.2kHz in allyl bromide.

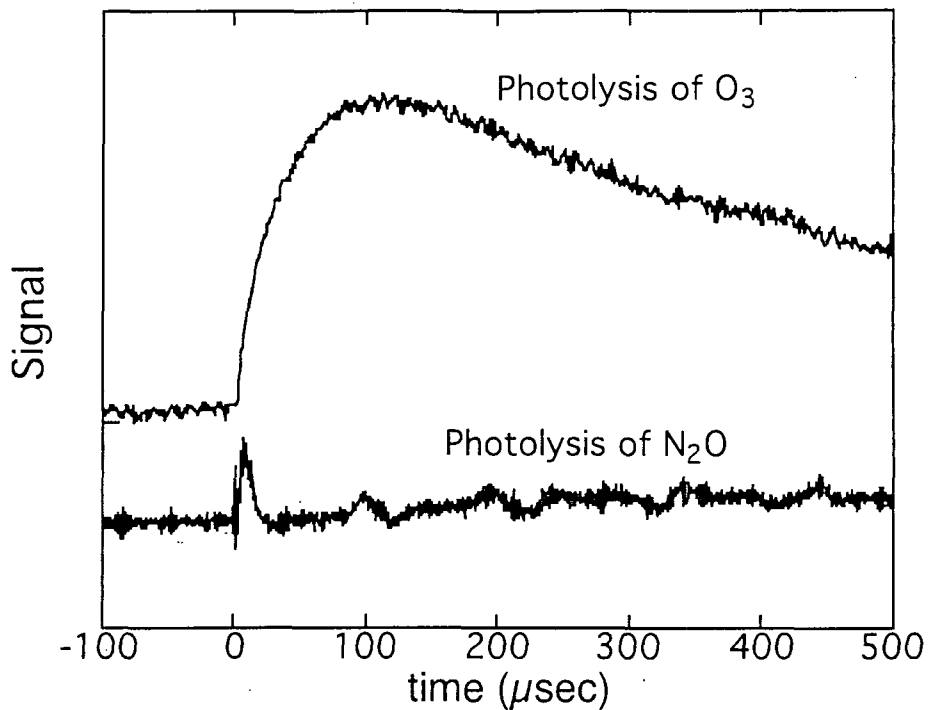


Fig. 2. Comparison of the OH decay rates using photolysis of O₃ at 248 nm as the source of O(¹D) with the best result we could obtain photolyzing N₂O at 193 nm as the O(¹D) source. The two signals are not on the same scale.

Vibrational Spectroscopy and Reactions of Highly Excited Transient Radicals

Hai-Lung Dai,

Department of Chemistry, University of Pennsylvania, Philadelphia, PA 19104-6323;
dai@sas.upenn.edu

I. Summary

Toward characterizing the spectroscopy and structure of unknown transient radicals that are important to energy production and consumption processes, an approach based on nanosecond time resolved Fourier Transform IR Emission Spectroscopy (TR-FTIRES) has been developed for investigating unknown radicals. The transient radical species is produced with high vibrational excitation through UV photolysis of a precursor molecule. The IR emission from the highly excited species through its IR active vibrational modes is detected with fast time resolution using the TR-FTIR technique. Inert gases are used as the ambient background gas for collision relaxation of the excited radical species, so the latter time spectral emission bands correspond to the fundamental transitions and rotational band analysis can reveal the structure of the radical.

To eliminate the possibility that emission bands from other excited product molecules from the photo-dissociation of the precursor, several precursors that may produce the radical as the common product can be used to ensure the correct identification of the radical emission bands. Two-dimension correlation technique can also be applied to reveal the group of emission bands that are from the same emitting species.

As a first demonstration of this approach we have detected all nine vibrational modes of the vinyl radical [J. Chem. Phys., 112, 9209 (2000)], for which only one vibrational mode was previously reported through experimental work. In the following we report the progress made in the past year on a couple of nitrogen containing radicals. These species, cyanovinyl and OCCN, are important to combustion environments where nitrogen is abundant and also to atmospheric chemistry. Their vibrational spectroscopy is experimentally characterized for the first time.

This approach also allows the reactions of the excited radical and the photodissociation reaction of the precursor molecules to be characterized. In the study of the vinyl radical, the dissociation induced by 193 nm photons of vinyl chloride was characterized through analyzing the product energy distribution revealed by the time-resolved IR emission spectra following photodissociation. In particular the dissociation channel resulting in the products of C_2H_2 and HCl are found to be through a three-centered transition state resulting in vinylidene and HCl [J. Chem. Phys., 115, 1734 (2001)]. The photodissociation dynamics of acrylonitrile has also been characterized. It is found that of the four dissociation channels at 193 nm, the one leading to molecular products is also primarily through a four-centered transition state resulting in HNC and

acetylene. All these observations are fundamentally important to the understanding of chemical dynamics as well as the combustion processes.

II. Structure and Vibrational Modes of the Cyanovinyl Radical

The structure and vibrational modes of the cyanovinyl radical have been characterized by using time-resolved Fourier Transform IR Emission Spectroscopy. The cyanovinyl radical was generated with internal excitation through photo-dissociation of acrylonitrile. IR emission, detected with sub-micro second time resolution, from reaction products following photo-dissociation revealed the vibrational modes. The two vibrational modes of the cyanovinyl radical with the strongest transition strength have been identified at their fundamental transition frequencies: the CN stretch mode at 2563 cm^{-1} and the CH_2 out of plane wag at 965 cm^{-1} . The assignments were made based on experiments with deuterated acrylonitrile and *ab initio* calculations. Rotational contour analysis of the CN emission band is consistent with a bent equilibrium structure that becomes more linear with vibrational excitation.

III. The OCCN Radical

The OCCN radical is produced through 193 nm photodissociation of carbonyl cyanide, $\text{CO}(\text{CN})_2$, pivaloyl cyanide, $\text{CO}(\text{CN})(\text{CH}_3)_3$, and methyl cyanofornate, $\text{CO}(\text{CN})(\text{OCH}_3)$. The dissociation reactions leave the radical and other products with sufficient internal excitation. Infrared and near-infrared emissions from all vibrationally excited species are detected by the nanosecond Fourier-transform infrared emission spectroscopy. The time resolved spectra following photodissociation of carbonyl cyanide is shown in Fig. 1. The emission features can be assigned to several species. In addition to frequency and relative intensity, the time dependence of the intensity may also be used for assignment as it indicates if the emitting species is created immediately following the dissociation or is a result of secondary reactions.

Since all three precursor molecules supposedly should all result in OCCN as the only common product in their dissociation, their emission spectra should reveal common features, appear immediately following photodissociation, that can be assigned to OCCN. Fig. 2 shows the emission spectra from the three different precursors. Indeed a strong feature can be identified in all three spectra as the CN stretch of the OCCN radical at 2093 cm^{-1} . This assignment is aided by *ab initio* calculations that show that for this radical the strongest vibrational transition, by more than one order of magnitude in emission intensity, is the CN stretch.

Revealing the weaker emission bands from this radical is much more challenging. A hetero-spectral correlation two-dimensional scheme, designed to correlate the same frequency and intensity time-dependence of the common features, is now being tested to identify these weaker features. Since the frequencies of the features shift with time as the emitting molecules are quenched by ambient gases, the correlation among the spectra from the different precursors, instead of among the emission features themselves, is tested.

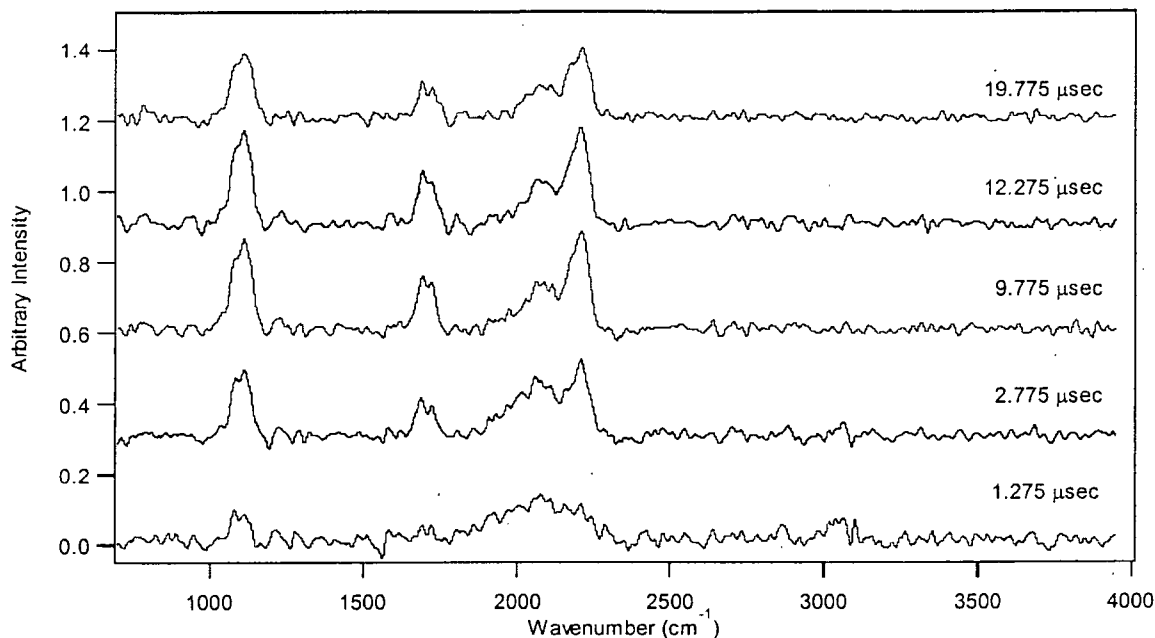


Figure 1: Time resolved emission spectra following the dissociation of carbonyl cyanide, 75 mTorr in a 4-Torr Ar bath, with laser power of 40 mJ/pulse. The feature at 2093 cm^{-1} is present in very early time slices and is a result of primary dissociation while those features at 1105 , 1703 , and 2199 cm^{-1} evolve later in time and are the result of secondary reactions.

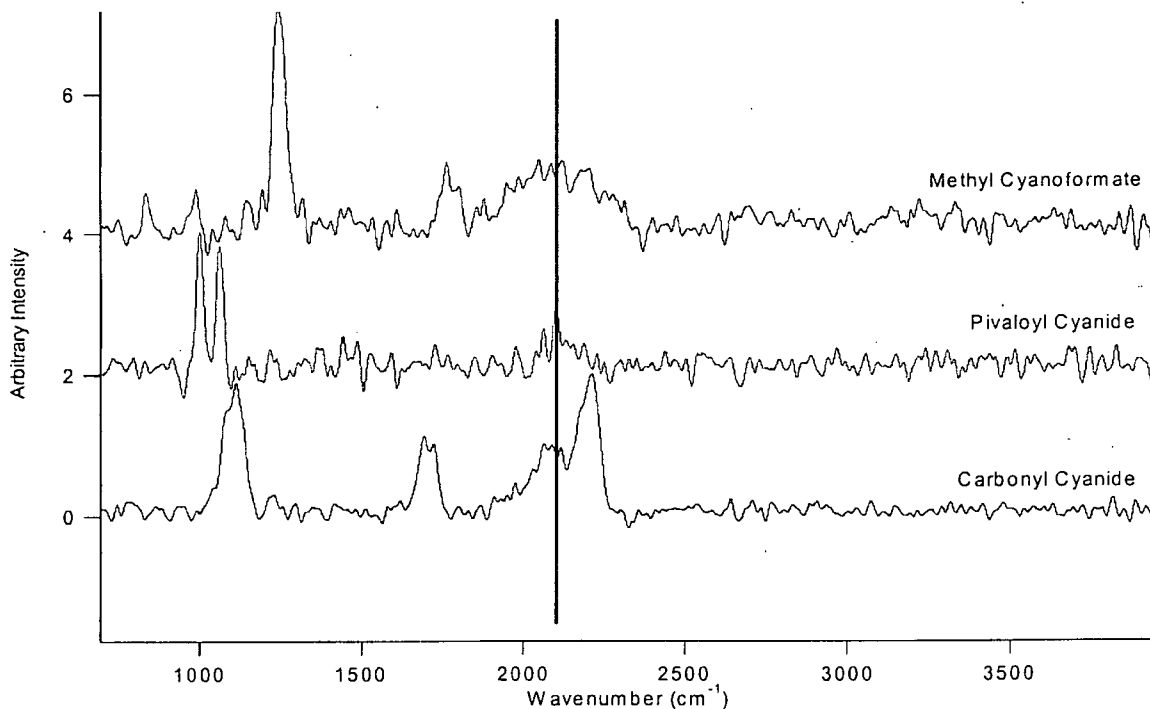


Figure 2: Emission features at $9.8\text{ }\mu\text{sec}$ into the experiment of the three precursors studied: carbonyl cyanide, pivaloyl cyanide and methyl cyanoformate. A common emission feature appears at 2093 cm^{-1} in all three precursors. This feature is assigned to the CN stretch of the OCCN radical.

IV. Photodissociation of Acrylonitrile: Determination of the Transition State Structure

Acrylonitrile, also known as vinyl cyanide, is an important molecule whose photodissociation reaction following UV irradiation has been intensively studied using molecular beam techniques by several laboratories. The TR-FIRES technique in our laboratory can be used to monitor the identity of the dissociation products as well as their internal energy content. The IR emission approach is complementary to the Mass spectrometry detection in molecular beam studies as the latter can discern the atomic make up of the molecule but the former may reveal its structure. Both advantages have proven valuable in the study of this dissociation reaction. Based on molecular beam studies one primary dissociation channel at 193 nm has been found to result in the HCN and acetylene products. Our time-resolved IR emission study shows that the hydrogen cyanide product appears primarily in the HNC isomer form. This finding suggests that the transition state is more likely to be four-centered, which is supported by some recent theoretical calculations

V. Publications since 1999 with support from this grant

Interfacing a Transient Digitizer to a Fourier Transform Spectrometer for Nanosecond Time-Resolved Spectroscopy

Rev. Sci. Instr., 70, 18-22 (1999)

Laura T. Letendre, Hai-Lung Dai, Ian A. McLaren, and Timothy J. Johnson

Structure and Dynamics of Highly Excited Molecules from Time-Resolved FTIR Emission Spectroscopy

Proceedings of the 12th International Conference on FT Spectroscopy, eds. K. Itoh and M. Tasumi (Waseda University Press, Tokyo, Japan, 1999), p. 115-8

L. Letendre, D. K. Liu, C. D. Pibel, J. B. Halpern, and H. L. Dai

Vibrational Spectroscopy of a Transient Species through Time-Resolved Fourier Transform Emission Spectroscopy: The Vinyl Radical

J. Chem. Phys., [communication], 112, 9209-12 (2000)

Laura Letendre, D-K Liu, Charles D. Pibel, Joshua B. Halpern and Hai-Lung Dai

V-V Energy Transfer from Highly Vibrationally Excited Molecules through Transition Dipole Coupling: A Quantitative Test on Energy Transfer from SO₂ to SF₆(3₁)

J. Phys. Chem. A, 104, 10460-3 (2000)

Dong Qin, Gregory V. Hartland and Hai-Lung Dai

Collisional Deactivation of Highly Vibrationally Excited SO₂: A Time Resolved Fourier Transform Emission Spectroscopy Study

Z. Phys. Chem., 214, 1501-19 (2000)

D. Qin, G.V. Hartland, C.L. Chen and H.L. Dai

193. nm Photolysis of Vinyl Bromide: Nascent Product Distribution of the C₂H₃Br → C₂H₂(vinylidene) + HBr Channel

J. Chem. Phys. 115, 1734-41 (2001)

Dean-Kuo Liu, Laura T. Letendre and Hai-Lung Dai

Structure and the CN Stretch Mode of the Cyanovinyl Radical: A Study by Time-Resolved FTIR Emission Spectroscopy

to appear in J. Phys. Chem.

Laura Letendre and Hai-Lung Dai

Bimolecular Dynamics of Combustion Reactions

H. Floyd Davis

Department of Chemistry and Chemical Biology
Baker Laboratory, Cornell University, Ithaca NY 14853-1301
hfd1@cornell.edu

I. Program Scope:

This aim of this project is to better understand the mechanisms and product energy disposal in bimolecular reactions fundamental to combustion chemistry. Using the crossed molecular beams method, a molecular beam containing highly reactive free radicals is crossed at right angles with a second molecular beam. The angular and velocity distributions of the products from single reactive collisions are measured.

II. Recent Progress:

a. Oxygen atom Rydberg Time-of-Flight Spectroscopy.

We have extended the hydrogen atom Rydberg time-of-flight (HRTOF) method, used previously in our laboratory and elsewhere, to the detection of ground state oxygen atoms, $O(^3P_J)$. A particular spin-orbit state of oxygen was "tagged" by a double-resonance two-photon excitation to high- n Rydberg states. By selecting appropriate VUV wavelengths near 130 nm, each of the three $O(^3P_{0,1,2})$ spin orbit levels may be excited to a common $O(^3S_1)$ state. A second photon near 304 nm then pumps the excited atoms to a selected Rydberg level. The Rydberg O atoms fly to a detector where they are field ionized and collected.

We have characterized this method by studying the photodissociation dynamics of NO_2 and ClO_2 in the near ultraviolet. Our studies demonstrated that ORTOF is a general way to accurately measure angular and velocity distributions of individual spin orbit states of oxygen ($J=0,1,2$) from photodissociation or bimolecular reactions. In particular, we have demonstrated that the lifetimes of oxygen Rydberg atoms are long compared to their flight time to the detector (100 μ s).

We have recently set up our crossed beams apparatus to study the bimolecular reaction $H + O_2 \rightarrow OH + O(^3P_J)$. This reaction is very important in combustion processes, and is known to produce OH primarily in $v = 0$ in high rotational levels. By measuring the $O(^3P_J)$ velocity distributions using Rydberg tagging, we expect to learn about the internal distribution of the OH counterfragment as a function of scattering angle. As indicated in Fig. 2, the

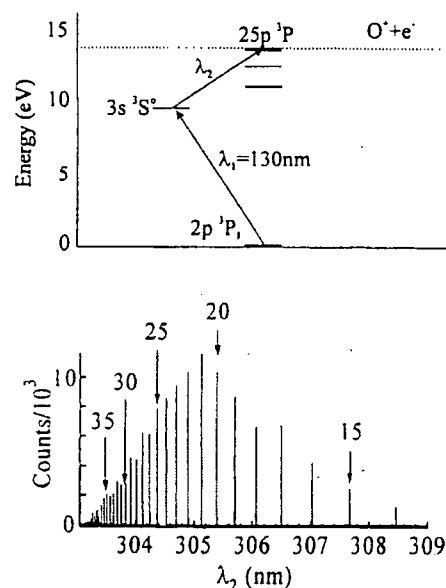


Fig. 1- Top: Oxygen atom Rydberg pumping scheme. Bottom: Rydberg Excitation spectrum obtained by scanning λ_1

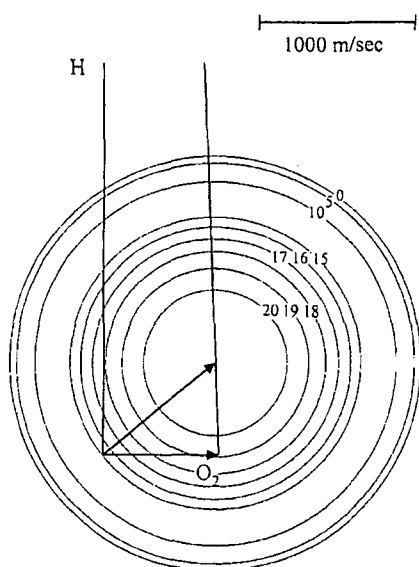


Fig. 2- Newton diagram in velocity space for $\text{H} + \text{O}_2 \rightarrow \text{OH} + \text{O}({}^3\text{P}_2)$ reaction at $E_{\text{coll}} = 1.8$ eV. Circles denote $\text{O}({}^3\text{P}_2)$ velocities for indicated rotational levels of OH ($v=0$)

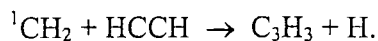
state through collisions, we found that with careful optimization of the nozzle-laser distance, a singlet methylene beam could be produced with sufficient intensity to allow reactive scattering studies. To our knowledge, this is the first time that the reactions of an electronically excited polyatomic radical have been studied in crossed molecular beams.

To characterize our source, we first studied the simplest reaction of singlet methylene:



Although our beam contains ground state triplet methylene, it is unable to react with H_2 . The raw undulator radiation near 10.5 eV was used to ionize the CH_3 products from the above reaction at the detector of endstation 1, a universal crossed molecular beams apparatus. Although the angular and velocity measurements are still under analysis, the data shows that the reaction mechanism primarily involves direct insertion of methylene into hydrogen followed by simple C-H bond fission.

Some preliminary studies of the reaction with acetylene were also performed:



This reaction is believed to be initiated by addition across the triple bond to form cyclopropene, which subsequently undergoes isomerization to propyne and H atom loss producing propargyl + H. Representative time-of-flight spectra for the propargyl radical

spacings between different levels of the OH product are sufficiently large that it may be possible to observe structure corresponding to different OH rotational states.

b. Crossed Beam Reaction Dynamics of Singlet Methylene (${}^1\text{CH}_2$).

In November 2001, and then again in January 2002, the PI spent a total of six weeks at beamline 9.0.2 at the Advanced Light Source, LBNL. In collaboration with Musa Ahmed and coworkers, we characterized and then utilized a pulsed molecular beam source of electronically excited singlet methylene (${}^1\text{CH}_2$) for crossed beam reactive scattering studies. The source, which was first developed and characterized at Cornell using fluorescence excitation spectroscopy, employs photolysis of ketene (CH_2CO) at 308 nm at the orifice of a supersonic nozzle. Although electronically excited singlet methylene is easily quenched to the ground triplet

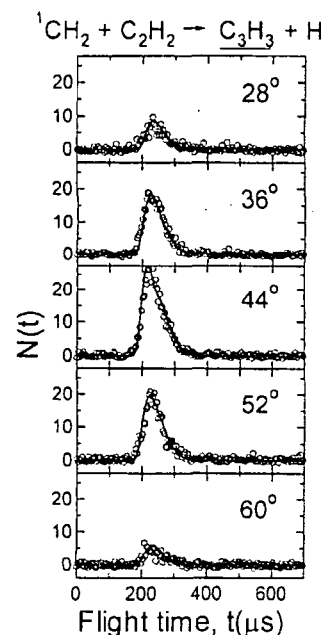


Fig. 3- Time-of-flight spectra of propargyl radical from $\text{CH}_2 + \text{C}_2\text{H}_2$ reaction at indicated laboratory angles.

products are shown in Fig. 3. The circles are the experimental data, and the solid lines are calculated TOF spectra based on the input translational energy $P(E)$ and center of mass angular $T(\Theta)$ distributions shown in Fig. 4. The propargyl radical is believed to be important in soot formation, as it may subsequently dimerize to form benzene or react to form other aromatic molecules.

We believe that with some further optimization of experimental conditions, a number of other interesting reactions involving $^1\text{CH}_2$ and $^1\text{CD}_2$ are feasible. In particular, reaction with H_2O is expected to involve insertion with formation of highly vibrationally excited methanol, which subsequently undergoes several competitive unimolecular decomposition processes such as simple bond fission producing $\text{OH} + \text{CH}_3$, or molecular elimination with formation of $\text{H}_2 + \text{H}_2\text{CO}$ or $\text{H}_2 + \text{HCOH}$.

c. Progress Towards Studies of $\text{OH} + \text{D}_2 (v=1) \rightarrow \text{HOD} + \text{D}$

During the first year of the funding period, we were able to demonstrate mode specific energy disposal in the $\text{OH} + \text{D}_2 \rightarrow \text{HOD} + \text{D}$ reaction (publication 1). In that case, translational energy was employed to surmount the potential energy barrier for reaction. Very recently, a number of groups have done quantum scattering calculations on the reaction $\text{OH} + \text{D}_2 (v=1) \rightarrow \text{HOD} + \text{D}$. An experimental study in which the HOD product vibrational distribution is measured as a function of scattering angle would provide an important test of the PES.

During the past year, we have configured our apparatus to study the title reaction. The D_2 is pumped to $v = 1$ by stimulated Raman pumping using two laser beams (532 nm and 633 nm, produced by Raman shifting in D_2). Although this method has been demonstrated by several groups to be very efficient, we have found that we are unable to pump a sufficient fraction of the D_2 molecules using our existing Nd:YAG laser, due to its broad linewidth (1 cm^{-1}). We have therefore set this project aside for the moment while we explore ways to acquire an injection-seeded Nd:YAG laser in order to complete these experiments.

III. Publications since 2000:

1. Mode Specific Energy Disposal in the 4-atom reaction $\text{OH} + \text{D}_2 \rightarrow \text{HOD} + \text{D}$. B. Strazisar, C. Lin and H.F. Davis, *Science* **290**, 958 (2000).
2. Vibrationally Inelastic Scattering of High-n Rydberg H atoms from N_2 and O_2 . B. Strazisar, C. Lin and H.F. Davis, *Physical Review Letters* **86**, 3997 (2001).

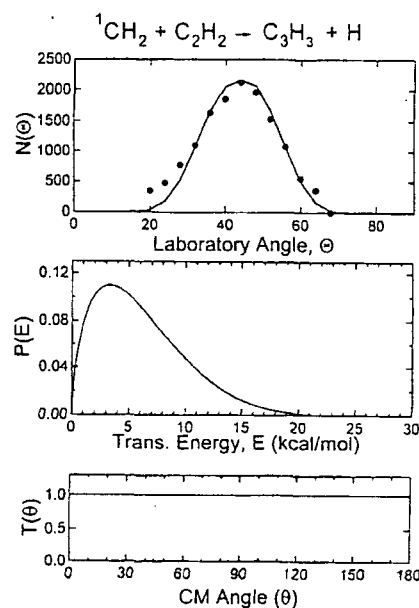


Fig. 4- Top: Laboratory angular distribution for propargyl from $^1\text{CH}_2 + \text{H}_2\text{C}_2$ reaction. Middle and Bottom: Translational energy $P(E)$ and center of mass angular distribution $T(\theta)$ for propargyl + H product channel.

Multiple-time-scale kinetics

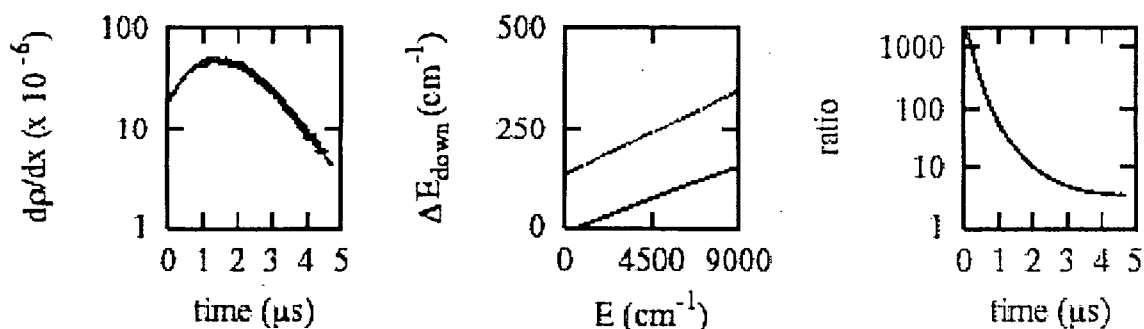
Michael J. Davis

Gas Phase Chemical Dynamics Group, Chemistry Division
Argonne National Laboratory
Argonne, IL 60439
Email: davis@tcg.anl.gov

Research in this program focuses on three interconnected areas. The first involves the study of intramolecular dynamics, particularly of highly excited systems. The second area involves the use of nonlinear dynamics as a tool for the study of molecular dynamics and complex kinetics. The third area is the study of the classical/quantum correspondence for highly excited systems, particularly systems exhibiting classical chaos.

Recent Progress

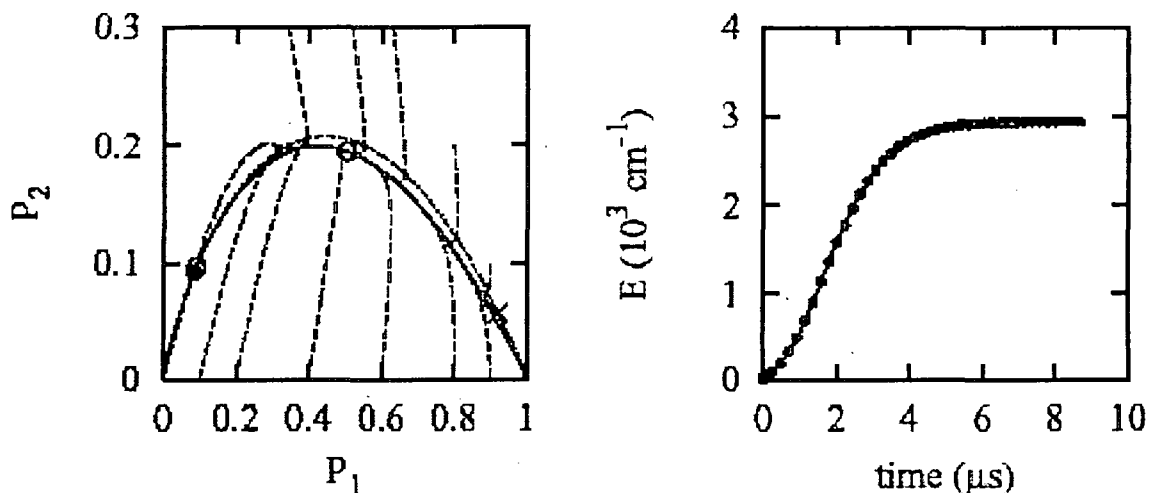
The study of nonlinear master equations relevant to vibrational relaxation and association dynamics has continued. Two projects were completed in the last year in this area. The first is a collaboration with Kiefer to fit results generated by his group, who also attempted to model the results with a linear master equation, which described only collisions with a buffer gas. This modeling was generally unsuccessful and led to the current project. The main type of experimental result is presented as a series of dots in the first panel of the figure, which show a distinct nonlinearity. The purpose of the project was to fit the



experiments with the nonlinear master equation, which is demonstrated to be very good, as shown by the solid line in the first panel. The nonlinearity of the master equation results from the inclusion of self-collisions terms, which in the experiments are oxirane-oxirane collisions, with the oxirane 3.92% dilute in krypton. In addition to self-collisions, the master equation included a temperature variation which results from the cooling of the bath as the vibrations of oxirane heat up. An exponential gap law was used for both self-collisions and buffer gas collisions and ΔE_{down} for both types of collisions was assumed to vary linearly with energy. The parameters in this functional form were

varied to fit the experimental results, as shown by the solid line in the first panel. Two types of results from our study are shown in the last two panels of the figure. It was found that ΔE_{down} (dashed line in the middle panel) was much larger for self-collisions than buffer gas collisions (solid line). Also, the forces for relaxation were generally much larger for self-collisions than buffer gas collisions, with the ratio of the two shown in the final panel. Note that the forces from self-collisions can be orders of magnitude larger than those for buffer gas collisions, despite the dilution of the oxirane.

The dynamics of the master equations were studied further. It was shown (first panel in figure below) that the systems generally possessed attractive one-dimensional manifolds which are analogous to the eigenvectors of a linear master equation. The



one-dimensional manifold is shown as a solid line in the panel. Trajectories (dashed lines) are attracted to it on the way to equilibrium (large solid dot). The experimental initial condition is shown as a large x in the panel, and the experimental observation time (1 – 5 μs) is shown as two open circles, the first being the one on the right. This panel demonstrates that total experimental observation occurs under quasi-steady-state conditions. Because motion is one-dimensional along the manifold it is possible to develop a one-dimensional nonlinear rate law in analogy to the typical one-dimensional linear rate law which is developed for linear master equations along an eigenvector. We found it possible to fit the motion along the one-dimensional manifolds to a Taylor series expansions away from the equilibrium point:

$$\frac{d\Delta E}{dt} = -\sum_i k_i (\Delta E)^i,$$

where ΔE refers to displacement from equilibrium. The dots in the right panel show a fifth order rate law fit, which demonstrates excellent agreement with the simulation, shown as a solid line.

The same sort of analysis can be applied to the nonlinear master equation describing association kinetics. A collaboration with Klippenstein (Sandia) has led to the result shown in the figure below. On the left column are shown a series of one-

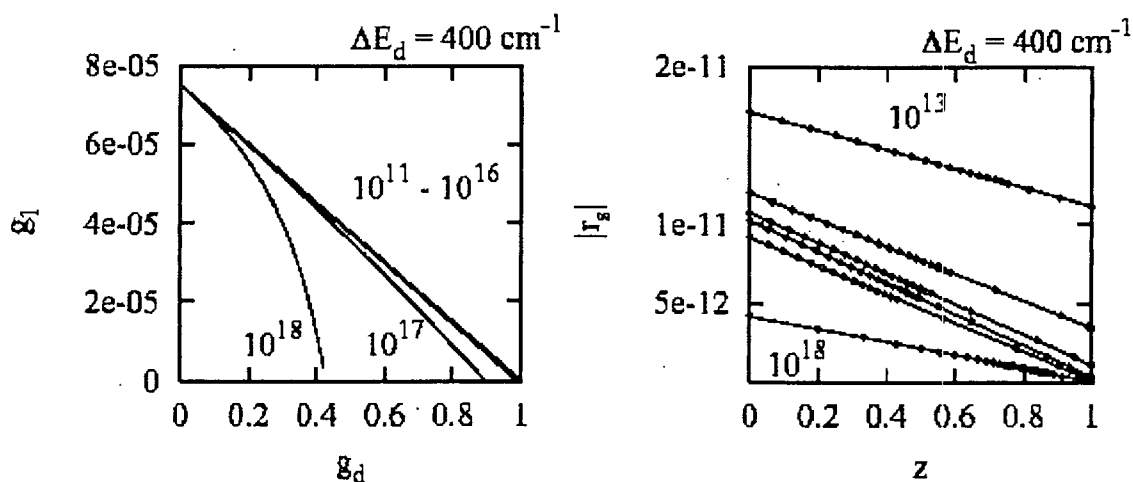
dimensional manifolds for methyl recombination at 1350 K for different dilutions of the reactive species in argon.

In the right panel of the figure is shown a fit of the local rate constant to a second-order rate law:

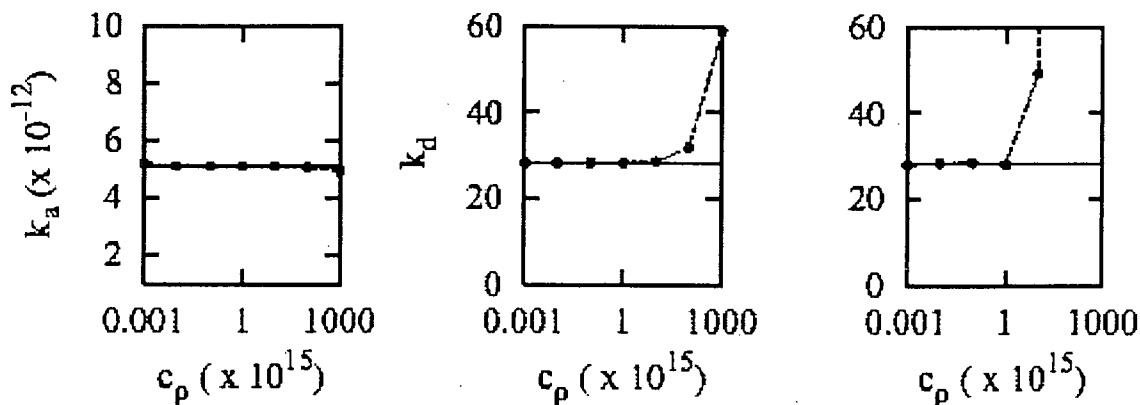
$$\frac{d\rho^{\text{CH}_3}}{dt} = \sum_{n=1} a_n (\rho^{\text{CH}_3} - \rho_{\text{eq}}^{\text{CH}_3})^n$$

$$r_s = \frac{1}{(\rho_{\text{CH}_3} - \rho_{\text{CH}_3}^{\text{eq}})} \frac{d\rho_{\text{CH}_3}}{dt},$$

with z a progress variable along the one-dimensional manifold.



The local rate constant can be fit to a line, resulting in a second-order rate law. This rate law is somewhat different than the typical second-order rate law, because it describes displacements away from equilibrium, but can be compared term by term to the typical second-order rate law, as is done in the figure below. In the leftmost panel the association rate constant is derived (dots) and is compared to the more typical calculation of the association rate constant which is made near equilibrium (solid line). Good agreement is



obtained at a number of dilutions, although there is some discrepancies at higher densities (compare the solid and dashed lines in the first panel). However the dissociation rate constant is not always accurately obtained, as demonstrated in the two panels on the right, where two different ways of generating it are shown. Although there is good agreement for dilute situations, the rate constant differs greatly from the near-equilibrium case at higher densities. This indicates that the notion of an equilibrium constant is breaking down along the one-dimensional manifold away from equilibrium.

In addition to the completed projects, two others have been initiated. The first is a collaboration with Kaper (Boston University) and Kaper (Mathematics and Computer Sciences, ANL) and involves the study of low-dimensional manifolds in reaction-diffusion equations and simple models of flames. A combination of asymptotic analysis and numerical simulations have been undertaken and preliminary results have been generated. A second project with Kellman and Tyng has also been initiated. This involves the assignment of the eigenstates of acetylene in classically chaotic regions of phase space.

Future Plans

Effort in the near term will be two-fold. There will be an increased effort to understand low-dimensional manifolds in systems with transport, including one-dimensional models of flames. There will also be an increased effort in studying the dynamics of nonlinear master equations with multiple wells, including the study of low-dimensional manifolds in these systems and their implications for extracting rate laws. In the longer term there will be an expanded effort in studying the geometry of the phase space of more realistic reactive flow problems.

Publications

M. J. Davis and R. T. Skodje, "Geometric investigation of low-dimensional manifolds in systems approaching equilibrium", *J. Chem. Phys.* **111**, 859 (1999).

M. J. Davis and R. T. Skodje, "Geometric approach to multiple-time-scale kinetics: A nonlinear master equation describing vibration-to-vibration relaxation", *Z. Phys. Chem.* **215**, 233 (2001).

R. T. Skodje and M. J. Davis, "Geometrical simplification of complex kinetic systems", *J. Phys. Chem. A.* **105**, 10356 (2001).

M. J. Davis and J. H. Kiefer, "Modeling of nonlinear vibrational relaxation of large molecules in shock waves with a nonlinear, temperature-varying master equation", *J. Chem. Phys.*, May 2002.

M. J. Davis, "Dynamics of a nonlinear master equation: Low-dimensional manifolds and the nature of vibrational relaxation", *J. Chem. Phys.*, May 2002.

M. J. Davis and S. J. Klippenstein, "Geometric investigation of association/dissociation kinetics with an application to the master equation for $\text{CH}_3 + \text{CH}_3 \leftrightarrow \text{C}_2\text{H}_6$ ", *J. Phys. Chem. A*, June 2002.

COMPREHENSIVE MECHANISMS FOR COMBUSTION CHEMISTRY: EXPERIMENT, MODELING, AND SENSITIVITY ANALYSIS

Frederick L. Dryer

*Department of Mechanical and Aerospace Engineering
Princeton University, Princeton, New Jersey 08544-5263*

fldryer@princeton.edu

Grant No. DE-FG02-86ER-13503

Program Scope

The experimental aspects of our work are conducted in a 10 cm-diameter variable pressure flow reactor (VPFR), at pressures from 0.3 to 20 atm, temperatures from 500 K to 1200 K, and with observed reaction times from 0.5×10^{-2} to 2 seconds. Measurements of stable reactant, intermediate, and product species provide a significantly constrained set of kinetic data for elucidating mechanistic behavior, validating detailed kinetic mechanisms, and extracting specific rate constant information. Continuing efforts of this program are: (1) utilizing the perturbations of the H_2/O_2 and $CO/H_2O/Oxidant$ reaction systems by the addition of small amounts of other species to further clarify elementary reaction properties; (2) further elucidating the reaction mechanisms for the pyrolysis and oxidation of small hydrocarbons (alkanes, olefins) and oxygenates (aldehydes, alcohols, and ethers).

Recent Progress

Recent progress, including selected summaries of published works, those in press, those in review for publication and some of the efforts currently underway, are presented below.

1. T. Carriere, P.R. Westmoreland, A. Kazakov, Y.S. Stein, and F.L. Dryer, "Modeling Ethylene Combustion From Low To High Pressure", 29th Proceedings of the Combustion Institute (to be published)

We have obtained new high-pressure data on ethene oxidation, and in collaboration with the group of Prof. Westmoreland, we have used these data to evaluate the state of several current ethene oxidation models as well as one being collaboratively developed. It was found that using the same reaction set, data from two ethylene-oxygen combustion systems at greatly different pressures could be reproduced satisfactorily. The new data from the VPFR were for the following conditions: temperature (850-950 K), pressure (5-10 atm), equivalence ratio ($\phi=2.5$). The second set of data (Bhargava and Westmoreland, *Combust. Flame* 113:333-347, 1998) were for a low-pressure (20 Torr), laminar premixed fuel-rich flame ($\phi=1.9$).

A key difference between the present mechanism and previous ones lies in the modeling of the complex $C_2H_3+O_2$ reaction. New rate constants were calculated based on recent findings regarding the potential energy surface of this system. In particular, the product set CH_2CHO+O was found to contribute much less than reported in earlier studies, and the $HCO+CH_2O$ channel was preferred at temperatures up to 2300 K. The present reaction set predicted the species profiles in both cases with reasonable accuracy, allowing us to interpret and compare the reaction pathways over a wide range of conditions.

In the low-pressure flame, C_2H_4 is mainly consumed by abstraction, while in the high-pressure system, abstraction (mainly by OH instead of H) competes with H-addition that forms C_2H_5 . In both cases, abstraction forms C_2H_3 that reacts with O_2 to make HCO and CH_2O and eventually CO and CO_2 . However, higher levels of C_2H_5 and HO_2 at the high-pressure, lower-temperature flow reactor condition drive distinct pathway differences. The key role of HO_2 chemistry is particularly emphasized through the reaction CH_2O+HO_2 . Model comparisons support a lower value of the rate constant for this reaction, consistent with that recommended by Hochgreb and Dryer (*Combust. Flame* 91:257-284, 1992).

2. J. Li, A. Kazakov, and F.L. Dryer, "Ethanol Pyrolysis Experiments in a Variable Pressure Flow Reactor", *Int. J. Chem. Kin.* 33:859-867 (2001).

Experimental profiles of stable species concentrations are reported for pyrolysis of ethanol in a variable pressure flow reactor at initial temperatures near 950 K and at constant pressures ranging from 3 to 12 atm. These pyrolysis data represent a unique contribution to the experimental database available for the development of comprehensive ethanol combustion mechanisms, for there are no other data for the pyrolysis at these temperatures. The data are particularly relevant in light of the recent work of Marinov (*Int. J. Chem. Kinet.*, 31:183-220, 1999) which suggests that the decomposition of ethanol into ethylene and water is a major source of ethylene in the oxidation of ethanol at flow reactor conditions. We show in the paper that the existence of this decomposition channel, which produces no radical driven reactions, and its relative rate in comparison to those decomposition channels which lead to further radical destruction of ethanol, result in reaction phenomena that do not permit reaction shifting techniques to be used in comparing flow reactor experimental data with computational results.

In the paper, we present a new technique for comparison of model predictions with experimental observations. Using this new technique, comparison of the experiments with the kinetic model of Marinov shows that the model underestimates the fuel consumption rate and the yields of H_2O and C_2H_4 , the main products of ethanol

decomposition, as well as CH_3HCO and CH_4 , species related to abstraction channels. Analyses also show the importance of H abstraction reactions by CH_3 and H atoms are underestimated at flow reactor conditions. Improvements in both the decomposition kinetics and abstraction channels will be required to develop mechanism improvements. Continuing efforts on the ethanol pyrolysis and oxidation reaction systems are discussed further below.

3. Continuing Work

In addition to the above published works, we have made significant progress on several other topics, briefly discussed below.

- **High Pressure Studies of Formaldehyde Oxidation**

In our earlier study of methyl radical reactions (Scire et al., *Int. J. Chem. Kin.* 33:75-100, 2001), we found that the uncertainty in the rate constant for the reaction



was a major contributor to the uncertainty in the determination of rate constants for the reaction of methyl radicals with HO_2 . Experiments have been conducted on the high-pressure oxidation of formaldehyde at pressures from 1.1 to 12.5 atm, covering a temperature range from 777 to 948 K, in order to determine the rate constant and uncertainty for reaction 1. Formaldehyde was generated through the decomposition of the formaldehyde trimer, 1,3,5-trioxane and delivered to the reactor in a solution with water. As a result of the experimental method, formaldehyde mole fractions up to only 400 ppm and only reaction temperatures greater than 750K could be studied. A global technique (Scire et al., *Int. J. Chem. Kin.* 33:789-802, 2001) was used to establish rigorous parametric uncertainties for the results. In the global parametric calculations, each of the rate constants in the mechanism, excluding the one being determined, was randomized, with the overall rate of the pressure-dependent reactions being randomized as well. It was found during the initial run of sample points, without importance sampling, that the weight function did not play a significant role in defining the uncertainty limits. The effective number of points used in the weight function was therefore set equal to the actual number of data points, and importance sampling was not used. At each of the reaction temperatures studied, at least 4000 points were used in the parametric calculations. For each of the experimental uncertainty calculations, at least 1200 points were used. The rate constant determinations, including their uncertainties are shown in Fig. 1 along with present literature data (Scire, Ph.D. Thesis, 2002). The datum of Baldwin and Walker (*Proc. Combust. Inst.* 17:525-533, 1979) is a factor of 2 lower than that reported by them, based upon a revised rate constant for $\text{HO}_2 + \text{HO}_2 \rightarrow \text{H}_2\text{O}_2 + \text{O}_2$. Most of the literature expressions pass close to their originally reported datum. The new determination at 777 K matches the originally reported datum within uncertainty. Therefore, the new rate constant values also match most of the literature expressions within uncertainty. More importantly, however, the new determination at 948 K, near the lower end of Hochgreb's experimental temperature range, agrees very well with Hochgreb's expression. The only experimental data spanning the temperature range covered by our work is that of Vandanyan and coworkers (*Combust. Flame.* 17:315-322, 1971). Their expression is inconsistent with the new rate constant values. The new data substantially disagree with the corrected value of the Baldwin and Walker recommendation, and the expression of Baulch et al. (*J. Phys. Chem. Ref. Data* 23:847-1033) is also low in comparison to these new measurements. This work is in preparation for publication and further details can be found in the Ph.D. Thesis of Scire (2002).

- **Pyrolysis of Ethanol in the Presence of Toluene**

Ethanol pyrolysis experiments with toluene as a radical trapper have been performed in the VPFR. During pure ethanol pyrolysis, the principal radicals CH_3 , H, and OH produced by ethanol decomposition reactions further react with ethanol via H-abstraction reactions, making it difficult to extract the contributions of the various decomposition channels. In the presence of a radical terminator such as tri-methylbenzene or toluene, the radicals formed in the secondary reactions primarily react with toluene and produce stable species (benzene, ethylbenzene, etc.). Toluene was chosen as the terminating species in the present work because the mutual solubility with ethanol simplifies the experimental aspects of the work and the existence of literature mechanisms for both ethanol and toluene permits numerical assistance in developing the appropriate experiments and in analysis of the resulting data. Using a combined mechanism from those for ethanol (Marinov *Int. J. Chem. Kinet.*, 31:183-220, 1999) and toluene (Emdee *J. Phys. Chem.*, 96:2151-2161, 1992), it appears that at our available experimental conditions, mole fraction ratios of toluene/ethanol greater than about 1 result in significant radical removal, and as a result, between 60-75% of the observed ethanol disappearance is produced by



We performed experiments at 3 atm, 1050 K with 0.12 % ethanol and 0.12 % toluene, and at 1.67 atm, 1068 K with 0.12 % ethanol and 0.12 % toluene. The combined model underestimates the observed ethanol consumption rate and production rates of H_2O and C_2H_4 , the main decomposition products. Experimentally, the yield of H_2O is slightly higher than that of C_2H_4 , apparently due to some H-abstraction reaction from ethanol by residual quantities

of OH. However, the model flux analysis for C₂H₄ production suggests that more than 93 % of C₂H₄ results from the reaction (2). Thus we have estimated the rate for reaction (2) based upon the experimental yield of C₂H₄. The average value over the experimental observation time is about 1.35 s⁻¹ for the experiments at 1050 K, and 2.28 s⁻¹ for the experiments at 1068 K. Figure 2 shows the comparison of experimental decomposition reaction rate with available literature data. The new result is in very close agreement with the RRKM calculations of Tsang (2nd Joint Meeting of the US Sections of the Combustion Institute, Paper 92, Oakland, CA, March 2001) and the expression of Herzler et al. (*J. Phys. Chem.*, 101:5500-5508, 1997) derived from shock tube experiments in which tri-methylbenzene was used as a radical terminator. The reaction rate constants of Marinov and those recently suggested by Park et al. (2001 Eastern States Section Fall Technical Meeting, Hilton Head Island, S.C., December) at these conditions are lower by a factor of 1.7 and 2.7-3.5, respectively.

• High-Pressure Propene Oxidation

A series of experiments on propene oxidation were performed in the Variable Pressure Flow Reactor (VPFR) within the following ranges of conditions: pressures from 3 to 12.5 atm, temperatures from 850 K to 1040 K, and equivalence ratios of $\phi=0.7$, $\phi=1.0$ and $\phi=1.3$. Carbon monoxide, ethene, methane, carbon dioxide, formaldehyde, acetylene, 1-butene, 1,3-butadiene and water were quantitatively detected by FTIR, GC and online analyzers. The comparison of the experimental data with the model of Davis et al. (*Combust. Flame*, 119:375-399, 1999), which was calibrated against the flow reactor data taken at atmospheric conditions, was found to be rather poor. The fuel consumption rate was severely over-predicted by the model. Another model produced recently by the same authors (Qin et al., *Proc. Combust. Inst.*, 28:1663-1669, 2000) yielded a much better agreement with experimental data (Fig. 3). The major species profiles agreed reasonably well. However, the model performance substantially deteriorates for minor species. We have also performed reactivity experiments on propene oxidation at 12.5 atm pressure and stoichiometric condition with a residence time of 1.8 s. Although static reactor experiments (Wilk et al., *Combust. Sci. Technol.*, 52:39-58, 1987; *Combust. Flame* 77:145-170, 1989) and recent numerical modeling work (Heyberger et al., *Combust. Flame* 126:1780-1802, 2001) suggest the existence of a “negative temperature coefficient” (NTC) phenomenon for the reaction between 600 and 800 K, we observe no such behavior. From the recent modeling work of Heyberger et al., it appears that the apparent NTC behavior, if it exists, is mainly due to the reversibility of the addition of molecular oxygen to C₃H₆OH radical. We conclude that either the prior experimental work in static reactors is aberrated by surface effects, or the characteristic reaction times over which this phenomenon becomes important are too long to be of consequence under combustion conditions. Further experiments and modeling on these issues is presently underway.

Plans

Reaction systems of present interest over the coming year, in addition to those discussed above, include the pyrolyses and oxidations of acetaldehyde, methyl formate, dimethoxy methane, and toluene, all over a range of pressures and temperatures.

Publications, 2000 - Present

1. J.J. Scire, “Determination of Elementary Rate Constants by Fitting Complex Reaction Mechanisms: Application to Intermediate-Temperature Hydrocarbon Kinetics”, PhD Thesis, Mechanical and Aerospace Engineering, Princeton University, Princeton, NJ, 2002, MAE 3101-T.
2. T. Carriere, P.R. Westmoreland, A. Kazakov, A., Y.S. Stein, and F.L. Dryer, “Modeling Ethylene Combustion From Low To High Pressure”, 29th International Symposium on Combustion (2002). Accepted for Publication.
3. J. Li, A. Kazakov, and F.L. Dryer, “Ethanol Pyrolysis Experiments in a Variable Pressure Flow Reactor”, *Int. J. Chem. Kin.* 33:859-867 (2001).
4. J.J. Scire, R.A. Yetter, and F.L. Dryer, “Comparison of Global and Local Sensitivity Techniques for Rate Constants Determined Using Complex Reaction Mechanisms”, *Int. J. Chem. Kin.*, 33:780-852 (2001).
5. J.J. Scire, Jr., S. D. Klotz, and F.L. Dryer, “Initial Observations of Ketene in Flow Reactor Kinetic Studies”, *Zeitschrift für Physikalische Chemie*, 215:1011-1023 (2001).
6. J.C. Lee, R.A. Yetter, F.L. Dryer, A.G. Tomboulides, and S.A. Orszag, “Simulation and Analysis of Laminar Flow Reactors”, *Combust. Sci and Tech.*, 159:199-212 (2001).
7. J.J. Scire, Jr., R.A. Yetter, and F.L. Dryer, “Flow Reactor Studies of Methyl Radical Oxidation Reactions in Methane Perturbed Moist Carbon Monoxide Oxidation at High Pressure with Model Sensitivity Analysis”, *Int. J. Chem. Kin.*, 33:75-100 (2000).
8. S.L. Fischer, H.J. Curran and F.L. Dryer, “A Flow Reactor Study of Dimethyl Ether. I: High Temperature Pyrolysis and Oxidation”, *Int. J. Chem. Kin.*, 32:713-740 (2000).
9. H.J. Curran, S.L. Fischer, and F.L. Dryer, “A Flow Reactor Study of Dimethyl Ether. II: Low Temperature Oxidation”, *Int. J. Chem. Kin.*, 32:741-759 (2000).
10. M.A. Mueller, “The Oxidation of Carbon Monoxide/Hydrogen/Oxygen/NO_x/SO_x Mixtures in a High Pressure Flow Reactor”, Ph.D. Thesis, Department of Mechanical and Aerospace Engineering, Princeton University, Princeton, NJ, 2000, MAE 3066-T.
11. M.A. Mueller, J.L. Gatto, T.J. Kim, R.A. Yetter, and F.L. Dryer, “Hydrogen/Nitrogen Dioxide Kinetics: Derived Rate Data for the Reaction H₂+NO₂ = HONO+H at 833 K”, *Combust. Flame*, 120:589-594 (2000).

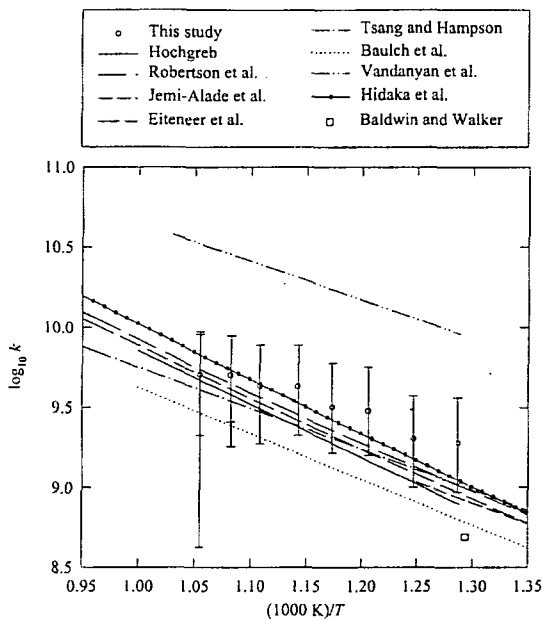


Figure 1 – Comparison of the new rate constant determinations for $\text{CH}_2\text{O} + \text{HO}_2$ with literature recommendations.

Data Sources:

- Hochgreb and Dryer, *Combust. Flame* 91:257-284 (1992)
- Robertson et al. *Elementary Reactions*. In Pilling, M.J. (Ed.), *Low-Temperature Combustion and Autoignition*, Elsevier (1997)
- Jemi-Alade et al., *Chem. Phys. Lett.* 195:25-31 (1992)
- Eiteneer et al., *J. Phys. Chem. A* 102:5196-5205 (1998)
- Tsang and Hampson, *J. Phys. Chem. Ref. Data* 15:1087-1279 (1986)
- Baulch et al., *J. Phys. Chem. Ref. Data* 23:847-1033 (1994)
- Vardanayan et al., *Combust. Flame*: 17:315-322 (1971)
- Hidaka et al., *Combust. Flame* 92:365-376 (1993)
- Baldwin and Walker, *Proc. Combust. Inst.* 17:525-533 (1979)

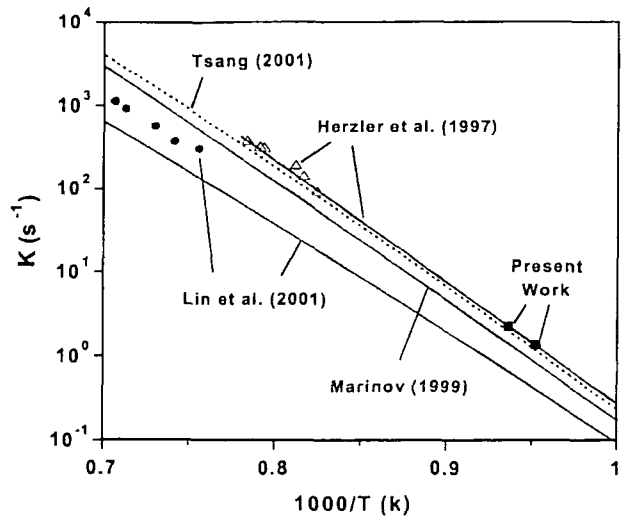


Figure 2 – Rate constant for $\text{C}_2\text{H}_5\text{OH} = \text{C}_2\text{H}_4 + \text{H}_2\text{O}$: RRKM calculations of Tsang (3 atm), Marinov (3 atm), Lin et al (1 atm), and the experimental data of present work (1.67 atm, 3 atm), Herzler et al. (1.5 - 2.0 bar), and Lin et al. (0.57 - 1.02 atm). Symbols - experimental data; lines - RRKM calculations (Tsang, Marinov, Lin et al.) and the fit of Herzler et al. (See text for data references).

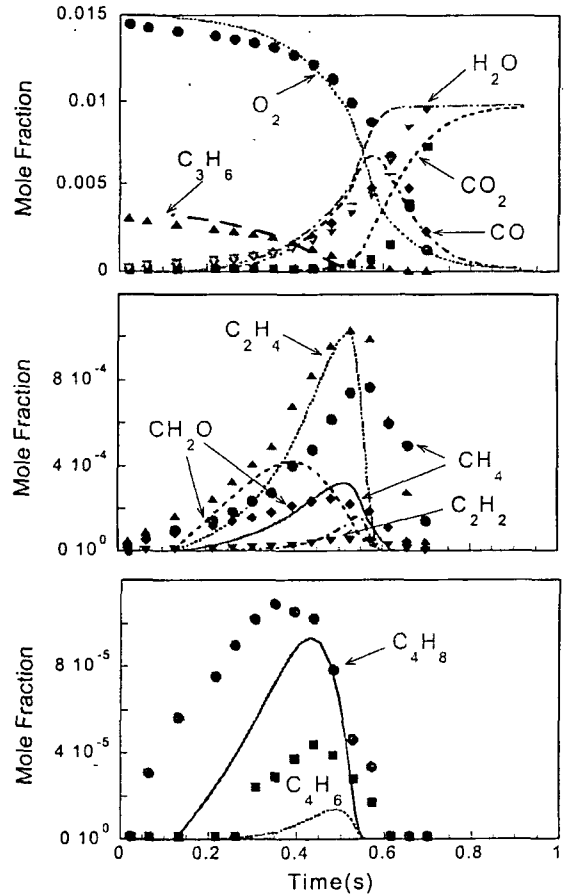


Figure 3 - Comparison of high pressure VPFR C_3H_6 oxidation data ($p=6.0$ atm, $T=1010$ K, $\phi=1.0$) with the predictions of the model of Qin et al. (2000).

LASER PHOTOELECTRON SPECTROSCOPY OF IONS

G. Barney Ellison
Department of Chemistry & Biochemistry
University of Colorado
Boulder, CO 80309-0215
Email: barney@JILA.colorado.edu

1. Methylperoxyl Radical, CH₃OO.

In addition to our earlier photodetachment spectra of the CH₃OO⁻ ion [J. Am. Chem. Soc., **123**, 9585-9596 (2001)], we have studied the matrix infrared spectroscopy of the methylperoxyl radical. We have used a tandem pair of supersonic nozzles to produce clean samples of CH₃OO radicals in cryogenic matrices. One hyperthermal nozzle decomposes azomethane (CH₃NNCH₃) to generate intense pulses of CH₃ radicals while the second nozzle alternately fires a burst of O₂/Ar at the 20 K matrix. The CH₃/O₂/20 K Argon radical-sandwich reacts to produce target methylperoxyl radicals: CH₃ + O₂ → CH₃OO. The absorption spectra of the radicals are monitored with a Fourier Transform infrared spectrometer. We report 10 of the 12 fundamental infrared bands of the methylperoxyl radical CH₃OO, \bar{X}^2A'' , in an argon matrix at 20 K. The experimental frequencies (cm⁻¹) and polarizations follow; the a' modes are 3032, 2957, 1448, 1410, 1180, 1109, 902, 492 while the a'' modes are 3024 and 1434. We can not detect the asymmetric CH₃ rocking mode, ν_{11} , nor the torsion, ν_{12} . The infrared spectra of CH₃¹⁸O¹⁸O, ¹³CH₃OO, and CD₃OO have been measured as well in order to determine the isotopic shifts. The experimental frequencies, { ν }, for the methylperoxyl radicals are compared to harmonic frequencies, { ω }, resulting from a UB3LYP/6-311G(d,p) electronic structure calculation. Linear dichroism spectra were measured with photo-oriented radical samples in order to establish the experimental polarizations of most vibrational bands. The methylperoxyl radical matrix frequencies listed above are within $\pm 2\%$ of the gas phase vibrational frequencies. A final set of vibrational frequencies for the CH₃OO radical are recommended.

2. Hydroperoxyl Radical, HOO

Ruscic *et al.* recently reported that the heat of formation of hydroxyl radical is revised from the longstanding value of $\Delta_f H_0(\text{OH}) = 9.35 \pm 0.05$ kcal mol⁻¹ and $\Delta_f H_{298}(\text{OH}) = 9.40 \pm 0.05$ kcal mol⁻¹ down to $\Delta_f H_0(\text{OH}) = 8.86 \pm 0.07$ kcal mol⁻¹ and $\Delta_f H_{298}(\text{OH}) = 8.92 \pm$

0.07 kcal mol⁻¹. [*J. Phys. Chem. A* **2001**, *105*, 1] The thermochemistry of many radicals has been measured by chemical cycles that involve OH. An example is the hydroperoxyl radical which has been studied by C.J. Howard [*J. Am. Chem. Soc.* **1980**, *102*, 6937; *J. Chem. Phys.* **1984**, *81*, 4458.]



From eqs 1 and 2 it is clear that a revision of $\Delta_f H_{298}(\text{OH})$ has implications for the heat of formation of hydroperoxyl radical.

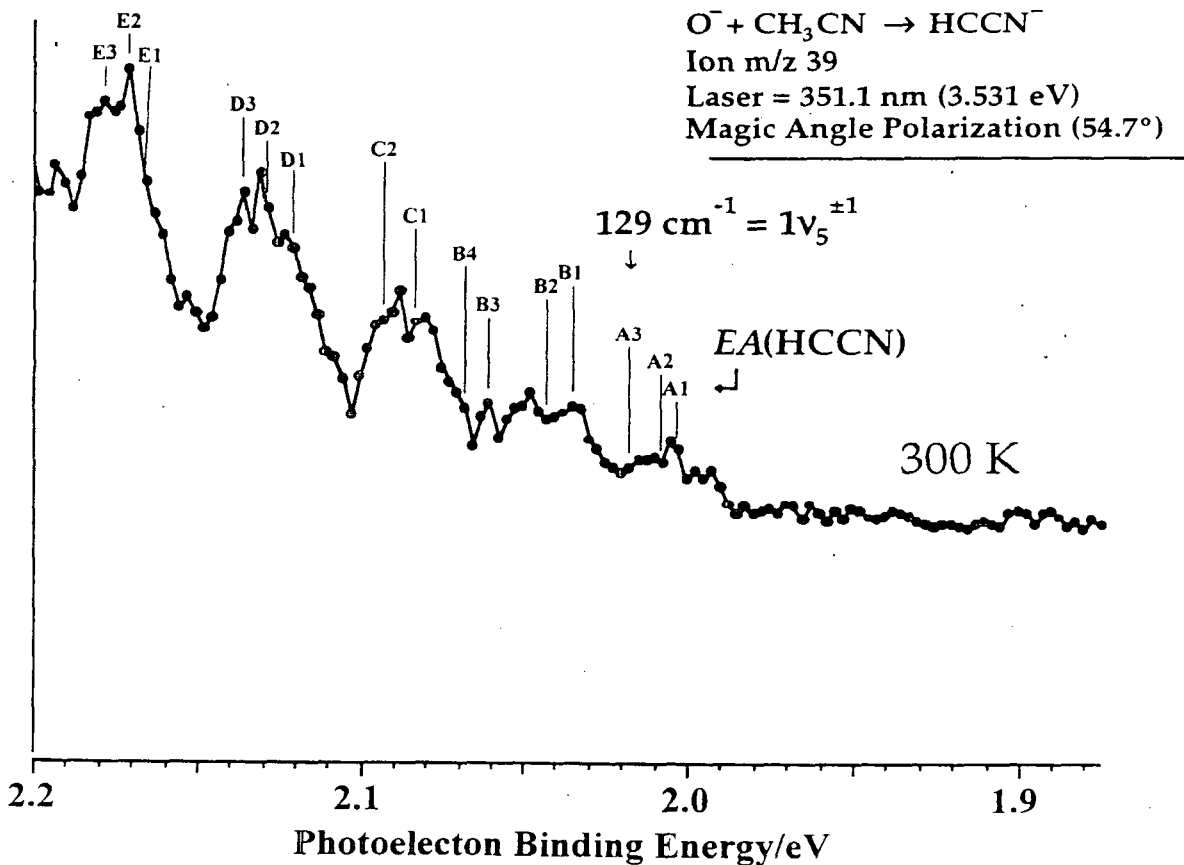
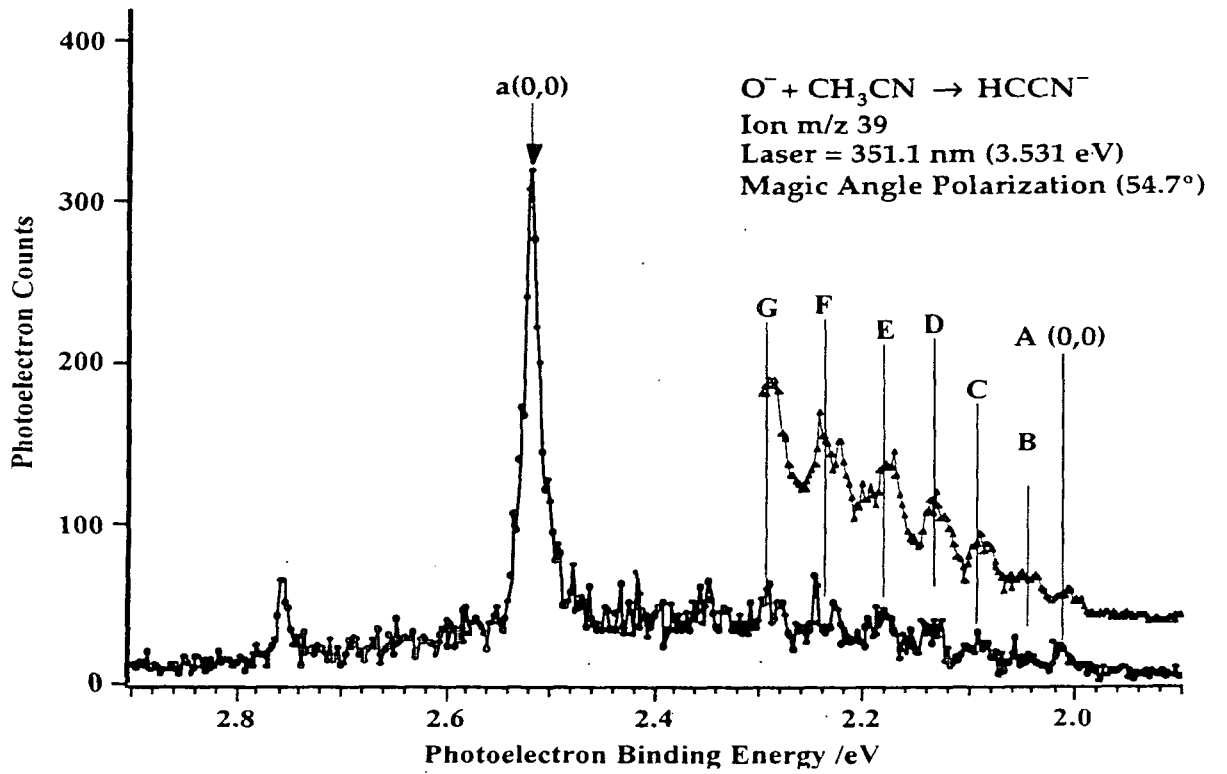
We present a determination of $\Delta_f H_{298}(\text{HOO})$ based upon a negative ion thermodynamic cycle. The photoelectron spectra of HOO^- and DOO^- were used to measure the molecular electron affinities (EAs). In a separate experiment a tandem flowing afterglow-selected ion flow tube (FA-SIFT) was used to measure the forward and reverse rate constants for $\text{HOO}^- + \text{HC}\equiv\text{CH} \rightleftharpoons \text{HOOH} + \text{HC}\equiv\text{C}^-$ at 298 K, which gave a value for $\Delta_{\text{acid}} H_{298}(\text{HOO-H})$. The experiments yield the following values: $EA(\text{HOO}) = 1.078 \pm 0.006$ eV; $T_0(X \text{ HOO} - \bar{A} \text{ HOO}) = 0.872 \pm 0.007$ eV; $EA(\text{DOO}) = 1.077 \pm 0.005$ eV; $T_0(X \text{ DOO} - \bar{A} \text{ DOO}) = 0.874 \pm 0.007$ eV; $\Delta_{\text{acid}} G_{298}(\text{HOO-H}) = 369.5 \pm 0.4$ kcal mol⁻¹; and $\Delta_{\text{acid}} H_{298}(\text{HOO-H}) = 376.5 \pm 0.4$ kcal mol⁻¹. The acidity/EA thermochemical cycle yields values for the bond enthalpies $DH_{298}(\text{HOO-H}) = 87.8 \pm 0.5$ kcal mol⁻¹ and $D_0(\text{HOO-H}) = 86.6 \pm 0.5$ kcal mol⁻¹. We recommend the following values for the heats of formation of the hydroperoxyl radical: $\Delta_f H_{298}(\text{HOO}) = 3.2 \pm 0.5$ kcal mol⁻¹ and $\Delta_f H_0(\text{HOO}) = 3.9 \pm 0.5$ kcal mol⁻¹; we recommend that these values supercede those listed in the current NIST-JANAF thermochemical tables.

The "acidity/EA" value for the heat of formation of the hydroperoxyl radical is in reasonable agreement with the value recommended in the review article of Shum and Benson, $\Delta_f H_{298}(\text{HOO}) = 3.5_{-0.5}^{+1.0}$ kcal mol⁻¹ and with the value derived by Fisher and Armentrout, $\Delta_f H_{298}(\text{HOO}) = 3.8 \pm 1.2$ kcal mol⁻¹. Our new heat of formation falls within the stated uncertainty of the $\Delta_f H_{298}(\text{HOO}) = 2.8 \pm 0.5$ kcal mol⁻¹ value recommended by Howard and co-workers, and also overlaps with the number chosen for the most recent Gurvich thermochemical tables, which was based on Howard's experiments. The Litorja and Ruscic measurement [*J. Electron Spectrosc. Relat. Phenom.* **1998**, *97*, 131] of the

bond dissociation energy, $D_0(\text{HOO-H}) = 86.7 \pm 0.8 \text{ kcal mol}^{-1}$, is in excellent agreement with our value. Since our "acidity/EA" bond energy of HOOH is so close to the "positive ion" PIMS value, the PIMS extracted heats of formation of the hydroperoxyl radical, $\Delta_f H_0(\text{HOO}) = 4.0 \pm 0.8 \text{ kcal mol}^{-1}$ and $\Delta_f H_{298}(\text{HOO}) = 3.3 \pm 0.8 \text{ kcal mol}^{-1}$, also agrees closely with our values.

2. Cyanocarbene and isocyanocarbene, HCCN and HCNC

Negative ion photoelectron spectroscopy has been used to study the HCCN⁻ and HCNC⁻ ions. The electron affinities of cyanocarbene have been measured to be $EA(\text{HCCN } \tilde{X}^3\Sigma^-) = 2.003 \pm 0.014 \text{ eV}$ and $EA(\text{DCCN } \tilde{X}^3\Sigma^-) = 2.009 \pm 0.020 \text{ eV}$. Photodetachment of HCCN⁻ shows a 0.4 eV long vibrational progression in ν_5 , the H-CCN bending mode; the HCCN⁻ photoelectron spectra reveal excitations up to 10 quanta in ν_5 . The term energies for the excited singlet state are found to be $T_0(\text{HCCN } \bar{a}^1A') = 0.515 \pm 0.016 \text{ eV}$ and $T_0(\text{DCCN } \bar{a}^1A') = 0.518 \pm 0.027 \text{ eV}$. For the isocyanocarbene, the two lowest states switch and HCNC has a singlet ground state and an excited triplet state. The electron affinities are $EA(\text{HCNC } \tilde{X}^1A') = 1.883 \pm 0.013 \text{ eV}$ and $EA(\tilde{X}^1A' \text{ DCNC}) = 1.877 \pm 0.010 \text{ eV}$. The term energy for the excited triplet state is $T_0(\text{HCNC } \bar{a}^3A'') = 0.050 \pm 0.028 \text{ eV}$ and $T_0(\text{DCNC } \bar{a}^3A'') = 0.063 \pm 0.030 \text{ eV}$. Proton transfer kinetics in a flowing afterglow apparatus were used to re-measure the enthalpy of deprotonation of CH₃NC to be $\Delta_{\text{acid}} H_{298}(\text{CH}_3\text{NC}) = 383.6 \pm 0.6 \text{ kcal mol}^{-1}$. The acidity/EA thermodynamic cycle was used to deduce $D_0(\text{H-CHCN}) = 104 \pm 2 \text{ kcal mol}^{-1}$ [$\Delta_f H_0(\text{HCCN}) = 110 \pm 4 \text{ kcal mol}^{-1}$] and $D_0(\text{H-CHNC}) = 106 \pm 4 \text{ kcal mol}^{-1}$ [$\Delta_f H_0(\text{HCNC}) = 133 \pm 5 \text{ kcal mol}^{-1}$]. The top Fig. is the photoelectron spectrum of HCCN⁻ where the ion is produced in a flowing afterglow source. The black connected dots (•) show the spectrum collected with liquid nitrogen cooling of the source, while the triangulated (♦) spectrum was collected without cooling. Peaks A to G arise from excitation into the ³HCCN while peak a arises from excitation into ¹HCCN. The bottom Fig. is an expanded view of the origin of the photoelectron spectrum of HCCN⁻. Semi-rigid bender (from Prof. R.F. Curl) energies for calculated transitions are shown with arrows and identities of these are shown in Table 1; the H-CCN bending fundamental, $1\nu_5^{\pm 1} = 128.9079687(40) \text{ cm}^{-1}$, reported by Allen *et al* is marked.



DOE Publications

- Carl R. Kemnitz, G. Barney Ellison, William L. Karney, and Weston Thatcher Borden, "CASSCF and CASPT2 *Ab Initio* Electronic Structure Calculations Find Singlet Methylnitrene Is an Energy Minimum", *J. Am. Chem. Soc.* **122**, 1098-1101 (2000).
- Jonathan C. Rienstra-Kiracofe, G. Barney Ellison, Brian C. Hoffman, and Henry F. Schaefer III, "The Electron Affinities of C₃O and C₄O," *J. Phys. Chem. A* **104**, 2273-2280 (2000).
- A. V. Friderichsen, E-J. Shin, R. J. Evans, M. R. Nimlos, D. C. Dayton, and G. B. Ellison, *Fuel*, **80**, 1747-1755 (2001).
- A. V. Friderichsen, J. G. Radziszewski, M. R. Nimlos, P. R. Winter, D. C. Dayton, D. E. David and G. B. Ellison, "The Infrared Spectrum of the Matrix-Isolated Phenyl Radical", *J. Am. Chem. Soc.*, **123**, 1977-1988 (2001).
- S. J. Blanksby, T. M. Ramond, G. E. Davico, M. R. Nimlos, S. Kato, V. M. Bierbaum, W. C. Lineberger, G. B. Ellison and M. Okumura, "Negative Ion Photoelectron Spectroscopy, Gas Phase Acidity, and Thermochemistry of the Peroxyl Radicals CH₃OO and CH₃CH₂OO", *J. Am. Chem. Soc.*, **123**, 9585-9596 (2001).
- S. Nandi, P. A. Arnold, B. K. Carpenter, M. R. Nimlos, D. C. Dayton and G. B. Ellison, "Polarized Infrared Absorption Spectrum of Matrix-Isolated Allyl Radicals", *J. Phys. Chem. A*, **105**, 7514-7524 (2001).
- J. C. Rienstra-Kiracofe, G. S. Tschumper, H. F. Schaefer III, S. Nandi and G. B. Ellison, "Atomic and Molecular Electron Affinities: Photoelectron Experiments and Theoretical Computations," *Chem. Revs.*, **102**, 231-282 (2002).
- S. Nandi, S. R. Blanksby, X. Zhang, M. R. Nimlos, D. R. Dayton and G. B. Ellison, "Polarized Infrared Absorption Spectra of Matrix-Isolated Methylperoxyl Radicals, CH₃OO \tilde{X}^2A'' ", *J. Phys. Chem. A*, (in press, 2002).
- T. M. Ramond, S. J. Blanksby, S. Kato, V. M. Bierbaum, G. E. Davico, R. L. Schwartz, W. C. Lineberger and G. B. Ellison, "The Heat of Formation of the Hydroperoxyl Radical HOO *via* Negative Ions", *J. Phys. Chem. A*, (in press, 2002).

Thermochemistry of Hydrocarbon Radicals: Guided Ion Beam Studies

Kent M. Ervin
Department of Chemistry/216
University of Nevada, Reno
Reno, Nevada 89557
Telephone: 775-784-6676
E-mail: ervin@chem.unr.edu

Project Scope

Gas phase negative ion chemistry methods are employed to determine enthalpies of formation of hydrocarbon radicals that are important in combustion processes and to investigate the dynamics of ion–molecule reactions. Using guided ion beam tandem mass spectrometry, we measure collisional threshold energies of endoergic proton transfer and hydrogen atom transfer reactions of hydrocarbon molecules with negative reagent ions. The measured reaction threshold energies for proton transfer yield the relative gas phase acidities. In an alternative methodology, competitive collision-induced dissociation of proton-bound ion–molecule complexes provides accurate gas phase acidities relative to a reference acid. Combined with the electron affinity of the R· radical, the gas phase acidity yields the RH bond dissociation energy of the corresponding neutral molecule, or equivalently the enthalpy of formation of the R· organic radical. The threshold energy for hydrogen abstraction from a hydrocarbon molecule yields its hydrogen atom affinity relative to the reagent anion, providing the RH bond dissociation energy directly. Electronic structure calculations are used to evaluate the possibility of potential energy barriers or dynamical constrictions along the reaction path, and as input for RRKM and phase space theory calculations.

Recent Progress

Polyynyl radical thermochemistry

We have completed experimental work on competitive threshold collision-induced dissociation of proton-bound complex anions containing $C_{2n}H^-$ species ($n = 1-4$).¹ Modeling the energy-dependent product branching ratios using RRKM theory yields the gas phase acidities of the polyynes, $HC_{2n}H$, which can be combined with known electron affinities to obtain the CH bond dissociation energies. Initial results on 1,3-butadiyne (diacetylene) have been published.² Rigorous analysis of the data for the larger species requires additional ab initio calculations on transition states and a major revision of our RRKM modeling code to handle decomposition on multi-well potentials. This work is continuing.

Improved gas-phase acidity scale

Combining experimental and theoretical results, we have evaluated and compiled gas phase acidities for a set of reference species to anchor gas phase acidity measurements at 0 K.³ The high-precision experimental results include recent revisions of benchmark thermochemical values in the literature (e.g., $D(\text{HO-H})^4$) and new threshold ion-pair production spectroscopy measurements.⁵ An investigation of theoretical calculations of the acidities at 0 K demonstrates excellent performance at the CCSD(T)/aug-cc-pVTZ//B3LYP/aug-cc-pVTZ level for 16 benchmark acids composed of elements through chlorine, with a mean error of -0.2 kJ/mol and a mean absolute error of 1.5 kJ/mol. The improved acidity scale can be employed to reevaluate experimental relative acidities for systems we and others have measured by gas-phase ion chemistry methods. For example, improved acidities for small alkanols (methyl to tert-butyl alcohol) from our laboratory^{3,6} combined with recent measurements of the alkoxy radical electron affinities⁷ yield their O-H bond dissociation energies within 3 kJ/mol.

Polycyclic aromatic hydrocarbons

In a step toward our goal of obtaining experimental C-H bond dissociation energies for polycyclic aromatic hydrocarbons (PAHs), we collaborated with the Lineberger group at the University of Colorado to measure the electron affinity of naphthyl radical.⁸ This project included a major upgrade of data analysis software for Franck-Condon fits to negative ion photoelectron spectra. Preliminary photoelectron spectra were also obtained for coronene and coronene- C_2H_2 anions. These experiments to obtain electron affinities complement measurements of gas phase acidities in our laboratory.

Application of statistical rate theory to the kinetic method

As a side project, we have used RRKM theory to model the “kinetic method”, which is a unimolecular dissociation product branching ratio measurement widely used by mass spectrometry groups to measure relative ion affinities.^{2,9} This work takes advantage of code in software we have developed for modeling our threshold collision-induced dissociation experiments.^{6,10} The theoretical basis for the thermochemical correlations used in the kinetic method has sometimes been misinterpreted in the literature; our numerical simulations provide guidance for mass spectrometrists using the method.

Product kinetic energy release distributions

We have recently modified our guided ion beam tandem mass spectrometer for measurements of the kinetic energies of products of activated ion-molecule reactions. The octopole beam guide has been split into two sections, with a reaction cell in the first section and a time-of-flight region in the second longer section. The ion beam is pulsed by a set of deflectors following the first mass spectrometer. The times-of-flights of reactant and product ions are measured and converted into product velocities or kinetic energies in the center-of-mass frame. Our first kinetic energy release measurements have been performed on the $\text{Cl}^- + \text{CH}_3\text{Br}$ reaction,¹¹ chosen as an initial system for testing the apparatus because of previous measurements on kinetic energy release distributions in the decomposition of metastable

Cl⁻(CH₃Br) complex anions.¹² We found a remarkable variation in the product velocity distributions with collision energy for the ClCH₃ + Br⁻ product channel. At the lowest collision energies (near thermal), the product velocities have an isotropic, statistical distribution (matching phase space theory) implying mediation via the ion–molecule complex. At intermediate energies, ClCH₃ is forward scattered, consistent with a more direct reaction mechanism. At high energies, there is strong backward scattering, which may be due to an impulsive rebound mechanism.

Future Directions

Our new experimental capability to distinguish reaction mechanisms via product energy distributions will enhance our understanding of proton transfer and hydrogen atom transfer reactions related to combustion chemistry. We further plan to use the energy release distributions for thermochemical measurements; as an adjunct to reaction threshold energy measurements. By fixing the reactant collision energy and measuring the product energies, we can use energy balance to determine reaction enthalpies (either directly from the maximum kinetic energy release or via models of the dynamics). This method should be useful for systems where we have previously found collision energy barriers in excess of the reaction endothermicity. For example, the hydrogen transfer reaction S⁻ + RH → SH⁻ + R with RH = H₂ gave a threshold energy precisely equal to the known reaction endothermicity,¹³ but when we tried the reaction with simple hydrocarbons (RH = CH₄, C₂H₆, C₂H₄, C₆H₆) we found significant barriers in excess of the endothermicities, preventing thermochemical determinations of Δ_rH(R).¹⁴ That behavior is contrary to the “typical” behavior that ion–molecule reactions have zero activation energies in excess of the endothermicities, except for specific situations such as a change of spin state along the reaction coordinate. We will examine these hydrogen transfer reactions with S⁻ both experimentally and theoretically to discover the dynamic or energetic reasons for the excess barriers and to develop the kinetic energy release method for thermochemical measurements.

References

- (1) Shi, Y.; Ervin, K. M. (to be published).
- (2) Ervin, K. M. *Int. J. Mass Spectrom.* **2000**, *195/196*, 271.
- (3) DeTuri, V. F.; Ervin, K. M. *J. Phys. Chem. A* (submitted).
- (4) Ruscic, B.; Feller, D.; Dixon, D. A.; Peterson, K. A.; Harding, L. B.; Asher, R. L.; Wagner, A. F. *J. Phys. Chem. A* **2001**, *105*, 1.
- (5) Martin, J. D. D.; Hepburn, J. W. *J. Chem. Phys.* **1998**, *109*, 8139.
- (6) DeTuri, V. F.; Ervin, K. M. *J. Phys. Chem. A* **1999**, *103*, 6911.
- (7) Ramond, T. M.; Davico, G. E.; Schwartz, R. L.; Lineberger, W. C. *J. Chem. Phys.* **2000**, *112*, 1158.
- (8) Ervin, K. M.; Ramond, T. M.; Davico, G. E.; Schwartz, R. L.; Casey, S. M.; Lineberger, W. C. *J. Phys. Chem. A* **2001**, *105*, 10822.
- (9) Ervin, K. M. *J. Am. Soc. Mass Spectrom.* **2002**, *13*, 435.
- (10) Rodgers, M. T.; Ervin, K. M.; Armentrout, P. B. *J. Chem. Phys.* **1997**, *106*, 4499.
- (11) Angel, L. A.; Ervin, K. M. (to be published).

- (12) Graul, S. T.; Bowers, M. T. *J. Am. Chem. Soc.* **1994**, *116*, 3875.
- (13) Rempala, K.; Ervin, K. M. *J. Chem. Phys.* **2000**, *112*, 4579.
- (14) Rempala, K.; Ervin, K. M. (unpublished).

Publications, 2000–present

“Gas phase acidity and C–H bond energy of diacetylene”, Y. Shi and K. M. Ervin, *Chem. Phys. Lett.* **318**, 149-154 (2000).

“Microcanonical analysis of the kinetic method. The meaning of the ‘effective temperature’”, K. M. Ervin, *Int. J. Mass Spectrom.* **195/196**, 271-284 (2000).

“Collisional activation of the endoergic hydrogen atom transfer reaction $S^-(^2P) + H_2 \rightarrow SH^- + H$ ”, K. Rempala and K. M. Ervin, *J. Chem. Phys.* **112**, 4579-4590 (2000).

“Experimental techniques in gas phase ion thermochemistry”, K. M. Ervin, *Chem. Rev.* **101**, 391-444 (2001). Erratum, *ibid.* **102**, 855 (2002).

“Dynamics of the gas-phase reactions of fluoride ions with chloromethane”, L. A. Angel and K. M. Ervin, *J. Phys. Chem. A*, **105**, 4042-4051 (2001).

“Naphthyl radical: Negative ion photoelectron spectroscopy, Franck-Condon simulation, and thermochemistry”, K. M. Ervin, T. M. Ramond, G. E. Davico, R. L. Schwartz, S. M. Casey, W. C. Lineberger, *J. Phys. Chem. A*, **105**, 10822-10831 (2001).

“Dynamics of the gas-phase reactions of chloride ions with fluoromethane”, L. A. Angel, S. P. Garcia, and K. M. Ervin, *J. Am. Chem. Soc.* **124**, 336-345 (2002).

“Microcanonical analysis of the kinetic method. The meaning of the ‘apparent entropy’”, K. M. Ervin, *J. Am. Soc. Mass Spectrom.* **13**, 435-452 (2002).

Low Energy Ion-Molecule Reactions: Gases and Interfaces

James M. Farrar
Department of Chemistry
University of Rochester
Rochester, NY 14627
E-mail: farrar@chem.rochester.edu

Program Scope

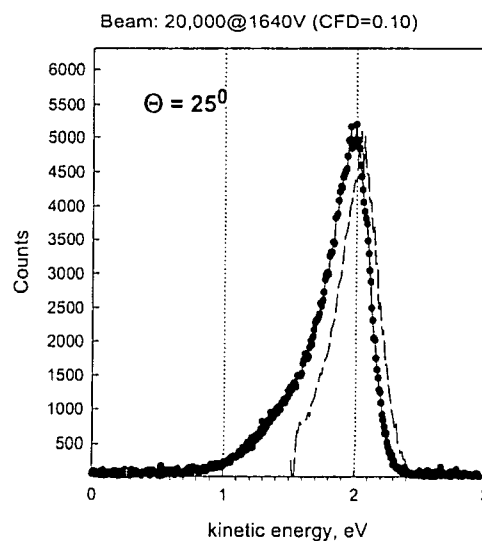
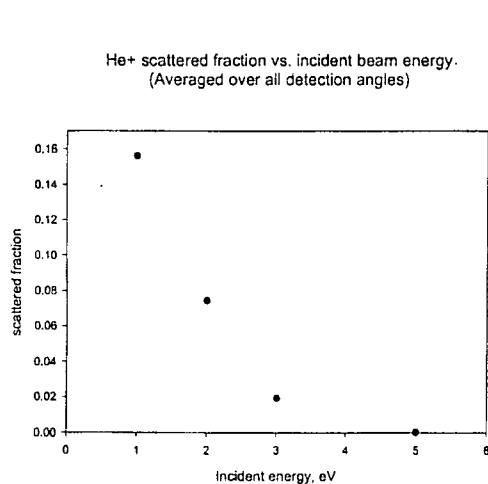
This objective of this project is to study the dynamics of the interactions of low energy ions important in combustion with small molecules in the gas phase and with liquid hydrocarbon surfaces. The first of these topics is a long-standing project in our laboratory devoted to probing the key features of potential energy surfaces that control chemical reactivity. The project provides detailed information on the utilization of specific forms of incident energy, the role of preferred reactant geometries, and the disposal of total reaction energy into product degrees of freedom. We employ crossed molecular beam methods under single collision conditions, at collision energies from below one eV to several eV, to probe potential surfaces over a broad range of distances and interaction energies. These studies allow us to test and validate dynamical models describing chemical reactivity. Measurements of energy and angular distributions of the reaction products with vibrational state resolution provide the key data for these studies. The second project requires us to apply these gas phase methods to probe interactions of low energy ions with liquid hydrocarbon systems. As a particular example, we are probing the interactions of low energy ions with the branched chain aliphatic hydrocarbon squalane, $C_{30}H_{62}$.

Recent Progress

The primary focus of our program, using the experimental methods developed in our laboratory for crossed beam studies of gas phase reactions, is the relatively unexplored problem of gas-liquid surface interactions and dynamical processes occurring at such interfaces. These processes are important in understanding the evaporation of multicomponent mixtures such as diesel fuels, the degradation of lubricants under harsh combustion conditions, the stability of polymers and other hydrocarbon-based materials in adverse environments, and the heating and fuel evaporation stages of droplet combustion. The collisional processes that lead to fuel heating and evaporation at interfaces are poorly known. The most straightforward approach to probing these issues is to direct projectiles at the surface of a hydrocarbon liquid having a very low vapor pressure, such that all collisions occur at the gas-liquid interface. To meet this objective, we employ the rotating disk source of Nathanson and collaborators,¹ in which a polished wheel rotates through a reservoir of the liquid of interest, allowing a film of thickness 100 μ to form. The surface is scraped mechanically just prior to interaction with the ion beam to remove surface contaminants. The work of Nathanson and co-workers demonstrates that surfaces prepared in this manner are uncontaminated by species adsorbed from the gas phase.

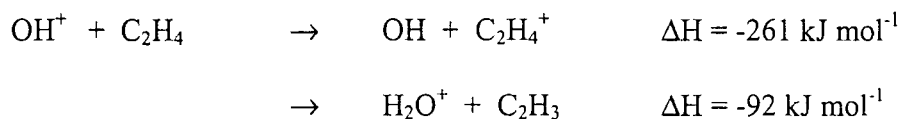
Previous studies of collisional processes at the gas-liquid interface have been concerned with probing the kinetic and/or internal energies of species that enter the gas phase following interaction with the surface. For example, the work of Nathanson has shown that the interactions of rare gas atoms and both polar and non-polar molecules with liquid surfaces near room temperature can be divided into direct inelastic scattering processes and trapping-desorption phenomena. In the former case, the scattered species suffer elastic or weakly inelastic collisions. The latter interactions, which occur as a result of a significant residence time on the liquid surface, are characterized by large energy transfers. The desorbed product distributions are qualitatively consistent with accommodation of kinetic energy by the liquid surface. However, work on the “soft landing” of ions on liquid surfaces² has shown that the sticking coefficients for polyatomic ions on a variety of surfaces can be very close to unity, leading to very low reflected fluxes. Initial results from our lab for the kinetic energy distributions of scattered particles were consistent with high degrees of charge trapping at the liquid surface. The development of significant amounts of surface charge made reproducible determination of scattered ion distributions quite difficult. Thus, it was necessary for us to carry out a series of measurements on the nature of reflected ions as a function of incident energy.

The results of this study have been surprising. Owing to the long range attractive potential of the ion with the polarizable hydrocarbon surface, we expected the reflection coefficient to *decrease* with decreasing collision energy – *i.e.*, sticking should increase with decreasing collision energy. We also expected the ions that actually did leave the surface would have experienced significant energy transfer to the surface, *i.e.*, the collisions should be “sticky”. In fact, we see very different results. In the case of He⁺ incident on the squalane surface at a collision energy of 5 eV, the data presented in the left panel below show that fewer than one percent of the ions reflect, but the reflected fraction increases to almost 20% at one eV collision energy. The right panel, portraying the kinetic energy distribution for ions scattered at the non-specular angle of 25° at an incident energy of 2 eV, shows that these events, which we would expect to show the greatest inelasticity, are remarkably elastic.



There is some trailing of the distribution to lower kinetic energies, but the majority of the scattered events are elastic. In addition, the experimental data for He^+ on squalane show that the angular distributions of scattered ions are essentially isotropic. This last observation is consistent with the pattern expected for trapping-desorption events, but the energy distributions and the reflection coefficients are not compatible with this picture. We expect that large scale molecular dynamics simulations will be necessary to understand the details of these interactions. Initially, to gain a qualitative understanding of the data, we are setting up simulations with a simple potential in which the liquid is represented as a Lennard-Jones fluid³ and the long range interaction of the ions with LJ spheres is modeled with a polarization interaction.

Another goal of this project is to observe and characterize reactive processes at the liquid interface. At this point, we have not yet observed reactive collisions. For the incident ion OH^+ , the principal reactive processes that we would expect to occur at the surface of a liquid aliphatic hydrocarbon are charge-transfer and hydrogen atom transfer. Direct observation of the former process cannot be accomplished (a neutral particle leaves the surface). In order to better characterize the latter process, that of hydrogen atom abstraction, and to understand the kinematics of similar collision processes with isolated molecular species, we have begun gas phase crossed beam studies of the reactions of OH^+ with C_2H_4 . Early studies have indicated appreciable rates for charge transfer and hydrogen atom transfer:



Experimental differential cross sections for these two reactions are currently being measured over the collision energy range from 0.5 eV to 3 eV.

Future Plans

We plan to continue our studies on inelastic processes at liquid hydrocarbon surfaces by measuring reflection coefficients for additional liquids (*e. g.*, perfluoropolyphenyl ethers and glycerol) and over a range of temperatures. *In situ* monitoring of the surface charge build-up will require the use of Kelvin probes, and we hope to implement that phase of the project in the next renewal period. We will proceed with molecular dynamics simulations as described above. We also expect to complete reactive scattering studies in the gas phase that will serve as precursor studies to reactive etching measurement on the liquid surface.

Publications, 2000-2002

Susan Troutman Lee, Elizabeth Richards O'Grady, Michael A. Carpenter, and James M. Farrar, "Dynamics of the Reaction of O⁻ with D₂ at Low Collision Energies: Reagent Rotational Energy Effects", *Phys. Chem. Chem. Phys.*, **2**, 679 (2000).

Susan Troutman Lee and James M. Farrar, "Dynamics of the OH⁻ + D₂ Isotope Exchange Reaction: Reactive and Nonreactive Decay of the Collision Complex", *J. Chem. Phys.* **112**, 581 (2000).

James M. Farrar, "Ion Kinetics and Energetics", in *Encyclopedia of Physical Science and Technology*, Third edition, Volume 8 (Academic, New York, 2001), pp. 65-82.

James M. Farrar, "Steric and Solvent Effects in Ionic Reactions", *Science* **295**, 2222 (2002).

References

1. See, for example, M. E. Saecker, S. T. Govoni, D. V. Kowalski, M. E. King, and G. M. Nathanson, *Science*, **252**, 1421 (1991).
2. A. A. Tsekouras, M. J. Iedema, G. B. Ellison, and J. P. Cowin, *Int. J. Mass Spectrom. Ion Proc.* **174**, 219 (1998); K. Wu, M. J. Iedema, and J. P. Cowin, *Science* **286**, 2482 (1999).
3. N. Lipkin, R. B. Gerber, N. Moiseyev, and G. M. Nathanson, *J. Chem. Phys.* **100**, 8408 (1994).

Nonlinear Raman spectroscopy of jet-cooled organic radicals and radical complexes

Peter M. Felker

Box 951569, Department of Chemistry, University of California
Los Angeles, CA 90095-1569
email: felker@chem.ucla.edu

Program Scope:

The DoE-sponsored project in this laboratory involves (a) the development of non-linear spectroscopic methods for use in characterizing the geometries, level structures and dynamics of species in sparse, gaseous samples and (b) the application of such techniques to the study of species, including organic free radicals and radical complexes, in cold, molecular beams.

Recent Progress:

In the past year we have advanced in the following areas: (1) We have made progress in the application of mass-selective, ionization-detected stimulated Raman spectroscopy (IDSRS) to the study of organic free radicals. (2) We have made significant strides in relating the information available from the vibrational and rotational spectroscopic methods employed in our laboratory to the intermolecular forces and dynamics that pertain to weakly bound molecular complexes and clusters.

1. Nonlinear Raman spectroscopy of organic free radicals

For several years we have been using mass-selective IDSRS to make species-selective measurements of the Raman spectra of molecules and molecular clusters at 0.03 cm^{-1} resolution (e.g., Refs. 1-3). A primary focus of the present DoE project is to extend such measurements to organic radicals and complexes thereof. In this regard we have made some progress, though there is certainly much more to do. Specifically, we have been successful in measuring intramolecular Raman spectra at 0.03 cm^{-1} resolution of the benzyl radical in a seeded supersonic molecular beam. The radical was generated by discharge-induced electrolysis of benzyl chloride. Mass-selective IDSRS was implemented with a photoionization probe involving two-color, resonantly-enhanced two-photon ionization (R2PI) via the vibronic band system of the species near $22,000\text{ cm}^{-1}$.⁴ Initial measurements have pertained to the ν_{12} fundamental (a CC stretch) of the species, which has been observed as a narrow, polarization-sensitive band near 988 cm^{-1} . The observation of other Raman bands has also been made. This study has given us a very good idea of the stringent requirements that must be met if one wishes to make routine measurements of nonlinear Raman spectra for jet-cooled radicals. We shall make use of this knowledge in future studies.

2. Studies of intermolecular forces and intermolecular dynamics

We have used mass-selective IDSRS and rotational coherence spectroscopy (RCS) to obtain a considerable body of data pertaining to the intermolecular level structures and geometries of weakly bound clusters, including clusters composed of molecules directly relevant to combustion processes. In principle, such results can be very informative as to intermolecular potential-energy surfaces (IPS's) and intermolecular dynamics. In practice, one often has significant difficulty in realizing this promise because the highly-coupled, large-amplitude nature of intermolecular motions complicates the interpretation of spectroscopic results. What one requires is close coupling between experiment and theoretical studies directed toward (a) the computation of IPS parameters and, subsequently, (b) the quantitative solution of the Schrödinger equation relevant to the intermolecular rotational-vibrational-tunneling states of a given species. Our group has made significant progress in the latter area.^{5,6} Specifically, we have developed and tested computer code applicable to a variety of types of cluster species (atom-molecule, linear molecule-nonlinear molecule, etc.) and to the calculation of properties such as transition moments, rotational constants, etc. Recently, we have also developed collaborations with Dr. Berta Fernández of the University of Sanitago Compostela and co-workers and with Prof. Samuel Leutwyler's group at the University of Bern to address the need for high-quality IPS computations. The upshot is that we are in an excellent position to begin to extract useful information about intermolecular forces and dynamics from experimental results relating to intermolecular transitions and cluster geometries.

The benzene-N₂ complex is the first species to which we have applied this comprehensive approach.⁷ The results of high-level *ab initio* calculations of IPS points from Dr. Fernandez's group were fit to an analytic function, which was then used in dynamically-exact five-dimensional (rigid monomer) calculations of $J = 0$ intermolecular states for several benzene-N₂ isotopomers. Rotational constants and Raman-scattering coefficients for the intermolecular states were also computed. The computational results relating to rotational constants are in excellent agreement with experimental results obtained by others for the zero-point level of the ground electronic state. More significant, the computed $J = 0$ intermolecular energies and Raman scattering coefficients have greatly facilitated the assignment of intermolecular Raman spectra (0 to 100 cm⁻¹) measured for the perprototated and perdeuterated species. Indeed, the major Raman features are reproduced in the computational results with a frequency accuracy of about 1 cm⁻¹ and with qualitatively correct relative intensities. The upshot is that we have obtained considerable understanding of the nature of, and dynamics on, the low-energy portion of the 5-D benzene-N₂ IPS. Further, we have contributed to the assessment of the quality of *ab initio* calculations required to yield IPS results suitable for quantitative interpretation of spectroscopic results on weakly bound species.

The 1-naphthol-(ammonia)₂ cluster is a species on which we have used RCS to measure rotational constants at ~MHz resolution. The species is of interest in large part because of the cluster-size dependence of excited-state proton-transfer dynamics that character-

izes the 1-naphthol-(ammonia)_n cluster series. Translating our RCS results into structural information on the cluster has been difficult owing to the species' twelve intermolecular degrees of freedom. Collaboration with the Leutwyler group, who have performed electronic structure calculations leading to minimum-energy geometries for the cluster, has significantly narrowed the range of likely geometries of the species to ones involving essentially a hydrogen-bonded ring.⁸ With this geometrical information now in hand, one is in a much stronger position to interpret results that we have obtained pertaining to the inter- and intramolecular Raman spectroscopy of the cluster. Further, one has better handle on interpreting RCS results relating to the structures of larger clusters in the 1-naphthol-(ammonia)_n series.

In addition to the two cluster species mentioned specifically above, IDSRS results on intermolecular transitions have been obtained for a number of other species in the present project period. These species include benzene-He, which is important for the information that its study can reveal about molecule-helium interactions, interactions whose characterization has become increasingly important given the marked increase in interest in doped helium clusters. They also include benzene-ammonia, whose study is relevant to an understanding of hydrogen bonding to π -electron proton acceptors. The results of these studies will be written up soon.

Future Work:

Our future work under the auspices of the DoE will be aimed largely toward measuring the ground-state vibrational spectra of organic free radicals involved in combustion systems and of complexes and clusters containing such radicals. These studies will involve excimer-laser photolysis generation, as well as pulsed-discharge generation of radicals in supersonic expansions. In addition, we also hope set up a thermolysis source of jet-cooled radicals, like the ones employed by the groups of Chen⁹ and Ellison,¹⁰ for example. We will focus initial attention on benzyl radical and complexes containing that species. Species targeted for subsequent Raman studies include the allyl, C₄H, and C₆H radicals.¹¹⁻¹³ The interest will be to characterize the vibrational level structures of these species in spectral regions difficult to access by other means. In regard to the experiments on complexes we hope to help in the effort to characterize the interactions between open-shell species and other molecules via intermolecular vibrational spectroscopy.

In addition to vibrational spectroscopic studies of organic radicals, we plan to continue to apply the combined experimental/computational approach that was described above for benzene-N₂ toward the characterization of intermolecular forces and dynamics in molecular complexes and clusters. In this area, there are numerous candidate species involving three, five, and six intermolecular degrees of freedom. We also plan to focus attention on the measurement and interpretation of intermolecular Raman spectra and rotational spectroscopic results on trimers and larger clusters. As part of this effort we shall make use of rigid-body diffusion Monte-Carlo methods¹⁴ to try to get a handle on zero-point-

averaged cluster structures.

References

1. W. Kim and P. M. Felker, *J. Chem. Phys.* **107**, 2193 (1997).
2. W. Kim and P. M. Felker, *J. Chem. Phys.* **108**, 6763 (1998).
3. W. Kim, M. W. Schaeffer, S. Lee, J. S. Chung, and P. M. Felker, *J. Chem. Phys.* **110**, 11264 (1999).
4. For example, G. C. Eiden and J. C. Weisshaar, *J. Chem. Phys.* **95**, 6194 (1991).
5. W. Kim, D. Neuhauser, M. R. Wall, and P. M. Felker, *J. Chem. Phys.* **110**, 8461 (1999).
6. For example, P. M. Felker, D. Neuhauser, and W. Kim, *J. Chem. Phys.* **114**, 1233 (2001). P. M. Felker, *J. Chem. Phys.* **114**, 1233 (2001).
7. P. M. Felker, B. Fernández, et al. – to be submitted.
8. S. Leutwyler, P. M. Felker, et al. – to be submitted.
9. D. W. Kohn, H. Clauberg, and P. Chen, *Rev. Sci. Instrum.* **63**, 4003 (1992).
10. A. V. Friderichsen, J. G. Radziszewski, M. R. Nimlos, P. R. Winter, D. C. Dayton, D. E. David, and G. B. Ellison, *J. Am. Chem. Soc.* **123**, 1977 (2001).
11. For example, A. D. Sappes and J. C. Weisshaar, *J. Phys. Chem.* **91**, 3731 (1987).
12. K. Hoshina, H. Kohguchi, Y. Ohshima, and Y. Endo, *J. Chem. Phys.* **108**, 3465 (1998).
13. M. Kotterer and J. P. Maier, *Chem. Phys. Lett.* **266**, 342 (1997).
14. V. Buch, *J. Chem. Phys.* **97**, 726 (1992).

Publications 2000-2002

1. P. M. Felker, D. Neuhauser, and W. Kim:
“Efficient calculation of molecular constants and transition intensities in weakly bound species from $J = 0$ eigenstates: Benzene-Ar as test case,”
J. Chem. Phys. **114**, 1233-1241 (2000).
2. P. M. Felker:
“Calculation of rovibrational states of weakly bound complexes by transformation from an Eckart frame: Benzene-N₂,”
J. Chem. Phys. **114**, 7901-7910 (2001).

Spectroscopic and Dynamical Studies of Highly Energized Small Polyatomic Molecules

Robert W. Field and Robert J. Silbey
Massachusetts Institute of Technology
Cambridge, MA 02139
rwfield@mit.edu

Program Definition: Our research program is centered on the development and application of experimental and theoretical methods for studying the dynamics (Intramolecular Vibrational Redistribution and Isomerization) and kinetics of combustion species. The primary focus is the dynamics of acetylene at internal energies above the acetylene \leftrightarrow vinylidene isomerization barrier in the $S_0 \tilde{X}$ state and the cis \leftrightarrow trans barrier in the $S_1 \tilde{A}$ state.

Recent Progress

It is rare that a molecule permits direct spectroscopic characterization of a potential energy surface isomerization barrier region. Our effort to illuminate spectroscopically the acetylene \leftrightarrow vinylidene isomerization barrier on the $S_0 \tilde{X}^1\Sigma_g^+$ potential energy surface has taken a dramatic detour. In order to gain systematic access to the isomerization barrier region on one potential surface, it is necessary to characterize and exploit the barrier region on another potential surface. Spectroscopic perturbations (anharmonic, Coriolis, spin-orbit) can provide spectroscopic access to classes of states to which access is nominally prohibited by the usual spectroscopic selection and propensity (Franck-Condon) rules. Our immediate goal is to more completely characterize the anharmonic and Coriolis perturbations on the $S_1 \tilde{A}^1A_u$ surface, particularly those involving the three bending modes (ν'_3 trans-bend, ν'_4 torsion, and ν'_6 asymmetric in-plane bend). This spectroscopic and dynamical information will provide a basis for systematic study of the S_0 state barrier region by "perturbation-facilitated transition state spectroscopy." Eigenstates that embody large amplitude motion along the S_0 state minimum energy isomerization path will be selectively illuminated and interrogated.

Our recent studies of the acetylene S_1 state have been *focused* by our previous studies of the structure and dynamics on the S_0 state potential surface. Previous studies of the $S_1 - S_0$ Dispersed Fluorescence spectrum have established that, from the acetylene side, the minimum energy isomerization path involves almost exclusively a local-bender motion of one CCH and that this local-bender motion becomes increasingly decoupled from other vibrational modes as one approaches the transition state. Thus, in order to illuminate spectroscopically the transition state, one needs a "local-bender pluck". Such a pluck cannot be achieved based on the Franck-Condon active normal modes. However, by exploiting spectroscopic perturbations between Franck-Condon bright and dark normal modes, nominally forbidden $S_1 \leftarrow S_0$ excitation transitions borrow sufficient intensity to provide an experimental basis for the necessary and elusive local-bender pluck.

Our studies of the acetylene S_1 state have also been *aided* by our previous analysis of the DF spectrum and calculation of $S_1 - S_0$ Franck-Condon factors. The S_0 state polyad model, derived from effective Hamiltonian fits to our DF spectra, provides unique spectroscopic signatures for each of the possible perturbers in the S_1 state. These signatures are predicted patterns in the DF spectrum, computed from a combination of Franck-Condon transition amplitudes and H_{eff} eigenvectors. There are several kinds of patterns. The global low-energy:high-energy intensity ratio provides a measure of the number of Franck-Condon bright ν'_3 (trans-bend) quanta in the S_1 state. The intrapolyad intensity pattern determines the number of quanta of non-totally-symmetric modes ($\nu'_4 + \nu'_6$) in the S_1 state. Intrapolyad interference effects among the states that contain different combinations of the vibrational angular momenta associated with the trans-bend (l''_4) and cis-bend (l''_5) that yield the same value of the total vibrational angular momentum (l''_{tot}) distinguish between the various members of S_1 state bending polyads [e.g. the $N'_{\text{bend}} = \nu'_4 + \nu'_6 = 4$ polyad contains anharmonically interacting (ν'_4, ν'_6) = (4, 0), (2, 2), and (0, 4) basis states]. What might appear as indescribable complexity in the DF spectrum is in fact the unique fingerprint for every eigenstate on the S_1 state potential surface.

An enormous amount of spectroscopic detective work must be done in order to characterize all of the relevant anharmonic and Coriolis perturbations on the S_1 state potential surface. We have initiated collaborations with several research groups with complementary expertise (and experimental data). Professor Soji Tsuchiya and Ms. Nami Yamakita (Japan Women's University and Waseda University) have recorded

$S_1 - S_0$ UV-only and IR-UV double resonance fluorescence excitation spectra. Professor F. Fleming Crim and Dr. Sarah Henton (University of Wisconsin) have also recorded IR-UV double resonance fluorescence spectra. Professor Anthony Merer's (University of British Columbia) analyses of spectroscopic perturbations have redefined the limits of spectroscopic detective work. Finally, Professor John Stanton (University of Texas) has computed a state-of-the-art acetylene S_1 -state potential energy surface.

John Stanton's calculations of anharmonic and Coriolis coupling terms on the acetylene S_1 state are proving crucial to our analyses of the complex web of spectroscopic perturbations and have identified and quantified the dominant mechanisms for intensity borrowing by nominally Franck-Condon dark states. Most notable among these are overtones of the antisymmetric in-plane-bend (ν_6'), which will provide a local-bender pluck of the S_0 acetylene \leftrightarrow vinylidene transition state. The near-degeneracy of ν_6' with ν_4' , the torsional mode, has made the exploitation of this pluck more challenging.

Starting with the extraordinary dynamic range of the supersonic jet UV-only LIF and IR-UV-LIF spectra from the Tsuchiya group, Anthony Merer has identified the vibrational bands which hold the keys to the analysis of the S_1 state perturbations. Some of those bands have been subjected to more detailed analysis at MIT by static gas cell Differential Temperature Laser Induced Fluorescence (DT-LIF) Spectroscopy, supplemented by Dispersed Fluorescence (DF) Spectroscopy. Figure 1 compares the JWU and MIT data in a 30-cm^{-1} -wide region about the $V_1^4 K_1^2$ band center (where V corresponds to ν_4'' in the S_0 state and ν_3' in the S_1 state). The initial DT-LIF spectra were recorded during a three-month visit by Ms. Yamakita to MIT. In DT-LIF, two LIF spectra are recorded simultaneously at two significantly different temperatures. Using the eXtended Cross Correlation (XCC) pattern-recognition algorithm, we are able to separate hot and cold bands based on their drastically distinct temperature-dependent intensities. The MIT spectra are recorded at higher resolution (0.05 vs. 1 cm^{-1}) and higher temperatures (350 and 250 K vs. 5 K) than the JWU spectra, and the DT-LIF scheme permitted overlapping hot and cold bands to be disentangled.

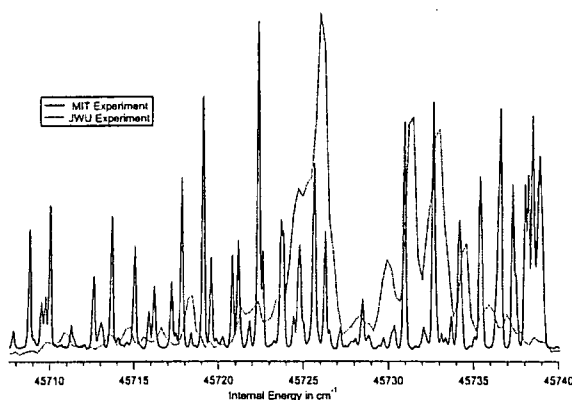


Figure 1: A comparison of MIT and JWU data. The MIT spectrum has superior resolution (0.05 vs. 1 cm^{-1}). The JWU spectrum has appreciable intensity only near the band center resulting from the low rotational temperature in the supersonic jet.

One central question in the analysis of new bands in the acetylene $S_1 - S_0$ spectra is which bands involve non-totally-symmetric bending modes, ν_4 and ν_6 , and which do not. This is answered by the K -structure, which is irregular for the bending overtones and combinations, owing to extremely strong and pervasive a -type Coriolis interactions. DF spectra also distinguish between assignment possibilities, both in the relative intensities of low- and high-energy regions of the spectrum and in details of the intra-polyad intensity patterns. Another challenging question addresses energy ordering within polyads. Owing to the nearly identical harmonic frequencies of the torsion and the asymmetric-in-plane-bend normal modes, the

non-totally-symmetric bending states form polyads, and it is necessary to determine the energy rank of each observed member of each bend polyad. The subset of observed states cannot be arranged into polyads without some spectroscopic clues as to which polyad the state belongs as well as the energy rank within that polyad. This is accomplished mostly by trial and error, but knowledge of the intensity borrowing mechanisms, primarily via cubic anharmonic coupling terms, from Franck-Condon bright states narrows the assignment possibilities. Based on tentative assignments (mostly due to Merer) of the global data set, a nearly complete set of ν_i and x_{ij} vibrational constants has been determined for the S_1 state. In addition, the cubic anharmonicity constants responsible for illuminating members of the Franck-Condon dark non-totally-symmetric bending polyads have been tentatively determined, and a few complete bend polyads have been observed and will soon yield an experimental value for the key Darling-Dennison quartic anharmonic coupling parameter, K_{4466} .

The IR-UV double resonance spectra recorded by Sarah Henton in the Crim group sample the high energy region of the S_1 state. The density of *observed* vibrational states is comparable to the *computed* density of symmetry-accessible vibrational states. Anharmonic and Coriolis coupling have become so pervasive that all traces of Franck-Condon selectivity have vanished. Our ongoing analysis of the lower-energy portion of the spectrum, in particular the intensity-borrowing mechanisms based on Stanton's *ab initio* cubic anharmonic constants, is prerequisite to any plausible assignment of the Henton-Crim spectra. Those spectra will in turn provide stringent tests for our model of the S_1 state in the region where the in-plane cis-trans isomerization barrier is strongly sampled.

Future Directions

The identification of $n\nu'_{\text{bend}}$ polyads in the $S_1 \tilde{A}$ state of acetylene unambiguously illuminates a new set of bright states in the $S_0 \tilde{X}$ state. A systematic series of DF and SEP experiments on $^{12}\text{C}_2\text{H}_2$ will be performed to take advantage of this source of local-bender pluck brightness.

We also plan to record LIF, DF, and SEP spectra of $^{13}\text{C}_2\text{H}_2$ using the ν'_6 local-bend pluck. The permutation doublets observable in the DF and SEP spectra will provide a unique class of spectroscopic information about the location of the small number of vibrational levels localized on the vinylidene side of the S_0 state isomerization barrier and the strength of the coupling of those levels with the very sparse manifold of acetylene-localized pure local-bender eigenstates that are uniquely capable of sampling the isomerization barrier at its lowest and thinnest region.

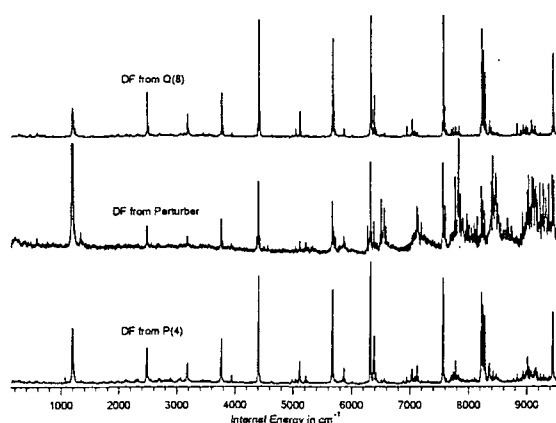


Figure 2: DF spectra recorded via three rotational lines ($Q(8)$, a $Q(8)$ perturber, and $P(4)$) in $4\nu'_3$. The buildup of intensity at high energy in the spectrum of the perturber demonstrates access to states with only 1 quantum of excitation in ν'_3 .

Recent DOE-Supported Publications (Since 2000)

1. M.P. Jacobson and R.W. Field, "Acetylene at the Threshold of Isomerization," *J. Phys. Chem.* 104, 3073-3086 (2000).
2. M.P. Jacobson and R.W. Field, "Visualizing Intramolecular Vibrational Redistribution: Expectation Values of Resonance Operators," *Chem. Phys. Lett.* 320, 553-560 (2000).
3. D.B. Moss, Z. Duan, M.P. Jacobson, J.P. O'Brien, and R.W. Field, "Observation of Coriolis Coupling Between $\nu_2 + 4\nu_4$ and $7\nu_4$ in Acetylene $^1\Sigma_g^+$ by Stimulated Emission Pumping Spectroscopy," *J. Mol. Spectrosc.* 199, 265-274 (2000).
4. H.K. Srivastava, A. Conjusteau, H. Mabuchi, A. Callegari, K.K. Lehmann, G. Scoles, M.L. Silva, and R.W. Field, "Rovibrational Spectroscopy of the $\nu = 6$ Manifold in $^{12}\text{C}_2\text{H}_2$ and $^{13}\text{C}_2\text{H}_2$," *J. Chem. Phys.* 113, 7376-7383 (2000).
5. M.L. Silva, M.P. Jacobson, Z. Duan, and R.W. Field, "Anomalous Simplicity of the Dispersed Fluorescence Spectrum of $^{13}\text{C}_2\text{H}_2$," *J. Mol. Struct.* 565, 87-91 (2001).
6. M.L. Silva, R. Jongma, R.W. Field, and A.M. Wodtke, "The Dynamics of 'Stretched Molecules': Experimental Studies of Highly Vibrationally Excited Molecules with Stimulated Emission Pumping," *Annu. Rev. Phys. Chem.* 52, 811-852 (2001).
7. K. Hoshina, A. Iwasaki, K. Yamanouchi, M.P. Jacobson, and R.W. Field, "The Infrared-Ultraviolet Dispersed Fluorescence Spectrum of Acetylene: New Classes of Bright States," *J. Phys. Chem. A* 114, 7424-7442 (2001).
8. M.L. Silva, M.P. Jacobson, Z. Duan, and R.W. Field, "Unexpected Simplicity in the $S_1 - S_0$ Dispersed Fluorescence Spectra of $^{13}\text{C}_2\text{H}_2$," *J. Chem. Phys.* 116, 93 (2002).

Laser Studies of Chemical Reaction and Collision Processes

George Flynn, Department of Chemistry, Columbia University
Mail Stop 3109, 3000 Broadway, New York, New York 10027
flynn@chem.columbia.edu

Introduction and Overview

Our work involves the study of energy transfer during collisions between molecules. We have focussed our attention on what we believe is the most important energy transfer problem in current studies of chemical and collision dynamics: the collisional cooling of molecules with "chemically significant" amounts of vibrational energy. A molecule with "chemically significant" energy is one that is sufficiently energetic to undergo chemical reaction or bond rupture. Our efforts are aimed at determining both a qualitative and quantitative picture of these collision processes. The qualitative picture constitutes the "mechanism" that controls relaxation for these high energy collision events. By mechanism we mean the quantum state resolved picture of the quenching process, which in turn provides insight into the relative effectiveness of short and long range forces in mediating the energy transfer. The quantitative measure of these collision events is contained in the energy transfer probability distribution function, $P(E,E')$, which gives the probability for transferring an amount of donor internal energy $\Delta E = E - E'$ during a collision.¹⁻¹⁶ A key result of our efforts over the past few years has been the development of a method to invert our data and obtain directly significant portions of this distribution function. $P(E,E')$ is the *sine qua non* for meaningful comparisons between experimental data and theoretical calculations. Despite its close connection to theoretical descriptions of energy transfer processes, this function is also of enormous practical significance since kinetic models of unimolecular reactions employing master equation techniques require $P(E,E')$ as input. We have had some notable successes in determining both the qualitative, mechanistic energy transfer picture for these high energy collision events and the quantitative shape and magnitude of $P(E,E')$. These results have left a number of well posed, unanswered questions about energy transfer for molecules with chemically significant amounts of energy that we plan to investigate over the next year. We hope through these experiments to improve our basic understanding of photochemical and photophysical phenomena and to provide dynamical and mechanistic data of fundamental interest for combustion and atmospheric reaction processes.

Our effort to understand and develop a quantum state resolved picture of the quenching of unimolecular reactions is one aspect of the more general field of vibrational energy transfer, the process by which molecules transfer their internal vibrational energy during collisions. The high energy of the quenched species distinguishes the present experimental studies from those vibrationally quantum state resolved investigations involving donors with only a few quanta of internal vibrational energy, carried out in the 1960's and 1970's at the dawn of the laser/energy transfer era. Similarly, the truly remarkable spectral resolution of the present experiments, providing as it does deep physical insight into the quenching process for these high energy molecules, distinguishes these investigations from most of the unimolecular reaction quenching studies carried out from roughly 1925 through 1990.

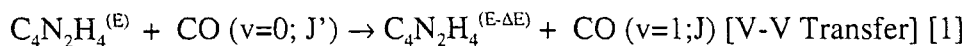
Experimental Approach

Our success in obtaining new levels of understanding about these high energy collision events has been based on the use of infrared diode lasers to probe the post collision quantum state population distributions of one of the collision partners.^{1,12-16} The application of infrared diode lasers to study time-dependent dynamic events was developed in our laboratory under D.O.E. sponsorship. The technique as applied to studies of dynamic molecular processes in our laboratory is by now well established. In brief, in the experimental approach that we are using to study these energy transfer processes, substrates (S) of essentially arbitrary complexity are

produced with high energy by laser pumping methods. The collision processes that relax these highly excited S* molecules are investigated by probing the quantum states of the bath molecules B' produced by the interaction between S* and B. By using relatively simple bath molecules and sophisticated laser probe methods to follow the quantum states of B', the nature of the mechanism for energy loss by S* can be "seen" through the behavior of the (small) energy acceptor molecule, B. To fully analyze the deactivation process for such highly vibrationally excited molecules as S*, however, the level of excitation, rotational profiles and translational recoils of *different* vibrational modes of the bath acceptor B' are required. Furthermore, the amount of energy transferred to the rotational and translational degrees of freedom of the *ground* (vibrationless) state of the bath molecules is also of interest. Our technique is capable of supplying all of this extremely valuable information.

Results: Probing Soft Collision Mediated Energy Transfer

The present molecular system that we are studying consists of highly excited pyrazine donor molecules, which have about 5 eV of internal vibrational energy, colliding with cold (roughly room temperature) CO molecules. In these kinds of experiments, CO is a particularly appealing bath acceptor for a number of reasons. Among these is the transition moment for the CO ($v=0 \rightarrow 1$) vibrational transition, which is relatively small, especially compared to the CO₂ molecule, a bath species that we have studied extensively. This transition moment is expected to be the controlling factor determining the energy transfer efficiency between highly excited donors such as pyrazine and room temperature CO for those collisions that produce vibrationally excited CO ($v=1$) in a vibration-vibration energy transfer process such as:



For this process we find that the dominant channels are those with $J' - J = \Delta J = \pm 1$, reminiscent of energy transfer by a long range, soft collision mechanism, mediated by the CO ($v=0 \rightarrow 1$) transition moment. The data from this study are now complete with the energy transfer process (1) having been investigated over a range of final ($v=1; J$) states in CO at a number of initial, ambient temperatures. The probability for excitation of the $v=1$ vibrationally excited state is temperature dependent and ranges from a factor of 4-10 smaller than the probability for excitation of the analogous state in CO₂ ($00^0 1$) in collisions with highly excited pyrazine. These results are consistent with the fact that the transition moment for the CO₂ ($00^0 0 \rightarrow 00^0 1$) transition is 10 times larger than that for CO ($v=0 \rightarrow 1$); however, the temperature dependence for this process with CO as an acceptor is noticeably different from the temperature dependence for the same process with CO₂ as an acceptor. This may be related to the presence of a small permanent dipole moment for CO and/or to the differences in mean velocity for CO and CO₂ at a given temperature. In both cases the absolute probability for the occurrence of an energy transfer process such as (1) is quite small, about 1% gas kinetic for CO₂ and about 0.1% gas kinetic for CO.¹⁷

Results: Probing Angular Momentum Constraints for Impulsive Collisions

The picture for collisions that leave CO in the $v=0$ state but cause a change in angular momentum J is completely different. This process can be described by the equation:

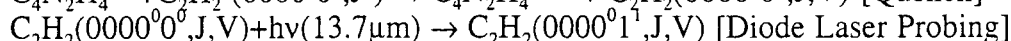
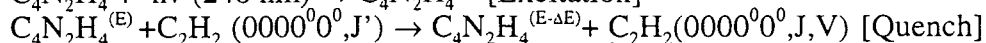
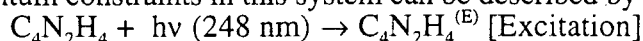


V is CO velocity. Here $J' - J = \Delta J \gg \pm 1$, and the line width for transitions such as CO ($v=0; J \rightarrow v=1; J \pm 1$) is found to be well above room temperature, indicating that the CO ($v=0; J; V$) produced by equation [2] is translationally hot. These are characteristics of hard, impulsive collisions in which the CO directly strikes one of the vibrating atoms on the highly excited pyrazine. The data from this study are now complete with the energy transfer process

(2) having been investigated over a range of final ($v=0$; J) states in CO at a number of initial, ambient temperatures. In these impulsive collisions we find a direct, linear correlation between the velocity recoil of a CO bath molecule and its rotational angular momentum quantum number. The maximum final J state observed in these experiments is roughly 40. Both of these features of the energy transfer process have also been confirmed in trajectory calculations.¹⁸ We now have all the data needed to construct the $P(E,E')$ energy transfer distribution function for hot pyrazine/CO collisions of the type described by equation (2).¹⁹

Present and Future Experimental Program

We plan to continue to use the high resolution, high speed infrared diode laser probe technique to determine final vibrational, rotational, and translational energy distributions for bath product species formed as the result of a collision event. In particular quantum state and velocity distributions will be determined for acetylene recoiling from high energy donor molecules. Acetylene provides an excellent probe molecule to investigate the importance of angular momentum constraints on the energy transfer process. The center of mass is in the middle of the $C\equiv C$ triple bond making the maximum impact length, b , roughly the length of a C-H bond plus half a $C\equiv C$ triple bond [a total length of 1.66 Å]. Experiments to test for angular momentum constraints in this system can be described by the following equations



For acetylene the mean J at room temperature is roughly 13 and we expect the mean ΔJ for this molecule to be approximately $(1.66/1.23)60=80$. (1.23 Å is the length of the C=O bond in CO_2 and 60 is the mean change in J for CO_2 undergoing collisions with highly excited pyrazine.) Thus, we predict a maximum ΔJ for these experiments to be around 93, noticeably higher than that for CO_2 and much larger than that found for CO ($\Delta J \approx 20$). These experiments require a complete change of optics for our experimental system in order to operate in the 12-14 μm infrared spectral region. The necessary optics have been purchased and are being tested. The model trajectory calculations carried out during the past year will be continued in order to determine the dependence of the shape and magnitude of the energy transfer distribution function, $P(E,E')$, on initial collision excitation energy, E , on angular momentum, and on the initial quantum state of the bath molecule.

References

1. C. A. Michaels and G. W. Flynn, *J. Chem. Phys.* **106**, 3558 (1997)
2. I. Oref and D.C. Tardy, *Chem. Rev.* **90**, 1407 (1990)
3. J. R. Barker, J. D. Brenner, and B. M. Toselli, *Advances in Chemical Kinetics and Dynamics*, **2B**, 393-425 (1995); John Barker, Ed.; JAI Press Inc., Greenwich, CT
4. I. Oref, *Advances in Chemical Kinetics and Dynamics*, **2B**, 285-298 (1995); John Barker, Ed.; JAI Press Inc., Greenwich, CT
5. F. A. Lindemann, *Trans. Faraday Soc.*, 1922, **17**, 598.
6. D. C. Tardy and B. S. Rabinovitch, *Chem. Rev.* **77**, 369 (1977)
7. J. Troe, *J. Chem. Phys.* **66**, 4745 (1977).
8. T. Lenzer, K. Luther, J. Troe, R. G. Gilbert, and K. F. Lim, *J. Chem. Phys.* **103**, 626 (1995).
9. J. Troe, *J. Chem. Phys.* **97**, 288 (1992).
10. V. Bernshtein and I. Oref, *J. Phys. Chem.* **97**, 12811 (1993).
11. J. R. Barker, *J. Phys. Chem.*, **96**, 7361 (1992); J. D. Brenner, J. P. Erinjeri, and J. R. Barker, *Chem. Phys.* **175**, 99 (1993).
12. Chris A. Michaels, Amy S. Mullin, Jeunghye Park, James Z. Chou, and George W. Flynn, *J. Chem. Phys.*, **108**, 2744-2755 (1998)
13. C. A. Michaels, Z. Lin, A. S. Mullin, H. C. Tapalian, and G. W. Flynn, *J. Chem. Phys.*, **106**, 7055-7071 (1997)

14. G. W. Flynn, C. A. Michaels, H. C. Tapalian, Z. Lin, E. Sevy, and M. A. Muyskens in *Highly Excited Molecules: Relaxation, Reaction, and Structure*, ACS Symposium Series, 678, pp134-149, Eds. Amy Mullin and George Schatz, American Chemical Society, Washington, DC, 1997
15. E.T. Sevy, C. A. Michaels, H. C. Tapalian, and G.W. Flynn, "Competition Between Photochemistry and Energy Transfer in UV-excited Diazabenzene: II. Identifying the Dominant Energy Donor for 'Supercollisions'", *J. Chem. Phys.*, 112, 5844-51 (2000)
16. E. T. Sevy, Seth Rubin, Z. Lin, and G. W. Flynn, "Translational and Rotational Excitation of the CO₂(00⁰) Vibrationless State in the Collisional quenching of Highly Vibrationally Excited 2-Methylpyrazine: Kinetics and Dynamics of Large Energy Transfers", *J. Chem. Phys.*, 113, 4912-4932 (2000)
17. Natalie Seiser, K. Kavita, and George Flynn, "Long Range Energy Transfer in Pyrazine-CO Collisions: Excitation of CO (v=1)", in preparation
18. Cortney Higgins, Quan Ju, Natalie Seiser, George Flynn and Sally Chapman, "Classical Trajectory Study of Energy Transfer in Pyrazine-CO Collisions", *J. Phys. Chem. A*, 105, 2858-2866, (2001)
19. Natalie Seiser, Quan Ju, Eric Sevy, and George Flynn, "Quenching of Pyrazine by CO: Angular Momentum Constraints for Impulsive Encounters", in preparation

DOE Publications: (2000-2002)

1. E.T. Sevy, M.A. Muyskens, S.M. Rubin, and G.W. Flynn, "Competition Between Photochemistry and Energy Transfer in UV-excited Diazabenzene: I. Photofragmentation Studies of Pyrazine at 248 nm and 266 nm", *J. Chem. Phys.*, 112, 5829-43 (2000)
2. E.T. Sevy, C. A. Michaels, H. C. Tapalian, and G.W. Flynn, "Competition Between Photochemistry and Energy Transfer in UV-excited Diazabenzene: II. Identifying the Dominant Energy Donor for 'Supercollisions'", *J. Chem. Phys.*, 112, 5844-51 (2000)
3. Jack M. Preses, Christopher Fockenber, and George Flynn, "A Measurement of the Yield of Carbon Monoxide from the Reaction of Methyl Radicals and Oxygen Atoms", *J. Phys. Chem.*, 104, 6758-6763 (2000)
4. E. T. Sevy, S. M. Rubin, Z. Lin, and G. W. Flynn, "Translational and Rotational Excitation of the CO₂(00⁰) Vibrationless State in the Collisional quenching of Highly Vibrationally Excited 2-Methylpyrazine: Kinetics and Dynamics of Large Energy Transfers", *J. Chem. Phys.*, 113, 4912-4932 (2000)
5. E. T. Sevy, M. A. Muyskens, Z. Lin, and G. W. Flynn, "Competition Between Photochemistry and Energy Transfer in UV-excited Diazabenzene: III. Photofragmentation and Collisional Quenching in Mixtures of 2-Methylpyrazine and Carbon Dioxide", *J. Phys. Chem. A*, 104, 10538-10544 (2000)
6. Cortney Higgins, Quan Ju, Natalie Seiser, George Flynn and Sally Chapman, "Classical Trajectory Study of Energy Transfer in Pyrazine-CO Collisions", *J. Phys. Chem. A*, 105, 2858-2866, (2001)
7. George W. Flynn, *Encyclopedia of Chemical Physics and Physical Chemistry*, Volume III: Applications, Part C3 Chemical Kinetics and Dynamics, "Energy Transfer in Gases", John Moore and Nicholas Spencer, Eds., pp 0000-0000, (2002)
8. Natalie Seiser, Quan Ju, Eric Sevy, and George Flynn, "Quenching of Pyrazine by CO: Angular Momentum Constraints for Impulsive Encounters", in preparation
9. Natalie Seiser, K. Kavita, and George Flynn, "Long Range Energy Transfer in Pyrazine-CO Collisions: Excitation of CO (v=1)", in preparation

GAS-PHASE MOLECULAR DYNAMICS: KINETICS OF RADICAL-RADICAL REACTIONS

Christopher Fockenberg and Jack M. Preses

Chemistry Department 555A, Brookhaven National Laboratory, Upton, NY 11973-5000
fknberg@bnl.gov, preses@bnl.gov

Program Scope

The goal of this research is the understanding of elementary chemical reactions important in the combustion of fossil fuels. Interest centers on reactions of short-lived chemical intermediates, which are investigated by using broadband mass spectrometric as well as molecule specific high-resolution laser absorption methods.

Recent Progress

Time resolved time-of-flight mass spectrometry (TOFMS): We measured the temperature and pressure dependence of the rate constant of the methyl-methyl recombination reaction with He as bath gas using our TOFMS apparatus:



This study was motivated by an earlier investigation of the reaction of $^3\text{CH}_2$ with CH_3 , in which a fairly substantial difference in the rate constant of reaction (1) was found between the literature and our results. Methyl radicals were produced by the 193-nm laser photolysis of acetone. In the observed temperature (300 – 700 K) and pressure (0.5 – 10 Torr) ranges the rate constant exhibits a negative temperature dependence and fall-off behavior typical of that for recombination reactions.

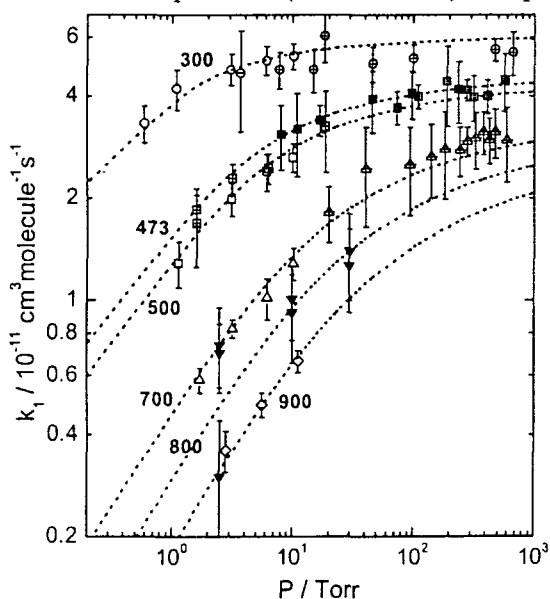


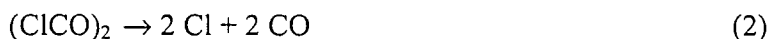
Fig. 1: Plots of the pressure dependence of the rate constants, k_1 , for He as bath gas at 300 K: \circ this work, \oplus ref. 1, \ominus ref. 2; 473 K: \blacksquare ref. 3; 500 K: \square this work; \boxplus ref. 3; 700 K: \triangle this work, \blacktriangle ref. 1; 800 K: \blacktriangledown ref. 2; 900 K: \diamond ref. 3. The dashed lines are global fit results using Troe's equation.

While the reaction rates obtained from the methyl profiles show a linear relationship with the initial methyl radical concentration, the production rate for ethane exhibits a peculiar drop off at larger methyl concentrations. However, the final ethane concentration does not appear to be affected by the kinetics and has been determined to be exactly half the initial methyl concentration. While the recombination rate constant at 300 K was again found to be higher than previously measured by other groups, the agreement between the literature and our data at higher temperatures is good. To check for systematic errors, we measured the rate constant for this reaction with Ar (1 Torr) as bath gas at 300 K. The measured rate

constant agrees very well with the literature. Interestingly, the rate constant obtained from ethane production is about 50% smaller than the value determined from the methyl decay. The ethane yield, however, is consistent with the initial methyl concentration.

In addition, rate constants were calculated theoretically using variable reaction coordinate transition state theory (TST) with a new potential energy surface built from high-level *ab initio* calculations. The *ab initio* and TST calculations were performed with the MOLPRO and VARIFLEX programs, respectively.^{4,5} The calculated high-pressure rate constants were fitted to a generalized Arrhenius expression giving: $k_{\infty}^{\text{theory}}(T) = 9.31 \times 10^{-11} (T/298 \text{ K})^{-0.925} e^{-129 \text{ K}/T} \text{ cm}^3 \text{ molecule}^{-1} \text{ s}^{-1}$. The pressure dependence of the recombination rate constant was calculated using the master equation formalism with a simple exponential model for the collisional energy transfer employing a set of energy transfer parameters, $\langle \Delta E_{\text{down}} \rangle$. By comparing the calculated and experimental fall-off curves, we found that at room temperature, He and H₂ are more efficient colliders than Ar. With increasing temperature, the difference in $\langle \Delta E_{\text{down}} \rangle$ between He and Ar becomes negligible. Troe's equation was fitted to a set of data comprised of rate constants determined here and found in the literature. With $k_{\infty}(T)$ set to be the high-pressure-limit rate constant calculated here, the two remaining parameters can be given by $k_0(T) = 5.36 \times 10^{-26} (T/298 \text{ K})^{-2.65} e^{-245 \text{ K}/T} \text{ cm}^6 \text{ molecule}^{-2} \text{ s}^{-1}$, and $F_{\text{cent}}(T) = e^{-T/479 \text{ K}}$ (see Fig. 1).

We have begun studying the products and yields from the 193-nm photolysis of oxalyl chloride and propargyl chloride.



Chlorine atoms were scavenged by the reaction with ethane or H₂ giving HCl as well as ethyl radicals or hydrogen atoms, respectively, at temperatures higher than 500 K. The drop in the precursor species was then compared to the production of HCl and CO. The observed increase at $m/e = 28$ is consistent with a $(95 \pm 5)\%$ yield of two CO molecules for each oxalyl chloride photolyzed. However, we find that only about half of the corresponding HCl molecules expected are generated initially. Moreover, there is no obvious correlation between HCl yield and H₂ concentration, which would have indicated that the loss of Cl atoms is caused by other, *e.g.*, heterogeneous, reactions in the reactor. Further investigations into this mystery are underway.

The motivation for this study is to find optimum conditions to produce hydrogen atoms and propargyl radicals, and to study their reaction kinetics:



Preliminary experiments (photolysis of propargyl chloride in H₂ at 500 K) show indeed the production of a species at $m/e = 40$. However, the main product under these conditions was C₆H₆. Interestingly, we clearly see C₃H₃Cl₂ as an intermediate species.

Tunable Diode Laser Absorption Spectroscopy (TDLAS): We previously measured the CO yield from the reaction of CH₃ and O atoms at room temperature using TDLAS. We separated CO produced by the radical-radical reaction from that generated by the 193-nm photolysis of the precursor substance, acetone, by using isotopically labeled acetone, ¹³CH₃¹²C(O)¹³CH₃, and observing absorption lines from ¹³C¹⁶O and ¹²C¹⁶O. We also showed that under our

experimental conditions, isotopic scrambling could be ignored. The measured yield was in excellent agreement with a calculation from the ANL group.⁶ Prompted by the same group's prediction of the CO yield from the reaction of CD₃ and O atoms, we have now measured this yield using the same method. In this case, the distinction between the two CO sources was made by using CD₃C(¹⁶O)CD₃ and S¹⁸O₂ (99.5 ¹⁸O atom %) and observing absorptions of ¹²C¹⁸O and ¹²C¹⁶O. The CO yield was determined to be 0.12 ± 0.01 (2σ), once again in excellent agreement with the ANL group's prediction (see Fig. 2). In the course of this work we confirmed the locations of several absorption lines of CD₂O in the ~2000 cm⁻¹ range of our CO diode that may be useful in the future.

We investigated the use of a 3000 cm⁻¹ laser diode for detection of C-H and H-X stretches and confirmed our ability to detect HCl $\nu = 0 \rightarrow \nu = 1$ absorptions. By operating this diode together with a 2070 cm⁻¹ laser diode, we will examine the photolysis of oxalyl chloride separately from the TOFMS investigation in order to precisely determine the yields of CO and chlorine atoms, which will be converted to HCl in the reaction with H₂ (see above). To study, *e.g.*, the kinetics of reaction (4), the concentration of H atoms can be directly determined from the concentration of HCl.

Future Plans

After completion of the investigation of the C₃H₃ + H reaction we will revisit the CH₃ + OH reaction. The main complication regarding the study of this reaction has been our inability to observe hydroxyl radicals so far. Since fragmentation is a serious problem using Ne ($h\nu > 16$ eV) in the discharge lamp, we have to use H₂ instead (many lines with the main line at $h\nu = 10.2$ eV), which, however, limits our sensitivity toward OH radicals (IP = 13 eV) and H₂O (IP = 12.6 eV). Choosing a larger diameter for the orifice: 1 mm instead of the 0.5 mm currently in use should give us a four times better signal. We will also examine the photolysis of hydrogen peroxide at 193 nm as a potential source for OH, which has a yield of ≈ 1.5 . Beyond this research, we plan to use our experience in the photolysis of oxalyl chloride to generate CH₂OH and HO₂ from Cl + CH₃OH \rightarrow CH₂OH + HCl and CH₂OH + O₂ \rightarrow HO₂ + CH₂O, and to study selected reactions of these radicals.

As part of the ongoing study of the kinetics of propargyl radicals with H atoms, we will use tunable diode laser spectroscopy to study the yield and kinetics of allene, C₃H₄, from this reaction. Propargyl radicals and H atoms will be produced as above from propargyl chloride,

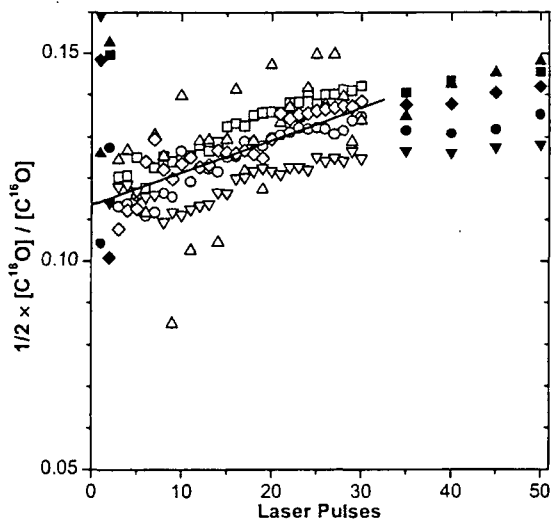


Fig. 2: ¹⁸O product yield vs. excimer laser pulses for five separate experiments. The line is a linear fit to all data points shown as open circles. Points not fitted include very low and high CO concentrations where the CO signal was comparable to the uncertainty in the measurement and where the influence of secondary chemistry begins to distort the CO concentrations.

oxalyl chloride, and H₂ for 193-nm photolysis; studies using 248-nm photolysis will use propargyl bromide as the source for propargyl radicals. We have obtained a very intense, single-mode diode that permits observation of the very strong C-H bends in allene near 1955 cm⁻¹. We have already located numerous allene absorption lines in this region. Since the internal degrees of freedom of allene produced in this reaction are likely to be equilibrated, we should be able to measure real-time allene kinetics during reaction in order to corroborate the TOFMS studies.

Acknowledgment

This work was performed at Brookhaven National Laboratory under Contract DE-AC02-98CH10886 with the U.S. Department of Energy and supported by its Division of Chemical Sciences, Office of Basic Energy Sciences.

Reference

- (1) Pereira, R. D. A.; Baulch, D. L.; Pilling, M. J.; Robertson, S. H.; Zeng, G. *J. Phys. Chem. A* **1997**, *101*, 9681.
- (2) Knyazev, V. D.; Slagle, I. R. *J. Phys. Chem. A* **2001**, *105*, 6490
- (3) Stoliarov, S. I.; Knyazev, V. D.; Slagle, I. R. *J. Phys. Chem. A* **2000**, *104*, 9687
- (4) Werner, H.-J.; Knowles, P. J.; Amos, R. D.; Bernhardsson, A.; Berning, A.; Celani, P.; Cooper, D. L.; Deegan, M. J. O.; Dobbyn, A. J.; Eckert, F.; Hampel, C.; Hetzer, G.; Korona, T.; Lindh, R.; Lloyd, A. W.; McNikolas, S. J.; Manby, F. R.; Meyer, W.; Mura, M. E.; Nicklass, A.; Palmieri, P.; Pitzer, R.; Rauhut, G.; Schuetz, M.; Stoll, H.; Stone, A. J.; Tarroni, R.; Thorsteinsson, T. MOLPRO 2000.
- (5) Klippenstein, S. J.; Wagner, A. F.; Dunbar, R. C.; Wardlaw, D. M.; Robertson, S. H. VARIFLEX; 1.0 ed., 1999.
- (6) Marcy, T. P.; Diaz, R. R.; Heard, D.; Leone, S. R.; Harding, L. B.; Klippenstein, S. J. *J. Phys. Chem. A* **2001**, *105*, 8361

Publications since 2000

Ion Yields for Tetramethylgermane Exposed to X-Rays near the Ge K-Edge, R. A. Holroyd, J. M. Preses, and T. K. Sham, *J. Phys. Chem. A* **104**, 2859-2864 (2000).

A Measurement of the Yield of Carbon Monoxide from the Reaction of Methyl Radicals and Oxygen Atoms, J. M. Preses, C. Fockenberg, and G. W. Flynn, *J. Phys. Chem. A* **104**, 6758-6763 (2000).

Radiation Chemical Effects of X-rays on Liquids, R. A. Holroyd and J. M. Preses in *Chemical Applications of Synchrotron Radiation*, Sham, T. K., ed.; World Scientific Publishing: in press.

A Direct Measurement of the Rate Constant for the CH₂(\tilde{X}^3B_1) + CH₃ Reaction at 300 K, B. Wang and C. Fockenberg, *J. Phys. Chem. A* **105**, 8449-8455 (2001)

Temperature Dependence of the Rate Constant and Product Distribution of the Reaction of CH₃ Radicals with O(³P) Atoms, C. Fockenberg and J. M. Preses, *J. Phys. Chem. A*, **106**, 2924 -2930 (2002)

Experimental and Theoretical Investigations on the Methyl-Methyl Recombination Reaction, B. Wang, H. Hou, and C. Fockenberg, *J. Phys. Chem. A*, submitted (2002)

Quantitative Imaging Diagnostics for Reacting Flows

Jonathan H. Frank

Combustion Research Facility
Sandia National Laboratories, MS 9051
Livermore, CA 94551
jhfrank@ca.sandia.gov

Program Scope

The primary objective of this project is the development and application of laser-based imaging diagnostics for studying reacting flows. Imaging diagnostics provide temporally and spatially resolved measurements of species, temperature, and velocity distributions over a wide range of length scales. Multi-dimensional measurements are necessary to determine spatial correlations, scalar and velocity gradients, flame orientation, curvature, and connectivity. Our current efforts focus on planar laser-induced fluorescence (PLIF) and Rayleigh scattering techniques for probing the detailed structure of both isolated flow-flame interactions and turbulent flames. The investigation of flow-flame interactions is of fundamental importance in understanding the coupling between turbulence and chemistry in turbulent flames. These studies require the development of a new suite of imaging diagnostics to measure key species in the hydrocarbon-chemistry mechanism as well as to image rates of reaction and scalar dissipation.

Recent Progress

Recent research has continued to emphasize the development of diagnostics for probing the detailed structure of reaction zones during flow-flame interactions. The coupling of measurements with simulations also remains an essential element of this program. Research activities have included the following: i) Reaction-rate imaging with CO and OH PLIF in vortex-flame interactions and turbulent jet flames ii) A demonstration of simultaneous 2-D measurements of mixture fraction, temperature, and reaction-rate in turbulent jet flames. iii) An initial study of a new imaging diagnostic for vinyl (C_2H_3) and acetylene (C_2H_2) to provide insight into the C_2 branch of reaction pathways in rich premixed flames. iv) Investigation of vortex-flame interactions with a focus on the effects of stoichiometry and flow configuration.

Reaction-rate Imaging Joint CO/OH PLIF imaging was used to perform 2-D measurements of the forward reaction rate of the reaction $CO + OH \Rightarrow CO_2 + H$ in both repeatable flow-flame interactions and turbulent jet flames. The diagnostic technique uses simultaneous CO and OH PLIF to derive an image of the forward rate of the reaction $CO + OH \Rightarrow CO_2 + H$. This reaction represents the primary pathway for the formation of CO_2 in a methane-air flame. The basic concept of the diagnostic involves using the product of simultaneous OH and CO PLIF measurements to obtain a signal that is proportional to the reaction rate. Recently, we demonstrated instantaneous CO/OH reaction-rate imaging in turbulent partially premixed CH_4 /air jet flames with varying levels of local extinction. In the flames with little extinction, the reaction-rate diagnostic was coupled with the mixture-fraction/temperature imaging technique described below. These measurements will allow us to analyze the instantaneous structure of the reaction-rate field and should provide insight into turbulence-chemistry interactions.

Mixture Fraction and Temperature Imaging We performed an initial demonstration of a three-scalar technique for 2-D measurements of mixture fraction (ξ) and temperature in partially premixed flames using a combination of polarized and depolarized Rayleigh scattering and CO LIF. Mixture fraction is a fundamental quantity of interest in nonpremixed and partially premixed combustion. Scalar dissipation ($\chi = 2D|\nabla\xi|^2$) is a metric for the rate of molecular mixing, which is a critical parameter in nonpremixed and partially premixed flames. To determine scalar dissipation requires a measurement of mixture fraction gradients. Mixture fraction imaging in a single plane provides two components of the gradient. Mixture fraction can be determined by measuring all major species. However, it is impractical to do this in two dimensions. Mixture fraction imaging thus requires the identification of a subset of measurements that can provide an accurate measure of mixture fraction with enough signal for 2-D measurements. Previous efforts have focused on a two-scalar approach that combines Rayleigh scattering and fuel concentration measurements. A fundamental difficulty with this approach is that it is not very sensitive near stoichiometric conditions where the fuel signal disappears and the Rayleigh signal does not vary greatly as a function of mixture fraction. Methods for obtaining fuel concentration have included laser-induced fluorescence of fuel tracers and Raman scattering from fuel. However, the pyrolysis of fluorescent tracers results in signal loss well on the rich side of the reaction zone. Fuel Raman imaging yields quite modest signal levels because Raman scattering cross-sections are very weak. A more promising technique, which we are investigating in collaboration with Prof. Marshall Long at Yale University, uses depolarized and polarized Rayleigh scattering to measure fuel concentration. To further improve sensitivity of the mixture fraction measurement near stoichiometric, we are exploring the use of CO LIF, which provides a signal that is a relatively strong function of mixture fraction near stoichiometric conditions. In our initial investigations, we have demonstrated single-shot measurements in laminar and turbulent jet flames.

Development of C₂-Species Imaging Diagnostic We have completed the first stage of an investigation into a new imaging diagnostic tool for probing C₂ chemical reaction pathways in premixed flames. Current chemical reaction mechanisms for hydrocarbon combustion have significant uncertainties with regard to C₂ chemistry. Consequently, computations of the effects of flow-flame interactions on C₂ reactions have considerable limitations, and experimental measurements are needed. However, there is a lack of diagnostic techniques for imaging C₂ species. We are investigating a novel imaging technique using Swan-band emission from laser-generated C₂* in premixed methane-air flames. The first stage of the study has identified multi-photon laser-induced fragmentation fluorescence (LIFF) from vinyl (C₂H₃) and acetylene (C₂H₂) as the two possible sources of laser-generated C₂* emission. We performed measurements of laser-generated C₂* emission with excitation wavelengths near 230 nm in a low-pressure cell and considered seven different absorbing species: C₂H₂, C₂H₃, C₂H₄, C₂H₆, C₃H₆, C₄H₆, and CH₄. Results showed that photolysis of C₂H₃ is between 200 and 1300 times more efficient at generating C₂* emission than is photolysis of C₂H₂. The relative efficiency depends on the initial internal excitation of the vinyl radical, which was produced by 193-nm photolysis of methyl vinyl ketone (CH₃COC₂H₃). The possible mechanisms for C₂H₃ LIFF include competing two-photon and three-photon processes. For lower initial internal excitation, the three-photon process dominates. Acetylene LIFF occurs via a three-photon process. Vinyl photolysis is considerably more efficient than acetylene because the initial H-atom abstraction is a single-photon process for vinyl and a two-photon process for acetylene. These initial studies indicate

that it may be possible to obtain single-pulse PLIF images of vinyl radical that would offer unique information about the flux of carbon through C_2 pathways. Further experiments are needed to verify the technique at the elevated temperatures in flames.

Study of OH in Flame-Vortex Interaction Efforts to resolve observed differences between experimental and computational studies of flame-vortex interactions have included a series of measurements in both V-flames and counterflow flames. Recently, an axisymmetric counterflow burner was built to study the response of strained premixed flames to a toroidal vortex ring. This burner operates over a broad range of flame-vortex conditions, and its optical access allows the use of a variety of imaging diagnostics. In initial studies using OH PLIF, the response of the counterflow flame to a toroidal vortex was compared with that of a V-flame to a line vortex pair. Dramatic differences were observed in the two configurations for rich ($\phi=1.2$) premixed flames with N_2 dilution. The abrupt burst in OH that occurred as the line-vortex pair propagated into the V-flame was not observed in the counterflow flame. Instead, the OH level along the centerline of the toroidal vortex decreased by approximately a factor of 3.8 relative to the steady unperturbed flame. Similar results were obtained for a range of vortex strengths. Further experiments in the counterflow burner showed the following trends: In richer flames, the OH decrease along the centerline was less dramatic, and an OH increase was observed along the sides of the vortex wake. As the flame pinched off a pocket of unburned reactants, we observed a sudden increase in the OH level. In a lean flame ($\phi=0.6$), the OH levels were not significantly affected by the toroidal vortex. Differences in the evolution of the OH field for the two burner configurations indicates the sensitivity of transient flame response to the dynamics of the flow.

Future Plans

In the near term, we will continue to expand our suite of novel laser-based imaging diagnostics and apply these techniques to the study of flow-flame interactions in highly reproducible, building-block flames. We will investigate the extension of diagnostics to single-shot measurements in turbulent flames. This represents a first step towards our long-term goal of using imaging diagnostics to apply our understanding of building-block flames to turbulent flow-flame interactions. In all of these endeavors, we will strive to couple our experimental measurements with simulation and modeling efforts.

Reaction-rate Imaging We plan to continue the development and application of diagnostics that provide imaging measurements of reaction-rates. In the near future, our primary emphasis will be further developing the simultaneous CO/OH measurement technique to obtain the spatial distribution of the forward reaction rate of the $CO + OH \Rightarrow CO_2 + H$ reaction in both reproducible flow-flame interactions and turbulent flames.

Mixture Fraction We will expand our initial demonstration of simultaneous 2-D mixture-fraction and temperature measurements by implementing the technique in a wider range of turbulent jet flames and repeatable flow-flame interactions. The diagnostic technique will be further evaluated using comparisons with results from multiscalar point and line measurements performed in collaboration with R. Barlow. Further developments are needed to accurately determine scalar dissipation rates and to extend the technique to flames having localized extinction. We will consider issues of spatial resolution in determining gradients of mixture fraction.

C₂-Species Diagnostic We will extend our understanding of laser-induced fragmentation fluorescence (LIFF) of vinyl (C₂H₃) and acetylene (C₂H₂) to a flame environment by combining measurements from LIFF and a photoionization mass spectrometer in a low pressure flame. The mass spectrometer will provide quantitative measurements of the vinyl and acetylene profiles in the flame. These profiles will be compared with the 2-D LIFF measurements to gain an understanding of the LIFF photophysics and verify the diagnostic technique at flame temperatures. The mass spectrometer requires a vuv photo-ionization source that can span the ionization potentials of both vinyl and acetylene. Consequently, the experiments will be conducted at Lawrence Berkeley Laboratory's Advanced Light Source. This research will be performed in collaboration with A. McIlroy and D. Osborn.

Flame-Vortex Interactions In the near future, studies on flame-vortex interactions will focus on understanding differences between interactions of the V-flame with a line vortex and the counterflow flame with a toroidal vortex. The local stretch rate of the vortex will be measured using simultaneous OH PLIF and particle image velocimetry (PIV). We will map out the response of the counterflow flame to a toroidal vortex over a range of stoichiometries, dilution levels, strain rates, and vortex sizes. We will couple experiments with computations by H. Najm.

DOE Supported Publications

J. H. Frank, S. A. Kaiser, and M. B. Long, "Reaction-rate, Mixture Fraction, and Temperature Imaging in Turbulent Methane/Air Jet Flames," *Proc. Combust. Inst.* Vol. 29, accepted (2002).

J. Fielding, J. H. Frank, S. A. Kaiser, M. D. Smooke, and M. B. Long, "Polarized/Depolarized Rayleigh Scattering for Determining Fuel Concentrations in Flames," *Proc. Combust. Inst.* Vol. 29, accepted (2002).

C. M. Vagelopoulos and J. H. Frank, "Effects of Flow and Chemistry on OH Levels in Premixed Flame-Vortex Interactions," *Proc. Combust. Inst.* Vol. 29, accepted (2002).

D. L. Osborn and J. H. Frank, "Laser-induced Fragmentation Fluorescence Detection of the Vinyl Radical and Acetylene", *Chem. Phys. Lett.* 349:43 (2001).

R. S. Barlow, A. N. Karpetsis, J. H. Frank, and J.-Y. Chen, "Scalar Profiles and NO Formation in Laminar Opposed-Flow Partially-Premixed Methane/Air Flames," *Combust. Flame* 127:2102 (2001).

J. H. Frank, R. S. Barlow, and C. Lundquist, "Radiation and Nitric Oxide Formation in Turbulent Nonpremixed Jet Flames," *Proc. Combust. Inst.*, 28:447 (2000).

P. A. Nooren, M. Versluis, T. H. van der Meer, R. S. Barlow, and J. H. Frank, "Raman-Rayleigh-LIF Measurements of Temperature and Species Concentrations in the Delft Piloted Turbulent Jet Diffusion Flame," *Applied Phys. B* 71:95 (2000).

MECHANISM AND DETAILED MODELING OF SOOT FORMATION

Principal Investigator: Michael Frenklach

Department of Mechanical Engineering

The University of California

Berkeley, CA 94720-1740

Phone: (510) 643-1676; E-mail: myf@me.berkeley.edu

Project Scope: Soot formation is one of the key environmental problems associated with operation of practical combustion devices. Mechanistic understanding of the phenomenon has advanced significantly in recent years, shifting the focus of discussion from conceptual possibilities to specifics of reaction kinetics. However, along with the success of initial models comes the realization of their shortcomings. This project focuses on fundamental aspects of physical and chemical phenomena critical to the development of predictive models of soot formation in the combustion of hydrocarbon fuels, as well as on computational techniques for the development of predictive reaction models and their economical application to CFD simulations. The work includes theoretical and numerical studies of gas-phase chemistry of gaseous soot particle precursors, soot particle surface processes, particle aggregation into fractal objects, and development of economical numerical approaches to reaction kinetics.

Recent Progress:

A Quantum Monte Carlo Study of Energy Differences in C₄H₃ and C₄H₅ Radicals (with X. Krokidis, N. W. Moriarty, and W. A. Lester, Jr.)

Elucidation of reaction pathways and associated rates for the formation of aromatics in high-temperature pyrolysis and oxidation of hydrocarbons is currently one of the most active areas of research in gas-phase chemical kinetics. The primary focus is on the formation of the first aromatic ring from small aliphatics, because this step is perceived to be the rate-limiting step in the reaction sequence to larger aromatics and eventually soot. Arguments revolve around several possibilities. Among these are the even-carbon-atom pathways that involve the addition of acetylene to *n*-C₄H₃ and *n*-C₄H₅,



The former, reaction 1, was suggested to play a key role in the formation of the first aromatic ring on the basis of detailed kinetic simulations of shock-tube acetylene pyrolysis,¹ the result reiterated in subsequent kinetic studies. These numerical simulations also identified reaction 2, suggested by Bittner and Howard,² as playing a role at lower temperatures.³

Reactions 1 and 2 were dismissed by Miller and Melius,⁴ who suggested that *n*-C₄H₃ and *n*-C₄H₅ could not be present in sufficiently high concentrations because these radicals transform rapidly to their corresponding resonantly stabilized isomers, *i*-C₄H₃ and *i*-C₄H₅. Past numerical analysis revealed that Miller and Melius' conclusion on the C₄H₃ and C₄H₅ abundances originated, primarily, from the much lower stabilities predicted by BAC-MP4 for the *n* forms relative to the corresponding *i* forms of these radicals, which is especially pronounced in the case of the C₄H₃ isomers. The BAC-MP4 predictions for standard enthalpy differences between the *n*

and *i* forms are 12 kcal/mol for the C₄H₅ isomers and 19 kcal/mol for the C₄H₃ isomers.⁴ In contrast, the enthalpy differences in the initial kinetics studies¹ were assumed to be about 8 kcal/mol, based on estimates of Benson. The 8 kcal/mol difference was incorporated into the group-additivity scheme of Stephen Stein, which served as a consistent thermodynamic set for the initial kinetic modeling.

Recent quantum-mechanical studies report differences in the range of 7–14 kcal/mol for the *n*-C₄H₅ isomers, and raised the standard enthalpy of formation of the *n*-C₄H₃ radical to 134 kcal/mol, as compared to the previous estimates of 127 and 130 kcal/mol (for a complete list of references see Ref. 7 from the Publication list below).

We employed several ab initio quantum techniques, but mostly focused on the Diffusion Monte Carlo (DMC) method, which offers high accuracy. The latter resulted in enthalpies of formation of 126.0, 119.4, 83.4, and 76.2 kcal/mol for *n*-C₄H₃, *i*-C₄H₃, *n*-C₄H₅, and *i*-C₄H₅, respectively, all with one standard deviation of 0.6 kcal/mol. These results translate into enthalpy differences of 6.6±1.2 kcal/mol for C₄H₃, and 7.2±1.2 kcal/mol for C₄H₅ radicals, which are substantially lower than the prior theoretical predictions. The DMC results suggest higher stability for the *n* radicals, bringing the difference between the *n* and *i* isomers essentially back to the Benson estimates. The higher stability of *n*-C₄H₃ and *n*-C₄H₅ predicted by DMC “restores” the importance of reactions 1 and 2.

Carlo Simulation of Soot Particle Aggregation with Simultaneous Surface Growth (with P. Mitchell)

Mature soot particles appear as fractal-like aggregates randomly formed by branched chains of nearly spherical primary particles. Soot particle formation is initiated by homogeneous nucleation of precursors in the gas phase. Condensed phase material coalesces, leading to the formation of the first recognizable primary particles. The earliest visible particles are typically on order of 1–2 nm. After this initial stage, there is a transition from purely coalescent growth to aggregation. Aggregation is the process whereby emerging particles floc together forming the larger, more complex particle agglomerates. Particles also grow due to surface deposition. Gas-phase species, such as acetylene, “attach” themselves to the surface of the growing particles during both the coalescent and aggregation stages of coagulation. Surface growth adds a layer of mass on the soot particle surface thereby generating most of the solid-phase material. This growth mechanism encourages a rounder, more uniform shape, countering a portion of the geometric randomness added by aggregation, and in the extreme forming perfectly spheroidal particles. Formation of primary particles precedes that of aggregates. However, the transition between the two modes of growth is not well understood.

We investigated this transition using dynamic Monte-Carlo simulations. The simulations construct soot particles via ensemble-averaged collisions between small, geometrically perfect spheres. Simultaneously with the collisions, the particle sphere surfaces grow at a prescribed rate. The result is a union of overlapping spheres. A point sampling algorithm was implemented to compute particle center of mass, volume, surface area, fractal dimension, and radius of gyration.

Examination of the transition necessitated the development of shape descriptors to quantify the geometric differences between particles. The descriptors, that we call δ and Δ , were developed to accomplish this task. Descriptor δ was used to quantify a particle’s geometric proximity to either a perfectly round ball or a chain-like aggregate. For a given shape, Δ was

used to quantify a particle's rate of geometric change. Using this approach, we developed a working definition of the transition between coalescent coagulation and fractal aggregation. The developed theory was tested on several examples.

Nucleation of Soot: Molecular Dynamics Simulations of Pyrene Dimerization (with C. A. Schuetz)

Experimental and numerical studies indicate that particle coagulation plays an important role in soot formation. However, to date, neither method has been able to conclusively determine the stage at which chemical precursors begin to coalesce. In the present study, molecular dynamics (MD) with "on-the-fly" quantum forces was used to investigate binary collisions between pyrene molecules. In the present study, the semiempirical PM3 Hamiltonian was used as the interatomic multi-body potential. At each time step of MD simulation, self-consistent-field (SCF) convergence of the PM3 wave function was achieved, providing the potential energy and the interatomic forces of the system. The numerical integration was performed using the predictor of Beeman's predictor-corrector method. By using a simulation time-step of 0.5 fs, the total energy of the system was maintained constant to within ~1 kcal/mol per 10 ps of simulation time.

Most of the runs were performed at 1600 K, within the temperature window of soot nucleation in flames. The MD simulations were successful in producing dimers with substantial collisional frequency and lifetimes far exceeding the equilibrium-based predictions, thus demonstrating that pyrene dimerization is physically realistic in flame environments. The principal finding of the present study is the development of internal rotors by colliding pyrene molecules. This phenomenon is responsible for stabilization of the forming dimer. Analysis of the MD results shows that the mechanism of stabilization is rooted in the pattern of energy transfer. The translational energy of the individual colliding molecules is "trapped" in internal rotors that emerge upon collision, and in the vibrational modes of the dimer, including the van der Waals bond established between the pyrene molecules. This model extends the view of stabilization of aromatic species dimerization, with the implication that aromatic dimers of species as small as pyrene can survive long enough to evolve into soot nuclei.

Reference:

1. M. Frenklach, D. W. Clary, W. C. Gardiner, Jr, and S. E. Stein, *Proc. Combust. Inst.* **20**, 887 (1985).
2. J. D. Bittner and J. D. Howard, *Proc. Combust. Inst.* **18**, 1105 (1981).
3. M. Frenklach and J. Warnatz, *Combust. Sci. Technol.* **51**, 265 (1987).
4. J. A. Miller and C. F. Melius, *Combust. Flame* **91**, 21 (1992).

Future Plans

1. *Soot Chemistry*: In collaboration with William Lester's group we will continue ab initio quantum-chemical analysis of reactions that are critical to the development of kinetic models of aromatic growth. It is planned to continue the careful study of small aliphatic unsaturated radicals of combustion interest for which alternative methods have provided heats of formation and atomization energies of uncertain accuracy. For this effort, it is essential that the saturated parents of the radicals be computed to serve as benchmarks for accuracy assessment. It is planned to complete studies of C₄ systems and to follow with the study of selected C₅ species.

One aspect of the procedures followed in DMC molecular computations that must be carefully addressed is the specification of geometries at critical points of the potential energy surface. For example, the usual procedure is to obtain the equilibrium geometry from non-QMC approaches such as second-order Moller-Plesset perturbation theory (MP2) or a generalized gradient approximation density functional method such as B3LYP. Although much success has been achieved for the systems studied to date, for the radicals and novel bonding systems that are contemplated for study, it is important to have a technique that is not dependent on other methods. We plan to apply the design matrix method and assess its usefulness for this purpose.

2. *Particle Aggregation*: As the fundamental parameters controlling the transition from coalescent coagulation to fractal aggregation are now established, our next objective is to develop a model that captures the essential physics of the original Monte Carlo model but in a numerical form amenable to incorporation into the method of moments used in our soot model. We will test then the new soot model in a series of actual flame simulations.
3. *Homogeneous Nucleation of Carbon Nanoparticles*. We will continue molecular dynamics simulations with “on-the-fly” quantum forces, exploring wider ranges of initial conditions. Our next objective is to investigate collisions of different-size aromatics.

Publications

1. “Kinetic Modeling of Soot Formation with Detailed Chemistry and Physics: Laminar Premixed Flames of C₂ Hydrocarbons,” J. Appel, H. Bockhorn, and M. Frenklach, *Combust. Flame* **121**, 122–136 (2000).
2. “Scaling and Efficiency of PRISM in Adaptive Simulations of Turbulent Premixed Flames,” J. B. Bell, N. J. Brown, M. S. Day, M. Frenklach, J. F. Grcar, R. M. Propp, and S. R. Tonse, *Proc. Combust. Inst.* **28**, 107–113 (2000).
3. “On Unimolecular Decomposition of Phenyl Radical,” H. Wang, A. Laskin, N. W. Moriarty, and M. Frenklach, *Proc. Combust. Inst.* **28**, 1545–1555 (2000).
4. “The Dependence of Chemistry on the Fuel Inlet Equivalence Ratio in Vortex-Flame Interactions,” J. B. Bell, N. J. Brown, M. S. Day, M. Frenklach, J. F. Grcar, and S. R. Tonse, *Proc. Combust. Inst.* **28**, 1933–1939 (2000).
5. “Ab Initio Study Of Naphthalene Formation By Addition Of Vinylacetylene to Phenyl,” N. W. Moriarty and M. Frenklach, *Proc. Combust. Inst.* **28**, 2563–2568 (2000).
6. “Solution Mapping Approach to Modeling Combustion,” M. Frenklach, in *Computational Fluid and Solid Mechanics*, K. J. Bathe, Ed., Elsevier, New York, 2001, pp. 1177–1179.
7. “A Quantum Monte Carlo Study of Energy Differences in C₄H₃ and C₄H₅ Isomers,” X. Krokidis, N. W. Moriarty, W. A. Lester, Jr., and M. Frenklach, *Int. J. Chem. Kinet.* **33**, 808–820 (2001).
8. “Reaction Mechanism of Soot Formation in Flames,” *Phys. Chem. Chem. Phys.*, in press.
9. “Method of Moments with Interpolative Closure,” *Chem. Eng. Sci.*, in press.
10. “Nucleation of Soot: Molecular Dynamics Simulations of Pyrene Dimerization,” C. A. Schuetz and M. Frenklach, *Proc. Combust. Inst.* **29**, accepted for publication.

Multiresonant Spectroscopy and the High-Resolution Threshold Photoionization of Combustion Free Radicals

Edward R. Grant
Department of Chemistry
Purdue University
West Lafayette, IN 47907
edgrant@purdue.edu

Program Definition/Scope

In this research we apply methods of multiresonant spectroscopy and rotationally resolved threshold photoionization to characterize the structure, thermochemistry and intramolecular dynamics of excited neutrals and cations derived from combustion free radicals. The objectives of this work are: (1) To measure ionization potentials with wavenumber accuracy for a broad set of polyatomic molecules of relevance to combustion and combustion modeling; (2) To determine vibrational structure for cations as yet uncharacterized by ion absorption and fluorescence spectroscopy, including the study of anharmonic coupling and intramolecular vibrational relaxation at energies approaching thresholds for isomerization; (3) By threshold photoionization scans, referenced in double resonance to specific cation rovibrational states, to obtain information on originating-state level structure useful for the development of neutral-species diagnostics; (4) To measure rotationally detailed state-to-state photoionization cross sections for comparison with theory; and (5) To spectroscopically study near-threshold electron-cation scattering dynamics of relevance, for example, to plasma processes such as dissociative recombination, by acquiring and analyzing rotationally resolved high-Rydberg spectra.

Recent Progress

Bend-Stretch Fermi Resonance in DCO⁺

Perturbations in the positions of higher vibrational states of polyatomic molecules confer information on the anharmonic properties of vibrational potentials that permit energy to flow between zeroth-order normal modes. Such details represent a challenge to theory in efforts to predict rates from *ab initio* calculations. Before our studies, there were no measurements on the positions of higher vibrationally excited states of either HCO⁺ or DCO⁺, but conjectures on anharmonicity were possible based on perturbations in rotational constants.

Now, with double-resonant Rydberg extrapolations that rotationally resolve limits associated with the bending-excited levels (030) and (040), we have direct information on the structure of the bend. Analysis of the rovibrational structure derived from the positions of the (030) thresholds fits with a simple parameterization extended from lower vibrational levels. For (040), however, we find that the vibrational angular momentum components (04⁰0) and (04²0) are *inverted* in energy, with the (04⁰0) component displaced approximately 20 cm⁻¹ to a position above that of (04²0). We interpret this perturbation to support a conjecture by Hirota that the vibrational structure of DCO⁺ is perturbed by a 4:1 bend-stretch Fermi resonance. Extending the pattern by which vibrational angular momentum components are split in (020) and (030), we can establish the unperturbed

position of (04⁰0), from which we estimate the matrix element for bend-stretch coupling. Analysis yields a moderate Fermi matrix element, $W_{(04^0 0)(10^0 0)}$, of 32.43 cm⁻¹, which is about two-thirds the magnitude of coupling found in the systems, CO₂ and NO₂⁺, where bend-stretch mixing significantly affects the character of higher vibrationally excited states.

Ion-dip absorption spectroscopy of the A ²A" State of HCO

Double-resonance spectroscopy has provided us with a great deal of information about the structure and thermochemistry of the formyl radical and its cation. The convergence of rovibrationally resolved Rydberg series isolated in transitions from single photoselected intermediate states determine state-to-state ionization energies of the radical as well as anharmonic properties of the vibrational potential of the formyl cation, including the characterization of a relatively strong quintic bend-stretch Fermi resonance in DCO⁺.

We can gain much more information on the anharmonic coupling of vibrational modes in HCO⁺/DCO⁺ if we extend our spectroscopic measurements to higher excited states. In principle, the way to achieve this is clear: In order to resolve series that converge to any vibrational limit of the formyl cation we need only to prepare the corresponding gateway level of the 3pπ ²Π intermediate Rydberg state. The main obstacle we face is a practical one. Levels above 3pπ ²Π (030) in HCO and (040) in DCO lie beyond the wavelength limit of simple frequency doubling. Access to a subset of these states is further challenged by poor Franck-Condon factors for bent-to-linear transitions: No levels excited in ν₁ have been observed in the 3pπ spectrum of either HCO or DCO. The CO-stretch fundamental is weak in HCO and unobserved for DCO. Shorter wavelengths can be prepared by sum-frequency mixing, and we are currently pursuing this strategy. However, higher first-photon energy does not help to overcome unfavorable Franck-Condon factors.

We have embarked on a more general approach. Our goal is to open a wide new range of higher excited states, within which we will be able to measure levels that will challenge the power of contemporary theory to capture essential details in the properties of anharmonic vibrational potentials. NO₂ provides a good model. First-photon absorption in the B ²B₂ ← X ²A₁ system of this molecule selects a single rotational level in an intermediate state of strongly mixed vibronic character. From each such photoselected state, there exists a very broad Franck-Condon envelope for transitions to the linear 3pσ ²Σ_u⁺ Rydberg state extending from (000) to higher levels of vibrational excitation in all three normal coordinates.

The same opportunity exists to span a broad range of bent-to-linear transitions for HCO and DCO. In analogy with NO₂, the low-lying A ²A" electronic state of the formyl radical forms a Renner-Teller pair with the X ²A' ground state. We plan to test the feasibility of executing double resonance transitions to stretching and higher excited bending levels of the 3pπ ²Π Rydberg state in this system as the first steps of an ultimate three-color triple-resonance strategy for isolating high-Rydberg series that converge to corresponding levels of the cation.

We have begun experiments to establish ²A" levels suitable for double resonance. Promising candidates have been observed in laser-induced fluorescence. This system has been well studied by a variety of other spectroscopic techniques, including four-wave mixing and photofragment excitation, as well as optogalvanic spectroscopy. All levels accessed in visible absorption predissociate with lifetimes varying from tens of picoseconds to hundreds of femtoseconds.

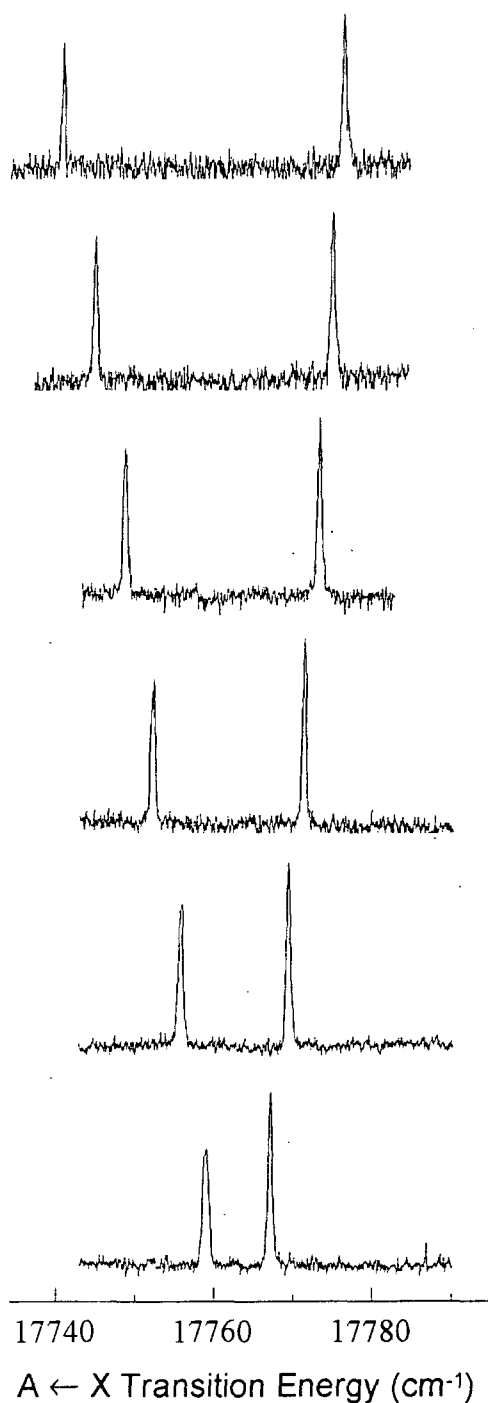


Figure 5 Ion dip spectra of the $A^2A''(0110) \leftarrow X^2A'(000)$ transition in HCO for a series of selected initial rotational states from $N'' = 1-6$

To identify $A^2A'' \leftarrow X^2A'$ transitions in our apparatus, we have performed ion-dip experiments. Tuning an ionization laser to transitions in the $3p\pi^2\Pi(030) \leftarrow X^2A'$ system, we dip the ion signal by pumping transitions from the selected X^2A' level to the A^2A'' state. Figure 1 to the right shows a sequence of scans over $A^2A''(011^00) \leftarrow X^2A'(000)$ for $3p\pi^2\Pi(030) \leftarrow X^2A'$ resonant ionization transitions fixed on initial rotational quantum numbers N'' from 0 to 9. These lines associated with an odd bending level of the $^2A''$ state appear comparatively sharp because predissociation to the underlying A' continuum requires indirect K-type and Coriolis coupling. Lifetimes determined by high-resolution observations lie in the range of tens of picoseconds. By comparison, Figure 2 below shows a spectrum of the $A^2A''(010^10) \leftarrow X^2A'(000)$ band recorded from the $N''=1$ level of the ground state. The simulations represent Lorentzians reflecting lifetimes of 150 fs.

Double resonance with the $A^2A''(0110)$ state offers a feasible means to populate higher bending excited levels of the $3p\pi^2\Pi$ state. From the measured lifetime, we can estimate that temporally overlapped 5 ns lasers will effect population transfers within a factor of 100 as large as those that could be achieved by one-photon excitation. Favorable Franck-Condon factors could well improve the effectiveness of this spectroscopic route, as will the reduction in non-resonant background that can be expected using longer wavelength light sources. In practice, however, our preliminary experiments have shown that required second photon frequencies produce background signal from ionization of our acetaldehyde precursor. The use of H_2CO should yield no such contaminating signal. We are developing a novel H-atom abstraction source to use as a means for efficiently generating HCO radicals from this precursor.

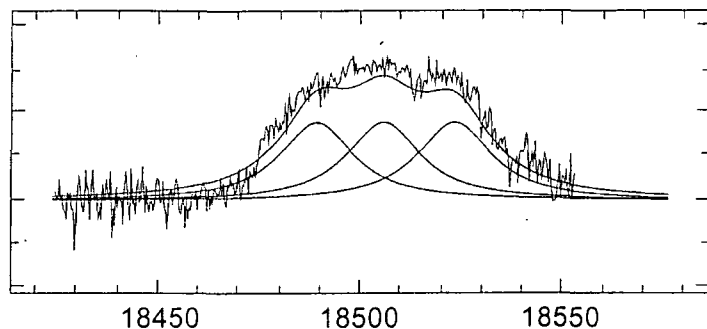


Figure 2 Ion dip spectra of the $A \leftarrow X$ ${}^2A''(0\ 12\ 0) \leftarrow X\ {}^2A'$ transition in HCO for an initial rotational states, $N'' = 6$. Simulations use $(0\ 11\ 0)$ rotational constants with Lorentzian widths corresponding to lifetimes of 150 fs.

$A \leftarrow X$ Transition Energy (cm^{-1})

References to publications of DOE sponsored research (2000-2002)

Experimental Characterization of the Higher Vibrationally Excited States of HCO^+ : Determination of ω_2 , x_{22} , g_{22} and $B_{[030]}$, R. J. Foltynowicz, J. D. Robinson, E. J. Zückerman, H. G. Hedderich and E. R. Grant, *J. Mol. Spectrosc.* **199**, 147-157 (2000).

Double-resonant photoionization efficiency (DR/PIE) spectroscopy: A precise determination of the adiabatic ionization potential of DCO, R. J. Foltynowicz, J. D. Robinson and E. R. Grant, *J. Chem. Phys.* **114**, 5224 (2001).

An experimental measure of anharmonicity in the bending of DCO^+ , J. D. Robinson, R. J. Foltynowicz and E. R. Grant, *J. Chem. Phys.* **114**, 878 (2001).

The $A\ {}^1\Pi \leftarrow X\ {}^1\Sigma^+(2,0)$ Transition in ${}^{11}\text{BH}$ and ${}^{10}\text{BH}$ Observed by (1+2)-Photon Resonance-Enhanced Multiphoton Ionization Spectroscopy, J. Clark, M. Konopka, L.-M. Zhang and E. R. Grant, *Chem. Phys. Lett.* **340**, 45 (2001).

Bend-Stretch Fermi Resonance in DCO^+ , J. D. Robinson, R. J. Foltynowicz, K. Prentice, P. Bell and E. R. Grant, *J. Chem. Phys.* **116**, 2370 (2002).

Laser-assisted (1+1')-photon ionization-detected absorption spectrum of the $3p\pi\ {}^2\Pi$ state of HCO and DCO, R. J. Foltynowicz, J. D. Robinson, K. Prentice, P. Bell and E. R. Grant, *J. Chem. Phys.* **116**, xxx (2002).

CHEMICAL DYNAMICS IN THE GAS PHASE: QUANTUM MECHANICS OF CHEMICAL REACTIONS

Stephen K. Gray
Gas Phase Chemical Dynamics Group, Chemistry Division
Argonne National Laboratory
Argonne, IL 60439

E-mail: gray@tcg.anl.gov

PROGRAM SCOPE

This work emphasizes the development and application of accurate quantum mechanical approaches for chemical reaction dynamics. Much of the work involves time-dependent or iterative quantum methods that, in addition to computational simplifications, can yield mechanistic insight. Applications to gas phase systems of current experimental interest, and of relevance to combustion, are emphasized. The calculations also allow one to assess the quality of the underlying potential energy surfaces and the reliability of approximate theoretical approaches such as classical trajectories and transition state theory.

RECENT PROGRESS

Accurate quantum dynamics calculations often involve representing the wavefunction or wave packet on a configuration space grid. The evaluation of the action of the Hamiltonian operator on the wavefunction, which is carried out many times in a typical calculation, is the major computational bottleneck to obtaining reaction probabilities and rate constants. The kinetic energy contribution to this action, which generally involves second derivatives, should be as efficient as possible. Simple finite difference (FD) methods are quite efficient for estimating the kinetic energy contribution, scaling linearly with the number of grid points. Moreover, FD methods are also very amenable to the high performance, parallel computing environment, suggesting that difficult, four-atom and larger systems might be more readily tackled from this perspective. Unfortunately, very small grid spacings are often required to achieve acceptable accuracy, which tends to nullify the potential advantages. As a consequence, most applications have involved either the fast Fourier transform (FFT) method, or related pseudospectral or discrete variable representations (DVRs) to provide approximations to the kinetic energy operator action. These approaches are highly accurate and can often be very efficiently implemented in traditional (one-processor) computing environments. However, they are not as amenable to parallelization. In collaboration with Goldfield, a new approach to finite difference approximation, called the dispersion fitted finite difference (DFFD) method, was developed [1]. It retains all the simplicity and ease of parallelization of ordinary FD methods, but improves (often by orders of magnitude) the accuracy of the underlying kinetic energy operator approximation. The idea is to consider the momentum (or Fourier) representation of the FD second derivative approximation, and design the coefficients of the method such that this momentum representation is a good approximation, to some pre-specified accuracy, of the correct one. The resulting DFFD methods are just like ordinary FD ones, except that the coefficients in the derivative approximations are different. It was demonstrated that these

methods can be of comparable accuracy and efficiency to the FFT method, and that they are much more efficient (for comparable accuracy) than most other DVR methods.

The real wave packet (RWP) method [2] was applied to understand the dynamics of several triatomic systems. The nature of unimolecular resonances in H_2O was explored with Goldfield [3]. The $\text{O}(^1\text{D}) + \text{HCl} \rightarrow \text{OCl} + \text{H} / \text{OH} + \text{Cl}$ reaction was examined with a high quality *ab initio* surface in work with Balint-Kurti and co-workers [4]. These calculations represent the first state-to-state quantum reactive scattering calculations for this atmospherically important chemical system. Branching ratios for the OCl vs OH product channels were obtained and agreed reasonably well with experimental results. The calculated vibrational state product distributions were also in reasonable accord with experiment, indicating an inverted OH vibrational state distribution. The first three-dimensional, fully quantum mechanical study the $\text{N}(^4\text{S}) + \text{O}_2(\Sigma_g^-) \rightarrow \text{NO}(^2\Pi) + \text{O}(^3\text{P})$ reaction, important in both combustion and atmospheric chemistry, was carried out with Petrongolo and co-workers [5]. Reactant state resolved reaction probabilities and cross sections, as well as thermal rate constants, were estimated. The reaction mechanism, which involves short-lived NOO intermediates, was explicitly mapped out by inspection of the evolving wave packet. The calculations also serve to confirm a previously proposed mixed quantum/classical model for the reaction, and indicate that variational transition state theory can exhibit significant errors for temperatures less than 500K.

The RWP approach [2], coupled with the use of DFFD approximations [1] and certain angular grid representations [6] allowed the construction of an efficient four-atom reactive scattering code [7]. As a non-trivial illustration, Goldfield and I also carried out extensive wave packet calculations on the $\text{H}_2 + \text{OH} \rightarrow \text{H}_2\text{O} + \text{H}$ reaction, with the recent, *ab initio* based potential surface of Wu and co-workers [8]. Rate constants were obtained and compared with experiment and transition state theory.

FUTURE PLANS

Our future work will focus on more challenging, four-atom and larger chemical reaction systems, extending the preliminary work we have already accomplished on the $\text{H}_2 + \text{OH}$ reaction [7]. In terms of methodology, we will develop efficient, parallel versions of our wave packet codes that will allow us to study the quantum dynamics of such systems. We will also work on hybrid or more approximate techniques for obtaining quantum mechanical information about the reaction dynamics.

We will begin to assess the role of entrance channel complexes on the $\text{OH} + \text{CO} \rightarrow \text{CO}_2 + \text{H}$ reaction using our new four-atom scattering code [8], high performance parallel computing techniques [6], and a recent potential energy function that includes the entrance channel wells [9]. We hope to obtain accurate, quantum mechanical rate constants for this important combustion reaction. We also plan to analyze aspects of the entrance channel complexes and correlate with recent experiment and theory of Lester and co-workers [10]. We will also continue to examine important triatomic systems, including aspects of the $\text{H} + \text{O}_2$ and $\text{N} + \text{O}_2$ reactions with our wave packet methodologies.

References

- [1] S. K. Gray and E. M. Goldfield, *J. Chem. Phys.* **115**, 8331 (2001).
- [2] S. K. Gray and G. G. Balint-Kurti, *J. Chem. Phys.* **108**, 950 (1998).
- [3] S. K. Gray and E. M. Goldfield, *J. Phys. Chem. A* **105**, 2634 (2001).
- [4] V. Piermarini, G. G. Balint-Kurti, S. K. Gray, F. Gögtas, A. Laganà* and M. L. Hernández, *J. Phys. Chem. A* **105**, 5743-5750 (2001).
- [5] P. Defazio, C. Petrongolo, S. K. Gray, and C. Oliva, *J. Chem. Phys.* **115**, 3208-3214 (2001).
- [6] E. M. Goldfield, *Comput. Phys. Comm.* **128**, 178 (2000).
- [7] E. M. Goldfield and S. K. Gray, *J. Chem. Phys.*, *submitted* (2002).
- [8] G. Wu, G. C. Schatz, G. Lendvay, D.-C. Fang, and L. B. Harding, *J. Chem. Phys.* **113**, 3150 (2000).
- [9] D. Troya, M. J. Lakin, G. C. Schatz, and M. Gonzalez, *J. Chem. Phys.*, *submitted* (2002).
- [10] M. I. Lester, B. V. Pond, D. T. Anderson, L. B. Harding, and A. F. Wagner, *J. Chem. Phys.* **113**, 9889 (2000).

PUBLICATIONS, S. K. Gray (2000-2002)

1. K. M. Forsythe and S. K. Gray, A transition state real wavepacket approach for obtaining the cumulative reaction probability, *J. Chem. Phys.* **112**, 2623-2633 (2000).
2. S. Nanbu, S. K. Gray, T. Kinoshita and M. Aoyagi, Theoretical study of the potential energy surfaces and bound states of HCP, *J. Chem. Phys.*, **112**, 5866-5876 (2000).
3. S. Skokov, T. Tsuchida, S. Nanbu, J. M. Bowman, and S. K. Gray, A comparative study of the quantum dynamics and rate constants of the $O(^3P) + HCl$ reaction described by two potential surfaces, *J. Chem. Phys.* **113**, 227-236 (2000).
4. S. K. Gray, G. G. Balint-Kurti, G.C. Schatz, J. J. Lin, X. Liu, S. Harich, and X. Yang, Probing the effect of H_2 rotational state in $O(^1D) + H_2 \rightarrow OH + H$: Theoretical dynamics including nonadiabatic effects and a crossed molecular beam study, *J. Chem. Phys.* **113**, 7330-7344 (2000).
5. M. Hankel, G. G. Balint-Kurti, and S. K. Gray, Quantum mechanical calculation of product state distributions for the $O(^1D) + H_2 \rightarrow OH + H$ reaction on the ground electronic state surface, *J. Chem. Phys.* **113**, 9658-9667(2000).
6. S. K. Gray, B. G. Sumpter, D. W. Noid, and M. D. Barnes, Quantum mechanical model of localized electrons on the surface of polymer nanospheres, *Chem. Phys. Lett.* **333**, 308-313 (2001).

7. M. Hankel, G.G. Balint-Kurti, and S. K. Gray, Quantum mechanical calculation of reaction probabilities and branching ratios for the $O(^1D) + HD \rightarrow OH(OD) + D(H)$ reaction on the $1A'$ and $1A''$ adiabatic potential energy surfaces, *J. Phys. Chem. A* **105**, 2330-2339 (2001).
8. S. K. Gray and E. M. Goldfield, Highly excited bound and low-lying resonance states of H_2O , *J. Phys. Chem. A* **105**, 2634-2641 (2001).
9. V. Piermarini, G. G. Balint-Kurti, S. K. Gray, F. Gögtas, A. Laganà* and M. L. Hernández, Wave packet calculation of cross sections, product state distributions, and branching ratios for the $O(^1D) + HCl$ reaction, *J. Phys. Chem. A* **105**, 5743-5750 (2001).
10. K. M. Forsythe, S. K. Gray, S. J. Klippenstein, and G. E. Hall, An *ab initio* molecular dynamics study of S_0 ketene fragmentation, *J. Chem. Phys.* **115**, 2134-2145 (2001).
11. P. Defazio, C. Petrongolo, S. K. Gray, and C. Oliva, Wave packet dynamics of the $N(^4S) + O_2 \rightarrow NO + O$ reaction on the X^2A' potential energy surface, *J. Chem. Phys.* **115**, 3208-3214 (2001).
12. S. K. Gray and E. M. Goldfield, Dispersion fitted finite difference method with applications to molecular quantum mechanics, *J. Chem. Phys.* **115**, 8331-8344 (2001).
13. M. Hankel, G. G. Balint-Kurti, and S. K. Gray, Sinc wavepackets: A new form of wavepacket for time-dependent quantum mechanical reactive scattering calculations, *Int. J. Quant. Chem.*, *in press* (2002).

SKG was supported by the Office of Basic Energy Sciences, Division of Chemical Sciences, Geosciences, and Biosciences, U.S. Department of Energy under Contract No. W-31-109-ENG-38

Computer-Aided Construction of Chemical Kinetic Models

William H. Green, Jr., MIT Department of Chemical Engineering,
77 Massachusetts Ave., Cambridge, MA 02139. email: whgreen@mit.edu

Project Scope

The combustion chemistry of even simple fuels can be extremely complex, involving hundreds or thousands of kinetically significant species. The most reasonable way to deal with this complexity is to use a computer not only to numerically solve the kinetic model, but also to construct the kinetic model in the first place. We are developing the methods needed to make computer-construction of accurate combustion models practical, as well as tools to make it feasible to handle and solve the resulting large kinetic models.

Our work during this grant period has focused on: 1) development of improved rapid reaction rate estimation techniques suitable for systems involving many large molecules, 2) methods for automating $k(T,P)$ calculations while building mechanisms with a computer, 3) development of a new "Adaptive Chemistry" method for coupling complex chemical kinetics into flame simulations, and 4) "Valid Range Analysis", i.e. methods for identifying the range of reaction conditions over which a kinetic model is valid.

Recent Progress

1. TS Group Additivity for Reaction Rate Estimates

Often the accuracy of combustion simulations is constrained primarily by the accuracy of the high-pressure-limit rate parameters employed. It is unlikely that either experiment or high-quality quantum calculations will be able to provide the very large number of rate constants needed. Instead, we are generalizing from a limited number of quantum calculations and experimental data, using the concept of functional groups. Benson's group additivity scheme very accurately describes thermochemical properties for stable species; we are extending this approach to predict the transition state properties (e.g. the free-energy of activation, needed to compute reaction rates). Our group additivity predictions are within 40% of the dozens of individual quantum (CBS-Q, canonical TST, Wigner tunneling) rates we have tested over the whole T range. One advantage of our approach over the more conventional linear free-energy relationship (LFER) approach is that group-additivity naturally predicts Arrhenius plot curvature. Our quantum-based group additivity estimates for H-abstraction reactions are generally within a factor of 5 of the best literature rates above 500 K.

We have published a few dozen transition-state group values for alkanes, and have developed non-nearest-neighbor corrections which allow this method to be accurate for reactions with polar and unsaturated substituents. We have summarized this work in three recent articles [8,9,12], and have submitted a fourth article to *Theoretical Chemistry Accounts*.

2. Automated $k(T,P)$ Calculations

We have continued to develop computer algorithms and software for rapidly and accurately computing $k(T,P)$ during computerized model construction.[1,6,7] This

involves using an accurate screening technique to compute only the isomerizations and dissociation channels which are numerically significant. We applied these techniques to a variety of reactions through chemically activated cycloalkyl radicals, where hundreds of wells and product channels were energetically accessible, and where experimental data was available for detailed comparison. We recently completed the integration of these screened $k(T,P)$ calculations into kinetic model generation software, and are now constructing hydrocarbon combustion models which for the first time account for the pressure-dependence effects on all the reactions.

Most of our $k(T,P)$ software development was done in collaboration with Jeff Grenda and Tony Dean of ExxonMobil, with financial support from a DOE Academic-Industrial partnership award. (Tony Dean is now at Colorado School of Mines.) Applications of these $k(T,P)$ calculation methods to aromatic hydrocarbon reactions [2-5] were done in collaboration with Jack Howard.

3. Adaptive Chemistry & Numerics for Reacting Flow Simulations

Reacting flow simulations are most valuable for reactors/combustors with large concentration or temperature gradients, where one expects the chemistry to be dramatically different in different spatial regions (or at different times in a dynamic simulation). However, currently most reacting flow simulations are performed using the same chemistry model at all mesh positions and at all times. These calculations typically require a very large amount of CPU time and computer memory, limiting most reacting-flow simulations of hydrocarbon combustion to oversimplified chemical kinetic models.

Computational efficiency without sacrificing chemical accuracy is possible by 'adapting' the chemistry model to the local reaction conditions in much the same way that modern simulations use adaptive time-steps and adaptive mesh refinement. The idea in all three cases is to use a lot of detail when it is necessary, but to use a less-detailed description whenever possible without sacrificing accuracy. Our Adaptive Chemistry [11] approach of ignoring chemical species where they are insignificant is very advantageous, since the best available methods for solving the kinetic equations and for computing the multicomponent diffusion coefficients both scale super-linearly with the number of chemical species considered. A paper detailing the methodology and presenting several applications has recently been submitted to *Combustion and Flame*.

In our quest to reduce the CPU time required to solve large combustion models, we have also developed a numerical method taking advantage of advances in sparse linear algebra and automatic differentiation technology. This approach reduces the CPU time required to solve the LLNL n-heptane model by a factor of 60, making it practical to use this type of very detailed model in rather complex simulations.[10]

4. Valid Range Analysis and Model Reduction

In any method that uses or generates multiple kinetic models, one is faced with the problem of identifying which kinetic model is valid for which reaction conditions. We have submitted the first paper that identifies a valid range for an arbitrary kinetic model to *Chemical Engineering Science*. We have also developed a computer program which identifies the smallest valid reduced model for a set of user-specified reaction conditions that it is possible to obtain by eliminating reactions, and used this to develop a reduced

model library for use in Adaptive Chemistry simulations. This work on optimal model reduction has recently been submitted to *Combustion and Flame*.

Future Plans

We will publish a database of high-pressure-limit reaction-family rate estimation rules. For kinetic models with thousands of reactions, it is more reasonable to compare these rules than to try to compare each reaction rate individually. Many of these rate estimates will be derived from the TS group additivity approach described above. Comparisons will be made with rate estimation rules already in the literature. We will also develop new thermochemical groups as required using high-level quantum chemistry and advanced models for hindered internal rotation.

We will also take existing large combustion mechanisms, and compute their pressure-dependencies and their valid ranges, so that users will know where these models can be used reliably. As part of this work, we will develop criteria to determine when a large-molecule reaction will be in the high-pressure-limit, and when a $k(T,P)$ calculation is necessary.

The rate estimation rules and automated $k(T,P)$ calculations will be coupled with computerized model-generation software to construct new combustion chemistry models, with larger valid ranges than existing models.

We will also develop the "Adaptive Chemistry" technique into a flexible software library which can be called by a variety of computational fluid dynamics codes. This software will include automated model reduction and valid range analysis tools, and software to facilitate control of model-truncation error.

Publications Resulting from DOE Sponsorship (Since 2000)

1. David M. Matheu & William H. Green, "A priori Falloff Analysis for OH + NO₂", *Int. J. Chem. Kinetics* **32**, 245-262 (2000).
2. Joanna L. DiNaro, Jack B. Howard, William H. Green, Jefferson W. Tester, and Joseph W. Bozzelli, "Analysis of an Elementary Reaction Mechanism for Benzene Oxidation in Supercritical Water", *Proc. Combust. Inst.* **28**, 1529-36 (2000).
3. J.L. DiNaro, J.B. Howard, W.H. Green, J.W. Tester, & J.W. Bozzelli, "Elementary Reaction Mechanism for Benzene Oxidation in Supercritical Water", *J. Phys. Chem. A* **104**, 10576-86 (2000).
4. H. Richter, T.G. Benish, O.A. Mazzyar, W.H. Green, and J.B. Howard, "Formation of Polycyclic Aromatic Hydrocarbons and their Radicals in a Nearly Sooting Premixed Benzene Flame", *Proc. Combust. Inst.* **28**, 2609-18 (2000).
5. H. Richter, O.A. Mazzyar, R. Sumathi, W.H. Green, J.B. Howard, and J.W. Bozzelli, "Detailed Kinetic Study of the Growth of Small Polycyclic Aromatic Hydrocarbons. I. 1-Naphthyl + Ethyne", *J. Phys. Chem. A* **105**, 1561-73 (2001).
6. W.H. Green, P.I. Barton, B. Bhattacharjee, D.M. Matheu, D.A. Schwer, J. Song, R. Sumathi, H.H. Carstensen, A.M. Dean, & J.M. Grenda, "Computer-Construction of Detailed Models for Gas-Phase Reactors", *Ind. Eng. Chem. Res.* **40**, 5362-5370 (2001).

7. David M. Matheu, Thomas A. Lada II, William H. Green, Anthony M. Dean, and Jeffrey M. Grenda, "Rate-Based Screening of Pressure-Dependent Reaction Networks", *Computer Physics Communications* **138**, 237-249 (2001).
8. Raman Sumathi, Hans-Heinrich Carstensen, and William H. Green, Jr. "Reaction Rate Prediction via Group Additivity, Part 1: H Abstraction from Alkanes by H and CH₃", *Journal of Physical Chemistry A* **105**, 6910-6925 (2001).
9. R. Sumathi, H.-H. Carstensen, and W.H. Green, "Reaction Rate Prediction via Group Additivity, Part 2: H Abstraction from Alkenes, Alkynes, Alcohols and Acids by H atoms", *Journal of Physical Chemistry A* **105**, 8969-8984 (2001).
10. D.A. Schwer, J.A. Tolsma, W.H. Green, and P.I. Barton, "On Upgrading the Numerics in Combustion Chemistry Codes", *Combust. Flame* **128**, 270-291 (2002).
11. William H. Green, Jr. and Douglas A. Schwer, "Adaptive Chemistry", in *Computational Fluid and Solid Mechanics: Proceedings of the First MIT Conference on Computational Fluid and Solid Mechanics, June 12-15, 2001*, ed. by K.J. Bathe (Elsevier, 2001).
12. R. Sumathi, H.-H. Carstensen, and W.H. Green, "Reaction Rate Prediction via Group Additivity, Part 3: Effect of Substituents with CH₂ as the Mediator", *J. Phys. Chem. A* (accepted).

SPECTROSCOPY AND DYNAMICS OF MOLECULAR FREE RADICALS

Gregory E. Hall (gehall@bnl.gov), Trevor J. Sears (sears@bnl.gov) and Arthur G. Suits (agsuits@bnl.gov)

Department of Chemistry, Brookhaven National Laboratory, Upton, NY 11973-5000

PROGRAM SCOPE

This research is carried out as part of the Gas Phase Molecular Dynamics group program in the Chemistry Department, Brookhaven National Laboratory. The goal is a fundamental understanding of factors affecting the structure, dynamics and chemical reactivity of short-lived intermediates in gas phase reactions. Sensitive, high resolution, optical and mass spectroscopic methods are developed and used to characterize and monitor transient species and gas phase reactions. Molecular beam and imaging techniques complement the optical studies and are applied to photo-induced unimolecular and bimolecular reactions. Aspects of the program focused on reaction kinetics and theory are highlighted in separate abstracts [C. Fockenberg and J. Preses, and J. Muckerman].

RECENT PROGRESS

Small carbenes have been a focus of several inter-related recent studies. Continuing near-infrared spectroscopic studies have provided a library of assignments that are essential for the dynamical studies of product state correlations and energy transfer. New theoretical approaches have been developed for the rovibronic problem of large amplitude motion in combination with the Renner effect, using substituted carbenes as a test case. Ion imaging studies of the CO product in coincidence with CH₂ are providing a view of the product state correlations in ketene dissociation complementary to our recent Doppler measurements of CH₂. Rotational energy transfer, collision induced intersystem crossing and chemical reaction of singlet CH₂ all compete during the first few collisions with Ar and ketene following the near ultraviolet dissociation of ketene at low pressures. Direct evidence for the importance of a few strongly mixed singlet-triplet rotational states, acting as "doorway states" for intersystem crossing, is obtained from the state-resolved kinetics, which probe the pre-steady-state regime of the master equation governing the relaxation. These studies are relevant to the use of ketene photodissociation in a jet-cooled singlet CH₂ source for crossed beam reaction studies by F. Davis [Cornell]. Finally, flow tube kinetics studies have recently been performed on some triplet CH₂ reactions, as described in another abstract [Fockenberg and Preses].

A new theoretical approach has been developed to treat the Renner-Teller effect in triatomic molecules, based on hyperspherical coordinates and an approximate adiabatic treatment of K, the projection of total angular momentum on the principal A axis. The method has been demonstrated for the case of HCB_r, where *ab initio* electronic structure calculations and high resolution spectroscopic results have been combined with the new dynamical treatment to give an accurate picture of the rovibronic structure. Alternate state-of-the-art theoretical approaches to this problem had failed, since sufficiently accurate analytic fits to the potential surface could not be found. The present grid-based formulation does not require fitting a potential.

The lowest energy singlet-singlet electronic transition in unsymmetrical carbenes, such as HCCl and HCB_r, is a perpendicular transition, yet one observes both parallel and perpendicular sub-bands. Classic work by Hougen and Watson explained the intensities of such "forbidden" parallel rovibronic bands as arising from an effect they called axis switching, which is related to a change in the reference geometry that is used to define the molecule-fixed axis system by the Eckart conditions. In spectra recorded previously, the parallel sub-bands appeared to be stronger than predicted on the basis of the usual theory. The additional influences of Coriolis mixing,

anharmonicity, and complications due to low frequency vibrational motion could in principle contribute, and we sought an example in which the geometrical structure of ground and excited states could be spectroscopically determined, fixing the axis-switching part of the problem. New spectra of allowed and forbidden near-infrared rovibronic bands in chloro-methylene were recorded for this purpose. $K=0-1$ and $K=0-0$ sub-bands of the $\tilde{A}''(0,1,0) - \tilde{X}'A'(0,0,0)$ transition have been assigned for four isotopomers of HCCl, while the $\tilde{A}(0,0,0) - \tilde{X}(0,0,0)$ was measured for the two chlorine isotopomers of the protonated species. The J-dependent relative intensities were measured for subsequent comparison with theory. The parallel band intensities derive from a combination of axis-switching and c-type Coriolis coupling. When both mechanisms were included in a model of the spectral intensities, satisfactory agreement with the experimental measurements was obtained for all the measured bands. The Coriolis contributions are small for these bands, but can add to or subtract from the axis-switching.

The reactions of ground state oxygen atoms with saturated hydrocarbons represent a cornerstone in our understanding of polyatomic reaction dynamics. However, despite two decades of investigation, essentially all experimental studies of the dynamics of these reactions have relied upon a probe of the OH product, and detailed translational energy and angular distributions have never been obtained. Use of crossed-beam velocity map imaging with VUV single photon ionization probe techniques has enabled us to investigate the global dynamics of these reactions for the first time, affording new and sometimes surprising insights into this classic problem. We obtained the differential cross sections and translational energy distributions for reaction of $O(^3P)$ with cyclohexane, n-butane and isobutane at a range of well-defined collision energies from 4.7 to 14.8 kcal/mol. The product alkyl radicals are largely backscattered with respect to the alkane beam at all collision energies, but the scattering distribution is clearly broadened with increasing collision energy. This is consistent with a picture of direct rebound dynamics but inconsistent with a recent result for the vibrationally excited OH component [H. Tsurumaki et al., *J. Chem Phys.* **112** 8338 (2000)], and we have explored the source of this inconsistency. More surprising is the large fraction of the available energy partitioned into internal degrees of freedom of the alkyl radical, showing that the simple triatomic picture of the reaction is inadequate to account for all of the observations. To explain the observed dynamics we propose a modification of the triatomic model in which the exoergicity is adjusted to reflect "vertical" rather than "adiabatic" H abstraction energetics, and this picture is supported by ab initio calculations and by detailed consideration of the translational energy release patterns.

We have recently developed a novel spectroscopic probe of cations not amenable to study by traditional techniques. This approach, termed ion pair imaging spectroscopy (IPIS), involves VUV dissociation of molecules to ion pair products with imaging detection of the resulting translational energy distributions. It is fully analogous to photoelectron spectroscopy but has the advantage that it may be applied to systems for which stable neutral precursors may not exist. In this case the departing anion plays the role of a "heavy electron," and the result for ion pair dissociation of a stable molecule is to give the cation associated with ionization of a radical. This approach has the further advantage that it is a much slower process than photoelectron ejection, so that in principle larger regions of the cation configuration space may be accessed. A potential disadvantage is that the larger mass of the departing anion may produce a broad rotational distribution in the cation that could interfere with accurate determination of its spectroscopic properties. We have recently shown that IPIS can provide rotationally resolved spectra, eliminating the uncertainty introduced by the rotational broadening and instead allowing determination of additional spectroscopic properties. We applied the technique under high-resolution conditions to study ion pair products of the vacuum ultraviolet photodissociation of methyl chloride to obtain a rotationally resolved and assigned spectrum for CH_3^+ . The results

afford new values for vibrational frequencies and rotational constants for this molecule that match well with those calculated in our group

FUTURE PLANS

The comparison of theory and experiment on axis switching intensities in DCCl is leading to some surprising insights into the rovibrational problem in floppy molecules. In the hyperspherical coordinate formulation of the Renner-Teller problem, rotation is defined using the instantaneous inertial tensor of the vibrating molecule. This implies substantially stronger mixing of rotational and vibrational degrees of freedom than in the usual spectroscopists' Eckart frame. Coriolis contributions to the same transitions are negligible in the small-amplitude theory of Hougen and Watson, due to the choice of the Eckart frame, in which rotation and vibration are maximally separated. In contrast, Coriolis interactions are large, but easily computed in the hyperspherical formulation, and they account for a substantial fraction of the observed intensity in the forbidden sub-bands. Incorporation of axis-switching into the hyperspherical coordinate problem is not completely understood and we continue to work in this area.

Preliminary data have been obtained in the region of the HCB_r $\tilde{A}(010) - \tilde{a}(000)$ singlet-triplet transition near 10800 cm⁻¹. What appears to be a Q-branch has been identified in a weak spectrum, however sub-bands of stronger singlet-singlet hot bands overlap the region making analysis difficult. However, the upper state involved in this transition has been characterized in earlier work, so we are hopeful that analysis of this spectrum will permit a determination of the triplet-singlet spacing in HCB_r to an accuracy of better than 0.01 cm⁻¹, a first for any methylene, including CH₂ itself.

Coincident state distributions for the energy selected unimolecular decomposition of ketene provide a probe of dynamical corrections to statistical rate theory. Frequency modulated Doppler spectroscopy of the singlet CH₂ fragment can be combined with CO ion imaging data to provide a cross-validated set of product correlations to compare with recent dynamical calculations starting from the variational RRKM transition state.

We plan to extend the crossed-beam imaging studies in two directions. One, we are now limited by our 7.9 eV probe, and we would like to extend our range a bit deeper into the VUV, opening a number of additional systems to study. We plan to implement an anti-Stokes Raman laser driven by an F₂ pump laser, to reach 8.3 eV. The second direction involves study of hydroxyl radical reaction dynamics with systems such as alkanes and alcohols to explore the generality of our picture of "vertical" H abstraction dynamics.

ACKNOWLEDGEMENT

Work at Brookhaven National Laboratory was carried out under Contract No. DE-AC02-98CH10886 with the U. S. Department of Energy and is supported by its Division of Chemical Sciences, Office of Basic Energy Sciences.

PUBLICATIONS SINCE 2000

1. B.-C. Chang, M.L. Costen, A.J. Marr, G. Ritchie, G.E. Hall, and T.J. Sears, *Near infrared spectroscopy of bromomethylene in a slit jet expansion*. *J. Molec. Spectrosc.*, 2000. **202**: p. 131-143.

2. K. Kobayashi, L.D. Pride, and T.J. Sears, *Absorption spectroscopy of CH₂ near 9500 cm⁻¹*. J. Phys. Chem. A, 2000. **104**: p. 10119-10124.
3. G.E. Hall and S.W. North, *Transient Laser Frequency Modulation Spectroscopy*, Annu. Rev. Phys. Chem. 2000. **51**: p. 243-274.
4. M.L. Costen, H. Katayanagi and G.E. Hall, *State correlations in the unimolecular dissociation of ketene*, J. Phys. Chem. A, 2000. **104**: p 10247-10258
5. T.C. Steimle, M.L. Costen, G.E. Hall, and T.J. Sears, *Transient frequency modulation absorption spectroscopy of molecules produced in a laser ablation supersonic expansion*. Chem. Phys. Letts., 2000. **319**: p. 363-367.
6. K. Kobayashi and T.J. Sears, *Absorption spectroscopy of singlet CH₂ near 11200 cm⁻¹*. Can J. Phys., 2001. **79**: p. 347-358.
7. K.M. Forsythe, S.K. Gray, S.J. Klippenstein and G.E. Hall, *An ab initio molecular dynamics study of S₀ ketene fragmentation*, J. Chem. Phys., 2001. **115**: p 2134-2145.
8. H.-G. Yu, T. Gonzalez-Lezana, A.J. Marr, J.T. Muckerman, and T.J. Sears, *Experimental and theoretical studies of the near-IR spectrum of bromomethylene*. J. Chem. Phys., 2001. **115**: p. 5433-5444.
9. H.-G. Yu, J.T. Muckerman, and T.J. Sears, *A theoretical study of the potential energy surface for the reaction OH+CO=H+CO₂*. Chem. Phys. Letts., 2001. **349**: p. 547-554.
10. F. Qi, O. Sorkhabi, A. G. Suits, S.-H. Chien and W.-K. Li, "Photodissociation of ethylene sulfide at 193nm : A photofragment translational spectroscopy study with VUV synchrotron radiation and ab initio calculations," *J. Am. Chem. Soc.*, **123**, 148 (2001).
11. Julie A. Mueller, Johanna L. Miller, Laurie J. Butler, Fei Qi, Osman Sorkhabi and Arthur G. Suits, "Internal Energy Dependence of the H + Allene / H + Propyne Product Branching from the Unimolecular Dissociation of 2-Propenyl Radicals," *J. Phys. Chem. A* **104**, 48 (2001).
12. O. Sorkhabi, F. Qi, A.H. Rizvi and A.G. Suits, "The ultraviolet photochemistry of phenylacetylene and the enthalpy of formation of 1,3,5-Hexatriyne," *J. Am. Chem. Soc.*, **123**, 671 (2001).
13. C. L. Berrie, C. A. Longfellow, A. G. Suits and Y. T. Lee, "Infrared multiphoton dissociation of acetone in a molecular beam," *J. Phys. Chem. A.*, **105**, 2557 (2001).
14. J. A. Mueller, B. F. Parsons, L. J. Butler, F. Qi, O. Sorkhabi and A. G. Suits, "Competing isomeric product channels in the 193 nm photolysis of 2-Chloropropene and in the unimolecular dissociation of the 2-propenyl radical," *J. Chem. Phys.* **114**, 4505 (2001).
15. M. Ahmed, D. S. Peterka, P. Regan, X. Liu and A. G. Suits, "Ion pair imaging spectroscopy: CH₃Cl → CH₃⁺ + Cl," *Chem. Phys. Lett.* **339**, 203 (2001).
16. A. G. Suits and F. Qi, "The photodissociation of cyclic sulfides probed with tunable undulator radiation," *J. Elect. Spec. Rel. Phenom.*, **119**, 127 (2001).
17. X. Liu, R. L. Gross and A. G. Suits, "'Heavy electron' photoelectron spectroscopy: rotationally resolved ion pair imaging of CH₃⁺," *Science* **294** 2527 (2001).
18. H.-G. Yu, J.T. Muckerman, and T.J. Sears, *A K-dependent adiabatic approximation to the Renner-Teller effect for triatomic molecules*. J. Chem. Phys., 2002. **116**: p. 1435-1442.
19. X. Liu, R. L. Gross and A. G. Suits, "Differential cross sections for O(³P) + alkane reactions by direct imaging," *J. Chem. Phys.* **116**, 5333 (2002). (Communication).
20. K. Kobayashi, G.E. Hall, J.T. Muckerman, T.J. Sears, and A.J. Merer, *The E-X spectrum of jet-cooled TiO observed in absorption*. J. Molec. Spectrosc., 2002. **XXX**: p. xxx-xxx (in press).
21. P. Regan, F. Qi, A. G. Suits, J. K. Lau and W. K. Lee, "New product channels observed from the 193-nm photodissociation of acrolein," J. Chem. Phys. (submitted 2001).
22. H.-G. Yu, and T.J. Sears, *Rovibronic energies of CH₃⁺*. J. Chem. Phys. (Submitted, 2002)
23. A. Lin, K. Kobayashi, H.-G. Yu, G.E. Hall, J.T. Muckerman, T.J. Sears, and A.J. Merer, *Axis-switching and Coriolis coupling in the A (010)-X (000) transitions of HCCl and DCCl*. J. Molec. Spectrosc. (submitted 2002).
24. X. Liu, R.L. Gross, G.E. Hall, J.T. Muckerman and A.G. Suits, *Imaging O(³P) + alkane reactions in crossed molecular beams: vertical vs. adiabatic H abstraction dynamics*, J. Chem. Phys. (submitted 2002).

SPECTROSCOPY AND KINETICS OF COMBUSTION GASES AT HIGH TEMPERATURES

Ronald K. Hanson and Craig T. Bowman
Department of Mechanical Engineering
Stanford University, Stanford, CA 94305-3032
hanson@me.stanford.edu, bowman@navier.stanford.edu

Program Scope

This program involves two complementary activities: (1) development and application of cw laser absorption methods for the measurement of concentration time-histories and fundamental spectroscopic parameters for species of interest in combustion; and (2) shock tube studies of reaction kinetics and thermochemistry relevant to combustion. Species investigated in the spectroscopic portion of the research include: OH using narrow-linewidth ring dye laser absorption; NH₂ using frequency-modulation laser absorption methods; CH₃ using external-cavity frequency-doubling laser absorption, and NO₂ using fixed-frequency laser absorption. Reactions of interest in the shock tube kinetics research include: NH₂ + NO → Products; NH₂ + NO₂ → Products; Benzylamine → Products; and CH₃ + O₂ → Products. An important new element of the research has been to measure the enthalpy of formation for OH using shock tube methods.

Recent Progress: Shock Tube Chemical Kinetics

NH₂ + NO → Products: We have nearly concluded a shock tube study of the two primary channels of the reaction of NH₂ and NO,



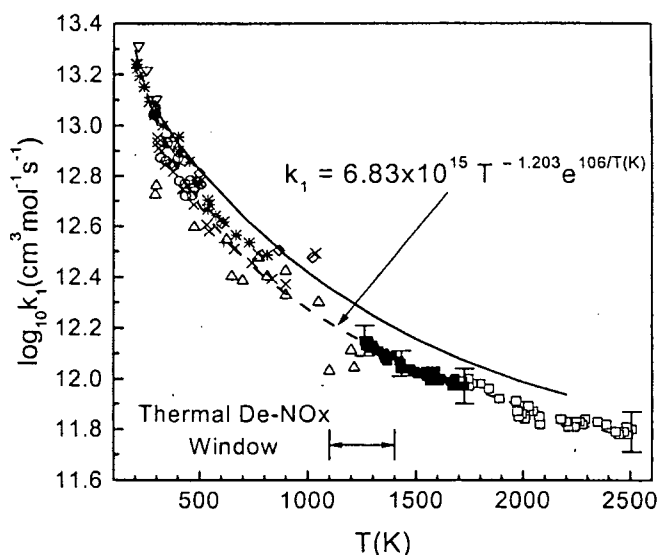
The branching ratio, $\alpha = k_{1a}/(k_{1a}+k_{1b})$, of these two primary channels is an important parameter in the modeling of NO_x reduction by the Thermal DeNO_x process. Our approach exploited the high sensitivity of NH₂ detection available with frequency-modulation (FM) spectroscopy methods to establish accurate high-temperature values of both the overall rate and the branching ratio. Using low (ppm level) concentrations of NH₂ generated by excimer laser photolysis of shock-heated NH₃/NO/Ar mixtures in the temperature range 1340 K - 1670 K, it was possible to nearly eliminate the dependence of α on the overall rate coefficient. This resulted in a very accurate determination of the branching ratio near $\alpha = 0.5$ that occurs near 1560 K. More recently we have measured the branching ratio in the higher temperature region, 1826-2159 K, using thermal decomposition of monomethylamine as a source of NH₂ in mixtures of CH₃NH₂, NH₃, NO and argon. In these experiments we found that the branching ratio increased from 0.59 at 1826 K, to 0.66 at 2159 K.

The overall rate coefficient of the reaction NH₂ + NO → products was also determined using FM detection of NH₂. NH₂ radicals were produced for these experiments using the thermal decomposition of two separate source compounds: CH₃NH₂, monomethylamine (MMA), and C₆H₅CH₂NH₂, benzylamine (BA). To determine k_{1a+1b} , a perturbation strategy was employed that is based on changes in the NH₂ profiles when NO is added to the MMA or BA/Ar mixtures. Sensitivity analysis shows that NH₂ profiles in these mixtures were sensitive primarily to the overall rate, with significantly lower sensitivity to the branching ratio and other NH₂ reactions. The measured NH₂ profiles were interpreted by detailed kinetic modeling to obtain k_{1a+1b} -values in the

temperature range 1700-2500 K using MMA, and were extended to 1300 K using BA. Results are shown in Fig. 1.

The present k_{1a+1b} -values are consistent with recent theoretical results of Miller and co-workers. There is no evidence of a positive activation energy for this reaction at elevated temperatures as reported in several other high-temperature experimental studies. Combining the present high-temperature data with lower temperature determinations yields the following simple expression for the overall reaction rate, $k_{1a+1b} = 6.83 \times 10^{15} T^{-1.203} e^{106/T(K)} \text{ cm}^3/\text{mol-s}$ for the temperature range 300-2500K.

Fig. 1. Summary of k_1 : ■ data from $\text{C}_6\text{H}_5\text{CH}_2\text{NH}_2$ experiments; □ data from CH_3NH_2 experiments [8]; ○ Lesclaux et al. (1975); △ Silver and Kolb (1982); ▽ Stief et al. (1982); ◇ Atakan et al. (1989); + Wolf et al. (1994); × Park and Lin (1997); * Wolf et al. (1997); — Miller and Klippenstein (2000); - - - Equation (1). The vertical bars represent the combined fitting errors and uncertainties associated with secondary reactions and absorption coefficient.



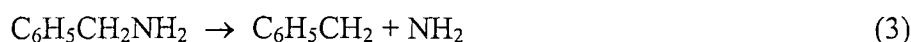
$\text{NH}_2 + \text{NO}_2 \rightarrow \text{Products}$: We are studying the overall rate coefficient and the branching ratio of the reaction of NH_2 with NO_2 . This reaction plays a role during Thermal De-NOx in the recycling of NO_2 back to NO and in N_2O formation. The primary channels and the definition of the branching ratio are



$$\alpha_2 = k_{2a}/(k_{2a}+k_{2b})$$

NH_2 was generated using thermal decomposition of small quantities of benzylamine that was added to NO_2/Ar mixtures. To determine the overall rate coefficient ($k_{2a}+k_{2b}$), we measure NH_2 using FM absorption. Since the sensitivity analysis shows that N_2O traces are sensitive to the branching ratio, we are employing IR emission to measure N_2O concentration. NO_2 is also monitored (in absorption) to verify the current reaction mechanism. We have found that the overall rate coefficient and the branching ratio are $5.5 \times 10^{12} \text{ cm}^3 \text{ mol}^{-1} \text{ s}^{-1}$, and 0.17 respectively for the temperature range 1320 – 1530 K and pressures near 1.35 atm.

Decomposition of Benzylamine: In connection with our measurements of the $\text{NH}_2 + \text{NO}$ and $\text{NH}_2 + \text{NO}_2$ reactions, we are studying the rate coefficient of the benzylamine (BA) decomposition reaction



Measuring the initial slope of NH_2 concentration during BA decomposition, we determine the decomposition rate of BA into benzyl and NH_2 radicals. In addition, we are performing RRKM

calculations that allow inference of the high-pressure-limit values of the decomposition rate of BA and the heat of formation of the benzyl radical.

OH Thermochemistry: We have measured the standard enthalpy of formation of OH using shock tube methods. Recently, workers in several laboratories have found evidence of a lower value for the enthalpy of formation of OH. This radical plays an important role in combustion chemistry and has such a profound effect on the kinetic modeling in our research that we felt it was necessary to mount a strong effort to verify this potential difference. Our strategy involved sensitive and accurate measurements of OH using narrow-linewidth laser absorption, in shock-heated high temperature H₂-O₂-Ar mixtures where the plateau levels of OH are strongly sensitive to the OH heat of formation and insensitive to kinetic parameters. Over the range of our experimental conditions (1720-2718 K) we found $\Delta H_{f,298}(\text{OH}) = 8.92 \pm 0.16$ kcal/mol, which is ~ 0.45 kcal/mol below the previously accepted value, and agrees with other recent experimental efforts and theoretical calculations.

Recent Progress: Absorption Diagnostics and Spectroscopy

FM Absorption: We have previously developed FM absorption spectroscopy methods for NH₂ detection. This method, similar to that used by Sears and colleagues at Brookhaven, allows direct subtraction of the noise caused by the interaction of the laser beam and the shock-induced flow. Using this method we have achieved a minimum detectable absorption of 0.01% in a single-pass configuration, representing a factor of 5-20 improvement in detection sensitivity over conventional laser absorption.

Building on this previous work, we have developed an improved, second-generation FM detection scheme using higher modulation frequencies (1.2 GHz, compared to the previous 600 MHz). This scheme has improved detection sensitivity for NH₂ by a factor of ~ 3 , as well as permitting application of this technique to species with broader absorption features.

OH Spectral Parameters: We have also investigated the collision-width and -shift parameters of several rotational lines in the OH A-X transition that are accessible with our ring dye laser, with the goal of providing missing spectroscopic data and extending the useful operating (pressure) range of the OH laser absorption diagnostic.

Future Plans

Complete high temperature studies of branching ratio α for the reaction NH₂ + NO.

Complete studies of benzylamine decomposition and heat of formation.

Complete investigation of the overall rate and branching ratio of the reaction of NH₂ + NO₂.

Complete investigation of the heat of formation of OH using shock tube methods. Investigate the consequences of this lower value of the enthalpy of formation of OH, previous rate coefficient determinations and other combustion parameters.

Investigate other applications of shock tube methods to measure thermochemical parameters relevant to combustion.

Develop external-cavity frequency-doubling methods for the generation of laser radiation at 216 nm as needed for the improved detection of CH₃.

Develop techniques to measure CH₃ quantitatively at high pressures using laser absorption at 216 nm.

Apply these frequency-doubling methods to other wavelengths of interest including the detection of HCO at 258 nm.

Recent Publications of DOE Sponsored Research: 2000-2002

1. J. T. Herbon, R. K. Hanson, D. M. Golden, and C. T. Bowman, "A Shock Tube Study of the Enthalpy of Formation of OH," Proceedings of the Combustion Institute **29**, in press.
2. S. H. Song, R. K. Hanson, C. T. Bowman, and D. M. Golden, "A Shock Tube Study of the NH_2+NO_2 Reaction," Proceedings of the Combustion Institute **29**, in press.
3. S. H. Song, D. M. Golden, R. K. Hanson, and C. T. Bowman, "A Shock Tube Study of Benzylamine Decomposition: Overall Rate Coefficient and Heat of Formation of the Benzyl Radical," submitted to Journal of Physical Chemistry A.
4. S. H. Song, R. K. Hanson, D. M. Golden, and C. T. Bowman, "A Shock Tube Study of the Product Branching Ratio of the NH_2+NO Reaction at High Temperatures," submitted to Journal of Physical Chemistry A.
5. R. W. Bates, D. M. Golden, R. K. Hanson, and C. T. Bowman, "Experimental Study and Modeling of the Reaction $\text{H} + \text{O}_2 + \text{M} \rightarrow \text{HO}_2 + \text{M}$ ($\text{M}=\text{Ar}, \text{N}_2, \text{H}_2\text{O}$) at Elevated Pressures and Temperatures between 1050 and 1250 K," Phys. Chem. Chem. Phys. **3**, 2337-2342 (2001).
6. D. F. Davidson and R. K. Hanson, "Chapter 5.2: Spectroscopic Diagnostics," *Handbook of Shock Waves: Volume 1*, G. Ben-Dor, O. Igra and T. Elperin, editors, Academic Press, San Diego, pp. 741-785, (2001).
7. J. T. Herbon and R. K. Hanson, "Measurements of Collision-Shift in Absorption Transitions of the OH A-X (0,0) Band Using a Shock Tube," Paper 5734, 23rd International Symposium on Shock Waves, Arlington, Texas (2001).
8. E. L. Petersen and R. K. Hanson, "Non-Ideal Effects Behind Reflected Shock Waves in a High-Pressure Shock Tube," Shock Waves **10**, 405-420 (2001).
9. S. Song, R. K. Hanson, C. T. Bowman, and D. M. Golden, "Shock Tube Determination of the Overall Rate of $\text{NH}_2+\text{NO} \rightarrow$ Products in the Thermal De-Nox Temperature Window," Paper 204 2nd Joint Meeting of the US Section of the Combustion Institute, March (2001).
10. S. Song, R. K. Hanson, C. T. Bowman, and D. M. Golden, "Shock Tube Determination of the Overall Rate of $\text{NH}_2+\text{NO} \rightarrow$ Products in the Thermal De-NOx Temperature Window," International J. Chemical Kinetics **33**, 715-721 (2001).
11. V. Nagali, D. F. Davidson and R. K. Hanson, "Measurements of Temperature-Dependent Argon-Broadened Half-Widths of H_2O Transitions in the 7117 cm^{-1} Region," J. Quant. Spectrosc. Radiat. Transfer **64**, 651-655 (2000).
12. S. Song, R. K. Hanson, C. T. Bowman, and D. M. Golden, "Shock Tube Determination of the Overall Rate of $\text{NH}_2+\text{NO} \rightarrow$ Products at High Temperatures," Proceedings of the Combustion Institute **28**, 2403-2409 (2000).

Theoretical Studies of Potential Energy Surfaces*

Lawrence B. Harding
Gas Phase Chemical Dynamics Group, Chemistry Division
Argonne National Laboratory
Argonne, IL 60439
harding@anl.gov

Program Scope

The goal of this program is to calculate accurate potential energy surfaces for both reactive and non-reactive systems. Our approach is to use state-of-the-art electronic structure methods (MR-CI, CCSD(T), etc.) to characterize multi-dimensional potential energy surfaces. Depending on the nature of the problem, the calculations may focus on local regions of a potential surface (for example, the vicinity of a minimum or transition state), or may cover the surface globally. A second aspect of this program is the development of techniques to fit multi-dimensional potential surfaces to convenient, global, analytic functions that can then be used in dynamics calculations. Finally a third part of this program involves the use of direct dynamics for high dimensional problems to by-pass the need for surface fitting.

Recent Results

C₂H₅+O → products: Direct dynamics/classical trajectory calculations using a B3LYP potential surface predict an unexpectedly large number of product channels are open in this reaction. The dominant product channels are, simple abstraction forming OH and C₂H₄, and addition followed by a simple bond cleavage, forming either H atom plus acetaldehyde or methyl radical plus formaldehyde. However, in addition to these channels we have also found trajectories that form CH₄+HCO, H₂+CH₃CO, H₂O+vinyl radical and H+ethylene oxide. The first three of these we believe would not be predicted by any simple statistical theory, i.e. there are no saddle points or reaction paths directly connecting the ethoxy radical minimum with any of these three sets of products.

CH₃+H: A four dimensional grid of points characterizing the reaction coordinate, the two transition modes and the CH₃ umbrella mode at a CAS+1+2/aug-cc-pvtz level of theory, has been fit. Variable reaction coordinate transition state theory (VRCTST) calculations, done in collaboration with S. Klippenstein (Sandia), yield predictions for the zero-pressure limit isotopic exchange rate constants that are about 15% greater than available experimental data. Trajectory simulations indicate that the transition state re-crossing factor for the capture process is 0.90, essentially independent of temperature and pressure. Correcting for this dynamical effect yields rate constants in good agreement with the experimental data. Variations in the umbrella mode of the methyl radical are predicted to have surprisingly little effect on the rate constant.

CH₃+O: Three, three dimensional, transitional mode surfaces have been fit (corresponding to the three states that correlate with ground state reactants). Two of the surfaces are found to be reactive while the third surface is repulsive. VRCTST calculations predict a rate constant that is essentially independent of temperature from 200°-2000°K. We again investigated the effect of allowing the umbrella mode of the CH₃ to relax and again found this to have little effect on the rate.

H+CH₃O and H+CH₂OH: Three dimensional surfaces have been fit for both H+CH₃O and H+CH₂OH in which the internal coordinates of the CH₃O (or CH₂OH) fragment are held fixed. Plots of these two potentials are shown in Figure 1. Preliminary VRCTST calculations (with

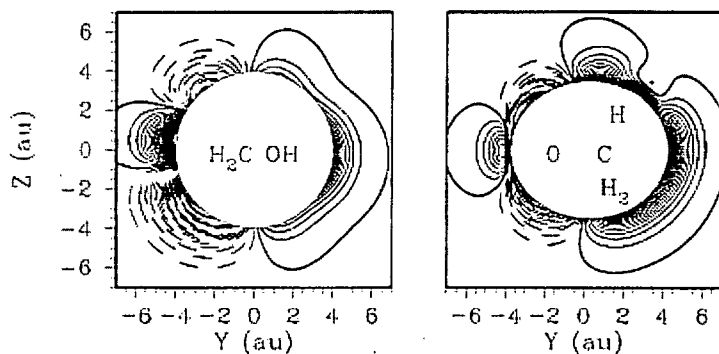


Figure 1: Interaction potentials for H+H₂COH and H+CH₃O. The contour increment is 2 kcal/mole. Solid contours denote repulsive interactions; dashed contours denote attractive interactions. The geometries of the CH₃O and CH₂OH fragments are fixed.

S. Klippenstein) yield room temperature, high pressure limit rate constants of 9×10^{-11} and 2×10^{-10} cm³/molecule sec for H+CH₃O and H+CH₂OH, respectively. These are both significantly higher than the most recent experimental estimates^{1,2} of 3.3×10^{-11} and 6.8×10^{-11} cm³/molecule sec.

One interesting feature of the H+CH₃O potential has to do with the transitional mode corresponding to rotation of the incoming H atom around the CO bond axis. A plot of the barrier for this hindered internal rotation as a function of R(OH) is shown in Figure 2. The calculations

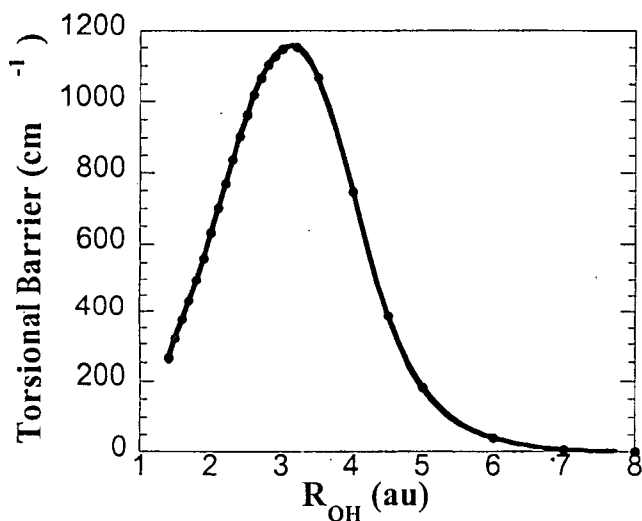


Figure 2. CAS+1+2/cc-pvdz torsional barrier for CH₃OH as a function of R_{OH}.

predict a maximum in the barrier height of 1150 cm⁻¹ at R(OH)=1.65 Å. This can be compared to the torsional barrier at R_e which is predicted to be 515 cm⁻¹. The conclusion that the torsional barrier of methanol increases when the OH bond is stretched is in agreement with recent experiments by Rueda et al³.

Future Plans

Our direct dynamics/classical trajectory studies on $O+CH_3$ and $O+C_2H_5$ have demonstrated that the decomposition of highly energized species can lead to unexpected products. In the coming year we plan to search for more examples of this kind of behavior. One specific system we will study is the dissociation of formaldehyde. At higher energies one might expect to find a new mechanism for the reaction $H_2CO \rightarrow H_2 + CO$ in which the molecule starts to dissociate towards $H+HCO$ but before the two fragments completely separate, an abstraction occurs forming the H_2+CO products.

In collaboration with Stephen Klippenstein we plan to develop methods for evaluating high temperature partition functions of molecules with large amplitude vibrational modes. One of the first applications will be to H_2COH .

Acknowledgement: This work was performed under the auspices of the Office of Basic Energy Sciences, Division of Chemical Sciences, Geosciences and Biosciences, U.S. Department of Energy, under Contract W-31-109-Eng-38.

References:

- (1) S. Dobe, T. Berces, and I. Szilagy, *J. Chem. Soc. Faraday Trans.* 87, 2331 (1991)
- (2) S. Dobe, T. Berces, F. Temps, H.Gg. Wagner and H. Ziemer, *J. Phys. Chem.* 98, 9792 (1994)
- (3) T. Rueda, O.V. Boyarkin, T.R. Rizzo, I. Mukhopadhyay and D. S. Perry, *J. Chem. Phys.* 116, 91 (2002)

PUBLICATIONS (2000 - Present):

Classical Trajectory Calculations of the High Pressure Limiting Rate Constants and of Specific Rate Constants for the Reaction $H+O_2 \rightarrow HO_2$: Dynamic Isotope Effects Between Tritium+ O_2 and Muonium+ O_2 , L.B. Harding, J. Troe, and V.G. Ushakov, *Phys. Chem. Chem. Phys.* 2, 631-642 (2000)

Potential Energy Surface of the A State of NH_2 and the role of Excited States in the $N(^2D)+H_2$ Reaction, L.A. Pederson, G.C. Schatz, T. Hollebeek, T.-S. Ho, H. Rabitz and L.B. Harding, *J. Phys. Chem.* 104,2301-2307 (2000)

A Summary of "A Direct Transition State Theory Based Study of Methyl Radical Recombination Kinetics", S.J. Klippenstein and L.B. Harding, *J. Phys. Chem.* 104,2351-2354 (2000)

Barrier to Methyl Internal Rotation of 1-Methylvinoxy Radical in the $X(^2A'')$ and $B(^2A')$ States: Experiment and Theory, S. Williams, L.B. Harding, J.F. Stanton, and J.C. Weisshaar, *J. Phys. Chem. A* 104,10131-10138(2000)

A New Potential Surface and Quasiclassical Trajectory Study of $H+H_2O \rightarrow OH+H_2$, G.-S. Wu, G.C. Schatz, G. Lendvay, D.-C. Fang, L.B. Harding, *J. Chem. Phys.* 113, 3150-3161 (2000)

Exploring the $OH+CO$ Reaction Coordinate via Infrared Spectroscopy of $OH-CO$ Reactant Complexes, M. I. Lester, B. V. Pond, D. T. Anderson, L. B. Harding, A. F. Wagner *J. Chem. Phys.* 113, 9889-9892 (2000)

Statistical Rate Theory for the $HO + O \leftrightarrow HO_2 \leftrightarrow H + O_2$ Reaction System: SACM/CT Calculations between 0 and 5000 K, L.B. Harding, A. I. Maergoiz, J. Troe, and V.G. Ushakov *J. Chem. Phys.* **113**, 11019-11034 (2000)

Barrier to Methyl Internal Rotation of Cis and Trans 2-Methylvinoxy Radical in the $X(^2A'')$ and $B(^2A'')$ States: Experiment and Theory, S. Williams, L.B. Harding, J.F. Stanton, and J.C. Weisshaar, *J. Phys. Chem. A*, **104**, 9906-9913 (2000)

Initiation in H_2/O_2 : Rate Constants for $H_2+O_2 \rightarrow H+HO_2$ at High Temperature, J.V. Michael, J.W. Sutherland, L.B. Harding, and A.F. Wagner, *28th Symposium (International) on Combustion*, **28**, 1471-1478 (2000)

Theoretical Kinetic Estimates for the Recombination of Hydrogen Atoms with Propargyl and Allyl Radicals, L.B. Harding and S.J. Klippenstein, *28th Symposium (International) on Combustion*, **28**, 1503-1509 (2000)

Evidence for a Lower Enthalpy of Formation of Hydroxyl Radical and a Lower Gas Phase Bond Dissociation Energy of Water, B. Ruscic, D. Feller, D. A. Dixon, K. A. Peterson, L. B. Harding, R. A. Asher, and A. F. Wagner. *J. Phys. Chem. A* **105**, 1-4 (2001)

Construction of reproducing kernel Hilbert space potential energy surfaces for the $1A''$ and $1A'$ states of the reaction $N(^2D)+H_2$, T. Hollebeck, T.-S. Ho, H. Rabitz and L.B. Harding, *J. Chem. Phys.* **114**, 3945-3948 (2001)

Mapping the $OH+CO \rightarrow HOCO$ reaction pathway through infrared spectroscopy of the $OH-CO$ reactant complex, M. I. Lester, B. V. Pond, M.D. Marshall, D. T. Anderson, L. B. Harding, A. F. Wagner, *Faraday Discussions*, **118**, 373-385(2001)

Comment on "On the High Pressure Rate Constants for the $H/Mu + O_2$ Addition Reactions", L.B. Harding, J. Troe, and V.G. Ushakov, *Phys. Chem. Chem. Phys.* **3**, 2630-2631 (2001)

A Direct Transition State Theory Based Analysis of the Branching in NH_2+NO , De-Cai Fang, L.B. Harding, S.J. Klippenstein and J.A. Miller, *Faraday Discussions*, **119**, 207-222(2001)

Theoretical and Experimental Investigation of the Dynamics of the Production of CO from the CH_3+O and CD_3+O Reactions, T.P. Marcy, R. R. Diaz, D. Heard, S.R. Leone, L.B. Harding and S.J. Klippenstein, *J. Phys. Chem. A* **105**, 8361-8369 (2001)

On the Enthalpy of Formation of Hydroxyl Radical and Gas Phase Bond Dissociation Energies of Water and Hydroxyl, B. Ruscic, A. F. Wagner, L. B. Harding, R. A. Asher, D. Feller, D. A. Dixon, K. A. Peterson, Y. Song, X. Qian, C.-Y. Ng, J. Liu and W. Chen, *J. Phys. Chem. A* **106**, 2727-2747(2002)

Resolving the Mystery of Prompt CO_2 : The $HCCO+O_2$ Reaction, S.J. Klippenstein, J. A. Miller, and L.B. Harding *28th Symposium (International) on Combustion*, **29**, (accepted)

A Theoretical Analysis of the CH_3+H Reaction: Isotope Effects, the High Pressure Limit and Transition State Recrossing, S.J. Klippenstein, Y. Georgievskii, and L.B. Harding *28th Symposium (International) on Combustion*, **29**, (accepted)

Femtosecond Laser Studies of Ultrafast Intramolecular Processes

Carl Hayden
Combustion Research Facility, MS9055
Sandia National Laboratories
Livermore, CA 94551-0969
CCHAYDE@SANDIA.GOV

Program Scope

The purpose of this research program is to characterize important fundamental chemical processes by probing them directly in time. In this work femtosecond laser pulses are used to initiate chemical processes and follow their progress. The development of new techniques that take advantage of the time resolution provided by femtosecond lasers for studies of chemical processes is an integral part of this research.

Our research focuses on studies of ultrafast energy relaxation and unimolecular reaction processes in very highly excited molecules. The goal of these studies is to provide measurements of the time scales for elementary chemical processes that play critical roles in the reaction mechanisms of highly excited reaction intermediates, such as those created in combustion environments by either thermal excitation or exothermic addition reactions. Over the past several years we have developed femtosecond time-resolved photoelectron spectroscopy as a method for studying ultrafast energy relaxation processes such as internal conversion and to measure the time scales for subsequent vibrational energy redistribution. To extend these studies to processes involving dissociation we recently developed the time-resolved photoelectron-photoion coincidence imaging technique. This approach provides a wealth of new information from femtosecond time-resolved experiments. Our recent work has emphasized collaborative studies with other research groups to both apply and extend these capabilities.

Recent Progress:

Time-resolved studies of CF₃I dissociative ionization

One recent focus of my research has been the measurement of femtosecond time-resolved photoelectron angular distributions. Photoelectron angular distributions (PADs) are potentially very useful probes of dynamics in molecules. PADs are sensitive to the nature of the molecular orbital that is ionized, the geometry and orientation of the molecule as the electron departs, and the dynamics of the photoionization process. Unfortunately, much of the information is lost when the PAD is measured from a randomly oriented sample of molecules and hence PADs have not been extensively studied. In femtosecond time-resolved experiments the time scale of the experiment is often short compared to molecular rotation times so it is possible to measure PADs from aligned or oriented molecules. Several recent theoretical studies have suggested the possibility of using femtosecond time-resolved PADs to probe ultrafast dynamics.^{1,2,3} Studies of ultrafast dynamics in molecules necessarily measure the evolution of broad superpositions of molecular states. When probed by a time-resolved method such as photoelectron spectroscopy the resulting spectrum of this superposition is broad and rapidly changing. It is frequently difficult to determine whether the evolution of the spectrum is due to changes in electronic configuration from processes such as internal conversion or from vibrational dynamics that result in changing Franck-Condon factors. Measurements of time-resolved PADs have the potential to distinguish between electronic and purely vibrational dynamics.

In an ongoing collaboration with Anouk Rijs and Dr. Maurice Janssen at Vrije University, Amsterdam, The Netherlands we have performed extensive measurements on the dissociative multiphoton ionization of CF_3I using coincidence imaging. In these studies the molecule is two-photon excited with a 264 nm pulse in the region of the 7s Rydberg state. The excited molecule is then probed by time-delayed ionization. Probe wavelengths between 396 and 365 nm have been used. There are several reasons to choose this system for study. The CF_3I molecule is one of the few polyatomic molecules for which PADs associated with dissociative ionization have been measured using a CW approach.^{4,5} Thus it is a good system for developing the techniques for our time-resolved PAD measurements. The use of two-photon excitation potentially prepares a very well aligned molecule from which to study the ionization. Finally, very interesting dynamics have been observed following excitation of CF_3I in this region and the coincidence imaging technique should supply information to help understand them.

The experiments are performed by crossing the femtosecond excitation and ionization pulses with a molecular beam containing CF_3I . The ions are imaged on a time and position sensitive detector while coincident electrons are imaged on a similar detector. Ion and electron images are accumulated at various time delays between excitation and ionization. The time and position sensitive detectors allow us to calculate the initial velocity vector of each detected fragment ion and its associated electron. The ion detection system also functions as a mass spectrometer, and data on all masses are collected simultaneously.

The ionization of CF_3I is strongly enhanced when the excitation and ionization pulses overlap in time. The primary ion products are CF_3I^+ , CF_3^+ , and I^+ . The maximum production of fragment ions occurs when the ionization pulse is delayed about 100 fs and the fragment ion yield decays with a time constant of approximately 250 fs. As shown in Fig. 1, the kinetic energy in the fragmentation decreases rapidly with time delay between the excitation and ionization. This change in the kinetic energy reflects evolution of the initially excited state in the neutral molecule because neither laser pulse creates a significant number of ions by itself. The photoelectron spectra coincident with the fragment ions show that the parent ion is initially generated upon ionization, with a very broad range of internal energies. These broad, time-resolved photoelectron spectra are not consistent with the ionization of a Rydberg state and indicate that the initially excited state is strongly coupled to another state with a substantially different geometry than the ion. The observed I^+ fragments are produced by immediate photodissociation of the highly vibrationally excited CF_3I^+ parent ions. The most highly excited parent ions fragment directly to produce CF_3^+ fragment ions.

As seen in Fig. 2, the photoelectron angular distributions coincident with I^+ formation show virtually no correlation between the ion recoil direction and the electron recoil velocity. This is consistent with the ionization and dissociation occurring in separate steps. On the other hand, the photoelectron angular distributions corresponding to CF_3^+ production show a relatively strong correlation between the ion recoil direction and the electron velocity vector. We believe this is due to essentially simultaneous ionization and dissociation. The multiple types of information available with the coincidence imaging method are enabling us to develop a consistent picture of this dissociative ionization process. The experiments probe both the time evolution of the highly excited neutral molecule and the ionization dynamics of the excited states.

Future Plans

My immediate future work involves the continuation of collaborative research projects. Experiments planned with Anouk Rijs and Dr. Maurice Janssen will use continue to use time-

delayed ionization to study photodissociation processes that yield small halogenated free radicals. Of particular interest is the photodissociation of multiply halogenated molecules that have several dissociation pathways. I also have an ongoing collaboration with Dr. James Shaffer at the University of Oklahoma and Albert Stolow at the Steacie Institute, NRC, Canada studying the UV photodissociation of NO dimers around 210 nm. This system has been extensively studied in the past,⁶ but the mechanism for the dissociation has not been determined. We have done a set of experiments exciting the NO dimer at 210 nm then probing with time delayed ionization in our coincidence imaging apparatus. The experiments demonstrate that the dissociation is not direct because no correlation is measured between the photofragment and photoelectron energies. The broad photoelectron energy spectrum shows that the dimer undergoes a very rapid geometry change upon excitation, and the new geometry preferentially ionizes to an excited state of the ion. Recently I have made some changes to the apparatus that result in a substantial reduction of the background in these experiments and will make more detailed measurements possible. We are also planning experiments to continue measurements of photoelectron angular distributions from larger polyatomic molecules. To compare with our previous measurements on the DABCO molecule we will study derivatives and analogs of DABCO that have different symmetry properties.

One goal for developing the coincidence imaging technique is to study isomerization in hot radicals generated by photolysis. We have constructed a second coincidence imaging apparatus with complementary capabilities to our first apparatus. A primary design feature of the new apparatus is an increased sample density achieved by moving the molecular beam source much closer to the detection region. This is an especially important consideration for experiments on hot radicals that must first be produced by photolysis because it will widen our choice of precursors to include those with weaker absorption cross sections. We will now bring this apparatus into operation by adding a new improved detection system.

References

1. Y. Arasaki, K. Takatsuka, K. Wang, and V. McKoy, *Chem. Phys. Lett.* **302**, 363 (1999).
2. S. C. Althorpe and T. Seiderman, *J. Chem. Phys.* **110**, 147 (1999).
3. T. Zuo, A. D. Bandrauk, and P. B. Corkum, *Chem. Phys. Lett.* **259**, 313 (1996).
4. K. G. Low, P. D. Hampton, and I. Powis, *Chem. Phys.* **100**, 401 (1985).
5. P. Downie and I. Powis, *J. Chem. Phys.* **111**, 4535 (1999).
6. V. Blanchet, A. Stolow, *J. Chem. Phys.*, **108**, 4371 (1998).

Publications: 2000-Present

- C. C. Hayden and A. Stolow, "Non-Adiabatic Dynamics Studied by Femtosecond Time-Resolved Photoelectron Spectroscopy", in *Adv. Ser. in Phys. Chem., Vol. 10: Photoionization and Photodetachment*, edited by C. Y. Ng, (World Scientific, Singapore, 2000).
- J. A. Davies, R. E. Continetti, D. W. Chandler, and C. C. Hayden, "Femtosecond Time-Resolved Photoelectron Angular Distributions Probed During Photodissociation of NO₂", *Phys. Rev. Lett.*, **84**, 5983 (2000).
- A. M. Rijs, C. C. Hayden, and M. H. M. Janssen, "Femtosecond Coincidence Imaging of Dissociative Ionization Dynamics in CF₃I", in *Femtochemistry and Femtobiology: Ultrafast Dynamics in Molecular Science*, (World Scientific) in press.
- E. A. Wade, J. I. Cline, K. T. Lorenz, C. C. Hayden and D. W. Chandler, "Direct Measurement of the Binding Energy of the NO Dimer", *J. Chem. Phys.*, accepted.

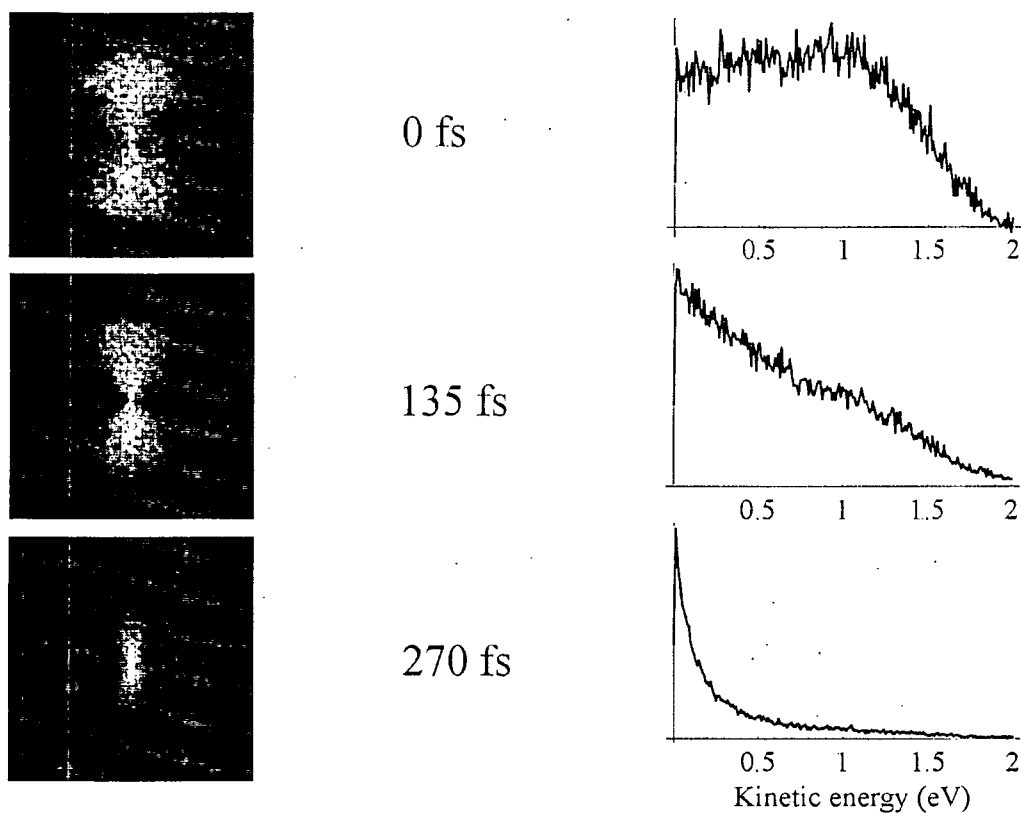


Figure 1. Ion images and kinetic energy distributions at increasing pump-probe time delays for the production of I^+ from CF_3I .

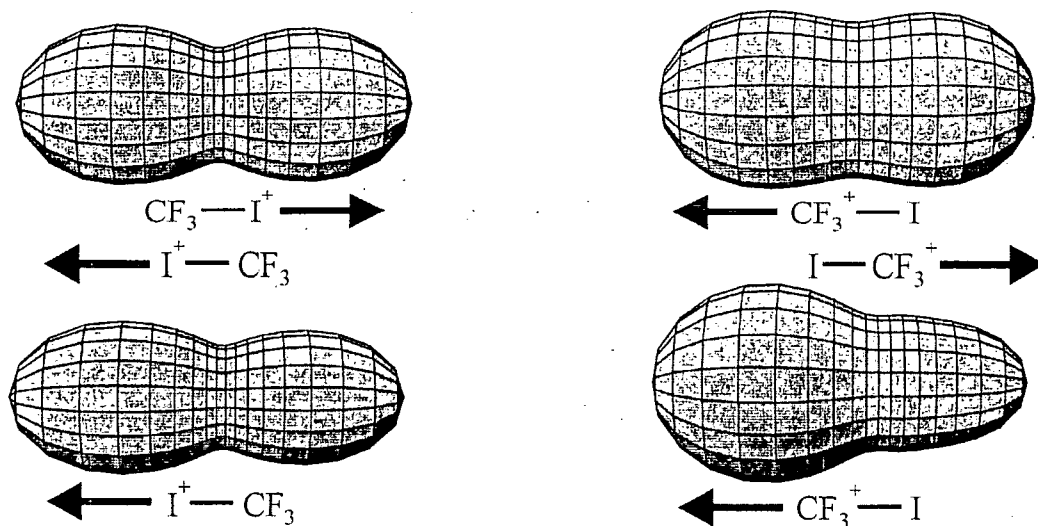


Figure 2. Photoelectron angular distributions coincident with the production of I^+ and CF_3^+ . The top row shows the overall angular distributions for horizontal laser polarizations, while the bottom row shows molecular frame distributions for fragments recoiling only to the left.

CHEMICAL ACCURACY FROM AB INITIO MOLECULAR ORBITAL CALCULATIONS

Martin Head-Gordon
Department of Chemistry, University of California, Berkeley, and,
Chemical Sciences Division, Lawrence Berkeley National Laboratory,
Berkeley, CA 94720.
mhg@cchem.berkeley.edu

1. Scope of Project.

Short-lived reactive radicals and intermediate reaction complexes are believed to play central roles in combustion, interstellar and atmospheric chemistry. Due to their transient nature, such molecules are challenging to study experimentally, and our knowledge of their structure, properties and reactivity is consequently quite limited. To expand this knowledge, we develop new theoretical methods for reliable computer-based prediction of the properties of such species. We apply our methods, as well as existing theoretical approaches, to study prototype radical reactions, often in collaboration with experimental efforts. These studies help to deepen understanding of the role of reactive intermediates in diverse areas of chemistry. At the same time, these challenging problems sometimes reveal frontiers where new theoretical developments are needed in order to permit better calculations in the future.

2. Summary of Recent Major Accomplishments.

2.1 *Time-dependent density functional theory calculations.*

Density functional theory is a simple and effective computational tool for computational studies of the ground and excited states of radicals. For excited states, time-dependent density functional theory (TDDFT) provides an in-principle exact framework for the calculation of excitation energies. We have previously shown that low-lying excited states of radicals can usually be adequately described using TDDFT with existing functionals. This is an exciting result because such states often involve substantial double excitation character that is tremendously difficult to describe within wavefunction-based approaches. This significantly expands the size range of radicals that are amenable to simulation by electronic structure methods.

Over the past year, we have completed three major applications of TDDFT. First, we have studied excited states of carotenoids involved in the light-harvesting complex of purple bacteria [14], after establishing the performance of TDDFT for related polyene oligomers [7]. Using our recently developed approach to describing intermolecular energy transfer within TDDFT [8], we were then able to describe Coulombic coupling leading to energy transfer from the carotenoid to neighboring bacteriochlorophyll molecules.

Second, we have performed calculations on the excited states of closed shell polycyclic aromatic hydrocarbon (PAH) cations which are known to be intermediates in sooting flames [9]. They may also be of relevance in the interstellar medium, and our

study of their electronic spectra suggests that experimental efforts to obtain laboratory spectra are worthwhile. A combined experimental and theoretical study of the fluorene cation has also been completed [16], where all key features seen in the experimental spectrum were assigned using electronic structure methods developed under the support of this program.

Third, we have studied the excited states of the phenyl peroxy radical, and related peroxy radicals, using TDDFT methods [15]. Experiments in solution by the Ingold group (NRC), and in the gas phase by Lim (Emory) showed that it has an absorption in the visible. This is in contrast to the vinyl peroxy radical which only absorbs in the UV, based on experiments by Fahr and Laufer. Furthermore, based on examination of the calculations, we are able to extract a simple and satisfying qualitative picture of the origin of the substituent effects [15]. We may attempt to extend this work to model solvation effects on the absorption.

2.2 *New methods for high accuracy electronic structure calculations.*

While density functional calculations are extremely valuable, the highest levels of accuracy currently possible come from wavefunction-based electronic structure calculations, such as CCSD(T) (which are also dramatically more expensive). We have performed systematic benchmarks of the performance of existing electronic structure methods for structure and vibrational frequency prediction for radicals [13]. We found that advanced coupled cluster methods performed significantly less well for radicals than for closed shell molecules, with the widely used CCSD(T) method offering no net improvement over CCSD.

To try to overcome the deficiencies of (T) corrections for radicals and for the related problem of bond-dissociation to radical fragments, we have developed a new correction to singles and doubles coupled cluster methods [3]. This new method is a true second order correction to a coupled cluster reference, and therefore we denote the correction as (2). The physics of this correction, when applied to a singles and doubles coupled cluster reference, is that it accounts for the leading 3 and 4-electron correlations between electrons. The reference itself only accounts for pair correlations.

In addition to the general formulation, we have developed specific versions to correct the optimized orbital coupled cluster doubles method, as OD(2) [1], the coupled cluster singles and doubles method, as CCSD(2) [10], and the quadratic coupled cluster doubles method, as QCCD(2) [17]. It will of course be some time before the strengths and weaknesses of our new (2) corrections relative to CCSD(T) are completely clear. The most striking result we have obtained to date is a 4 to 5-fold reduction in error for QCCD(2) versus CCSD(T) for predicting the structure and harmonic frequency of N₂ (errors are relative to exact calculations). The level of accuracy obtained by QCCD(2) for this problem actually approaches CCSDTQ! This provides strong incentive for further testing and development of the (2) corrections.

2.3 *How compact can the exact many-body wavefunction be?*

An exciting theoretical result was obtained [11] on the ability to write the exact wave function in a very compact form, similar to a generalized coupled cluster doubles wave

function, and depending on a number of variables only equal to the degrees of freedom in the two-particle density matrix. The usual linear expansion of the exact wavefunction involves a factorial number of degrees of freedom! This compact form may offer a way around the problems of n-representability that have plagued attempts to develop electronic structure theory based on the 2-particle density matrix. While (as far as we can tell!) not directly useful for practical calculations, this may be a basis for novel approximations in the future.

3. Summary of Research Plans.

3.1 *Density functional theory for excited states of radicals.*

We are planning further development and application of the time-dependent density functional (TDDFT) approach to excited states of large molecules, particularly radicals. We are performing a combined theoretical and experimental study of the perylene, terrylene (C₃₀H₁₆) and quaterrylene (C₄₀H₂₀) series, examining neutral, radical cation and radical anion of each species. We hope to assign the main peak seen experimentally and explain trends in oscillator strength. We are also calculating excitation energies and oscillator strengths for other large PAH molecules, including coronene, circumcoronene, and ovalene, looking for the origin of trends in oscillator strength and excitation energy. We are also working on extensions of TDDFT to explore excited potential energy surfaces via gradient and possibly hessian evaluation. This should later permit prediction of lineshapes, and possibly also non-radiative lifetimes.

3.2 *Accurate electronic structure methods.*

Based on the very exciting preliminary results we have obtained so far, we plan to assess the strengths and weaknesses of our new (2) approach to performing high accuracy corrections to singles and doubles coupled cluster theory. The code will be made more efficient and tests for reaction barriers, accurate thermochemistry and spectroscopic constants of small radicals will be performed. Separately we are working on the problem of developing new wavefunction-based methods for the description of radicals that are spin-pure, rather than the usual approach of breaking spin-symmetry. This will build on ideas of perfect pairing, and observations we have made earlier on the importance of "spin-flip" configurations in the excited states of radicals.

4. Publications from DOE Sponsored Work, 2000-present.

- [1] "A Second Order Correction to Singles and Doubles Coupled Cluster Methods Based on a Perturbative Expansion of a Similarity-Transformed Hamiltonian", S.R.Gwaltney and M.Head-Gordon, Chem. Phys. Lett. 323, 21-28 (2000).
- [2] "Complete Basis Set Extrapolations for Low-lying Triplet Electronic States of Acetylene and Vinylidene", C.D.Sherrill, E.F.C.Byrd, and M.Head-Gordon, J. Chem. Phys. 113, 1447-1454 (2000).
- [3] "Second Order Perturbation Corrections to Singles and Doubles Coupled Cluster Methods: General Theory and Application to the Valence Optimized Doubles Model", S.R.Gwaltney, C.D.Sherrill, M.Head-Gordon, and A.I.Krylov, J. Chem. Phys. 113, 3548-3560 (2000).

- [4] "Excited States Theory for Optimized Orbitals and Valence Optimized Orbitals Coupled-Cluster Doubles Models", A.I.Krylov, C.D.Sherrill, and M.Head-Gordon, *J. Chem. Phys.* 113, 6509-6527 (2000).
- [5] "Q-Chem 2.0: A High Performance Ab Initio Electronic Structure Program Package", J.Kong, C.A.White, A.I.Krylov, C.D.Sherrill, R.D.Adamson, T.R.Furlani, M.S.Lee, A.M.Lee, S.R.Gwaltney, T.R.Adams, C.Ochsenfeld, A.T.B.Gilbert, G.S.Kedziora, V.A.Rassolov, D.R.Maurice, N.Nair, Y.Shao, N.A.Besley, P.E.Maslen, J.P.Dombroski, H.Daschel, W.Zhang, P.P.Korambath, J.Baker, E.F.C.Byrd, T.Van Voorhis, M.Oumi, S.Hirata, C.-P.Hsu, N.Ishikawa, J.Florian, A.Warshel, B.G.Johnson, P.M.W.Gill, M.Head-Gordon, J.A.Pople, *J. Comput. Chem.* 21, 1532-1548 (2000).
- [6] "Tensors in Electronic Structure Theory: Basic Concepts and Applications to Electron Correlation Models", M. Head-Gordon, M. S. Lee, P.E.Maslen, T. van Voorhis and S. R. Gwaltney, in "Modern Methods and Algorithms of Quantum Chemistry", edited by J.Grotendorst, NIC Series Volume 3, Second Edition (NIC Directors, Juelich, 2000), pp. 593-638.
- [7] "Excitation Energies from Time-Dependent Density Functional Theory for Linear Polyene Oligomers: Butadiene to Decapentaene", C.-P.Hsu, S.Hirata and M.Head-Gordon, *J. Phys. Chem. A* 105, 451-458 (2001).
- [8] "Excitation Energy Transfer in Condensed Media", C.-P. Hsu, G.R. Fleming, M. Head-Gordon, and T. Head-Gordon, *J. Chem. Phys.* 114, 3065-3072 (2001).
- [9] "Electronic Spectra and Ionization Potentials of a Stable Class of Closed Shell Polycyclic Aromatic Hydrocarbon Cations", J. L. Weisman, T. J. Lee, and M. Head-Gordon, *Spectrochim. Acta A*, 57, 931-945 (2001).
- [10] "A second order correction to the coupled cluster singles and doubles method: CCSD(2)", S. R. Gwaltney and M. Head-Gordon, *J. Chem. Phys.* 115, 2014-2021 (2001).
- [11] "Two body coupled cluster expansions", T. Van Voorhis and M. Head-Gordon, *J. Chem. Phys.* 115, 5033-5040 (2001).
- [12] "Calculating the Equilibrium Structure of the BNB Molecule: Real Versus Artificial Symmetry Breaking", S.R. Gwaltney and M. Head-Gordon, *Phys. Chem. Chem. Phys.* 3, 4495-4500 (2001).
- [13] "The theoretical prediction of molecular radical species: a systematic study of equilibrium geometries and harmonic vibrational frequencies", E.F.C. Byrd, C.D. Sherrill, and M. Head-Gordon, *J. Phys. Chem. A* 105, 9736-9747 (2001).
- [14] "The role of the S1 state of carotenoids in photosynthetic energy transfer: the light harvesting complex II of purple bacteria", C.-P. Hsu, P.J. Walla, M. Head-Gordon, and G.R. Fleming, *J. Phys. Chem. B* 155, 11016-11025 (2001).
- [15] "On the Origin of Substituent Effects in the Absorption Spectra of Substituted Peroxy Radicals: Time-Dependent Density Functional Theory Calculations", J.L. Weisman and M. Head-Gordon, *J. Am. Chem. Soc.* 123, 11686-11694 (2001).
- [16] "Vibrational and Electronic Spectroscopy of the Fluorene Cation", J. Szczepanski, J. Banisaukas, M. Vala, S. Hirata, R.J. Bartlett, and M. Head-Gordon, *J. Phys. Chem. A* 106, 63-73 (2002).
- [17] "A Perturbative Correction to the Quadratic Coupled Cluster Doubles Method for Higher Excitations", S. R. Gwaltney, E. F. C. Byrd, T. Van Voorhis, and M. Head-Gordon, *Chem. Phys. Lett.* 353, 359-367 (2002).

**Laser Studies of the
Combustion Chemistry of Nitrogen**

John F. Hershberger

**Department of Chemistry
North Dakota State University
Fargo, ND 58105
john.hershberger@ndsu.nodak.edu**

Time-resolved infrared diode laser spectroscopy is used in our laboratory to study the kinetics and product channel dynamics of chemical reactions of importance in the gas-phase combustion chemistry of nitrogen-containing radicals. This program is aimed at improving the kinetic database of reactions crucial to the modeling of NO_x control strategies such as Thermal de-NO_x, RAPRENO_x, and NO-reburning. The data obtained is also useful in the modeling of propellant chemistry. The emphasis in our study is the quantitative measurement of both total rate constants and product branching ratios.

HCCl + NO_x Reactions

We have completed our investigation of reactions of the HCCl radical using both laser-induced fluorescence and infrared absorption techniques. This radical is of interest in modeling the combustion of chlorinated hydrocarbons. We form HCCl from 193-nm photolysis of HCClBr₂, and detect it by LIF spectroscopy at 602.53 nm. We have measured rate constants for HCCl + NO and HCCl + NO₂ over the temperature ranges 298-572 and 298-476 K, respectively. Using LIF detection of HCCl and standard pseudofirst order kinetics, we obtain a total rate constant of $(2.75 \pm 0.2) \times 10^{-11} \text{ cm}^3 \text{ molecule}^{-1} \text{ s}^{-1}$ at 296 K for HCCl+NO, which is somewhat higher than the one previous report¹ of $(1.5 \pm 0.5) \times 10^{-11}$. For the HCCl + NO₂ reaction, we obtain $k = (1.10 \pm 0.02) \times 10^{-10} \text{ cm}^3 \text{ molecule}^{-1} \text{ s}^{-1}$ at 296.

For HCCl+NO, several product channels are possible:



Using infrared diode absorption spectroscopy, we have detected HCNO, N₂O, and CO₂ product molecules upon photolysis of CHClBr₂/NO/SF₆ mixtures. We attribute the formation of N₂O and CO₂ to the secondary reaction:



Previous experiments in several laboratories including our own have shown that this reaction is fast and produces N₂O and CO₂ in roughly equal yields. Our best numbers are $\phi_{2a}=0.44$ and $\phi_{2b}=0.56$, independent of temperature over the range 296-500 K.²

Calibration of N₂O and CO₂ signals is straightforward using published linestrengths. Our results show that the relative yields of these molecules is consistent with the statement that they originated entirely from the NCO+NO reaction. By measuring the 193-nm absorption coefficient of HCClBr₂ and assuming a quantum yield for HCCl production of unity, we obtain a branching ratio of 0.24 ± 0.04 into channel (1c)

HCNO (fulminic acid) is the major product of this reaction. Calibration of these signals is more difficult, and is described in detail in our publication. We obtained an estimate of $\phi_{1a} = 0.68\pm 0.06$ at 296 K. Since $\phi_{1a}+\phi_{1c}$ is close to unity, we conclude that our assumptions about unity photolysis quantum yields are correct, and that no other channel makes a major contribution.

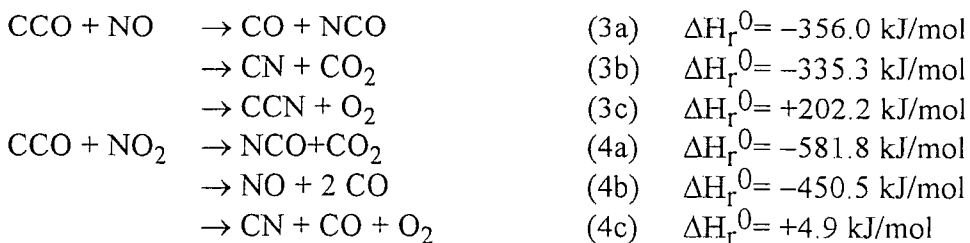
CCO + NO_x Reactions

We are currently investigating reactions of CCO radicals with NO and NO₂. We have detected infrared absorption signals near 1970 cm⁻¹ assignable³ to CCO upon photolysis of carbon suboxide (C₃O₂). When using 193 nm radiation, the transients have rather long risetimes of ~50 μsec, possibly because CCO is initially formed in an excited singlet electronic state. Upon 248 nm photolysis, somewhat faster risetimes are observed, which is consistent with other reports that mostly ground electronic state CCO is produced at this wavelength. As a result, most of our kinetic data have been collected using 248 nm. We have measured the following total rate constants (in cm³ molecule⁻¹ s⁻¹):

$$k(\text{CCO}+\text{NO}) = (1.25\pm 0.5)\times 10^{-10} \exp[-(274\pm 149)/T] \quad (T=298-605 \text{ K})$$

$$k(\text{CCO}+\text{NO}_2) = (6.38\pm 0.3)\times 10^{-11} \exp[-(2.2\pm 2.4)/T] \quad (T=298-598 \text{ K})$$

Possible product channels include:



NCO formed in channels (3a) would then be expected to react with NO via reaction (2), producing CO, CO₂, and N₂O products. We have detected CO and N₂O products in the CCO+NO system. One complication is that CO is formed in large amounts in the C₃O₂ photolysis. We have measured the contribution of channel (3a), however, by measuring the N₂O yield, and assuming that reaction (2a) is the primary source of this molecule. A preliminary estimate of the branching ratio is $\phi_{3a}=0.3\pm 0.05$ at 298 K. We are also doing ab initio calculations on this system to further elucidate the mechanism. The potential surface is

complicated, with several three-member ring intermediates and transition states, but it appears that low energy routes to both (3a) and (3b) exist.

CCN Kinetics

We have begun work on kinetic measurements of the CCN radical. At present, the best precursor we have for this species is HBr_2CCN . This precursor is known to produce HCCN upon 193 nm photolysis.⁴ We have found that by weakly focusing the excimer beam, we produce significant amounts of CCN via multiphoton dissociation. CCN is then detected by laser-induced fluorescence at ~ 403 nm. Although use of focused photolysis light introduces some additional problems, this approach is adequate for total rate constant measurements using LIF, and we have a preliminary estimate of the CCN+NO rate constant of $(2.98 \pm 0.8) \times 10^{-12} \text{ cm}^3 \text{ molecule}^{-1} \text{ s}^{-1}$ at 300 K. We are currently investigating the temperature and pressure dependence of this reaction.

Several product channels are possible:



Unfortunately, our photolytic precursor is not particularly suitable for product yield measurements, because of the HCCN that is also produced. We do see some differences between product yields when comparing experiments with focused and unfocused beams. For example, CO is produced in much higher yield relative to N₂O and CO₂ when using focused photolysis light. This CO could have come from channels (5d) or (5e), or from secondary chemistry of NCO or CCO from (5a) or (5b). We do not believe it is practical to obtain more than qualitative information from the data using this precursor.

One future plan is to try an alternative precursor: the synthesis of NCCNO, variously called cyanofulminate or cyanogen N-oxide, has been reported recently.⁵ The photodissociation channels have not been investigated. If this molecule produces CCN+NO upon photolysis, it would make an excellent precursor for CCN radical studies. On the other hand, if it produces CN+CNO, it might make a good precursor for CNO, which is a less well studied isomer of the NCO radical. In the near future, we plan to investigate the photolysis channels of this molecule.

NCN Kinetics

NCN has been suggested as a possible intermediate in the prompt-NO process. The kinetics of this species are therefore of interest. We have started work on kinetic measurements of the NCN+NO_x reactions. We form NCN by a very old technique:⁶ photolysis of a mixture of C₂N₂ and CH₂N₂. Several species, including CN and CH₂ are formed in this system. It is not clear exactly how the NCN is produced, but possibilities

include reactions such as ${}^1\text{CH}_2 + \text{C}_2\text{N}_2 \rightarrow \text{C}_2\text{H}_2 + \text{NCN}$, or $\text{CN} + \text{CH}_2\text{N}_2 \rightarrow \text{NCN} + \text{CH}_2\text{N}$. We detect NCN using previously characterized LIF spectroscopy at 329 nm. Several products are possible:



We observe a pressure-dependent rate constant for NCN+NO, suggesting that NCNNO complex stabilization is a significant product channel. Only trace amounts of N_2O and CO_2 products are observed. At low total pressures (1-3 Torr), a rate constant of $(2.88 \pm 0.2) \times 10^{-13} \text{ cm}^3 \text{ molec}^{-1} \text{ s}^{-1}$ at 298 K is observed, with a negative temperature dependence. The NCN+ NO_2 reaction is very slow at low pressures; we are still investigating whether the rate constant increases at higher pressures.

References

1. R. Wagener, H. Gg. Wagner, *Z. Phys. Chem.* 175, 9 (1992).
2. W.F. Cooper, J. Park, J.F. Hershberger, *J. Phys. Chem.* 97, 3283 (1993).
3. C. Yamada, H. Kanamori, H. Horiguchi, S. Tsuchiya, E. Hirota, *J. Chem. Phys.* 84, 2573 (1986).
4. J.D. Adamson, J.D. DeSain, R.F. Curl, and G.P. Glass, *J. Phys. Chem. A* 101, 874 (1997).
5. T. Pasinszki, N.P.C. Westwood, *J. Phys. Chem.* 100, 16856 (1996).
6. G. Herzberg, D.N. Travis, *Can. J. Phys.* 42, 1658 (1964).

Publications acknowledging DOE support (1999-present)

“Temperature Dependence of the Product Branching Ratio of the $\text{CN} + \text{O}_2$ Reaction”, K.T. Rim and J.F. Hershberger, *J. Phys. Chem. A* **103**, 3721 (1999).

“Kinetics of the NCS Radical”, R.E. Baren and J.F. Hershberger, *J. Phys. Chem. A* **103**, 11340 (1999).

“Product Branching Ratio of the $\text{HCCO} + \text{NO}$ Reaction”, K.T. Rim and J.F. Hershberger, *J. Phys. Chem. A* **104**, 293 (2000).

“Recent Progress in Infrared Absorption techniques for Elementary Gas Phase Reaction Kinetics”, C. Taatjes and J.F. Hershberger, *Ann. Rev. Phys. Chem.* **52**, 41 (2001).

“Kinetics of $\text{HCCl} + \text{NO}_x$ Reactions”, R.E. Baren, M. Erickson, and J.F. Hershberger, *Int. J. Chem. Kinet.* **34**, 12 (2002).

“Kinetics of the NCN Radical”, R.E. Baren and J.F. Hershberger, *J. Phys. Chem. A*, submitted.

Small-Angle X-ray Scattering Studies of Soot Inception and Growth

Jan P. Hessler

Chemistry Division, Argonne National Laboratory
9700 South Cass Avenue, Argonne, Illinois 60439-4831
E-mail: hessler@anl.gov

1. Scope

Under fuel-rich conditions hydrocarbon fuels produce soot, which appears as an ensemble of ultra-fine particles that range in size up to a few hundred nanometers. A comprehensive theory or model that is capable of predicting the inception and growth of soot over a wide range of chemical and physical conditions is just beginning to emerge. Such a model is needed to help reduce the health hazards associated with soot production, improve the radiative transfer of energy in industrial applications, and devise efficient production processes that use soot in various applications. The high spectral intensity of x-rays produced by the undulator at the Basic Energy Sciences Synchrotron Radiation Center of Argonne's Advanced Photon Source has allowed us to perform small-angle x-ray scattering (SAXS) studies of the initial distribution of soot particles formed by various fuels. SAXS provides an *in situ* probe of the morphology of soot in the region from less than 1 to 100 nm and complements the *ex situ* technique of electron microscopy. Recently, we reviewed the salient features of SAXS that are needed to study the kinetics of soot formation.[1]

2. Recent Progress

2.1. Bimodal distributions and transition regions

Kinetic information about soot formation is obtained by measuring the intensity of the scattered x-rays as a function of the magnitude of the transferred momentum, $q = (4\pi/\lambda)\sin(\theta/2)$ where θ is the scattering angle. In March of last year we obtained data at several heights above our burner and several positions with respect to the axis of the flame. These allowed us to perform Abel inversions and, thereby, extract the radial dependence of the scattering intensity. We identified a spatially-dependent background due to the reduced density of scatters near the flame front. This background is more

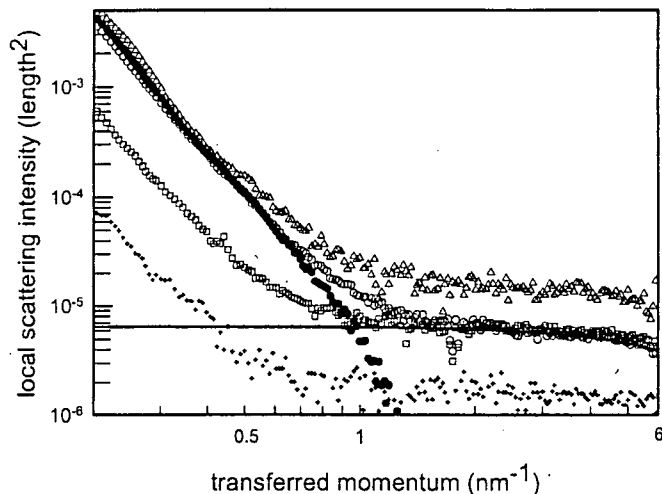


Figure 2.1: Measured SAXS profiles at several different positions with respect to the axis of a propylene diffusion flame.

pronounced in a self-sustaining flame such as an acetylene diffusion flame than in the pyrolysis of toluene in the post-flame region of a methane/hydrogen flat-flame. After this background, which may be approximated by a parabola, has been subtracted we perform the Abel inversion at each value of transferred momentum and then reconstruct the radial dependence of the local scattering intensity. An example of the local scattering intensity at several different radial positions is shown in figure 2.1. This and other data suggest that at least a bimodal distribution is needed to describe the SAXS data. The slowly varying part of the intensity for $q \geq 1 \text{ nm}^{-1}$ indicates that we are observing scattering from relatively small structures. As a test of the capabilities of SAXS, with S. Seifert and R. E. Winans, we have measured the scattering from effusive beams of Naphthalene, Anthracene, *tert*-Butylanthracene, Phenanthrene, and Pyrene. The details of the behavior for $q \leq 1 \text{ nm}^{-1}$ are best shown in a plot of $q^4 I(q)$ vs. q , which amplifies the deviations from q^{-4} behavior. An example is shown in figure 2.2. The location of the dip in the 0.9 mm profile at $q \simeq 0.35 \text{ nm}^{-1}$ indicates the particles have a mean radius of gyration, $\langle R_g \rangle$, of about 10 nm while the depth of the dip indicates that the polydispersity of a Schultz distribution, $\sigma / \langle R_g \rangle$, is about 0.3. We refer to these as primary soot particles. As we move from 0.9 to 1.3 mm the profiles change systematically until the first dip becomes stable at 0.2 nm^{-1} . Particles at this and larger

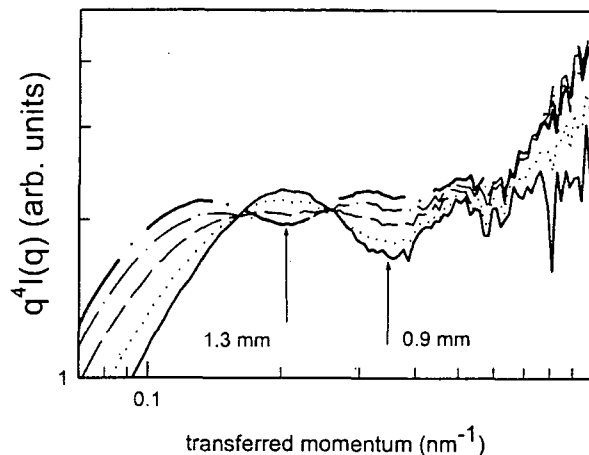


Figure 2.2: Plot of $\log[q^4 I(q)]$ vs. $\log [q]$ at distances of 0.9, 1.0, 1.1, 1.2, and 1.3 mm from the axis of a propane flame.

distances from the center of the flame have $\langle R_g \rangle \simeq 21$ nm and $\sigma / \langle R_g \rangle \simeq 0.2$. We note that the profiles at 1.3 mm and beyond have minima that are within 20% of those observed by Sornsen, Oh, Schmidt, and Rieker who studied SAXS from various types of mature soot.[2] From similar observations at different heights we may construct the following description of soot formation. At short times, close to the source of the fuel, the small species dominate. As we move up in the flame we begin to see highly dispersed primary particles. The mean size of these particles is the same on both the fuel rich and lean side of the flame front. Near the widest part of the flame we begin to see the transition region shown in figure 2.2. As we continue higher the extent of this transition region increases. Clearly, the description of soot morphology that we obtain with x-ray scattering contains detailed information that simply has not been previously observed.

2.2. A detector for time-resolved SAXS

The prototype of the annular detector that we have designed to have a temporal resolution that will match the revolution time of an electron bunch at the APS, 3.68 μ s was tested by observing scattering from a burning droplet as it fell through the x-ray beam. With a similar detector we will be able to monitor the formation of soot in a shock tube in the critical period that is not accessible to elastic scattering in the optical region.

3. Future Plans

The small species that scatter significantly above 1 nm^{-1} must be identified. In addition to our work on effusive molecular beams mentioned above, we note that Chen and Dobbins[3] have observed diffraction maxima from disordered carbons at $q \simeq 13 \text{ nm}^{-1}$. We plan to observe this diffraction peak in a flame. The width of this peak will provide information about the size of the particles that contain the disordered carbon. If we can characterize the spatial and temporal dependence of x-ray scattering from $0.1 \leq q(\text{nm}^{-1}) \leq 15$ or 20 we should have the most detailed description of soot inception and formation that may be obtained with an *in situ* technique. We now feel that we have developed enough experience in SAXS that we can obtain scattering information that can be used to develop and test models of soot formation. We plan to perform experiments that are designed to identify and test critical aspects of these models.

References

- [1] J. P. Hessler, S. Seifert, R. E. Winans, and T. H. Fletcher, *Faraday Discuss.*, 2001, **119**, 395-407.
- [2] C. M. Sornsen, C. Oh, P. W. Schmidt, and T. P. Rieker, *Phys. Rev. E*, 1998, **58**, 4666-4672.
- [3] H. X. Chen and R. A. Dobbins, *Combust. Sci. and Tech.*, 2000, **159**, 109-128.

Publications Supported by this Program 2000-present

Small-angle X-ray studies of soot inception and growth

J. P. Hessler, S. Seifert, R. E. Winans, and T. H. Fletcher, *Faraday Discuss.*, 2001, **119**, 395-407.

Spatially Resolved Small-Angle X-ray Scattering Studies of Soot Morphology During Inception and Growth

J. P. Hessler, S. Seifert, and R. E. Winans, to be published in *Proc. Comb. Inst.* 2002, **29**

Small-Angle X-ray Scattering for Studies of Soot Inception and Formation

J. P. Hessler, S. Seifert, and R. E. Winans, to be published in *Preprints of Symposia*, Division of Fuel Chemistry, 224th National Meeting of the American Chemical Society, Aug 18-22, 2002, Boston, Mass.

PRODUCT IMAGING OF COMBUSTION DYNAMICS

P. L. Houston
Department of Chemistry
Cornell University
Ithaca, NY 14853-1301
plh2@cornell.edu

Program Scope

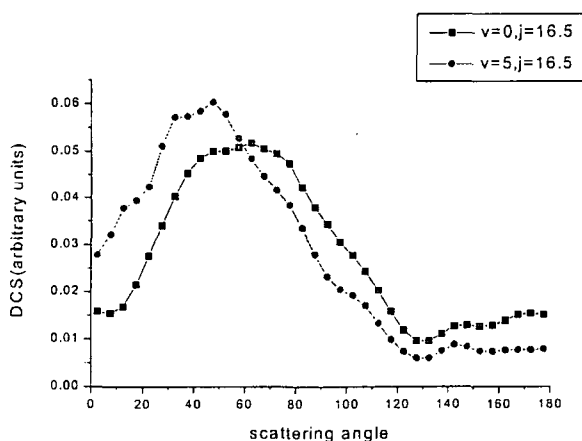
The technique of product imaging is being used to investigate several processes important to a fundamental understanding of combustion. The imaging technique produces a "snapshot" of the three-dimensional velocity distribution of a state-selected reaction product.

Research in three main areas is planned. First, the imaging technique will be used to measure rotationally inelastic energy transfer on collision of closed-shell species with several important combustion radicals. Such measurements improve our knowledge of intramolecular potentials and provide important tests of *ab initio* calculations. Second, product imaging will be used to investigate the reactive scattering of radicals or atoms with species important in combustion. These experiments, while more difficult than studies of inelastic scattering, are now becoming feasible. They provide both product distributions of important processes as well as *angular information important to the interpretation of reaction mechanisms*. Finally, experiments using product imaging at the Advanced Light Source will explore the vacuum ultraviolet photodissociation of CO₂ and other important species. Little is known about the highly excited electronic states of these molecules and, in particular, how they dissociate. These studies will provide product vibrational energy distributions as well as angular information that can aid in understanding the symmetry and crossings among the excited electronic states.

Recent Progress

Rotational Differential Cross Sections for Vibrational Excited States

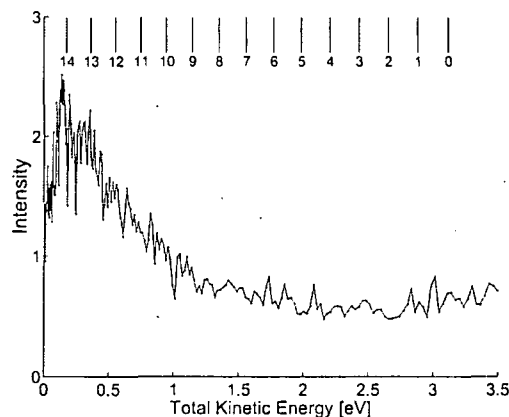
Rotationally inelastic scattering of vibrationally excited NO($v=5$) from Ar was studied with a crossed molecular beam ion imaging apparatus. Vibrationally excited NO was generated at the exit of a pulsed nozzle by the photo-initiated reaction between O(¹D) and N₂O. The results for rotational excitation in vibrationally excited NO were compared to those in the vibrational ground state at a collision energy of 1460 cm⁻¹. The final rotational state of NO, populated by scattering from Ar, was detected by a 1+1 REMPI via the A(²Σ⁺)←X(²Π_{1/2}) electronic transition. The R₂₁ transition was used to probe the final scattered state in both cases. As shown in the figure for $J=16.5$, the rotational rainbow maxima are observed at slightly smaller angles in the scattering of vibrationally excited NO from



Ar compared to the scattering of NO in the vibrational ground state from Ar. A hard ellipse potential model was used to investigate the effect of initial vibrational excitation on the rotational energy transfer process. The small shifts observed in the rainbow maxima are evidence for a slight enhancement in angular anisotropy in the intermolecular potential for NO($v=5$)/Ar compared to NO($v=0$)/Ar.

N(2D) Product Velocity Mapped Imaging in the VUV Photolysis of Nitrous Oxide at 118.2 nm

Resonance-enhanced multiphoton ionization with time-of-flight product imaging of the N(2D) atoms has been used to study the N₂O photodissociation at 118.2 nm and the two-photon dissociation at 268.9 nm. These imaging experiments allowed the determination of the total kinetic energy distributions of the NO(X) and N($^2D_{5/2}$) products. The NO(X) fragments resulting from the photodissociation processes are produced in highly vibrationally excited states. The two-photon photodissociation process yields a broad NO(X) vibrational energy distribution, while the 118.2 nm dissociation appears to produce a vibrational distribution sharply peaked at NO(X, $v=14$), as shown in the figure.



Total kinetic energy distribution of N($^2D_{5/2}$) + NO(X)

Future Directions

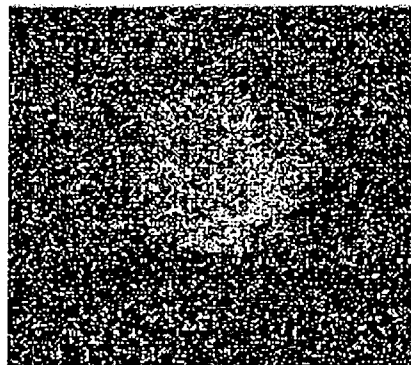
Our success in measuring differential cross sections for rare gas collisions with the densities of NO(v, J) that we can produce in our photolysis source gives us confidence that we can use the capabilities of our source to study differential cross sections for collisions of rare gas atoms with various radical species. Members of our group (as well as others) have extensive experience in creating radicals by photolysis, and many of these can be ionized by simple REMPI schemes. For example, for comparison to the work of Bowman and co-workers, we could create HCO from 308 nm photolysis of acetaldehyde and detect the product rotational states by ionization. Other systems amenable to study by this technique include collisions of rare gases or small molecules with the following radicals: SO, SH, PO, NH, CH₃ and CH₃O.

For example, we are currently using a crossed molecular beam ion imaging system for studying the scattering of SO radicals from Ar. The SO radicals are generated by photolysis of 20% SO₂/Ar by 193 nm excimer laser (Lambda Physik, Compex 200). The 193 nm light is focused at the exit of a piezoelectric nozzle. The beam of SO radicals travels a distance of about 10 cm and then crosses a beam of Ar at a right angle. Scattered SO is detected by a 1+1 REMPI ionization scheme using the B-X transition (3-0 band). The Ar beam is toggled between on and off states every 60 shots, and the signal is recorded for each toggle state. The difference of the signal from the two toggle states corrects for the background population that might be present in the radical beam. Ion optics accelerate the ions perpendicular to the

scattering plane. The Newton sphere is imaged on a detector comprising of chevron mounted MCPs and phosphor assembly. A CCD camera (Xybion CCD-50) images the phosphor.

The (3-0) B-X band was scanned in the range 231.35-231.6 nm. An etalon was used to scan the wavelength. Rotational lines from the resolved spectrum were used to image state specific differential scattering cross section for SO from Ar.

The figure at right presents the results for scattering into the $P_2(J''=10)$ line. A dim outline of the Newton sphere is visible, as most of the scattering is in the forward direction (lower right).



We also plan to investigate differential cross sections for reactive collisions. A start has been made on the $O(^1D) + N_2O$ system and the $OH + CO$ system, but improvements to the apparatus will be required to make these practical.

A third area of future investigation is determination of vibrational distributions following VUV photodissociation of small molecules. The N_2O work reported above was an evaluation experiment to see what could be done with laboratory-based lasers; we found that even for the most strongly absorbing systems, the experiment is difficult. This may explain why, despite the large absorption coefficients of small molecules in the vacuum ultraviolet region of the spectrum, little is known either about their excited states or about the products they dissociate to. The availability of a beam line at the Advanced Light Source now makes it possible to investigate the dynamics of energy release for small molecules following absorption of a VUV photon. Typical absorption cross sections in the region from 110-140 nm are on the order of $1 \times 10^{-16} \text{ cm}^2$. For triatomics, multiphoton ionization of the atomic photodissociation fragment can be performed with very high efficiency. It should thus be possible using the product imaging facilities of End Station Three at the ALS to image the atomic fragment, thereby determining the vibrational distribution of the sibling diatomic fragment. Such information should help in understanding what bonds in addition to the dissociative one either lengthen or bend during the dissociation process. Angular distributions of products also provide information about the symmetry of the excited state and the time scale for dissociation.

Publications Prepared with DOE Support 2001-2002

P. L. Houston, B. R. Cosofret, A. Dixit, S. M. Dylewski, J. D. Geiser, J. A. Mueller, R. J. Wilson, P. J. Pisano, M. S. Westley, K. T. Lorenz, and D. W. Chandler, "Product Imaging Studies of Photodissociation and Bimolecular Reaction Dynamics," *J. Chinese Chem. Soc.*, **48**, 309-318 (2001).

A. A. Dixit, P. J. Pisano, and P. L. Houston, "Differential cross section for rotationally inelastic scattering of vibrationally excited NO($v=5$) scattered from Ar," *J. Phys. Chem.* **105**, 11165-11170 (2001).

P. L. Houston, "Charged Particle Imaging in Chemical Dynamics: An Historical Perspective," in *Imaging in Molecular Dynamics: Technology and Applications*, B. Whitaker, ed. (Cambridge University Press, in press).

Bogdan R. Cosofret, H. Mark Lambert, and Paul L. Houston, "N(2 D) Product Velocity Mapped Imaging in the VUV Photolysis of Nitrous Oxide at 118.2 nm," *J. Korean Chem. Soc.*, *accepted*, (K.-H. Jung commemorative issue).

AROMATICS OXIDATION AND SOOT FORMATION IN FLAMES

J. B. Howard and H. Richter
MIT Department of Chemical Engineering
77 Massachusetts Avenue
Cambridge, MA 02139-4307
Email: jbhoward@mit.edu

Scope

This project is concerned with the kinetics and mechanisms of aromatics oxidation and soot and fullerenes formation in flames. The overall objective of the aromatics oxidation work is to extend the study of benzene oxidation by measuring concentration profiles for important benzene decomposition intermediates such as phenyl and phenoxy radicals which could not be adequately measured with molecular-beam mass spectrometry to permit definitive testing of benzene oxidation mechanisms. The focus includes polycyclic aromatic hydrocarbons (PAH) radicals which are of major importance under fuel-rich conditions although their concentrations are in many cases too low to permit measurement with conventional molecular beam mass spectrometry. The radical species measurements are used in critical testing and improvement of benzene oxidation and PAH growth mechanisms. The overall objective of the research on soot formation is to extend the measurement of radicals into the overlapping region of large molecular radicals and small soot particles with radical sites. The ultimate goal is to understand how nascent soot particles are formed from high molecular weight compounds, including the roles of planar and curved PAH and the relationships between soot and fullerenes. The specific aims are to characterize both the high molecular weight compounds involved in the nucleation of soot particles and the structure of soot including internal nanoscale features indicative of contributions of planar and/or curved PAH to particle inception.

Recent Progress

The development of a kinetic model describing the oxidation of hydrocarbons has been continued. Currently, the mechanism consists of 256 species and 1101 reactions and the corresponding thermodynamic and transport property data have been assembled. Thermodynamic property data were taken from the literature or were determined by means of density functional theory (DFT). In some cases *ab initio* calculations on a complete basis set level (CBS-Q and CBS-RAD) were carried out [1]. Isodesmic reactions were used for the heats of formation of most radical species while vibrational analysis allowed for the determination entropies and heat capacities. Quantum Rice-Ramsperger-Kassel (QRRK) [2] analysis was conducted in order to determine pressure-dependent rate constants of chemically activated reactions.

The use of kinetic modeling for practical combustion devices requires sufficient predictive capabilities for a large range of conditions, i.e., type of fuel, equivalence ratio, pressure and temperature. The model has been extensively tested for acetylene [3,4], ethylene [5,6], benzene [7-10] and methane [11] combustion. Structures of low-pressure laminar premixed flames have been taken from the literature [3-11]. All computation have been conducted with the Premix code of the Chemkin software package [12] using experimental temperature profiles as input. The determination of rates of production of selected species using a feature in the postprocessor of the flame code [12] allowed for the quantification of the contributions of specific reactions to the formation and consumption of selected species.

The investigated flames covered equivalence ratios from lean [5] to stoichiometric [11] and rich [3,4,6-10] allowing for the assessment of the competition between oxidation and growth processes leading to polycyclic aromatic hydrocarbons (PAH) of increasing size and ultimately to soot. Flat PAH containing exclusively condensed hexagons up to coronene (C₂₄H₁₂, 300 amu) and molecules containing five-membered rings are included in the model.

The kick-off of the sequential formation of PAH of increasing size is widely determined by the competition between oxidation and growth reactions. Therefore, a detailed knowledge of the formation and consumption of the first aromatic structure, particularly benzene and also naphthalene, is essential for a correct description of combustion processes under fuel-rich conditions. Benzene formation has been investigated in rich premixed acetylene [3,4] and ethylene [6] flames. Self-combination of propargyl (HCCCH₂) was found to be the dominant benzene formation pathway in both rich acetylene and ethylene flames. In addition, reaction of vinyl with vinylacetylene, i.e., C₄H₄ + C₂H₃ ⇌ benzene + H, contributed to benzene formation in the rich ethylene flame [13]. Reactions of ¹CH₂ and ³CH₂ with acetylene were found to be the major propargyl formation route. Pressure dependence of these reactions was taken into account. Hydrogen abstraction by H and to some extent OH radicals, to form C₃H₂ observed experimentally by mass spectrometry [3,4-7], was identified as the dominant propargyl consumption route. In agreement with Mebel et al. [14], the structure HCCCH (propargylene) was assigned to the C₃H₂ species, its thermodynamic properties were determined based on a CBS-Q optimized structure [1].

The kinetic model has been also applied to two low-pressure premixed stoichiometric methane/air flames with and without the addition of 1.5% of benzene, investigated by molecular beam sampling coupled to mass spectrometry and gas chromatography. Methane consumption was found to be initiated by hydrogen abstraction by H, OH and O while the resulting methyl radicals were oxidized by reaction with O to formyl, CH₃ + O ⇌ HCO + H₂, and formaldehyde, CH₃ + O ⇌ CH₂O + H. In agreement with the observation in the benzene/oxygen flame [7,8], hydrogen abstraction with OH and H leading to phenyl and phenoxy formation via reaction with O radicals, i.e., benzene + O ⇌ phenoxy + H were identified as major initial reaction steps. Phenoxy is also formed by phenyl oxidation with O₂, with reaction to o-benzoquinone as competing pathway. Five-membered ring species, such as cyclopentadienyl are key intermediates in the subsequent degradation process.

The growth of PAH has been investigated in two premixed low pressure benzene flames. Experimental flame structures were determined by a) nozzle beam sampling followed by scavenging with dimethyl disulfide (DMDS) and analysis by gas chromatography coupled to mass spectrometry (GC-MS) [8] and b) probe sampling followed by solvent extraction and gas and liquid chromatography (GC-MS and HPLC) [10]. The predictive capability of the model for PAH radicals such as 1,3,4,5-acenaphthyl and 1,2,4-pyrenyl measured by means of the scavenging technique in a benzene/oxygen/argon flame with an equivalence ratio of $\phi = 1.8$ [8] was assessed. The comparison of model predictions for PAH containing up to five condensed aromatic rings (e.g., benzo[a]pyrene and benzo[b]fluoranthene) with experimental data measured after probe sampling in the benzene/oxygen/argon flame with an equivalence ratio of $\phi = 2.4$ [10], showed encouraging agreement. Reaction path analysis showed reaction of PAH with PAH radicals to be essential for the formation of certain PAH, e.g., fluoranthene and benzo[b]fluoranthene. Sequential hydrogen-abstraction/acetylene addition was confirmed to play a significant role in PAH growth. The overprediction of acetylene in the postflame zone of both rich benzene flames was found to be an important contributor in the underpredicted depletion far from the burner of PAH formed via the hydrogen-abstraction/acetylene addition pathway, such as acenaphthylene, cyclopenta[cd]pyrene and their derivatives, including substituted PAH. Ring-ring condensation, initially suggested for

phenanthrene formation [15], was extended to larger species and reaction between phenylacetylene and its radical was found to contribute to pyrene formation. Underpredictions of larger PAH in the $\phi = 1.8$ benzene flame [8] might indicate contributions of additional pathways such as isomerization of biphenylene-type species formed by recombination of benzyne-like compounds.

Future Plans

The work will include finishing and reporting PAH radical concentration measurements in two benzene oxygen flames, and extension of flame modeling calculations to include the assessment of predictions against experimental measurements.

References

1. Sumathi, R., personal communication, Massachusetts Institute of Technology, 2001.
2. Chang, A. Y., Bozzelli, J. W. and Dean, A. M. Kinetic Analysis of Complex Chemical Activation and Unimolecular Dissociation Reactions Using QRRK Theory and the Modified Strong Collision Approximation. *Z. Phys. Chem.* **214**, 1533-1568 (2000).
3. Westmoreland, P. R., Howard, J. B. and Longwell, J. B. Tests of Published Mechanisms by Comparison with Measured Laminar Flame Structure in Fuel-Rich Acetylene Combustion. *Proc. Combust. Inst.* **21**, 773-782 (1986).
4. Westmoreland, P. R. Experimental and Theoretical Analysis of Oxidation and Growth Chemistry in a Fuel-Rich Acetylene Flame. Ph.D. thesis, Massachusetts Institute of Technology, Cambridge, MA 1986.
5. Bhargava, A. and Westmoreland, P. R. MBMS Analysis of a Fuel-Lean Ethylene Flame. *Combust. Flame* **115**, 456-467 (1998).
6. Bhargava, A. and Westmoreland, P. R. Measured Flame Structure of Kinetics in a Fuel-Rich Ethylene Flame. *Combust. Flame* **113**, 333-347 (1998).
7. Bittner, J. D. and Howard, J. B. Composition Profiles and Reaction Mechanisms in a Near-Sooting Premixed Benzene/Oxygen/Argon flame. *Proc. Combust. Inst.* **18**, 1105-1116 (1981).
8. Benish, T. G., PAH Radical Scavenging in Fuel-Rich Premixed Benzene Flames. Ph.D. thesis, Massachusetts Institute of Technology, Cambridge, MA 1999.
9. McKinnon, J. T. and Howard, J. B., The Role of PAH and Acetylene in Soot Nucleation and Growth. *Proc. Combust. Inst.* **24**, 965-971 (1992).
10. Grieco, W. J., Lafleur, A. L., Swallow, K. C., Richter, H., Taghizadeh, K. and Howard, J. B. Fullerenes and PAH in Low-Pressure Premixed Benzene/Oxygen Flames. *Proc. Combust. Inst.* **27**, 1669-1675 (1998).
11. Dupont, L. Etude expérimentale et modélisation cinétique de la dégradation thermique des composés organiques volatils aromatiques benzène, toluène et para-xylène dans des flammes de méthane. Ph.D. thesis, Université des Sciences et Technologies de Lille, February 2001.
12. Kee, R. J., Rupley, F. M., Miller, J. A., Coltrin, M. E., Grcar, J. F., Meeks, E., Moffat, H. K., Lutz, A. E., Dixon-Lewis, G., Smooke, M. D., Warnatz, J., Evans, G. H., Larson, R. S., Mitchell, R. E., Petzold, L. R., Reynolds, W. C., Caracotsios, M., Stewart, W. E., Glarborg, P., Wang, C., and Adigun, O. *CHEMKIN Collection*, Release 3.6, Reaction Design, Inc., San Diego, CA (2000).

13. Richter, H. and Howard, J. B., Formation and Consumption of Single-Ring Aromatic Hydrocarbons and Their Precursors in Premixed Acetylene, Ethylene and Benzene Flames. Accepted for publication in *Physical Chemistry Chemical Physics*.
14. Mebel, A. M., Jackson, W. M., Chang, A. H. H., and Lin, S. H. Photodissociation Dynamics of Propyne and Allene: A View from ab Initio Calculations of C_3H_n ($n= 1- 4$) Species and the Isomerization Mechanism for C_3H_2 . *J. Am. Chem. Soc.* **120**, 5751- 5763 (1998).
15. Appel, J., Bockhorn, H. and Frenklach, M., Kinetic Modeling of Soot Formation with Detailed Chemistry and Physics: Laminar Premixed Flames of C_2 Hydrocarbons. *Combust. Flame* **121**, 122-136 (2000).

Publications of DOE Sponsored Research, 2000-2002

1. Richter, H. Benish, T.G., Ayala, F. and Howard, J.B.: "Kinetic Modeling of the Formation of Polycyclic Aromatic Hydrocarbons," *A.C.S. Fuel Chem. Div. Preprints* **45(2)**, 273-277, 2000.
2. Grieco, W.J., Howard, J.B., Rainey, L.C. and Vander Sande, J.B.: "Fullerene Carbon in Combustion-Generated Soot," *Carbon* **38**, 597-614, 2000.
3. Richter, H. and Howard, J.B.: "Formation of Polycyclic Aromatic Hydrocarbons and their Growth to Soot – A Review of Chemical Reaction Pathways," *Prog. Energy and Combust. Sci.* **26**, 367-380, 2000.
4. Kronholm, D.F. and Howard, J.B.: "Analysis of Soot Surface Growth Pathways using Published Plug-Flow Reactor Data with New Particle Size Distribution Measurements and Published Premixed Flame Data," *Proc. Combust. Inst.*, **28**, 2555-2561, 2001.
5. Richter, H., Benish, T.G., Mazyar, O.A., Green, W.H. and Howard, J.B.: "Formation of Polycyclic Aromatic Hydrocarbons and Their Radicals in a Nearly Sooting Premixed Benzene Flame," *Proc. Combust. Inst.*, **28**, 2609-2618, 2001.
6. Hebgen, P., Goel, A., Howard, J.B., Rainey, L.C. and Vander Sande, J.B.: "Synthesis of Fullerenes and Fullerene Nanostructures in a Low Pressure Benzene/Oxygen Diffusion Flame," *Proc. Combust. Inst.*, **28**, 1397-1404, 2001.
7. Richter, H., Mazyar, O.A., Green, W.H., Howard, J.B. and Bozzelli, J.W.: "A Detailed Kinetic Study of the Growth of Small Polycyclic Aromatic Hydrocarbons," *J.Phys Chem. A*, **105**, 1561-1573, 2001.
8. Goel, A., Hebgen, P., Vander Sande, J.B. and Howard, J.B.: "Combustion Synthesis of Fullerenes and Fullerene Nanostructures," *Carbon*, **40**, 177-182, 2002.
9. Richter, H. and Howard, J.B.: "Formation and Consumption of Single-Ring Aromatic Hydrocarbons and Their Precursors in Premixed Acetylene, Ethylene and Benzene Flames", *Phy.Chem.Chem.Phys.* (in press).

IONIZATION PROBES OF MOLECULAR STRUCTURE AND CHEMISTRY

Philip M. Johnson
Department of Chemistry
State University of New York, Stony Brook, NY 11794
Philip.Johnson@sunysb.edu

PROGRAM SCOPE

Photoionization processes provide very sensitive probes for the detection and understanding of molecules and chemical pathways relevant to combustion processes. Laser based ionization processes can be species-selective by using resonances in the excitation of the neutral molecule under study or by exploiting the fact that different molecules have different sets of ionization potentials. Therefore the structure and dynamics of individual molecules can be studied, or species monitored, even in a mixed sample. We are continuing to develop methods for the selective spectroscopic detection of molecules by ionization, to use these spectra for the greater understanding of molecular structure, and to use these methods for the study of some molecules of interest to combustion science.

RECENT PROGRESS

The exploitation of Rydberg molecules has enabled orders-of-magnitude increases in the resolution available for recording the spectra of molecular ions. These spectra provide information equivalent to photoelectron spectra, but contain much more information by virtue of that resolution and the versatility of laser preparation of the states involved.

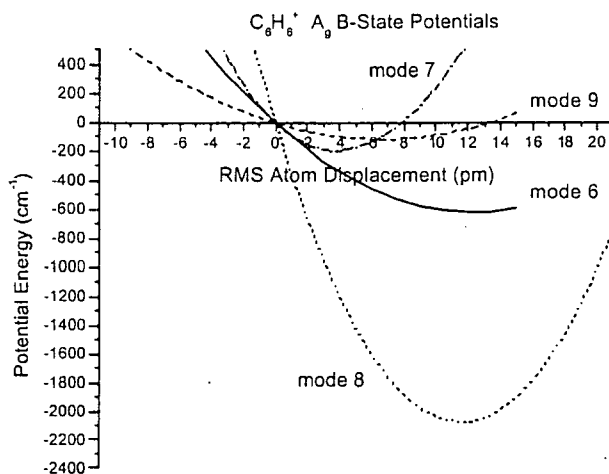
We primarily use previously developed techniques called mass analyzed threshold ionization spectroscopy (MATI) and photoinduced Rydberg ionization spectroscopy (PIRI) to provide high resolution access to the spectroscopy of the electronic states of ions. To accomplish this we create high Rydbergs state just below an ionic threshold. A small field is used to separate the prompt ions from the Rydberg molecules and then after a delay of a few microseconds either a small electrical pulse field ionizes the Rydbergs (MATI) or a tunable laser beam is sent through the Rydberg molecules (PIRI). In the latter, if this laser is resonant with a transition of the ionic core, core-excited Rydberg molecules are created which promptly autoionize. These ions are again separated from the remaining Rydbergs and after a further few microseconds the various ion packets are sent into a TOF mass spectrometer, where they arrive as a distinct groups whose intensity can be recorded as the either the Rydberg preparation laser or the final laser is scanned. The resonant nature of MATI and PIRI are of great use in sorting out the vibrational structure of some ionic states.

I. Calculations of the Jahn-Teller potentials for the lower states of benzene cation

The higher vibronic levels in the MATI spectra of benzene cation ground state and the PIRI spectra of the first excited state are very difficult to understand because of uncertainties concerning the relative coupling strengths of the various Jahn-Teller active modes. Only one of the four active modes is easily identifiable in the spectra, leaving the effects of the others to speculation.

The unique symmetry of benzene fortuitously allows the direct calculation of the electronic structure

of the lowest four states of the cation (three of these are degenerate) because they each have different electronic symmetry, even when the molecule vibrates along a D_{2h} coordinate. For this reason, it is possible to get accurate electronic energies and gradients using restricted open shell density functional theory, allowing the direct calculation of optimum geometries, vibrational frequencies and vectors, and potential energy curves along the D_{2h} modes of each state, as shown at right for the $C_6H_6^+$ B state. Since Jahn-Teller parameters are simply related to features of the potential energy curves, they are easily obtained from the calculations.



It has been found possible to calculate some known state energies, vibrational frequencies and Jahn-Teller parameters with almost spectroscopic accuracy, lending credence to the overall procedure. The calculated linear coupling parameters for the e_{2g} modes of the three lowest degenerate states of benzene cation are found to be:

C_6H_6 mode	X^2E_{1g}	B^2E_{2g}	D^2E_{1u}	C_6D_6 mode	X^2E_{1g}	B^2E_{2g}
6	0.48	0.93	4.12	6	0.44	0.66
9	0.10	0.10	0.06	9	0.12	0.49
8	0.30	1.36	0.15	8	0.37	1.11
7	0.00	0.07	0.06	7	0.00	0.21

A remarkable feature of these results is the magnitude of the coupling in the excited states of the cation. A parameter of one is considered to be the dividing line between a static Jahn-Teller effect, where the molecule is permanently distorted, and a dynamic effect where the molecule can sample the entire vibration phase space with its zero point motions. The B and D states are well into the static regime, with mode 6 of the D state having a distorted potential well that can support several vibrational levels.

Another important result is the importance of mode 8 in the coupling of the X and B states, indicating that it must be included in any thorough Jahn-Teller treatments of these states. It is hoped that these results may enable it to be identified in the spectra, enabling a more complete experimental analysis of the vibronic coupling in this prototype system.

These theoretical results necessitate a reassessment of the vibrational assignments in the PIRI and MATI spectra of benzene via new Jahn-Teller modeling. Preliminary results indicate that the new experimental assignments will be consistent with parameters close to the ones presented above.

II. Nanoclusters

In a collaboration with Trevor Sears and Michael White we have been using our laser ionization TOF mass spectrometry apparatus to develop efficient sources of metal (Ti, V, Mo) carbide, nitride, and

sulfide nanoparticles. These sources will be used for surface chemistry and spectroscopic studies of these important catalytic species.

FUTURE PLANS

We are in the process of setting up a pulsed amplified CW dye laser system in order to obtain higher resolution electronic spectra of molecular cations using the multiphoton dissociation, and PIRI techniques. This system will enable rotational resolution to be obtained for medium sized molecule and molecular clusters. The pulse nature of this high resolution source will couple well with our established spectroscopic techniques and with the pulsed coherent vuv generation used to prepare Rydberg states. It will also enable the generation of infrared wavelengths for the measurement of low-lying electronic states and for vibrational spectroscopy. The goal is to develop a general method for cation spectroscopy with orders of magnitude higher optical resolution than current techniques.

DOE PUBLICATIONS

“Reassessing the orbitals of pi systems using photoinduced Rydberg ionization spectroscopy,” Philip Johnson, Richa Anand, Jason Hofstein and Jeffrey LeClaire, *J. Electron Spect. and Related Phenom.*, **108**, 177-187 (2000).

“Mass-analyzed cation spectroscopy using Rydberg states: MATI and PIRI”, Philip M. Johnson, *Adv. Ser. in Phys. Chem.*, Vol. 10A, *Photoionization and Photodetachment*, edited by C. Y. Ng (World Scientific, Singapore, 2000).

Andrew Burrill and Philip Johnson, “Torsional analyses of trans-2-butene and propene cations: A comparative investigation of two prototypical ions with different degrees of symmetry”, *Journal of Chemical Physics*, **115**, 133 (2001).

Andrew Burrill and Philip Johnson, “The ionization potential and ground state cation vibrational structure of 1,4-dioxane”, *Chemical Physics Letters*, **350**, 473 (2001).

DYNAMICAL ANALYSIS OF HIGHLY EXCITED MOLECULAR SPECTRA

Michael E. Kellman

Department of Chemistry, University of Oregon, Eugene, OR 97403

kellman@oregon.uoregon.edu

PROGRAM SCOPE:

Spectra of highly excited molecules are essential to understanding intramolecular processes of fundamental importance for combustion. The objective of our program is to develop new theoretical tools to unlock knowledge of intramolecular dynamics encoded in highly excited experimental spectra. Because of the breakdown of the standard normal modes picture in highly excited vibrational states, new theoretical tools are needed to interpret the information about ultrafast internal molecular motion contained in high energy spectra. The marked departure from ordinary normal mode behavior in highly excited states includes the birth in bifurcations of new anharmonic modes, and the onset of widespread chaotic classical dynamics. In a bifurcation, a normal mode changes character, with an abrupt change in the natural motions of the molecule. This results in severe disturbance of the ordinary spectral patterns associated with normal modes.

Currently, the goal is to handle dynamics of increasing complexity in larger systems, including spectra of isomerizing systems up to and above the isomerization barrier. For this, we have been assembling a systematic array of theoretical tools, tested over past years. Where needed, significant further development of these methods is underway, for example, for systems with multiple barriers. Several specific molecular systems are of greatest interest for the near future. Acetylene appears to be the system where there is greatest likelihood that experimental access will become possible to all the dynamical problems of interest to us.

RECENT PROGRESS: DECODING ULTRAFAST DYNAMICS FROM SPECTRA.

Bifurcation analysis: Branchings of the normal modes into new anharmonic modes. The approach we have taken for analysis of highly excited vibrational spectra uses bifurcation analysis of the classical version of the effective Hamiltonian used to fit spectra. This bifurcation approach was first applied to a number of spectra fit with a Hamiltonian containing just a single resonance coupling. Important cases are the appearance in coupled stretch systems of local as well as normal modes; and 2:1 Fermi resonance coupling, for example, between a stretch and bend.

A key challenge has been to extend this approach to systems with more than two modes, coupled by multiple resonances. We successfully analyzed the bifurcations of the full three-mode system for a number of triatomics. We now have now applied this to a bifurcation analysis of the bend degrees of freedom of acetylene [in preparation]. The

pure bending system is a stepping-stone to the planned inclusion of the stretch degrees of freedom and an attack on the above-barrier isomerization problem for vinylidene-acetylene isomerization, both described below.

Visualization of complex molecular dynamics. One of the most important goals of our research is to convert the fairly abstract dynamical knowledge of the bifurcation analysis into a directly visualizable representation. For this, we are using computer animation techniques to make movies of the anharmonic modes born in bifurcations. Examples of our animations can be found on a web-site at [http://darkwing.uoregon.edu/\\$\sim\\$meklab/](http://darkwing.uoregon.edu/\simmeklab/), which the interested reader is urged to access.

Spectral patterns of chaotic acetylene: Assigning spectra with diabatic correlation diagrams. We certainly would like to detect directly in spectra the effects of bifurcations and resulting birth of new anharmonic modes. We learned early on how to do this for relatively simple systems with a single resonance, identifying spectral patterns characteristic of distinct kinds of bifurcations. But are analogous patterns and their detection possible in chaotic systems involving many modes and multiple resonances, such as the acetylene bends system?

In earlier years, we have shown how to identify and understand patterns using a diabatic correlation diagram technique. We have now applied this diabatic correlation procedure to acetylene spectra, and have succeeded in identifying novel energy and intensity patterns [3,4].

FUTURE PLANS: COMPLEXITY AND REACTIVE DYNAMICS IN LARGER SYSTEMS.

The biggest questions at present are whether this progress can be extended to larger systems of greater complexity, and to the realm of reactive phenomena such as unimolecular rearrangements involving a potential barrier. The key challenges are: (1) whether current methods are practical for larger, more complex systems, with more degrees of freedom, and if so, making the results intelligibly understood and utilized; and (2) the very difficult problem of extending the spectroscopic Hamiltonian to handle qualitatively new physical situations, in particular, motion in multiple potential wells, and very large-amplitude motion above two or more wells. We are interested in the particular chemical problem of the acetylene-vinylidene isomerization.

The Challenge of complexity. As the systems become ever larger, the challenge is whether the desired analysis can be performed at all, and if so, whether it will be understandable in a useful way. The problems all basically stem from the higher dimensionality of the systems. We work in phase space, so a system with N degrees of freedom has a $2N$ -dimensional phase space.

How can one analyze the dynamics of such a system? The standard procedure for a two degree of freedom system is to make Poincare surfaces of section by taking slices in

phase space of numerically integrated classical trajectories. Clearly, analysis using purely numerical methods is going to be very difficult, if not for all practical purposes completely intractable, for these four-atom systems.

We take a different approach, which we believe is the key to making the analysis of larger systems tractable. This involves the polyad quantum number in a key role. What has not been as widely appreciated as it might be is that the presence of the polyad number in the spectroscopic Hamiltonian is of enormous value in bifurcation analysis, because it makes solution for the bifurcations of the normal modes essentially analytic - avoiding the alternative of numerical searching of computational solutions of Hamilton's equations. This is true even for many degrees of freedom with multiple resonances couplings and chaos. The bifurcation problem thereby is reduced from numerical searching to the much simpler task of finding the solutions of analytical (polynomial) equations.

Probing the pathway to isomerization. Developing methods to uncover the molecular motion involved in the isomerization is one of the central goals of our research. It leads us to explore three distinct, but related sets of problems. (1) What is the fate of the pure local bending mode, the supposed isomerization mode, as the barrier is approached and surmounted? (2) Is the isomerization process one that really involves only the bending modes? We believe not, and that in answer to both questions, it is necessary to include the stretches to achieve isomerization. (3) Finally, suppose spectroscopy does access the isomerization. This will involve vibrations of acetylene below the top of the barrier; motion on the other side of the barrier in the small vinylidene well; and motion above the barrier that samples both the acetylene and vinylidene regions. Can one build a spectroscopic Hamiltonian to accommodate all of these phenomena? This has not previously been done; if feasible, it will involve a significant extension of the use of effective spectroscopic Hamiltonians. Then, what will be the signatures in the vibrational spectrum of the isomerization process?

Inclusion of stretch modes. It is entirely possible that access to the isomerization of necessity must include some C-H stretch quanta: after all, attempts so far to access the isomerization with pure bending excitation apparently have not been successful. There are independent reasons why it is important to understand the dynamics of acetylene with stretch excitation included. Consider, for example, the question of what happens when energy is placed in a pure C-H stretch overtone with energy above the isomerization barrier. How quickly, and by what pathway, does this energy reach the isomerization?

The bifurcation analysis for the full stretch-bend system involves a 12-dimensional phase space. More precisely, assuming three good polyad numbers, as indicated by existing spectroscopy, the relevant phase space is 8-dimensional. As discussed above, this is where exploiting the analytical solvability of the bifurcation analysis will provide a crucial advantage. Graphical presentation and interpretation of the resulting bifurcation diagrams will be a challenge. We expect the use of computer animations like those exemplified in the website mentioned above to be of tremendous value for visualizing the complex dynamics that are certain to be found.

Spectroscopic Hamiltonians for multiple wells and above barrier spectroscopy. The most challenging problem of all in approaching isomerization problems along the lines of our work is to include above barrier spectroscopy, and multiple wells, in the spectroscopic Hamiltonian; and to develop techniques such as bifurcation analysis to obtain dynamical information. We believe the time is ripe for this development.

We are extending our techniques to build a spectroscopic Hamiltonian for isomerization problems. Until experimental data become available, we will work with model systems, extending current data and models in as realistic a way as possible.

Recent publications (in print or in press since 2000) related to DOE supported research:

1. M. Joyeux, D. Sugny, V. Tyng, M.E. Kellman, H. Ishikawa, R.W. Field, C. Beck, and R. Schinke, "Semiclassical Study of the Isomerization States of HCP", *J. Chem. Phys.* 112, 4162 (2000.)
2. S. Yang and M.E. Kellman, "Direct Trajectory Method for Semiclassical Wavefunctions", *Phys Rev A* 62, 022105 (2000).
3. J.P. Rose and M.E. Kellman, "Spectral Patterns of Chaotic Acetylene", *J. Phys. Chem. A.* 104, 10471 (2000).
4. M.E. Kellman, J.P. Rose, and Vivian Tyng, "Spectral Patterns and Dynamics of Planar Acetylene", *European Physical Journal D* 14, 225 (2001).
5. M.E. Kellman, "Internal Molecular Motion", *Encyclopedia of Chemical Physics and Physical Chemistry*, J.H. Moore, Ed. (Institute of Physics, London, 2001).
6. S. Yang and M.E. Kellman, "Addendum: Direct Trajectory Method for Semiclassical Wavefunctions", in press, *Phys Rev A*.
7. S. Yang and M.E. Kellman, "Semiclassical Wave Function Near a Strong Resonance", in press, *Phys. Rev. A*.
8. C.Zhou, D. Xie, R.Chen, G.Yan, H.Guo, V. Tyng, and M.E. Kellman, "Highly Excited Vibrational Energy Levels of $\text{CS}_2(\tilde{X})$ on a New Empirical Potential Energy Surface and Semiclassical Analysis of the 1:2 Fermi Resonance", in press, *Spetrcchimica Acta A*.

KINETICS OF COMBUSTION-RELATED PROCESSES AT HIGH TEMPERATURES

J. H. Kiefer and R.S. Tranter
Department of Chemical Engineering
University of Illinois at Chicago
Chicago, IL 60607
(kiefer@uic.edu)

Program Scope

This program involves the use of the shock tube with laser-schlieren, laser-flash absorption, and dump-tank GC/MS analysis diagnostics to explore reactions and energy transfer processes over an extremely wide range of temperatures and pressures. We are interested primarily in the kinetics of unimolecular reactions at combustion temperatures, and, in particular, the effect of unimolecular falloff. We have continued some of the work reported last year and have also initiated some new projects.

Recent progress

The study of early precursors to soot formation: the pyrolysis of propargyl iodide.

Last year we reported the first results of experiments on this pyrolysis and a tentative model of the process (see last-year's abstract for a more complete introduction to this problem).

It is generally believed that aromatic rings are essential for efficient soot formation, and the most popular current route for these from aliphatic species is still propargyl recombination to benzene ($2\text{C}_3\text{H}_3 \rightarrow \text{C}_6\text{H}_6$). Scherer, Just and Frank [1] have shown that $\text{C}_3\text{H}_3\text{I} \rightarrow \text{C}_3\text{H}_3 + \text{I}$ is a quantitative pyrolytic source of C_3H_3 over 1.5-2.2 bar, and 1100-2100K, so reactions of propargyl can be investigated with this as a good source in the shock tube.

We have now observed this decomposition and the subsequent reactions of propargyl using the laser-schlieren technique on some 80 shockwave experiments in 2 and 5% $\text{C}_3\text{H}_3/\text{Kr}$ over 800 – 1500K and at low pressures, in the range from <20 to 160 torr. Some informative examples are shown in the last-page figure. For the highest and lowest temperatures with low pressures (top right), the gradients are initially positive and stay that way, showing little beyond $\text{C}_3\text{H}_3\text{I}$ dissociation. From such experiments we have extracted low-pressure rate constants for this dissociation, rates then used to construct a RRKM model. In the figure one sees that for higher temperatures/pressures, this positive gradient is followed by decisively negative values (exothermic reaction) that always accurately return to zero late in the process (late time data not shown).

The possible C_6H_6 products of propargyl combination are ($\Delta_f H^\circ_{298}$): 1,5-hexadiyne TT (99), and the other two direct addition products 1,2,4,5-hexatetraene HH (98), and 1,2-hexadien-5-yne HT (99); there are also the H-atom shift isomer 1,3-hexadien-5-yne (87); and the cyclics 3,4-dimethylenecyclobut-1-ene (80), fulvene (52) and benzene (20). Formation of phenyl + H has now been excluded (1), so the possible short-time reactions in this system reduce to: $\text{C}_3\text{H}_3\text{I} \rightarrow \text{C}_3\text{H}_3 + \text{I}$ and $2\text{C}_3\text{H}_3 \rightarrow$ (some set of) C_6H_6 .

As explained in the earlier abstract, the complexity of the mechanism may be reduced by recognizing that when propargyl is steady state, only fulvene or benzene formation is

sufficiently exothermic to produce a negative gradient. Thus we have the surprising observation that fulvene and/or benzene must be formed and stabilized at extremely low pressures, ~20 torr, and for temperatures higher than 1500K (note the upper left figure).

Previously we modeled the experiments assuming benzene formation was the sole source of negative gradients. Since then two important theoretical treatments of the combination have appeared (2,3) and these establish quite convincingly that, in the absence of H-atoms, isomerization of fulvene to benzene cannot occur on the short time period of these experiments. Thus we believe the negative gradients actually indicate fulvene formation early in the reaction, and, as before, the gradient returns to zero simply because of depletion of the C_3H_3 by formation of some proportion of the first six isomers listed above, all of which only produce small positive or negligible negative values.

In the figure we compare two possible models. Both use our RRKM rate of C_3H_3 decomposition, differing only in the rates to the various C_6H_6 . Carstensen and Dean (4) provide a large mechanism that can be tested, and the results with this scheme are shown in the figure as the dashed lines, using their full mechanism, without modification, and their thermochemistry. This mechanism does offer some negative gradient (bottom left figure) but they are always much too small and too late. Although this mechanism was designed for argon pressures of two atm, deactivation/stabilization is inadequate even for the present much lower pressures.

In an attempt to rectify the above problem we have retained the key reactions of the Carstensen/Dean mechanism, i. e., those controlling the gradient, which are now the four forming the linear isomers HT, TT, and HH (equal rates) and fulvene. Formation of the dimethylenecyclobutene was ignored; this is near a net thermoneutral and easily compensated by trivial adjustments in the other rates. In addition we have made all four reactions equally pressure dependent, with third-order rates larger by a factor two at 100 torr. The results are heavy lines in the figure. As seen, this works quite well (these gradients are *very* small) and of course some dependence on pressure is unsurprising for such low pressures. Deactivation remains surprisingly efficient; the chosen recombination rates are all above 10^{12} cc/mol-sec for 100 torr.

Pyrolysis of 1,1,1-trifluoroethane.

We have completed a study of the molecular dissociation $CF_3CH_3 \rightarrow HF + CF_2=CH_2$, a popular "chemical thermometer" for single pulse studies. This investigation was discussed in the last abstract. This work is now complete, the results further tested and verified, and a publication is in preparation.

Decomposition of oxirane and acetaldehyde.

We have been working on these problems for some time. We hope to produce a paper on the acetaldehyde work very soon. The oxirane may still need further experiments and analysis.

Decomposition of neopentane and Isobutane at very high temperatures.

These two are new projects that were started during the past year. Disagreement on the C-C bond strength in neopentane and/or the heat of formation of the *tert*-butyl radical has continued, with the best current electronic structure calculations still lying substantially higher than experiment (4). A common feature in RRKM models of dissociation, even for

large molecules, is the persistence of unimolecular falloff. Even a small drop of 10 or 20% in rate, almost kinetically negligible, can bring along as much as a 5 kcal/mol reduction in apparent E_a . Thus it seems prudent to perform experiments that clearly demonstrate significant falloff, develop a RRKM model based on these, and then apply it to the available dissociation data.

At high temperatures, neopentane dissociation involves the overall process: $C_5H_{12} \rightarrow CH_3 + H + C_4H_8$ (isobutene). At lower temperatures the subsequent decomposition of the isobutene (overall $C_4H_8 \rightarrow H + CH_3 + C_3H_4$) is certainly insignificant, but at very high temperatures this may not be true. There are no reliable data on this reaction, so we have also done a study of this reaction under similar conditions. The latter study is nearly complete, we have a good RRKM model for use in the neopentane modeling. This shows that the reaction remains of minor import, but is nonetheless needed for an accurate full modeling of neopentane laser-schlieren profiles.

Future plans.

We plan first to extend and complete the above projects. We need additional data on the propargyl reactions at higher temperatures and over a somewhat larger temperature range. The neopentane experiments are still quite incomplete. When they are in more finished form, we plan to get into the interesting if difficult problem of RRKM modeling of this dissociation. In the longer term, we are considering a return to the unresolved butadiene dissociation/isomerization using some improved methods now available.

References

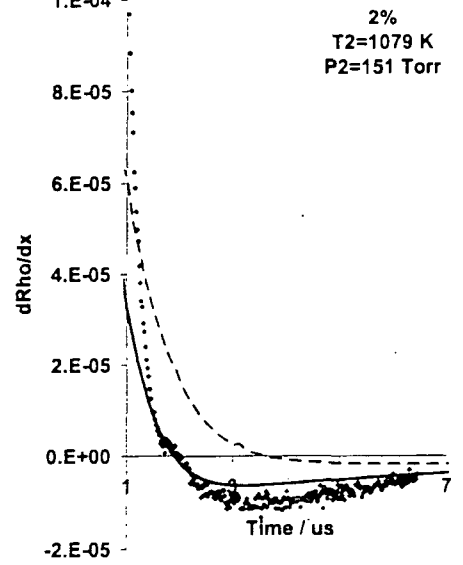
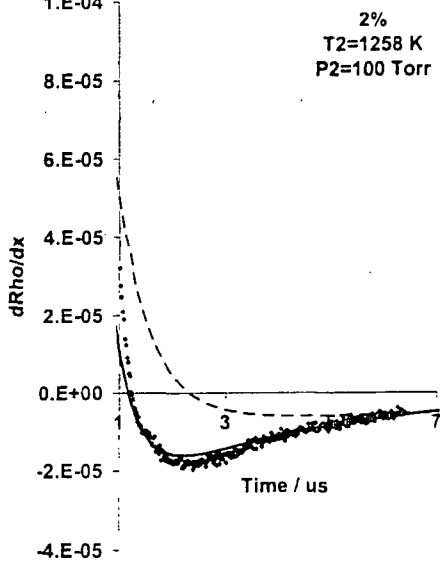
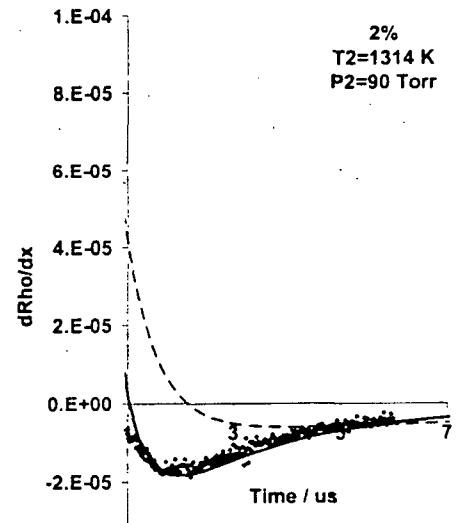
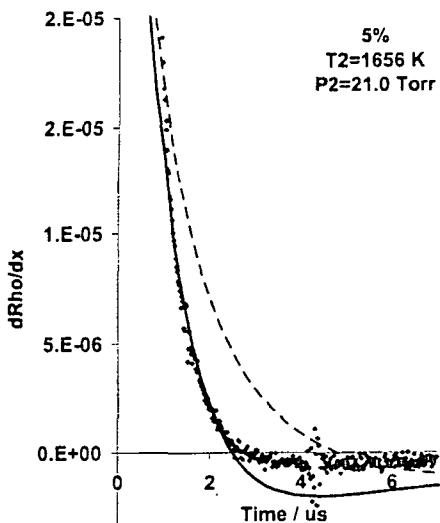
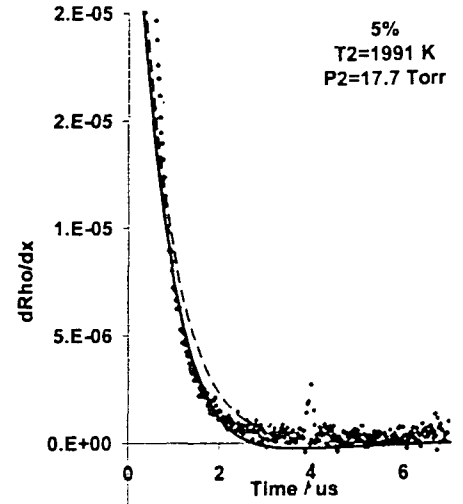
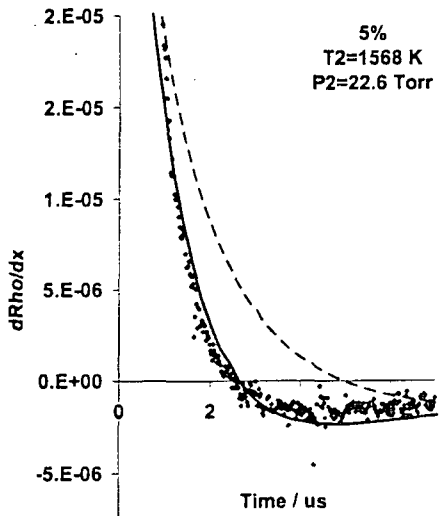
- 1) S. Scherer, Th. Just, and P. Frank, Proc. Combust. Inst. **28**: 1511 (2000).
- 2) J. A. Miller and S. J. Klippenstein, J. Phys. Chem. **105**, 7254 (2001).
- 3) H-H. Carstensen and A. M. Dean, Phys. Chem. Chem. Phys., in press.
- 4) B. J. Smith and L. Radom, J. Phys. Chem. **102**, 10787 (1998).

Publications of DOE Sponsored Research During 2000-2002.

"The Application of Densitometric Methods to the Measurement of Rate Processes in Shock Waves", J. H. Kiefer, in "Handbook of Shock Waves" Chapter 16.2, Academic Press, New York; p. 29 - 76 (2001).

Thermodynamic Functions for the Cyclopentadienyl Radical: The Effect of Jahn-Teller Distortion, J. H. Kiefer, R. S. Tranter, H. Wang and A. F. Wagner, Int. J. Chem. Kinet. **33**, 834 (2001).

Modeling of Nonlinear Vibrational Relaxation of Large Molecules in Shock Waves with a Nonlinear, Temperature-varying Master Equation, M. J. Davis and J. H. Kiefer, J. Chem. Phys. **116**, (2002). In press



THEORETICAL CHEMICAL KINETICS

Stephen J. Klippenstein
Combustion Research Facility
Sandia National Laboratories
Livermore, CA, 94551-0969
E-mail: sjklipp@sandia.gov

Program Scope

The focus of this program is the theoretical estimation of the kinetics of elementary reaction steps of importance in combustion chemistry. The research involves a combination of *ab initio* quantum chemistry, variational transition state theory, direct dynamics, and master equation simulations. The emphasis of our current applications is on (i) reactions of importance in soot formation, (ii) radical oxidation reactions, and (iii) NO_x chemistry. We are also interested in a detailed understanding of the limits of validity of and, where feasible, improvements in the accuracy of specific implementations of transition state theory. Detailed comparisons with experiments, and with other theoretical methods are used to explore and improve the predictive properties of the transition state theory models. Direct dynamics simulations are being performed as a means for testing the statistical assumptions, for exploring reaction mechanisms, and for generating theoretical estimates where statistical predictions are clearly inadequate. Master equation simulations are used to study the pressure dependence of the kinetics and to produce phenomenological rate coefficients for use in kinetic modeling.

Recent Progress

From the Master Equation to Kinetics

In collaboration with Jim Miller, we have derived a procedure for relating the rate coefficients in a phenomenological rate model to the eigenvectors and eigenvalues of the master equation transition matrix. This procedure is easily automated and provides a straightforward means for transforming transition state theory models for the individual isomerization and dissociation channels into a kinetic model for the overall reaction. Importantly, this procedure results in a kinetic model that reproduces the time-dependent populations from the master equations for *all timescales* longer than the energy transfer time. A description of this procedure is provided in Jim Miller's abstract.

In a separate collaboration with Jim Miller, we have investigated the dissociation of CH₄ in the low-pressure limit. In this work, a new choice of variables (total E and total J, as opposed to active energy ϵ and total J) was considered for the 2-D to 1-D reduction in the master equation, and a variety of energy transfer functions were studied. The E,J model is found to give more reasonable values for the average energy transferred than the ϵ , J model, and the comparison of E and E,J models indicates that the rotational degrees of freedom behave more and more as if they are active as the temperature rises. A more detailed summary is again provided in Jim Miller's abstract.

In collaboration with Mike Davis at Argonne National Laboratory we have performed a geometric investigation of the association/dissociation kinetics in $\text{CH}_3 + \text{CH}_3$. The variation of the geometry of phase space with temperature, pressure, and density of reactive species was studied for the phenomenological rate law, a Lindemann mechanism, and the master equation. We also showed that a good way of investigating the asymptotic motion of this nonlinear problem was by studying the approach and subsequent motion on a one-dimensional manifold that is the nonlinear analogue of the appropriate eigenvector of the linear master equation. A new method for calculating association rate constants and ultimately a new rate law for the association/dissociation process was also developed (cf. the abstract of Mike Davis).

Propargyl Radical Kinetics

We have discovered the importance of a new route for forming benzene in the recombination of propargyl radicals. This new pathway involves a 1,5-H transfer from $\text{CH}_2\text{CCHCHCCH}_2$ to form $\text{CH}_2\text{CHCHCHCCH}$, which can then cyclize to one of a variety of C6 ring species. With this new pathway, master equation simulations predict a total rate coefficient of $5 \times 10^{12} \text{ cm}^3 \text{ mole}^{-1} \text{ s}^{-1}$ at 1500 K and 1 atm. This value, which is increased by a factor of 5 from our prior prediction, is in good agreement with the values used in modeling soot formation. Furthermore, this new pathway helps explain the simultaneous observation of fulvene and benzene in the thermal isomerization of $\text{CHCCH}_2\text{CH}_2\text{CCH}$. We are in the process of obtaining a complete kinetic model for the propargyl recombination via master equation simulations incorporating this new pathway. This work was performed in collaboration with Jim Miller.

As described in Jim Miller's abstract, we have also extended our prior analysis of the $\text{H} + \text{C}_3\text{H}_3$ recombination to include an analysis of the pressure dependence of the propyne/cyclopropene/allene isomerization/dissociation kinetics.

Radical Oxidation

In collaboration with Jim Miller and Larry Harding (Argonne National Laboratory) we have solved the mystery of prompt CO_2 formation during acetylene combustion via a theoretical characterization of the $\text{HCCO} + \text{O}_2$ reaction. A combination of electronic structure theory, RRKM theory, and master equation and direct trajectory simulations indicate that the primary products of this reaction are $\text{CO}_2 + \text{CO} + \text{H}$. The sequence



then yields simultaneous formation of CO and CO_2 as originally observed in Kistiakowsky's laboratory in the 1960's. The simulations also predict the formation of $\text{OCHCO} + \text{O}$, and $\text{CO} + \text{CO} + \text{OH}$ as minor (<~10%) secondary products. Interestingly, the $\text{CO} + \text{CO} + \text{OH}$ products arise in part from an H atom abstraction from HCO to CO_2 during the initial bimolecular product formation. As in our earlier study of the $\text{CH}_3 + \text{O}$ reaction, this process appears to occur in the absence of any saddle point. The low value observed for the total rate coefficient ($\sim 10^{-12} \text{ cm}^3 \text{ molecules}^{-1} \text{ s}^{-1}$) is primarily the result of a modest entrance channel barrier arising from the need to break the resonances in HCCO and O_2 during the adduct formation process.

In collaboration with Craig Taatjes and John DeSain we have applied the master equation to kinetic phenomenology procedure to generate rate coefficients for each of the channels in the ethyl and propyl + O_2 reactions. These rate coefficients were implemented in a kinetic model for the Cl initiated oxidation of ethane and propane. Comparisons were made between the predicted and observed time-dependent HO_2 and OH concentrations. For HO_2 , the observations provide a

direct test of the model for the radical + O₂ kinetics. Meanwhile, for OH, others reactions such as R + HO₂, RO₂ + OH, and C₃H₆OOH + O₂ also played a key role in the predicted time dependence.

In a related collaboration with Craig Taatjes and John DeSain we have studied the reaction of cyclo-propyl radical with O₂. A quantum chemical mapping of the reaction pathways suggests that the primary products are CH₂CHCHO + OH; arising from an H transfer from the ring to the terminal O atom, followed by OO bond fission in concert with fission of the cyclo-propyl ring. The maximum barrier for this process is predicted to be 2 kcal/mol below reactants. Thus, the overall reaction should be fairly rapid, in reasonable agreement with experiment. In contrast, the barriers for all other pathways leading to bimolecular products are predicted to lie at least 4 kcal/mol above reactants. As a result, it is difficult to explain the experimentally observed formation of HO₂ on the same timescale as OH.

Dynamics

In collaboration with Larry Harding (Argonne National Laboratory) and Yuri Georgievskii we have studied the reaction of methyl radicals with hydrogen atoms via a combination of *ab initio* quantum chemistry, variational transition state theory, and classical trajectory simulations. These calculations focused on an analysis of transition state recrossing effects for the high-pressure limit, and on the prediction of isotopic exchange rate constants. The interaction between the two radicals, including the umbrella mode of the methyl radical, was first examined at the CAS+1+2 level using the aug-cc-pvtz basis. Variable reaction coordinate transition state theory estimates based on these *ab initio* results were found to be in good agreement with trajectory simulations; generally overestimating the reactive flux by only about 10%. The dynamically corrected theoretical predictions for the isotopic exchange and the high-pressure addition rate constants were in good agreement with experiment (generally within ~15%).

Future Directions

The additions of acetylene to C₄H₃ and/or C₄H₅ have been postulated to be key steps in the formation of aromatic ring compounds. We will investigate each of these reactions, considering both the *n* and *i* isomers for each one, since they are effectively separate species with quite different kinetic properties. This study will build on the earlier quantum chemical work of Walch, but will include a more wide-ranging analysis of the reaction pathways. The temperature and pressure dependence of the rate constant will again be estimated via master equation analyses.

The accuracy of transition state theory will be examined for the CH₃ + CH₃ reaction via direct dynamics simulations. This study will indicate whether or not the deviations from experiment for our related direct transition state theory calculations are the result of nonstatistical effects. An understanding of the reason for such deviations has important implications for transition state theory based modeling in general.

In collaboration with Larry Harding we will develop and implement methodologies for directly evaluating classical anharmonic and nonrigidity corrections to molecular state densities at the dissociation threshold and canonical partition functions at high temperatures. Initial applications will be to CH₄, CH₃, CH₂OH, and H₂CO.

DOE Supported Publications, 2000-Present

1. James A. Miller and Stephen J. Klippenstein, *Theoretical Considerations in the $\text{NH}_2 + \text{NO}$ Reaction*, J. Phys. Chem. A, **104**, 2061-2069 (2000).
2. Stephen J. Klippenstein and Lawrence B. Harding, *A Summary of "A Direct Transition State Theory Based Study of Methyl Radical Recombination Kinetics"*, J. Phys. Chem. A, **104**, 2351-2354 (2000).
3. James A. Miller and Stephen J. Klippenstein, *A Theoretical Analysis of the Reaction Between Vinyl and Acetylene: Quantum Chemistry and Solution of the Master Equation*, J. Phys. Chem. A, **104**, 7525-7536, (2000); see also J. Phys. Chem. A, **104**, 9806 (2000).
4. James A. Miller, Stephen J. Klippenstein, and Struan H. Robertson, *A Theoretical Analysis of the Reaction Between Ethyl and Oxygen*, Proc. Combust. Inst, **28**, 1479-1486, (2000).
5. Stephen J. Klippenstein, and Lawrence B. Harding, *Theoretical Kinetic Estimates for the Recombination of Hydrogen Atoms with Propargyl and Allyl Radicals*, Proc. Combust. Inst., **28**, 1503-1509, (2000).
6. Holger Thiesemann, Eileen P. Clifford, Craig A. Taatjes and Stephen J. Klippenstein, *Temperature Dependence and Deuterium Kinetic Isotope Effects in the $\text{CH}(\text{CD}) + \text{C}_2\text{H}_4(\text{C}_2\text{D}_4)$ Reaction Between 295 and 726 K*, J. Phys. Chem. A, **105**, 5393-5401 (2001).
7. James A. Miller and Stephen J. Klippenstein, *The Recombination of Propargyl Radicals: Solving the Master Equation*, J. Phys. Chem. A, **105**, 7254-7266, (2001).
8. Kelsey M. Forsythe, Stephen K. Gray, Stephen J. Klippenstein, and Gregory E. Hall, *An Ab Initio Molecular Dynamics Study of S_0 Ketene Fragmentation*, J. Chem. Phys., **115**, 2134-2145, (2001).
9. Timothy P. Marcy, Robert R. Diaz, Dwayne Heard, Stephen R. Leone, Lawrence B. Harding, and Stephen J. Klippenstein, *Theoretical and Experimental Investigation of the Dynamics of the Production of CO from the $\text{CH}_3 + \text{O}$ and $\text{CD}_3 + \text{O}$ Reactions*, J. Phys. Chem. A, **105**, 8361-8369, (2001).
10. Craig A. Taatjes and Stephen J. Klippenstein, *Kinetic Isotope Effects and Variable Reaction Coordinates in Barrierless Recombination Reactions*, J. Phys. Chem. A, **105**, 8567-8578, (2001).
11. James A. Miller and Stephen J. Klippenstein, *The Reaction Between Ethyl and Molecular Oxygen II: Further Analysis*, Int. J. Chem. Kinet., **33**, 654-668, (2001).
12. David K. Hahn, Stephen J. Klippenstein, and James A. Miller, *A Theoretical Analysis of the Reaction Between Propargyl and Molecular Oxygen*, Faraday Disc., **119**, 79-100, (2001).
13. John. D. DeSain, Craig A. Taatjes, James A. Miller, Stephen J. Klippenstein, and David K. Hahn, *Infrared Frequency-Modulation Probing of Product Formation in Alkyl + O_2 Reactions: IV. Reactions of Propyl and Butyl Radicals with O_2* , Faraday Disc., **119**, 101-120, (2001).
14. De-Cai Fang, Lawrence B. Harding, Stephen J. Klippenstein, and James A. Miller, *A Direct Transition State Theory Based Analysis of the Branching in $\text{NH}_2 + \text{NO}$* , Faraday Disc., **119**, 207-222, (2001).
15. James A. Miller, Stephen J. Klippenstein, and Christophe Raffy, *Solution Of Some One- And Two-Dimensional Master Equation Models For Thermal Dissociation: The Dissociation Of Methane In The Low-Pressure Limit*, J. Phys. Chem. A, *in press* (2002).
16. Michael J. Davis and Stephen J. Klippenstein, *Geometric Investigation of Association/Dissociation Kinetics with an Application to the Master Equation for $\text{CH}_3 + \text{CH}_3 \leftrightarrow \text{C}_2\text{H}_6$* , J. Phys. Chem. A, *in press* (2002).
17. Lawrence B. Harding and Stephen J. Klippenstein, *A Theoretical Analysis of the $\text{CH}_3 + \text{H}$ Recombination Reaction*, Proc. Comb. Inst., **29**, *in press* (2002).
18. Stephen J. Klippenstein, James A. Miller, and Lawrence B. Harding, *Theoretical Kinetic Estimates for the Reaction of HCCO with O_2* , Proc. Comb. Inst., **29**, *in press* (2002).

TIME-RESOLVED FTIR EMISSION STUDIES OF LASER PHOTOFRAGMENTATION AND RADICAL REACTIONS

Stephen R. Leone
JILA and Department of Chemistry and Biochemistry
University of Colorado
Boulder, Colorado 80309-0440
(303) 492-5128 srl@jila.colorado.edu

Scope of the Project

This project explores laser-initiated radical reactions, radical-radical reactions, photofragmentation events, and energy transfer processes related to problems in combustion dynamics. The vibrationally and low-lying electronically excited species generated in such processes are probed by time-resolved Fourier transform infrared (FTIR) emission spectroscopy. Dynamics measurements are obtained by acquiring time-resolved signals from a high repetition rate pulsed excimer laser at each mirror position of the spectrometer. These signals are then assembled into interferograms at a series of time delays, to obtain spectra at each time delay. This is a relatively unique facility, applicable to spectrally detect the diatomic and small polyatomic species that are the products of photofragmentation and radical reactions. The current research involves several major thrusts. One is to study radical reactions to determine the nascent product species and states formed in a variety of important radical-radical and radical-molecule processes. The other thrust is to study photofragmentation involving polyatomic molecules and radical species to obtain nascent vibrational and rotational state detail.

Product State Distributions of Photofragmentation

A large block of earlier published work involved the development of new tools for spectroscopic pattern recognition and the use of these tools to study complex photodissociation pathways in ammonia and deuterated ammonia molecules. The method of time-resolved FTIR spectroscopy permits the experimentalist to study the progress of many simultaneous reaction pathways, monitoring the infrared-emitting product state distributions and branching ratios of different reaction channels. Detailed analyses of the spectroscopic data obtained, and their variation with reaction conditions, are a necessary prerequisite to the interpretation of other chemical reaction systems under study, as well as to learn about the dynamics on complex polyatomic potential surfaces.

With the previous successes in this laboratory to study the photofragmentation of ammonia with a jet-cooled source, a new slit jet source was developed to produce a longer path length of jet-cooled species. The slit jet that was constructed is 4 cm long and 0.005 cm in width and operates from 10-50 Hz. This new source has been tested with the emission from NH_2 produced from ammonia, and to study the dissociation of acetylene, under jet-cooled conditions, both with 193 nm dissociating pulses. For ammonia dissociation, the spectral features observed with the slit jet reproduce those obtained earlier with a circular pinhole jet for the low-lying electronically excited state of NH_2 . More challenging new experiments, which should be possible with the long slit jet, are now being performed. The first was to detect vibrational emission from the ground electronic state of NH_2 upon dissociation of ammonia, but this experiment has not yet been successful. Work is continuing to improve the signal to noise to perform this more difficult experiment. The

investigation of the C_2H radical from the dissociation of C_2H_2 has produced several identifiable C_2H bands at 3772, 3786, 4012, and 4108 cm^{-1} . Additional peaks at 3590 cm^{-1} and between 6000-10000 cm^{-1} are identified to be from C_2 produced by a two photon dissociation. The C_2H transitions have less rotational width than previous studies with room temperature samples. Thus work is progressing to obtain high quality spectra that can be analyzed to study the dynamics of the dissociation of the jet-cooled parent acetylene with rotational state detail.

$CD_3/CH_3 + O$ Radical-Radical Reactions

In a joint experimental and theoretical work, together with Larry Harding and Stephen Klippenstein, the relative production of CO in the reactions of $CD_3/CH_3 + O$ was investigated. The yield of $CO(v=1)$ from the deuterated methyl + O reaction was measured to be $69 \pm 10\%$ of the yield of $CO(v=1)$ from the hydrogenated methyl + O reaction. Classical trajectory studies confirm the CO producing channel, arising from the sequence $CH_3O \rightarrow HCO + H_2 \rightarrow CO(v) + H + H_2$. The calculations also indicate the experimentally observed lower yield of CO in the deuterated reaction. Finally, the calculations show the importance of the reaction mechanism. This reaction, which proceeds through methoxy, CH_3O , has no transition state in the potential surface for the production of H_2 from the methoxy intermediate. Instead, the calculations show that the H_2 product is formed by passing over a high energy ridge in the potential, rather than via a minimum energy path. This surprising result explains the theoretical and experimental controversy over the CO producing channel in the methyl + O reaction. The results also mean that such new types of reactive mechanisms must be considered for other highly energized systems, which may not proceed through saddle point transition states.

Ethyl, *n*-Propyl, Isopropyl, and *n*-Butyl Radical Reactions with O atoms

In recent work, a group of symmetric ketones are photodissociated in the presence of SO_2 to study the reactions of larger hydrocarbon radicals with O atoms. The symmetric ketones, acetone, diethyl ketone, di-*n*-propyl ketone, diisopropyl ketone, and di-*n*-butyl ketone, are dissociated with 193 nm light, while the photodissociation of SO_2 produces O atoms simultaneously. The products of the reactions of $O(^3P)$ with methyl, ethyl, *n*-propyl, isopropyl, and *n*-butyl radicals are then observed under low resolution with the FTIR. In earlier work, the reactions of methyl and ethyl were studied in detail, and the CO-producing channel was verified completely. Here the methyl and ethyl reactions are compared with the reactions of the larger hydrocarbons. The reactions of these larger radicals with $O(^3P)$ can yield aldehydes or CO as primary products. Evidence is found that the CO-producing channel occurs for all the alkyl radicals studied, and the kinetic dependence for the *n*-propyl reaction is studied in detail to verify the CO production. In addition, the absorption cross sections for the series of symmetric ketones are quantified at 193 nm and used to set limits on the production of the alkyl radical yields and the relative $CO(v)$ yields from the reactions. The lower limit on the yields of ethyl, *n*-propyl, *i*-propyl, and *n*-butyl in the photodissociation of the ketones, normalized to 2 for methyl, are 1.3 ± 0.2 , 0.8 ± 0.2 , 1.8 ± 0.7 and 0.86 ± 0.14 , respectively. The relative CO yields from the reactions with O atoms, normalizing to methyl + O as unity (the actual CO yield measured by the Brookhaven group is 0.18), are 0.74-1.04, 0.35-1.06, 0.58-0.64, and 0.074-0.017, respectively, for the same series of radicals. This work is currently being prepared for publication and these preliminary numbers may be altered with further analysis (Timothy P. Marcy, Robert Richard Díaz, Dwayne Heard, Stephen R.

Leone, "Reactions of O(³P) with alkyl radicals produced by 193 nm photolysis of symmetric ketones,")

NH₂ + NO, Thermal De-NO_x Reaction with Additional Vibrational Excitation

A new study was performed on the reaction of NH₂ with NO, in which the initial NH₂ is formed with electronic and vibrational excitation. Emission is observed from vibrationally excited NO, N₂O, and H₂O. The NO emission occurs by energy transfer from the initially excited NH₂. The N₂O is formed only by the availability of the extra excitation energy, requiring passage over a high barrier. The vibrationally excited H₂O is formed only in a delayed kinetic process that exhibits an induction period. Experimental investigations of this induction period suggest that the water vapor product is only formed after vibrational excitation is removed from the NH₂ radical by collisions. The results provide additional evidence for the interesting temperature dependence of the product branching ratios in the NH₂ + NO reaction and the narrow temperature range over which the water vapor product is formed. With the presence of vibrational excitation in the NH₂, there is a significant probability that the collisions of NO with vibrationally excited NH₂ occur by deactivation and dissociation of the reactive complex, without reaction to form H₂O. This is reasonable, since for the reaction to occur it has to pass through many transition states, breaking all the initial bonds in the reactants and reforming new ones in the products.

Future Plans

New studies of radical reactions and photofragmentation will be pursued, including: C₂H reactions with O atoms and photofragmentation studies that produce small radicals using jet cooled precursors, to obtain vibrational distributions of radical products.

Recent Publications

Richard A. Loomis, Jonathan P. Reid, and Stephen R. Leone, "Photofragmentation of ammonia at 193.3 nm: Bimodal rotational distributions and vibrational excitation of NH₂(\tilde{A})," *J. Chem. Phys.* **112**, 658 (2000).

Jonathan P. Reid, Richard A. Loomis and Stephen R. Leone, "Characterization of dynamical product-state distributions by spectral extended cross-correlation: Vibrational dynamics in the photofragmentation of NH₂D and ND₂H," *J. Chem. Phys.*, **112**, 3181 (2000).

Jonathan P. Reid, Timothy P. Marcy, Seppe Kuehn and Stephen R. Leone, "The Direct Production of CO($v=1-9$) in the Reaction of O(³P) with the Ethyl Radical," *J. Chem. Phys.* **113**, 4572 (2000).

Jonathan P. Reid, Richard A. Loomis and Stephen R. Leone, "The effect of parent zero-point motion on the ND₂(\tilde{A}) rotational state distribution in the 193.3 nm photolysis of ND₃, *Chem Phys Lett*, **324**, 240 (2000).

Jonathan P. Reid, Richard A. Loomis and Stephen R. Leone, "Competition Between N-H and N-D Bond Cleavage in the Photodissociation of NH₂D and ND₂H," *J. Phys Chem.* **104**, 10139 (2000).

Jonathan P. Reid, Charles X.W. Qian and Stephen R. Leone, "Probing the cyclic transition state in the reaction O(³P) + alkyl iodides to form HOI: Electronic, steric and thermodynamic factors influencing the reaction pathway," *Phys. Chem. Chem. Phys.*, **2**, 853 (2000).

Timothy P. Marcy, Jonathan P. Reid, Charles X. W. Qian, and Stephen R. Leone, "Addition-insertion-elimination reactions of O(³P) with halogenated iodoalkanes producing HF(v) and HCl(v)," *J. Chem. Phys.* **114**, 2251 (2001).

Timothy P. Marcy, Robert Richard Díaz, Dwayne Heard, Stephen R. Leone, Lawrence B. Harding, and Stephen J. Klippenstein, "Theoretical and experimental investigation of the dynamics of the production of CO from the CH₃ + O and CD₃ + O reactions," *J. Phys. Chem. A* **105**, 8361 (2001).

Timothy P. Marcy, Dwayne Heard, Stephen R. Leone, "Product studies of inelastic and reactive collisions of NH₂ + NO: Effect of vibrationally and electronically excited NH₂," *J. Phys. Chem. A* (In press, D. Setser special issue).

INTERMOLECULAR INTERACTIONS OF HYDROXYL RADICALS ON REACTIVE POTENTIAL ENERGY SURFACES

Marsha I. Lester
Department of Chemistry
University of Pennsylvania
Philadelphia, PA 19104-6323
milester@sas.upenn.edu

PROGRAM SCOPE

A primary objective of the DOE supported work in this laboratory is to examine the interaction potential and reaction dynamics of the $\text{CH}_4 + \text{OH}$ system, one of the key initiation steps in the combustion of methane. The goal of this study is to map out the reaction pathway from the entrance valley through the transition state via spectroscopic and dynamical studies of $\text{CH}_4\text{-OH}$ entrance channel complexes. Our approach is to stabilize the $\text{CH}_4 + \text{OH}$ reactants in a weakly bound complex in the entrance channel to reaction and then to use stimulated Raman, infrared, and/or electronic excitation for spectroscopic characterization of the system.¹⁻⁴ Vibrational or electronic excitation of one of the reactants induces a reactive and/or inelastic scattering process that starts from a well-defined initial state under the restricted geometric conditions imposed by the complex. We explore these dynamical processes through the lifetime of the vibrationally activated complexes and the quantum state distribution of the products. The results of these experiments yield a wealth of new information on the $\text{CH}_4 + \text{OH} \rightarrow \text{CH}_3 + \text{H}_2\text{O}$ potential energy surface. These studies are being extended to reactant complexes of OH radicals with other molecular partners of combustion importance, namely ethylene, acetylene, and acetaldehyde.

VIBRATIONAL SPECTROSCOPY OF $\text{CH}_4\text{-OH}$

Infrared action spectroscopy has been utilized to examine the structure, stability, and vibrational decay dynamics of $\text{CH}_4\text{-OH}$ complexes that have been trapped in the entrance channel to the fundamental $\text{CH}_4 + \text{OH} \rightarrow \text{CH}_3 + \text{H}_2\text{O}$ hydrogen abstraction reaction. Rotationally resolved infrared spectra of the $\text{CH}_4\text{-OH}$ complex have been obtained in the OH fundamental and overtone regions.² Structural parameters derived from the spectra indicated that the centers of mass of the CH_4 and OH partners are separated by $R=3.66(1)$ Å. In addition, the projection quantum number showed that the OH bond axis lies along the intermolecular axis in the ground state of $\text{CH}_4\text{-OH}$. These experimental observations were consistent with complementary *ab initio* calculations that predict a C_{3v} minimum energy configuration for $\text{CH}_4\text{-OH}$ with the hydrogen of OH pointing toward one of four equivalent faces of the CH_4 tetrahedron at an equilibrium separation distance of $R_e=3.47$ Å.

The infrared spectra in the OH stretching regions also exhibited homogeneous line broadening arising from the rapid decay of vibrationally activated $\text{CH}_4\text{-OH}$ complexes due to vibrational predissociation and/or reaction. Homogeneous linewidths of $0.14(2)$ and $0.21(2)$ cm^{-1} have been observed for the pure OH stretching bands in the fundamental and overtone regions, corresponding to $38(5)$ and $25(3)$ ps lifetimes for vibrationally activated complexes with one and

two quanta of OH stretching excitation, respectively. These lifetimes are surprisingly short and suggest that both inelastic and reactive channels contribute to the rapid decay of CH₄-OH (ν_{OH}) and ($2\nu_{\text{OH}}$) as found in a recent collision study of OH ($\nu=1, 2$) + CH₄.⁵ The nascent distribution of the OH products from vibrational predissociation of CH₄-OH ($2\nu_{\text{OH}}$) also showed that the dominant inelastic decay channel involves the transfer of one quantum of OH stretch to the pentad of CH₄ vibrational states with energies near 3000 cm⁻¹.

Additional studies have focused on the infrared spectroscopy and subsequent decay dynamics of CH₄-OH reactant complexes in the CH₄ antisymmetric stretching region (ν_3) at 3.3 μm .³ Infrared excitation of the CH₄ ν_3 mode resulted in an intense, yet enormously broad spectrum extending over 40 cm⁻¹. The appearance of the spectrum has been explained in terms of a model in which the CH₄ unit is freely rotating within the CH₄-OH complex, as found for other CH₄ complexes.⁶ In the ν_3 region, the CH₄-OH complex can undergo a multitude of possible transitions, each associated with a rovibrational transition of free methane, which give rise to the enormous span of the CH₄-OH spectrum. The spectrum also exhibited extensive homogeneous broadening (≥ 1 cm⁻¹) arising from the rapid decay of vibrationally activated CH₄-OH complexes due to vibrational predissociation and/or reaction. This broadening consistent with quantum reactive scattering calculations that predict a large enhancement in the CH₄ + OH reaction rate in full collisions upon vibrational activation of the C-H stretching mode.⁷ The OH fragments from CH₄-OH (ν_3) were produced with minimal rotational excitation, indicating that vibrational predissociation proceeds via near-resonant vibrational energy transfer within the CH₄ unit from the initially prepared asymmetric stretch (ν_3) to an overtone bend state.

Our most recent study examined the changes in the spectroscopic properties and decay dynamics of the CH₄-OH complex upon deuteration of the hydroxyl moiety.⁴ The pure OD overtone spectrum of CH₄-OD is remarkably similar to that of CH₄-OH in the OH overtone region, with similar spectral shifts and rotational band structures. The rotationally resolved infrared spectrum of the pure OD overtone band of CH₄-OD is located at 5165.68(1) cm⁻¹ (origin). The spectrum exhibits homogeneous line broadening, which is estimated to have a zero power linewidth of 0.10(1) cm⁻¹, corresponding to a lifetime for CH₄-OD ($2\nu_{\text{OD}}$) of 53(5) ns. The CH₄-OD spectrum exhibits less extensive homogeneous line broadening than that seen for CH₄-OH, indicating that CH₄-OD ($2\nu_{\text{OD}}$) decays about a factor of two times slower due to inelastic recoil and/or chemical reaction than CH₄-OH ($2\nu_{\text{OH}}$).

The OD ($\nu=1$) fragments from vibrational predissociation of CH₄-OD ($2\nu_{\text{OD}}$) are highly rotationally excited, while the OH ($\nu=1$) fragments from CH₄-OH ($2\nu_{\text{OH}}$) have minimal rotational excitation. The significantly lower vibrational frequency of OD causes the near-resonant vibrational energy transfer to the pentad of CH₄ vibrational states near 3000 cm⁻¹ to become energetically closed for CH₄-OD ($2\nu_{\text{OD}}$). Instead, vibrational predissociation of CH₄-OD ($2\nu_{\text{OD}}$) proceeds through a less energetically favorable transfer to low frequency bending modes of CH₄. The larger energy gap associated with inelastic decay of CH₄-OD ($2\nu_{\text{OD}}$) implies a slower rate of vibrational predissociation, suggesting that more time will be available for reaction within the vibrationally activated complex. If the rate coefficient for reaction within the complex remains essentially unchanged upon deuteration, as found in full collision studies, then the branching fraction for reaction could also be significantly increased in CH₄-OD ($2\nu_{\text{OD}}$).

FUTURE PLANS

During the next three years, we plan to extend and expand our very successful efforts to characterize OH reactant complexes with partners of combustion relevance (e.g. H₂/D₂, CH₄, and CO). We will investigate several more complicated systems where molecular associations of OH radicals have already been predicted to play a critical role in the reaction mechanism. These systems have strong intermolecular interactions (2.5–4.2 kcal mol⁻¹), very low barriers to reaction (often lying below the reactant asymptote), and fast overall rates of reaction. Specific examples include the addition reaction of OH radicals to the double bond of ethylene (C₂H₄), where recent high-level *ab initio* calculations by Garrett and coworkers have identified a hydrogen-bonded complex between OH and the π -bond of C₂H₄ as an important precursor to reaction.⁸ An analogous T-shaped complex has been predicted on the reaction path for OH addition to acetylene (C₂H₂).⁹ Another example is the CH₃CHO-HO complex, which has been inferred via kinetic modeling as a key intermediate species in the OH hydrogen abstraction from acetaldehyde. *Ab initio* calculations indicate that this hydrogen-bonded complex has a five membered ringlike structure composed of the H-C=O of the aldehyde and the hydroxyl radical.^{10,11}

REFERENCES

- ¹ M. Tsiouris, M. D. Wheeler, and M. I. Lester, *Chem. Phys. Lett.* **302**, 192 (1999).
- ² M. D. Wheeler, M. Tsiouris, M. I. Lester, and G. Lendvay, *J. Chem. Phys.* **112**, 6590 (2000).
- ³ M. Tsiouris, M. D. Wheeler, and M. I. Lester, *J. Chem. Phys.* **114**, 187 (2001).
- ⁴ M. Tsiouris, I. B. Pollack, and M. I. Lester, *J. Phys. Chem. A*, submitted for publication (2002).
- ⁵ K. Yamasaki, A. Watanabe, T. Kakuda, N. Ichikawa, and I. Tokue, *J. Phys. Chem. A* **103**, 451 (1999).
- ⁶ R. E. Miller, T. G. A. Heijmen, P. E. S. Wormer, A. van der Avoird, and R. Moszynski, *J. Chem. Phys.* **110**, 5651 (1999).
- ⁷ G. Nyman and D. C. Clary, *J. Chem. Phys.* **101**, 5756 (1994).
- ⁸ S. M. Kathmann, M. Dupuis, and B. C. Garrett, personal communication (2001).
- ⁹ C. Sosa and H. B. Schlegel, *J. Am. Chem. Soc.* **109**, 4193 (1987).
- ¹⁰ S. Aloisio and J. S. Francisco, *J. Phys. Chem. A* **104**, 3211 (2000).
- ¹¹ J. R. Alvarez-Idaboy, N. Mora-Diez, R. J. Boyd, and A. Vivier-Bunge, *J. Am. Chem. Soc.* **123**, 2018 (2001).

**DOE SUPPORTED PUBLICATIONS
2000-2002**

1. M. D. Wheeler, M. Tsiouris, M. I. Lester, and G. Lendvay, "OH Vibrational Activation and Decay Dynamics of CH₄-OH Entrance Channel Complexes", *J. Chem. Phys.* **112**, 6590-6602 (2000).
2. M. W. Todd, D. T. Anderson, and M. I. Lester, "Infrared Spectroscopy and Inelastic Recoil Dynamics of OH Radicals in Complexes with *ortho*- and *para*-D₂", *J. Phys. Chem. A* **104**, 6532-6544 (2000).
3. M. D. Wheeler, D. T. Anderson, and M. I. Lester, "Probing Reactive Potential Energy Surfaces by Vibrational Activation of H₂-OH Entrance Channel Complexes", *Int. Rev. Phys. Chem.* **19**, 501-529 (2000).
4. M. Tsiouris, M. D. Wheeler, and M. I. Lester, "Activation of CH Stretching Vibrations in CH₄-OH Entrance Channel Complexes: Spectroscopy and Dynamics", *J. Chem. Phys.* **114**, 187-197 (2001).
5. M. W. Todd, D. T. Anderson, and M. I. Lester, "Reactive Quenching of OH A ²Σ⁺ in Collisions with Molecular Deuterium via Nonadiabatic Passage through a Conical Intersection", *J. Phys. Chem. A* **105**, 10031-10036 (2001).

Theoretical Studies of Molecular Systems

William A. Lester, Jr.
Chemical Sciences Division,
Ernest Orlando Lawrence Berkeley National Laboratory and
Kenneth S. Pitzer Center for Theoretical Chemistry,
Department of Chemistry, University of California, Berkeley
Berkeley, California 94720-1460
walester@lbl.gov

Program Scope

This research program is directed at extending fundamental knowledge of atoms and molecules. The approach combines the use of ab initio basis set methods and the quantum Monte Carlo (QMC) method to describe the electronic structure, energetics, and reaction pathways of systems of primarily combustion interest.

Recent Progress

Quantum Monte Carlo Study of the CO interaction with a model surface for Cr(110) (with O. El Akramine, X. Krokidis, C. A. Taft, A. C. Pavão, T. C. Guimãraes, and R. Zhu)

The interaction of diatomic molecules such as CO with transition metal (TM) surfaces is an important step in understanding heterogeneous catalysis. Evaluating quantitatively the interaction energy between a gas molecule and a TM surface, despite its importance, still presents computational difficulties; for recent reviews, see refs. [1,2]. Much effort has been devoted to the investigation of the specific behavior of each TM and the influence of surface structure of the metal on the interaction with a diatomic molecule.

In a previous ab initio restricted Hartree-Fock (HF) study we considered Cr_2CO and Cr_4CO surface cluster models to simulate CO adsorption on the Cr(110) surface in perpendicular and tilted states [3]. The latter state was identified by us and others to account for the unusually low carbon-oxygen stretching frequencies observed in CO adsorption on TM surfaces and to be a predissociative molecular state.

In general, the direct and the precursor state models, are used to describe the dissociation of a molecule on a surface [4]. In direct dissociative chemisorption, the incident molecule dissociates into adsorbed fragments immediately upon collision with the surface. In dissociative chemisorption through a precursor state, the molecule is adsorbed intact before dissociating. It is well known that CO is adsorbed with the carbon atom closest to the surface. On most densely packed metal surfaces, CO is adsorbed with the molecular axis parallel to the surface normal [5]. We note that the more common Blyholder model [6] does not take into account the existence of

CO tilted states [7] because at the time of publication there was no experimental evidence for their existence.

We have focused on CO adsorption and dissociation on a model transition metal surface for Cr(110). The Cr(110) surface is described by a Cr_2 system with the interatomic distance set to the experimental lattice separation of Cr(110). There have been numerous experimental investigations of CO chemisorption on single crystal transition metals using various experimental techniques including high-resolution electron-energy-loss spectroscopy (HREELS), electron-stimulated desorption ion angular distribution (ESDIAD), low-energy electron diffraction (LEED), Auger-electron spectroscopy (AES), and core valence photoemission. In addition, there have been a number of theoretical studies of the adsorption/dissociation of diatomic molecules on metallic surfaces, of which we cite only a few, using unrestricted Hartree Fock (UHF) combined with the resonating valence bond theory and multiple-scattering X_α formalism [5], the Hückel method [8], ab initio UHF [9], in addition to the ab initio HF investigation of Cr_nCO clusters [3].

The aim of the present study is to carry out a quantum Monte Carlo (QMC) study in the diffusion Monte Carlo (DMC) approach of CO adsorption and dissociation on the Cr(110) model surface both to assess our previous ab initio HF study, and to gain insight on the use of the DMC method for quantitative description of gas-surface interactions. To these ends we computed the total energy of the system in the same configurations as previously investigated and identified the more stable binding mode.

The present results are consistent with various experiments that show the tilted/near-parallel configuration to be a more stable orientation mode at low CO coverage than the perpendicular arrangement. We have determined the energy difference between these two modes of CO-surface interaction to high accuracy. The DMC calculations of adsorption of CO on the model surface have been analyzed in terms of the topological representation of the electron localization function (ELF). This procedure provides clear understanding and insight on the electron rearrangement and reorganization during the interaction of CO with the metallic surface. The CO dissociation on 3d-metal surfaces is confirmed to be a two-step (metal \rightarrow CO and CO \rightarrow metal) charge transfer process and the near-parallel orientation (tilted state) is identified as the precursor state to the dissociation.

REFERENCES

- [1] C. A. Taft, T. C. Guimarães, A. C. Pavão, and W.A. Lester, Jr., *Int. J. Phys. Chem.* **18**, 163 (1999).
- [2] (C. A. Taft, please provide a recent review reference to the work and authors. Thanks).
- [3] A. C. Pavão, B. L. Hammond, M. M. Soto, W.A. Lester, Jr. and C. A. Taft, *Surf. Sci.* **323**, 340 (1995).
- [4] S. T. Ceyer, *Ann. Rev. Phys. Chem.* **39**, 479 (1988).
- [5] (a) T. C. Guimarães, A. C. Pavão, C. A. Taft, and W.A. Lester, Jr. *Phys. Rev. B*, **56**, 7001 (1997), (b) A. C. Pavão, M. Braga, and C. A. Taft, B.L. Hammond and W.A. Lester Jr., *Phys. Rev. B* **44**, 1910 (1991).

- [6] G. Blyholder, J. Chem. Phys. **68**, 2772, (1964).
- [7] A. C. Pavão, M. M. Soto and W.A. Lester Jr., S. K. Lie, B.L. Hammond and C. A. Taft, Phys. Rev. B **50**, 1868 (1994).
- [8] S. P. Mehandru and A. B. Anderson, Surf. Sci. **169**, (1986) L281.
- [9] (a) P. S. Bagus, C. J. Nelin, C. W. Bauschlicher, J. Chem. Phys. **28** (1983) 5423, (b) C. W. Bauschlicher, P. S. Bagus, C. J. Nelin, B. O. Roos, J. Chem. Phys. **85** (1986).

A Quantum Monte Carlo Study of Energy Differences in C₄H₃ and C₄H₅ Isomers (with X. Krokidis, N. W. Moriarty, and M. Frenklach)

Quantum Monte Carlo and a series of other ab initio as well as density functional theory calculations were performed for the enthalpy of formation of C₄H₃ and C₄H₅ radicals. The enthalpy differences between the *n* and *i* isomers of C₄H₃ and C₄H₅ are predicted to be substantially lower than those obtained in other recent theoretical studies. The nature of the middle C-C bond in these radicals was examined using the electron localization function topological analysis performed with bonding evolution theory for partitioning the molecular space into regions with clear chemical meaning. This analysis showed that the *n* isomers are represented by a unique Lewis structure while the *i* isomers are represented by a resonance description. For the latter systems, the middle C-C bond is only mildly conjugated and the corresponding degree of conjugation was calculated. These results signify higher prominence of the even-carbon-atom reaction pathways in the formation of the first aromatic ring in hydrocarbon pyrolysis and oxidation, consistent with past kinetic modeling and recent experimental studies.

Future Plans

Future work will continue in the direction of establishing fundamental understanding of mechanisms leading to soot formation as well as other molecular species of combustion interest. In addition, there will be an enhanced effort to develop an efficient scheme for the calculation of optimized geometries in the DMC method.

DOE Supported Publications 2000-2002

1. J. C. Grossman, W. A. Lester, Jr., and S. G. Louie, "Quantum Monte Carlo and Density Functional Theory Characterization of 2-Cyclopentenone and 3-Cyclopentenone Formation from O(³P) + Cyclopentadiene, J. Am. Chem. Soc. **122**, 705 (2000).
2. J. A. W. Harkless and W. A. Lester, Jr., "Quantum Monte Carlo for Atoms and Molecules, "Proceedings of the Workshop on Contemporary Problems in Mathematical Physics, World Scientific Publishing (Singapore), p. 153, 2000.
3. J. A. W. Harkless and W. A. Lester, Jr., "Quantum Monte Carlo Determination of the Atomization Energy and Heat of Formation of Propargyl Radical," J. Chem. Phys. **113**, 2680 (2000).

4. C. A. Taft, E. Longo, F. Sensato, J. B. L. Martins, R. Sambrano, A. L. Almeida, and W. A. Lester, Jr., "Interaction of Water, Gases, and Other Complexes with Metal Oxide Surfaces", *Recent Res. Devel. Quantum Chem.* **1**, 105 (2000).
5. R. N. Barnett, Z. Sun, and W. A. Lester, Jr., "Improved Trial Wave Functions in Quantum Monte Carlo: Application to Acetylene and Its Dissociation Fragments," *J. Chem. Phys.* **114**, 2013 (2001).
6. A. C. Pavão, C. A. Taft, T. C. F. Guimarães, M. B. C. Leão, J. R. Mohallem, and W. A. Lester, Jr. "Interdisciplinary Applications of Pauling's Metallic Orbital and Unsynchronized Resonance to Problems of Modern Physical Chemistry: Conductivity, Magnetism, Molecular Stability, Superconductivity, Catalysis, Photoconductivity and Chemical Reaction," (feature article), *J. Phys. Chem.* **105**, 5 (2001).
7. I. Ovcharenko, A. Aspuru-Guzik, and W. A. Lester, Jr., "Soft Pseudopotentials for Efficient Quantum Monte Carlo Calculations: From Be to Ne and Al to Ar," *J. Chem. Phys.* **114**, 7790 (2001).
8. W. A. Lester, Jr., "Research Developments and Progress During the Nineties," *J. Mol. Struct. (THEOCHEM)* **573**, 55 (2001).
9. X. Krokidis, N. W. Moriarty, W. A. Lester, Jr., and M. Frenklach, "A Quantum Monte Carlo Study of Energy Differences in C₄H₃ and C₄H₅ Isomers," *Int. J. Chem. Kinetics* **33**, 808 (2001).

Quantum Dynamics of Fast Chemical Reactions

DE-FG02-87ER13679

April 2002

John C. Light

The James Franck Institute and Department of Chemistry

The University of Chicago, Chicago, Illinois 60637

j-light@uchicago.edu

Scope:

The aims of this research and are to develop theoretical infrastructure and computational methods and to apply these methods to determine theoretically reaction rates and other dynamical quantities of interest for chemical reactions.

During the past year we have focused primarily on two areas: development of better representations for dynamical calculations on larger systems and applications to understand the vibration/rotation structure of molecules of interest in combustion problems. This year we focused primarily protonated acetylene (HHCCH^+). Substantial work on semiclassical methods and the diagonal Born-Oppenheimer approximation was also published in 2001 which we briefly describe first.

Recent Results:

Semiclassical scattering:

A major problem in using semiclassical initial value representation methods (IVR or HK) for detailed calculations on reactive systems is the sensitivity of the S-matrix elements, and thus the state-to-state reaction probabilities to the large oscillatory term in the integrand over initial values due to the action accumulated over the trajectory. This can be partially compensated using the Moeller wave operator formalism of quantum scattering which generates action only due to the difference of a reference Hamiltonian, H_0 , and the true Hamiltonian, $H[1]$. When coupled with an improved method for calculating the monodromy matrix[2], this makes the calculation of semiclassical state-to-state reactive scattering substantially more efficient. However, it remains a difficult task to generate the reactive scattering S-matrix semiclassically.

Basis Representations:

For the large amplitude dynamics of molecular systems the size of standard quantum representations (essentially basis sets) such as DVR's[3] scale with number of particles, n , as N^{3n-6} where N , the number of basis functions per degree of freedom is usually ≥ 10 . Thus the utility of these direct product approaches is limited to systems with fewer than six or seven large amplitude motions. Improvements in extracting eigenvalues and eigenfunctions such as filter diagonalization[4, 5] and other iterative methods[6] are very important but do not change the basic scaling problem - addition of a "floppy" atom to a "floppy" molecule increases the size of a direct product basis by roughly a factor of 10^2 to 10^3 . Current alternatives either limit

the large amplitude motions (e.g. normal modes or adiabatic separations) or use self consistent vibrational field approaches[7, 8].

The use of correlated bases such as distributed Gaussians[9] for multidimensional systems was explored many years ago and has been adopted for some calculations since then. However, the recent "Quasi-random distributed Gaussian basis" method (QDGB)[10] permits the basis to cover more efficiently the requisite portion of phase space required for vibrational levels up to a given energy. This has been extended to *angular* variables as described below for the $C_2H_3^+$ system.

The alternative development of an optimal direct product basis based on similar phase space considerations[11-13] substantially improves the direct product DVR, but does not directly attack the exponential dependence of basis size on dimensionality.

DOE Supported publications, 2001

Quasi-random distributed Gaussian bases for bound problems Sophia Garashchuk and J. C. Light, J. Chem. Phys 114, 3929 (2001)

Semiclassical application of the Moeller operators in reactive scattering Sophia Garashchuk and J. C. Light, J. Chem. Phys 114, 1060 (2001)

Phase Space Optimization of Quantum Representations: Three-body Systems and the Bound States of HCO B. Poirier and J. C. Light, J. Chem. Phys. 114, 6562 (2001)

The diagonal Born-Oppenheimer correction to molecular dynamical properties. S. Garashchuk and J. C. Light and V. A. Rassolov Chem. Phys. Lett. 333, 459 (2001)

Ongoing Projects:

We are continuing studies on improved representations as well as dynamical calculations on interesting systems.

Angular Representations:

Direct product angular DVR's

For systems of more than three atoms the internal coordinate systems usually contain more than one angle and a coupled angular basis is required to impose a specific value of the angular momentum. Thus one of the additional difficulties for larger systems is the use of large angular bases (we used about 8000 for the acetylene system[14]). For four atom systems with three internal angles we showed that the coupled angular basis may be replaced by a 3D direct product DVR[14]. This is surprising since the basis is not correct at the boundaries where effective potential singularities occur (e.g. 0 and π). However, since the effective potentials are repulsive, the wave function goes to zero at the boundaries and the eigenvalues are given very accurately by the angular DVR basis.

The direct product angular basis is substantially more efficient to use than the coupled angular basis and will permit the calculations on acetylene to be extended to the energy regime of the acetylene/vinylidene isomerization.

Gaussian bases in angles and radial coordinates:

The QDGB may also be extended to angular coordinates, albeit with some additional complexity[15]. One problem is that Gaussians extend to $(-\infty, \infty)$ whereas all angular coordinates have finite ranges or are periodic. However, the Gaussian basis can be limited to the finite range by a quadratic polynomial in angle which forces zero or zero derivative boundary conditions at the boundaries (e.g. $\theta(\theta - \pi)$). Similarly

Gaussians in radial distances can be forced to zero as $r \rightarrow 0$. The required error function type integrals are not computationally difficult.

These have been used for the study of protonated acetylene.

Theoretical Spectroscopy:

The work on the protonated acetylene molecule is essentially complete. The $C_2H_5^+$ molecule is of interest both in combustion and in interstellar chemistry. With five atoms there are 9 degrees of freedom for $J = 0$, five angles and four distances in the modified Radau coordinates of choice. Preliminary spectra have indicated that the molecule is planar at low energy with the proton being bound to the C=C double bond at the equilibrium configuration. At relatively low energies the molecule can tunnel between equivalent configurations through a shallow metastable minimum at the "classical" $H_2C=CH^+$ configuration.

Quite extensive calculations of the PES for this system showed that

- a) the system remains planar during the isomerization;
- b) as two H's rotate to the "classical" configuration, the CCH moiety remains essentially linear with essentially no change in distances.
- c) the HCH angle of the "rotating" H's also remains quite constant along the isomerization reaction path, although the HC distance changes appreciably.
- d) it was determined that G3MP3LargeBasis quantum calculations were adequate to describe the PES near the reaction path quite accurately.

This suggested that a reduced dimensionality calculation on the planar system involving two CH distances and two HCC angles would be sufficient to characterize the vibrational dynamics of the isomerization, and this calculation was done. The calculation of matrix elements of the potential in the Gaussian basis using the grid of calculated points was quite difficult. In fact a local analytic representation of the potential was required for accuracy. This was accomplished using the new Hermite interpolation method of Bowman's group [16, 17]. Approximately 500 Gaussians distributed in 4-D were required for convergence of the lowest 10 or so levels of each symmetry.

The energy levels are given in Table I below. The very small (anti-symmetric - symmetric) splittings of the lowest 3 levels indicates that these levels are localized at the non-classical minimum configuration.

REFERENCES

- [1] Sophya Garashchuk and J. C. Light. Semiclassical application of the Moeller operators in reactive scattering. *J. Chem. Phys.*, 114:1060, 2001.
- [2] Sophya Garashchuk and J. C. Light. Simplified calculation of the stability matrix for semiclassical propagation. *J. Chem. Phys.*, 113:9390, 2000.
- [3] J. C. Light and T. Carrington, Jr. Discrete variable representations and their utilization. *Adv. Chem. Phys.*, 114:263, 2000.
- [4] M. R. Wall and D. Neuhauser. Extraction, through filter-diagonalization, of general quantum eigenvalues or classical normal-mode frequencies from a small number of residues or a short-time segment of a signal .1. theory and application to a quantum-dynamics model. *J. Chem. Phys.*, 102:8011-8022, 1995.
- [5] V. A. Mandelshtam and H. S. Taylor. *J. Chem. Phys.*, 106:5085, 1997.

TABLE I: Energies, splittings and splitting convergence of the energy levels for 4D calculation. Column I contains symmetric energy levels, E^{sym} . Columns II - IV are the energy differences, $E^{asym}-E^{sym}$, for bases A, B and C, respectively, as described in text. Columns V and VI show the difference of the splittings for bases A and C (column V), B and C (column VI). All quantities are in cm^{-1} .

Level	I	II	III	IV	V	VI
1	3909.0	1.1×10^{-6}	-2.6×10^{-7}	-1.1×10^{-6}	2.2×10^{-6}	8.0×10^{-7}
2	4576.7	2.2×10^{-6}	4.6×10^{-6}	2.4×10^{-6}	-2.1×10^{-7}	2.3×10^{-6}
3	5095.7	8.5×10^{-3}	8.5×10^{-3}	8.4×10^{-3}	7.8×10^{-5}	7.9×10^{-5}
4	5196.7	0.093	0.093	0.092	0.0012	0.0008
5	5373.4	168.9	168.8	168.6	0.32	0.24
6	5587.5	77.7	77.6	77.8	-0.12	-0.14
7	5752.1	37.0	37.1	37.1	-0.11	0.0041
8	5882.0	135.3	135.3	135.2	0.075	0.11
9	6148.5	46.6	46.7	46.5	0.12	0.19
10	6202.6	62.8	62.5	62.5	0.22	-0.031

- [6] Hua-Gen Yu and G. Nyman. Quantum dynamics of the $\text{O}^3\text{P} + \text{CH}_4 \rightarrow \text{OH} + \text{CH}_3$ reaction: An application of the rotating bond umbrella model and spectral transform sub space iteration. *J. Chem. Phys.*, 112:238, 2000.
- [7] I. Burghardt, H.-D. Meyer, and L.S. Cederbaum. Approaches to the approximate treatment of complex molecular systems by the multiconfiguration time dependent Hartree method. *J. Chem. Phys.*, 111:2927, 1999.
- [8] C. Cattarius, G.A. Worth, H.-D. Meyer, and L.S. Cederbaum. All mode dynamics at the conical intersection of an octa-atomic molecule: MCTDH investigation on the butatriene cation. *J. Chem. Phys.*, 115:2088, 2001.
- [9] I. P. Hamilton and J. C. Light. On distributed gaussian bases for simple model multidimensional vibrational problems. *J. Chem. Phys.*, 84:306, 1986.
- [10] Sophia Garashchuk and J. C. Light. Quasi-random distributed Gaussian bases for bound problems. *J. Chem. Phys.*, 114:3929-3939, 2001.
- [11] Bill Poirier and J. C. Light. Phase space optimization of quantum representations: Direct product basis sets. *J. Chem. Phys.*, 111:4869, 1999.
- [12] B. Poirier and J. C. Light. Phase space optimization of quantum representations: Three-body systems and the bound states of HCO. *J. Chem. Phys.*, 114:6562, 2001.
- [13] B. Poirier. Algebraically self-consistent semi-classical quantization on phase space. *Found. Phys.*, 30:1191, 2000.
- [14] Hua Chen. *Theoretical Spectra of Floppy Molecules*. PhD thesis, University of Chicago, Chicago, IL, 60637, 2000.
- [15] S. Garashchuk and J. C. Light. Theoretical study of protonated acetylene. *In preparation*.
- [16] S. Carter, J. M. Bowman, and B. J. Braams. *Chem. Phys. Lett.*, 342:636, 2001.
- [17] B. J. Braams. *MELKES package, Private Communication*.

Kinetics of Elementary Processes Relevant to Incipient Soot Formation

M. C. Lin
Department of Chemistry
Emory University
Atlanta, GA 30322
chemmcl@emory.edu

I. Program Scope

Soot formation and abatement processes are some of the most important and challenging problems in hydrocarbon combustion. The key reactions involved in the formation of polycyclic aromatic hydrocarbons (PAH's), the precursors to soot, remain elusive. Small aromatic species such as C_5H_5 , C_6H_6 and their derivatives are believed to play a pivotal role in incipient soot formation.

The goal of this project is to establish a kinetic database for elementary reactions relevant to soot formation in its incipient stages. In the past year, our major focus has been placed on the experimental studies on several reactions of C_6H_5 with alkanes and computational studies on the reaction of CH_3 with HO_2 , the reaction of OH and CH_3 radicals with C_6H_6 as well as the reaction of H atoms with C_5H_6 at the G2M level of theory.¹ These results are briefly summarized below.

II. Recent Progress

A. Experimental studies

We have developed three complementary methods for determination of the kinetics and mechanisms for C_6H_5 reactions with combustion species, including small alkenes and small aromatics. Combination of these methods: cavity ring-down spectrometry (CRDS), pyrolysis/Fourier transform infrared spectrometry (P/FTIRS) and pulsed laser photolysis/mass spectrometry (PLP/MS), allows us to cover a broad temperature range, 300 - 1000 K. The results of our recent studies on the reactions of C_6H_5 with C_3H_8 and $n-C_6H_{14}$, and the oxidation of C_6H_5NO by NO_2 are briefly summarized below.

1. $C_6H_5 + C_3H_8$ Reaction

The kinetics for the $C_6H_5 + C_3H_8$ reaction has been measured by PLP/MS using C_6H_5NO as the radical source in the temperature range $419 < T < 773$ K. The results can be represented by $k(C_3H_8) = 7.5 \times 10^{11} \exp(-1940/T) \text{ cm}^3 \text{ mole}^{-1} \text{ s}^{-1}$. This preliminary result will be further confirmed by experiments using acetophenone as the radical source to cover temperatures up to 1000 K.

2. $C_6H_5 + n-C_6H_{14}$

The kinetics for the $C_6H_5 + n-C_6H_{14}$ reaction has been measured by PLP/MS in the temperature range $403 < T < 775$ K. The results can be represented by $k(C_6H_{14}) = 3.0 \times 10^{12} \exp(-2000/T) \text{ cm}^3 \text{ mole}^{-1} \text{ s}^{-1}$. Similar to the propane reaction cited above, experiments with acetophenone as the radical source for higher temperatures are under way. A full analysis of these data will be carried out to extract their secondary C-H abstraction rate constants upon completion of the studies, which will include $n-C_4H_{10}$ and $n-C_8H_{18}$ also.

3. Kinetics of C_6H_5NO oxidation by NO_2

In our recent study of the $C_6H_5 + H_2$ and CH_4 reactions by P/FTIRS,^{2,3} we discovered that a long standing mixture of C_6H_5NO and NO at room temperature produced $C_6H_5NO_2$, resulting perhaps from a series of redox reactions involving nitric oxide and nitrosobenzene, which generated NO_2 initially, followed by the direct oxidation of nitrosobenzene by nitrogen dioxide. To substantiate the last process, we have carried out a pyrolytic study of the $C_6H_5NO + NO_2$ reaction in the temperature range 373 - 473 K by P/FTIRS.⁴ The results suggest that the reaction does occur and is strictly bimolecular; the rate constant for the direct O-exchange reaction, $C_6H_5NO + NO_2 \rightarrow C_6H_5NO_2 + NO$, $k_1 = (9.62 \pm 0.35)$

$\times 10^{10} \exp [-(6500 \pm 144)/T] \text{ cm}^3 \text{ mol}^{-1} \text{ s}^{-1}$, could be satisfactorily accounted for by the transition state theory with the energy barrier, $E_1^0 = 10.0 \pm 0.3 \text{ kcal/mol}$ at 0 K, using the geometric parameters and frequencies obtained by B3LYP/cc-pVDZ calculations.

B. Computational Studies

1. $\text{CH}_3 + \text{HO}_2 \rightarrow \text{CH}_3\text{O}_2\text{H}$, $\text{CH}_3\text{O} + \text{OH}$, and $\text{CH}_4 + \text{O}_2$

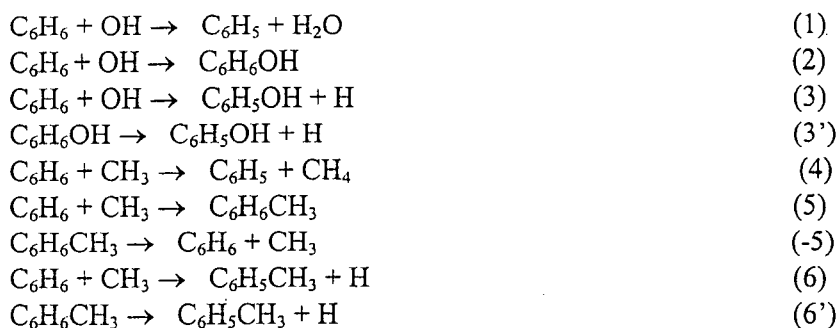
The combustion of alkanes in general under high-pressure conditions is strongly affected by the kinetics of the CH_3 reaction with HO_2 . We have performed a detailed analysis of the reaction system⁵ at the G2M level of theory, in conjunction with variational RRKM calculations.⁶ The reaction was shown to take place by several product channels producing (a) $\text{CH}_4 + \text{O}_2$ ($^3 \Sigma_g^-$) and (b) $\text{CH}_4 + \text{O}_2$ ($^1 \Delta$) by direct H-abstraction, and (c) $\text{CH}_3\text{O} + \text{OH}$ and (d) $\text{CH}_2\text{O} + \text{H}_2\text{O}$ by association/decomposition mechanism via CH_3OOH . The bimolecular reaction rate constants for the formation of these products have been calculated for the temperature range 300-3000 K and found to be pressure independent up to 50 atm. The Arrhenius equations for the two major channels (a) and (c) were found to be strongly curved; they can be represented by $k_a = 4.23 \cdot 10^{-16} T^{1.25} \exp(828/T)$ for 300-800 K, $k_a = 3.02 \cdot 10^{-21} T^{2.83} \exp(1877/T)$ for 800-3000 K, and $k_c = 2.97 \cdot 10^{-10} T^{-0.24} \exp(182/T)$ for 300-1000 K and $1.02 \cdot 10^{-13} T^{0.76} \exp(1195/T)$ for 1000-3000 K, in units of $\text{cm}^3 \text{ molecule}^{-1} \cdot \text{s}^{-1}$. In the abstraction channel (a), the effect of multiple reflections above its molecular complex ($\text{CH}_3 \cdots \text{HO}_2$), which lies 1.9 kcal/mol below the reactants with a 1.2 kcal/mol barrier leading to the formation of the $\text{CH}_4 + \text{O}_2$ ($^3 \Sigma_g^-$) products, was found to be quite significant at low temperatures ($T < 300 \text{ K}$). In addition, the predicted rate constant for the unimolecular decomposition of CH_3OOH agrees closely with the available experimental data using the heats of formation of CH_3O ($5.4 \pm 0.5 \text{ kcal/mol}$) and CH_3OOH ($-29.0 \pm 1.0 \text{ kcal/mol}$) calculated with the isodesmic method at 0 K. These rate constants are recommended for kinetic modeling of incipient soot formation.

2. $\text{C}_6\text{H}_5 + \text{C}_2\text{H}_4$ Reaction

The $\text{C}_6\text{H}_5 + \text{C}_2\text{H}_4$ reaction is relevant to the formation of PAH's and soot. Its kinetics had been studied by CRDS several years ago by Yu and Lin,⁷ whose result could be correlated with those reported earlier by Fahr et al.^{8,9} acquired under very low pressure conditions by RRKM calculations using assumed transition state parameters.⁷ The mechanism employed in our interpretation of the kinetic data included the addition producing the excited $\text{C}_6\text{H}_5\text{C}_2\text{H}_4$ radical followed by either stabilization or decomposition producing $\text{C}_6\text{H}_5\text{C}_2\text{H}_3 + \text{H}$. This mechanism, though sufficient for interpretation of the overall kinetics, is clearly over-simplified, according to the result of our *ab initio* calculation based on the G2M method.¹ The $\text{C}_6\text{H}_5\text{C}_2\text{H}_4$ radical adduct can in fact undergo numerous isomerization and decomposition reactions forming stable double ring compounds including [4,2,0]- C_8H_9 , [3,3,0]- C_8H_9 (with C_1 and C_s symmetries), spiro- C_8H_9 and $\text{C}_6\text{H}_5\text{CHCH}_3$, which is more stable than $\text{C}_6\text{H}_5\text{C}_2\text{H}_4$ by 11.7 kcal/mole. The predicted addition barrier, 2.0 kcal/mol, correlates our CRDS and Fahr's low-pressure data very well.

3. $\text{OH} + \text{C}_6\text{H}_6$ Reaction

The reaction of OH with C_6H_6 at high temperatures plays a pivotal role in soot formation chemistry. Under combustion conditions, there are only limited reliable kinetic data for computer simulation of soot formation. We have carried out a detailed analysis of the reaction by G2M/RRKM calculations. The reaction was found to occur by a pre-reaction complex. The molecular structure, stabilization energy and the nature of bonding interactions of the $[\text{C}_6\text{H}_6 \cdots \text{OH}]$ complex have been characterized. Accurate thermochemistry for major reaction channels was established by making a combined use of experimental and theoretical parameters. A multistep kinetic model for the OH-addition channel was proposed and the effects of T, P and reaction time on the apparent rate constants were evaluated by weak collision master equation/RRKM analysis. Available experimental kinetic data for all relevant reactions are critically analyzed and correlated with modeled effective rate constants. Combination of these and previous results for the CH_3 - C_6H_6 system,¹⁰ we obtained the following thermochemical and kinetics data:



$$\begin{aligned} \Delta H_{(1)}(0 \text{ K}) &= -5.6 \pm 0.8 \text{ kcal/mol}, & \Delta H_{(4)}(0 \text{ K}) &= 8.5 \pm 0.9 \text{ kcal/mol}, \\ \Delta H_{(2)}(0 \text{ K}) &= -17.0 \pm 3 \text{ kcal/mol}, & \Delta H_{(5)}(0 \text{ K}) &= -10.7 \pm 3 \text{ kcal/mol}, \\ \Delta H_{(3)}(0 \text{ K}) &= 0.3 \pm 0.4 \text{ kcal/mol}, & \Delta H_{(6)}(0 \text{ K}) &= 9.4 \pm 0.4 \text{ kcal/mol}, \\ \Delta H_{(-3')}(0 \text{ K}) &= -17.3 \pm 3 \text{ kcal/mol}, & \Delta H_{(-6')}(0 \text{ K}) &= -20.1 \pm 3 \text{ kcal/mol}. \end{aligned}$$

Equilibrium constants (T = 200 – 2500 K):

$$\begin{aligned} K_1 &= 130 \times T^{-0.26} \exp(2643/T), \\ K_2 &= 6.15 \times 10^{-32} \times T^{2.00} \exp(9460/T) \text{ cm}^3 \text{ molecule}^{-1}, \\ K_3 &= 5.65 \times 10^{-7} \times T^{1.62} \exp(310/T). \end{aligned}$$

Rate constants fitted from the experiment (T = 200 – 2500 K):

$$\begin{aligned} k_1 &= 6.70 \times 10^{-22} T^{3.33} \exp(-732.4/T) \text{ cm}^3 \text{ molecule}^{-1} \text{ s}^{-1} \\ k_{(-3)} &= 8.9 \times 10^{-18} T^{2.0} \exp(-2753 \pm 250/T) \text{ cm}^3 \text{ molecule}^{-1} \text{ s}^{-1} \end{aligned}$$

Derived based on reverse rate constants and known thermochemistry:

$$\begin{aligned} k_{(-1)} &= k_1/K_1 = 5.2 \times 10^{-24} T^{3.59} \exp(-3375/T) \text{ cm}^3 \text{ molecule}^{-1} \text{ s}^{-1} \\ k_3 &= K_3 * k_{(-3)} = 5.0 \times 10^{-24} T^{3.62} \exp(-2443 \pm 250/T) \text{ cm}^3 \text{ molecule}^{-1} \text{ s}^{-1} \end{aligned}$$

4. CH₃ + C₆H₆ Reaction

The kinetics for the CH₃ + C₆H₆ reaction has been investigated by modeling the existing data obtained by Holt and Kerr.¹¹ The result of the modeling suggests that the yields of CH₄ measured in the UV photolysis of mixtures of (CH₃CO)₂, *i*-C₄H₁₀ and C₆H₆ and employed in their analysis of the CH₃ + C₆H₆ kinetics could be quantitatively predicted by the reactions of CH₃ with *i*-C₄H₁₀ and alkyl radicals present in the system, *independent of the CH₃ + C₆H₆ reaction*.¹² The CH₃ + C₆H₆ reaction was concluded to be insignificant under the conditions employed on account of the instability of the C₇H₉ radical adduct and the strong C-H bonds in benzene which prevent the occurrence of the simple abstraction process.

5. H + C₅H₆ Reaction

The H + *c*-C₅H₆ reaction, critical to the formation of the cyclopentadienyl radical under sooting conditions, has been studied at the G2M level of theory.¹³ Statistical theory calculations have been performed using theoretical potential energy surface and molecular parameters. It has been shown that the reaction can occur by both the abstraction and addition mechanisms. The latter process has not been considered in combustion modeling to date. Theoretical rate constants have been calculated for the low-lying product channels and relative contributions of the addition and abstraction channels have been assessed. The potential role of open-chain intermediates produced by the addition process in kinetic data analysis has been suggested and corresponding rate constants have been recommended for inclusion in the modeling of the H + *c*-C₅H₆ reaction for 1000 K ≤ T ≤ 3000 K:

Direct abstraction producing $H_2 + C_5H_5$:

$$k_{2a} = 3.03 \times 10^8 \cdot T^{1.71} \cdot \exp(-2813/T) \text{ cm}^3/\text{mol}\cdot\text{s};$$

Addition reaction producing *c*- C_5H_7 :

$$k_{2b} (1 \text{ atm}) = 5.64 \times 10^{113} \cdot T^{-29.2} \cdot \exp(-31294/T) \text{ cm}^3/\text{mol}\cdot\text{s};$$

Addition reaction producing $CH_2=CH-CH-CH=CH_2$:

$$k_{2c} (1 \text{ atm}) = 8.27 \times 10^{126} \cdot T^{-32.3} \cdot \exp(-41439/T) \text{ cm}^3/\text{mol}\cdot\text{s};$$

III. Future Plans

Currently, we continue the acquisition of kinetic data for C_6H_5 reactions by CRDS and PLP/MS techniques to determine the reactivity of the phenyl toward s-CH bonds and the determination of total rate constants and product branching probabilities in the C_6H_5 reactions with C_3H_4 , ketene, acetaldehyde and alcohols. Computationally, we will carry out high-level *ab initio* MO calculations to improve our predictive capability for the rate constant and product branching ratios of C_6H_5 reaction with O_2 . We also plan to extend the calculations to include the reaction of C_6H_5 radicals with alkanes to correlate the kinetic data obtained for the abstraction reactions.

IV. References (DOE publications, 2000-present, denoted by #)

1. A. M. Mebel, K. Morokuma and M. C. Lin, *J. Chem. Phys.*, 103, 7414 (1995).
2. J. Park, I. V. Dyakov, and M. C. Lin., *J. Phys. Chem. A*, 101, 8839 (1997).
3. I. V. Tokmakov, J. Park, S. Gheyas and M. C. Lin, *J. Phys. Chem. A*, 103, 3636 (1999).
- #4. J. Park, Y. M. Choi, I. V. Dyakov and M. C. Lin, *J. Phys. Chem., A*, 106, 2903 (2002).
- #5. R. S. Zhu and M. C. Lin, *J. Phys. Chem. A.*, 105, 243 (2001).
6. S. J. Klippenstein, A. F. Wagner, R. C. Dunbar, D. M. Wardlaw, and S. H. Robertson, VARIFLEX: VERSION 1.00, 1999.
7. T. Yu and M. C. Lin, *Combust. Flame*, 100, 169 (1995).
8. A. Fahr, W. G. Mallard, S. E. Stein, 21st Symp. (Int.) on Combust., The Combustion Institute, 1986, p. 825.
9. A. Fahr and S. E. Stein, 22nd Symp. (Int.) on Combust., The Combust. Institute, 1988, 1023.
- #10. I. V. Tokmakov and M. C. Lin, *Int. J. Chem. Kinet.*, 33, 633 (2001).
11. P. M. Holt. and J. A. Kerr, *Int J Chem Kinet* 9, 185, 1977.
- #12. J. Park and M. C. Lin, *Int. J. Chem. Kinet.*, 33, 803 (2001).
- #13. L. V. Moskaleva and M. C. Lin, *Proc. Combust. Inst.* 29, in press.

Other DOE Publications Not Cited in the Text:

1. Gi-Jung Nam, W. Xia, J. Park and M. C. Lin, *J. Phys. Chem. A*, 104, 1233 (2000).
2. Y. M. Choi, Wensheng Xia, J. Park and M. C. Lin, *J. Phys. Chem. A*, 104, 7030 (2000).
3. L. V. Moskaleva and M. C. Lin, *J. Comput. Chem.* 21, 415 (2000).
9. L. V. Moskaleva, W. S. Xia and M. C. Lin, *Chem. Phys. Lett.*, 331, 269 (2000).
5. L. V. Moskaleva and M. C. Lin, *Proc. Combust. Inst.*, 28 (Part II), 2393 (2000).
6. L. V. Moskaleve and M. C. Lin., *Z. Phys. Chem.*, 215, 1043-54 (2001).
7. A. M. Mebel, M. C. Lin, D. Chakraborty, J. Park, S. H. Lin and Y. T. Lee, *J. Chem. Phys.* 114, 8421 (2001).
8. R. S. Zhu, C.-C. Hsu and M. C. Lin, *J. Chem. Phys.* 115, 195 (2001).
9. W. S. Xia, R. S. Zhu, M. C. Lin and A. M. Mebel, *Faraday Discuss.*, 119, 191(2001).
10. J. Park, S. Gheyas and M. C. Lin, *Int. J. Chem. Kinet.*, 33, 64 (2001).

INVESTIGATION OF POLARIZATION SPECTROSCOPY AND DEGENERATE FOUR-WAVE MIXING FOR QUANTITATIVE CONCENTRATION MEASUREMENTS

Principal Investigator: Robert P. Lucht

Department of Mechanical Engineering, Texas A&M University, Mail Stop 3123, College Station, TX 77843-3123 (rlucht@tamu.edu)

I. PROGRAM SCOPE

Polarization spectroscopy (PS) and degenerate four-wave mixing (DFWM) are techniques that show great promise for sensitive measurements of transient gas-phase species, and diagnostic applications of these techniques are being pursued actively at laboratories throughout the world. However, significant questions remain regarding strategies for quantitative concentration measurements using polarization spectroscopy and DFWM. The objective of this research program is to develop and test strategies for quantitative concentration measurements in flames and plasmas. We are investigating the physics of these processes by direct numerical integration (DNI) of the time-dependent density matrix equations that describe the resonant interaction. Significantly fewer restrictive assumptions are required using this DNI approach compared with the assumptions required to obtain analytical solutions. Inclusion of the Zeeman state structure of degenerate levels has enabled us to investigate the physics of polarization spectroscopy and of polarization effects in DFWM. Recently, we have incorporated the effects of hyperfine structure in our numerical calculations of PS signal generation. We have successfully incorporated the multi-axial-mode laser structure that is characteristic of commercial dye lasers into our polarization spectroscopy calculations. Experimental measurements are performed in well-characterized flames, gas cells, or nonreacting flows for comparison with our theoretical calculations.

II. RECENT PROGRESS

A. *Theoretical Analysis of Short-Pulse Polarization Spectroscopy*

The potential advantages of short-pulse laser excitation for reducing or eliminating the effects of collisions in laser diagnostic measurements in combustion have long been recognized. A laser with a nominal pulse length of 10-100 psec is ideal for diagnostics of atmospheric pressure flames because the laser pulse length is shorter than the characteristic collisional times in the medium. In addition, the nominal laser bandwidth (Fourier transform limit) of 1.5 to 0.15 cm^{-1} is low enough that the laser radiation can couple efficiently with molecular resonances. We have performed an extensive theoretical study of short-pulse PS. The direct numerical integration (DNI) method that we have developed over the last few years is particularly well-suited for the investigation of the physics of this technique. The time-dependent density matrix equations for these levels are integrated numerically and the PS signal is calculated from the time-dependent third-order polarization induced in the medium by the interaction of the pump and probe beams. Our calculations [1] and the results of previous experiments [2] indicate that there is a very significant reduction in the sensitivity of the PS signal to the collision rate for short-pulse laser excitation. Saturated short-pulse PS seems to be a very promising technique for quantitative concentration measurements of minor species in flames.

We have investigated the laser excitation dynamics in detail by examining the temporal dependence of the Zeeman populations and the induced coherences for the allowed Zeeman transitions

[1]. The laser excitation dynamics for the $P_{12}(2)$ transition are shown in Fig. 1 for low and high pump beam intensities.

B. Effects of Pump Polarization and Hyperfine Structure on PS Signal Intensities

We completed an experimental investigation of the effect of pump polarization and have investigated the effect of hyperfine structure on PS signal generation. The hyperfine structure of the $Q_1(4)$ resonance of the OH (0,0) band in the $A^2\Sigma^+ - X^2\Pi$ electronic transition is shown in Fig. 2. The $\Delta F = \Delta J$ hyperfine components have a Q-branch character, while the $\Delta F \neq \Delta J$ hyperfine components have P- or R-branch character. We have performed OH polarization spectroscopy experiments in atmospheric pressure, near-adiabatic flames in which we have inserted a 1/4-waveplate in the pump beam path to change the polarization of the pump beam from circular to linear in a smooth fashion. The results of spectral scans of the $Q_1(4)$ and $P_{12}(4)$ transitions are shown in Fig. 3. The scans were performed by scanning the wavelength of a frequency-doubled, Nd:YAG-pumped dye laser through the transitions of interest. For the $Q_1(4)$ transition, $\Delta J = 0$, while $\Delta J = -1$ for the $P_{12}(4)$ transition. Consequently the pump polarization dependence of the main branch transition and the satellite transition are quite different. In Fig. 3(a), note that for the case of circular polarization that essentially no PS signal is evident for the $Q_1(4)$ transition. For the saturated conditions shown in Fig. 3(b), however, some signal is evident for the $Q_1(4)$ transition. Our first hypothesis was that this saturated PS signal for the circularly polarized pump was arising from the $\Delta F \neq \Delta J$ hyperfine components. However, we incorporated the hyperfine structure of the resonance into our DNI code and modeled the experiment, as shown in Fig. 4. The appearance of the PS signal for the $Q_1(4)$ resonance under saturation conditions for a circularly polarized pump beam is due to the laser excitation dynamics; as shown in Fig. 1 these dynamics can be quite complicated at high pump intensities. At pump intensities of around 10^{12} W/m², the PS signals for the cases of linearly and circularly polarized pump beams will actually be nearly equal.

C. Infrared Polarization Spectroscopy Measurements of the CO₂ Molecule

We have performed mid-infrared polarization spectroscopy experiments on the CO₂ molecule in Dr. Andrew McIlroy's laboratory at the Combustion Research Facility at Sandia National Laboratories. The experiments were performed using a Continuum Mirage 3000 optical parametric generator to produce single-mode laser radiation at 2700 nm. The experimental line shapes and absolute signal levels have now been compared with the results of numerical calculations. PS spectra were acquired for the P(13) and P(14) lines from pure CO₂ at room temperature and pressure. The calculated line shapes and the experimental line shapes are in excellent agreement. In addition, the calculated strength of the PS signal, normalized by the input intensity of the probe laser beam, agrees with experiment to within a factor of approximately five. The numerical calculations for the P(14) line involve 58 Zeeman states and two bath levels. The excellent agreement between theory and experiment is very encouraging and suggests that the DNI code will be quite valuable for analysis and of infrared polarization spectroscopy signals and for assessment of expected signal-to-noise ratios for proposed experiments.

III. FUTURE WORK

Our investigation of the physics of short-pulse PS will continue; the reduced dependence of the picosecond PS signal on collision rate for both low and high laser intensities is very encouraging. We are presently examining the development of orientation, alignment, and higher order moments of these

quantities in the medium and attempting to relate these quantities directly to the PS signal generation process. We will perform PS measurements in low-pressure flames for comparison with our multi-mode calculations and investigate the potential of two-color PS for sensitive concentration measurements, especially for atomic species. The DNI code will be modified for modeling two-color PS. Further infrared PS experiments in collaboration with Dr. McIlroy at Sandia are planned. We are also collaborating with a group at Lund University on modeling their PS data collected from a low-pressure flame using a multi-mode optical parametric generator, and in modeling ongoing experiments with a new single-mode laser system. We are also in the process of developing our own injection-seeded single-mode OPO laser sources for PS experiments. The generation of DFWM signals from molecules with anisotropic Zeeman state distributions [3] will be investigated theoretically.

IV. REFERENCES

1. S. Roy, R. P. Lucht, and T. A. Reichardt, "Polarization Spectroscopy Using Short-Pulse Lasers: Theoretical Analysis," *Journal of Chemical Physics* **116** (2), 571-580 (2002).
2. T. A. Reichardt, F. Di Teodoro, R. L. Farrow, S. Roy, and R. P. Lucht, *J. of Chem. Phys.* **113**, 2263-2269 (2000).
3. T. Müller, T. A. W. Wasserman, P. H. Vaccaro, and B. R. Johnson **108**, 7713-7738 (1998).

V. BES-SUPPORTED PUBLICATIONS 1999-2001

1. T. A. Reichardt, W. C. Giancola, and R. P. Lucht, "Experimental Investigation of Saturated Polarization Spectroscopy for Quantitative Concentration Measurements," *Applied Optics* **39**, 2002-2008 (2000).
2. W. C. Giancola, T. A. Reichardt, and R. P. Lucht, "Multi-Axial-Mode Laser Effects in Polarization Spectroscopy," *Journal of the Optical Society of America B* **17**, 1781-1794 (2000).
3. T. A. Reichardt, F. Di Teodoro, R. L. Farrow, S. Roy, and R. P. Lucht, "Collisional Dependence of Polarization Spectroscopy with a Picosecond Laser," *Journal of Chemical Physics* **113**, 2263-2269 (2000).
4. J. Walewski, C. F. Kaminski, S. F. Hanna, and R. P. Lucht, "Dependence of Partially Saturated Polarization Spectroscopy Signals on Pump Intensity and Collision Rate," *Physical Review A* **64** (6), 3816-3827 (2001).
5. S. Roy, R. P. Lucht, and T. A. Reichardt, "Polarization Spectroscopy Using Short-Pulse Lasers: Theoretical Analysis," *Journal of Chemical Physics* **116** (2), 571-580 (2002).
6. R. P. Lucht, S. Roy, and T. A. Reichardt, "Polarization Effects in Combustion Diagnostics and Calculation of Radiative Transition Rates," *Progress in Energy and Combustion Science*, submitted for publication (2002).
7. S. Roy, R. P. Lucht, and A. McIlroy, "Mid-Infrared Polarization Spectroscopy of Carbon Dioxide: Experimental and Theoretical Investigation," *Applied Physics B*, submitted for publication (2002).

VI. GRADUATE DISSERTATIONS RESULTING FROM DOE/BES SUPPORT 1999-2001

1. Sukesh Roy, "Laser Diagnostic Investigation of Low-Pressure Diamond-Forming Flames," Ph.D. Thesis, Texas A&M (2002), supported 50% on BES grant.
2. Sherif F. Hanna, "Investigation of Pump Polarization Effects on Polarization Spectroscopy in Atmospheric Pressure Flames," M.S. Thesis, Texas A&M (2001).

Graduate Students Supported at Present Time: Waruna Kulatilaka, Jonathan DuBois

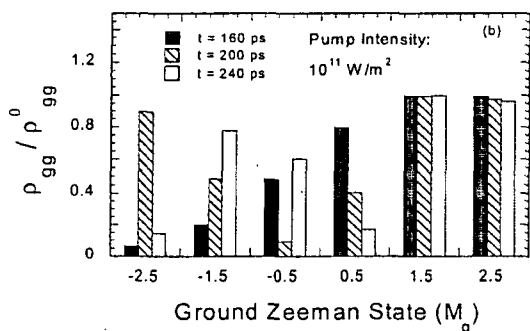
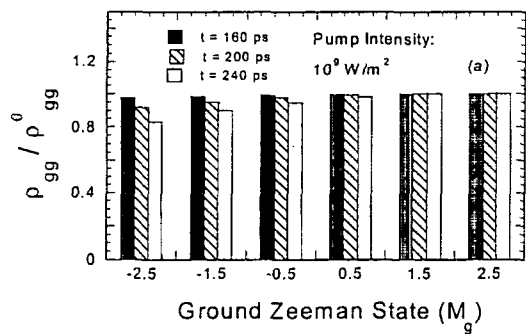
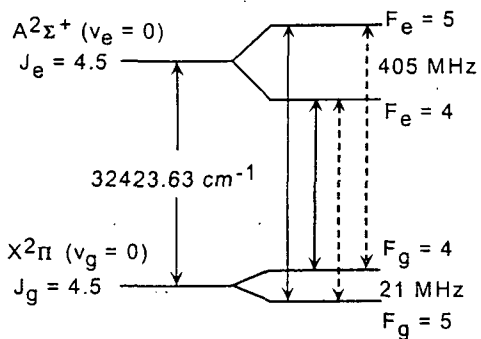


Figure 1. Population of the ground Zeeman states for the $P_1(2)$ resonance for a 100-psec FWHM laser pulse for (a) low pump intensity and (b) high pump intensity. The laser pulse peaks at $t = 200$ ps.



Solid Lines: $\Delta F = \Delta J$
Dashed Lines: $\Delta F \neq \Delta J$

Figure 2. Hyperfine structure of the OH $Q_1(4)$ line.

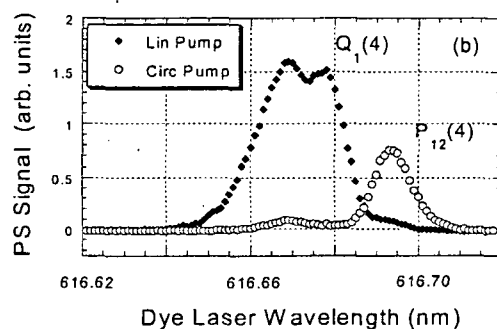
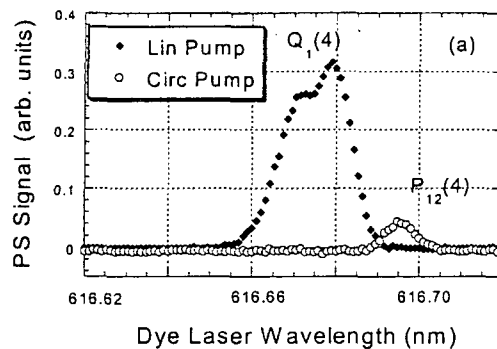


Figure 3. PS signals obtained for linearly polarized pump and circularly polarized pump under conditions of (a) low pump intensity and (b) high pump intensity. The $Q_1(4)$ and $P_{12}(4)$ transitions were probed.

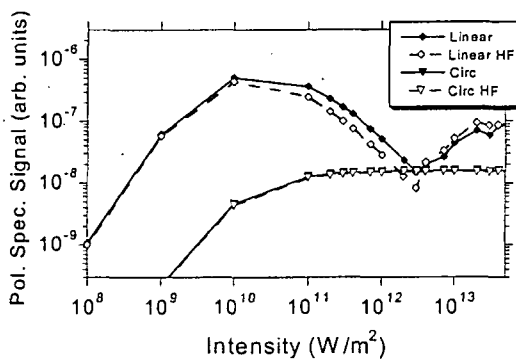


Figure 4. PS saturation curves for the $Q_1(4)$ resonance for linearly polarized pump and a circularly polarized pump with and without the inclusion of the hyperfine structure.

Time-Resolved Infrared Absorption Studies of the Dynamics of Radical Reactions

R. G. Macdonald
Chemistry Division
Argonne National Laboratory
Argonne, IL 60439
Email: macdonald@anlchm.chm.anl.gov

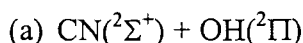
Background

There is very little information available about the dynamics of radical-radical reactions. These processes are important in combustion being chain termination steps as well as processes leading to new molecular species. For almost all radical-radical reactions, multiple product channels are possible, and the determination of product channels will be a central focus of this experimental effort. Two approaches will be taken to study radical-radical reactions. In the first, one of the species of interest will be produced in a microwave discharge flow system with a constant known concentration and the second by pulsed-laser photolysis of a suitable photolyte. The rate constant will be determined under pseudo-first order conditions. In the second approach, both transient species will be produced by the same photolysis laser pulse, and both followed simultaneously using two different continuous-wave laser sources. This approach allows for the direct determination of the second-order rate constant under any concentration conditions if the appropriate absorption cross sections have been measured. In both approaches, the time dependence of individual ro-vibrational states of the reactants and/or products will be followed by frequency- and time-resolved absorption spectroscopy. In order to determine branching ratios and second-order rate constants, it is necessary to measure state-specific absorption coefficients and transition moments of radicals and these measurements will play an important role in this experimental study.

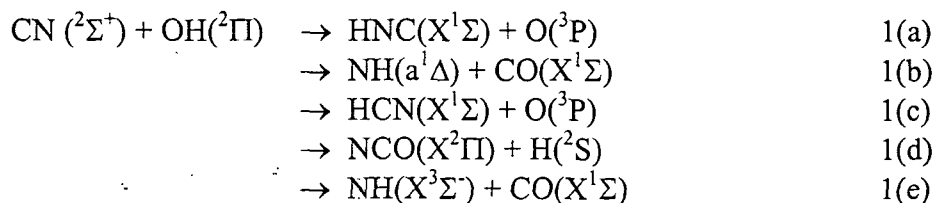
Recent Results

The difficulty in studying radical-radical reactions is the necessity to know the time dependence of the absolute concentration of two transient species. In some cases, it may be possible to make measurements in environments where the concentration of one species is in great excess over the other, and its absolute concentration established. These circumstances result in pseudo first-order conditions, and only the time dependence of the radical with the smaller concentration need be determined, not its absolute concentration. However, such conditions are difficult to generate in practice because of the reactive nature of radicals and self-radical-radical recombination.

In the current work, the above difficulty was eliminated by simultaneously monitoring the time dependence of the absolute concentration of two radical species using state-specific time-resolved absorption spectroscopy. These experiments also illustrate the utility of the time-resolved absorption technique, and the power of infrared spectroscopy to probe a variety of molecular and/or transient species at the individual ro-vibration state level of detail.



The key process in NO_x production in combustion is the breaking of the CN triple bond. In both the prompt NO and the fuel-fixed nitrogen mechanism for NO_x production, the $\text{CN}(^2\Sigma^+) + \text{OH}(^2\Pi)$ radical-radical reaction can be a limiting step in this process at high temperatures and rich flames. This reaction exemplifies all of the possible features of radical-radical reactions: multiple potential energy surfaces, multiple spin manifolds and multiple product channels. In C_s geometry, there are only two electronic surfaces that correlate with the reactants in each of the singlet and triplet manifolds, i.e. $^1A'$ and $^1A''$ and $^3A'$ and $^3A''$. Neglecting stabilization products, there are five possible exothermic product channels, in increasing exothermicity:



Some of these product channels involve either the singlet (1(b) and 1(d)), triplet (1(a), 1(c), 1(d) and 1(e)) or both 1(d) manifolds. There has been no previous direct measurement of the thermal rate constant or a determination of the product branching ratios.

Time-resolved absorption spectroscopy was used to monitor the reactants, CN and OH, as well as a transient species from each of the possible product channels. The CN radical was monitored in the CN "Red" system using the $\text{CN}(A^2\Pi \leftarrow X^2\Sigma)(2,0)$ band at 790 nm, while the other species OH, HNC, NH, HCN, and NCO were monitored in the infrared using a tunable infrared laser. The CN radical was generated by the excimer laser photolysis of $(\text{CN})_2$ at 193 nm and the OH radical from the reaction of O^1D with either H_2 or H_2O . The latter source of the OH radical has several advantages: there is very little generation of HCN from the slow $\text{CN} + \text{H}_2\text{O}$ reaction and there is much less vibrational excitation in the OH reactant. Initial radical concentrations were in the range 3×10^{12} to 2×10^{13} molecules cm^{-3} . The experiments were carried out at a total pressure of 3 - 6 Torr.

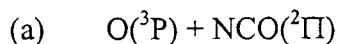
The time dependences of $[\text{CN}]$ and $[\text{OH}]$ were measured simultaneously on the same photolysis laser pulse. The rate constant for reaction 1, $k_{\text{CN}+\text{OH}}$, was determined using an integrated profiles method suggested by Yamasaki and coworkers.¹ The removal of CN is dominated by the reaction with OH, as illustrated in Figure 1; thus, the rate equation describing the time dependence of $[\text{CN}]$ can be written as the removal by second, reaction 1, and first order processes, k_{1st} , and directly integrated using the experimentally determined concentration profiles for CN and OH giving:

$$[\text{CN}]_t - [\text{CN}]_0 = k_{\text{CN}+\text{OH}} \int_0^t [\text{CN}][\text{OH}] dt - k_{1st} \int_0^t [\text{CN}] dt.$$

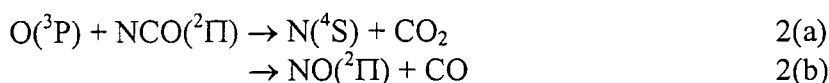
The left and right hand sides were evaluated at various time intervals and a multi-linear regression analysis determined $k_{\text{CN}+\text{OH}}$ and k_{1st} directly using the experimental concentration profiles. The $k_{\text{CN}+\text{OH}}$ evaluated by the integrated profiles method were in good agreement with those determined using a detailed kinetic model to simulate the

[CN] profiles. The directly measured rate constant at room temperature is in reasonable accord (a factor of two) with the inferred rate constant at 2000 K used in modeling studies.

Four of the five product channels have been observed with channel (b) not being detected. The NCO + H channel, (d) dominates the product channels with about 90% of the reaction leading to these products. (This was also the inferred product at high temperatures in modeling studies.) To determine the exact product channel distribution several reaction rate constants will need to be determined, namely the rate constant for NCO + O and NCO + N₂O, these measurements are currently being carried out.



The atom-radical reaction, $O(^3P) + NCO(^2\Pi)$, has two possible reaction channels



The complexity of the multiple potential energy surface nature of radical-radical interactions becomes much larger for this system as the reactants correlate, in C_s symmetry, to 3A' and 3A'' electronic surfaces each in a doublet or quartet spin manifold. The likely product channel, 2(b), only correlates to ²A' and ²A'' surfaces. Equal concentrations of [O] and [NCO] were created by the photolysis of (CN)₂ and the subsequent rapid reaction of CN + O₂ to generate O and NCO. The time dependence of the absolute [NCO] was followed using the infrared combination (10⁰1) ← (00⁰0) band. To investigate three body effects, the reaction was studied with Ar and CF₄ as a bath gas over a modest pressure range of 1 – 4 Torr. The rate constant was found to be large 2.4 x 10⁻¹⁰ cm³ molecule⁻¹s⁻¹ in CF₄ and slightly smaller in Ar. The rate constant was determined using a model to simulate the [NCO] profiles. A reaction-contribution-factor analysis showed that the O + NCO reaction accounted for over 80% removal of NCO.

Future Work

The study of the CN + OH reaction is proceeding on several fronts, namely the final branching ratio measurements are waiting for the determination of the NCO + N₂O reaction rate constant. The measurements on the CN + OH system will be extended to higher temperatures. In addition, theoretical studies of the CN + OH reaction (see the abstract of A. Wagner) are being planned.

The experimental techniques used here can be applied to reactions with reactants or products with one or two heavy atoms (C, O, N) with any additional atoms being H. Studies involving the reactions of small hydrocarbon radicals (methyl and vinyl) are being investigated.

References

1)K. Yamasaki, A. Watanabe, T. Kakuda, and I. Tokue, , J. Phys. Chem. 104A, 9081 (2000).

Publications 2000-2002.

Rotational and vibrational state distribution of HNC(0v0) from the hot H atom reaction: H + (CN)₂ → HNC + CN.

-R. G. Macdonald

J. Phys. Chem. 104A, 10202-10211, (2000).

Determination of the branching ratios for the reaction of hot H atoms with BrCN and ClCN.

-B. K. Decker, G. He, I. Tokue, and R. G. Macdonald

J. Phys. Chem. 105A, 5759-5767, (2001).

Channeling of products in the hot atom reaction: $H + (CN)_2 \rightarrow HCN/HNC + CN$, and the reaction of CN with CH_3SH .

-B. K. Decker and R. G. Macdonald

J. Phys. Chem. 105A, 6817-6825, (2001)

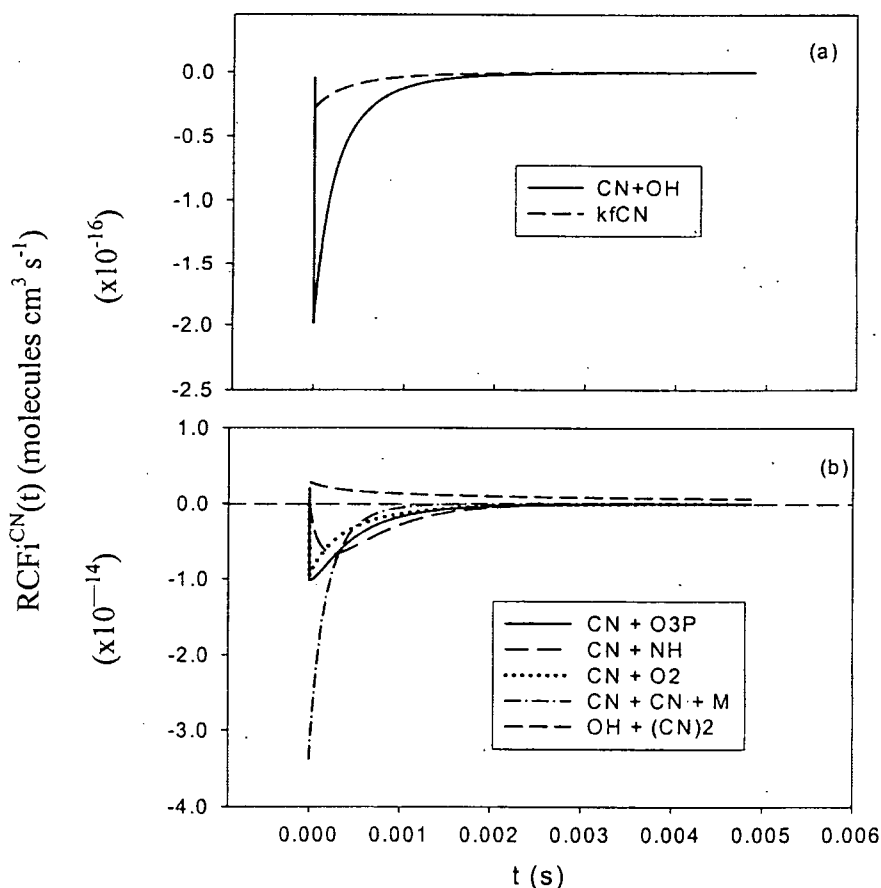


Figure 1. Reaction-contribution-factors, $RCF_i^{CN}(t)$, for the CN radical removal rate processes for a typical experiment. The reaction-contribution factor gives the time dependent flux of molecules for the removal (negative) or production (positive) for a given species (CN) by other species (i) in the system. The RCF for any first order loss process is given by k_{fCN} in (a) and for minor processes in (b). $RCF_i^{CN}(t)$ for the $CN + OH$ reaction is two-orders of magnitude larger than for any reaction, indicating that the $CN + OH$ reaction dominates the CN decay and is shown separately in (a). The initial experimental conditions were: $[CN]_0 = 7.5 \times 10^{12}$, $[OH]_0 = 1.24 \times 10^{13}$, $[(CN)_2] = 2.68 \times 10^{15}$, $[N_2O] = 1.01 \times 10^{16}$, $[H_2O] = 1.53 \times 10^{16}$, and $[Ar] = 1.11 \times 10^{17}$.

Flame Chemistry and Diagnostics

Andrew McIlroy
Combustion Research Facility
Sandia National Laboratories, MS 9055
Livermore, CA 94551-0969
Phone: (925) 294-3054
Email: amcrlr@sandia.gov

Program Scope

The goal of this program is to elucidate the chemical mechanisms of combustion through a combination of experiments based on state-of-the-art diagnostics and detailed chemical kinetic modeling. The experimental program concentrates on the development and application of combustion diagnostics for the measurement of key chemical species concentrations. Although much work has been done to develop diagnostics for combustion species, many common radicals such as CH_3 and CH_2 remain challenging to study on a routine basis and many larger radicals remain difficult to detect at all. Comparison of experimental data to models employing detailed chemical kinetics allows us to determine the important chemical kinetic pathways for combustion, to test the accuracy of published models, and to develop new models. For the development and validation of chemical kinetic models, low pressure, one-dimensional laminar flames are studied. Transport issues are minimized in this configuration and well-developed models including detailed chemical kinetics, such as the Sandia PREMIX code, are available. As turbulent combustion models become increasingly sophisticated, accurate chemical kinetic mechanisms will play a larger role in computations of realistic combustion systems. Validated and well-characterized models will be required as inputs to these reactive flow codes. Only after rigorous comparisons of calculated and experimental results for a given chemical kinetic flame model over a wide range of steady conditions can these models be used with any confidence in turbulent codes. Recent studies of transiently strained flame structure indicate that even this stringent level of validation may be insufficient^{1,2}.

Recent Progress

Recently, we have carried out work in several general areas: the development and application of new laser and mass spectrometer diagnostics, and the testing of chemical kinetic models of combustion by careful measurements of stable species and radical intermediates. This work is briefly summarized below.

In collaboration with Prof. Terry Cool of Cornell University and Prof. Phil Westmoreland of the University of Massachusetts, we have constructed a low-pressure flame, molecular beam sampling mass spectrometer system at the Lawrence Berkeley National Laboratory Advanced Light Source (ALS) Chemical Dynamics Beamline. The new instrument takes advantage of the high VUV photon flux and wide tunability available at the ALS to extend photoionization mass spectrometry (PIMS) methods developed at Cornell and the CRF. Construction of the new instrument was completed this last year and initial data on ethylene flames has been collected. We have demonstrated the sufficient sensitivity to detect radicals generated in flames with only a few minutes of signal averaging. Our 1.3 m flight tube is providing unit mass resolution to ~300

amu. We expect significant improvements in sensitivity as detection methods are optimized in the next few months.

Although the molecular beam (MB) method is often used to study the structure of low-pressure flames, typically combined with mass spectrometric (MS) detection, it is poorly characterized. The temperature of the MB must be known especially if species concentrations are to be measured with spectroscopic methods, such as resonance enhanced multiphoton ionization spectroscopy (REMPI). In collaboration with Burak Atakan and coworkers at the University of Bielefeld, two independent MBMS instruments, which are very similar to those used previously by different groups, were investigated starting with pressures of 40 and 50 mbar in the burner chamber. The rotational temperatures of NO and benzene were determined using REMPI spectroscopy for different initial conditions, the ions were separated by time-of-flight mass spectrometers. Two REMPI excitation schemes were applied, for NO the first step always being the excitation of the A-X transition near 225 nm, while benzene was excited and ionized at wavelengths near 259 nm. Unexpectedly, molecular beams from cold gas flows were cooled very slightly by 10-25%. In the molecular beams derived from low-pressure flames, the cooling effect was stronger, with final temperatures of 300-400 K, but the MB temperature was virtually independent of the initial temperature. A possible explanation of this finding would be, that the cooling takes to a large extent by wall collisions within the nozzle and to a lesser degree by intermolecular collisions.

While the propargyl radical recombination reaction has been identified as the primary pathway to benzene from C1-C3 fuels³, the reaction pathways of larger fuels remain unclear. In particular, the importance of benzene formation from acetylene addition to C4 radicals is uncertain. We are continuing a study of 1,3-butadiene combustion in doped H₂/O₂/Ar flames with the goal of understanding the mechanism of benzene ring formation from this prototype C4 fuel. Electron impact mass spectrometer and PIMS data have been collected for two candidate flames at several ionization energies. Temperature and OH concentration profiles have been measured by OH laser-induced fluorescence. Benzene and toluene formation have been observed in the mass spectra from both flames. In addition, signals have been tentatively identified for several C3, C4, and C5 radicals, including signals likely from propargyl and cyclopentadienyl radicals. The mass spectra reveal the presence of oxygenated species, not in current models. More detailed studies of individual species ionization energies are required for positive identification of these flame species. We will then be able to make meaningful comparisons to detailed chemical kinetic models of molecular weight growth in flames also being developed by Miller and coworkers at Sandia.

Our cavity ringdown spectroscopy (CRDS) studies of radical intermediates in combustion have been quite successful, but the future development of this technique is hampered by several factors. Most significantly, the current sensitivity is limited by the presence of uncorrelated baseline noise, which is believed to be due to scattering in the flame. An additional problem is the limited dynamic range when using medium resolution pulsed dye lasers due to multi-exponential decays present on strong transition, such as those of OH and CH. We have undertaken a program to develop new combustion diagnostics utilizing recently developed cw laser-based, high sensitivity direct absorption methods. We are developing of a prototype system

to implement the NICE-OHMS and AC cavity ringdown methods developed at JILA by Hall, Ye and coworkers^{4,5}. Both these methods are high resolution, frequency modulated, intracavity absorption techniques that make true differential absorption measurements, directly addressing the weaknesses of pulsed laser CRDS. We have completed construction of the servo locked laser system necessary for these techniques.

We have undertaken a study of the application of infrared (IR) polarization spectroscopy (PS) to combustion diagnostics. Previous laser diagnostic efforts in the IR⁶ have suffered from spectral congestion due to overlapping bands from the many species present in flames. Polarization spectroscopy has the potential to select for study individual branches of a given spectrum, thus reducing spectral congestion⁷⁻⁹. Although polarization spectroscopy has been widely applied in the visible and ultraviolet regions of the spectrum, there have been no previous studies of its utility in the IR. Using cells and cold jets of CO₂, we have begun to assess the performance of IR-PS with the eventual goal of extending this work into a combustion environment. The P(13) and P(14) lines of the (0 0⁰ 0)-(1 0⁰ 1) transition of CO₂ were probed using a single-mode optical parametric generator system at approximately 2.7 μm. The experimental results were compared with the results of the time-dependent density-matrix equations using direct numerical integration. The measured and calculated PS line shapes were in excellent agreement, and the absolute experimental signal level agreed with the theoretical calculation to within a factor of four. This work was performed with Prof. Bob Lucht and his student Sukesh Roy of Texas A&M University.

Future Plans

The flame sampling PIMS systems at Sandia and the LBL/ALS are ideal for studying the formation of soot precursors such as polycyclicaromatic hydrocarbons (PAH), which are easily fragmented by other ionization techniques. In order to investigate the formation of the first aromatic ring in rich combustion, we will continue our studies of several simple unsaturated fuels. Acetylene, ethylene, allene and 1,3-butadiene all provide excellent opportunities to investigate the initial stages of molecular weight growth. Our initial focus is on 1,3-butadiene flames. In collaboration with Cool and Westmoreland, we will investigate several remaining uncertainties in ethylene flames, including the identity of the mass 78 species. GC/MS analysis of rich ethylene flames indicates the presence of at least four species in addition to benzene at mass 78. Benzene, a component of gasoline, is a fuel that readily produces high concentrations of PAHs and soot. It has been used in a number of studies by Howard's group¹⁰⁻¹⁵ and others^{16,17} to investigate the mechanism of formation of PAHs and fullerenes. These fuels have been investigated by traditional sampling EI-Q-MS and in optical studies, however, our new photoionization instrument will be better able to detect many of the low concentration, larger molecular weight species that are not well quantified in these previous studies.

With the development of new high sensitivity absorption diagnostics such as NICE-OHMS and AC-CRDS, we will attempt to detect *in situ* new C₂ and C₃ radicals in flames. Few species with two or more heavy atoms have been directly detected in flames. These species have congested spectra and large partition functions, which hinder their detection by traditional laser spectroscopies. Vinyl and propargyl radicals are of particular interest due to their importance

and ubiquity in hydrocarbon combustion. Neither of these species has been detected previously in flames, except by probe sampling techniques. Detection of C₂ and C₂H will also be pursued.

Recent BES Publications

J. W. Thoman, Jr., A. McIlroy, "Absolute CH concentrations in rich low-pressure methane-oxygen-argon flames via cavity ringdown spectroscopy of the A²Δ-X²Π transition," *Journal of Physical Chemistry A* **104**, 4953 (2000).

A. McIlroy, T. D. Hain, H. A. Michelsen, T. A. Cool, "A laser and molecular beam mass spectrometer study of low-pressure dimethyl ether flames," 28th *International Symposium on Combustion*, 2000, 1647.

H. N. Najm, P. H. Paul, O. M. Knio, A. McIlroy, "A numerical and experimental investigation of premixed methane-air flame transient response," *Combustion and Flame* **125**, 879 (2001).

A. McIlroy and J. B. Jeffries, "Cavity ring-down spectroscopy for concentration measurements," in *Applied Combustion Diagnostic*, Eds. K. Kohse-Hoeinghaus and J. B. Jeffries, Taylor and Francis: London, in press.

M. Shahu, C.-H. Yang, C. D. Pibel, A. McIlroy, C. A. Taatjes and J. B. Halpern "Vinyl radical visible spectroscopy and excited state dynamics," *Journal of Chemical Physics* **116**, 1 (2002)..

Cited References

- (1) Najm, H. N.; Knio, O. M.; Paul, P. H.; Wyckoff, P. S. *Combustion Theory and Modelling* **1999**, *3*, 709-725.
- (2) Najm, H. N.; Paul, P. H.; Knio, O. M.; McIlroy, A. *Combustion and Flame* **2001**, in press.
- (3) Pope, C. J.; Miller, J. A. *Proceedings of the Combustion Institute* **2000**, 28.
- (4) Ye, J.; Ma, L.-S.; Hall, J. L. *Journal Of The Optical Society Of America B-Optical Physics* **1998**, *15*, 6-15.
- (5) Gianfrani, L.; Fox, R. W.; Hollberg, L. *Journal of The Optical Society of America B-Optical Physics* **1999**, *16*, 2247-2254.
- (6) Scherer, J. J.; Aniolek, K. W.; Cernansky, N. P.; Rakestraw, D. J. *Journal of Chemical Physics* **1997**, *107*, 6196-6203.
- (7) Reichardt, T. A.; DiTeodoro, F.; Farrow, R. L.; Roy, S.; Lucht, R. P. *Journal of Chemical Physics* **2000**, *113*, 2263-2269.
- (8) Reichardt, T. A.; Giancola, W. C.; Lucht, R. P. *Applied Optics* **2000**, *39*, 2002-2008.
- (9) Giancola, W. C.; Reichardt, T. A.; Lucht, R. P. *Journal of the Optical Society of America B-Optical Physics* **2000**, *17*, 1781-1794.
- (10) Howard, J. B.; McKinnon, J. T.; Johnson, M. E.; Makarovskiy, Y.; Lafleur, A. L. *Journal of Physical Chemistry* **1992**, *96*, 6657-6662.
- (11) Howard, J. B. *Proceedings of the Combustion Institute* **1992**, *24*, 933-946.
- (12) Pope, C. J.; Howard, J. B. *Proceedings of the Combustion Institute* **1994**, *25*, 671-678.
- (13) Richter, H.; Taghizadeh, K.; Grieco, W. J.; Lafleur, A. L.; Howard, J. B. *Journal of Physical Chemistry* **1996**, *100*, 19603-19610.
- (14) McKinnon, J. T.; Howard, J. B. *Proceedings of the Combustion Institute* **1992**, *24*, 965-971.
- (15) Vaughn, C. B.; Howard, J. B.; Longwell, J. P. *Combustion and Flame* **1991**, *87*, 278-288.
- (16) Bachman, M.; Wiese, W.; Homann, K.-H. *Combustion and Flame* **1995**, *101*, 548-550.
- (17) Smith, R. D.; Johnson, A. L. *Combustion and Flame* **1983**, *51*, 1-22.

FLASH PHOTOLYSIS-SHOCK TUBE STUDIES

Joe V. Michael

Gas Phase Chemical Dynamics Group, Chemistry Division
Argonne National Laboratory, Argonne, IL 60439
e-mail: michael@anlchm.chm.anl.gov

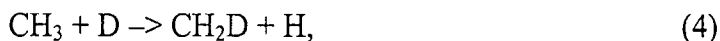
During the past year, rate studies on one unimolecular and several bimolecular reactions have been completed. The ARAS and radical absorption methods were used for detection in reflected shock wave experiments.

The shock tube technique with D-atom atomic resonance absorption spectrometry (ARAS) detection has been used to study the thermal decomposition of C₂D₅I,



over the temperature range, 924-1370 K.¹ The C₂D₅ radicals formed in reaction (1) decompose to give C₂D₄ + D effectively instantaneously on the time scale of the experiment. Hence, absolute [D] formation rates can be used to measure the rate constants for C₂D₅I decomposition. The present experiments are very similar to those already reported from this laboratory for C₂H₅I decomposition.² The first-order rate constant results can be summarized by the Arrhenius equation, $k_{\text{C}_2\text{D}_5\text{I}} = 2.49 \times 10^{10} \exp(-17729 \text{ K}/T) \text{ s}^{-1}$ where $k_{\text{C}_2\text{D}_5\text{I}} = k_1 + k_2$. The branching ratio between product channels, C₂D₅ + I and C₂D₄ + DI, was also determined.

The thermal decomposition results coupled with the fast decomposition of C₂D₅-radicals were then used to prepare [D]. [CH₃]₀ was generated from the concurrent thermal decomposition of CH₃I, and, in subsequent kinetics experiments, D + CH₃ was measured.



Reaction (3) has already been studied in our laboratory.³ Experiments were then performed by observing both absolute [D] depletion and [H] formation. The results were modeled with a thirty-three step mechanism; however, because of the high sensitivity for H- and/or D-detection,⁴ the mechanism could be reduced to effectively four reactions, two of which are known (reactions (1) and (3)) and the other is the reverse of reaction (4). Hence, reaction (-4) is completely specified by k_4 and the calculated equilibrium constant, $K_{4,-4}$.

Within experimental error, the rate constants for reaction (4) were found to be temperature independent with $k_4 = (2.20 \pm 0.22) \times 10^{10} \text{ cm}^3 \text{ molecule}^{-1} \text{ s}^{-1}$ for 1294 $\leq T \leq$ 753 K. The present data have been combined with earlier lower temperature determinations,⁵ and the resultant database has been examined with unimolecular rate

theory. Pressure stabilization was found to be negligible. $k_4 = k_{4\infty} \langle k_{fE} / (k_{fE} + k_{bE}) \rangle = k_{4\infty} F$ from theory. Using the frequencies and structures given in Seakins et al.⁵ and Sutherland et al.⁶ we find $F(300 \text{ K})$ is 0.928 in good agreement with Seakins et al. Klippenstein, Goergievski, and Harding⁷ have also carried out extensive theoretical calculations on reaction (4) and find that F varies from 0.92 to 0.79 over the same T -range. We obtain $F(1800 \text{ K}) = 0.857$. The implications of the present study can be generalized to supply a reliable value for the high-pressure limiting rate constant for methane dissociation.

A sabbatical appointee, Professor Lev N. Krasnoperov from the New Jersey Institute of Technology, visited our laboratory during the past year. We were able to evaluate the feasibility of a novel multi-pass absorption technique in combination with a shock tube for sensitive monitoring of free radical concentrations in high-temperature kinetics studies. This method has been applied for studying several of hydroxyl radical reactions.

The multi-pass cell consists of two dielectric mirrors comprising a stable cavity. Light from a traditional light source (such as Xe or Hg arc lamp, hollow cathode lamp, MW discharge resonance lamp, etc.) is used to monitor the transient absorption of the species inside the cell. The increase in the sensitivity is due to the multiple passes of the photons inside the cell and is controlled by the reflectivities of the mirrors and cell losses (from cell window reflection and/or slight window absorption) at the monitoring wavelength. No coherent effects are involved. The "gain" of the cell is related to the one pass loss by:

$$\text{Gain} = (\text{One Pass Loss})^{-1}. \quad (5)$$

An increase in the sensitivity from 10 to 100 times is easily achieved using inexpensive dielectric mirrors and AR coated windows. This method allows the use of lower initial free radical concentrations, and the elementary reactions of interest can be better isolated.

Hydroxyl radicals were monitored using a MW excited OH resonance lamp selected using a narrow band interference filter. The cell was made of a spherical ($R = 20 \text{ cm}$) and a planar dielectric mirrors (97.67 and 97.10% reflectances). The cell gain was 38 without the windows and 14 with AR coated windows. Single-shot kinetics with the initial concentration of OH-radicals as low as $5 \times 10^{12} \text{ molecule cm}^{-3}$ were recorded. The majority of the measurements were performed with the $[\text{OH}]_0 = 1 \text{ to } 2 \times 10^{13} \text{ molecule cm}^{-3}$.

Several OH-radical sources were investigated, including pyrolyses of $\text{C}_2\text{H}_5/\text{NO}_2$ mixtures, HNO_3 , $(\text{CH}_3)_3\text{COOH}$, and CH_3OH . In the latter cases, both OH and CH_3 are simultaneously produced. The hydroxyl reactions studied were:



The results for reactions (6) and (7) are in good agreement with the literature. The reaction of hydroxyl- with methyl-radicals, reaction (9), was studied in the most detail.

The results are shown in Fig. 1. Reaction of methylene with hydroxyl, reaction (10), is a potential interfering reaction; the rate constant of this reaction was evaluated using

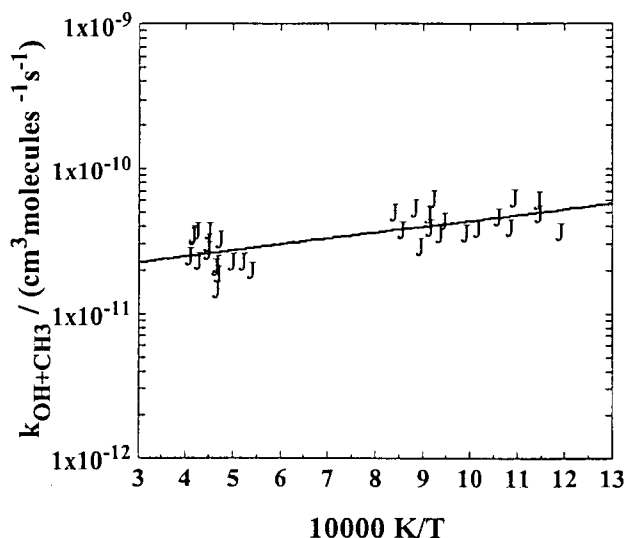


Fig. 1: Arrhenius plot for $\text{CH}_3 + \text{OH}$

ketene as an additional source of methylene.

Additional atom and radical with molecule reaction studies (e. g. Cl + hydrocarbons, OH + hydrocarbons, $\text{CF}_2 + \text{O}_2$, etc.) and, also, thermal decomposition investigations (e. g. C_2H_5 , C_2H_3 , etc.) are in the planning stage at the present time. These reaction studies are of theoretical interest to chemical kinetics and of practical interest in hydrocarbon combustion or waste incineration.

This work was supported by the U. S. Department of Energy, Office of Basic Energy Sciences, Division of Chemical Sciences, under Contract No. W-31-109-ENG-38.

References

1. M.-C. Su and J. V. Michael, Proc. Combust. Inst. **29**, accepted.
2. S. S. Kumaran, M.-C. Su, K. P. Lim, and J. V. Michael, Proc. Combust. Inst. **26**, 605 (1996).
3. S. S. Kumaran, M.-C. Su, and J. V. Michael, Int. J. Chem. Kinet. **29**, 535 (1997).
4. J. V. Michael and Assa Lifshitz, in *Handbook of Shock Waves, Vol. 3*; G. Ben-Dor, O. Igra, T. Elperin, and A. Lifshitz, Eds., Academic Press, New York, 2001, pp. 77-105.
5. P. W. Seakins, S. H. Robertson, M. J. Pilling, D. M. Wardlaw, F. L. Nesbitt, R. P. Thorne, W. A. Payne, and L. J. Stief, J. Phys. Chem. A **101**, 9974 (1997).
6. J. W. Sutherland, M.-C. Su, and J. V. Michael, Int. J. Chem. Kinet., **33**, 669 (2001).
7. S. J. Klippenstein, Y. Goergievski, and L. B. Harding, Proc. Combust. Inst. **29**, accepted

PUBLICATIONS FROM DOE SPONSORED WORK FROM 2000-2002

- *Thermal Rate Constants over Thirty Orders of Magnitude for the $\text{I} + \text{H}_2$ Reaction*, J. V. Michael, S. S. Kumaran, M.-C. Su, and K. P. Lim, Chem. Phys. Lett. **319**, 99 (2000).
- *Photolysis of Ketene at 193 nm and the Rate Constant for $\text{H} + \text{HCCO}$ at 297 K*, G. P. Glass, S. S. Kumaran, and J. V. Michael, J. Phys. Chem. A **104**, 8360 (2000).

- *Reply to comment on "Rate Constants for $\text{CH}_3 + \text{O}_2 \rightleftharpoons \text{CH}_3\text{O} + \text{O}$ at High Temperature and Evidence for $\text{H}_2\text{CO} + \text{O}_2 \rightleftharpoons \text{HCO} + \text{HO}_2$ ", J. V. Michael, S. S. Kumaran, and M.-C. Su, J. Phys. Chem. A **104**, 9800 (2000).*
- *Initiation in H_2/O_2 : Rate Constants for $\text{H}_2 + \text{O}_2 \rightleftharpoons \text{H} + \text{HO}_2$ at High Temperature, J. V. Michael, J. W. Sutherland, L. B. Harding, and A. F. Wagner, Proc. Combust. Inst. **28**, 1471 (2000).*
- *Atomic Resonance Absorption Spectroscopy with Flash or Laser Photolysis in Shock Waves Experiments, J. V. Michael and Assa Lifshitz, in Handbook of Shock Waves, Vol. 3 ; G. Ben-Dor, O. Igra, T. Elperin, and A. Lifshitz, Eds., Academic Press, New York, 2001, pp. 77-105.*
- *Rate Constants for $\text{H} + \text{CH}_4$, $\text{CH}_3 + \text{H}_2$, and CH_4 Dissociation at High Temperature, J. W. Sutherland, M.-C. Su, and J. V. Michael, Int. J. Chem. Kinet., **33**, 669 (2001).*
- *Rate Constants, $1100 \leq T \leq 2000$ K, $\text{H} + \text{NO}_2 \rightleftharpoons \text{OH} + \text{NO}$, Using Two Shock Tube Techniques: Comparison of Theory to Experiment, M.-C. Su, S. S. Kumaran, K. P. Lim, J. V. Michael, A. F. Wagner, L. B. Harding, and D.-C. Fang, J. Phys. Chem. A, in press.*
- *Rate Constants for $\text{H} + \text{O}_2 + \text{M} \rightleftharpoons \text{HO}_2 + \text{M}$ in Seven Bath Gases, J. V. Michael, M.-C. Su, J. W. Sutherland, J. J. Carroll, and A. F. Wagner, J. Phys. Chem. A, in press.*
- *$\text{C}_2\text{D}_5\text{I}$ Dissociation and $\text{D} + \text{CH}_3 \rightleftharpoons \text{CH}_2\text{D} + \text{H}$ at High Temperature: Implications to the High Pressure Rate Constant for CH_4 Dissociation, M.-C. Su and J. V. Michael, Proc. Combust. Inst., accepted.*

Particle Diagnostics Development

H. A. Michelsen

Sandia National Labs, MS 9055, P. O. Box 969, Livermore, CA 94551

hamiche@ca.sandia.gov

1. Program Scope

A growing concern about adverse health, economic, and environmental effects of small particles has prompted strict regulations of fine particulate emissions and has intensified research on the formation and impact of combustion-generated particles. Studies of particle formation, however, are hindered by a lack of sensitive, accurate, noninvasive measurements of particle physical characteristics. Our research program focuses on the development of optical diagnostics for particles, primarily soot particles, in combustion environments. The goal of this work is in situ measurements of volume fraction, size, and morphology of such particles with fast time response and high sensitivity. Combustion-generated soot particles consist of small (5-50 nm diameter) carbon spheroids held firmly together at points of contact to form fractal-like, branched-chain aggregates. Small primary particle sizes and non-spherical aggregate shapes complicate optical schemes for measuring sizes and volume fractions of air-borne particles. Over the past year our research has been aimed at assessing the applicability of laser-induced incandescence (LII) for quantitative volume fraction measurements. This work involves experimental measurements of LII from soot produced in flames combined with the development of a comprehensive model of the response of soot particles to laser irradiation over a wide range of laser fluences.

2a. Recent Progress Related to Particle Diagnostics

LII has been used to make qualitative observations of soot temporal and spatial distributions in engines, engine exhaust, and flames.¹⁻³ This technique involves heating the particles with a laser and measuring the resulting blackbody emission. LII has recently been used to determine soot volume fraction and primary particle size quantitatively.³⁻⁷ Quantitative measurements of volume fraction generally require accurate calibrations,^{3-5,7} and quantitative particle size measurements rely heavily on models of particle cooling rates.^{5,6,8-10} The results appear to be extremely sensitive to measurement conditions (e.g., ambient temperature and pressure, particle composition and morphology, laser beam spatial profile), and the general applicability of the technique has not been demonstrated conclusively. Primary particle sizing is also dependent on the accuracy of LII models, which exhibit large discrepancies with experimental data. The goal of our current project is to develop a detailed understanding of the microphysical mechanisms involved in laser heating and subsequent cooling of particles, which is required for quantitative application of LII to combustion studies.

Our research program combines experimental and modeling studies to develop an accurate description of LII. We have constructed a model that accounts for particle heating by laser absorption and oxidation and cooling by sublimation, conduction, and radiation, includes convective and diffusive heat and mass transfer processes, and incorporates mechanisms for annealing and melting. Recently published experimental data were used to determine the temperature dependence of important parameters included in the model. The most substantial advances in this model over previous models are the inclusion of (1) temperature-dependent thermodynamic parameters for calculating sublimation, conduction, and internal energy storage, (2) wavelength-dependent optical parameters to describe absorption and emission, (3) the introduction of a nonthermal mechanism for evaporative heat and mass loss, (4) the influence of annealing on absorption, emission, and sublimation, and (5) a thermal accommodation coefficient more appropriate for high-temperature conductive cooling. Our goal is to test the model under a wide range of conditions and refine it to the point that it can be used for quantitative analysis of LII signals in a variety of combustion environments.

In our LII experiments the particles are heated with pulses of ~ 7 ns duration (10 Hz) at 532 nm from an injection-seeded Nd:YAG laser. An aperture is placed in the laser beam and imaged into the flame to provide a homogeneous spatial profile. Since LII is extremely nonlinear with laser fluence, a homogeneous beam profile is critical for interpreting the results. The signal is imaged onto a fast Si photodiode and collected between 570 and 1100 nm. We have collected data to fluences as high as 1 J/cm^2 with a temporal resolution of 0.3 ns. We have varied the fuel, burner dimensions, and flow rates to test the sensitivity of the technique to different conditions.

Comparison of the model with these experimental data has provided valuable insight into the sensitivity of LII signals to measurement conditions and has highlighted uncertainties in the model that result from a lack of understanding of the microphysical mechanisms involved in the LII process. In general the model reproduces the steep rise in LII signal as the particles heat and the decay as the particles cool. At fluences below $\sim 0.2 \text{ J/cm}^2$, temperatures increase rapidly during the laser pulse and slowly decay (on microsecond timescales) following the laser pulse. This slow decay is predominantly attributable to conductive cooling. At higher fluences particles quickly reach and surpass the sublimation temperature of $\sim 4000 \text{ K}$, becoming superheated, and then cool rapidly via sublimation back to the sublimation point. Sublimation also causes particles to decrease in size at these higher fluences, whereas at lower temperatures particles swell slightly with increasing temperature as density decreases.

Soot particles have been shown to anneal at temperatures above $\sim 2500 \text{ K}$ into multi-shell carbon onions.^{11,12} These nested fullerene structures can also form during laser heating.¹³ Furthermore, graphite surfaces have been shown to melt at atmospheric pressure when heated rapidly with a laser.¹⁴⁻¹⁷ Changes in the phase of soot primary particles via annealing and melting are likely to influence heating and cooling rates because of differences in physical properties, such as (1) the index of refraction, which controls rates of light absorption and emission, (2) enthalpies and entropies of formation of carbon clusters, which control sublimation rates, and (3) thermal accommodation coefficients, which determine the rate of heat conduction to the ambient atmosphere. Soot annealing rates have not been measured under the conditions encountered during laser heating on nanosecond timescales and are inferred from annealing rates measured on graphite at lower temperatures on longer timescales. At low fluences (temperatures), annealing is associated with di-interstitial migration parallel to the graphite crystallite basal plane and recombination with stationary vacancies.¹⁸ At higher fluences, the shapes and magnitudes of the temporal profiles are strongly influenced by high-temperature annealing processes associated with interstitial and vacancy formation and migration.

Understanding absorption and emission rates is crucial to the analysis of LII signals. There are large uncertainties associated with the wavelength-, temperature-, composition-, and phase-dependence of the optical properties of soot, however, which lead to substantial uncertainties in interpreting LII measurements. The model results incorporate the measured emissivity of unannealed soot with values for the annealed particles based on pyrolytic graphite. As particles anneal, their emissivity and absorptivity decrease, leading to a decrease in LII signal.

The model descriptions of cooling and mass loss by sublimation and photodissociation are the most important terms for calculating the temporal behavior and magnitude of the LII signal at fluences above 0.1 J/cm^2 . This part of the model is also the most complex and, in the case of photodissociation, the most uncertain. Although previous studies have suggested that laser photodesorption of carbon clusters from graphite can proceed by a nonthermal mechanism,¹⁹ the nature of this mechanism, including the number of photons required, is not known. Our model includes such a mechanism with a cross section and enthalpy of reaction approximated by comparing the results with the data. Including the nonthermal photolysis term allows the model to reproduce the lack of fluence dependence of the peak signal at fluences above 0.1 J/cm^2 .

Future work, described below, will include performing experiments under widely varying conditions to test our understanding of LII. We will also perform experiments to narrow some of the uncertainties associated with our description of the response of particles to laser irradiation.

2b. Other BES-Supported Work

The reaction of atomic chlorine with methane has been identified as the mechanism that initiates the production of higher molecular weight hydrocarbons and soot during the combustion of CH_4 in the presence of chlorinated species.²⁰ In addition, the deprotonation of CH_4 by Cl can be used to accelerate the growth of diamond films by chemical vapor deposition.²¹ This reaction also plays a significant role in atmospheric chemistry.^{22,23} Although this reaction has been studied extensively, the thermal rate constants needed for combustion and atmospheric modeling studies are uncertain. We have used a simple model to combine information gained from state-specific cross section experiments of the Cl+ CH_4 reaction to narrow the uncertainties associated with thermal rate constants used in models. This approach provides a means for integrating all available data into a more complete description of this reaction, enabling extrapolation of the measurements to conditions that are difficult to access experimentally. The goal is to combine disparate data sets for practical applications without relying on the development of accurate potential energy surfaces or complex theoretical methodologies.

We have fit the available thermal kinetic data with a model that includes separate terms for the ground state, the excited symmetric and asymmetric stretching modes, and the umbrella bend mode. Each term is derived by calculating the overlap of a Maxwell distribution with a function representing the translational energy dependence of the reaction probability, assumed to be given by the transmission function for tunneling through an asymmetric Eckart barrier with an adjustable barrier and scaling (steric) factor. Each term is weighted by the Boltzmann factor. The results demonstrate that curvature in the Arrhenius plot at temperatures above room temperature can be explained by enhancement of the reaction rate when the symmetric or asymmetric stretch of CH_4 is excited. At low temperatures, the observed curvature can be explained by tunneling and modest reaction-rate enhancement by a low frequency bending mode of CH_4 . An analysis of dynamical and thermal measurements of the kinetic isotope effect for the reaction of Cl with $^{13}\text{CH}_4$, $^{12}\text{CH}_3\text{D}$, $^{12}\text{CH}_2\text{D}_2$, $^{12}\text{CHD}_3$, and $^{12}\text{CD}_4$ indicates that tunneling enhances the reaction probability of hydrogen-atom abstraction by partially relaxing the steric restrictions for the collinear geometry of the transition state. This analysis provides a prediction of rate constants at combustion temperatures for which measurements are not currently available.

3. Future plans

1. Our next set of experiments will use a longer wavelength (1064 nm instead of 532 nm) to heat the particles. Heating the particles with IR light will give us more information about the wavelength response of the nonthermal sublimation component. Our data are consistent with a mechanism that requires at least two photons at 532 nm and is likely to require more photons at 1064 nm.

2. We are currently using a laser with a pulse duration of ~ 7 nanoseconds. We will further test our understanding of the high temperature physics and chemistry of soot particles by using a laser with a significantly shorter pulse duration (115 picoseconds). This set of experiments will allow us to isolate mechanisms that take place on short timescales (e.g., absorption, nonthermal photolytic desorption) from processes that are predicted to evolve over longer (nanosecond) timescales (e.g., thermal sublimation, annealing).

3. In the experiments described above we collected broadband LII signal. We have purchased a spectrometer with a gatable array detector, which will allow us to record time-resolved emission spectra during and after the laser pulse. Temperatures will be inferred from these spectra using the Planck function with a gray-body assumption and compared with model-predicted temperatures.

4. We are in the process of designing a soot source that will extract soot from a flame and cool it before heating it with the laser. A Scanning Mobility Particle Sizer (SMPS) will be attached to the source for measuring aggregate size distributions. We will use the new source to investigate the sensitivity of the LII temporal profiles to the initial and ambient temperatures and aggregate size.

5. If LII proves to be applicable over a wide range of combustion conditions, this work will be extended to include investigations of the utility of combining LII with other optical techniques, such as laser-light scattering (LLS) in which light elastically scattered from the sample is measured at one or more angles and multipass extinction.

4. References

1. Dec, J. E.; zur Loye, A. O.; Siebers, D. L. *Proc. SAE* **1991**, SAE Paper No. 910224.
2. Tait, N. P.; Greenhalgh, D. A. *Ber. Bunsenges. Phys. Chem.* **1993**, *97*, 1619.
3. Vander Wal, R. L.; Dietrich, D. L. *Appl. Opt.* **1995**, *34*, 1103.
4. Ni, T.; Pinson, J. A.; Gupta, S.; Santoro, R. J. *Appl. Opt.* **1995**, *34*, 7083.
5. Mewes, B.; Seitzman, J. M. *Appl. Opt.* **1997**, *36*, 709.
6. Roth, P.; Filippov, A. V. *J. Aerosol Sci.* **1996**, *27*, 95.
7. Shaddix, C. R.; Smyth, K. C. *Comb. Flame* **1996**, *107*, 418.
8. Will, S.; Schraml, S.; Leipertz, A. *Opt. Lett.* **1995**, *20*, 2342.
9. Schraml, S.; Dankers, S.; Bader, K.; Will, S.; Leipertz, A. *Comb. Flame* **2000**, *120*, 439.
10. Smallwood, G. J.; Snelling, D.; Liu, F.; Gülder, Ö. L. *J. Heat Transf., Trans. ASME* **2001**, *123*, 814.
11. Bacsa, W. S.; de Heer, W. A.; Ugarte, D.; Châtelain, A. *Chem. Phys. Lett.* **1993**, *211*, 346.
12. de Heer, W. A.; Ugarte, D. *Chem. Phys. Lett.* **1993**, *207*, 480.
13. Vander Wal, R. L.; Ticich, T. M.; Stephens, A. B. *Appl. Phys. B* **1998**, *67*, 115.
14. Venkatesan, T.; Jacobson, D. C.; Gibson, J. M.; Elman, B. S.; Braunstein, G.; Dresselhaus, M. S.; Dresselhaus, G. *Phys. Rev. Lett.* **1984**, *53*, 360.
15. Heremans, J.; Olk, C. H.; Eesley, G. L.; Steinbeck, J.; Dresselhaus, G. *Phys. Rev. Lett.* **1988**, *60*, 452.
16. Malvezzi, A. M.; Bloembergen, N.; Huang, C. Y. *Phys. Rev. Lett.* **1986**, *57*, 146.
17. Reitze, D. H.; Wang, X.; Ahn, H.; Downer, M. C. *Physical Review B* **1989**, *40*, 11.
18. Banhart, F.; Füller, T.; Redlich, P.; Ajayan, P. M. *Chem. Phys. Lett.* **1997**, *269*, 349.
19. Krajnovich, D. J. *J. Chem. Phys.* **1995**, *102*, 726.
20. Franklach, M. *Comb. Sci. Technol.* **1990**, *74*, 283.
21. Wu, J.-J.; Hong, C.-N. *J. Appl. Phys.* **1997**, *81*, 3647.
22. Solomon, S. *Rev. Geophys.* **1999**, *37*, 275.
23. Keene, W. C.; Jacob, D. J.; Fan, S.-M. *Atmos. Environ.* **1996**, *30*, i.

5. BES peer-reviewed publications

P. O. Witze, S. Hochgreb, D. Kayes, H. A. Michelsen, and C. R. Shaddix, "Time-resolved laser-induced incandescence and laser elastic scattering measurements in a propane diffusion flame", *Appl. Opt.* **40**, 2443-2452 (2001).

H. A. Michelsen, "The reaction of Cl with CH₄: A connection between kinetics and dynamics", *Acc. Chem. Res.* **34**, 331-337 (2001).

H. A. Michelsen, "Carbon and hydrogen kinetic isotope effects for the reaction of Cl with CH₄: Consolidating chemical kinetics and molecular dynamics measurements", *J. Geophys. Res.* **106**, 12,267-12,274 (2001).

H. A. Michelsen and W. R. Simpson, "Relating state-dependent cross sections to non-Arrhenius behavior for the Cl+CH₄ reaction", *J. Phys. Chem. A* **105**, 1476-1488 (2001).

A. McIlroy, T. D. Hain, H. A. Michelsen, and T. A. Cool, "A laser and molecular beam mass spectrometer study of low-pressure dimethyl ether flames", *Twenty-eighth Symposium (International) on Combustion*, (Edinburgh, Scotland, July 30-August 4, 2000) pp. 1647-1653.

Chemical Kinetics and Combustion Modeling

James A. Miller

Combustion Research Facility
Sandia National Laboratories
Livermore, CA 94551-0969
e:mail: jamille@ca.sandia.gov

Program Scope

The goal of this program is to gain qualitative insight into how pollutants are formed in combustion systems and to develop quantitative mathematical models to predict their formation rates. The approach is an integrated one, combining low-pressure flame experiments, chemical kinetics modeling, reaction rate theory, and kinetics experiments (microscopic and macroscopic) to gain as clear a picture as possible of the processes in question. My efforts and those of my collaborators are focused on problems involved with the nitrogen chemistry of combustion systems and the formation of soot and PAH in flames, as well as on general problems in hydrocarbon combustion.

Recent Results

Solution of Some One- and Two-Dimensional Master Equation Models for Thermal Dissociation: The Dissociation of Methane in the Low-Pressure Limit
(with Stephen J. Klippenstein and Christophe Raffy)

Using three formulations of the master equation (ME), we have investigated theoretically the dissociation of methane in the low-pressure limit. The 3 forms of the ME are as follows:

1. A one-dimensional model in which E , the total energy, is the independent variable (the E model)
2. The two-dimensional strong-collision-in-J model of Smith and Gilbert (Int. J. Chem. Kinet. 1998, 20, 307-329) in which ϵ , the energy in the active degrees of freedom, and J , the total angular momentum quantum number, are the independent variables (the ϵ, J model).
3. A two-dimensional variant of the ϵ, J model in which E and J are the independent variables (the E,J model).

The third form of the ME is the most physically realistic, and for this model we have investigated the dependence of values of the energy transfer moments ($\langle \Delta E_d \rangle$, $-\langle \Delta E \rangle$, and $\langle \Delta E^2 \rangle^{1/2}$) deduced from experiment on assumed forms of the energy transfer function, $P(E, E')$, and on temperature. All three moments increase as the temperature rises; $-\langle \Delta E \rangle$ increases from 20-25 cm^{-1} at 300K to 110-120 cm^{-1} at 4000K.

The variation in the energy transfer moments with the form of $P(E, E')$ depends on the particular moment and the temperature, but generally the variation is not greater than 25%. For the same input to the models, the E and E,J models give similar values of the rate coefficient at high temperature, implying that the rotational degrees of freedom behave increasingly as if they are active as temperature is increased. For $T > 3000\text{K}$, the dissociation perturbs the equilibrium energy distribution of the molecule so much that the detailed-balance condition begins to fail, i.e. $k_0(T)/k_r(T) \neq K_{\text{eq}}(T)$, where $k_0(T)$ and $k_r(T)$ are the dissociation and recombination rate coefficients, and $K_{\text{eq}}(T)$ is the equilibrium constant.

*Determining Phenomenological Rate Constants from the
Multiple-Well Master Equation*
(with Stephen J. Klippenstein)

We have developed a method of calculating all the dissociation/recombination and isomerization rate constants on a multiple-well potential energy surface from the eigenvalues and eigenvectors of G , the transition matrix of the master equation. In general, one can write the rate constant for reaction from configuration A to configuration B as

$$k_{AB} = - \sum_{j=1}^{N_{\text{chem}}} \lambda_j \Delta X_{Bj}^{(A)},$$

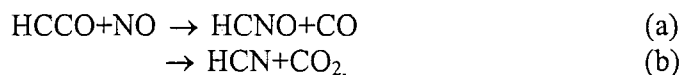
where N_{chem} is the number of chemically significant eigenpairs, λ_j is the j^{th} eigenvalue of G , and $\Delta X_{Bj}^{(A)}$ is the change in population of B that accompanies the time evolution of the j^{th} eigenpair from $t = 0$ to $t = \infty$ when A is the reactant. The quantity $\Delta X_{Bj}^{(A)}$ can be trivially calculated from the eigenvectors of G . We have reanalyzed our previous work on $\text{C}_2\text{H}_3 + \text{C}_2\text{H}_2$ and $\text{C}_3\text{H}_3 + \text{C}_3\text{H}_3$ using this method. A paper on this work is complete and will be submitted for publication shortly.

*An Analysis of Some Chemical Reactions Occurring on the
C₃H₄ Potential Energy Surface*
(with Stephen J. Klippenstein)

We have studied theoretically a number of chemical reactions on the C_3H_4 potential energy surface. This work utilizes the multiple-well master-equation methods described above (and in previous publications) with a potential energy surface based on new QCISD(T) electronic structure calculations complementing the previous work of Klippenstein and Harding on $\text{C}_3\text{H}_3 + \text{H}$. With very modest modifications to 2 isomerization barriers we have been able to predict a wide range of experimental results, including rate constants and product distributions for cyclopropene isomerization to allene and propyne, rate constants for isomerization of allene to propyne and the reverse, and rate constants for allene and propyne dissociation. Our preliminary results indicate that allene dissociates to $\text{C}_3\text{H}_3 + \text{H}$ slightly faster than propyne, in disagreement with conclusions drawn from shock tube experiments. (*J. Phys. Chem. A* **101**, 4057-4071 (1997)). Our preliminary analysis further indicates that the experiments should not be able to detect any difference between the rates of allene and propyne dissociation, because the allene \rightleftharpoons propyne isomerization equilibrates so rapidly that a dissociation experiment can detect only the equilibrated pair dissociating in tandem.

NO_x Reburning
(with Peter Glarborg and Stephen J. Klippenstein)

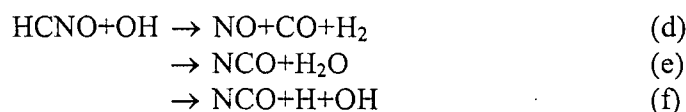
We have made some substantial changes in our NO_x reburn mechanism. These changes were brought about by recent experimental and theoretical work that show that the HCCO+NO reaction,



is dominated by reaction (a) rather than (b). Careful analysis of the consequences of this change forced us to look carefully at the reaction of HCNO with OH, searching for alternatives to the reaction,



We found a number of other energetically accessible products of this reaction, namely



The latter 2 reactions allow the effective removal of NO without the concomitant formation of hydrogen cyanide, a desirable feature for predicting the results of flow reactor experiments on reburning with C₁- and C₂- hydrocarbon fuels. We expect to write a paper on these results within the next year.

Other Work

We have also completed an extensive analysis of the HCCO+O₂ reaction and substantially extended our previous analysis of propargyl recombination. Both of these efforts are in collaboration with Stephen Klippenstein and are discussed in his abstract.

Future Directions

Our work in the next year will largely focus on the cyclization and pre-cyclization chemistry of flames fueled (or partially fueled) by 1, 3 butadiene. This work will involve both theory and modeling and will proceed in parallel with the experiments in Andy McIlroy's lab at Sandia, where he is measuring the structure of a H₂/O₂/Ar-C₄H₆ flame.

We shall also complete our investigation of the C₃H₃+C₃H₃ reaction including a detailed comparison with experiment. Particular issues concerning the nitrogen chemistry of combustion will continue to be of interest, especially those that impact the modeling of NO_x control techniques such as Thermal De-NO_x, RAPRENO_x, and reburning.

Publications of James A. Miller 2000 – Present

S.J. Klippenstein, J.A. Miller, and L.B. Harding, "Resolving the Mystery of Prompt CO₂: The HCCO + O₂ Reaction," *Proceedings of the Combustion Institute* **29**, accepted (2002).

J.A. Miller, S.J. Klippenstein, and C. Raffy "Solution of Some One- and Two-Dimensional Master Equation Models for Thermal Dissociation: The Dissociation of Methane in the Low-Pressure Limit", *J. Phys. Chem. A*, accepted (2002).

J.A. Miller "Concluding Remarks", *Faraday Discussions of the Royal Society of Chemistry* **119**, 461-475 (2001).

J.A. Miller and S.J. Klippenstein, "The Recombination of Propargyl Radicals: Solving the Master Equation," *J. Phys. Chem. A* **105**, 7254-7266 (2001).

J.A. Miller and S.J. Klippenstein, "The Reaction Between Ethyl and Molecular Oxygen II: Further Analysis," *International Journal of Chemical Kinetics* **33**, 654-668 (2001).

D.K. Hahn, S.J. Klippenstein, and J.A. Miller, "A Theoretical Analysis of the Reaction Between Propargyl and Molecular Oxygen," *Faraday Discussions of the Royal Society of Chemistry* **119**, 79-100 (2001).

D.-C. Fang, L.B. Harding, S.J. Klippenstein, and J.A. Miller, "A Direct Transition State Theory Analysis of the Branching in NH₂ + NO," *Faraday Discussions of the Royal Society of Chemistry* **119**, 207-222 (2001).

J.D. DeSain, C.A. Taatjes, D.K. Hahn, J.A. Miller, and S.J. Klippenstein, "Infrared Frequency-Modulation Probing of Product Formation in Alkyl + O₂ Reactions: IV Reactions of Propyl and Butyl Radicals with O₂ between 295 and 750K" *Faraday Discussions of the Royal Society of Chemistry* **119**, 101-120 (2001).

J.A. Miller, S.J. Klippenstein, and S.H. Robertson, "A Theoretical Analysis of the Reaction Between Ethyl and Molecular Oxygen," *Proceedings of the Combustion Institute* **28**, 1479-1486 (2000).

J.A. Miller, S.J. Klippenstein, and S.H. Robertson, "A Theoretical Analysis of the Reaction Between Vinyl and Acetylene: Quantum Chemistry and Solution of the Master Equation," *J. Phys. Chem. A* **104**, 7525-7536 (2000), see also *J. Phys. Chem. A* **104**, 9806 (2000).

C.J. Pope and J.A. Miller, "Exploring Old and New Benzene Formation Pathways in Low-Pressure Premixed Flames of Aliphatic Fuels," *Proceedings of the Combustion Institute* **28**, 1519-1527 (2000).

J.A. Miller and S.J. Klippenstein, "Theoretical Considerations in the NH₂ + NO Reaction" *J. Phys. Chem. A* **104**, 2061-2069 (2000).

Detection and Characterization of Free Radicals Relevant to Combustion Processes

Terry A. Miller
Laser Spectroscopy Facility, Department of Chemistry
The Ohio State University, Columbus OH 43210, email: tamiller+@osu.edu

1 Program Scope

The chemistry of combustion is well-known to be extremely complex. Modern computer codes used to describe this chemistry often employ hundreds of reactions with correspondingly large numbers of chemical intermediates.¹⁻³ In more cases than one would like, the rate constants for these reactions are “estimates” and the intermediates and their concentrations posited but not experimentally verified. While precise measurements of all these quantities is probably an unrealizable goal, the obtainment of experimental values for the benchmarking of computational results will likely remain an important task for the foreseeable future.

Notwithstanding the overall complexity of combustion chemistry, it is reasonable to speak of certain reactions and corresponding intermediates playing particularly important roles under given conditions. In the combustion of hydrocarbons at all temperatures, alkyl radicals are critical intermediates. In the low temperature regime, the alkyl radical ($R\cdot$) reaction,



with the production of peroxy radicals, $RO_2\cdot$, has been termed the single most important step.²

The $RO_2\cdot$ formed in Eq. (1) leads to a complex set of “oxy” radicals. Some, although not all, of the fates of $RO_2\cdot$ include reaction with $R'\cdot$ to form alkoxy radicals, $RO\cdot$, and $R'O\cdot$, and isomerization with internal H atom abstraction to yield a hydroperoxy-alkyl radical, $\cdot QOOH$ which in turn may add O_2 to yield the peroxyalkylhydroperoxide radical, $\cdot O_2QOOH$. Additional reactions involving these radicals (including $HO_2\cdot$) can lead to non-radical species, e.g., olefins, epoxides, etc., which may well subsequently decompose into other radical species.

While the “oxy radicals” are clearly critical intermediates in combustion, very little is known about them experimentally. In particular most of these species lack good spectroscopic identification and analysis. It is one of the principal aims of our work to remedy this inadequacy by obtaining and analyzing representative spectra of these species. The resulting information will fundamentally characterize the radicals’ geometric and electronic structures as well as their spectroscopic response. The data will be used in a benchmark fashion with *ab initio* calculations to iteratively obtain the most comprehensive picture possible of the radical’s characteristics and thermodynamic properties. The results will allow simulation of the radical’s spectrum under a variety of conditions. Such approaches may ultimately lead to detection and concentration-mapping techniques applicable to actual combustion environments. At the least, the assigned spectra provide reliable diagnostics for these radicals in experiments designed to measure their dynamics and reaction kinetics. Indeed we have found in our initial studies of alkoxy radicals that spectroscopy and dynamics are inseparable.

2 Recent Progress

Our DOE support commenced in August, 2001. However, we had performed a variety of work on the peroxy and alkoxy radicals prior to that date which “set the stage” for our present efforts. We will first describe recent aspects of that work and then present our present efforts.

2.1 Alkoxy Radicals

The spectroscopy of the alkoxy radicals began roughly 50 years ago with the observation of the methoxy emission spectrum⁴ and has continued to the present with most recent efforts involving laser induced fluorescence (LIF) observations on its easily accessible near UV transition. Similar LIF studies on the ethoxy^{5,6} and 2-propoxy⁷ radicals have been performed for roughly twenty years now. However until very recently no larger alkoxy radical spectra were known, even though clearly the existence of larger alkanes in conventional fuels, e.g., octane, might have led to the expectation of roles for the corresponding alkoxy radicals, e.g. octoxy, in their combustion.

However, the conventional wisdom with respect to the LIF spectroscopy of larger alkoxy radicals has apparently been that they were unattractive targets, as their quantum yields might well be expected to decrease as non-radiative decay paths became more probable in the larger radicals. Additionally it was expected that even if some LIF spectra were observed, they might well not be very informative because of extreme complexity and congestion.

The first evidence to the contrary came in two recent reports by Dibble and co-workers^{8,9} who searched for LIF spectra from 14 structural isomers of butoxy, pentoxy, and hexoxy. They reported finding structured LIF spectra for 4 of the 14 isomers, which under their experimental conditions were indeed relatively congested. This work, while hardly overturning the existing paradigm, stimulated us to search for LIF spectra of a number of the larger alkoxy radicals under free jet expansion conditions. As is illustrated in Fig. 1, we have now observed¹⁰ the spectra of all the primary alkoxy radicals, $C_nH_{2n+1}O$, with $n \leq 10$. We have also made similar observations for many of the secondary and tertiary structural isomers of the corresponding alkoxy radicals. These results have created a new paradigm which suggests that strong LIF spectral signatures can be expected from any alkoxy radical under favorable conditions.

We have commenced detailed analysis of the spectra shown in Fig. 1. It is important to remember the previously^{4,5,11,12} observed spectra of smaller alkoxy radicals, i.e., methoxy, ethoxy, and 2-propoxy, show strong C-O stretch progressions with >5 members. However for the radicals shown in Fig. 1, no long C-O (or any other) progressions can be identified.

Since most of the lines in Fig. 1 cannot be explained as vibrational progressions, the question of their assignment naturally arises. Detailed rotational analyses¹³ beyond the scope of this project have demonstrated that the observed lines correspond to a number of different conformers of the given structural isomer of the radical "frozen out" in a non-equilibrium distribution in the jet. The assignment of various lines to

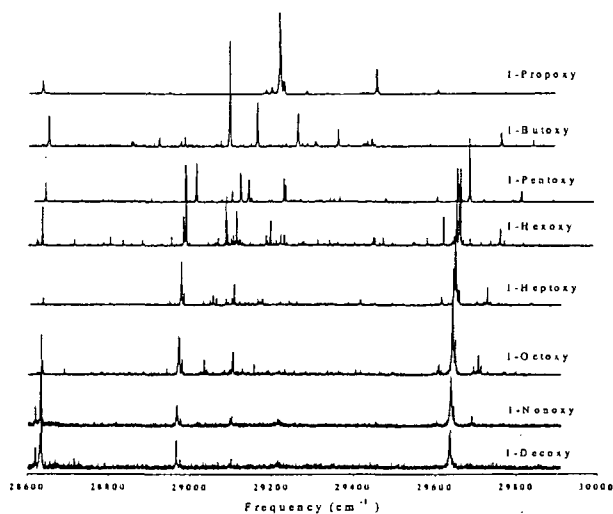


Figure 1: LIF spectra of the primary alkoxy radicals $C_nH_{2n+1}O$ with $n = 3 - 10$ under free jet conditions

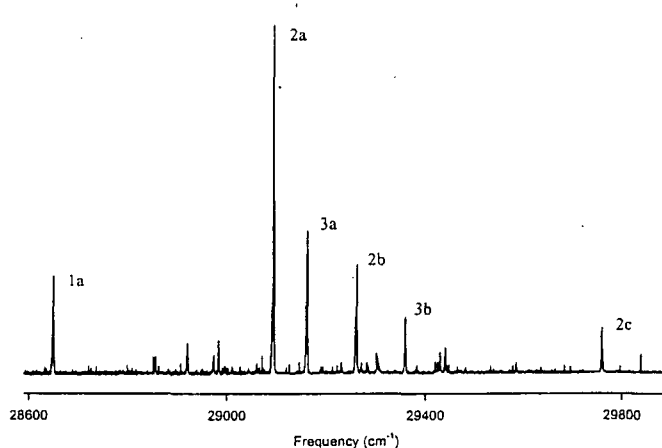


Figure 2: LIF spectrum of the 1-butoxy radical. The origin bands of three different conformers are denoted by the labels 1a, 2a, and 3a with excited vibrational levels being denoted as b, c, etc.

particular conformers is shown in Fig. 2 for the case of 1-butoxy. So far we have identified in Fig. 2, 3 of the 6 conformers of 1-butoxy predicted by *ab initio* calculations. They are a C_s structure (conformer 2); a species (conformer 1) in which the C_s symmetry is removed by having the oxygen-out-of-plane; and finally a species (conformer 3) where the C_s symmetry is removed by the "tail" methyl group being twisted out of plane. Work is presently proceeding to assign as many lines in our observed alkoxy spectra to specific conformers of given structural isomers of $C_nH_{2n+1}O$ as possible.

Since this DOE grant has commenced we have also set up an apparatus capable of resolving the fluorescence from the individual lines in the LIF excitation spectra of Figs. 1 and 2. Such a dispersed fluorescence spectrum from the conformer #1 of 1-butoxy is shown in Fig. 3. The analysis of this data is just beginning, but it is clear from Fig. 3 that the spectrum shows movement from sharp line structure near the origin to a relatively broad and congested spectra at lower frequencies. The energy at which the broadening becomes pronounced is, perhaps coincidentally, very similar to the calculated¹⁴ barrier height for the H atom isomerization that converts the species from an alkoxy to an alkyl radical. We have preliminary data that show the wavelength resolved spectrum for different conformers exhibit fairly significantly different structure. A good deal of additional work will be required to understand these results in detail.

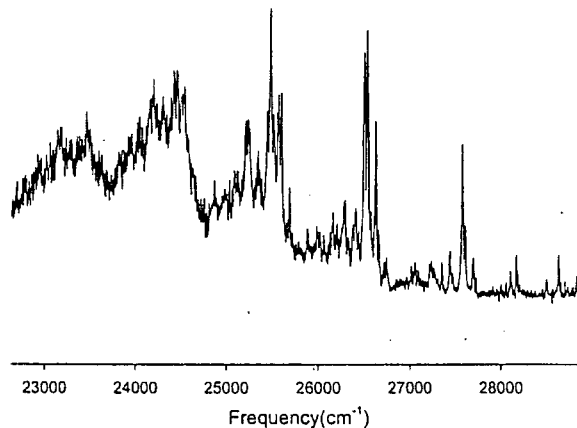


Figure 3: Dispersed fluorescence spectrum of 1-butoxy following excitation of the band marked 1a in Fig. 2

2.2 Peroxy Radicals

While the alkyl peroxy radicals are arguably more important in combustion chemistry, the available spectroscopic information is certainly sparser than for the alkoxy radicals. Historically the only spectroscopic diagnostic of the peroxy radicals has been a broad, unstructured $\tilde{B} - \tilde{X}$ absorption¹⁵ in the UV which does not allow one to distinguish $RO_2\cdot$ from $R'O_2\cdot$. There is a second $\tilde{A} - \tilde{X}$ transition in the near IR, but because it is very weak, very little attention¹⁶ has been given it. Recently we have demonstrated^{17,18} that cavity ringdown spectroscopy (CRDS) can be used to detect alkyl peroxy radicals and give rise to spectra that readily distinguish one alkyl radical from another. Recently we have reported¹⁷ the first CRDS spectra of the $\tilde{A} - \tilde{X}$ transition of CH_3O_2 , $C_2H_5O_2$ and $2-C_3H_7O_2$.

3 Future Plans

For the alkoxy radicals, the observation of LIF excitation spectra that are specific to conformer and structural isomer of a given empirical formula $C_nH_{2n+1}O$ opens the door to a host of future work. On-going efforts to assign specific lines in the observed spectra to individual conformer origins, and excited vibrational levels, will continue. As assignments are made, wavelength resolved emission spectra will be taken for given lines to ascertain the ground state structure and dynamics for the very specifically defined conformer and isomer of a given alkoxy radical.

For the peroxy radicals, efforts are being made to extend the frequency range and sensitivity of our CRDS apparatus. The primary aim of this effort is to detect the $\tilde{A} - \tilde{X}$ transition of other organic peroxy radicals relevant to combustion, e.g., larger alkyl peroxy radicals and/or unsaturated radicals like vinyl or propargyl peroxy.

Acknowledgement We wish to acknowledge the support of the grant DE-FG02-01ER15172 by the Chemical Sciences, Geosciences and Biosciences Division, Office of Basic Energy Sciences, Office of Science, U.S. Department of Energy.

References

- [1] "A Flow Reactor Study of Neopentane Oxidation at 8 Atmospheres: Experiments and Modeling," S. Wang, D. L. Miller, N. P. Cernansky, H. J. Curran, W. J. Pitz, and C. K. Westbrook, *Combustion and Flame* **118**, 415 (1999).
- [2] "A Comprehensive Modeling Study of *n*-Heptane Oxidation," H. J. Curran, P. Gaffuri, W. J. Pitz, and C. K. Westbrook, *Combustion and Flame* **114**, 149 (1998).
- [3] C. K. Westbrook, W. J. Pitz, and W. R. Leppard, *SAE Technical Paper Series* (International Fuels and Lubricants Meeting and Exposition, Toronto, Canada, October 7-10, 1991).
- [4] "Fluorescent Spectra from Ethyl Nitrate. Part 1. - Supposed Emissions from Alkoxy Radicals and NO₂," D. W. G. Style and J. C. Ward, *Trans. Farad. Soc.* **49**, 999 (1953).
- [5] "Laser-Induced Fluorescence of the C₂H₅O Radical," G. Inoue, M. Okuda, and H. Akimoto, *J. Chem. Phys.* **75**, 2060 (1981).
- [6] "Rotationally Resolved Electronic Excitation Spectra of the Ethoxy $\bar{B} \leftarrow \bar{X}$ Transition," X. Q. Tan, J. M. Williamson, S. C. Foster, and T. A. Miller, *J. Phys. Chem.* **97**, 9311 (1993).
- [7] "The Implications of the Rotationally Resolved Spectra of the Alkoxy Radicals for Their Electronic Structure," S. C. Foster, Y.-C. Hsu, C. P. Damo, X. Liu, C.-Y. Kung, and T. A. Miller, *J. Phys. Chem.* **90**, 6766 (1986).
- [8] "Laser-Induced Fluorescence Excitation Spectra of *tert*-Butoxy and 2-Butoxy Radicals," C. Wang, L. G. Shemesh, W. Deng, M. D. Lilien, and T. S. Dibble, *J. Phys. Chem. A* **103**, 8207 (1999).
- [9] "Laser-Induced Fluorescence Spectroscopy of *tert*-Pentoxy and 3-Pentoxy Radicals," C. Wang, W. Deng, L. Shemesh, M. D. Lilien, D. R. Katz, and T. S. Dibble, *J. Phys. Chem. A* **104**, 10368 (2000).
- [10] "Laser Excitation Spectra of Large Alkoxy Radicals Containing 5 to 12 Carbon Atoms," S. Gopalakrishnan, C. C. Carter, J. Atwell, and T. A. Miller, *J. Phys. Chem.* **105**, 2925 (2001).
- [11] "Jet-Cooled Laser Induced Fluorescence Spectroscopy of Some Alkoxy Radicals," C. C. Carter, J. Atwell, S. Gopalakrishnan, and T. A. Miller, *J. Phys. Chem. A* **104**, 9165 (2000).
- [12] "Rovibronic Analysis of Laser Induced Fluorescence Excitation Spectrum of the Jet-Cooled Methoxy Radical," D. E. Powers, M. Pushkarsky, and T. A. Miller, *J. Chem. Phys.* **106**, 6863 (1997).
- [13] "High Resolution LIF Spectroscopy of the 1-Alkoxy Radicals Containing from 3 to 8 Carbon Atoms," S. Gopalakrishnan, C. C. Carter, V. Stakhursky, and T. A. Miller, *J. Chem. Phys.* (to be published).
- [14] "Ab Initio Studies of the Isomerization and Decomposition Reactions of the 1-Butoxy Radical," G. Lendvay and B. Viskolcz, *J. Phys. Chem. A* **102**, 10777 (1998).
- [15] "Organic Peroxy Radicals: Kinetics, Spectroscopy and Tropospheric Chemistry," P. D. Lightfoot, R. A. Cox, J. N. Crowley, M. Destriau, G. D. Hayman, M. E. Jenkin, G. K. Moortgat, and F. Zabel, *Atmos. Environ.* **26A**, 1805 (1992).
- [16] "Electronic Absorption Spectra of Organic Peroxyl Radicals in the Near Infrared," H. E. Hunziker and H. R. Wendt, *J. Chem. Phys.* **64**, 3488 (1976).
- [17] "Detection and Characterization of Alkyl Peroxy Radicals Using Cavity Ringdown Spectroscopy," M. B. Pushkarsky, S. J. Zalyubovsky, and T. A. Miller, *J. Chem. Phys.* **112**, 10695 (2000).
- [18] "Observation of the $\bar{A} - \bar{X}$ Electronic Transition of the CF₃O₂ Radical," S. J. Zalyubovsky, D. Wang, and T. A. Miller, *Chem. Phys. Letts.* **335**, 298 (2001).

Reaction Dynamics in Polyatomic Molecular Systems

William H. Miller

Department of Chemistry, University of California, and
Chemical Sciences Division, Lawrence Berkeley National Laboratory
Berkeley, California 94720-1460
miller@cchem.berkeley.edu

Program Scope or Definition

The goal of this program is the development of theoretical methods and models for describing the dynamics of chemical reactions, with specific interest for application to polyatomic molecular systems of special interest and relevance. There is interest in developing the most rigorous possible theoretical approaches and also in more approximate treatments that are more readily applicable to complex systems.

Recent Progress

Classical molecular dynamics (CMD) simulations (\equiv classical trajectory calculations) are widely used to describe a variety of dynamical processes in complex molecular systems, e.g., chemical reactions rates involving polyatomic molecules. Classical mechanics, of course, cannot describe quantum mechanical effects such as coherence/interference, tunneling, zero-point energy constraints, etc., features that sometimes make significant contributions to the process of interest. The current focus of our research efforts is to develop practical ways for adding quantum effects to CMD by using the initial value representation (IVR) of semiclassical (SC) theory. Ref. 9 gives a comprehensive summary of the theoretical development and surveys numerous recent SC-IVR applications.

For complex molecular systems, the dynamical quantity of interest is typically expressed in terms of a time correlation function of the form

$$C_{AB}(t) = \text{tr} \left[\hat{A} e^{i\hat{H}t/\hbar} \hat{B} e^{-i\hat{H}t/\hbar} \right], \quad (1)$$

where \hat{A} and \hat{B} are hermitian operators depending on the property of interest, and \hat{H} is the Hamiltonian of the system. E.g., the reaction rate for a chemical reaction is the $t \rightarrow \infty$ limit of Eq. (1), where \hat{A} is the Boltmannized-flux operator and \hat{B} a Heaviside function that is 1 (0) on the product reactant side of a dividing surface in configuration space. If, as is often the case, \hat{B} is a local function of the form $B[s(\mathbf{q})]$, then the 'forward-backward' (FB) version of SC-IVR theory (cf. ref. 9) gives the correlation function of Eq. (1) as

$$C_{AB}(t) = (2\pi\hbar)^{-F} \int d\mathbf{p}_0 \int d\mathbf{q}_0 \int dp_s \tilde{B}(p_s) \langle \mathbf{p}_0, \mathbf{q}_0 | \hat{A} | \mathbf{p}_0', \mathbf{q}_0' \rangle C_0(\mathbf{p}_0, \mathbf{q}_0; p_s) e^{iS_0(\mathbf{p}_0, \mathbf{q}_0; p_s)/\hbar}, \quad (2)$$

where $(\mathbf{p}_0, \mathbf{q}_0)$ are the initial conditions for classical trajectories that arrive at phase point $(\mathbf{p}_t, \mathbf{q}_t)$ at time t ; at time t there is a momentum 'jump',

$$\mathbf{p}_t \rightarrow \mathbf{p}_t + p_s \frac{s(\mathbf{q}_t)}{q_t}, \quad (3)$$

and the trajectory is then evolved backward in time to $t = 0$; $(\mathbf{p}_0', \mathbf{q}_0')$ is the final phase point, S_0 the action integral along this FB trajectory, and C_0 a factor involving the derivatives of final values $(\mathbf{p}_0', \mathbf{q}_0')$ with respect to initial ones $(\mathbf{p}_0, \mathbf{q}_0)$. $\tilde{B}(p_s)$ is the Fourier transform of the function $B(s)$, and $|\mathbf{p}_0, \mathbf{q}_0\rangle$ and $|\mathbf{p}_0', \mathbf{q}_0'\rangle$ are coherent states.

An important example of the above methodology is to the calculation of thermal rate constants for

chemical reactions: the rate constant $k(T)$ is given by the long time limit of the flux-side correlation function,¹

$$K(T) = Q_r(T)^{-1} C_{fs}(t \rightarrow \infty), \quad (4)$$

where Q_r is the reactant partition function (per unit volume), and $C_{fs}(t)$ is the correlation function of Eq. (1) with

$$\hat{A} = e^{-\frac{\beta \hat{H}}{2}} \hat{F} e^{-\frac{\beta \hat{H}}{2}}, \quad (5a)$$

$$\hat{B} = h(s(\mathbf{q})) \quad (5b)$$

\hat{F} being the flux operator, $\frac{i}{\hbar} [H, h(s(\mathbf{q}))]$, and $h(s(\mathbf{q}))$ the Heaviside function.

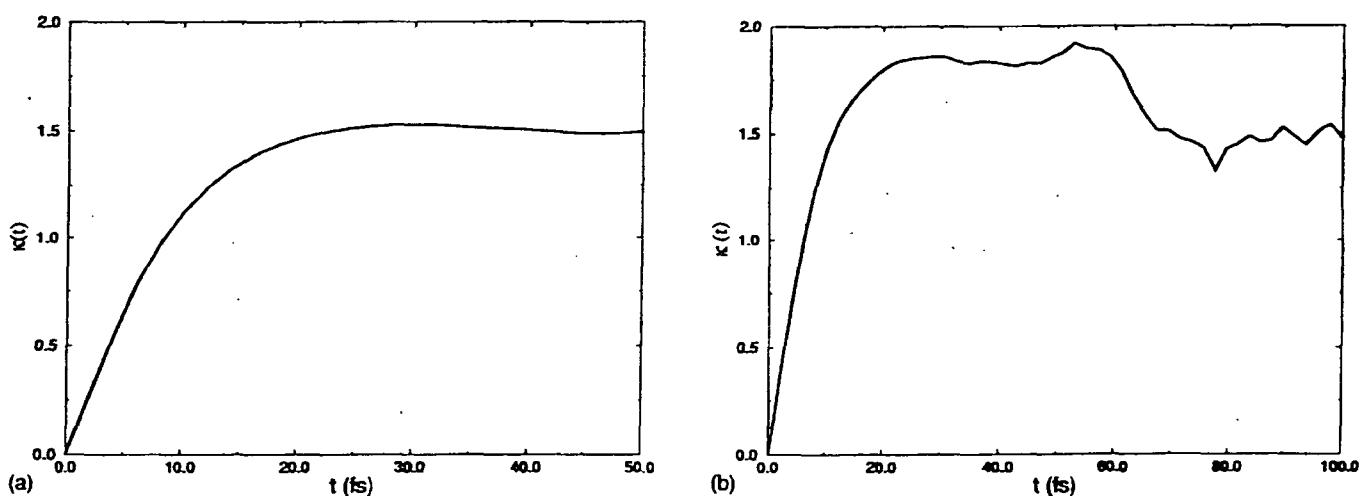
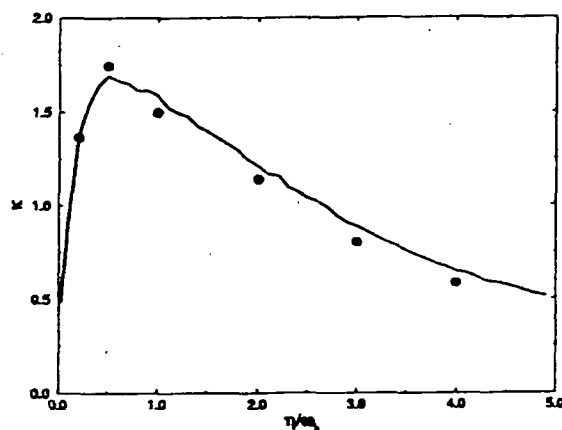


Figure 1. Flux correlation function for two cases at $T = 300$ K: (a) $\eta/\omega_b = 1.0$; (b) $\eta/\omega_b = 0.3$

Figure 2. Transmission coefficient $\kappa = k/k_{TST,CL}$ as a function of coupling parameter η/ω_b at $T = 300$ K; the solid circles are the FB-IVR result, and the solid line is from the accurate quantum path integral calculations, ref. 2.



Figures 1 and 2 show some results from ref. 2, the model system being a double well potential (a model of an isomerization reaction) coupled to a 'bath' of harmonic oscillators (modeling the other degrees of freedom, e.g., in a polyatomic molecule, or solvent degrees of freedom in solution). Figure 1 shows $C_{fs}(t)$ for two different values of the coupling strength (the parameter η); in Figure 1a, the coupling is

sufficiently strong that no re-crossing of the transition state dividing surface takes place, while there is such re-crossing behavior in the weaker coupling of Figure 1b. Figure 2 shows the transmission coefficient (the rate constant with the classical transition state theory value divided out) as a function of coupling strength. It shows the typical 'Kramer's turn-over' behavior, and is in excellent agreement with fully quantum calculations by Topaler and Makri.²

Future Plans

With the validation of the above SC-IVR methodology for non-trivial model problems, work is underway to apply it to real molecular systems, both gas phase reactions and reactions in complex environments.

References

1. W. H. Miller, *J. Chem. Phys.* **61**, 1823 (1974); W. H. Miller S. D. Schwartz and J. W. Tromp, *J. Chem. Phys.* **79**, 4889 (1983).
2. M. Topaler and N. Makri, *J. Chem. Phys.* **101**, 7500 (1994).

2000 - 2002 (to date) DOE Publications

1. W. H. Miller, Using Mechanics in a Quantum Framework: Perspective on "Semiclassical Description of Scattering", *Theo. Chem. Accts.* **103**, 236-237 (2000); LBNL-42905.
2. H. Wang, M. Thoss, and W. H. Miller, Forward-Backward Initial Value Representation for the Calculation of Thermal Rate Constants for Reactions in Complex Molecular Systems, *J. Chem. Phys.* **112**, 47-55 (2000); LBNL-44637.
3. E. A. Coronado, Victor S. Batista, and W. H. Miller, Nonadiabatic Photodissociation Dynamics of *ICN* in the \bar{A} Continuum: A Semiclassical Initial Value Representation Study, *J. Chem. Phys.* **112**, 5566-5575 (2000); LBNL-44723.
4. M. Thoss, W. H. Miller and G. Stock, Semiclassical Description of Nonadiabatic Quantum Dynamics: Application to the S_1 - S_2 Conical Intersection in Pyrazine, *J. Chem. Phys.* **112**, 10282-10292 (2000); LBNL-44877.
5. R. Gelabert, X. Gimenez, M. Thoss, H. Wang and W. H. Miller, A Log-Derivative Formulation of the Prefactor for the Semiclassical Herman-Kluk Propagator, *J. Phys. Chem.* **104**, 10321-10327 (2000); LBNL-45437.
6. V. Guallar, V. S. Batista and W. H. Miller, Semiclassical Molecular Dynamics Simulations of Intramolecular Proton Transfer in Photo-Excited 2-(2'-hydroxyphenyl)-oxazole, *J. Chem. Phys.* **113**, 9510-9522 (2000); LBNL-46405.
7. H. Wang, M. Thoss, K. Sorge, R. Gelabert, X. Gimenez and W. H. Miller, Semiclassical Description of Quantum Coherence Effects and Their Quenching: A Forward-Backward Initial Value Representation Study, *J. Chem. Phys.* **114**, 2562-2571 (2001); LBNL-46836.
8. R. Gelabert, X. Gimenez, M. Thoss, H. Wang and W. H. Miller, Semiclassical Description of Diffraction and Its Quenching by the Forward-Backward Version of the Initial Value Representation, *J. Chem. Phys.* **114**, 2572-2597 (2001); LBNL-46837.
9. W. H. Miller, The Semiclassical Initial Value Representation: A Potentially Practical Way for Adding Quantum Effects to Classical Molecular Dynamics Simulations, *J. Phys. Chem.* **105**, 2942-2955 (2001); LBNL-46935.

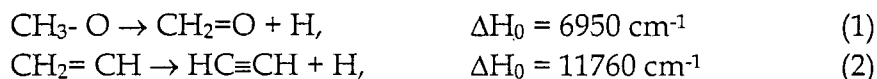
10. M. Thoss, H. Wang and W. H. Miller, "Generalized Forward-Backward Initial Value Representation for the Calculation of Correlation Functions in Complex Systems," *J. Chem. Phys.* **114**, 9220-9235 (2001); LBNL-47268.
11. J. Xing, E. A. Coronado and W. H. Miller, "Some New Classical and Semiclassical Models for Describing Tunneling Processes with Real-Valued Classical Trajectories," *J. Phys. Chem. A* **105**, 6574-6578 (2001); LBNL-47268.
12. H. Wang, M. Thoss and W. H. Miller, "Systematic Convergence in the Dynamical Hybrid Approach for Complex Systems: A Numerically Exact Methodology," *J. Chem. Phys.* **115**, 2979-2990 (2001); LBNL-47557.
13. M. Thoss, H. Wang and W. H. Miller, "Self-Consistent Hybrid Approach for Complex Systems: Application to the Spin-Boson Model with Debye Spectral Density," *J. Chem. Phys.* **115**, 2991-3005 (2001); LBNL-47558.
14. H. Wang, D. E. Manolopoulos and W. H. Miller, "Generalized Filinov Transformation of the Semiclassical Initial Value Representation," *J. Chem. Phys.* 6317-6326 (2001); LBNL-48140.
15. W. H. Miller, "Adding Quantum Effects to Classical Molecular Dynamics Simulations via the Semiclassical Initial Value Representation," *SIMU Newsletter*, Issue 3, 51-62 (2001); LBNL-47984.
16. E. A. Coronado, J. Xing, and W. H. Miller, "Ultrafast Non-Adiabatic Dynamics of Systems with Multiple Surface Crossings: A Test of the Meyer-Miller Hamiltonian with Semiclassical Initial Value Representation Methods," *Chem. Phys. Lett.* **349**, 521-529, (2001); LBNL-47694.
17. W. H. Miller, "Using the Semiclassical Initial Value Representation to Include Quantum Effects in Molecular Dynamics" in Wide-Amplitude Rovibrational Bound States in Polyatomic Molecules, ed. I. N. Kozin, M. M. Law, and J. N. L. Connor, CCP6, Daresbury, UK (2001); LBNL-49021.
18. W. H. Miller, An Alternate Derivation of the Hermann-Kluk (Coherent State) Semiclassical Initial Value Representation of the Time Evolution Operator, *Mol. Phys.* **100**, 397-400 (2002); LBNL-47781.
19. V. Guallar, V. S. Batista, W. H. Miller and D. L. Harris, Proton Transfer Dynamics in the Activation of Cytochrome P450eryF, *J. Am. Chem. Soc.* **124**, 1430-1437 (2002); LBNL-48392.
20. V. Guallar, B. F. Gherman, W. H. Miller, S. J. Lippard and R. A. Friesner, Dynamics of Alkane Hydroxylation at the Non-heme Diiron Center in Methane Monooxygenase, *J. Am. Chem. Soc.* (accepted); LBNL-49467.
21. T. Yamamoto, H. Wang, and W. H. Miller, Combining Semiclassical Time Evolution and Quantum Boltzmann Operator to Evaluate Reactive Flux Correlation Function for Thermal Rate Constants of Complex Systems, *J. Chem. Phys.* (accepted); LBNL-49465.
22. W. H. Miller, On the Relation between the Semiclassical Initial Value Representation and an Exact Quantum Expansion in Time-Dependent Coherent States, *J. Phys. Chem.* (submitted); LBNL-49606.

Unimolecular Reaction Dynamics of Free Radicals*

C. Bradley Moore, Investigator
Department of Chemistry
The Ohio State University
Columbus, OH 43210-1106
moore.1@osu.edu

Program Scope

The fundamental goal of this work is a quantitative understanding of the unimolecular reactions of free radicals. These reactions are of crucial importance in combustion and in atmospheric chemistry. Reliable theoretical models for predicting the rates and products of these reactions are required for modeling combustion and atmospheric chemistry systems. In contrast to the benchmark reactions, $\text{CH}_2\text{CO} \rightarrow {}^{1,3}\text{CH}_2 + \text{CO}$, the reactions of free radicals occur over barriers sufficiently low that the hypothesis of rapid energy randomization upon which statistical transition state theories depend is in doubt. A study of the rates and dynamics of methoxy and vinyl radicals in their ground electronic states is in progress:



These should serve as benchmarks for this important class of reactions. The dissociation of CH_3O has a very low barrier, about $8,000 \text{ cm}^{-1}$. As for many other free radicals, this low barrier results from the simultaneous increase in the bond order of C-O as the C-H bond is broken.

The statistical Transition State Theory (TST), i.e. RRKM and its variants, depends on the basic postulate that complete intramolecular vibrational energy redistribution (IVR) is much faster than the chemical reactions of interest. TSTs give reaction rates that are functions of total energy and angular momentum. While TSTs are consistent with much experimental data and have gained practical importance for computational modeling of complex reaction systems, some small and moderate size molecular systems, e.g., HCO and HF₂CO, are observed to decompose at rates that depend systematically on rovibrational quantum numbers. The dissociation of HCO is quantitatively understood in terms of the coupling of modestly perturbed single quantum states to the H+CO continuum. Lower barriers result in limited IVR due to

* This work was supported by the Director, Office of Energy Research, Office of Basic Energy Sciences, Chemical Sciences Division of the U. S. Department of Energy under Contract No. DE-FG02-02ER15284.

lower vibrational level densities and smaller matrix elements for mode coupling and level mixing at the lower energies.

Methoxy and vinyl will provide benchmark models for unimolecular dynamics in systems that lie between the statistical and single-quantum-state extremes. Other radicals important in combustion and atmospheric chemistry will also be explored including members of the RO₂ family.

The experiments use a wide range of time and wavelength resolved laser spectroscopies. Radicals are produced by laser flash photolysis of precursors in supersonic jets. Products are observed by laser-induced fluorescence and by state-selective Resonance-Enhanced Multiphoton Ionization (REMPI) with velocity map ion imaging. This allows complete spectroscopic study of the radicals including the intramolecular vibrational couplings revealed in the spectra of highly excited ground electronic state rovibrational energy levels.

Decay time and linewidth measurements then give the dissociation rates of well-characterized rovibronic energy levels. Ion imaging and Doppler-resolved REMPI measurements give vector and scalar correlations of the product energy state distributions.

Recent Progress

Electronic Spectroscopy of Jet-Cooled Vinyl Radical

M. B. Pushkarsky, A. M. Mann, J. S. Yeston, and C. B. Moore

The vibrationally resolved spectra of the $\tilde{A}^2A'' \leftarrow \tilde{X}^2A'$ electronic transition of jet-cooled vinyl radical (CH₂CH) and its partially deuterated isotopomer CD₂CH in the range of 443 – 516 nm have been obtained via action spectroscopy.

The appearance of the H or D fragment was monitored via 1+1' REMPI through the Lyman- α transition. The vibrational structure of the \tilde{A}^2A_1 state was resolved and analyzed. About 20 vibrational bands of CH₂CH and 15 vibrational bands of CD₂CH were assigned. The experimental vibrational frequencies agree well with *ab initio* calculations performed using B3LYP/6-311(d)G theory level.

The simulation of the rotational structure of several bands recorded with rotational resolution (0.1 cm⁻¹) reinforces vibrational assignments and exhibits lifetime broadening due to predissociation for both partially deuterated and nondeuterated vinyl radicals in the \tilde{A}^2A'' state. For these bands with resolved rotational structure, the corresponding rate constants of predissociation and their dependence on the type of vibrational mode excited were measured through the spectral lifetime broadening. It was concluded that predissociation proceeds in two steps, rate-limiting internal conversion into highly vibrationally excited levels of the \tilde{X}^2A' ground electronic state followed by dissociation to acetylene (HCCH) and H atom.

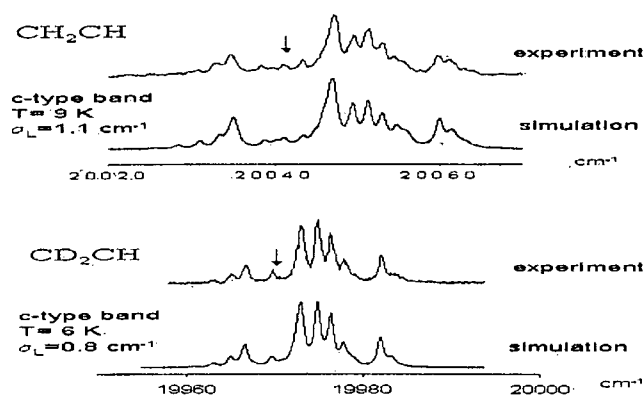


Fig 1. Examples of the experimental and simulated rotationally resolved spectra of the band origins of CH_2CH and CD_2CH radicals. The arrows indicate positions of the origin, T_0 . The component of transition dipole moment, rotational temperature, and Lorentzian linewidth are given for each simulation.

Future Plans

Extensive rotationally resolved Laser Induced Fluorescence (LIF) measurements of the $\tilde{A}^2A' \leftarrow \tilde{X}^2E$ electronic transition of partially deuterated isotopomers CHD_2O and CH_2DO will shed the light on the detailed rotational and vibrational structures of their upper electronic states \tilde{A}^2A' . Based on known spectroscopy of the CH_3O \tilde{A}^2A' upper electronic state Stimulated Emission Pumping (SEP) will be used to selectively prepare the CH_3O radical with the desired type and quantity of vibrational-rotational excitation in the ground CH_3O \tilde{X}^2E electronic state.

Measurements of H^+ and D^+ ion velocity maps to reveal the energy partitioning mechanism between H(D) and acetylene (vinylidene) and their corresponding deuterated isotopomers are in progress.

In a collaboration with Karl Kompa, a Director of the Max Planck Institute for Quantum Optics near Munich, an exploration of the selectivity of femtosecond ir multiphoton dissociation reactions has been initiated. Dr. Jake Yeston from our lab spent the past 6 months in Munich. He participated in a series of experiments on metal carbonyls and initiated studies on diazomethane. Dissociation was induced by single pulses of 100 fs duration and will be reported in the near future.

Publications 2001

1. M.B. Pushkarsky, A.M. Mann, J.S. Yeston, and C.B. Moore, "Electronic Spectroscopy of Jet-Cooled Vinyl Radical," *J. Chem. Phys.* 115, 10738-10744 (2001).

GAS-PHASE MOLECULAR DYNAMICS: THEORETICAL STUDIES OF REACTION DYNAMICS AND SPECTROSCOPY

James T. Muckerman (muckerma@bnl.gov) and Hua-Gen Yu[†] (hgy@bnl.gov)
Chemistry Department, Brookhaven National Laboratory, Upton, NY 11973-5000

Program Scope

This research is carried out as part of the Gas-Phase Molecular Dynamics group program in the Chemistry Department at Brookhaven National Laboratory. The goal is a theoretical description of the spectroscopy of radical species related to combustion, and the energetics, dynamics and kinetics of elementary chemical reactions in which they are involved.

Recent Progress

Near-infrared spectrum of bromomethylene. Experimental work in spectroscopy in our program is complemented by extensive *ab initio* calculations of the electronic potential energy surfaces combined with dynamical solution of the vibrational problem to estimate anharmonic frequencies and vibronic transition moments as an aid to understanding the observed spectra. Calculations on HCB_r were performed using the MOLPRO 2000 program package.¹ The potential energy surfaces for the three electronic states of HCB_r were obtained by performing a CASSCF calculation involving the twelve valence electrons and nine valence orbitals followed by an IC-MRCI calculation² of the three target states at each point of a direct-product discrete-variable representation (DVR) grid in CH–Br Jacobi coordinates. The resulting two singlet surfaces yielded stretching frequencies that were slightly (*ca.* 6.5%) lower than those observed experimentally. The CH and CBr distances were therefore scaled by a common linear scaling factor³ on all three surfaces to achieve better agreement with the experimental stretching frequencies. This scaling preserves the global features of the potential energy surfaces such as the degeneracy of the two singlet surfaces for all linear HCB_r geometries. The three surfaces are shown in Fig. 1 along a cut at the calculated equilibrium value of r_{CH} in the \tilde{X}^1A' state. The T_{00} value for the singlet-to-singlet transition is calculated to be within 500 cm^{-1} of the experimental value. An analysis of our observed bending intervals in the \tilde{A}^1A'' state suggested that the calculated T_{00} value of the triplet state was about 250 cm^{-1} too small. Making this shift and including spin-orbit coupling between the \tilde{X} and \tilde{a} states, the calculations make testable predictions of the position of the triplet and singlet state vibronic levels. Our predicted value of the $\tilde{a} - \tilde{X}$ singlet-triplet splitting is 2028 cm^{-1} . While this work was in progress, Tsai *et al.*⁴ reported wavelength dispersed laser-induced fluorescence spectra of bromomethylene that confirm the conclusions and predictions of our model.

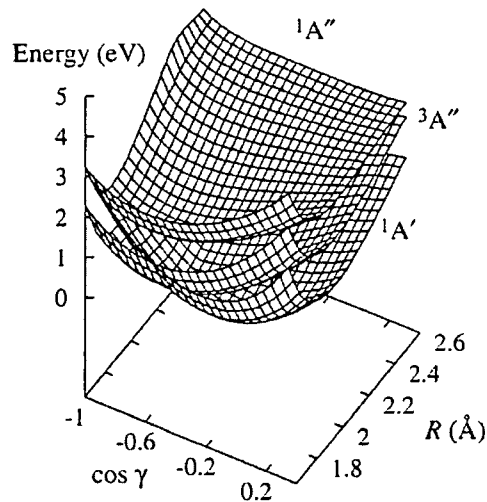


Fig. 1. Potential energy surfaces for the three lowest-lying electronic states of HCB_r from the scaled *ab initio* MRCI calculation with the cc-pVTZ basis described in the text. Here R is the distance from the center of mass of the CH moiety to the Br atom, and γ is the angle between \mathbf{R} and \mathbf{r} , the C-to-H distance. Note the intersection of the X^1A' and a^3A'' surfaces at intermediate values of $\cos \gamma$, and the degeneracy of the two singlet surfaces at all linear configurations ($\cos \gamma = -1$) as the two components of a $^1\Delta$ state.

[†] Gertrude and Maurice Goldhaber distinguished postdoctoral fellow

Potential energy surface for HOCO. Stationary points on the OH + CO potential energy surface were calculated using an extrapolated full-coupled-cluster, complete-basis-set (FCC/CBS) method. The *trans*-HOCO intermediate was found to lie 30.10 kcal/mol below the OH + CO dissociation limit. For the forward reaction, the vibrationally adiabatic ground-state barrier height was predicted to be 1.03 kcal/mol. There is also a van der Waals complex in the OH + CO entrance channel that may play some role in the reaction dynamics. A many-body expansion potential energy surface was obtained by refitting the potential of Schatz *et al.*^{5,6} to the new *ab initio* data. A FORTRAN subroutine for evaluating this potential is available upon request.

Collision dynamics and kinetics of the OH + CO reaction. In collaboration with G. D. Billing (Univ. of Copenhagen), we have employed the quantum dressed classical mechanics (or time-dependent Gauss-

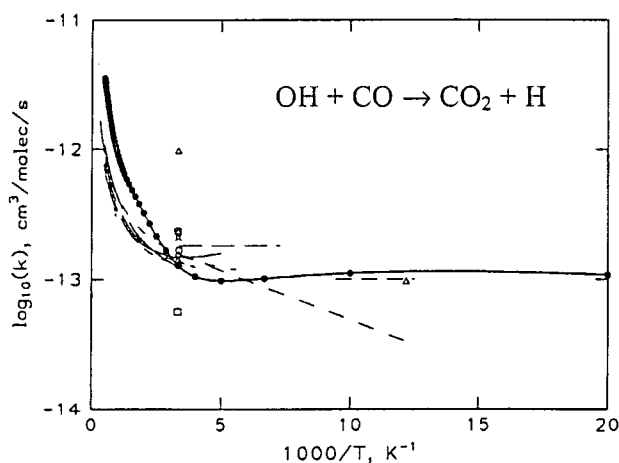


Fig. 2. Temperature dependence of rate constant for the reaction $\text{OH} + \text{CO} \rightarrow \text{CO}_2 + \text{H}$ calculated using the TDGH-DVR method and our fit to stationary points on an *ab initio* potential energy surface (solid line and filled points). Also shown are all the experimental data in the NIST database reported since 1984 (dashed lines and open symbols).

Hermite discrete variable representation, TDGH) method⁷ to calculate the energy dependent cross section and temperature dependent rate constant for the OH + CO reaction on the many-body expansion potential energy surface described above. Only the OH and CO bond distances were treated with more than one grid point; the single grid point used for the remaining four coordinates amounts to treating them with classical mechanics. We used 129 points along the OH coordinate and 21 points along the CO coordinate. In all, over 3000 trajectories were computed of which only a small fraction (*ca.* 20) were classically reactive. The reaction probability was computed from the amplitude of the wavefunction at grid points with the OH distance larger than 2.9 Å. Tunneling in the OH coordinate makes a significant contribution to the overall reactivity. The

lowest-energy trajectories are important in determining the rate constant in the 50 to 100 K range, but have long lifetimes (several ps) and require a large amount of cpu time to compute. This consideration limits the accuracy of the computed rate constant, shown in Fig. 2, at 50 K (estimated error 50-100%) compared to that above 100 K (estimated error 20-30%). The calculated rate constant is seen to exhibit a strongly non-Arrhenius behavior, being almost constant at low temperature.

Photoinduced unimolecular dissociation of *trans*-HOCO. To further test the features of our HOCO potential energy surface, the quantum dissociation dynamics of HOCO photoexcited to the $\nu_{\text{OH}} = 3$ overtone have been studied using a time-dependent wavepacket approach. The dynamics calculations were carried out using a four-dimensional planar model in which the terminal C=O bond is treated as a spectator and fixed at its equilibrium geometry in the *trans* conformer on our potential surface. The branching fraction into $\text{H} + \text{CO}_2$ and $\text{OH} + \text{CO}$ products, and the resonance states associated with the $\nu_{\text{OH}} = 3$ overtone were investigated in detail.

The initial wavepacket, prepared as a separable product of a $\nu = 3$ wavefunction in the OH coordinate and a 3D ground-state wavefunction in the remaining coordinates, was found to be dominated by three

resonance states: $(\nu_{\text{OH}}, \nu_{\text{CO}}, \nu_{\text{HOC}}, \nu_{\text{CO}}) = (3,0,0,0)$, $(3,1,0,0)$ and $(3,0,0,1)$. The time-integrated probabilities for dissociation into the two energetically allowed product channels are shown in Fig. 3. Also shown is the time dependence of the branching fraction into the H + CO₂ products. At short times (less than 120 fs) the molecule dissociates almost exclusively into the H + CO₂ products owing to rapid H atom escape. At long times, however, the branching fraction falls to 0.26. This is consistent with *trans*-HOCO having a slightly lower barrier to form the OH + CO products than to form H + CO₂ on our potential energy surface even though the latter products are energetically favored. The lifetimes of the $(3,0,0,0)$, $(3,1,0,0)$ and $(3,0,0,1)$ resonances are 3.05, 1.38 and 0.94 ps, respectively. Their branching fractions are 0.33, 0.14 and 0.12, respectively.

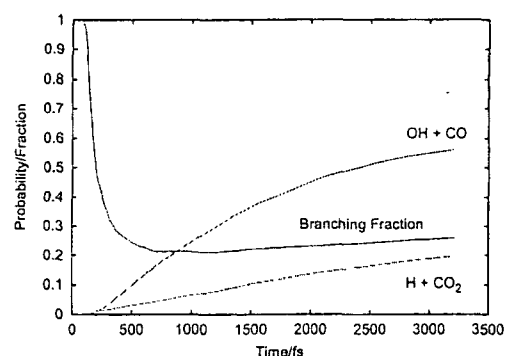


Fig. 3. Calculated yields (probabilities) of photodissociation products and the branching fraction into the H + CO₂ channel as a function of time.

A *K*-dependent adiabatic approximation to the Renner-Teller effect for triatomic molecules. A *K*-dependent adiabatic approach using a two-dimensional Hilbert space in the electronic degree of freedom has been developed to study the Renner-Teller effect in triatomic molecules. The theory is developed in hyperspherical coordinates, and approximately includes electronic spin-orbit interaction. The adiabatic Hamiltonians are expressed in terms of a *K*-dependent effective potential energy surface. Eigenpairs are calculated by solving the time-independent Schrödinger equation, which is represented in a mixed grid/basis set. The method has been applied to the $\tilde{A} \leftarrow \tilde{X}$ band system of bromomethylene (H/DCBr). The results obtained show that the Renner-Teller effect in this molecule is pronounced, particularly in the excited $\tilde{A} \ ^1A''$ state, and are in good agreement with recent experimental measurements made in the experimental part of this program.

A general variational algorithm to calculate vibrational energy levels of tetra-atomic molecules. We have developed a general variational method to calculate vibrational energy levels of tetra-atomic molecules in which the quantum mechanical Hamiltonian of the system is expressed in a set of coordinates defined by three orthogonalized vectors in the body-fixed frame without any dynamical approximation. The eigenvalue problem is solved by a Lanczos iterative diagonalization algorithm, which requires the evaluation of the action of the Hamiltonian operator on a vector. The Lanczos recursion is carried out in a mixed grid/basis set, *i.e.*, a direct product discrete variable representation (DVR) for the radial coordinates, and a non-direct product finite basis representation (FBR) for the angular coordinates. The action of the potential energy operator on a vector is accomplished *via* a pseudo-spectral transform method. Six types of orthogonal coordinates are implemented in this algorithm, which is capable of describing most four-atom systems with small and/or large amplitude vibrational motions. Preliminary applications of the algorithm to the test-case molecules H₂CO, NH₃, HOOH, and the van der Waals cluster He₂Cl₂ have been quite successful. The FORTRAN code implementing this algorithm is being made available to the scientific community free of charge.

Future Plans

Future theoretical studies related to combustion will focus on the further development and application of a *K*-dependent adiabatic approximation to the Renner-Teller effect for triatomic molecules such as HCCl and DCCl, the development and testing of an exact variational method for calculating vibrational energies of five-atom molecules in polyspherical coordinates, studies of the energetics and dynamics of radical-radical reactions such as CH₃ + OH, and theoretical characterization of the electronic states and oscillator

strengths for key species such as C₂ and C₃. Other studies related to catalysis will focus on the electronic structure of transition metal-containing radicals and clusters, and the energetics and dynamics of catalytic reactions on clusters and surfaces.

References

1. MOLPRO is a package of *ab initio* programs written by H.-J. Werner and P. J. Knowles, with contributions from R. D. Amos, A. Bernhardsson, A. Berning, P. Celani, D.L. Cooper, J. J. O. Deegan, A. J. Dobbyn, F. Eckert, C. Hampel, G. Hetzer, T. Korona, R. Lindh, A. W. Lloyd, S. J. McNicholas, F. R. Manby, W. Meyer, M. E. Mura, A. Nicklass, P. Palmieri, R. Pitzer, G. Rauhut, M. Schütz, H. Stoll, A. J. Stone, R. Tarroni, and T. Thorsteinsson.
2. R. Lindh, U. Ryu, and B. Liu, *J. Chem. Phys.* **95**, 5889 (1991); H.-J. Werner and P. J. Knowles, *J. Chem. Phys.* **82**, 5053 (1985); P. J. Knowles and H.-J. Werner, *Chem. Phys. Lett.* **115**, 259 (1985); H.-J. Werner and P. J. Knowles, *J. Chem. Phys.* **89**, 5803 (1988); P. J. Knowles and H.-J. Werner, *Chem. Phys. Lett.* **145**, 514 (1988); P. J. Knowles and H.-J. Werner, *Theor. Chim. Acta* **84**, 95 (1992).
3. J. M. Bowman and B. Gazdy, *J. Chem. Phys.* **94**, 816 (1990); *J. Chem. Phys.* **95**, 6309 (1991).
4. T.-C. Tsai, C.-W. Chen and B.-C. Chang, *J. Chem. Phys.* **115**, 766 (2001).
5. K. S. Bradley and G. C. Schatz, *J. Chem. Phys.* **106**, 8464 (1997).
6. G. C. Schatz, M. S. Fitzcharles and L. B. Harding, *Faraday Discuss.* **84**, 359 (1987).
7. G. D. Billing, *J. Chem. Phys.* **107**, 4286 (1997); *ibid* **110**, 5526 (1999).

Publications since 2000

- Competition Between Photochemistry and Energy Transfer in UV-Excited Diazabenzene: I. Photofragmentation Studies of Pyrazine at 248 nm and 266 nm*, E. T. Sevy, M. A. Muyskens, S. M. Rubin, G. W. Flynn and J. T. Muckerman, *J. Chem. Phys.* **112**, 5829-5843 (2000).
- Experimental and Theoretical Studies of the Near-IR Spectrum of Bromomethylene*, H.-G. Yu, T. Gonzalez-Lezana, A. J. Marr, J. T. Muckerman and T. J. Sears, *J. Chem. Phys.* **115**, 5433 (2001).
- A theoretical study of the potential energy surface for the reaction OH + CO → H + CO₂*, H.-G. Yu, J. T. Muckerman and T. J. Sears, *Chem. Phys. Lett.* **349**, 547 (2001).
- A K-dependent adiabatic approximation to the Renner-Teller effect for triatomic molecules*, H.-G. Yu, J. T. Muckerman and T. J. Sears, *J. Chem. Phys.* **116**, 1435 (2002).
- The E-X Spectrum of Jet-Cooled TiO Observed in Absorption*, K. Kobayashi, G. E. Hall, J. T. Muckerman, T. J. Sears and A. J. Merer, *J. Molec. Spectrosc.* **XX**, xxxx (2002).
- Axis-switching and Coriolis coupling in the A (010) – X (000) transitions of HCCL and DCCL*, A. Lin, K. Kobayashi, H.-G. Yu, G. E. Hall, J.T. Muckerman, T. J. Sears and A. J. Merer, *J. Molec. Spectrosc.*, submitted (2002).
- Imaging O(³P) + alkane reactions in crossed molecular beams: vertical vs. adiabatic H abstraction dynamics*, X. Liu, R. L. Gross, G. E. Hall, J. T. Muckerman and A. G. Suits, *J. Chem. Phys.*, submitted (2002).
- A general variational algorithm to calculate vibrational energy levels of tetra-atomic molecules*, H.-G. Yu and J. T. Muckerman, *J. Molec. Spectrosc.*, submitted (2002).
- Vibrational energy levels of the methyl cation*, H.-G. Yu and T. J. Sears, *J. Chem. Phys.*, submitted (2002).
- An exact variational method to calculate vibrational energies of five-atom molecules beyond the normal mode approach*, H.-G. Yu, *J. Chem. Phys.*, submitted (2002).
- Quantum dynamics of the photoinitiated unimolecular dissociation of HOCO*, H.-G. Yu and J. T. Muckerman, *J. Chem. Phys.*, submitted (2002).
- Vibrational energy transfer and reactivity in OH + CO collisions*, G. D. Billing, J. T. Muckerman and H.-G. Yu, *J. Chem. Phys.*, submitted (2002).

Acknowledgment

Work at Brookhaven National Laboratory was carried out under Contract No. DE-AC02-98CH10886 with the U.S. Department of Energy and is supported by its Division of Chemical Sciences, Office of Science.

Reacting Flow Modeling with Detailed Chemical Kinetics

Habib N. Najm

Combustion Research Facility
Sandia National Laboratories, MS 9051
Livermore, CA 94551
hnnajm@ca.sandia.gov

1. Program Scope

The purpose of this research program is to understand the transient behaviour of flames in turbulent flow, thereby improving the state of the art in predictive modeling of combustion systems. As such, the work involves: (1) Using advanced computational tools to investigate the structure and dynamical behaviour of flames in unsteady vortical laboratory-scale flows. (2) Performing detailed validation studies with matched experimental-numerical comparisons to assess the validity of existing flame chemistry and transport models. (3) Developing advanced techniques for the analysis of, and extraction of information from, multidimensional reacting flow computations. (4) Developing improved numerical methods for discretizing large scale reacting flow systems of equations with detailed kinetics and transport. (5) Developing efficient massively parallel programming approaches for computing large scale reacting flow with detailed kinetics.

2. Recent Progress

2.1 Premixed Flame-Vortex Interactions

Using GRI_{mech}1.2 with mixture-averaged transport, a parametric premixed methane-air flame-vortex-pair interaction study was conducted to investigate the effects of vortex-pair shape and strength on the transient response of the flame ($\Phi = 1.2$). Analysis of the evolution of various concentration profiles on the centerline indicates that, while the details of the interaction are quantitatively affected by the vortex shape and strength, only weak qualitative differences are observed between the various cases. In particular, the analysis indicates that the response of the flame structure in different cases can be related through the prevailing transient strain. We also found similar transient flame response from both the GRI_{mech}1.2 and GRI_{mech}3.0 mechanisms.

Using C_1 kinetics and temperature-dependent transport, we conducted a parametric flame-vortex-pair study varying vortex-pair size and strength. Results were used to validate and refine an embedded flame model that solves the 1D (opposed-jet) local flame structure along slices across a flame surface which is *embedded* in a large-scale computation. The transient response of heat release rate in the 2D computations was found to be in agreement with the 1D flame model when an appropriate representation of the 2D flow strain-rate time-history is imposed on the 1D flame. This is found to be the case even when the flame was not strictly "thin" with respect to flow structures in the 2D computations.

2.2 Uncertainty Quantification (UQ)

We constructed a UQ formulation for general low Mach number reacting flow based on a spectral polynomial chaos stochastic representation. We developed an efficient pseudo-spectral formulation of this construction, as well as a non-intrusive version that is based on Monte-Carlo (MC) realizations of the deterministic system. We applied the spectral approach

to non-reacting incompressible flow in a channel. Computations were used to examine the uncertainty in the velocity and pressure fields resulting from uncertainty in viscosity. We also applied the spectral approach for homogeneous isothermal ignition of a H₂-O₂ mixture at supercritical water oxidation conditions and validated results with published literature.

We applied the non-intrusive UQ approach to a 1D H₂-O₂ flame at supercritical conditions using MC realizations with the Chemkin Premix code. Both reaction rate constants and species enthalpies were uncertain, per known experimental error bands. Results indicated *significant* amplification of uncertainty in the primary flame reaction zone, particularly for H₂O₂ where the standard deviation of the mass fraction field was about 100% of the mean. Results also highlighted parameters with largest contribution to uncertainty in the concentration fields. Reduction of these parametric uncertainties through additional measurements will have a large impact on the confidence in this model predictions.

2.3 Lifted Jet Flame

We found that the computed edge flames at the base of a lifted methane-air jet flame were skewed such that their rich branches were essentially non-existent. The jet mixing layer exhibits steeper equivalence ratio gradients on the rich side than on the lean side, hence the skewed edge flame structure. Consistent with methanol triple flames, peak heat release was on the lean side of the edge flame. The OH and CO fields are in qualitative agreement with experimental PLIF measurements at the base of an axisymmetric lifted jet, with a sickle-like topology of CO consistent with the absence of the rich branch. We found that the product of the CO and OH signals may be used as a measure of the forward rate of $\text{CO} + \text{OH} \rightleftharpoons \text{H} + \text{CO}_2$. On the other hand, it is evident that the reverse rate is such that the peak net production of CO₂ is in the flame edge, while the peak of the [CO][OH] product and the forward rate of the above reaction is in the trailing diffusion flame. We also found that the concentration product [CH₂O][OH] was peaked around the premixed edge flame in a similar manner to HCO and global heat release rate.

2.4 SciDAC – Computational Singular Perturbation (CSP)

The need for inclusion of convection and diffusion as driving processes led us to modify and generalize the CSP canonic form of the governing equations such that chemical, diffusional, and convective processes are included. The presence of cold unburnt reactants required refinement of the criterion used to find the number of modes representing truly equilibrated processes and to discriminate between these latter ones and the modes associated with frozen processes. Further, our results highlighted the need for high accuracy in the numerical solution, which also helped us in assessing the effects of adopting different time integration schemes. We also adopted a special error-reduction procedure which accounts for nonlinearities by allowing iterative improvement of the estimates of the CSP basis vectors and in so doing decreasing the mode mixing between fast and slow modes.

We used CSP to analyze the computed interaction of a premixed methane-air flame (using GRI_{mech}1.2) with a counter-rotating vortex pair. Results identified local equilibrium manifolds at each mesh point which can be grouped into three distinct equilibrium manifolds, one in each of the reacting flow zones: the reactants, the products, and the primary flame reaction zone. We used this information to automatically derive simplified mechanisms for each region given predefined error thresholds. Results were also used to examine importance indices outlining the role of each reaction in the transient evolution of given species.

2.5 SciDAC – Computational Tools

We identified and used the GrACE Adaptive Mesh Refinement (AMR) mesh code as a suitable mesh functionality, and developed it into a Common Component Architecture (CCA) mesh component. GrACE includes parallelism and dynamic load balancing. We have also developed our thermodynamic and chemistry reacting flow code units into corresponding components under CCA. We have demonstrated the component-based assembly of codes for computing zero-dimensional ignition of $\text{H}_2\text{-O}_2$ and methane-air mixtures using CVODE, and for a 2D reaction-diffusion problem using GrACE for mesh refinement, based on an operator split construction around the stiff chemistry integration by CVODE. Work is in progress on the development of high order AMR spatial derivatives discretizations and interpolations.

3. Future Plans

3.1 Premixed Flame-Vortex Interactions

We plan to continue our investigations into transient flame response in unsteady vortical flow using parametric runs based on additional information from CSP and UQ analysis techniques. We plan variations in specific rate constants, with particular emphasis on reactions involved in low-temperature flame chemistry, in order to examine the effect on resulting flame response in relation to experimental measurements. The focus on the low-temperature flame zone is motivated by the following facts : (a) low-temperature flame chemistry is perhaps the least understood (hence most uncertain) aspect of hydrocarbon flames, and (b) computational evidence suggests that the low-temperature region of the flame is the most perturbed region during a flame-vortex interaction.

3.2 Uncertainty Quantification

We will build transport and momentum solutions into the spectral UQ flame code under development. We will use this code to evaluate uncertainty propagation in time-evolving 1D flames, and compare to results and performance of other non-intrusive approaches. Results will be used to evaluate the uncertainty in predicted flame structure and to understand the role of different parameters in the observed uncertainty. Extension to 2D flames will be investigated.

3.3 Lifted Jet Flame

We will extend our investigation of the stabilization and structure of lifted methane-air jet flames to span ranges of jet and coflow flowrate and mixture conditions. We will also pursue detailed comparisons with existing and planned experimental measurements of the internal structure of the lifted jet flame base structure at the CRF. We will also investigate computations of flameless oxidation (FLOX) in this geometry and compare with available experimental measurements on reaction-zone structure.

3.4 SciDAC – Computational Singular Perturbation

We will continue to work on improving robustness and accuracy of the analysis results by pursuing Hessian information for refinement of the CSP basis vectors. We will also reformulate the CSP codes into components under CCA, and will demonstrate their use for postprocessing of GrACE/AMR reacting flow data. We also plan to develop and implement automatic chemical simplification and reduction tools under CCA, based on CSP analysis.

3.5 SciDAC – Computational Tools

We will finalize development and optimization of the chemistry and thermodynamics components. We will develop and demonstrate a mixture-averaged transport property component. These components will be combined with AMR GrACE components to demonstrate a reaction-diffusion AMR CCA computation. We will work on developing and implementing high-order spatial derivative constructions for GrACE meshes. We will also work on implementing a low Mach number momentum AMR solver in the GrACE/CCA framework. This will require either importing or building projection scheme and poisson equation solutions on adaptive meshes. These will be coupled with the reaction-diffusion components to arrive at a full low Mach number reacting flow code with GrACE/AMR under CCA. We will also investigate the use of PRISM for tabulation of reacting flow solutions for efficient time integration of reacting flow.

DOE - Supported Publications [2000-2002]

- [1] Najm, H.N., Knio, O.M., and Paul, P.H., Role of Transport Properties in the Transient Response of Premixed Methane-Air Flames, *Proc. Comb. Inst.*, 29 (2002) accepted.
- [2] Le Maître, O.P., Reagan, M.T., Najm, H.N., Ghanem, R.G., and Knio, O.M., A Stochastic Projection Method for Fluid Flow II. Random Processes, *J. Comp. Phys.* (2002) to appear.
- [3] Najm, H.N., Paul, P.H., McIlroy, A., and Knio, O.M., A Numerical and Experimental Investigation of Premixed Methane-Air Flame Transient Response, *Combustion and Flame*, 125(1-2):879–892 (2001).
- [4] Knio, O.M., and Najm, H.N., Numerical Simulation of Unsteady Reacting Flow with Detailed Kinetics, in *Computational Fluid and Solid Mechanics* (K. Bathe, Ed.), volume 2, Elsevier, 2001, , pp. 1261–1264.
- [5] Le Maître, O.P., Knio, O.M., Najm, H.N., and Ghanem, R.G., A Stochastic Projection Method for Fluid Flow I. Basic Formulation, *J. Comp. Phys.*, 173:481–511 (2001).
- [6] Najm, H.N., Paul, P.H., Knio, O.M., and McIlroy, A., Transient Response of Premixed Methane-Air Flames, in *Computational Fluid and Solid Mechanics* (K. Bathe, Ed.), volume 2, Elsevier, 2001, , pp. 1334–1337.
- [7] Ashurst, Wm.T., Najm, H.N., and Paul, P.H., Chemical Reaction and Diffusion: a Comparison of Molecular Dynamics Simulations with Continuum Solutions, *Combustion Theory and Modeling*, 4:139–157 (2000).
- [8] Knio, O.M., and Najm, H.N., Effect of Stoichiometry and Strain-Rate on Transient Flame Response, *Proc. Comb. Inst.*, 28:1851–1857 (2000).
- [9] Marzouk, Y.M., Ghoniem, A.F., and Najm, H.N., Dynamic Response of Strained Premixed Flames to Equivalence Ratio Gradients, *Proc. Comb. Inst.*, 28:1859–1866 (2000).
- [10] Ray, J., Najm, H.N., Milne, R.B., Devine, K.D., and Kempka, S.N., Triple Flame Structure and Dynamics at the Stabilization Point of an Unsteady Lifted Jet Diffusion Flame, *Proc. Comb. Inst.*, 28:219–226 (2000).

Radical Chemistry and Photochemistry

Daniel M. Neumark
Chemical Sciences Division
Lawrence Berkeley National Laboratory
Berkeley, CA 94720
neumark@cchem.berkeley.edu

Program Scope

This research program is aimed at elucidating the photodissociation dynamics and bimolecular chemistry of free radicals and hydrocarbons, with particular emphasis on species that play a role in combustion chemistry. Our experiments yield primary chemistry and photochemistry, bond dissociation energies, heats of formation, and excited state dynamics. This fundamental information is vital for the development of accurate models of reaction mechanisms in combustion.

Although much time and effort has been invested in modeling combustion chemistry, many of the primary processes involved in combustion are poorly understood. As a result, one has a situation where sophisticated kinetics models stand on a weak foundation, because the primary chemistry of the reactions in the models and the thermochemistry of the species involved in these reactions are not known. Examples include the reactions leading to soot formation in flames, and reactions in which NO is produced as a by-product of combustion. Our program is focused on fundamental studies of species and reactions relevant to combustion chemistry. We have developed a state-of-the-art instrument for studying the photodissociation dynamics of free radicals. In addition, a crossed molecular/laser beam instrument is used to investigate the primary chemistry and photochemistry of both closed-shell hydrocarbons and hydrocarbon radicals.

Three instruments are used in these studies: a fast radical beam photofragment translational spectrometer, in which radicals are generated by photodetachment of mass-selected negative ions, and two neutral beam instruments, one with electron impact ionization of products and the other (at the Advanced Light Source) with tunable vacuum ultraviolet.

Recent Progress

The photodissociation dynamics of NCO have been examined using fast beam photofragment translational spectroscopy. Excitation of the 1_0^2 , 3_0^1 , and $1_0^2 3_0^2$ transitions of the $\tilde{B}^2\Pi \leftarrow \tilde{X}^2\Pi$ band produces $N(^4S) + CO$ photofragments exclusively, while excitation of the $1_0^3 3_0^3$ transition yields primarily $N(^2D) + CO$ photoproducts. The translational energy ($P(E_T)$) distributions yield $D_0(N-CO) = 2.34 \pm 0.03$ eV, and $\Delta H_{f,0}^0(NCO) = 1.36 \pm 0.03$ eV. The $P(E_T)$ distributions exhibit vibrationally resolved structure reflecting the vibrational and rotational distributions of the CO product. The

$N(^2D) + CO$ distribution can be fit by phase space theory (PST), while the higher degree of CO rotational excitation for $N(^4S) + CO$ products implies that NCO passes through a bent geometry upon dissociation. The $P(E_T)$ distributions suggest that when the $\bar{B}^2\Pi \leftarrow \tilde{X}^2\Pi$ band is excited, NCO undergoes internal conversion to its ground electronic state prior to dissociation. Excitation of NCO at 193 nm clearly leads to the production of $N(^2D) + CO$ fragments. While conclusive evidence for the higher energy $O(^3P) + CN(X^2\Sigma^+)$ channel was not observed, the presence of this dissociation pathway could not be excluded.

The photodissociation spectroscopy and dynamics of the HNCN and HCNN free radicals have been investigated by fast beam photofragment translational spectroscopy. In HNCN, predissociative transitions for both the $B^2A' \leftarrow X^2A''$ band and a higher energy band system assigned to the $C^2A'' \leftarrow X^2A''$ band were observed. Photofragment mass distributions indicate that N_2 loss is the primary dissociation pathway. Translational energy distributions reveal resolved vibrational structure of the N_2 fragment, suggesting that the HNCN radical first isomerizes to a cyclic-HCN₂ intermediate. A dissociation mechanism is proposed in which electronically excited HNCN undergoes internal conversion to the ground state, followed by isomerization to cyclic HCN₂ and dissociation through a tight three-center transition state. The HNCN bond dissociation energy D_0 and heat of formation $\Delta_f H_0(HNCN)$ were determined to be 2.80 ± 0.03 eV and 3.35 ± 0.03 eV respectively. HCNN was also found to dissociate exclusively to $CH + N_2$. Although this process could occur without a barrier on the ground state surface, the kinetic energy distributions suggest a more complicated mechanism that is still under investigation.

Photofragment translational spectroscopy has been used to investigate the dissociation dynamics of 1,2-butadiene at 193 nm. Ionization of scattered photoproducts was accomplished using tunable VUV synchrotron radiation at the Advanced Light Source. Two product channels are observed: $CH_3 + C_3H_3$ and $C_4H_5 + H$. Both are bond fission channels; no evidence of products from isomerization to 1,3-butadiene was observed. The C_3H_3 product can be identified as the propargyl radical through measurement of its photoionization efficiency curve, whereas the C_4H_5 product cannot be identified definitively. The translational energy $P(E_T)$ distributions suggest that both channels result from internal conversion to the ground electronic state followed by dissociation. The $P(E_T)$ distribution for the C_4H_5 product was sharply truncated below 7 kcal/mol, indicating spontaneous decomposition of the slowest C_4H_5 product.

The photodissociation dynamics of 1,3-butadiene at 193 nm have been investigated with photofragment translational spectroscopy coupled with product photoionization using tunable VUV synchrotron radiation. Five product channels are evident from this study: $C_4H_5 + H$, $C_3H_3 + CH_3$, $C_2H_3 + C_2H_3$, $C_4H_4 + H_2$, and $C_2H_4 + C_2H_2$. The translational energy ($P(E_T)$) distributions suggest that these channels result from internal conversion to the ground electronic state followed by dissociation. In order to investigate the dissociation dynamics in more detail, further studies were carried out using 1,3-butadiene-1,1,4,4-d₄. While the radical channels produced by the dissociation of 1,3-

butadiene-1,1,4,4-d₄ could be fit with the P(E_T) distributions obtained from 1,3-butadiene dissociation, the molecular channels required a unique P(E_T) distribution for each product isotopic combination. Branching ratios were determined for the channels listed above using a molecular beam photodissociation instrument with electron impact ionization. These measurements showed C₃H₃ + CH₃ to be the dominant channel. This channel arises from isomerization to 1,2-butadiene on the ground state surface followed by C-C bond fission.

Future plans

A major overhaul of the detection scheme on the fast radical instrument is underway. The current detector based on a dual wedge-and-strip anode provides time- and position-sensitive measurements for two photofragments. It cannot, however, be used if three fragments are produced from either a single or multiple photodissociation events, and its collection efficiency is low for slow photofragments. These problems will be solved with a new design, in which a CCD camera is used to record the positions of all photofragments with high precision, and a photomultiplier tube with a segmented anode records their arrival times. By correlating the two measurements after each laser shot one obtains position and time information for all photofragments. This design will also result in improved photofragment collection efficiency. This detector concept has been developed and used on several ion storage ring experiments in Europe and holds considerable promise for our radical photodissociation experiment.

The radical photodissociation work on the fast radical instrument will be complemented by photodissociation and crossed beam studies of radicals on the neutral molecular instruments in our laboratory and at the ALS. We have constructed pyrolysis and photolysis sources for free radicals and intend to use them to generate hydrocarbon species such as vinyl, phenyl, and CH radicals for use in photodissociation and reactive scattering experiments. Optimization of these neutral radical sources will be accomplished in a new chamber, currently under construction, in which photoionization mass spectrometry at 10.5 eV is used to selectively detect radicals produced in the source, but not the closed-shell precursors to the radicals.

Publications

H. Choi, R. T. Bise, A. A. Hoops, D. H. Mordaunt, D. M. Neumark, "Photodissociation of Linear Carbon Clusters C_n (n=4-6)," *J. Phys. Chem. A* 104, 2025, (2000).

H. Choi, R. T. Bise, A. A. Hoops, D. M. Neumark, "Photodissociation dynamics of the triiodide anion (I₃⁻)." *J. Chem. Phys.* 113, 2255, (2000).

R.T. Bise, A. A. Hoops, H. Choi, D. M. Neumark, "Photodissociation dynamics of the CNN free radical". *J. Chem. Phys.* 113, 4179, (2000).

H. Choi, R. T. Bise, D. M. Neumark, "Photodissociation dynamics of the ethoxy radical (C₂H₅O)". *J. Phys. Chem. A* 104, 10112, (2000).

R. T. Bise, A. A. Hoops, H. Choi, D. M. Neumark, "Photoisomerization and photodissociation dynamics of the NCN, CNN and HNCN free radicals". ACS Symposium Series 770 296, (2001).

R. T. Bise, A. A. Hoops, D.M. Neumark, "Photodissociation and photoisomerization pathways of the HNCN free radical". Chem. Phys. Lett. 114, 9000, (2001).

A. A. Hoops, R. T. Bise, J. R. Gascooke, D. M. Neumark, "State-resolved translation energy distributions for NCO photodissociation". J. Phys. Chem. 114, 9020, (2001).

J. Robinson, W. Sun, S. Harris, F. Qi, D. M. Neumark, "Photofragment translational spectroscopy of 1,2-butadiene at 193 nm" J. Chem. Phys. 115, 8359, (2001).

J. C. Robinson, S. A. Harris, W. Sun, D. M. Neumark, "Photofragment translational spectroscopy of 1,3-butadiene and 1,3-butadiene-1,1,4,4-d₄ at 193nm" (Submitted to Journal of American Chemical Society).

High-Resolution Photoionization and Photoelectron Studies: Determination of Accurate Energetic Database for Combustion Chemistry

C. Y. Ng

*Department of Chemistry, University of California at Davis
One Shields Avenue, Davis, California 95616
E-mail Address: cyng@chem.ucdavis.edu*

We have developed a unique high-resolution vacuum ultraviolet (VUV) photoion-photoelectron facility at the Chemical Dynamics Beamline of the Advanced Light Source (ALS).¹⁻³ Using this facility, we have introduced novel synchrotron-based pulsed field ionization (PFI)-photoelectron (PFI-PE) schemes,⁴ attaining resolutions of $1\text{-}5\text{ cm}^{-1}$ (full width at half maximum, FWHM). We have also established a generally applicable synchrotron-based PFI-PE-photoion coincidence (PFI-PEPICO) method⁵ for state- or energy-selected unimolecular dissociation studies of ions with resolutions only limited by the PFI-PE measurement. Recent studies have shown that by combining PFI-PE and PFI-PEPICO measurements, highly reliable energetic data, such as ionization energies (IEs), 0 K dissociative photoionization thresholds or appearance energies (AEs), 0 K bond dissociation energies (D_0 's), and 0 K heats of formation ($\Delta H_{f,0}^\circ$'s), for a range of small molecules and their ions can be obtained with unprecedented precision.²⁻⁸ An improvement of this PFI-PEPICO scheme using the radio frequency octopole ion guide technique should made possible the application of the PFI-PEPICO scheme for reliable measurements of 0 K AEs of medium size molecules. We have recently shown that by employing a wired ion gate to reject false coincidences, the signal-to-noise for PFI-PEPICO measurements can be significantly improved.⁹

We have also engaged in laboratory VUV laser photoionization studies. A comprehensive VUV laser system [tunable range = 6-19 eV, optical bandwidth = 0.12 cm^{-1} (FWHM)] based on four-wave sum- or difference- frequency mixing schemes, together with a reflectron time-of-flight mass spectrometer and a PFI-PE detector, has also been constructed in our laboratory.¹⁰ Since the VUV laser is operated at 30 Hz, it is ideal to couple with a molecular beam-excimer laser photodissociation source¹¹ for radical preparation. The PFI-PE measurements of radicals thus prepared using the VUV laser photoionization apparatus are expected to complement the PFI-PE and PFI-PEPICO studies at the ALS. These experimental developments in our laboratory and at the ALS have opened up a unique opportunity for initiating an experimental program for a systematic PFI-PE and PFI-PEPICO measurement of small and medium sizes molecules and radicals of relevance to combustion, atmospheric, and plasma chemistry. Highly accurate IEs, 0 K AEs, D_0 's, and $\Delta H_{f,0}^\circ$'s for selected polyatomic neutrals and their ions obtained in this study are expected to form a needed database for development of the next generation of *ab initio* quantum chemical computational procedures.

References:

1. C. Y. Ng, in "Photoionization, and Photodetachment", edited by C. Y. Ng (World Scientific, Singapore, 2000), *Adv. Ser. Phys. Chem.* **10A**, Chapter 9, p.394-538.
2. C. Y. Ng, *J. Electron Spectroscopy & Related Phenomena*, **112**, 31 (2000).
3. C. Y. Ng, *Int. J. Mass Spectrometry*, **200**, 357 (2000).
4. G. K. Jarvis, Y. Song, and C. Y. Ng, *Rev. Sci. Instrum.* **70**, 2615 (1999).

5. G. K. Jarvis, K.-M. Weitzel, M. Malow, T. Baer, Y. Song, and C. Y. Ng, *Rev. Sci. Instrum.* **70**, 3892 (1999).
6. K.-M. Weitzel, G. Jarvis, M. Malow, Y. T. Baer, Song, and C. Y. Ng, *Phys. Rev. Lett.* **86**, 3526 (2001).
7. Y. Song, X.-M. Qian, K.-C. Lau, C. Y. Ng, J. Liu and W. Chen, *J. Chem. Phys.* **115**, 2582, 4095 (2001).
8. X.-M. Qian, Y. Song, K.-C. Lau, C. Y. Ng, J. Liu, W. Chen, and G.-Z. He, *Chem. Phys. Lett.*, in press.
9. X.-M. Qian, T. Zhang, P. Wang, C. Y. Ng, R. A. Dressler, S. Miller, Y.-H. Chiu and D. J. Levandier, T. Baer, and D. S. Peterka, *Rev. Sci. Instrum.*, to be submitted.
10. H. K. Woo, J. Zhan, K.-C. Lau, C. Y. Ng, and Y.-S. Cheung, *J. Chem. Phys.*, submitted.
11. S. Nourbakhsh, K. Norwood, G.-Z. He, and C. Y. Ng, *J. Am. Chem. Soc.* **113**, 6311 (1991).

Publications of DOE sponsored research (2000-present)

- 1 C. Y. Ng, "Advances in photoionization and photoelectron studies using third generation synchrotron radiation and UV/VUV lasers", in "Photoionization, and Photodetachment", edited by C. Y. Ng (World Scientific, Singapore, 2000), *Adv. Ser Phys. Chem.* **10A**, Chapter 9, p.394-538.
- 2 C. Y. Ng, editor, "Photoionization and Photodetachment I" (World Scientific, Singapore, 2000), *Adv. Ser Phys. Chem.*, Vol. **10A**, 713 pages.
- 3 C. Y. Ng, editor "Photoionization and Photodetachment II" (World Scientific, Singapore, 2000), *Adv. Ser Phys. Chem.*, Vol. **10B**, 664 pages.
- 4 Y. Song, M. Evans, C. Y. Ng, C.-W. Hsu, and G. K. Jarvis, "Rotational-Resolved Pulsed Field Ionization Photoelectron Study of $O_2^+(A^2\Pi_u, v^+=0-12)$ in the Energy Range of 17.0-18.2 eV", *J. Chem. Phys.* **112**, 1271-1278 (2000).
- 5 Y. Song, M. Evans, C. Y. Ng, C.-W. Hsu, and G. K. Jarvis, "Rotationally Resolved Pulsed Field Ionization Photoelectron Study of $O_2^+(a^4\Pi_u, v^+=0-18)$ in the Energy Range of 16.0-18.0 eV", *J. Chem. Phys.* **112**, 1306-1315 (2000).
- 6 T. Baer, Y. Song, C. Y. Ng, J. Liu, and W. Chen, "High-Resolution PFI-PEPICO Studies of Ionic Dissociation at the Advanced Light Source", *Faraday Discussion* **115**, 137-145 (2000).
- 7 A. Yench, M. C. A. Lopes, G. C. King, M. Hochlaf, Y. Song, and C. Y. Ng, "Ion-Pair Formation Observed in a Pulsed-Field Ionization Photoelectron Spectroscopic Study of HF", *Faraday Discussion* **115**, 355-362 (2000).
- 8 G. K. Jarvis, R. C. Shiell, J. Hepburn, Y. Song, and C. Y. Ng, "Pulsed Field Ionization-Photoion Spectroscopy Using two-bunch Synchrotron Radiation: Time-of-Flight Selection Scheme", *Rev. Sci. Instrum.* **71**, 1325 (2000).
- 9 C. Y. Ng, "Advances in Photoionization and Photoelectron Studies Using Third Generation Synchrotron Radiation", *J. Electron Spectroscopy & Related Phenomena*, **108**, 41-45 (2000).
- 10 T. Baer, Y. Song, C. Y. Ng, W. Chen, and J. Liu, "The Heat of Formation of $C_3H_7^+$ and Proton Affinity of C_3H_6 Determined by Pulsed Field Ionization-Photoelectron Photoion Coincidence Spectroscopy", *J. Phys. Chem.* **104**, 1959 (2000).
- 11 K.-C. Lau, W.-K. Li, C. Y. Ng, H. Baumgärtel, and K.-M. Weitzel, "Gaussian-2 and Gaussian-3 Study of the Energetics and Structure of Cl_2O_n and $Cl_2O_n^+$, $n=1-7$ ", *J. Phys Chem.* **104**, 3197 (2000).
- 12 Jianbo Lau, Wenwu Chen, C.-W. Hsu, M. Hochlaf, M. Evans, S. Stimson, and C. Y. Ng, "High-Resolution Pulsed Field Ionization-Photoelectron Study of $CO_2^+(X^2\Pi_g)$ in the energy range of 13.6-14.7 eV", *J. Chem. Phys.* **112**, 10767 (2000).

- 13 H. Lefebvre-Brion and C. Y. Ng, "Pulsed Field Ionization Photoelectron Spectrum for $\text{CO}^+(\text{A}^2\Pi_u, v^+=1)$ ", *Chem. Phys. Lett.* **327**, 404-408 (2000).
- 14 C. Y. Ng, "Pulsed Field Ionization Photoelectron-Photoion Spectroscopy: Determination of Accurate Bond Dissociation Energies for Neutrals and Cations", *J. Electron Spectroscopy & Related Phenomena* (invited article), **112**, 31-46 (2000).
- 15 Jianbo Liu, M. Hochlaf, and C. Y. Ng, "Pulsed Field Ionization-Photoelectron Bands of $\text{CO}_2^+(\text{A}^2\Pi_u$ and $\text{B}^2\Sigma_u^+)$: An Experimental and Theoretical Study", *J. Chem. Phys.* **113**, 7988 (2000).
- 16 C. Y. Ng, "Vacuum Ultraviolet Photoionization and Photoelectron Studies in the New Millennium: Recent Developments and Applications", *Int. J. Mass Spectrometry*, special issue for year 2000 (invited article), **200**, 357-386 (2000).
- 17 Jianbo Liu, M. Hochlaf, G. Chambaud, P. Rosmus, and C. Y. Ng, "High Resolution Pulsed Field Ionization-Photoelectron Bands for $\text{CS}_2^+(\text{A}^2\Pi_u)$: An Experimental and Theoretical Study", *J. Phys. Chem.* **105**, 2183 (2001).
- 18 K.-M. Weitzel, G. Jarvis, M. Malow, Y. T. Baer, Song, and C. Y. Ng, "Observation of Accurate Ion Dissociation Thresholds in Pulsed Field Ionization Photoelectron Studies", *Phys. Rev. Lett.* **86**, 3526 (2001).
- 19 Y. Song, C. Y. Ng, G. Jarvis, and R. A. Dressler, "Rotational-Resolved Pulsed Field Ionization-Photoelectron Study of $\text{NO}^+(\text{A}^1\Sigma^-, v^+ = 0-17)$ in the Energy Range of 17.79-20.10 eV", *J. Chem. Phys.* **115**, 2101-2108 (2001).
- 20 Y. Song, X.-M. Qian, K.-C. Lau, C. Y. Ng, J. Liu and W. Chen, "High Resolution Energy-Selected Study of the Reaction $\text{NH}_3^+ \rightarrow \text{NH}_2^+ + \text{H}$: Accurate Thermochemistry for the $\text{NH}_2/\text{NH}_2^+$ and $\text{NH}_3/\text{NH}_3^+$ Systems", *J. Chem. Phys.* **115**, 2582-2589 (2001).
- 21 Y. Song, X.-M. Qian, K.-C. Lau, C. Y. Ng, J. Liu and W. Chen, "High Resolution Energy-Selected Study of the Reactions $\text{CH}_3\text{X}^+ \rightarrow \text{CH}_3^+ + \text{X}$: Accurate Thermochemistry for the $\text{CH}_3\text{X}/\text{CH}_3\text{X}^+$ (X= Br and I) System", *J. Chem. Phys.* **115**, 4095 (2001).
- 22 X.-M. Qian, Y. Song, K.-C. Lau, C. Y. Ng, J. Liu and W. Chen, "A Pulsed Field Ionization Study of the Dissociative Photoionization Reaction $\text{CD}_4 + h\nu \rightarrow \text{CD}_3^+ + \text{D} + e^-$ ", *Chem. Phys. Lett.* **347**, 51-58 (2001).
- 23 D. G. Fedorov, M. S. Gordon, Y. Song, and C. Y. Ng, "A Theoretical Study of the Spin-orbit coupling in $\text{O}_2^+(\text{A}^2\Pi_{3/2,1/2u}, v^+=0-15; \text{a}^4\Pi_{5/2,3/2,1/2,-1/2u}, v^+=0-18)$ ", *J. Chem. Phys.* **115**, 7393-7400 (2001).
- 24 X.-M. Qian, Y. Song, K.-C. Lau, C. Y. Ng, J. Liu, W. Chen, and G.-Z. He, "A Pulsed Field Ionization Study of the Reaction $\text{D}_2\text{O} + h\nu \rightarrow \text{OD}^+ + \text{D} + e^-$ ", *Chem. Phys. Lett.*, in press.
- 25 Branko Ruscic, Albert F. Wagner, Lawrence B. Harding, Robert L. Asher, David Feller, Kirk A. Peterson, Yang Song, Ximei Qian, C.Y. Ng, Jianbo Liu, and Wenwu Chen, "On the Enthalpy of Formation of Hydroxyl Radical and Gas-Phase Dissociation energies of Water and Hydroxyl", *J. Phys. Chem.*, in press.
- 26 C. Y. Ng, "Vacuum Ultraviolet Spectroscopy and Chemistry Using Photoionization and Photoelectron Methods", *Ann. Rev. Phys. Chem.* **54**, 101-140 (2002).
- 27 Wenwu Chen, M. Hochlaf, P. Rosmus, G.-Z. He, and C. Y. Ng, "Vacuum Ultraviolet Pulsed Field Ionization Photoelectron Study of OCS in the Energy range of 15.0-19.0 eV", *J. Chem. Phys.*, in press.

KINETICS AND DYNAMICS OF COMBUSTION CHEMISTRY

David L. Osborn

Combustion Research Facility, Mail Stop 9055

Sandia National Laboratories

Livermore, CA 94551-0969

Telephone: (925) 294-4622

Email: dlosbor@sandia.gov

PROGRAM SCOPE

The goal of this program is to elucidate mechanisms of elementary combustion reactions through the use of absorption and emission-based spectroscopy. The main technique employed is time-resolved Fourier transform spectroscopy (TR-FTS) to probe multiple reactants and products with broad spectral coverage ($> 1000 \text{ cm}^{-1}$), moderate spectral resolution (0.1 cm^{-1}) and a wide range of temporal resolution (ns – ms). The inherently multiplexed nature of TR-FTS makes it possible to simultaneously measure product branching ratios, internal energy distributions, energy transfer, and spectroscopy of radical intermediates. Together with total rate coefficients, this additional information provides further constraints upon and insights into the potential energy surfaces that control chemical reactivity.

For reactions producing vibrationally or electronically excited molecules, emission-based TR-FTS may be used to study product state distributions, energy transfer kinetics, and product branching ratios. While several groups have made great progress in gas phase emission-based TR-FTS,¹⁻⁷ there is little work in absorption.⁸ Absorption techniques are also being pursued in this program because they are more general than emission methods, and are not complicated by fluorescence lifetime effects or predissociation. Another thrust of this program is toward kinetic measurements of larger molecules. The development of absorption-based TR-FTS in the mid-infrared fingerprint region will enable reactivity studies of larger hydrocarbons (C3 – C6) found in practical fuels. Fourier transform spectroscopy offers well-known throughput and multiplex advantages over dispersive instruments when used in the infrared. Finally, the broadband spectral detection offered by FTS can allow the identification of unexpected product channels that might go unnoticed by narrow-band detection techniques.

RECENT PROGRESS

Photodissociation of dicyclopropyl ketone: cyclopropyl or allyl radicals

We have recently completed a set of experiments on the photodissociation dynamics of dicyclopropyl ketone (DCPK), a symmetric ketone analogous to acetone. The original goal of this study was to determine whether DCPK is a suitable photolytic precursor for cyclopropyl radicals. Cyclopropyl (*c*-C₃H₅) is a prototype for radical isomerizations, a critically important process in combustion chemistry. The cyclopropyl radical can ring open to the allyl radical (CH₂CHCH₂) over a (calculated) 20 kcal/mol barrier, with an exothermicity of 32 kcal/mol. A clean source of cyclopropyl radicals is crucial to studying this isomerization.

When acetone is excited to the S_2 state at 193 nm, it undergoes ISC to the T_1 surface followed by dissociation over a barrier to produce CH₃ + CH₃CO.⁹ Internal conversion to S_0 is not believed to be important. Secondary dissociation of CH₃CO to CH₃ + CO also occurs over a barrier, with a total quantum yield for CH₃ $\phi > 1.9$.¹⁰ The translational energy in both bond-breaking events peaks away from $E_T = 0$, and the CO vibrational and rotational distributions are hotter than predicted by statistical models.^{11,12}

We have investigated the 193 nm photodissociation of DCPK using time-resolved FT emission spectroscopy from 800 – 4000 cm^{-1} . Following photolysis, prompt emission is seen from free CO, implying that the dissociation products are $\text{CO} + 2\text{C}_3\text{H}_5$. Prompt emission is also seen in the C-H stretching region, and in the IR fingerprint region from 800 – 1600 cm^{-1} , both of which are assigned to C_3H_5 . The C-H emission decays within $\sim 25 \mu\text{s}$, consistent with its assignment as emission from a radical species. At later times additional features appear, which can be definitively assigned to emission from DCPK. The temporal profile of decreasing emission from C_3H_5 and increasing emission from DCPK is consistent with energy transfer from the hot radicals to the cold parent molecules. The main question is whether the nascent hydrocarbon emission is due to cyclopropyl, allyl, or a mixture of the two radicals. To better characterize the CO fragment and its energy content, we have in addition probed the rotational and translational energy distributions of CO using REMPI and photofragment translational spectroscopy.

By examining the time-resolved CO emission with 0.1 cm^{-1} resolution, we obtain the nascent vibrational distribution, which is fairly well described by a temperature of 1800 K, or $\langle E_{\text{vib}} \rangle = 1.3 \text{ kcal/mol}$. Similarly, from the CO REMPI spectrum, taken under collisionless conditions, we find a rotational temperature of ~ 2600 , corresponding to $\langle E_{\text{rot}} \rangle(\text{CO}) \sim 5 \text{ kcal/mol}$. The CO internal energy distributions are somewhat colder than those observed from acetone or diethyl ketone. Measurement of the translational energy deposited into CO is ill defined in this three-body dissociation. Nevertheless we can gain some insight into the CO translational energy by measuring the lab-frame energy distribution, which peaks at 5 kcal/mol, and provides an upper limit for the average center-of-mass translational energy. The total energy ($T + V + R$) in CO is therefore estimated as 8 – 10 kcal/mol.

We have performed B3LYP/DFT and higher level CBS-Q calculations to characterize important stationary points on both the S_0 and T_1 surfaces, benchmarking against acetone calculations at the same level of theory. The calculations demonstrate several differences between the thermodynamics of acetone and DCPK. In DCPK, photodissociation at 193 nm to $\text{CO} + 2(\text{c-C}_3\text{H}_5)$ leaves only 29 kcal/mol available energy (compared to 53 in acetone). In contrast, photodissociation to the ring-opened products, $\text{CO} + 2(\text{allyl})$, yields 92 kcal/mol. Furthermore, a transition state to ring opening in the parent molecule exists on the ground state surface. Therefore the amount of energy remaining in the photofragments should offer clues to the dissociation mechanism and the isomerization of C_3H_5 .

To predict product distributions in the statistical limit, we have used a two-step phase-space-theory model for the vibrational distribution of CO for both possible product channels. For the ISC mechanism (which would give cyclopropyl radicals), the PST model predicts that $> 99\%$ of the CO molecules will be in the zero-point level, clearly inconsistent with the data, even when the modest exit barriers on this surface are taken into account.

We conclude that the mechanism most consistent with the experimental and theoretical data is internal conversion of the initially excited DCPK to S_0 , followed by ring-opening isomerization of the parent molecule and dissociation producing $\text{CO} + \text{allyl} + \text{allyl}$. The availability of internal isomerization pathways and the influence of electron delocalization make the dissociation of DCPK qualitatively different from aliphatic ketones.

Multiphoton dissociation of C_2H_3 – a possible LIFF diagnostic in methane flames

The vinyl radical is an important intermediate in the chain of C2 species in methane/air flames. Unfortunately, direct detection of vinyl using LIF is not possible due to strong

predissociation. However, PLIF imaging experiments of rich methane-air flames in the Advanced Imaging Lab at the CRF show strong C_2 ($d^3\Pi_g \rightarrow a^3\Pi_u$) Swan band fluorescence that is laser-prompt with 230 nm excitation of the flame. The production of electronically excited C_2 from multiphoton dissociation of a precursor is termed laser-induced fragmentation fluorescence (LIFF), and could provide a method to study the C_2 chemistry branch in methane flames if the parent molecule(s) responsible for Swan band fluorescence can be identified. The narrow spatial distribution (500 μm FWHM) of C_2 LIFF signal along the flame propagation direction implies that the parent molecule is a short-lived species. The vinyl radical (C_2H_3) and acetylene (C_2H_2) are the most chemically reasonable choices for the parent molecule responsible for this LIFF.

We have conducted low-pressure cell experiments to measure the efficiency, photon energy dependence, and product state distribution of C_2 fluorescence from 230 nm multiphoton excitation of many candidate molecules that may be present in the flame or the cell environment, namely: CH_4 , C_2H_2 , C_2H_3 , C_2H_4 , C_2H_6 , C_3H_6 , and C_4H_6 . The vinyl radical was generated by photolysis of methyl vinyl ketone (MVK) at 193 nm, and LIFF from C_2 was collected using a gated, image-intensified CCD monochromator. The yield of vinyl radicals is calibrated by simultaneous collection of 2 photon LIF from the CO that is produced in equal numbers via photolysis of MVK. The only molecules that create significant LIFF signal are C_2H_2 , C_2H_3 , and C_4H_6 . While C_4H_6 is formed from the vinyl self-reaction in low pressure cell experiments, it is highly unlikely that it would be present in methane flame chemistry.

The LIFF photon energy dependence shows that both C_2H_2 and C_2H_3 require 3 photons to dissociate to electronically excited C_2 , consistent with spin-allowed dissociation pathways. The vinyl radical is photolytically produced with large amounts of internal energy, and is cooled by collisional energy transfer. By monitoring the LIFF signal as a function of time delay after the photolysis pulse, we find that the C_2 LIFF signal decreases by a factor of 6.5 due to a decrease in internal energy in the parent vinyl radical. When we compare the LIFF cross sections of C_2H_2 and C_2H_3 , we find that vinyl is more efficient than acetylene by a factor of 1300 – 200, depending on the internal energy of the vinyl radical. Even though the mechanism for dissociation of C_2H_3 passes through a C_2H_2 intermediate, the key difference in the observed cross sections lies in the loss of the first H atom. For vinyl, a strong one-photon absorption leads to H atom loss, while for acetylene the first photon absorption is at least three orders of magnitude weaker, and two photons are required for fission of the first C-H bond.

This photodissociation process may therefore be promising as a specific diagnostic for vinyl radicals in methane flames. However, it is likely that the LIFF cross section for acetylene will also increase with internal excitation, and further studies will be required to determine if this LIFF scheme will be a useful diagnostic in methane flames.

Time-resolved FTIR absorption spectroscopy

During the last year we have recorded the first data in this laboratory using time-resolved Fourier transform absorption spectroscopy. The apparatus consists of a small flow cell with White-type multipass optics for the broadband modulated probe beam. A photolysis laser propagating perpendicular to the probe beam is used to initiate the reaction. For these proof-of-principle experiments we have chosen to study the reaction $Cl + CH_4 \rightarrow HCl + CH_3$. This slightly endothermic reaction ($\Delta H_{rxn} = +1.6$ kcal/mol) is an ideal candidate because the product molecules are born in their ground vibrational levels, minimizing chemiluminescence and quantum state dilution. While it is clear that absorption-based time-resolved FTS is substantially

more difficult than emission-based FTS, the advantages of absorption spectroscopy make this technique more generally applicable to kinetics studies than emission spectroscopy.

Future Plans

Another area of interest is chemical reactions that may not occur solely on the ground state potential energy surface, but produce radical products in low-lying electronically excited states. For example, in $C_2H_5 + O_2 \rightarrow C_2H_4 + HO_2$, production of HO_2 in its excited \tilde{A} (${}^2A'$) state is energetically allowed, and is a possible explanation for inconsistencies in data comparing the forward and reverse reactions. Detection of this species by TR-FTS via the \tilde{A} (${}^2A'$) \rightarrow \tilde{X} (${}^2A''$) electronic emission would provide clear evidence that multiple electronic surfaces participate in this reaction.

Finally, high spectral brightness broadband sources for use in absorption-based FT spectroscopy will be investigated. Two avenues are being pursued. Self-phase modulation in dispersion-tuned microstructured fibers has recently been used to create quasi-cw ultra-broadband radiation. We will explore the use of these fibers in FT absorption spectroscopy. A second approach centers on optical parametric generation in quasi phase-matched nonlinear materials. A brighter, more collimated source of IR radiation would increase the detection sensitivity of FT absorption spectroscopy.

BES sponsored publications

David L. Osborn and Jonathan H. Frank, "Laser-induced fragmentation fluorescence detection of the vinyl radical and acetylene," *Chem. Phys. Lett.* **349**, 43 (2001).

References

- ¹ R. E. Murphy and H. Sakai, in *Proceedings of the Aspen International Conference on Fourier Transform Spectroscopy*, Aspen, p. 301 (1970).
- ² G. Hancock and D. E. Heard, *Adv. Photochem.* **18**, 1 (1993).
- ³ T. R. Fletcher and S. R. Leone, *J. Chem. Phys.* **88**, 4720 (1988).
- ⁴ J. J. Sloan and E. J. Kruus, in *Time Resolved Spectroscopy*, ed. R. J. H. Clark and R. E. Hester, John Wiley & Sons, p. 219 (1989).
- ⁵ G. V. Hartland, W. Xie, H. L. Dai, A. Simon, and M. J. Anderson, *Rev. Sci. Instrum.* **63**, 3261 (1992).
- ⁶ P. W. Seakins, in *The Chemical Dynamics and Kinetics of Small Radicals*, ed. K. Liu and A. Wagner, Singapore, p. 250 (1995).
- ⁷ G. E. Hall, J. T. Muckerman, J. M. Preses, R. E. Weston, and G. W. Flynn, *Chem. Phys. Lett.* **193**, 77 (1992).
- ⁸ J. Eberhard, P. S. Yeh, and Y. P. Lee, *J. Chem. Phys.* **107**, 6499 (1997).
- ⁹ S. W. North, D. A. Blank, J. D. Gezelter, C. A. Longfellow, and Y. T. Lee, *J. Chem. Phys.* **102**, 4447 (1995).
- ¹⁰ P. D. Lightfoot, S. P. Kirwan, and M. J. Pilling, *J. Phys. Chem.* **92**, 4938 (1988).
- ¹¹ E. L. Woodbridge, T. R. Fletcher, and S. R. Leone, *J. Phys. Chem.* **92**, 5387 (1988).
- ¹² G. E. Hall, H. W. Metzler, J. T. Muckerman, J. M. Preses, and R. E. Weston Jr., *J. Chem. Phys.* **102**, 6660 (1995).

The effect of large amplitude motion on the vibrational level structure and dynamics of internal rotor molecules

David S. Perry, Principal Investigator
University of Akron, Akron OH 44325-3601
DPerry@UAkron.edu

This project involves several different spectroscopic approaches to understanding large amplitude vibrational motion in methanol and its role in vibrational energy couplings. The methods employed include high-resolution spectroscopy in the 1.5 and 3 micron regions at the University Akron and IRLAPS spectroscopy up to the higher overtones in collaboration with Rizzo's group in Lausanne Switzerland. In addition to these laser-based methods, high resolution FTIR in the far-, mid-, and near-infrared regions are obtained in collaboration with Dr. Horneman at the U. of Oulu, Finland, Drs. Klee and Lock at Liebig U. in Gissen Germany, and Dr. Robert Sams at the Pacific Northwest National Laboratory. Publications acknowledging this project that have appeared since 2000 are referenced as numbers in parenthesis ().

A. Methanol

1. Torsional Coupling with the OH Stretch

The coupling of small amplitude vibrations to torsional motion is most directly revealed by accessing combination states involving excitation of both torsional motion and a small amplitude vibration. Because the first excited torsional state $v_{12}=1$ is close to the top of the torsional barrier and $v_{12}=2$ is well above it, these states allow all torsional conformations to be sampled. We have discovered that such torsional combination states can be observed as direct excitations from the vibrational ground state. The large torsional tunneling splitting in these states causes the spectra to be spread out over 100's of cm^{-1} . As a result, the structure of these bands is readily assignable and analyzable even in moderately low resolution single resonance spectra. The spectra have been fit to a global Hamiltonian to yield the vibrational dependence of the torsional parameters (5), and the observed trends are supported by *ab initio* calculations (3). A Franck-Condon model was developed (5) to account for the selection rules and relative intensities of these off-diagonal transitions. The capability of direct excitation of torsional combination states makes possible some of the experiments described below and other experiments that are planned.

Because much of the vibrational dynamics of methanol appears to be controlled by the "accidental" resonance of coupled states, spectra of ^{13}C methanol provide a needed check on the validity of the interpretation. The ^{13}C methanol spectra confirm the pattern and magnitude of torsion-vibration coupling found for ^{12}C methanol (6).

2. Torsional Coupling with the CH Stretch

In the fundamental region, our high resolution spectra have shown that the torsional tunneling splittings for the v_2 and v_9 vibrations are inverted relative to the ground state. Because this energy level structure was not consistent with existing Hamiltonians, we developed an internal coordinate Hamiltonian to explain the results.

The model takes into account torsional motion that interchanges the identities of the CH bonds that are *anti* and *gauche* to the OH bond. The coupling of the CH stretches with the torsion is strong enough to produce a spectral splitting of 42 cm^{-1} .

Based on symmetry considerations in systems with 3-fold internal rotation and on an analysis of our Hamiltonian, we proposed that inverted torsional structure should be a general phenomenon applicable to other modes and other systems. That expectation is now supported by *ab initio* calculations¹ and confirmed by L.-H. Xu and R.M. Lees by the assignment by of high resolution methanol spectra of the methyl rock² and HCH bends. Hougen has recently generalized the group theoretical framework for this effect.³

Because the torsional tunnelling splitting is an order of magnitude larger in torsionally excited states ($v_{12} \geq 1$) than in the lowest torsional state ($v_{12}=0$), CH-stretch-torsion combinations provide a much more sensitive probe of the torsional coupling parameters. The successful direct excitation of OH+torsional combinations, as described above, led us to look for CH+torsion combinations in the "empty" spectral region between the CH and OH fundamentals (3100 to 3500 cm^{-1}). This region was recorded for us by V.M. Horneman using a high-resolution FTIR and a 500 m multipass cell. The spectrum contains a good number of prominent spectral branches and many weaker lines. Assignments are continuing and up to now follow the pattern of our model calculation.

CH+OH combinations provide a useful probe of torsionally-mediated couplings involving the CH and OH stretches. OH stretch excitation is not expected to change the ordering of levels in the CH region but it will change the frequencies and splittings to allow a check on the form of the model Hamiltonian. Because this region is very weak and is expected to be just as congested as the CH fundamental region, we have implemented CW cavity ringdown detection with our slit-jet apparatus. This technique has shown good sensitivity and well-resolved spectra of one major band have been recorded.

3. Torsion-Rotation Coupling

Through a collaboration with Yun-Bo Duan, we have contributed to the optimization of the methanol Hamiltonian for high levels of excitation of both torsion and rotation. The best previous Hamiltonian was only able to fit the microwave and far-infrared data up to the first torsionally excited state to spectroscopic accuracy. The new approach provides a systematic way of optimizing the choice of spectroscopic parameters. Duan *et al.*⁴ have developed the theory and we are helping with the applications to certain methanol datasets. We have now been able to fit the data up to the second torsionally excited state to spectroscopic accuracy without increasing the number of parameters and we anticipate reasonable fits up to the highest torsional levels observed. This work involves several methanol isotopomers and we have discovered interspecies transitions in the asymmetric isotopomer, CH_2DOH (7).

4. Global Spectral Data

We now have complete coverage of the overtone spectrum of methanol from $4,900$ to $14,000\text{ cm}^{-1}$ and in specific regions as high as $28,000\text{ cm}^{-1}$. In addition to the OH stretch overtones, this region contains the CH overtones and several OH combinations with the COH bend and the CO stretch. The band positions have been fit to an anharmonic Hamiltonian. In the far infrared region, we have assignments for several

torsional overtones that have not yet appeared in the literature. Based on this work, on unpublished FIR and FTIR data, and on published work, we have compiled an extensive catalog of experimental vibrational energy levels that are the targets needed for modelling and for quantum calculations of the nuclear motion.

5. The Role of a Potentially Reactive Pathway

Consider two results from our recent publications on vibrational mode coupling in methanol:

1. The 50 cm^{-1} splitting observed in the $5\nu_1$ region of the OH stretch overtone manifold is assigned to an interaction between the OH and CH stretch vibrations. The coupling matrix element (23.5 cm^{-1}) between the $5\nu_1$ and $4\nu_1+\nu_2$ bands is thought to arise predominantly from the coupling of the CH bond anti to the OH bond.

2. Rotationally resolved and state-selected spectra in the OH stretch manifold show an increase in the torsional barrier height from 373 cm^{-1} in the vibrational ground state to more than 600 cm^{-1} when 6 quanta of the OH stretch are excited. The variation of the torsional barrier with OH stretch excitation reflects a strong coupling between these degrees of freedom.

Our *ab initio* calculations on methanol (MP2/6-311+G(2d,p) and higher levels) show how these two observations are related. When both the OH and anti CH bonds are substantially extended, the CO bond shortens and the geometry adjusts to reflect the potentially reactive pathway



Because of the formation of a CO double bond in formaldehyde, the resulting energy is substantially less than would be predicted by independent OH and CH bond extensions. The *ab initio* calculations show that the effect of this potentially reactive pathway extends well down into the bound region. The formaldehyde channel accounts for the observed OH – CH coupling (result 1. above) and it predicts induced partial double bond character on the C-O bond – and hence a higher torsional barrier – as the O-H bond is excited (result 2. above).

B. Nitromethane

Because the four heavy atoms are planar, nitromethane has a very low 6-fold barrier ($V_6=2.1\text{ cm}^{-1}$) to internal rotation. In methanol, we found an anomalous ordering of the torsional levels built on the asymmetric CH stretch vibrations. The treatment that we developed indicates that this should be a very general phenomenon, and nitromethane provides the opportunity to extend the concepts to a 6-fold potential. The low resolution work of Cavagnat and Lespade⁵ indicates very strong torsion vibration coupling in nitromethane.

High-resolution slit-jet FTIR spectra of the asymmetric NO stretch have been recorded for us at PNNL by Bob Sams. Assignments on this well-resolved low-temperature spectrum have begun.

C. Future Plans

During the next year, effort will be focused on analysis of the existing spectra noted above in sections A.2., A.3., and B. and on continued development and extension

of the CW cavity ringdown slit-jet experiment. Manuscripts on sections A.4. and A.5. are in preparation.

D. Footnotes

- ¹ L.-H. Xu, *J. Chem. Phys.* **113**, 3980 (2000).
- ² R. M. Lees and L.-H. Xu, *Phys. Rev. Lett.* **84**, 3815 (2000).
- ³ J. T. Hougen, *J. Mol. Spectrosc.* **207**, 60 (2001).
- ⁴ Y.-B. Duan, L. Wang, I. Mukhopadhyay, and K. Takagi, *J. Chem. Phys.* **110** (2), 927 (1999); Y.-B. Duan, L. Wang, X. T. Wu, I. Mukhopadhyay, and K. Takagi, *J. Chem. Phys.* **111** (6), 2385 (1999).
- ⁵ D. Cavagnat and L. Lespade, *J. Chem. Phys.* **106** (19), 7946 (1997).

E. Publications from this work, 2000 – 2002

- (1) A. V. Chirokolava, D. S. Perry, and L.-H. Xu, Sub-Doppler infrared spectra of the O-H stretch fundamental of ¹³C-methanol, *J. Mol. Spectrosc.* **203**, 320–329 (2000).
- (2) A. Chirokolava, D.S. Perry, O.V. Boyarkin, M. Schmidt, and T.R. Rizzo, Intramolecular energy transfer in highly vibrationally excited methanol. IV. Spectroscopy and dynamics of ¹³CH₃OH, *J. Chem. Phys.* **113**, 10068-10072 (2000).
- (3) M.A. Temsamani, L.-H. Xu, and D. S. Perry, Vibrational dependence of the torsional tunneling splitting and the a to b intensity evolution in the OH overtone spectra of CH₃OH, *Can. J. Phys.* **79**, 467-477 (2001).
- (4) L. Wang, Y.-B. Duan, I. Mukhopadhyay, D. S. Perry, and K. Takagi, On the physical interpretation of torsion-rotational parameters for CH₃OD isotopomers, *Chem. Phys.* **263**, 263-279 (2001).
- (5) David Rueda, Oleg V. Boyarkin, Thomas R. Rizzo, Indranath Mukhopadhyay and David S. Perry, Torsion-rotation analysis of OH stretch overtone-torsion combination bands in methanol, *J. Chem. Phys.* **116**, 91-100 (2002).
- (6) A. Chirokolava, David S. Perry, O.V. Boyarkin, M. Schmid, and T.R. Rizzo, Rotational and torsional analysis of the OH-stretch third overtone in ¹³CH₃OH, *J. Mol. Spectrosc.* **211**, XXX-XXX (2002).
- (7) Indranath Mukhopadhyay, David S. Perry, Yun-Bo Duan, John C. Pearson, S. Albert, Rebecca A.H. Butler, Eric Herbst, and Frank C. De Lucia, Observation and analysis of high-J inter-species transitions in CH₂DOH, *J. Chem. Phys.* **116**, 3710-3717 (2002).

Partially-Premixed Flames in Internal Combustion Engines

Professor Robert W. Pitz, Program Manager and Principal Investigator
Department of Mechanical Engineering, Vanderbilt University, Nashville, TN 37235
robert.w.pitz@vanderbilt.edu

Dr. Michael C. Drake and Dr. Todd D. Fansler, Co-Principal Investigators
General Motors R & D Center, 30500 Mound Road, Warren, MI 48090-9055
michael.c.drake@gm.com todd.d.fansler@gm.com

Professor Volker Sick, Co-Principal Investigator
Department of Mechanical Engineering, University of Michigan
2023 W. E. Lay Automotive Laboratory, Ann Arbor, MI 48109-2121
vsick@umich.edu

Program scope

The purposes of this joint university-industry research program are: 1) to use advanced laser diagnostics and detailed chemistry models to understand partially-premixed flames in unique laboratory burners, 2) to use advanced laser diagnostics to observe and characterize partially-premixed combustion in optically-accessible direct injection gasoline engines, and 3) to more fully develop laser diagnostic techniques for temperature and flame front imaging in partially-premixed flames and IC engines. The work is being done primarily at Vanderbilt University, General Motors Research and Development Center, and the University of Michigan.

The goals of this research are 1) a better understanding of the effects of strain and curvature on partially-premixed flame structure, 2) better conceptual models of partially-premixed combustion in highly stratified direct injection engines for automotive applications, and 3) improved and more robust laser diagnostic methods for use in university and industrial environments.

Recent progress

At Vanderbilt, a visible laser-based Raman system has been developed to obtain relatively-interference-free Raman signals in hydrocarbon and hydrogen flames (Osborne et al. 2000). Figure 1 shows a schematic of this system, which uses a frequency-doubled, Q-switched Nd-YAG laser as the Raman excitation source and a cryogenically-cooled CCD as the detector. This system has been applied to the analysis of opposed jet flames burning C_3H_8 (Wehrmeyer et al. 2001, 2002; Cheng et al. 2002), with these flames chosen in order to simulate what is expected to occur in a stratified-charge direct injection spark ignition (DISI) engine, where hot products impinge upon a zone of either lean or rich reactants. Various combinations of partial premixedness were studied, and in particular several flows involved a very lean C_3H_8 -air reactant jet impinging upon hot products produced by a lean H_2 -air flame. Most recently curved, premixed hydrogen-air tubular flames have been examined using the visible Raman system and a unique cylindrical burner developed at Vanderbilt (Mosbacher et al. 2001, 2002a, 2002b).

Figure 2 shows a schematic of the Vanderbilt cylindrical burner. A premixed combustible mixture is introduced to the outer circular chamber via a plenum with 16 circumferentially spaced inlet ports. The reactant mixture diffuses through fine gauge stainless steel wool (used to provide a uniform radial pressure drop in the flow chamber) and exits through a converging cylindrical nozzle of 1.5 cm radius and 2 cm height. A premixed tubular flame, with products exiting radially inward from the flame and the reactants flowing radially inward toward the flame, is formed around the cylindrical axis of the burner. The flame location is the radial position where the burning velocity balances with the upstream radial velocity of the unburned mixture. In this manner, premixed tubular flames of various radii can be formed by adjusting the reactant mixture velocity, thus controlling the degree of curvature and aerodynamic straining. A unique feature of the tubular burner is the provision of three optical access ports. Two laser access ports, located at 180° from each other, are 25 mm in diameter. A third 50 mm diameter optical port, located at right angles to the laser ports, is used by the light detection system to collect scattered light.

The axisymmetric flow-field in the tubular burner radially converges and axially diverges. Consequently, the tubular flame is stabilized by a finite rate of stretch. A specific expression for the global stretch rate, κ , in the tubular flame can be derived from this expression and is given as

$$\kappa \cong \frac{2V}{R},$$

where V is the radial inlet velocity, and R is the nozzle radius (1.5 cm).

In order to numerically model premixed tubular flames, the standard Oppdif program was modified to account for the radial geometry. Oppdif normally models opposed jet flames of axial symmetry, where the reactants originate along the symmetry axis and exit radially away from the axis. Flame structure is then mapped onto the axial dimension. In a tubular flame, the radial coordinate, instead of the axial coordinate, is used as the spatial dimension through which flame structure is mapped. By transforming the spatial coordinate and seeking a similarity solution of the two-dimensional conservation equations, the tubular flame can be modeled as a two-point boundary value problem. For this current work, the Oppdif program was modified for the tubular flame geometry.

Numerical simulations for the experimental premixed H_2 -air tubular flames examined were performed with detailed transport and complex chemistry. Several H_2/O_2 chemical kinetic mechanisms were examined. Gas phase radiation in the optically-thin limit was assumed.

Figure 3 shows a comparison of Raman temperature measurements with numerical simulations using four different chemical kinetic reaction mechanisms including thermal diffusion effects. Data from both sides of the tubular flame centerline are plotted versus radius to illustrate the axisymmetric structure of the flame. The adiabatic equilibrium flame temperature is also shown by the horizontal line at ~ 875 K to emphasize thermal-diffusion/curvature effects. Figure 3 is for a flame with a stretch rate of 90 s^{-1} and measured temperature of ~ 1295 K, which is ~ 420 K above the adiabatic flame temperature. Comparison of the mechanisms reveals that the kinetics of Mueller et al. and Yetter et al. are the strongest, leading to higher flame speeds, larger flame radii, less fuel focusing, and lower flame temperatures. Reaction mechanism trends illustrated in Fig. 3 are representative of all the stretch rates examined. At higher stretch rates significant differences are detected among the experimental and numerical data sets, indicating low temperature H_2/O_2 chemical kinetics models may need improvements.

At General Motors, graduate students from the University of Michigan (B. Stojkovic) and Vanderbilt University (M. Mosbacher) worked with Drs. Drake and Fansler during the Summer of 2001 to examine ultraviolet and visible combustion emission spectra in a DISI engine for different operating conditions. Drawing on the results of this study, experiments to combine spectrally resolved high-speed combustion imaging (Fansler et al. 2001a) with simultaneous spark-emission spectroscopy measurements of local fuel-air equivalence ratio were begun. The spark-spectroscopy technique was originally developed at GM in 2000-2001 with Stojkovic's collaboration under GM funding (Fansler et al. 2001b). Extension and systematic application of this combined approach during 2002 will be included in Stojkovic's doctoral thesis. A recent report of this work is in Fansler et al. (2002).

At the University of Michigan, quantitative two-dimensional measurements of equivalence ratios were pursued in an optically-accessible direct-injection gasoline engine. Because of the unique quenching properties of toluene, which are essentially dominated by collisions with molecular oxygen, the laser induced fluorescence signal of toluene is proportional to the number density of toluene molecules (used as a tracer in the non-fluorescing fuel, iso-octane) and is inversely proportional to the number density of molecular oxygen. This results from the quenching rate being directly proportional to the number density of molecular oxygen. Thus, irrespective of the absolute number density of fuel, local measurements of equivalence ratios are possible.

Calibration of equivalence ratio measurements was performed by several means. The amount of fuel injected is known from the injector characteristics, and the amount of air trapped in the cylinder could be determined via flow rate measurements using critical orifices. This measurement is confirmed via a commercial lambda meter that was used in the engine exhaust.

However, several issues remain. Local inhomogeneities in the equivalence ratio do not allow an unambiguous calibration. Therefore, the calibration is performed for engine operation conditions where the fuel is injected very early and thus has time to completely evaporate and mix. A high level of homogeneity was achieved through this procedure.

A KrF excimer laser was used to excite toluene fluorescence. It is known that the fluorescence signals of this excitation scheme will exhibit a substantial temperature dependence that has to be taken into account for quantitative measurements. However, two-dimensional in-situ temperature measurements in engines are very difficult and need further development. It had been demonstrated by Einecke et al. (2000) that this can be achieved with a two-line excitation approach and a similar technique has been proposed to DOE in a recent proposal by using toluene as a fluorescent temperature indicator. This would have the advantage of higher signal strength compared to 3-pentanone as used by Einecke et al. (2000) and it would also directly yield equivalence ratios at the same time.

For homogenous fuel distributions, as in the described study, one can measure the signal strength as a function of crank angle and hence, temperature and pressure variation. Since it is known that the equivalence ratio is constant and homogenous the temperature influence can actually be determined. As the LIF signal is both proportional to the number density of tracer and oxygen the signal can only vary because of temperature changes. Figure 4 shows the relative toluene signal as a function of crank angle, normalized to the signal at top dead center.

Future plans in the current project period

At Vanderbilt, the effect of flame curvature on cylindrical partially premixed flames will be assessed numerically and experimentally. To accomplish this a sintered metal tube will be inserted into the cylindrical burner to allow two different radial flows to be created. The visible Raman system will be applied to this reconfigured burner by obtaining Raman data along an off-center chord that pierces the tubular flame at two locations.

At the University of Michigan, it is hoped that DOE will fund work that will investigate the temperature dependent LIF signals of toluene as it is expected that a robust temperature imaging diagnostic technique can be developed. For the remainder of the ongoing project, the use of the simple 'temperature correction' strategy for homogenous conditions will be evaluated for applications under firing conditions and late injection, i. e. inhomogeneous conditions.

Publications acknowledging DOE support

- Cheng, Z., J. A. Wehrmeyer, and R. W. Pitz. 2002. "Opposed Jet Flames of Lean Premixed Hydrocarbon-Air Reactants vs. Hot Products." Paper presented at the Spring Technical Meeting of the Combustion Institute Central States Section, Knoxville, TN, April 8-9.
- Fansler, T. D., B. Stojkovic, M. C. Drake, and M. E. Rosalik. 2002. "Spark-Emission-Spectroscopy Measurements of Local Fuel-Air Ratio in Internal Combustion Engines", Paper presented at the Spring Technical Meeting of the Combustion Institute Central States Section, Knoxville, TN, April 8-9.
- Mosbacher, D. M., J. A. Wehrmeyer, and R. W. Pitz. 2002a. "Experimental and Numerical Investigation of Tubular Flames." accepted for publication, 29th Symposium (International) on Combustion.
- Mosbacher, D. M., J. A. Wehrmeyer, R. W. Pitz, C.-J. Sung, and J. L. Byrd. 2002b. "Experimental and Numerical Investigation of Premixed Cylindrical Flames." Paper presented at the 40th AIAA Aerospace Sciences Meeting, Reno, NV, Jan. 14-17.
- Mosbacher, D. M., J. A. Wehrmeyer, R. J. Osborne, Z. Cheng, R. W. Pitz, and C. J. Sung. 2001. "Investigation of Partially-Premixed Cylindrical and Axial Opposed Jet Propane-Air Flames," Paper presented at the Joint Meeting of the United States Sections of the Combustion Institute, Oakland, CA, March 25-28.
- Osborne R. J., J. A. Wehrmeyer, and R. W. Pitz. 2000. "A Comparison of UV Raman and Visible Raman Techniques for Measuring Non-Sooting Partially Premixed Hydrocarbon Flames," AIAA 38th Aerospace Sciences Meeting, Paper No. AIAA-2000-0776, Reno, Nevada, January 10-13.
- Sick, V., B. Stojkovic. 2001. "Attenuation Effects on Imaging Diagnostics of Hollow-Cone Sprays," *Applied Optics*, 40, (15) pp. 1-8.
- Stojkovic, B., V. Sick. 2001. "Evolution and Impingement of an Automotive Fuel Spray Investigated with Simultaneous Mie/LIF Techniques," *Applied Physics B* 73:75-83.
- Wehrmeyer, J. A., Z. Cheng, D. M. Mosbacher, and R. W. Pitz. 2002. "Opposed Jet Flames of Lean or Rich Premixed Propane-Air Reactants vs. Hot Products." *Combustion and Flame* 128: 2232-241.
- Wehrmeyer, J. A., R. J. Osborne, D. M. Mosbacher, Z. Cheng, R. W. Pitz, and C.-J. Sung. 2001. "Investigation of Partially Premixed Propane-Air Flames with Flame Curvature," AIAA 39th Aerospace Sciences Meeting, Paper No. AIAA-2001-1083, Reno, Nevada, January 8-11.

Other references cited above

- Einecke, S., Schulz, C., Sick, V. 2000. "Measurement of Temperature, Fuel Concentration and Equivalence Ratio Fields using Tracer LIF in IC Engine Combustion," *Applied Physics B* 71, pp. 717-723.
- Fansler, T. D., M.C. Drake, B. Stojkovic, M.E. Rosalik. 2001a. "Optical Studies of Mixture Preparation, Ignition and Combustion in a Spark-Ignited Direct-Injection Engine," submitted to *Intl. J. Engine Research*.
- Fansler, T. D., B.E. Stojkovic, M.C. Drake and M.E. Rosalik. 2001b. "Local Fuel-Air Ratio Measurements in Internal Combustion Engines Using Spark-Emission Spectroscopy," submitted to *Applied Physics B*.

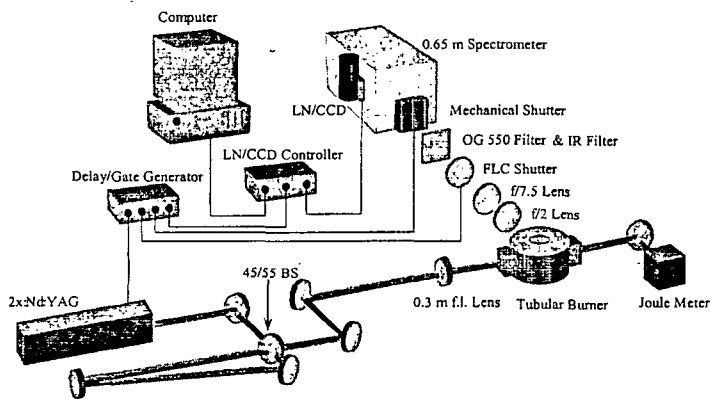


Fig. 1. Schematic of visible Raman system using cryogenically-cooled CCD camera.

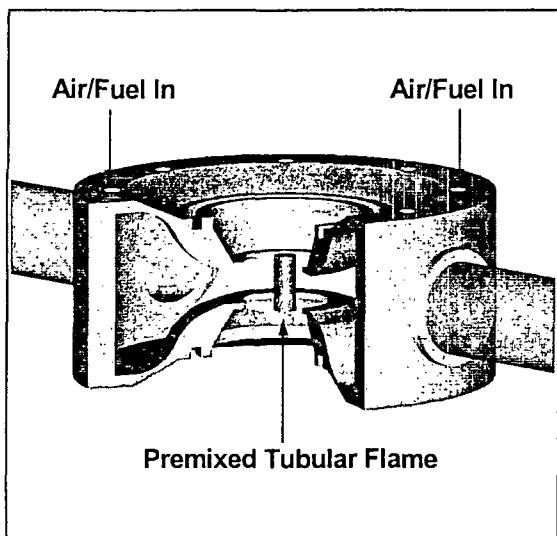


Fig. 2. Schematic of Vanderbilt Cylindrical Burner.

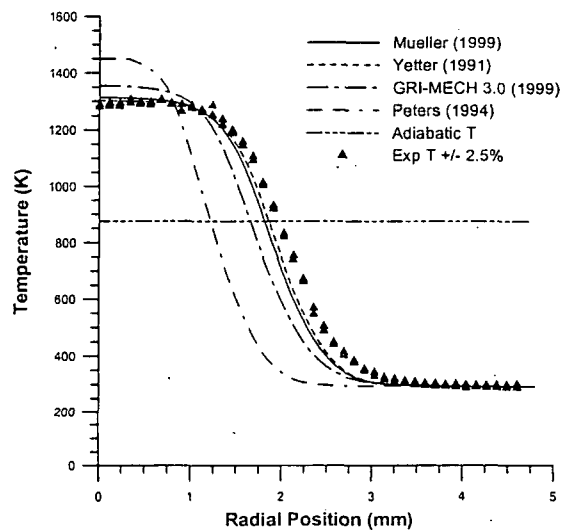


Fig. 3. Comparison of predicted temperature profiles from 4 reaction mechanisms in a premixed H_2 -air tubular flame ($\phi=0.175$, $\kappa=90 \text{ s}^{-1}$).

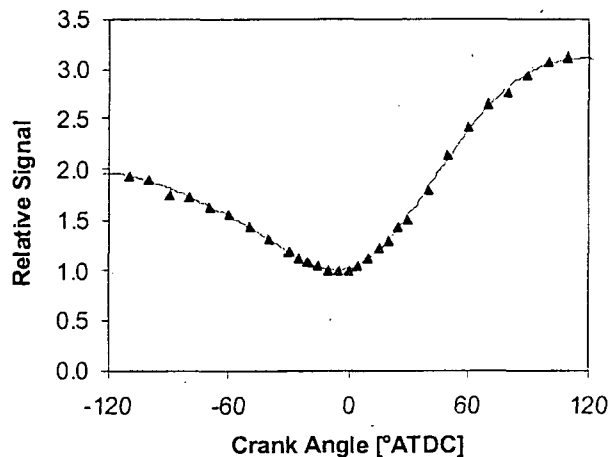


Fig. 4. Relative toluene signal as a function of crank angle, normalized to the signal at top dead center.

INVESTIGATION OF NON-PREMIXED TURBULENT COMBUSTION

Grant: DE-FG02-90ER14128

Principal Investigator: Stephen B. Pope
Sibley School of Mechanical & Aerospace Engineering
Cornell University
Ithaca, NY 14853
pope@mae.cornell.edu

Introduction

It is desirable to design combustion equipment to maximize the efficient utilization of the fuel, while minimizing the environmental impact of the combustion products. In most of the industries involved, turbulent combustion models are employed as a primary design tool. These are computer models that predict the combustion performance by solving a set of equations that model the fundamental physical and chemical processes involved. The turbulent combustion models considered in this project are PDF methods, in which a modelled transport equation is solved for the joint probability density function of velocity, turbulence frequency, and the thermochemical composition of the fluid (species mass fractions and enthalpy). The modelled PDF equation is solved numerically using a particle/mesh method.

An emphasis of the research is making detailed comparisons between the PDF model calculations and the experimental data obtained at Sandia (e.g., Barlow & Frank 1998). In the last several years, much attention has been devoted to the numerical methods used to solve the PDF equations. Several substantial advances have been made (outlined below) which have improved both the numerical accuracy of the calculations and their computational efficiency. In addition, work is continuing on making PDF calculations of bluff body flames with detailed chemistry and comparing the results with the available experimental data (e.g., Dally et al. 1998). We expect this work to be presented in July 2002 at TNF6 (the Sixth International Workshop on the Measurement and Computation of Nonpremixed Turbulent Flames).

The Consistent Hybrid Algorithm

The work of Muradoglu et al. (2001) is an important step in the development of improved PDF algorithms, and it draws together previous contributions of Jenny et al. (2001a,b).

The hybrid method solves the modelled transport equation for the joint PDF of velocity, turbulence frequency and compositions for turbulent reactive flows. A finite-volume (FV) method is used to solve the mean conservation equations for mass, momentum and energy and the mean equation of state; and a particle method is used to solve the modelled PDF equation. The method is completely consistent at the level of the governing equations solved by the FV and particle algorithms. The conditions to be fulfilled for full consistency at the numerical solution level are determined and the independent consistency conditions are identified. Correction algorithms are developed to enforce these independent consistency conditions to achieve full consistency at the numerical solution level. In addition, a new formulation of the energy equation and the equation of state is developed which is both general and simple. The hybrid method is applied to a non-premixed piloted jet flame, and the numerical results show that the correction algorithms are completely successful in achieving consistency. The convergence of the method is demonstrated; and, in particular, it is shown that the bias error is dramatically reduced (compared to that in previous PDF calculations). In addition, the results are shown to be in a good agreement with some earlier PDF calculations and also with the available experimental data. Because of the substantially

reduced numerical error (for given grid size and number of particles), the hybrid method represents a significant advance in the computational efficiency of particle/mesh method for the solution of PDF equations.

Local Time Stepping

A local time stepping algorithm has been developed (Muradoglu & Pope 2002) to improve the numerical efficiency of Lagrangian particle-based Monte Carlo methods for obtaining the steady-state solutions of the modelled PDF equations of turbulent reacting flows. On each step in the pseudo-time marching algorithm, the properties of each particle are advanced by a time step, the magnitude of which depends on the particle's spatial location. This algorithm has been incorporated into the consistent hybrid finite volume (FV)/particle method. The performance of the local time stepping method is evaluated in terms of numerical efficiency and accuracy through application to a non-reacting bluff body flow. For this test case, it is found that local time stepping can accelerate the global convergence of the hybrid method by as much as an order of magnitude, depending on the grid stretching. Additionally, local time stepping is found to improve significantly the robustness of the hybrid method mainly due to the accelerated convection of error waves out of the computational domain. The method is very simple to implement, and the small increase in CPU time per step (typically 3%) is a negligible penalty compared to the substantial reduction in the number of time steps required to reach convergence.

Transport Algorithm for Composition PDF Methods

In the composition PDF method (in contrast to the velocity-composition PDF method), computational particles move in space according to a stochastic differential equation (SDE). Such equations are difficult to integrate accurately and efficiently, and most schemes in use are only first-order accurate.

In the work of Cao & Pope (2002), a weak second-order accurate mid-point scheme for the stochastic differential equations (SDE's) arising in the composition PDF method for turbulent reactive flows is proposed and tested. The results are compared with two other schemes which are commonly used in the composition PDF method. In contrast to most higher-order schemes for SDE's, the present scheme uses a mid-point, which makes it especially suitable for the implementation of the position-advance fractional step in the composition PDF method. The scheme can also be applied to the PDF method used in conjunction with large eddy simulation (LES), since the SDE's considered include explicit time dependence of the drift and diffusion coefficients. Test calculations, including a 2D unsteady case, demonstrate the weak second-order accuracy of the scheme. A new methodology for developing higher-order schemes for SDE's (by comparing the moments of the increments of the numerical approximation with those of the exact increments) is used to develop this scheme.

Bluff Body Stabilized Flames

In the work of Muradoglu, Liu and Pope (2002), the velocity-turbulent frequency-composition PDF method combined with the consistent hybrid finite volume (FV)/particle solution algorithm is applied to a bluff-body stabilized turbulent flame. The statistical stationarity of the solution is shown, and the performance of the PDF method is assessed by comparing the mean yields with the available experimental data. The effects of the model constants C_{ω_1} (in the turbulence frequency model) and C_{ϕ} (in the mixing model) on the solutions are examined and it is found that all the mean fields are very sensitive to the changes in C_{ω_1} , while only the mixture fraction variance is sensitive to the changes in C_{ϕ} . The spatial and bias errors are also examined and it is shown that the hybrid method is second-order accurate in space, and that the bias error is vanishingly small in all the

mean fields. The required grid size and the number of particles per cell are determined for a 5% error tolerance.

Current Work and Future Plans

In the work just described, the simplest possible treatment of the chemistry is used, namely a steady flamelet/PDF model. Our current work on the bluff body flames uses a 19-species augmented reduced mechanism implemented via the ISAT algorithm (Pope 1997). Results are expected in time for the TNF6 meeting in Japan in July, 2002. Calculations may also be performed of swirling bluff body flames using detailed chemistry, to extend the work of Masri et al. (2000).

References

1. R.S. Barlow and J.M. Frank (1998) Twenty-seventh Symp. (Int'l) on Combust., p. 1087, Pittsburgh, The Combustion Institute.
2. R. Cao and S.B. Pope (2002) "Numerical integration of stochastic differential equations: weak second-order mid-point scheme for applications in the composition PDF method," J. Comput. Phys. (submitted).
3. B.B. Dally, D.F. Fletcher and A.R. Masri (1998) "Flow and mixing fields of turbulent bluff body jets and flames." *Combust. Theory Modelling*, **2**, 193-219.
4. P. Jenny, S.B. Pope, M. Muradoglu and D.A. Caughey (2001a) "A hybrid algorithm for the joint PDF equation for turbulent reactive flows," *J. Comp. Phys.* **166**, 281-252.
5. P. Jenny, M. Muradoglu, K. Liu, S.B. Pope, D.A. Caughey (2001b) "PDF simulations of a bluff-body stabilized flow," *J. Comp. Phys.* **169**, 1-23.
6. A.R. Masri, S. B. Pope and B.B. Dally (2000) "PDF computations of a strongly swirling nonpremixed flame stabilised on a new burner," *Proceedings of the Combustion Institute*, **28**, 123-131.
7. M. Muradoglu, S.B. Pope and D.A. Caughey (2001) "The hybrid method for the PDF equations of turbulent reactive flows: consistency conditions and correction algorithms," *J. Comp. Phys.* **172**, 841-878.
8. M. Muradoglu, K. Liu and S.B. Pope (2002) "PDF Modeling of a Bluff-Body Stabilized Turbulent Flame," *Combust. Flame* (submitted).
9. M. Muradoglu and S.B. Pope (2002) "A local time stepping algorithm for solving the PDF equations of turbulent reacting flows", *AIAA Journal* (to be published).
10. S.B. Pope (1997) "Computationally Efficient Implementation of Combustion Chemistry using In Situ Adaptive Tabulation," *Combustion Theory and Modelling*, **1**, 41-63

Publications from DOE Research 2000-2002

1. R. Cao and S.B. Pope (2002) "Numerical integration of stochastic differential equations: weak second-order mid-point scheme for applications in the composition PDF method," *J. Comput. Phys.* (submitted).
2. P. Jenny, S.B. Pope, M. Muradoglu and D.A. Caughey (2001) "A hybrid algorithm for the joint PDF equation for turbulent reactive flows," *J. Comp. Phys.* **166**, 281-252.
3. P. Jenny, M. Muradoglu, K. Liu, S.B. Pope, D.A. Caughey (2001) "PDF simulations of a bluff-body stabilized flow," *J. Comp. Phys.* **169**, 1-23.
4. A.R. Masri, S.B. Pope and B.B. Dally (2000) "PDF computations of a strongly swirling nonpremixed flame stabilised on a new burner," *Proceedings of the Combustion Institute*, **28**, 123-131.
5. M. Muradoglu, K. Liu and S.B. Pope (2002) "PDF Modeling of a Bluff-Body Stabilized Turbulent Flame," *Combust. Flame* (submitted).
6. M. Muradoglu and S.B. Pope (2002) "A local time stepping algorithm for solving the PDF equations of turbulent reacting flows", *AIAA Journal* (to be published).
7. M. Muradoglu, S.B. Pope and D.A. Caughey (2001) "The hybrid method for the PDF equations of turbulent reactive flows: consistency conditions and correction algorithms," *J. Comp. Phys.* **172**, 841-878.

OPTICAL PROBES OF ATOMIC AND MOLECULAR DECAY PROCESSES

S.T. Pratt

Gas Phase Chemical Dynamics Group, Chemistry Division
Argonne National Laboratory
Argonne, Illinois 60439

Telephone: (630) 252-4199

E-mail: spratt@anl.gov

PROJECT SCOPE

Molecular photoionization and photodissociation dynamics can provide considerable insight into how energy and angular momentum flow among the electronic, vibrational, and rotational degrees of freedom in isolated, highly energized molecules. This project involves the study of these dynamics in small polyatomic molecules, with an emphasis on understanding the mechanisms of intramolecular energy flow and determining how these mechanisms influence decay rates and product branching ratios. The experimental approach combines double-resonance laser techniques, which are used to prepare selected highly excited species, with mass spectrometry and high-resolution photoelectron spectroscopy, which are used to characterize the decay of the selected species. Additional techniques, including excited-state absorption spectroscopy by fluorescence-dip techniques and zero-kinetic energy-photoelectron spectroscopy are used as necessary. Ion-imaging capabilities are also currently being developed to characterize predissociation branching ratios and product angular distributions.

RECENT PROGRESS

In the past year, a significant effort was made on our continuing studies of the normal-mode dependence of vibrational autoionization in the Rydberg states of ammonia. Previously, the relative rates of autoionization via the symmetric stretch, ν_1 , and the umbrella vibration, ν_2 , were characterized by using photoelectron spectroscopy. Vibrational state distributions following autoionization of Rydberg states in which both normal modes were excited show that autoionization via the loss of one quantum from the umbrella mode dominates over autoionization via the loss of one quantum from the symmetric stretch. This observation was rationalized in terms of how the Rydberg orbitals change along the two normal coordinates. This year, analogous studies were performed on Rydberg states in which the umbrella mode and the asymmetric bending mode, ν_4 , were excited. In contrast to the results on ν_1 and ν_2 , in the new experiments the branching between decay via ν_2 and ν_4 was strongly dependent on the specific Rydberg state excited: in some cases, loss of a ν_2 quantum dominated, in others, loss of a ν_4 quantum dominated, and in yet others the two processes are equally important. Although these results can also be rationalized in terms of the normal-mode dependence of the Rydberg orbital, a detailed understanding will require more comprehensive spectroscopic assignments of the Rydberg series under study. The new experiments on ammonia also required the characterization of photoelectron spectra of the vibronic levels of the B $^1E''$ state that were used as the intermediates in the double-resonance experiments. Single-color photoelectron spectra recorded for the combination bands allowed us to identify a number of unassigned features in earlier photoelectron spectra of the B $^1E''$ state.

Progress was also made in my collaboration with Wally Glab of Texas Tech University to study the photoionization dynamics of water. In particular, difference frequency generation was used to produce VUV light to excite the $3p\ ^1B_2$ Rydberg state, which is based on the first excited state of the ion, the linear $A\ ^2A_1$ state. A probe laser was then used to excite higher Rydberg states converging to vibrationally excited levels of the $A\ ^2A_1$ state, and photoelectron spectra were recorded for selected resonances. Above the $H_2O^+ X\ ^2B_1$ state threshold, these resonances can undergo electronic autoionization into the $X\ ^2B_1$ continua, and above the $A\ ^2A_1(000)$ threshold, they can also undergo vibrational autoionization into the $A\ ^2A_1$ continuum. These studies are important for several reasons. First, they will aid in the assignment of double-resonance spectra of Rydberg series converging to excited vibrational levels of the ground state of H_2O^+ . These spectra are quite complicated due to interloping levels converging to the $A\ ^2A_1$ state of the ion, and the new spectra will allow the identification of the latter states. These spectra will also help in the interpretation of multichannel quantum defect theory calculations of the spectrum of H_2O that are currently being performed by Mark Child. In addition, the photoelectron spectra will provide insight into the competition between electronic and vibrational autoionization. Although photoelectron spectra for a number of states of interest were recorded in the past year, the laser frequencies used to generate the VUV light for the pump transition also caused significant ionization on their own. This additional source of ions degraded the resolution of the electron spectrometer and made it difficult to calibrate the spectra. This year, Wally has developed a simple method to separate the generating beams from the VUV light, and his approach will be implemented at Argonne this summer. Thus, it is expected that we will be able to record high quality photoelectron spectra for autoionizing resonances of water in the next few months.

A collaboration has recently been developed with Ed Grant of Purdue University to use photoelectron spectroscopy to study the vibrational autoionization dynamics of high Rydberg states of NO_2 . These studies will follow along the lines of the measurements on NH_3 . The spectroscopy of the NO_2 Rydberg states of interest has been characterized by Ed's group, and the photoelectron measurements to be performed at Argonne will be used to determine product branching ratios and the relative rates for autoionization via different normal modes of the molecule. Initial work will focus on two studies. In the first, we will characterize the ionic products following autoionization of series with one quantum in the symmetric stretch and one in the bending vibration. This work will allow the determination of the relative autoionization rates for the two modes. In the second study, we will attempt to characterize the effect of the Fermi resonance of one quantum in the symmetric stretch and two in the bend on the vibrational autoionization dynamics. This work is currently underway, and a student from Ed's group will work with us at Argonne for the next two months.

In general, the high Rydberg states of molecules can undergo predissociation as well as autoionization, and because the initial energy is usually considerably larger than the dissociation energy, the predissociation products can be formed in a distribution of final states. These final state branching fractions provide considerable information on the dynamics of the predissociation process. In the past, I have used resonance enhanced multiphoton ionization and traditional detection techniques to probe specific product channels. Ion-imaging techniques can produce a much fuller description of the dissociation dynamics by providing information on the branching ratios and product angular distributions directly. For this reason, an ion-imaging spectrometer has been constructed and a previously characterized photodissociation processes in O_2 has been

used for initial testing. This testing is now complete, and the apparatus is now being used to characterize dissociation processes relevant to the photoionization studies of NO_2 described above.

In collaboration with Timothy Zwier of Purdue University, we attempted to use photoelectron spectroscopy to characterize radiationless transitions from the $1^1\Delta_u$ state of diacetylene into the triplet manifold. In these experiments, we sought to pump the $1^1\Delta_u$ state in a supersonic expansion and to probe the products of the radiationless transition by using single-photon VUV photoionization with photoelectron energy analysis. Unfortunately, we did not succeed in recording a VUV photoelectron spectrum of the triplet species. We believe the reason for this lack of success is that the Franck-Condon factors between the triplet states and the ionic state spread the intensity in the photoelectron spectra over a large range of kinetic energies, and that the resulting signal was simply too weak to distinguish from the background signal. However, photoelectron spectra were recorded for a number of vibronic levels within the $1^1\Delta_u$ state, and a paper discussing these results was published in the *Journal of Chemical Physics*.

A similar approach to the study of radiationless transitions was applied more successfully in diazabicyclo-octane (DABCO). Earlier studies by Wallace and coworkers had shown that excitation of the S_2 origin band of DABCO resulted in a fast radiationless transition to the S_1 level. Double-resonance spectra obtained by pumping the S_2 origin showed only a weak threshold corresponding to the direct photoionization of the S_2 level, and a very intense threshold falling at the position expected for vertical photoionization of vibrationally excited DABCO in the S_1 state. Wallace and coworkers observed additional structure between these two thresholds, which they interpreted as resulting from photoionization of the previously unobserved S_- level. They suggested that this level was also populated by radiationless transitions from the S_2 level, and their analysis placed the level approximately midway between the S_1 and S_2 levels. This conclusion is at odds with quantum chemical calculations that place the S_- level at nearly the same energy as the S_2 level. I have recorded photoelectron spectra following excitation of the S_2 origin band, and, as suggested by Wallace and coworkers, these new data are completely consistent with a rapid radiationless transition from the S_2 level to the S_1 level. However, the spectra suggest an alternative explanation to the features previously assigned to photoionization of the S_- level. In particular, these features are reassigned as arising from the vibrational autoionization of Rydberg series accessed from vibrationally excited levels of the S_1 state and converging to the corresponding vibrationally excited state of the ion. This interpretation is consistent with double-resonance spectra recorded via low-lying vibrational levels of the S_1 state, and with the well-known propensity rule for vibrational autoionization. This conclusion suggests that the S_- level remains unobserved, and that, as has been suggested previously, the $S_- \leftarrow S_0$ transition lies buried beneath the much stronger features of the $S_2 \leftarrow S_0$ transition in the photoabsorption spectrum.

FUTURE PLANS

Much of the work in the near future will involve the continuation and extension of projects discussed above. In particular, studies of the photoionization dynamics of NH_3 will focus on approaches to preparing low-lying Rydberg states in which both the umbrella mode and the asymmetric stretch (ν_3) are excited; these states will then be used as intermediates to prepare autoionizing Rydberg states that will allow the comparison of autoionization rates for these two

modes. At this time, the most promising approach is to use single-photon VUV excitation of combination bands in the B ¹E" state. When combined with previous studies from my group, these experiments will allow the comparison of vibrational autoionization rates and mechanisms for all four normal modes in NH₃, and it is expected that this data set will provide significant input for the development of more complete models of vibrational autoionization in polyatomic molecules. In this regard, a theoretical study involving our group (see abstract of R. Shepard) and C. Green (NIST) will combine high order electronic structure methods with multichannel quantum defect theory to calculate the vibrational dependence of autoionization for comparison to our measurements. I am also reinitiating a collaboration with Christian Jungen of Orsay, France to develop ideas related to the theory of vibrational autoionization in polyatomic molecules, particularly with respect to processes involving degenerate electronic states. High-resolution photoelectron spectroscopy will also be used in the series of experiments on NO₂ in collaboration with Ed Grant, and in the experiments on H₂O in collaboration with Wally Glab. Finally, ion-imaging techniques will be applied to study the predissociation of high Rydberg states of NO and NO₂. Such studies are expected to provide important new insight on the interplay between predissociation and autoionization.

DOE-SPONSORED PUBLICATIONS SINCE 2000

1. C. A. Raptis, J. A. Bacon, and S. T. Pratt
DOUBLE-RESONANCE SPECTROSCOPY OF AUTOIONIZING STATES OF AMMONIA
J. Chem. Phys., **112**, 2815-2825 (2000).
2. J. A. Bacon and S. T. Pratt
PHOTOELECTRON SPECTROSCOPY OF AUTOIONIZING RYDBERG STATES AMMONIA
J. Chem. Phys. **112**, 4153-4161 (2000).
3. C. A. Raptis and S. T. Pratt
VIBRATIONAL AUTOIONIZATION IN RYDBERG STATES OF AMMONIA
Phys. Rev. Lett., **84**, 5078-5081 (2000).
4. C. A. Raptis and S. T. Pratt
MODE-DEPENDENT VIBRATIONAL AUTOIONIZATION IN ANILINE
J. Chem. Phys., **113**, 4190-4202 (2000).
5. J. A. Bacon and S. T. Pratt
PHOTOELECTRON SPECTROSCOPY OF AMMONIA: MODE DEPENDENT VIBRATIONAL AUTOIONIZATION
J. Chem. Phys. **113**, 7188-7196 (2000).
6. C. A. Raptis and S. T. Pratt
TWO-PHOTON SPECTROSCOPY OF AUTOIONIZING STATES OF AMMONIA
J. Chem. Phys. **115**, 2483-2491 (2001).
7. C. Ramos, P. R. Winter, T. S. Zwier, and S. T. Pratt
PHOTOELECTRON SPECTROSCOPY VIA THE 1 ¹Δ_u STATE OF DIACETYLENE
J. Chem. Phys., **116**, 4011-4022 (2002).
8. S. T. Pratt, J. A. Bacon, and C. A. Raptis
VIBRATIONAL AUTOIONIZATION IN POLYATOMIC MOLECULES
to appear in *Dissociative Recombination*, Edited by S. Guberman, Kluwer, New York, in press.

STUDIES IN CHEMICAL DYNAMICS

Herschel Rabitz and Tak-San Ho

Department of Chemistry

Princeton University

Princeton, NJ 08544

hrabitz@princeton.edu, tsho@princeton.edu

Program Scope

During the past year, research was done in the following three areas: (A) construction of accurate and fast-to-evaluate potential energy surfaces and calculations of corresponding dynamics for chemical reactions, (B) development and implementation of multivariate function approximation method to solve multi-dimensional quantum dynamics, and (C) development of accurate global, nonlinear mapping schemes between potential energy surfaces and laboratory data.

In category (A), in a close collaboration with Rex Skodje (University of Colorado) and Mebel (Institute of Atomic and Molecular Science, Academia Sinica), research on the reaction $S + H_2$ has been carried out. A global potential energy surface (PES) for the $1 A'$ state of the $S + H_2$ reaction has been obtained using high quality *ab initio* data at the multi-reference configuration interaction level with augmented polarized quadruple zeta basis sets. The resulting potential energy surface is analytic, first-order differentiable, and fast-to-evaluate. Extensive quasi-classical trajectory calculations, of 10,000-20,000 trajectories per energy and initial state, have also been performed for three isotopic cases: $S(D) + H_2/D_2/HD$. The calculated results for excitation functions and total differential cross sections are in good agreement with recent experimental measurements. Moreover, we have been implementing a new interpolation scheme, a successive decomposition method based on the blending-function method of Gordon and Reproducing Kernel Hilbert Space (RKHS) theory, for the accurate and efficient construction of multi-dimensional PESs. Preliminary studies of this new method on a number of triatomic systems, including $C+H_2$, $S+H_2$ and $O+H_2$, have shown that when compared to the conventional tensor product approach the new method can achieve a specified accuracy with much (\sim twice) fewer *ab initio* data.

In category (B), research has been concentrated on developing robust multivariate rational approximation methods using only scattered data, aiming to efficiently and accurately solve time-dependent multi-dimensional quantum fluid dynamics (QFD) equations in the Lagrangian description. The procedure holds promise as a rigorous means to accelerate the solution of multi-dimensional reactive dynamics.

To this end, two particular representations of the method, in conjunction with an effective domain decomposition technique, have been formulated and implemented. Numerical examples, for three- and six-dimensional cases, have demonstrated that the new method is reliable in generating accurate approximations, not only for the functional values but also for the corresponding first- and second-order derivatives. Preliminary study on photo-dissociation dynamics showed that the current method is robust and allows for long-time propagation of the QFD wave packets.

In category (C), research has pursued the construction of high quality potential energy surfaces from measurements of laboratory data. To this end, a recently developed non-iterative, global algorithm, the high-dimensional representation method (HDMR) has been implemented and applied to two demonstration systems: Na_2 and Ar-HCl . In both cases, a nonlinear potential laboratory data map was constructed to facilitate the search through a family of potentials and a nonlinear analysis was performed on the error propagation from the measured data to the family of potentials. In the Na_2 case, using the ro-vibrational spectral data for the $X^1\Sigma_g^+$ and $a^3\Sigma_u^+$ states, 90% confidence intervals around the mean Na_2 potentials have been accurately identified. In the Ar-HCl case, using both ro-vibrational spectral data and rotationally resolved state-state inelastic cross sections of David Chandler, a global Ar-HCl interaction potential with reliable error bars that are consistent with all of the experimental data has been obtained. These techniques are generic and should be applicable to extracting potentials from other emerging laboratory data.

Future Plans

In the coming year, we will continue to conduct our research in the following three general areas: (A) potential energy representation from ab initio data, (B) time-dependent reaction dynamics, and (C) global mapping between potential energy surfaces and laboratory data.

(A) Potential Energy Representation from ab initio Data. Various techniques including the fast grid interpolation for partially filled data, regularization, fast algorithms via pre-summations, and multivariate rational approximation are being developed and implemented for the construction of multidimensional potential energy surfaces. We plan on continuing the work to construct the five lowest singlet states $1A'$, $2A'$, $3A'$, $1A''$, and $2A''$ of the $\text{S} + \text{H}_2$, in collaboration with Rex Skodje (University of Colorado) and Alexander Mebel (Institute of Atomic and Molecular Science, Academia Sinica). Moreover, we plan on further exploring various blending-function techniques to deal with smooth potential functions of high dimensionality, aiming to drastically reducing the number of ab initio data necessary

for constructing accurate global poly-atomic potential energy surfaces of four and more atoms.

(B) Time-Dependent Reaction Dynamics. Robust rational approximation scheme for multivariate scattered data, in conjunction with domain decomposition techniques, is being developed and implemented for efficiently and accurately solving quantum fluid dynamics (QFD) equations in the moving grid Lagrangian framework. We plan on investigating various photo-dissociation processes and the reactive dynamics of systems of relevance to chemical combustions.

(C) Global Mapping between Potential Energy Surfaces and Laboratory Data. A new algorithm will be established aiming at determining the optimal laboratory data for extracting potential surfaces. Optimality will be achieved by relying on the ability to shape laser pulse to manipulate molecular dynamics guided by the desire to obtain the best possible information about the system potential. The research will explicitly consider the current laboratory capability to execute such experiments with the aim of providing the necessary algorithms to guide the experiments and extract their valuable potential surface information. We expect to make use of our recently developed high dimensional model representation technique to facilitate the inversion of the laboratory data.

Publications of DOE Sponsored Research(2000 - Present)

1. Potential Energy Surface of the A State of NH_2 and the Role of Excited States in the $\text{N}(^2\text{D}) + \text{H}_2$ Reaction, L. A. Pederson, G. C. Schatz, T. Hollebeek, T. S. Ho, H. Rabitz, and L. B. Harding; *J. Phys. Chem.*, **104**, 2301 (2000).
2. On the Importance of Exchange Effects in Three-Body Interactions: The Lowest Quartet State of Na_3 , J. Higgins, T. Hollebeek, J. Reho, T.-S. Ho, K.K. Lehmann, H. Rabitz, G. Scoles, and M. Gutowski; *J. Chem. Phys.*, **112**, 5751 (2000).
3. Reproducing Kernel Technique for Extracting Accurate Potentials from Spectral Data: Potential Curves of the Two-Lowest States $X^1\Sigma_g^+$ and $a^3\Sigma_u^+$ of the Sodium Dimer, T.-S. Ho, H. Rabitz, and G. Scoles; *J. Chem. Phys.*, **112**, 6218 (2000).
4. Solving the Bound-State Schrödinger Equation by Reproducing Kernel Interpolation, X.-G. Hu, T.-S. Ho, and H. Rabitz; *Phys. Rev. E*, **61**, 2074 (2000).
5. Solutions to Quantum Fluid Dynamics using Radial Basis Functions, X.-G. Hu, T.-S. Ho, and H. Rabitz; *Phys. Rev. E*, **61**, 5967 (2000).

6. Proper Construction of *ab initio* Global Potential Surfaces with Accurate Long-range Interactions, T.-S. Ho and H. Rabitz; J. Chem. Phys., **113**, 3960 (2000).
7. Determining quantum molecular potentials from spectroscopic energy levels using parametric equations of motion, D. A. Mazziotti and H. Rabitz, J. Phys. Chem. A, **104**, 9770 (2000).
8. Efficient Potential Energy Surfaces from Partially Filled *ab initio* Data over Arbitrarily Shaped Regions, T. Hollebeek, T.-S. Ho, and H. Rabitz, J. Chem. Phys., **114**, 3940 (2001).
9. Construction of Reproducing Kernel Hilbert Space Potential Energy Surfaces for the $1A''$ and $1A'$ States of the Reaction $N(^2D) + H_2$, T. Hollebeek, T.-S. Ho, H. Rabitz, and L. B. Harding, J. Chem. Phys., **114**, 3945 (2001).
10. The Ar-HCl potential energy surface from a global map-facilitated inversion of state-to-state rotationally resolved differential scattering cross sections and rovibrational spectral data, JM Geremia and H. Rabitz, J. Chem. Phys., **115**, 8899 (2001).
11. A global smooth *ab initio* potential energy surface of the $1A'$ state for the reaction $S(^1D) + H_2$, T.-S. Ho, T. Hollebeek, H. Rabitz, S. D. Chao, R. T. Skodje, A. S. Zyubin, and A. M. Mebel, J. Chem. Phys., **116**, 4124 (2002).
12. Multivariate radial basis interpolation for solving quantum fluid dynamics equations, X.-G. Hu, T.-S. Ho, H. Rabitz, and A. Askar, Computer and Mathematics with Application, **43**, 525 (2002).
13. Rational approximation with multi-dimensional scattered data, X.-G. Hu, T.-S. Ho, and H. Rabitz, Phys. Rev. E, in press.

Reactions of Atoms and Radicals in Pulsed Molecular Beams

Hanna Reisler
Department of Chemistry, University of Southern California
Los Angeles, CA 90089-0482
reisler@usc.edu

Program Scope

We study photoinitiated reactions of molecules and free radicals that involve competitive pathways and/or isomerization by exploiting multiple-resonance excitation schemes, state-selected product detection, and photofragment translational spectroscopy and ion imaging for generation of correlated distributions. Reaction thresholds are reached either via radiationless transitions from electronically excited states, or by vibrational excitation in the ground state.

Photodissociative Spectroscopy of CH₂OH in the 3p_x and 3s States

The hydroxymethyl radical (CH₂OH) is a significant product in the reaction of O(¹D) with methane. Similarly, reactions of Cl atoms and OH radicals with methanol yield predominantly CH₂OH. Because both CH₂OH and CH₃O have low barriers to dissociation, the photoisomerization CH₂OH ↔ CH₃O has commanded much theoretical interest. According to *ab initio* calculations, the lowest excited electronic states of CH₂OH have a predominant Rydberg character; specifically, the 3s, 3p_x, 3p_y, and 3p_z states.¹ Of these four states, only the 3p_y state does not carry oscillator strength, while the transitions to 3p_x and 3p_z are the strongest.¹⁻³ The Rydberg states are obtained by promoting the electron in the half-occupied π*CO antibonding molecular orbital to a Rydberg orbital localized on the carbon atom.

The assignment of the transitions to these Rydberg states has been the subject of some controversy. The experimentally observed absorption system, whose band origin is at 41,062 cm⁻¹ was initially assigned as the origin band of the 2²A'(3p_x) ← 1²A" transition.¹ Based on spectroscopic simulations of rotational contours for selected vibronic bands, Aristov *et al.* reassigned this system as the 2²A"(3p_z) ← 1²A" electronic transition.⁴ *Ab initio* calculations carried out by Bruna and Grein supported this assignment,² but a later computation by Chen and Davidson⁵ favored the initial assignment of the upper state as 3p_x, and ignored the experimental evidence to the contrary. The recalculated adiabatic transition energies to these states by Bruna and Grein³ reconfirmed their original assignments, and predicted a much lower energy for the 3s state than in the previous theoretical works.³

In previous publications, we reported on the molecular beam spectroscopy and photodissociation dynamics of the hydroxymethyl radical in the 3p_z Rydberg state.⁴ We estimated the lifetime of the 3p_z state at 0.5 ± 0.1 ps, and established that H + CH₂O (S₀) was a major dissociation channel following origin-band excitation. These studies, however, left uncertain the role of sequential surface crossings in accessing the dissociative state. The two lowest excited states, 3s and 3p_x, have never been identified in molecular beam spectroscopy. Their origins were tentatively assigned based on the UV absorption spectrum obtained at room temperature,⁶ the same spectrum for which the bands assigned to the 3p_z state were later reassigned as 3p_x.

We carried out the first molecular beam study of the excitation of CH₂OH(D) to the 3s and 3p_x states, assigned the origins for the two transitions, estimated the lifetimes of the excited states, and identified the channels responsible for the H dissociation products originating from these two states. By using the recent results of Hoffman and Yarkony on the conical intersections between the ground and the low-lying Rydberg states of CH₂OH,⁷ we were able also to describe the pathways leading from the initially excited electronic states to H(D)-products.

Three types of spectra were recorded: (a) depletion spectra; (b) H and D photofragment-yield spectra from CH₂OD; (c) 2+2 REMPI spectra. The depletion method can access the 3*p_x* and the 3*s* states. The probe laser frequency is fixed at 487.07 nm (41,062 cm⁻¹) to access (by 2+1 REMPI) the peak of the 2²A''(3*p_z*) ← 1²A'' origin band. The pump laser was scanned from 26,000 to 42,000 cm⁻¹, encompassing the range of the anticipated transitions to the 3*p_x* and 3*s* states. The population of the ground state was depleted whenever photon absorption to a lower state occurred, thereby causing an attenuation in the CH₂OH ion signal. H and D photofragments from CH₂OD were detected by (1+1') REMPI via the L-α transition at 121.6 nm. In the 1-color 2+2 REMPI method, simultaneous absorption of two photons excited the radical resonantly to the 3*p_x* Rydberg state, while additional two photons of the same wavelength were required to ionize the excited molecules.

As shown in Fig. 1, we observe several vibronic peaks in the depletion spectrum over the range 32,000-42,000 cm⁻¹. The first peak, at 35,063 cm⁻¹, is assigned as the origin band of the 2²A'(3*p_x*) ← 1²A'' transition. This assignment is based on the most recent theoretical calculations, and the fact that it is the first in a series of distinct bands. The second peak, which is 1607 cm⁻¹ higher in energy than the first, is assigned as the C-O stretch, 6₀¹. Since in the supersonic beam the spectral broadening due to rotational structure is effectively eliminated by the rotational cooling, it becomes obvious that the vibronic bands in the 2²A'(3*p_x*) ← 1²A'' transition are much broader than those in the corresponding transition to the 3*p_z* state, indicating that the 3*p_x* state is rapidly dissociating, with a lifetime much shorter than that of the 3*p_z* state. For comparison, also shown in Fig. 1 is the assigned 2+1 REMPI spectrum of CH₂OH in the region 41,000- 45,000 cm⁻¹, which shows vibronic bands belonging to the 2²A''(3*p_z*) ← 1²A'' system.⁴ This spectrum exhibits a progression in the C-O stretch deriving from the large C-O bond-length difference between the ground and the upper states. The vibrational progressions in the transitions terminating in the 3*p_x* and 3*p_z* states are quite similar, as expected for Rydberg states that converge to the ground state of the core ion, CH₂OH⁺. In order to identify the dissociation pathways, we measured the photofragment yield spectrum of the isotopic analog CH₂OD, and detected both H and D fragments following 3*p_x* excitation.

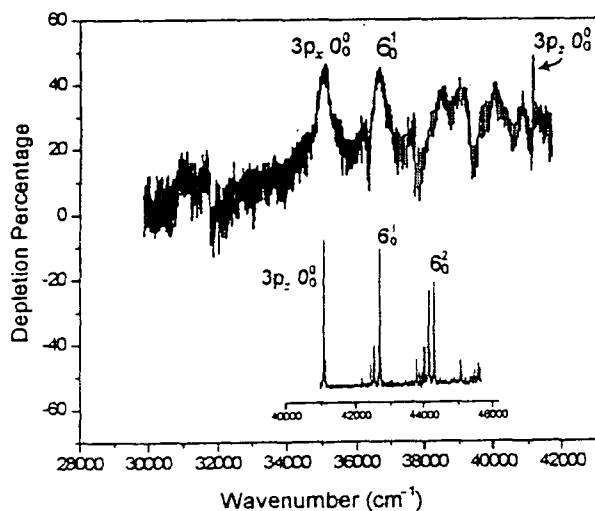


Fig. 1: Depletion spectrum in the region of the origin of the transition to the 3*p_x* state. The origin band to the 3*p_z* state served as the probe transition, and is shown as the narrow band at high energy. The inset shows the assigned vibronic spectrum of the 2²A''(3*p_z*) ← 1²A'' system.

Since the 3*s* state is the lowest excited state of CH₂OH, studying its photodissociation dynamics should simplify interpretation, as it would involve fewer possible surface couplings. We therefore searched for its origin near the wavelength predicted by the *ab initio* calculations (3.31 eV). We were unable to observe a REMPI spectrum in this region, but using the depletion method,

we detected a broad and structureless absorption feature starting at 26,000 cm^{-1} (3.21 eV), which is shown in Fig. 2. This absorption constitutes also the underlying continuum in the regions of the band origins of the transitions to the $3p_x$ and $3p_z$ states. The dissociative nature of the $3s$ state explains the absence of a REMPI spectrum. Our assignment of this depletion spectrum to the $3s \leftarrow 1^2A''$ transition is based on the proximity of the onset of the absorption to the theoretical prediction, and the fact that this is the lowest energy at which absorption can be recorded. This is the first time that absorption in this region is detected, and this band edge is also confirmed by the D photofragment yield spectrum of CH_2OD . No H atoms are observed near the origin.

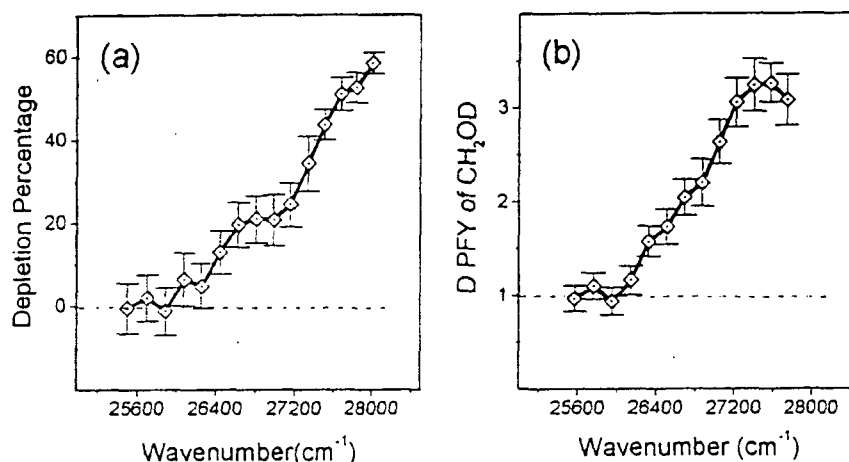


Fig. 2: Depletion and D photofragment yield spectra in the origin region of the transition to the $3s$ state.

Our results on the energy positions of the $3s$, and $3p_x$ states are in excellent agreement with the results of Bruna and Grein:

State	T_0^E (eV) Chen & Davidson ⁵	T_0^E (eV) Bruna & Grein ³	T_0 (eV) Exp.
$3s$	4.12	3.31	3.22
$3p_x$	5.20	4.41	4.34
$3p_z$	5.80	5.06	5.09

Considering the fact that the $3s$, $3p_x$ and $3p_z$ states are predominantly Rydberg in character and that they have identical ionic cores (the ground state of CH_2OH^+), the observation that the transition to the $3s$ state shows no structure is intriguing. Excitation of CH_2OH in the frequency range 25,000-40,000 cm^{-1} accesses the $3s$ and $3p_x$ Rydberg states, which are not correlated with $\text{H} + \text{CH}_2\text{O}(S_0)$. Therefore, searching for the surface crossing between $3p_x$ and $3s$, as well as between $3s$ and the ground state becomes important. The conical intersection calculations carried out recently by Hoffman and Yarkony identify pathways for radiationless decay, which play an essential role in the photodissociation dynamics on the $3s$ and $3p_x$ states.

An efficient vertical conical intersection between $3s$ and the ground state has been revealed. A seam was found at 2.9 eV for an O-H distance of about 2.8 Å. Following the $3s$ /ground state coupling, CH_2OH (CH_2OD) dissociates directly to $\text{H}_2\text{CO} + \text{H}(\text{D})$. No local minimum is found in this route. Our observation of D production in CH_2OD is consistent with this mechanism. Considering

the bound-free nature of the transition to the 3s state, it is not surprising that the spectrum appears structureless.

The photochemistry of the $3p_x$ state is more complicated due to multiple coupling pathways. According to the calculations, after the radical reaches the $3p_x$ state, it first couples to the 3s state, and subsequently to the ground state as described above. Because of the proximity of the $3p_x$ to the 3s state, Franck-Condon considerations would favor initial coupling between these two states. Two different paths then lead to intersections between the 3s and the ground state, and they provide readily accessible routes to either HCOH (HCO) + H or H₂CO (S₀) + H (D) products.

Future Plans

We plan to study the photochemistry on the 3s Rydberg state, in order to examine the roles of isomerization and C-H and O-H bond fission pathways. We are also setting up experiments in which the OH or CH vibrational excitation will precede electronic excitation, as well as studies of vibrational overtone excitation. The spectroscopy and photodissociation dynamics of higher hydroxyalkyl radicals will be then examined.

- ¹S. Rettrup, P. Pagsberg, and C. Anastasi, *Chem. Phys* **122**, 45 (1988).
- ²P. J. Bruna and F. Grein, *J. Phys. Chem. A* **102**, 3141(1998).
- ³P. J. Bruna and F. Grein, *J. Phys. Chem. A* **105**, 8599 (2001).
- ⁴V. Aristov, D. Conroy, and H. Reisler, *Chem. Phys. Lett* **318**, 393 (2000).
- ⁵F. Chen and E. R. Davidson, *J. Phys. Chem. A* **105**, 4558 (2001).
- ⁶J. Munk, P. Pagsberg, E. Ratajczak, and A. Sillesen, *J. Phys. Chem.*, **90**, 2752 (1986).
- ⁷B. C. Hoffman and D. R. Yarkony, to be submitted (2002).

Publications in 2000-2002:

- Symmetry and lifetime of the hydroxymethyl radical in the 3p_z Rydberg state*, V. Aristov, D. Conroy and H. Reisler, *Chem. Phys. Lett.*, **318**, 393 (2000).
- HCO rovibrational distributions from the unimolecular decomposition of H₂CO at excess energies 1100-2655 cm⁻¹*. L. Valachovic, M.J. Dulligan, M.F. Tuchler, Th. Droz-Georget, M. Zyrianov, A. Kolessov, H. Reisler and C. Wittig, *J. Chem. Phys.*, **112**, 2752 (2000).
- The electronic origin and vibrational levels of the first excited singlet state of isocyanic Acid (HNCO)*, H. Laine Berghout, F. Fleming Crim, Mikhail Zyrianov and Hanna Reisler, *J. Chem. Phys.*, **112**, 6678 (2000).
- Photodissociation of the hydroxymethyl radical in the 3p_z Rydberg state: formaldehyde + hydrogen atom channel*, D. Conroy, V. Aristov, L. Feng and H. Reisler, *J. Phys. Chem. A*, **104**, 10288 (2000).
- Competitive pathways and nonadiabatic transitions in photodissociation*, D. Conroy, V. Aristov, L. Feng, A. Sanov, and H. Reisler, *Acc. Chem. Res.*, **34**, 625-632 (2001).

Photoionization Studies of Transient and Metastable Species

Branko Ruscic

Chemistry Division, Argonne National Laboratory, 9700 South Cass Avenue, Argonne, IL 60439
ruscic@anl.gov

Program Scope

In most general terms, the fundamental goal of this program is to explore, understand, and utilize the basic processes of interaction of vacuum UV light with atoms and molecules. More specifically, the program uses photoionization mass spectrometry and other related methods to study transient and metastable species that are either intimately connected to energy-producing processes, such as combustion, or play prominent roles in the associated environmental issues. The ephemeral species of interest are produced *in situ* using various suitable techniques, such as sublimation, pyrolysis, microwave discharge, chemical abstraction reactions with H or F atoms, laser photodissociation, on-line synthesis, and others. The desired information is obtained by applying appropriate photoionization techniques, which use both conventional and coherent light sources in the vacuum UV region. The *spiritus movens* of our studies is the need to provide the chemical community with essential information on the species of interest to energy-related processes, such as accurate and reliable thermochemical, spectroscopic and structural data, and thus contribute to the global comprehension of the underlying chemical reactions. The scientific motivation is additionally fueled by the intent to extract, when possible, useful generalities such as bonding patterns within a class of related compounds, or unveil systematic behavior in the ubiquitous autoionization processes and other phenomena occurring during photoionization. In addition, results obtained in this program serve as testing ground for the state-of-the-art electronic structure calculations, and have historically generated a significant impetus for further theoretical developments. The experimental work of this program is coordinated with related experimental and theoretical efforts within the Argonne Chemical Dynamics Group to provide a broad perspective on this area of science.

Recent Progress

Finalization of the New Value for the Bond Dissociation Energy of Water and the Enthalpy of Formation of Hydroxyl

Last year we have announced¹ the significant finding that the generally accepted bond dissociation energy of water is too high by ~ 0.5 kcal/mol. Since then, the full paper,² which provides definitive evidence on the subject and engages in an exhaustive discussion of all relevant details, has been completed and it has just appeared in *J. Phys. Chem. A*. The associated front page artwork on that journal issues helps draw attention to this work. The full paper demonstrates how three components, consisting of a) carefully executed and analyzed photoionization mass-spectrometric measurements, b) an exhaustive analysis of spectroscopic data on OH, and c) very high-level ab initio calculations, all converge to the consensus values for the three tightly correlated quantities: $D_0(\text{H-OH}) = 41128 \pm 24 \text{ cm}^{-1} = 117.59 \pm 0.07 \text{ kcal/mol}$ ($118.81 \pm 0.07 \text{ kcal/mol}$ at 298.15 K), $D_0(\text{OH}) = 35593 \pm 24 \text{ cm}^{-1} = 101.76 \pm 0.07 \text{ kcal/mol}$ ($102.75 \pm 0.07 \text{ kcal/mol}$ at 298.15 K) and $\Delta H_f^\circ(\text{OH}) = 8.85 \pm 0.07 \text{ kcal/mol}$ ($8.91 \pm 0.07 \text{ kcal/mol}$ at 298.15 K). The final quantities are very slightly ($2\text{-}3 \text{ cm}^{-1}$, $<0.01 \text{ kcal/mol}$) different than those reported here last year. The new value affects many other thermochemical quantities – most of them in ways that are not readily transparent. The full paper illustrates this point by discussing+ several immediately obvious consequences of the new values. The full impact of this (and other similar new measurements affecting key thermochemical values) will become easier to asses once the Active Thermochemical Tables become fully operational.

Thermochemical Network Approach to $D_0(\text{H-OH})$, $D_0(\text{OH})$, and $\Delta H_{f0}(\text{OH})$

In order to incorporate the latest kinetic measurement³ of $\Delta H_{f0}(\text{OH})$, and make use of data involving H_2O_2 , as well as to address a small residual discrepancy² regarding the bond dissociation energy of water, we have explored the thermochemical network approach. The residual discrepancy alluded to above refers to the difference in $D_0(\text{H-OH})$ of $\sim 20 \text{ cm}^{-1}$ between the Rydberg tagging experiment,⁴ and our recommended value.² Albeit not profoundly relevant on the scale of normal thermochemical sensitivities, the discrepancy somewhat limits the error bar of the recommended value and is potentially pointing to some systematic difficulties. At the same time, the existing determination⁵ of $D_0(\text{HO-OH})$ seems to be congruent with our new value for $\Delta H_{f0}(\text{OH})$, but it crucially depends on the enthalpy of H_2O_2 . As opposed to water, no particular value for the enthalpy of formation of H_2O_2 has been endorsed by CODATA, and the values recommended by JANAF and the Russian compilation differ. The explored thermochemical network includes 26+ relevant measurements, and, *inter alia*, probes the foundation which supports the enthalpies of formation of H_2O and H_2O_2 . The network also allows further exploration and development of various statistical strategies leading to the network solution and related to the development of Active Tables. To that end, the current network is not "localized" (which is the approach that we have taken previously). When all available data is used, the network suggests quite unambiguously that the Rydberg tagging experiment is slightly off, and produces the following refined values: $D_0(\text{H-OH}) = 41129 \pm 5 \text{ cm}^{-1} = 117.59 \pm 0.01 \text{ kcal/mol}$ ($118.81 \pm 0.01 \text{ kcal/mol}$ at 298.15 K), $D_0(\text{OH}) = 35590 \pm 9 \text{ cm}^{-1} = 101.76 \pm 0.03 \text{ kcal/mol}$ ($102.75 \pm 0.03 \text{ kcal/mol}$ at 298.15 K) and $\Delta H_{f0}(\text{OH}) = 8.86 \pm 0.01 \text{ kcal/mol}$ ($8.92 \pm 0.01 \text{ kcal/mol}$ at 298.15 K). These coincide within 1-3 cm^{-1} with the recommended values, but have a significantly tighter uncertainty, since they are statistically supported by more data. The network also indicates that while the selection of core data defining the enthalpy of H_2O_2 is not hugely different between the Russian compilation and JANAF, the latter produces a wrong 298 K value. We have also used the network to test the (unlikely) hypothesis² that the photoionization measurements inherently refer to $J=1$ of the ground state of water (excited by 23.8 cm^{-1}); the network approach shows quite convincingly that this hypothesis is unattainable. This effort also clarifies some of the confusion introduced by a recent paper,⁶ where a value for $\Delta H_{f0}(\text{OH})$ very close to our recommended value¹ (but with an apparently lower uncertainty) is developed by simply averaging the values implied by the Rydberg tagging experiment and by the measurement of the HO-OH dissociation limit, but in the process it not only relies on the incorrect enthalpy increments for H_2O_2 found in JANAF, but it also misquotes the Rydberg tagging result by $\sim 10 \text{ cm}^{-1}$, which makes it appear closer to the other data.

Progress on the Enthalpy of Formation of HO_2

We have recently determined $\Delta H_{f0}^{\circ}(\text{HO}_2) = 4.0 \pm 0.8 \text{ kcal/mol}$ from a photoionization study of HO_2 and H_2O_2 . This value has been obtained from a positive ion cycle that involves two measurements: the photoionization appearance energy of HO_2^+ from H_2O_2 , $\text{AE}_0(\text{HO}_2^+/\text{H}_2\text{O}_2)$, and the measured adiabatic ionization energy of the HO_2 radical, $\text{IE}(\text{HO}_2)$. Due to idiosyncrasies in the appearance threshold, the value of $\text{AE}_0(\text{HO}_2^+/\text{H}_2\text{O}_2)$, relies indirectly on the analysis of the nearby threshold for the OH^+ fragment and hence depends (nonlinearly) on $\Delta H_f(\text{OH})$. A new analysis of this threshold (in light of the new value for the enthalpy of OH) suggests a lower 0 K value for HO_2 of $3.6 \pm 0.6 \text{ kcal/mol}$. Surprisingly, new negative ion cycle data⁸ produced $3.9 \pm 0.5 \text{ kcal/mol}$, in accord with our prior value. It should be noted that, at least at this point, the error bars are sufficiently large to allow overlap between all these values. We are currently expanding the OH thermochemical network to include HO_2 ; the solution of such network should produce a value that is both more reliable and has a lower uncertainty. Part of the network encompasses measurements of kinetic equilibria. Those measurements that involve reactions with OH are nominally (linearly) shifted by the amount of revision of the OH enthalpy (0.5 kcal/mol). For example, the data of Howard⁹ shifts from 3.2 ± 0.4

kcal/mol to 2.7 kcal/mol, and the data of Hills and Howard from 3.7 ± 0.4 kcal/mol to 3.2 kcal/mol. However, a novel statistical analysis (beyond pure network considerations) of the thermal dependence of the just quoted kinetic measurements appear to suggest that a more consistent choice would be 3.4 ± 0.6 kcal/mol and 3.6 ± 0.4 kcal/mol. This type of analysis of kinetic measurements is currently under development within the conceptual explorations related to the development of Active Kinetic Rate Tables, that parallels the current development of Active Thermochemical Tables.

Rotational Autoionization in the Ionization Threshold Region of CH₃

The interpretation of high-resolution spectra of the ionization threshold of CH₃, which explicitly reveals the previously¹¹ postulated existence of seldom-observed purely-rotational autoionization (i.e. not accompanied by vibrational autoionization), proves to be rather complex. The spectra have been obtained using our VUV laser setup and a novel approach that utilizes laser photolysis to generate radicals well-equilibrated at a known temperature (which is needed here both to have a known initial population of neutral CH₃ and to control the population of higher J states, for which this phenomenon is more promptly discerned). While confirming our previous suggestion that the rotational autoionization process involves a loss of both even and odd number of rotational quanta, up to the maximum allowable by selection rules and energetic constraints, the current analysis suggests that the observed peaks are composites that reflect peculiar "banding" effects occurring in the region of interest.

Development of Active Thermochemical Tables

We are currently pursuing the development of Active Thermochemical Tables. At the core of Active Tables is the explicit utilization and statistical treatment of underlying interdependences between various quantities, most conveniently expressed through a network of relationships. A more exhaustive description of Active Tables will be given at a later time. Suffices it to say here that, as opposed to conventional approaches, the Tables will produce globally consistent thermochemical values, allow instant updates with new data, allow "what if" explorations, isolate "weakest links" and hence suggest future high-impact experiments and/or calculations, etc While the conceptual and practical advances involving thermochemical networks and the underlying statistical analysis are a direct and continuing product of this project, the development of Active Tables is highly leveraged by other funding sources (DOE MICS), which will cover the actual software development.

Other progress

We have started a collaboration with J. A. Pople (NWU) and L. Curtiss (ANL) that aims to develop an approach that will produce individual uncertainties for G3-type calculations. We had again a successful collaboration with L. Butler (U. of C.) on the characterization of photodissociation products using experimental and theoretical techniques. Pending the technical readiness of the Chemical Reaction Dynamics Beamline at ALS and availability of beam-time, we will continue the process of implementing radical sources for the ALS at Berkeley. Finally, we are involved in an IUPAC Task Force that aims to critically evaluate thermochemical quantities of radicals that are important in combustion and subsequent atmospheric chemistry.

Future Plans

Future plans of this program pivot around the continued investigation of radicals and transient species that are intimately related to combustion processes, particularly those that potentially define the initial attack of O₂ on hydrocarbon moieties during combustion, as well as other ephemeral species that are implicated in subsequent atmospheric chemistry (particularly hydrocarbon moieties

that contain oxygen and/or nitrogen). In the lab we have made the instrumental modifications necessary to pursue the elucidation of these radicals, many of which are poorly understood, yet quite important in combustion as well as in atmospheric chemistry. These investigations will be complemented with measurements taking advantage of the Advanced Light Source at Lawrence Berkeley Laboratory. In collaboration with the theorists in the Argonne Chemical Dynamics Group, we also plan on determining in quantitative ways the effect of hindered rotations on thermochemical quantities of both transient and stable species. We also intend to further test and enhance our fitting methods for accurate determination of fragment appearance potentials. Last, but not least, we intend to devote a concerted effort to the development of Active Thermochemical Tables.

This work is supported by the U.S. Department of Energy, Office of Basic Energy Sciences, Division of Chemical Sciences, under Contract W-31-109-ENG-38

References

- ¹ B. Ruscic, D. Feller, D. A. Dixon, K. A. Peterson, L. B. Harding, R. L. Asher, and A. F. Wagner, *J. Phys. Chem. A* **105**, 1 (2001)
- ² B. Ruscic, A. F. Wagner, L. B. Harding, R. L. Asher, D. Feller, D. A. Dixon, K. A. Peterson, Y. Song, X. Qian, C. Y. Ng, J. Liu, W. Chen, and D. W. Schwenke, *J. Phys. Chem. A* **106**, 2727 (2002).
- ³ Herbon, J. T.; Hanson, R. K., Golden, D. M.; Bowman, C. T. , submitted to 29th International Symposium on Combustion, to be held in Hokkaido, Japan, July 21-26, 2002.
- ⁴ S. A. Harich; D. W. H. Hwang, X. Yang, J. J. Lin, X. Yang, R. N. Dixon, *J. Chem. Phys.* **113**, 10073 (2000).
- ⁵ Luo, X.; Fleming, P. R.; Rizzo, T. R. *J. Chem. Phys.* **96**, 5659 (1992).
- ⁶ Joens, J. A. *J. Phys. Chem. A*, **105**, 11041 (2001).
- ⁷ M. Litorja and B. Ruscic, *J. Electron Spectrosc.* **97** 131 (1998) .
- ⁸ T. M. Ramond, S. J. Blanksby, S. Kato, V. M. Bierbaum, G. E. Davico, R. L. Schwartz, W. C. Lineberger, and G. B. Ellison, *J. Phys. Chem. A* submitted
- ⁹ C. J. Howard, *J. Am. Chem. Soc.* **102**, 6937 (1980)
- ¹⁰ A. J. Hills and C. J. Howard, *J. Chem. Phys.* **81**, 4458 (1984).
- ¹¹ M. Litorja and B. Ruscic, *J. Chem. Phys.* **107**, 9852(1997)

Publications Resulting from DOE Sponsored Research (2000-2001)

- *Photoionization of HOCO Revisited: A New Upper Limit to the Adiabatic Ionization Energy and Lower Limit to the Enthalpy of Formation*, B. Ruscic and M. Litorja, *Chem. Phys. Lett.* **316**, 45-50 (2000)
- *Characterization of Nitrogen-Containing Radical Products from the Photodissociation of Trimethylamine at 193 nm Using Photoionization Detection*, N. R. Forde, L. J. Butler, B. Ruscic, O. Shorkabi, F. Qi, and A. Suits, *J. Chem. Phys.* **113**, 3088-3097 (2000)
- *Photoionization Mass Spectroscopic Studies of Free Radicals in Gas Phase: Why and How*, B. Ruscic, *Res. Adv. Phys. Chem.* **1**, 39-75 (2000)
- *Evidence for a Lower Enthalpy of Formation of Hydroxyl Radical and a Lower Gas-Phase Bond Dissociation Energy of Water*, B. Ruscic, D. Feller, D. A. Dixon, K. A. Peterson, L. B. Harding, R. L. Asher, and A. F. Wagner, *J. Phys. Chem. A* **105**, 1-4 (2001)
- *Theoretical Investigation of the Transition States Leading to HCl Elimination in 2-Chloropropene*, B. Parsons, L. Butler, and B. Ruscic, *Mol. Phys.* **100**, 865-874 (2002)
- *On the Enthalpy of Formation of Hydroxyl Radical and Gas-Phase Bond-Dissociation Energies of Water and Hydroxyl*, B. Ruscic, A. F. Wagner, L. B. Harding, R. L. Asher, D. Feller, D. A. Dixon, K. A. Peterson, Y. Song, X. Qian, C. Y. Ng, J. Liu, W. Chen, and D. W. Schwenke, *J. Phys. Chem. A* **106**, 2727-2747 (2002).

Reaction of the Phenyl Radical with Propyne

Henry F. Schaefer III

Center for Computational Quantum Chemistry, University of Georgia

Athens, Georgia 30602-2525

Email: hfsiii@uga.edu

(706)542-2067

The complicated potential energy surface (PES) for the phenyl + propyne reaction, which may contribute to the growth of polycyclic aromatic hydrocarbons (PAH's) under a wide variety of reaction conditions, is described. The PES was initially characterized with two different density functional methods. The energies of the entrance transition states, a direct hydrogen transfer channel and two addition reactions leading to chemically activated $C_9H_9^+$ intermediates, were evaluated using coupled cluster theory including connected triple excitations. An extensive set of unimolecular reactions was examined for these activated $C_9H_9^+$ intermediates, comprising 70 equilibrium structures and over 150 transition states, and product formation channels leading to substituted acetylenes and allenes such as PhCCH, PhCCCH₃, and PhCHCCH₂ were identified. The overall hypersurface scheme is illustrated in the figure on the next page. Systems such as this are so complicated that theoretical guidance may be essential for future experimental ventures. The lowest energy pathway leads to indene, a prototype PAH molecule containing a five-membered ring. The title reaction thus is an example of possible direct formation of a PAH containing a five-membered ring, necessary to explain the formation of non-planar PAH structures, from an aromatic radical unit and an unsaturated hydrocarbon bearing an odd number of carbons.

The importance of the phenyl + propyne and similar reactions to PAH formation can only be definitively assessed after theoretical studies of rate coefficients and product distributions have been completed (and these results have been incorporated into modeling studies). However, some important observations may already be made. The barrier to reaction for phenyl radicals + propyne is of height comparable to that for other alkenes and alkynes, such as acetylene, so it is expected that the rate coefficients of these reactions will be of similar order of magnitude. In combustion systems, acetylene is often present in quite high concentrations, but contributions from a number of unsaturated species with odd numbers of carbons could contribute to a significant additional PAH-growth channel.

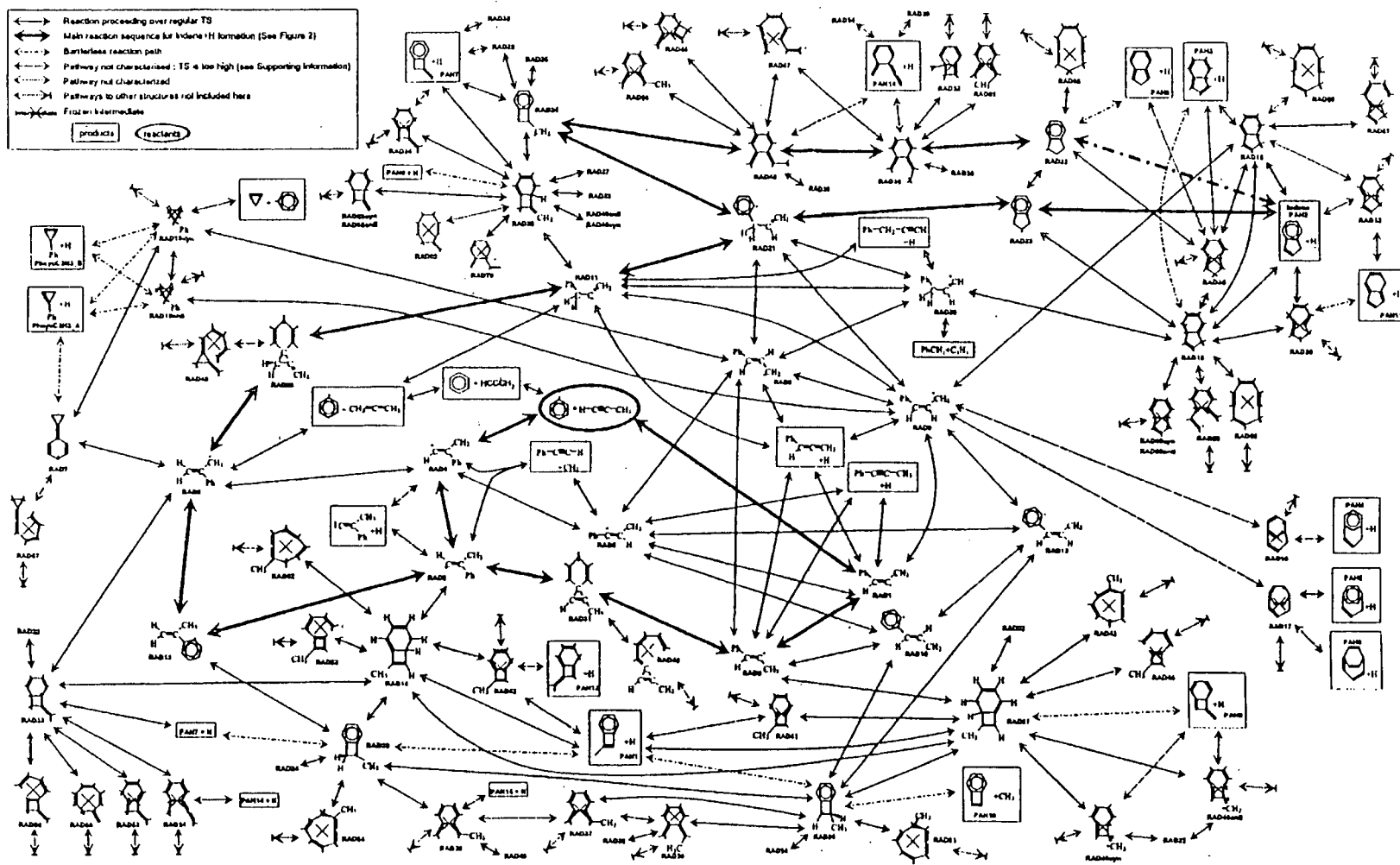


Figure 1. Reaction scheme for the phenyl + propyne reaction.

Research Support by the U. S. Department of Energy 2000, 2001, 2002

1. J. C. Rienstra-Kiracofe, G. B. Ellison, B. C. Hoffman and H. F. Schaefer, "The Electron Affinities of C₃O and C₄O," *William A. Goddard Issue, J. Phys. Chem. A* **104**, 2273 (2000).
2. R. A. King, W. D. Allen, and H. F. Schaefer, "On Apparent Quantized Transition-State Thresholds in the Photofragmentation of Acetaldehyde", *J. Chem. Phys.* **112**, 5585 (2000).
3. R. I. Kaiser, O. Asvany, Y. T. Lee, H. F. Bettinger, P. R. Schleyer, and H. F. Schaefer, "Crossed Beam Reaction of Phenyl Radicals with Unsaturated Hydrocarbon Molecules. I. Chemical Dynamics of Phenylmethylacetylene (C₆H₅CCCH₃; X ¹A') Formation from Reaction of C₆H₅ (X ²A₁) with Methylacetylene, CH₃CCH (X ¹A₁)", *J. Chem. Phys.* **112**, 4994 (2000).
4. S. T. Brown, Y. Yamaguchi, and H. F. Schaefer, "The $\tilde{X}^3\Sigma^-$ and $\tilde{A}^3\Pi$ Electronic States of Ketenylidene (CCO): Analysis of the Renner-Teller Effect in the Upper State", *Marilyn Jacox Issue, J. Phys. Chem. A* **104**, 3603 (2000).
5. A. G. Csaszar, W. D. Allen, Y. Yamaguchi, and H. F. Schaefer, "Ab Initio Determination of Accurate Ground Electronic State Potential Energy Hypersurfaces for Small Molecules", pages 15-68 in *Computational Molecular Spectroscopy*, editors P. R. Bunker and P. Jensen (Wiley, New York, 2000).
6. T. D. Crawford, S. S. Wesolowski, E. F. Valeev, R. A. King, M. L. Leininger, and H. F. Schaefer, "The Past, Present, and Future of Quantum Chemistry", pages 219 - 246 in *Chemistry for the 21st Century*, editors E. Keinan and I. Schechter (Wiley-VCH, Weinheim, Germany, 2001).
7. I. S. Ignatyev, H. F. Schaefer, and P. R. Schleyer, "Triplet States of Carbenium and Silylium Cations", *Chem. Phys. Lett.* **337**, 158 (2001).
8. M. Hofmann and H. F. Schaefer, "Structure and Reactivity of the Vinylcyclopropane Radical Cation", *Alfred Bauder Issue, J. Mol. Structure*
9. Y. Xie and H. F. Schaefer, "The Puzzling Infrared Spectra of the Nitric Oxide Dimer Radical Cation: A Systematic Application of Brueckner Methods", *Molecular Physics* **98**, 955 (2000).
10. J. C. Rienstra-Kiracofe, W. D. Allen, and H. F. Schaefer", "The C₂H₅+O₂ Reaction Mechanism: High-Level Ab Initio Characterizations", *Feature Article, J. Phys. Chem. A* **104**, 9823 (2000).
11. S.-J. Kim and H. F. Schaefer, "Dimethyldioxirane, Carbonyl Oxide, and the Transition State Connecting Them: Electronic Structures, Relative Energies, and Vibrational Frequencies", *J. Phys. Chem. A* **104**, 7892 (2000).
12. H. F. Bettinger, P. R. Schleyer, P. R. Schreiner, H. F. Schaefer, R. I. Kaiser, and Y. T. Lee, "The Reaction of Benzene with Ground State Carbon Atom, C(³P_j)", *J. Chem. Phys.* **113**, 4250 (2000).
13. C. J. Barden and H. F. Schaefer, "The Singlet-Triplet Separation in Dichlorocarbene: A Surprising Difference between Theory and Experiment", *J. Chem. Phys.* **112**, 6515 (2000).
14. H. F. Schaefer, "Quantum Mechanical Computations of Potential Energy Hypersurfaces", a vignette published on pages 882 - 888 of the Second Edition of *Physical Chemistry*, by R. S. Berry, S. A. Rice, and J. Ross (Oxford University Press, New York, 2000).
15. R. I. Kaiser, C. C. Chiong, O. Asvany, Y. T. Lee, F. Stahl, P. R. Schleyer, and H. F. Schaefer, "Chemical Dynamics of d₁-Methyldiacetylene (CH₃CCCCD; X ¹A₁) and d₁-Ethylnylallene (H₂CCCH(C₂D); X ¹A') Formation from Reaction of C₂D(X ²Σ⁺) with Methylacetylene, CH₃CCH (X ¹A₁)", *J. Chem. Phys.* **114**, 3488 (2001).
16. F. Stahl, P. R. Schleyer, H. F. Bettinger, R. I. Kaiser, Y. T. Lee, and H. F. Schaefer, "Reaction of the Ethynyl Radical, C₂H, with Methylacetylene, CH₃CCH, Under Single Collision Conditions: Implications for Astrochemistry", *J. Chem. Phys.* **114**, 3476 (2001).

17. C. J. Barden and H. F. Schaefer, "Quantum Chemistry in the Twenty-First Century", Cover Article, *Pure and Applied Chemistry* **72**, 1405 (2000).
18. E. F. Valeev, A. G. Csaszar, W. D. Allen, and H. F. Schaefer, "MP2 Limit for the Barrier to Linearity of Water", *J. Chem. Phys.* **114**, 2875 (2001).
19. E. F. Valeev, W. D. Allen, H. F. Schaefer, A. G. Csaszar, and A. L. L. East, "Interlocking Triplet Electronic States of Isocyanic Acid: Sources of Nonadiabatic Photofragmentation Dynamics", *William H. Miller Issue, J. Phys. Chem. A* **105**, 2716 (2001).
20. R. I. Kaiser, T. N. Le, T. L. Nguyen, A. M. Mebel, N. Balucani, Y. T. Lee, F. Stahl, P. R. Schleyer, and H. F. Schaefer, "A Combined Crossed Molecular Beam and *Ab Initio* Investigation of C₂ and C₃ Elementary Reactions with Unsaturated Hydrocarbons - Pathways to Hydrogen Deficient Radicals in Combustion Flames", *Faraday Discussions of the Chemical Society* **19**, 51 (2001).
21. F. Stahl, P. R. Schleyer, H. F. Schaefer, and R. I. Kaiser, "The Reactions of Ethynyl Radicals as a Source C₄ and C₅ Hydrocarbons in Titan's Atmosphere", *Planetary and Space Sciences*
22. B. G. Rocque, J. M. Gonzales, and H. F. Schaefer, "An Analysis of the Conformers of 1,5-Hexadiene", *Ernest R. Davidson Issue, Mol. Phys.* **100**, 441 (2002).
23. I. Hahndorf, Y. T. Lee, R. I. Kaiser, L. Vereecken, J. Peeters, H. F. Bettinger, P. R. Schreiner, P. R. Schleyer, W. D. Allen, and H. F. Schaefer, "A Combined Crossed Beam, *Ab Initio*, and RRKM Investigation of the Reaction of Carbon Species with Aromatic Molecules I: Benzene, C₆H₆ (X ¹A_{1g}) and d₆-Benzene, C₆D₆(X ¹A_{1g})", *J. Chem. Phys.* **116**, 3248 (2002).
24. H. F. Schaefer, "Computers and molecular Quantum Mechanics: 1965-2001, A Personal Perspective", *J. Molecular Structure* **573**, 129 (2001).
25. J. P. Kenny, K. M. Krueger, J. C. Rienstra-Kiracofe, and H. F. Schaefer, "C₅H₄: Pyramidine and Its Low Lying Isomers", *J. Phys. Chem. A* **105**, 7745 (2001).
26. L. Vereecken, J. Peeters, H. F. Bettinger, R. I. Kaiser, P. R. Schleyer, and H. F. Schaefer, "Reaction of Phenyl Radicals with Propyne", *J. Amer. Chem. Soc.* **124**, 2781 (2002).
27. J. C. Reinstra-Kiracofe, G. S. Tschumper, H. F. Schaefer, S. Nandi, and G. B. Ellison, "Atomic and Molecular Electron Affinities: Photoelectron Experiments and Theoretical Computations", *Chem. Revs.* **102**, 231 (2002).
28. N. R. Brinkmann, N. A. Richardson, S. S. Wesolowski, Y. Yamaguchi, and H. F. Schaefer, "Characterization of the X ²A₁ and \tilde{a} ⁴A₂ Electronic States of CH₂⁺", *Chem. Phys. Lett.* **352**, 505 (2002).
29. R. I. Kaiser, I. Hahndorf, O. Asvany, Y. T. Lee, L. Vereecken, J. Peeters, H. F. Bettinger, P. R. Schleyer, and H. F. Schaefer, "Neutral-Neutral Reactions in the Interstellar Medium: Elementary Reactions of C₆H₅ and C₆H₆", *Astronomy and Astrophysics*
30. R. I. Kaiser, F. Stahl, P. R. Schleyer, O. Asvany, Y. T. Lee, and H. F. Schaefer, "Atomic and Molecular Hydrogen Elimination in the Crossed Beam Reaction of d₁-Ethynyl Radicals C₂D(X ²Σ⁺) with Acetylene, C₂H₂(X ¹Σ_g⁺): Dynamics of d₁-Diacyetylene (HCCCCD) and d₁-Butadiynyl (DCCCC) Formation", *Phys. Chem. Chem. Phys.*
31. N. D. K. Petraco, W. D. Allen, and H. F. Schaefer, "The Fragmentation Path for Hydrogen Dissociation from Methoxy Radical", *J. Chem. Phys.*
32. L. Horny, N. D. K. Petraco, C. Pak, and H. F. Schaefer, "What Is the Nature of Polyacetylene Neutral and Anionic Chains HC_{2n}H and HC_{2n}H⁺ (n=6-12) that Have Been Recently Observed in Neon Matrices?", *J. Amer. Chem. Soc.*
33. P. Jensen, S. S. Wesolowski, N. R. Brinkmann, N. A. Richardson, Y. Yamaguchi, H. F. Schaefer, and P. R. Bunker, "A Theoretical Study of \tilde{a} ⁴A₂ CH₂⁺", *J. Mol. Spectroscopy*
34. D. Moran, F. Stahl, E. D. Jemmis, H. F. Schaefer, and P. R. Schleyer, "Structures, Stabilities and Ionization Potentials of Dodecahedane Endohedral Complexes", *J. Phys. Chem.*
35. Q. Li, J. F. Zhao, Y. Xie, and H. F. Schaefer, "Electron Affinities, Molecular Structures, and Thermochemistry of the Fluorine, Chlorine, and Bromine Substituted Methyl Radicals", *J. Phys. Chem.*

Nonlinear Diagnostic Techniques and Strategies

T. B. Settersten
Combustion Research Facility, Sandia National Laboratories
P.O. Box 969, MS 9056
Livermore, CA 94509-0969
Telephone: (925) 294-4701, email: tbsette@sandia.gov

Program Scope

The primary objective of this program is the development of novel laser-based techniques for application in combustion chemistry and reacting flow research. The program focuses on two aspects of diagnostic research. First is the design of innovative sensing strategies for important combustion species. Second is the fundamental investigation of the physics and chemistry of laser-atom/molecule interactions in systems that are perturbed by inter-molecular collisions. This includes the study of fundamental spectroscopy, energy transfer, and photochemical processes. This aspect of the research is essential to the correct interpretation of diagnostic signals. We are particularly interested in resonant nonlinear optical techniques because they can provide high sensitivity, spatial resolution, and species selectivity. Furthermore, we are investigating the use of near-transform-limited picosecond laser pulses because they provide high-peak power and adequate temporal and spectral resolution for measurements resulting from nonlinear laser-atom/molecule interactions in gas-phase systems.

Recent Progress

IR-UV double-resonance spectroscopy. We are addressing the pronounced need for spatially precise methods to measure important combustion species whose detection is hindered by either spectral interferences in the IR or predissociation in the UV using IR-UV double-resonance spectroscopy. Here, the double-resonance condition overcomes these problems. Techniques based on IR-UV double-resonance spectroscopy are spatially-resolved, absorption-based techniques in which an IR laser pumps a ro-vibrational transition and an UV laser probes an electronic transition from the labeled level. The IR-UV techniques simplify complex electronic spectra, and can provide important characterization of electronic states that predissociate or internally convert, which is essential for the development of future diagnostics that involve these states.

Several detection schemes are possible for IR-UV double-resonance experiments. Pump-probe absorption spectroscopy is a differential-absorption technique in which the IR and UV laser beams are crossed in the sample, and the IR laser pulse modifies the absorption experienced by the UV pulse. In two-color polarization spectroscopy (TC-PS), the IR laser induces birefringence and dichroism in the sample, which modifies the polarization of the transmitted UV probe pulse. Measurement of the polarization of the probe is then related to the properties of the sample. In two-color resonant four-wave mixing (TC-RFWM), the IR laser is split into two pump beams that are crossed in the sample. Interference of the pump pulses produces a population and polarization grating in the

sample, and the UV laser is scattered from the grating when the Bragg condition is satisfied. In all cases described here, the UV pulse is used as a probe so that high-quantum efficiency detectors with excellent noise characteristics can be used. A final technique, which relies on fluorescence detection is two-color laser-induced fluorescence (TC-LIF). Here, a UV pulse excites fluorescence and an IR pulse modifies the ground-state population. The change in the LIF signal induced by the IR pulse is related to the species concentration.

We investigated detection of OH in a lean methane-air flame by three double-resonance techniques.¹ These included TC-PS, TC-RFWM, and TC-LIF. The IR laser pulses were tuned to rotational lines in the fundamental vibrational band of OH $X^2\Pi$, while the UV pulses probed population in $X^2\Pi$ ($\nu=1$) using electronic transitions in the $A^2\Sigma \leftarrow X^2\Pi$ (1,1) system. The detection limits for TC-PS and TC-RFWM were both estimated to be approximately $5 \times 10^{12} \text{ cm}^{-3}$ per quantum state with impressive signal-to-background ratios of greater than $10^6:1$. Whereas TC-PS and TC-RFWM are nominally background-free techniques, the TC-LIF signal resides on a significant background (50-75 % of peak) due to LIF of the thermal population in $X^2\Pi$ ($\nu=1$).

We also tested the utility of these techniques for detecting CH_3 ,² which exhibits diffuse UV absorption in the $B^2A_1' \leftarrow X^2A_2''$ absorption band at 216 nm and does not fluoresce. The IR pump laser excited rotational lines in the ν_3 fundamental C-H stretching mode, and shared common ground states with the UV probe. We were not able to detect CH_3 in an atmospheric-pressure methane-air flame using the TC techniques, mainly as a result of energy partitioning at flame temperatures and the state specificity of the TC techniques; at 293 K, 5% of the population resides in $N=K=6$, while at 2000 K, this fraction is 0.1%. Instead, experiments were conducted at 293 K. Methyl radical was produced by photolyzing acetone or methyl iodide with a 266-nm laser pulse, and experiments were conducted at low pressure (~ 1 -5 Torr) and at atmospheric pressure. TC-RFWM spectra demonstrated the ability to resolve single rotational lines in the diffuse $B \leftarrow X$ absorption band. For example, when the pump laser excited the $R_3(6)$ line and the UV probe was scanned. P, Q, and R transitions out of the $N=6, K=3$ state were resolved, whereas the UV absorption spectrum is broad and featureless. Using TC-RFWM, the line positions of 20 rotational lines in the $B \leftarrow X$ band were measured and used to assign a new band origin. Uncertainties in the band origin affect the accuracy of absorption-based concentration measurements at high temperature, and we expect that this new assignment will improve such measurements.

Quenching of two-photon LIF of CO at elevated temperatures. Quantification of LIF measurements requires knowledge of quenching cross sections appropriate to the collisional environment. We previously conducted experiments to determine the temperature- and species-dependent quenching cross sections for 12 colliders in the temperature range $293 \text{ K} \leq T \leq 1031 \text{ K}$. Investigated species included He, Ne, Ar, Kr, Xe, H_2 , N_2 , O_2 , CO, H_2O , CO_2 , and CH_4 . The CO $B^1\Sigma^+$ ($\nu=0$) state was populated via two-photon excitation ($B^1\Sigma^+ \leftarrow \leftarrow X^1\Sigma^+$)³ using the frequency-tripled output of a distributed-feedback dye laser. The $B^1\Sigma^+ \rightarrow A^1\Pi$ fluorescence decay was collected with sub-ns resolution using a microchannel-plate photomultiplier tube. Recently,

approximately 2000 fluorescence decays were analyzed using a 6-parameter fitting routine that accounted for the instrument response function, photon transit-time spreading, non-resonant fluorescence background, and dc baseline shifts. Quenching rate coefficients (and thermally averaged cross sections) were determined from the dependence of the fluorescence-decay rate on quencher-gas pressure.⁴

Photolytic interferences in two-photon LIF of O-atom and CO. Two-photon LIF detection of CO and atomic oxygen require UV pulses of sufficiently high energies that ambient, high-temperature CO₂ may be photolyzed to produce O(³P) and CO(*X* ¹Σ⁺).⁵ With a 5- to 10-ns UV laser pulse, ground-state O and CO are photolytically produced and detected by the same pulse, limiting the detection sensitivity for the native species. We are characterizing the photolysis of CO₂ as a function of wavelength, temperature, and pulse energy to quantify the interference in TP-LIF measurements of CO at 230 nm (*B* ¹Σ⁺ ← ← *X* ¹Σ⁺)³ and 217 nm (*C* ¹Σ⁺ ← ← *X* ¹Σ⁺)⁶ as well as the interference to O-atom detection using TP-LIF at 226 nm (*3p* ³P ← ← *2p* ³P). The experiment employs a tunable ns laser to photodissociate CO₂, and a delayed ps laser to probe the products with TP-LIF.

Future Plans

Picosecond IR-UV double-resonance spectroscopy. The results of our proof-of-principle experiments that used ns IR-UV double-resonance spectroscopy to detect OH and CH₃ were promising for both the detection of and spectroscopic investigation of dark species. Single-mode lasers having a pulse duration of ca. 50 ps will be somewhat better sources for IR-UV double resonance techniques because they are short enough to avoid collisional effects but still long enough to allow for sufficient spectral resolution. Reducing mode fluctuations will result in lower limits of detection and allow more transient radicals to be monitored. High peak power will enable very efficient wavelength conversions and allow even weak transitions to be saturated. Studies at higher pressures will also be possible.

Quenching of two-photon LIF of CO at flame temperatures. Previous measurements characterized the species- and temperature-dependent quenching of the CO *B* ¹Σ⁺ (*v*=0) state in the temperature range 293 K ≤ *T* ≤ 1031 K. We will extend our measurements to temperatures approaching 2000 K using premixed, low-pressure flames. Under low-pressure flame conditions (~ 30 Torr), we expect that the fluorescence decay rate for CO will be on the order of 10⁸ s⁻¹. Using ps excitation and sub-ns LIF detection, we will temporally resolve the fluorescence decays, and infer cross sections from computed species concentrations and temperature in a series of engineered flames. A variety of premixed low-pressure flames, using various fuels, oxidizers, diluents, and flow rates will be utilized to achieve desired conditions. We expect to measure quenching cross sections for H₂O, H₂, CO₂, and N₂. We will validate the power-law temperature dependence that currently describes measured quenching rate coefficients for 293 K ≤ *T* ≤ 1031 K, or develop other models that ensure accurate prediction of the quenching cross sections at flame temperatures.

Photolytic interferences in two-photon LIF of O-atom and CO. We will continue our experiments to elucidate the photolysis mechanisms at play in two-photon LIF measurements of O-atom and CO concentrations. In addition to characterizing the CO₂ photolysis process at 217, 226, and 230 nm, we will characterize photolytic interferences to O-atom detection from other precursors. As suggested by other researchers, we expect contributions from the dissociation of O₂ following one-photon absorption in the Schumann-Runge bands. Scanning of the photolysis laser wavelength will be automated to enable the identification of any spectral signatures of the dissociation process and to determine the wavelength dependence of the photolysis cross section. Dependence on the laser fluence will be used to determine whether the photodissociation is due to a single-photon absorption or a higher-order process.

References

1. J. A. Gray, T. B. Settersten, and R. L. Farrow, "IR-UV double-resonance spectroscopy of OH in a flame," in preparation for submission to Chem. Phys. Lett.
2. J. A. Gray, T. B. Settersten, and R. L. Farrow, "IR-UV double-resonance spectroscopy of CH₃," in preparation for submission to Chem. Phys. Lett.
3. see, for example, S. Agrup and M. Aldén, Appl. Spectrosc. **48**, 1118 (1994).
4. see ref. 2 below.
5. A. P. Nefedov, V. A. Sinel'shchikov, A. D. Usachev, and A. V. Zobnin, Appl. Opt. **37**, 7729 (1998).
6. S. Linow, A. Dreizler, J. Janicka, E. P. Hassel, Appl. Phys. **B71**, 689 (2000).

BES-Supported Publications

1. T. B. Settersten and M. A. Linne, "Modeling Short-Pulse Excitation for Gas-Phase Laser Diagnostics," J. Opt. Soc. Am. B **19**, 954 (2002).
2. T. B. Settersten, A. Dreizler, and R. L. Farrow, "Temperature- and species-dependent quenching of CO $B^1\Sigma^+$ ($v=0$) probed by two-photon laser-induced fluorescence using a picosecond laser," J. Chem. Phys., submitted

Theoretical Studies of Potential Energy Surfaces and Computational Methods

Ron Shepard
Chemistry Division
Argonne National Laboratory
Argonne, IL 60439
[email: shepard@tcg.anl.gov]

Program Scope: This project involves the development, implementation, and application of theoretical methods for the calculation and characterization of potential energy surfaces (PES) involving molecular species that occur in hydrocarbon combustion. These potential energy surfaces require an accurate and balanced treatment of reactants, intermediates, and products. This difficult challenge is met with general multiconfiguration self-consistent-field (MCSCF) and multireference single- and double-excitation configuration interaction (MRSDCI) methods. In contrast to the more common single-reference electronic structure methods, this approach is capable of describing accurately molecular systems that are highly distorted away from their equilibrium geometries, including reactant, fragment, and transition-state geometries, and of describing regions of the potential surface that are associated with electronic wave functions of widely varying nature. The MCSCF reference wave functions are designed to be sufficiently flexible to describe qualitatively the changes in the electronic structure over the broad range of molecular geometries of interest. The necessary mixing of ionic, covalent, and Rydberg contributions, along with the appropriate treatment of the different electron-spin components (e.g. closed shell, high-spin open-shell, low-spin open shell, radical, diradical, etc.) of the wave functions are treated correctly at this level. Further treatment of electron correlation effects is included using large scale multireference CI wave functions, particularly including the single and double excitations relative to the MCSCF reference space. This leads to the most flexible and accurate large-scale MRSDCI wave functions that have been used to date in global PES studies.

Electronic Structure Code Maintenance, Development, and Applications: A major component of this project is the development and maintenance of the COLUMBUS Program System. The COLUMBUS Program System computes MCSCF and MRSDCI wave functions, MR-ACPF (averaged coupled-pair functional) energies, MR-AQCC (averaged quadratic coupled cluster) energies, spin-orbit CI energies, and analytic energy gradients. Geometry optimizations to equilibrium and saddle-point structures can be done automatically for both ground and excited electronic states. The COLUMBUS Program System is maintained and developed collaboratively with several researchers including Isaiah Shavitt and Russell M. Pitzer (Ohio State University), and Hans Lischka (University of Vienna, Austria). The COLUMBUS Program System of electronic structure codes has been maintained on the various machines used for production calculations by the Argonne Theoretical Chemistry Group, including IBM RS6000 workstations, DEC/COMPAC ALPHA workstations, the parallel IBM SP QUAD machine at ANL, the parallel IBM SP at NERSC, and the Theoretical Chemistry Group's IBM SP parallel supercomputer. Most recently, the codes have been ported to the 512-CPU Linux cluster, Chiba City, at Argonne, and to the new Theoretical Chemistry Group Linux cluster that was installed in November, 2001. The COLUMBUS codes also have been ported recently to the Macintosh personal computer, allowing sophisticated production-level electronic structure calculations on desktop and laptop computers. These computer codes are used in the production-level molecular applications by members and visitors of the Argonne Theoretical Chemistry Group. The next major release of the COLUMBUS codes will begin to incorporate the newer language features of F90/F95. This will facilitate future development and maintenance effort.

The submitted manuscript has been authored by a contractor of the U. S. Government under contract No. W-31-109-ENG-38. Accordingly, the U. S. Government retains a nonexclusive, royalty-free license to publish or reproduce the published form of this contribution, or allow others to do so, for U. S. Government purposes.

In collaboration with Hans Lischka (University of Vienna, Austria) and Robert Harrison (Pacific Northwest National Laboratory), the parallel version of the CI diagonalization program CIUDG has been developed and ported to several large parallel machines. Using the widely available TCGMSG and MPI libraries, this program also runs on networks of workstations, small-scale shared-memory parallel machines (e.g. Cray), and small-scale distributed memory machines (e.g. Linux clusters). The latest version of this parallel code uses the Global Array library, which allows for the elimination of unnecessary synchronization steps from earlier versions of this code and reduces the overall communications requirements for larger numbers of nodes. Excellent scalability on as many as 256 nodes of the IBM SP and 512 nodes on the Cray T3D and T3E have been demonstrated, and calculations on the 512-CPU Linux Cluster at Argonne are in progress. One benchmark calculation on Cr_2 by Dachsel, et al [*J. Phys. Chem. A*, **103**, 152-155 (1999)] using this code employed a $1.3\text{E}9$ CSF expansion of the wave function, the largest MRSDCI wave function ever reported. This is the first successful attempt to parallelize a production-level MRSDCI code, and this effort represents a major step toward using effectively the large-scale parallel supercomputers that are becoming available to scientists. Generalizations of the method are planned that will allow treatment of larger molecular systems. Future effort will be directed also to integrate the parallel version of the code with other parts of the COLUMBUS Program System to allow production-level PES calculations.

Initial applications of the MRSDCI analytic energy gradient code have begun and have included both ground and excited electronic states, and a variety of states including both closed- and open-shell systems and states of mixed valence and Rydberg character. A study of geometry optimizations for several small molecules has been initiated with the current code. This allows direct comparisons with experimental results and with other electronic structure methods. These geometry comparisons demonstrate that even with modest MCSCF reference spaces, the MRSDCI geometries compare very well with the very best single-reference methods currently in use. This is encouraging because the flexible MRSDCI wave functions are expected to be comparably accurate over the entire PES, whereas it is known that the accuracy of single-reference methods is biased toward those regions of the PES that are dominated by the reference determinant (such as near equilibrium conformations). These initial comparisons are for ground-state singlet molecules, and future work will include similar comparisons for high-spin states, radicals, and excited electronic states. Another recent application has been the study of the $1^1\text{B}_1(\sigma-\pi^*)$ and the $2^1\text{A}_1(\pi-\pi^*)$ excited states of formaldehyde for which it was found that, with flexible and accurate multireference wave functions, these two states form a conical intersection. Optimization of the geometry using analytic energy gradient methods reveals a nonplanar structure, in contrast to the findings of previous theoretical studies of this state. The critical feature of the electronic structure that must be correct in order to describe this conical intersection accurately is the accurate description of the ionic wave function contributions to the C–O bond. Another recent application is the barrier to predissociation of the lowest Rydberg excited state of NH_3 . This capability to characterize PESs of Rydberg states is important to the experimental work of S. Pratt in our group, and a multichannel quantum defect study of NH_3 will be undertaken next year in this context.

The bondlength statistics from the above systematic studies have suggested a hypothesis to explain some of the general trends of various electronic structure methods. This hypothesis is that the change in computed bondlengths is due not to the change in the kinetic energy (which is largely responsible for the overall minimum in the potential energy curve), but rather to the change in the electron-nuclear attraction. For example, single-configuration wave functions typically have spurious ionic contamination at long bond lengths, and these ionic terms in the wave function distort the electron-nuclear attraction

energy even near the equilibrium geometry. This hypothesis will be tested for various single reference and multireference wave functions. If this hypothesis proves to be correct, it may allow a way to compute improved molecular properties using simpler, and cheaper, wave function expansions.

Public Distribution of the COLUMBUS Program System: The COLUMBUS Program System is available using the *anonymous ftp* facility of the internet. The codes and online documentation are now also available from the web address <http://www.itc.univie.ac.at/~hans/Columbus/columbus.html>. The latest code version, 5.8.1, was released in September, 2001, and a new version 5.9 is imminent. In addition to the source code, the complete online documentation, installation scripts, sample calculations, and numerous other utilities are included in the distribution. A partial implementation of an IEEE POSIX 1009.3 library has been developed and is also available from <ftp://ftp.tcg.anl.gov>. This library simplifies the porting effort required for the COLUMBUS codes, and also may be used independently for other Fortran programming applications.

Iterative Matrix Diagonalization: A new iterative subspace diagonalization approach, called the Subspace Projected Approximate Matrix (SPAM) method, has been developed. In a subspace method, a new trial vector is added to an existing vector subspace each iteration. The choice of expansion vectors determines the convergence rate. The traditional Davidson and Lanczos methods are examples of iterative subspace methods. In the SPAM approach, an approximate matrix is constructed each iteration using a projection operator approach, and the eigenvector of this approximate matrix is used to define the new expansion vector. The convergence rate is improved in the SPAM method over the Davidson and Lanczos approaches because of these improved expansion vectors. The efficiency of the procedure depends on the relative expense of forming approximate and exact matrix-vector products. The SPAM method allows for the simultaneous optimization of several roots and it allows for an arbitrary number of levels of matrix approximations. This results in a multiroot-multilevel SPAM algorithm that has a wide range of possible applications. This matrix diagonalization method has been applied to a wide range of eigenvalue problems, including optimization of the lowest eigenpairs, the highest eigenpairs, and interior eigenpairs using both root-homing and vector-following. Approximations have been generated by neglecting small matrix elements, by tensor-product approximation, by expansion truncation, by neglect of off-diagonal matrix blocks, and by operator approximation. These applications demonstrate the wide range of applicability of the SPAM diagonalization method. Work in progress is directed toward approximation of MRSDCI Hamiltonian matrices based on repulsion integral approximation. Other planned extensions of this method include application to the generalized symmetric eigenvalue problem, the complex hermitian eigenvalue problem, the complex hermitian generalized eigenvalue problem, and the general (nonhermitian) eigenvalue problem. The application to other linear and nonlinear problems (including the coupled-cluster equation solution will also be considered. The source code and documentation for the multiroot-multilevel SPAM method are available from <ftp://ftp.tcg.anl.gov/pub/spam>.

The TCG Beowulf Linux Cluster: The Argonne Theoretical Chemistry Group historically has maintained an advanced computer system. Over the years, these have included the FPS attached processor (1982), the Stardent Titan workstations (1988), the Alliant FX-8 (1989), and the FX-2800 (1992) shared-memory parallel computers, and more recently the IBM SP distributed memory parallel computer system (1994) which now consists of 44 nodes. It is now possible to configure commodity hardware and software with free (or relatively inexpensive) operating system software to create a machine capable of supplying much of the computational requirements of the Group. We have started to grow such a system with the recent purchase of a 16 node (32 CPUs) system. The group's Linux cluster was delivered in November 2001, the COLUMBUS codes were ported and

installed in December, 2001, and it has been in production mode since January 2002. Over the next few years, we will expand this system to 64, or more, nodes. This allows the group to exploit the rapidly dropping costs of CPUs, memory, switching technology, and disk storage, and the rapidly increasing processing power of commodity CPUs.

This work was supported by the U.S. Department of Energy, Office of Basic Energy Sciences, Division of Chemical Sciences, under Contract No. W-31-109-ENG-38.

Publications:

- "High-Performance Computational Chemistry: Hartree-Fock Electronic Structure Calculations on Massively Parallel Processors," J. L. Tilson, M. Minkoff, A. F. Wagner, R. Shepard, P. Sutton, R. J. Harrison, R. A. Kendall, A. T. Wong, *The Int. J. High Performance Computing Applications* **13**, 291-302 (1999).
- "Ab Initio Determination of Americium Ionization Potentials," J. L. Tilson, R. Shepard, C. Naleway, A. F. Wagner, and W. C. Ermler, *J. Chem. Phys.* **112**, 2292-2300 (2000).
- "The Subspace Projected Approximate Matrix (SPAM) Modification of the Davidson Method," R. Shepard, A. F. Wagner, J. L. Tilson, and M. Minkoff, *J. Comp. Phys.* **172**, 472-514 (2001).
- "High-Level Multireference Methods in the Quantum-Chemistry Program System COLUMBUS: Analytic MR-CISD and MR-AQCC Gradients and MR-AQCC-LRT for Excited States, GUGA Spin-Orbit CI, and Parallel CI," H. Lischka, R. Shepard, R. M. Pitzer, I. Shavitt, M. Dallos, T. Muller, P. G. Szalay, M. Seth, G. S. Kedziora, S. Yabushita, and Z. Zhang, *Phys. Chem. Chem. Phys.* **3**, 664-673 (2001).
- "Geometry Optimization of Excited Valence States of Formaldehyde Using Analytical Multireference Configuration Interaction Singles and Doubles and Multireference Averaged Quadratic Coupled-Cluster Gradients, and the Conical Intersection Formed by the $1^1B_1(\sigma-\pi^*)$ and the $2^1A_1(\pi-\pi^*)$ States," M. Dallos, T. Muller, H. Lischka, and R. Shepard, *J. Chem. Phys.* **114**, 746-757 (2001).
- "The Calculation of f-f Spectra of Lanthanide and Actinide Ions by the MCDF-CI Method," M. Seth, K. G. Dyall, R. Shepard, and A. Wagner, *J. Phys. B: At. Mol. Opt. Phys.* **34**, 2383-2406 (2001).
- "An Ab Initio Study of the f-f Spectroscopy of Americium⁺³," J. L. Tilson, C. Naleway, M. Seth, R. Shepard, A. F. Wagner, and W. C. Ermler, *J. Chem. Phys.* (*in press*).
- "An Ab Initio Study of the Ionization Potentials and the f-f Spectroscopy of Europium Atoms and Ions," C. Naleway, M. Seth, R. Shepard, A. F. Wagner, J. L. Tilson, W. C. Ermler, and S. R. Brozell, (*in press*).
- "Analytic MRCI Gradient for Excited States: Formalism and Application to the $n-\pi^*$ valence- and $n-(3s,3p)$ Rydberg States of Formaldehyde," H. Lischka, M. Dallos, and R. Shepard, *Mol. Phys.* (*in press*).
- "Reducing I/O Costs For The Eigenvalue Procedure In Large-Scale CI Calculations," R. Shepard, I. Shavitt, and H. Lischka, *J. Computational Chem.*, (*in press*).

COMPUTATIONAL AND EXPERIMENTAL STUDY OF LAMINAR FLAMES

M. D. Smooke and M. B. Long
Department of Mechanical Engineering
Yale University
New Haven, CT 06520
mitchell.smooke@yale.edu

Program Scope

Our research has centered on an investigation of the effects of complex chemistry and detailed transport on the structure and extinction of hydrocarbon flames in coflowing axisymmetric configurations. We have pursued both computational and experimental aspects of the research in parallel. The computational work has focused on the application of accurate and efficient numerical methods for the solution of the boundary value problems describing the various reacting systems. Detailed experimental measurements were performed on axisymmetric coflow flames using two-dimensional imaging techniques. Spontaneous Raman scattering and laser-induced fluorescence were used to measure the temperature, major and minor species profiles. Laser-induced incandescence has been used to measure soot volume fractions. Our goal has been to obtain a more fundamental understanding of the important fluid dynamic and chemical interactions in these flames so that this information can be used effectively in combustion modeling.

Recent Progress

The major portion of our work during the past year has focused on a combined computational and experimental study of time varying, axisymmetric, laminar unconfined methane-air diffusion flames and on a combined computational and experimental study of the formation of soot in axisymmetric, laminar ethylene-air diffusion flames. The time varying systems can enable the investigator to bridge the gap between laminar and fully turbulent systems. In addition, time varying flames offer a much wider range of interactions between chemistry and fluid dynamics than do steady-state configurations. The sooting flames can enable the investigator to understand the detailed inception, oxidation and surface growth processes by which soot is formed in hydrocarbon flames.

Time-Varying Flames

Atmospheric pressure, overventilated, axisymmetric, coflowing, nonpremixed laminar flames were generated with a burner in which the fuel flows from an uncooled 4.0 mm inner diameter vertical brass tube (wall thickness 0.038 mm) and the oxidizer flows from the annular region between this tube and a 50 mm diameter concentric tube. The oxidizer is air while the fuel is a mixture containing methane and nitrogen 65%/35% by volume, to eliminate soot. The burner includes a small loudspeaker in the plenum of the fuel jet, which allows a periodic perturbation to be imposed on the exit parabolic velocity profile. Perturbations of 30% and 50% of the average velocity have been investigated. Because the flame is slightly lifted, there is no appreciable heat loss to the burner.

Two-dimensional profiles of temperature, mixture fraction, and mole fractions of N₂, CO₂, CH₄, H₂, CO, and H₂O as well as CH* emission have been measured in the time-varying flame. We obtain CH* relative concentration from flame chemiluminescence, and species concentrations and temperature with vibrational Stokes-shifted Raman scattering and Rayleigh scattering using

the second harmonic of a Nd:YAG laser. Each measurement is averaged over 1200 laser pulses, with separate data acquisitions for each orthogonal polarization of the scattered light. Measurements are performed at heights above the burner ranging from 2.5 mm to 50 mm, in 0.5 mm increments. These line measurements are then tiled together to form images. Data are acquired for the steady state flame, and for five equally spaced phases of the forced flame over one period.

The modulated flame length increases in time, until the flame begins to pinch off downstream, forming two slightly attached high temperature regions. For the 50% modulation, the two regions break apart, leaving unattached high temperature zones. Eventually the downstream region moves farther downstream, and burns out. The pinch-off phenomenon is more drastic in the 50% modulation than the 30% modulation. For the 50% case, the flame has a larger curvature than for the 30% case. The flame width at the flame anchoring point varies significantly over time, with a larger fluctuation seen for the 50% case. The lift off height stays the same over time, comparable to the steady flame lift off height.

Computationally we have generalized the velocity-vorticity model to solve time-dependent problems such as the forced time varying flame. We use a C1 mechanism with an optically thin radiation submodel. The velocity-vorticity model avoids the hyperbolic nature of the continuity equation and the accompanying numerical constructions required to suppress spurious wave propagation. For a time-dependent system, the computer effort required to calculate the solution at each time step scales approximately linearly with the number of grid points used to discretize the domain. To employ a reduced number of grid points efficiently, we have applied the local rectangular refinement (LRR) solution-adaptive gridding method [1] --- an orthogonal, unstructured gridding technique for solving systems of coupled nonlinear elliptic PDEs --- to the two periodically time-varying axisymmetric laminar diffusion flames.

The time-dependent LRR method is similar to the steady-state LRR method [1], with the following three exceptions. First, in the time-dependent method, the grid undergoes remeshing every several time steps, as needed. Remeshing is an automatic process in which any unnecessary refinement is removed and any required additional refinement is added. Second, in the current work, temporal partial derivatives are discretized using second order backward differences. Third, time steps are chosen adaptively based on the requirement that the CFL number not exceed unity.

In both the numerical and experimental results for each case, temporal fluctuations are apparent, although they are present to a lesser degree in the numerical results, presumably because the upwind discretizations used on the convective terms (for stability reasons) artificially increase the numerical diffusion. The "wishbone" structure is always present in the high temperature region near the flame's base; however, very hot gases also exist downstream during some parts of the periodic cycle. Despite dramatic fluctuations in the downstream region, the liftoff height remains nearly constant with time.

Soot Modeling

Soot kinetics are modeled as coalescing, solid carbon spheroids undergoing surface growth in the free molecule limit. The particle mass range of interest is divided into sections and an equation is written for each section including coalescence, surface growth, and oxidation. For the smallest section, an inception source term is included. The transport conservation equation for each section includes thermophoresis, an effective bin diffusion rate, and source terms for gas-phase scrubbing. The gas and soot equations are additionally coupled through non-adiabatic radiative

loss in the optically-thin approximation. The inception model employed here is based on an estimate of the formation rate of two- and three-ringed aromatic species (naphthalene and phenanthrene), and is a function of local acetylene, benzene, phenyl and molecular hydrogen concentrations. Oxidation of soot is by O₂ and OH. The surface growth rate is based upon that of Harris and Weiner [2] with an activation energy as suggested by Hura and Glassman [3].

Gas temperatures were measured with thermocouples and corrected for radiation heat transfer effects using standard techniques. A rapid insertion procedure was used to minimize errors due to soot deposition onto the thermocouple. Species concentrations were measured by extracting gas samples from the flames with a narrow-tipped quartz microprobe and analyzing these samples with on-line mass spectrometry. Acetylene and ethylene were quantified with an Extrel C50 variable-ionization-energy electron impact/quadrupole mass spectrometer, and C₃ to C₁₂ hydrocarbons with a custom-built photoionization/time-of-flight mass spectrometer. Measurements were directly calibrated and have an absolute uncertainty of 30%. Using planar laser imaging, we obtain two-dimensional fields of temperature, fuel concentration, and soot volume fraction in the C₂H₄/N₂ flame. The temperature field is determined using the two scalar approach of Starner et al. [4]. The soot volume fraction field is determined by laser-induced incandescence (LII). At sufficient laser intensities, the LII signal has been shown to be directly proportional to the soot volume fraction. Probe measurements of the soot volume fraction are used for calibration.

Fuel and nitrogen are introduced through the center tube (4mm id) utilizing a parabolic velocity profile and air through the outer coflow with a plug flow profile. Both velocity profiles were those employed in the experiments. Flames containing 40% (60%), 60% (40%) and 80% (20%) mole fractions of ethylene (nitrogen) with a bulk averaged velocity of 35 cm/sec were studied. The coflow air velocity was 35 cm/sec. Reactant temperatures were assumed to be 298 K. All radial velocities were assigned to zero at the flame base. Calculations were performed on an SGI Origin 2000 computer. The computations included 20 soot sections.

We have found that by placing an upper bound on the size of the soot particles for which surface growth is allowed, we have dramatically improved the comparisons between the predicted soot volume fractions of the model and the experiments, though the magnitude and orientation of some key species still contain significant differences. These results clearly indicate that the ability to make quantitative soot predictions remains limited by some fundamental uncertainties in the soot model (including the lack of aging and aggregate formation effects), by the ability of the chemical kinetic mechanism to predict accurately the concentrations of important species (benzene, propargyl, acetylene and diacetylene) and possibly by the lack of quantitative information concerning the production of translucent particles.

Future Plans

During the next year we hope to expand our research in two main areas. First, we will continue our study of sooting hydrocarbon flames with the goal of understanding the differences in soot distribution between the computational and experimental results. Second, we will continue our study of flickering diffusion flames with the goal of incorporating a C₂ mechanism and high order spatial approximations into the model. We will then begin incorporating a detailed soot model into the gas phase system with the goal of predicting soot volume fractions as a function of time. Laser induced incandescence (LII) will be used to measure soot volume fractions.

References

1. Bennett, B.A.V. and Smooke, M.D., *Combust. Theory Model.*, **2**, p. 221, (1998).
2. Harris, S.J., and Weiner, A.M., *Combust. Sci. Tech.*, **31**, p. 155, (1983).
3. Hura, H.S. and Glassman, I., *Proceedings of the Combustion Institute*, **22**, p. 371, (1988).
4. Starner, S., Bilger, R. W., Dibble, R. W., Barlow, R. S., *Combust. Sci. Tech.*, **86**, p. 223, (1992).
5. Bowman, C.T., Hanson, R.K., Davidson, D.F., Gardiner, Jr., W.C. Lissianski, Smith, G.P., Golden, D.M., Frenklach, M., Wang, H., and Goldenberg, M., GRI-Mech version 2.11, <http://www.gri.org> (1995).

DOE Sponsored Publications since 2000

1. J. Luque, J. B. Jeffries, G. P. Smith, D. R. Crosley, K. T. Walsh, M. B. Long, and M. D. Smooke, "CH(A-X) and OH(A-X) Optical Emission in an Axisymmetric Laminar Diffusion Flame," *Comb. and Flame*, **122**, (2000).
2. B. A. V. Bennett, C. McEnally, L. Pfefferle, and M. D. Smooke, "Computational and Experimental Study of Axisymmetric Coflow Partially Premixed Methane/Air Flames," *Comb. and Flame*, **123**, (2000).
3. K.T. Walsh, J. Fielding, M.D. Smooke, and M.B. Long, "Experimental and Computational Study of Temperature, Species, and Soot in Buoyant and Nonbuoyant Coflow Laminar Diffusion Flames," *Proceedings of the Combustion Institute*, **28**, (2000).
4. C.S. McEnally, L.D. Pfefferle, A.M. Schaffer, M.B. Long, R.K. Mohammed, M.D. Smooke, and M.B. Colket, "Characterization of a Coflowing Methane Air Nonpremixed Flame with Computer Modelling, Rayleigh-Raman Imaging, and On-Line Mass Spectrometry," *Proceedings of the Combustion Institute*, **28**, (2000).
5. M. D. Smooke and B. V. Bennett, "Modeling Coflow Diffusion Flames with Local mesh Refinement," in *Computational Fluid Dynamics in Industrial Combustion*, eds. C. E. Baukal, Jr., V. Y. Gershtein, and X. Li, CRC Press, New York, (2000).
6. B.A.V. Bennett, C.S. McEnally, L.D. Pfefferle, M.D. Smooke, and M.B. Colket, "Computational and Experimental Study of Axisymmetric Coflow Partially Premixed Ethylene/Air Flames," *Comb. and Flame*, **127**, (2001).
7. B.A.V. Bennett and M.D. Smooke, "The Effect of Overall Discretization Scheme on Jacobian Structure, Convergence Rate, and Solution Accuracy within the Local Rectangular Refinement Method," *Numerical Linear Algebra with Applications*, **8**, (2001).

STUDIES OF COMBUSTION KINETICS AND MECHANISMS

Irene R. Slagle
Research Center for Chemical Kinetics
Department of Chemistry
The Catholic University of America
Washington, DC 20064
slagle@cua.edu

PROGRAM SCOPE

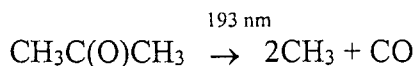
The objective of the current research program is to gain new quantitative knowledge of the kinetics and mechanisms of polyatomic free radicals that are important in hydrocarbon combustion processes. Experimental studies are carried out in a heatable fast-flow reactor coupled to a photoionization mass-spectrometer. Polyatomic free radicals (R) are generated in situ by excimer laser photolysis (193 or 248 nm) of suitable radical precursors and the radical decay is monitored in real-time experiments. Where possible, these experimental studies are coupled with theoretical ones to obtain an improved understanding of the factors governing reactivity.

RECENT PROGRESS

During the current reporting period our work has focused on two general types of free radical reactions: radical-radical reactions (which may lead to chain termination and molecular mass growth) and reactions of radicals with acetylene (reactions which may eventually lead to the formation of PAHs).

I. Reactions of CH₃ with Hydrocarbon Radicals

The reactions of methyl radicals with three unsaturated free radicals (vinyl, propargyl and allyl) and three n-alkyl radicals (C₂H₅, n-C₃H₇, and n-C₄H₉) have been studied using a kinetic method similar to that suggested by Garland and Bayes (*J. Phys. Chem.* **1990**, *94*, 4941). Initial conditions are chosen such that the concentration of methyl radicals is much greater than that of the unsaturated radicals. The only appreciable loss of methyl radicals comes from the self-reaction of methyl with minor contributions from heterogeneous loss. Because the concentration of unsaturated or n-alkyl radicals is kept sufficiently low that their rate of self-reaction is negligibly slow, the loss of these radicals occurs only by their reaction with CH₃ and a slow heterogeneous reaction. Because the heterogeneous rate constants can be determined directly in ancillary experiments, the rate constant for the reaction of CH₃ with another radical can be determined from temporal decay profiles of both radicals. The advantage of this method is that it is not necessary that the concentration of the unsaturated radical be known with any degree of accuracy. The initial concentration of CH₃ can be determined from the extent of decomposition of the CH₃-radical precursor, acetone.



1. CH₃ + C₂H₃

The most interesting of these reactions is the CH₃ + C₂H₃ reaction because of the many possible reaction paths that are energetically feasible. The overall rate constant is independent of pressure and demonstrates a slight negative temperature dependence, $k_{\text{C}_2\text{H}_3-\text{CH}_3} = 5.1 \times 10^{-7} \text{T}^{-1.26} \exp(-362/\text{T}) \text{ cm}^3 \text{ molecule}^{-1} \text{ s}^{-1}$. Propene, acetylene and allyl radicals

were identified as primary products of the $\text{CH}_3 + \text{C}_2\text{H}_3$ reaction. At room temperature propene and acetylene are the major products of the reaction whereas at 900K production of allyl radicals becomes the dominating channel. On the basis of these experimental results, a mechanism consisting of two major routes is proposed. One route proceeds via direct abstraction of a hydrogen atom from the vinyl radical by the methyl radical resulting in the formation of acetylene and methane. The other route proceeds via the formation of chemically activated propene that can undergo either collisional stabilization or further decomposition into allyl radical and hydrogen atom.

The mechanism of the radical-radical reaction $\text{C}_2\text{H}_3 + \text{CH}_3$ was also studied by quantum chemical methods. The pathways of reaction channels observed in the experimental studies, as well as those of other potential channels, were investigated. The results of the quantum chemical study and of the experimental work were used to create a model of the chemically activated route ($\text{C}_2\text{H}_3 + \text{CH}_3 \rightleftharpoons \text{C}_3\text{H}_6 \rightarrow \text{H} + \text{C}_3\text{H}_5$). In this model, energy- and angular momentum-dependent rate constants are calculated using the RRKM method in combination with the microcanonical variational selection of the transition states. Pressure effects are described by solution of the master equation. Temperature and pressure dependences of the rate constants and product yields were investigated. The model was used to predict the rate constants and branching fractions of the $\text{C}_2\text{H}_3 + \text{CH}_3$ reaction at temperatures and pressures outside the experimental ranges. The same model was used to analyze kinetics of two other reactions which occur on the same potential energy surface: the thermal decomposition of propene and the reaction of H atom with allyl radical, $\text{H} + \text{C}_3\text{H}_5 \rightleftharpoons \text{C}_3\text{H}_6 \rightarrow \text{C}_2\text{H}_3 + \text{CH}_3$. The results demonstrate the increasing importance of the $\text{CH}_3 + \text{C}_2\text{H}_3$ channels in both reactions at high temperatures (above ~ 1500 K).

2. $\text{CH}_3 + \text{C}_3\text{H}_5$ and $\text{CH}_3 + \text{C}_3\text{H}_3$

Unlike the reaction with vinyl, the only products observed in the allyl-methyl and propargyl-methyl reactions are the collisionally stabilized adducts. Reactions were studied over the temperature range 301-800K and bath gas (He) densities ($3 - 36 \times 10^{16}$ atoms cm^{-3}). The only product observed for the $\text{C}_3\text{H}_5 + \text{CH}_3$ reaction was C_4H_8 . Master equation modeling of collisional effects indicates that this reaction is near its high pressure limit under all experimental conditions used. Minor corrections for fall-off effect (on average, 18% at the highest temperatures) result in the high-pressure-limit rate constant $k^\infty_{\text{C}_3\text{H}_5-\text{CH}_3} = 1.55 \times 10^{-9} T^{-0.54} \exp(117\text{K}/T) \text{ cm}^3 \text{ molecule}^{-1} \text{ s}^{-1}$.

On the other hand, master equation modeling indicates that the reaction of propargyl with methyl is not near the high-pressure limit under our experimental conditions. Falloff corrections applied to this reaction reach, on average, a factor of two at 800K and introduce uncertainties in the high-pressure-limit rate constant values, $k^\infty_{\text{C}_3\text{H}_3-\text{CH}_3} = 6.80 \times 10^{-11} \exp(130\text{K}/T) \text{ cm}^3 \text{ molecule}^{-1} \text{ s}^{-1}$. The only product for the $\text{C}_3\text{H}_3 + \text{CH}_3$ reaction is C_4H_6 .

3. $\text{CH}_3 + n\text{-Alkyl Radicals}$

Overall rate constants of the reactions of methyl radical with three n-alkyl radicals (C_2H_5 , n- C_3H_7 , and n- C_4H_9) were obtained in direct real-time experiments in the temperature region 297-800 K and bath gas (helium) density $(3-36) \times 10^{16}$ atom cm^{-3} . The observed overall $\text{C}_2\text{H}_5 + \text{CH}_3$ (1), n- $\text{C}_3\text{H}_7 + \text{CH}_3$ (2), and n- $\text{C}_4\text{H}_9 + \text{CH}_3$ (3) rate constants demonstrate negative temperature dependences. Master equation modeling of collisional effects indicates that the n- $\text{C}_3\text{H}_7 + \text{CH}_3$ and the n- $\text{C}_4\text{H}_9 + \text{CH}_3$ reactions are at the high-pressure limit under all experimental conditions used. The $\text{C}_2\text{H}_5 + \text{CH}_3$ reaction is not at the high-pressure limit and falloff in reaction 1 cannot be neglected at 800 K. Falloff corrections applied to reaction 1, on average, reach 45% at 800 K and introduce noticeable uncertainties in the extrapolated high-pressure-limit rate constant values. The following expressions for the high-pressure-limit rate

constants of reaction 1 – 3 were obtained: $k_1^\infty = 2.36 \times 10^{-11} \exp(433 \text{ K} / T)$, $k_2^\infty = 3.06 \times 10^{-11} \exp(387 \text{ K} / T)$, and $k_3^\infty = 2.28 \times 10^{-11} \exp(473 \text{ K} / T) \text{ cm}^3 \text{ molecule}^{-1} \text{ s}^{-1}$. C_3H_8 was detected as a product of reaction 1 and C_5H_{12} and C_4H_8 were detected as products of reaction 3.

II. Propargyl Radical Self Reaction

The kinetics of the propargyl radical self reaction has been studied over the temperature interval 500 – 1000 K and bath gas (He) density $(3 - 6) \times 10^{16} \text{ molecule cm}^{-3}$. Propargyl radicals were produced by 248-nm laser photolysis of oxalyl chloride ($(\text{CClO})_2 \rightarrow 2\text{Cl} + 2\text{CO}$) followed by the instantaneous conversion of the chlorine atoms into propargyl radicals by the reaction with propyne ($\text{Cl} + \text{C}_3\text{H}_4 \rightarrow \text{C}_3\text{H}_3 + \text{HCl}$). Thus, no active species other than C_3H_3 were present in the system during the kinetics of C_3H_3 decay. Initial concentrations of the C_3H_3 radical were determined using the measured production of HCl. The kinetics of C_3H_3 decay was monitored in real time and the values of the rate constant were determined from the $[\text{C}_3\text{H}_3]$ temporal profiles. The rate constant was found to decrease with temperature from $3.3 \times 10^{-11} \text{ cm}^3 \text{ molecule}^{-1} \text{ s}^{-1}$ at 500 K to $2.8 \times 10^{-11} \text{ cm}^3 \text{ molecule}^{-1} \text{ s}^{-1}$ at 700K and $1.3 \times 10^{-11} \text{ cm}^3 \text{ molecule}^{-1} \text{ s}^{-1}$ at 1000K. The low value at 1000 K is likely to be due to the falloff effects. Products of the reaction were studied in real-time experiments as well as by GC/MS analysis. In the real-time experiments, only formation of products at mass of C_6H_6 was observed with no contribution of the $\text{C}_6\text{H}_5 + \text{H}$ channel. GC/MS analysis demonstrated dependence of the distribution of products on temperature.

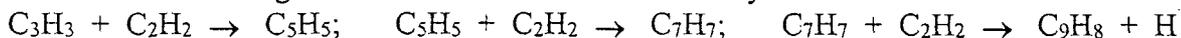
III. Reactions of Radicals with Acetylene

Numerous studies aimed at the elucidation of the chemical pathways leading to the formation of the first aromatic ring in the combustion of hydrocarbons have invoked the reactions of free radicals with acetylene (H. Richter and J.B. Howard, Prog. Energy Combust. Sci. 2000, 26, 565). Two reactions of acetylene (with propargyl and with methyl radicals) have been isolated for study with initial conditions selected to provide low radical concentrations so that potential side reactions such as reactions between radical products have negligible rates compared to that of the reaction of interest. Experiments were conducted under pseudo-first-order conditions with acetylene in large excess over the radical concentration. The photolysing laser intensity was kept low ($0.11 - 5.33 \text{ mJ pulse}^{-1} \text{ cm}^{-2}$) to ensure that products of the photodissociation of acetylene do not interfere with the reaction with propargyl or methyl.

1. $\text{C}_3\text{H}_3 + \text{C}_2\text{H}_2$

The reaction between the propargyl radical and acetylene was studied in the temperature range 800 – 1100 K and bath gas (helium) densities $[\text{He}] = (1.2 - 2.4) \times 10^{17} \text{ atom cm}^{-3}$. Propargyl radicals (C_3H_3) were produced by the pulsed 248-nm laser photolysis of 1,3-butadiene. The temperature dependence of the rate constant can be described by the Arrhenius expression: $k_1 = 3.9 \times 10^{-13} \exp(-5030 \text{ K} / T) \text{ cm}^3 \text{ molecule}^{-1} \text{ s}^{-1}$. The low value of the preexponential factor is consistent with the formation of C_5H_5 in a chemically activated mechanism characterized by a “loose” entrance and a “tight” exit transition states.

C_5H_5 was identified as a primary product of the reaction with the characteristic growth time of the C_5H_5 signal matching that of the C_3H_3 decay. Formation of C_7H_7 was observed with kinetics corresponding to that of a secondary reaction and formation of C_9H_8 was also observed at even longer reaction times. The kinetics of product formation suggest the following sequence of reactions occurring under the conditions of excess acetylene used in the current work:



2. CH₃ + C₂H₂

Rate constants of the reaction of methyl with acetylene were determined from 750 to 1000 K and were found to be independent of bath gas density within the experimental range, $[M] = [\text{He}] + [\text{C}_2\text{H}_2] = (6 - 24) \times 10^{16}$ molecule cm^{-3} . C₃H₄ was detected as a primary product of the reaction. The rate constant under these conditions can be described by the Arrhenius expression, $k = (6.3 \pm 2.9) \times 10^{-13} \exp((-5011 \pm 422) \text{ K}/T)$ $\text{cm}^3 \text{ molecule}^{-1} \text{ sec}^{-1}$.

FUTURE PLANS

The GC/MS study of the propargyl radical self reaction will be continued in order to determine the nature and distribution of the isomers of the C₆H₆ products. The self reaction of ethyl radicals will be determined as a function of temperature and density and the temperature dependence of the disproportionation to recombination ratio will be studied.

PUBLICATIONS ACKNOWLEDGING SUPPORT OF THIS GRANT

(2000 – present)

M. N. Kislitsyn, I. R. Slagle, V. D. Knyazev. Kinetics of the Reaction Between Methyl Radical and Acetylene. Symp. Int. Comb. Proc. Accepted for publication.

S. I. Stoliarov, V. D. Knyazev, I. R. Slagle. Computational Study of the Mechanism and Product Yields in the Reaction Systems $\text{C}_2\text{H}_3 + \text{CH}_3 \rightleftharpoons \text{C}_3\text{H}_6 \rightleftharpoons \text{H} + \text{C}_3\text{H}_5$ and $\text{C}_2\text{H}_3 + \text{CH}_3 \rightarrow \text{CH}_4 + \text{C}_2\text{H}_2$. J. Phys. Chem. A. Accepted for publication.

V. D. Knyazev. Theoretical Study of the Channel of Formation of CO in the Reaction of O Atoms with CH₃: Reaction Over a barrier but not Through a Saddle Point. J. Phys. Chem. A. Submitted for Publication.

V. D. Knyazev, I. R. Slagle. Kinetics of the Reactions of n-Alkyl (C₂H₅, n-C₃H₇, and n-C₄H₉) Radicals with CH₃. J. Phys. Chem. A, 105, 6490 (2001).

V. D. Knyazev, I. R. Slagle. Kinetics of the Reactions of Allyl and Propargyl Radicals with CH₃. J. Phys. Chem. A, 105, 3196 (2001).

S. I. Stoliarov, A. Bencsura, E. Shafir, V. D. Knyazev, I. R. Slagle. Kinetics of the Reaction of the CHCl₂ Radical With Oxygen Atoms. J. Phys. Chem. A, 105, 76 (2001).

V. D. Knyazev, W. Tsang. Chemically and Thermally Activated Decomposition of Secondary Butyl Radical. J. Phys. Chem. A, 104, 10747 (2000).

S. I. Stoliarov, V. D. Knyazev, I. R. Slagle. Experimental Study of the Reaction between Vinyl and Methyl Radicals in the Gas Phase. Temperature and Pressure Dependence of Overall Rate Constants and Product Yields. J. Phys. Chem. A, 104, 9687 (2000).

Elementary Reaction Kinetics of Combustion Species

Craig A. Taatjes

Combustion Research Facility, Mail Stop 9055, Sandia National Laboratories,
Livermore, CA 94551-0969

cataatj@ca.sandia.gov

www.ca.sandia.gov/CRF/staff/taatjes.html

SCOPE OF THE PROGRAM

The scope of this program is to develop new laser-based methods for studying chemical kinetics and to apply these methods to the investigation of fundamental chemistry relevant to combustion science. The central goal is to perform accurate measurements over wide temperature ranges of the rates at which important free radicals react with stable molecules. In the past several years, the program has concentrated on the investigation of CH, C₂H, and Cl + stable molecule reactions, applying the extraordinarily precise techniques of laser photolysis/continuous-wave laser-induced fluorescence (LP/cwLIF) and laser photolysis/continuous-wave infrared long-path absorption (LP/cwIRLPA). The precision of these methods enables kinetic measurements to probe reaction mechanisms, utilizing thermal rate constant and product distribution measurements as indicators of detailed global reaction paths. Another aim has been the investigation and application of new detection methods for precise and accurate kinetics measurements. Absorption-based techniques are emphasized, since many radicals critical to combustion are not amenable to fluorescence detection. As an additional advantage, absorption-based techniques can be straightforwardly applied to determination of absolute concentrations in reacting systems.

RECENT PROGRESS

The efforts of the laboratory center on extending the capabilities of the laser-induced-fluorescence method to new reaction systems, on developing high-sensitivity absorption-based techniques for kinetics measurements, and on applying these techniques to investigate important combustion reactions. In the last year we have continued to concentrate on the application of cw infrared frequency-modulation spectroscopy to measuring product formation in the reaction of alkyl radicals with O₂. We have also used cw LIF detection of HCO in the *B* ← *X* band to investigate kinetic isotope effects in the HCO + O₂ and HCO + NO reactions, and begun measuring reactions of the vinyl radical using visible absorption in the *A* ← *X* band. Absorption-based techniques for probing reactions, principally in the infrared, are extensively used.

IR FM Measurements of Product Formation in Alkyl + O₂ reactions

Neopentyl + O₂. We have performed time-resolved measurements of HO₂ formation in the Cl-atom initiated oxidation of *neo*-pentane using diode-laser absorption in the overtone of the O-H stretch. In these experiments, *neo*-pentyl radicals are produced by the reaction of *neo*-pentane with Cl atoms from Cl₂ photolysis at 355 nm. The direct

formation of HO₂ + alkene, which dominates many other alkyl + O₂ reactions, cannot occur in the *neo*-pentyl + O₂ reaction (because the conjugate alkene does not exist). The HO₂ observed in the neopentane oxidation must arise from secondary reactions, including subsequent chemistry of the QOOH intermediate. A significant overall yield of HO₂ is observed above 600 K, increasing with temperature. At 673 K, the HO₂ yield ([HO₂]/[Cl]₀) depends strongly on O₂ concentration. At the highest O₂ concentrations an apparent yield greater than unity is observed, indicating significant chain branching. This result is consistent with QOOH + O₂ reaction as a key step in chain branching. Ab initio (QCISD(T) and B3LYP) calculations of stationary states in the *neo*-pentyl + O₂ system (carried out by Stephen Klippenstein at the CRF) confirm the importance of the RO₂ ↔ QOOH isomerization and will be used in devising a more detailed model of the Cl-initiated *neo*-pentane oxidation.

C₂D₅ + O₂. In collaboration with Atsumu Tezaki (University of Tokyo) we have accomplished direct laser probing of the electronic transition in HO₂ and DO₂, using difference frequency mixing of a cw Nd:YAG laser and a dye laser in bulk LiNbO₃. Our first experiments have focused on detection of DO₂ from the reaction of C₂D₅ with O₂. The kinetic isotope effect in the DO₂ production will be a convolution of kinetic isotope effects for the stabilization, redissociation, and elimination channels, and successful modeling of the deuterated system will place additional demands on the theoretical description of the ethyl + O₂ potential energy surface. Our preliminary results establish that the “prompt” DO₂ yield is significantly smaller than the analogous HO₂ yield in C₂H₅ + O₂, presumably reflecting a longer lifetime of the RO₂ because of the increased adduct density of states. Further experiments are underway to characterize the contributions of DO₂ elimination from C₂D₅O₂.

Cyclopropyl + O₂. The production of HO₂ and OH in the Cl-initiated oxidation of cyclopropane was previously investigated in our laboratory using laser photolysis / CW infrared frequency modulation spectroscopy. In collaboration with Tim Wallington and Michael Hurley at Ford Motor Company, we have modeled the product formation in the *c*-C₃H₅ + O₂ reaction. In our experiments significant OH (~15%) and HO₂ (~25%) production is observed at 296 K and both [OH]/[Cl]₀ and [HO₂]/[Cl]₀ increase slowly with increased temperature until ~ 600 K where a sharper increase with temperature occurs. The Ford experiments identify ethene and oxirane as products following the reaction of cyclopropyl radicals with O₂. We propose that HO₂ is not a primary product of the cyclopropyl + O₂ reaction but arises from secondary reactions of HCO or HCO₂ products formed in conjunction with oxirane or ethene.

Pulsed LIF Detection of OH Formation in R + O₂ Reactions

In order to more thoroughly characterize the reaction of alkyl radicals with O₂, we have continued measurements of the time-resolved OH concentration in Cl-initiated oxidation reactions similar to those used in the investigations of HO₂ production. The results of master equation simulations and ab initio calculations on the ethyl and propyl reactions with O₂ have been combined with LIF and FM measurements of product formation in these reactions to produce and validate a phenomenological model capable

of explaining the body of kinetic data on these reactions. The master equations are in moderate to good agreement with the literature rate constants and the observed HO₂ and OH production curves over the 295-700 K temperature range. This work provides a rigorous basis for kinetic modeling of ethyl and propyl + O₂ which may be extended to analogous larger R + O₂ systems.

Laser Photolysis/cwLPA Measurements of C₂H₃ Reactions

We have begun to apply long-path absorption spectroscopy of the vinyl radical to kinetic investigations of its reactions with stable species. The vinyl radical is detected using a vibrational band of the $A \leftarrow X$ transition near 403 nm after 266 nm photolysis of C₂H₃I. The reaction of vinyl with NO is one of the first targets of investigation; this reaction has been calculated to proceed via a stable C₂H₃NO species, and to form HCN + CH₂O at elevated temperature. Preliminary measurements at room temperature (296 K) yield a rate coefficient for the addition of $1.5 \pm 0.25 \times 10^{-11} \text{ cm}^3 \text{ molecule}^{-1} \text{ s}^{-1}$, with no discernable pressure dependence between 10 and 80 Torr of He.

Laser Photolysis/cwLPA Detection of HCl ($v=1$) Production

The fraction of vibrationally excited HCl ($v=1$) produced in the reactions of Cl with CH₃OH, CH₃CHO, toluene, and *i*-butane has been measured at 298 K using the LP/cwIRLPA method. The fraction of available energy partitioned into HCl vibration (using the accepted thermochemistry of the corresponding radical products) is relatively high in all these reactions, and in fact vibrational population inversion is observed in the HCl product from the Cl + CH₃CHO reaction. The HCl vibrational fraction is consistent with a direct abstraction mechanism for all four reactions.

Laser Photolysis/cwLIF Detection of HCO Kinetics

The formyl radical, HCO, is a key intermediate in hydrocarbon combustion, and because of its position as a gateway for oxidation of all hydrocarbons, is an excellent marker for heat release in flames. We have recently found that a ring laser operating with Coumarin 521, previously used as a pulsed laser dye, produces laser light between 505 and 560 nm with remarkable efficiency and stability when pumped by the 457.9 Ar⁺ line. Doubling this light allows dependable detection of HCO.

The reactions HCO (DCO) + O₂ have been measured by the laser photolysis / CW laser-induced fluorescence (LIF) method from 296 to 673 K, probing the ($\tilde{B}^2A' \leftarrow \tilde{X}^2A'$) HCO (DCO) system. The HCO (DCO) + O₂ rate coefficients are 5.63 ± 0.31 and $5.61 \pm 0.23 \times 10^{-12} \text{ cm}^3 \text{ molecule}^{-1} \text{ s}^{-1}$, respectively, at 296 K; both are nearly independent of temperature between 296 and 673 K. The observed deuterium kinetic isotope effect is within the error estimate of previous measurements but is significantly smaller than recent theoretical predictions.

The reactions HCO (DCO) + NO have been measured by the laser photolysis / CW laser-induced fluorescence (LIF) method from 296 to 623 K, probing the ($\tilde{B}^2A' \leftarrow \tilde{X}^2A'$) HCO (DCO) system. The HCO (DCO) + NO rate coefficients are $1.81 \pm 0.10 \times 10^{-11} \text{ cm}^3 \text{ s}^{-1}$ and $1.61 \pm 0.12 \text{ cm}^3 \text{ s}^{-1}$, respectively, at 296 K. The reaction rate

decreases with increased temperature between 296 and 623 K. The kinetic isotope effect is measured to be $k_H/k_D = 1.12 \pm 0.15$ at 296 K and increases to 1.25 ± 0.15 at 296 K. The normal kinetic isotope effect is in disagreement with the single previous literature determination and is consistent with a significant contribution from direct abstraction.

FUTURE DIRECTIONS

Our characterization of $R + O_2$ reactions will continue, with the ability to simultaneously probe various reactants and products playing a key role in extending these measurements. In future experiments, photolysis of selected alkyl halides or reactions of Br with alkanes may be used to generate individual alkyl isomers. Selective deuteration also may make it possible to distinguish among different internal abstraction pathways in $R + O_2$ reactions. Interpretation of isotopic labeling experiments will require detection of both HO_2 and DO_2 and an understanding of the kinetic isotope effects on the overall reaction. Probing the electronic transition of the DO_2 using difference frequency generation of a cw Nd:YAG and a dye laser in $LiNbO_3$ will enable simultaneous detection of HO_2 (in the H-O overtone) and DO_2 (in the $A \leftarrow X$ band). In the long term, detection of the hydroperoxy radical intermediate in the $R + O_2 \rightarrow RO_2 \rightarrow QOOH \rightarrow QO + OH$ mechanism might be possible in the infrared.

Publications acknowledging BES support since 2000

1. Eileen P. Clifford, John T. Farrell, John D. DeSain, and Craig A. Taatjes, "Infrared Frequency-Modulation Probing of Product Formation in Alkyl + O_2 Reactions: I. The Reaction of C_2H_5 with O_2 between 295 and 698 K," *J. Phys. Chem. A*, **104**, 11549-11560 (2000).
2. John D. DeSain, Eileen P. Clifford, and Craig A. Taatjes, "Infrared Frequency-Modulation Probing of Product Formation in Alkyl + O_2 Reactions: II. The Reaction of C_3H_7 with O_2 between 296 and 683 K," *J. Phys. Chem. A*, **105**, 3205-3213 (2001).
3. Craig A. Taatjes and John F. Hershberger, "Recent Progress in Infrared Absorption Probing of Elementary Reaction Kinetics," *Annu. Rev. Phys. Chem.* **52**, 41-70 (2001).
4. Holger Thiesemann, Eileen P. Clifford, Craig A. Taatjes, and Stephen J. Klippenstein, "Temperature Dependence and Deuterium Kinetic Isotope Effects in the $CH(CD) + C_2H_4(C_2D_4)$ Reaction between 295 and 726 K," *J. Phys. Chem. A*, **105**, 5393-5401 (2001).
5. Leonard E. Jusinski and Craig A. Taatjes, "Efficient and Stable Operation of an Ar^+ -Pumped Continuous-Wave Ring Laser from 505-560 nm Using a Coumarin Laser Dye," *Rev. Sci. Instrum.* **72**, 2837-2838 (2001).
6. John D. DeSain and Craig A. Taatjes, "Infrared Frequency-Modulation Probing of Product Formation in Alkyl + O_2 Reactions: III. The Reaction of Cyclopentyl Radical ($c-C_5H_9$) with O_2 ," *J. Phys. Chem. A* **105**, 6646-6654 (2001).
7. John D. DeSain, Craig A. Taatjes, James A. Miller, Stephen J. Klippenstein, and David K. Hahn, "Infrared Frequency-Modulation Probing of Product Formation in Alkyl + O_2 Reactions: IV. Reactions of Propyl and Butyl Radicals with O_2 ," *Faraday Discuss.* **119**, 101-120 (2001).
8. Craig A. Taatjes and Stephen J. Klippenstein, "Kinetic Isotope Effects and Variable Reaction Coordinates in Barrierless Recombination Reactions," *J. Phys. Chem. A* **105**, 8567-8578 (2001).
9. John D. DeSain, Leonard E. Jusinski, Andrew D. Ho, and Craig A. Taatjes, "Temperature Dependence and Kinetic Isotope Effect in the Reaction of HCO (DCO) with O_2 between 298 and 673 K," *Chem. Phys. Lett.*, **347**, 79-86 (2001).
10. Milena Shahu, Chun-Hui Yang, Charles D. Pibel, Andrew McIlroy, Craig A. Taatjes, and Joshua B. Halpern, "Vinyl Radical Visible Spectroscopy and Excited State Dynamics", *J. Chem. Phys.*, in press.

THE EXTRACTION OF UNDERLYING MOLECULAR VIBRATIONAL DYNAMICS FROM COMPLEX SPECTRAL REGIONS

H.S. Taylor, Principal Investigator
Department of Chemistry, SSC 704
University of Southern California
Los Angeles, CA 90089-0482
E-mail: taylor@usc.edu
Phone: (213) 740-4112; Fax: (213) 740-3972

The object of this research program is to take the results of measured "complex" spectra on the high vibrational levels of polyatomic molecules and to extract from them the various internal motions that when quantized give rise to these spectra. In short we are learning how the atoms in the molecules move and how energy is transferred when specific amounts of energy are put into the molecule. All this can be done if the experimental results can be represented by a spectroscopic Hamiltonian. No potential surfaces or large-scale calculations are needed.

The assignments and dynamics of DCO and N₂O have been completed in the last year.^[1,2] The DCO results will be presented at the conference.

A most notable advance that grew out of these works besides the assignments themselves was the realization that for the systems treated so far, that, given the spectroscopic Hamiltonian the assignments and extraction of dynamics could be done for DCO and N₂O by analysis alone without any classical or quantum computation. For the spectra of CHBrClF^[3] only one extremely simple trajectory need be computed. In our published work so far,^[1,2,3,4,5] we did classical calculations in reduced phase space to uncover the classical periodic orbit organizing structures that supported, again in reduced configuration space, the quantum wave functions. These wave functions were trivially constructed from the final transformation matrix used by the experimentalist when fitting the parameters of spectroscopic Hamiltonian.

We no longer need to do extra calculations as we can infer to the degree necessary for our aims, the qualitative structure of the orbits in reduced dimension angle space from the principles of semiclassical dynamics and nonlinear dynamics. We can then anticipate wave function types, which are much simpler to view in the reduce configuration space of angle variables than they are in the original normal or local displacement coordinates. Importantly, by exhibiting each state's wave function intensity and phase (in angle space even bound state wave function will be complex) we can sort the wave functions into "ladder classes" and by counting nodes and phase advances we have been able to assign quantum numbers. Actual real world motions can be inferred by transforming prototype orbits expected from theory and confirmed by wave function shapes, back to displacement coordinate space. Alternatively, we can often from first principles figure out the motions from simple considerations once we know a state is for example, Fermi resonance or Darling-Dennison resonance dominated etc. This shall all be demonstrated for DCO.

As is known from previous papers,^[3,5] the spectral complexity is due for the most part to the interleaving of several ladders of states each of which is based on a different elementary classical motion which exhibits in reduced action space simple and unique looking wave

functions i.e. intensity and phase patterns. This uniqueness is what allows the sorting of states into ladders of state analogous to sorting cards in suites in a deck of playing cards. Node and phase counting allows ordering within the "suite". It is sometimes observed that some ladder rungs are missing and some wave functions do not fit the expected or observed simple patterns. These "complex" wave functions most often arise from the fact that two missing rungs on the same ladder are nearly degenerate due to local anharmonicities that lead to the energetic equivalence of populating difference modes (for example "along" and "perpendicular") on the same organizing structure. We have found a simple way to demix these states and always find the missing rungs and proper patterns. Such mixed states are due to quantum mixing of simple classical motions.

A small number of complex state were analyzed and discovered to result in a predictable way, form a classical "mixing" of the simple (Fermi, D-D, local, normal mode etc.) motions. The classical motion which the complex wave function reflects, is a motion made by stringing together (again in a predictable way uncovered from the principles of non-linear dynamics) sequences of the simple elementary motions into a resulting motion. The quantum and classical mixed states of course contributed to unique and qualitatively understandable (again, without calculation) different patterns of IVR.

In the future we shall address two basic problems.

First, we shall attempt to apply and extend our analysis to molecules in which the number of vibrational degrees of freedom minus the number of constants of motion (e.g. Polyad bending angular momentum etc, as the case may be) is greater than two. We already are working on Quack's spectra on CF_3CHF_2 .^[6] Here H_{eff} has four degrees of freedom. We have already had some success here having assigned at least one hundred states in an upper Polyad containing about two hundred states. We are also looking into what is known as time-frequency analysis using wavelet transforms to find organizing structures in reduced phase space. This method seems to be able to work in high dimension.

Another problem we are addressing is to extend the concept of effective spectroscopic Hamiltonian to spectral regions near barriers (as in double wells). There are deep theoretical problems here and we are treating the special case of a symmetric barrier where one can work on half the potential if proper boundary conditions are used. We are testing some new ideas here and hope to be able to derive an effective Hamiltonian from theoretically calculated levels of HO_2 . HO_2 has a low barrier to H atom reflection in the plane containing the O_2 bond and cannot be treated by spectroscopic Hamiltonian methods.

What if the wells are not symmetrical? We have no idea what to do here but we will keep studying this.

Publications (*) for the past year and references.

- 1*. Semicalssical Assigment of the Vibrational Spectra of N₂O, H. Waalkens, C. Jung, and H.S. Taylor, J. Chem. Phys., In press (2002).
- 2*. Extraction of the Vibrational Dynamics from Spectra of Highly Excited Polyuatomics: DCO, C. Jung, E. Atilgan and H.S. Taylor, J. Phys. Chem., In press (2002).
3. Extracting the CH Chromophore Vibrational Dynamics of CHBrClF Directly from Spectra: Unexpected Constants of the Motion and Symmetries, C. Jung, E. Ziemniak and H.S. Taylor, J. Chem. Phys., 115, 2449 (2001).
4. State-by State Assignment of the Bending Spectrum of Acetylene at 15000 cm⁻¹: A Case Study of Quantum-Classical Correspondence, with M. P. Jacobson, C. Jung, and R.W. Field, J. Chem. Phys., 111, 600-618 (1999)
5. The Acetylene Bending spectrum at ~10,000 cm⁻¹: Quantum Assignment in the Midst of Classical Chaos, C. Jung, M. Jacobson and H.S. Taylor, J. Phys. Chem. A, 105, 681 (2001).
6. J. Pochert, M. Quack, J. Stohner and M. Willeke, J. Chem. Phys. 115, 2719 (2000)

Terascale High-Fidelity Simulations of Turbulent Combustion with Detailed Chemistry

<http://scidac.psc.edu/>

SciDAC: Computational Chemistry

(DOE Office of Science, Basic Energy Sciences: Chemical Sciences, Program Manager: Walter J. Stevens)

Work-in-progress Report – Period from 09/01/01 to 03/31/02

List of Principal Investigators

- Arnaud Trouvé (Univ. Maryland, UMD, atrouve@eng.umd.edu)
- Jacqueline Chen (Sandia Natl. Lab., SNL, jhchen@ca.sandia.gov)
- Hong G. Im (Univ. Michigan, UMI, hgim@umich.edu)
- Christopher J. Rutland (Univ. Wisconsin, UW, rutland@engr.wisc.edu)
- Raghurama Reddy, Sergiu Sanielevici (Pittsburgh Supercomputing Center, PSC, Carnegie Mellon Univ., rreddy@psc.edu, sergiu@psc.edu)

Project Summary

Direct numerical simulation (DNS) is a mature and productive research tool in combustion science that is used to provide high-fidelity computer-based observations of the micro-physics found in turbulent reacting flows. DNS is also a unique tool for the development and validation of reduced model descriptions used in macro-scale simulations of engineering-level systems. Because of its high demand for computational power, current (gigascale) state-of-the-art DNS remains limited to small computational domains (*i.e.* small Reynolds numbers) and to simplified problems corresponding to adiabatic, non-sooting, gaseous flames in simple geometries. The objective of this research project is to use terascale technology to overcome many of the current DNS limitations.

The effort will leverage an existing SNL DNS capability, named S3D, and a PSC/SNL collaborative effort for efficient implementation of S3D on massively parallel processors (MPP) computers. S3D is a compressible Navier-Stokes solver coupled with an integrator for detailed chemistry, and is based on high-order finite differencing, high-order explicit time integration, and conventional structured meshing. The objective here is to both re-design S3D for effective use on terascale high-performance computing platforms, and to enhance the code with new numerical and physical modeling capabilities. The list of proposed numerical developments includes: an implicit/explicit additive Runge-Kutta method for efficient time integration; an immersed boundary method to allow for geometrical complexity; and an adaptive mesh refinement (AMR) capability to provide flexible spatial resolution. The list of proposed physical modeling developments includes: a thermal radiation capability; and a multi-phase capability including soot particles and liquid fuel droplets.

The new MPP S3D software will be object-oriented and adapted to fit into an advanced software framework, known as the Grid Adaptive Computational Engine (GrACE) framework. GrACE is a MPP framework targeted for AMR applications and includes load-balancing capabilities. In addition, S3D will be made compliant to a software interoperability standard, the Common Component Architecture (CCA) developed by a consortium of DOE laboratories and academic

institutions [1]. The CCA environment will allow exchanging software components developed by different teams working on complementary tasks. It will allow in particular the re-use of components developed by a separate SNL-led research project [2]. The SNL-led effort is closely related to, and coordinated with, the present project, and focuses for instance on developing an AMR component.

We plan to demonstrate the performance and capabilities of the new DNS code in a series of demonstration studies selected for both their technical challenge and scientific value. This includes: the simulation of compression-ignition of a gaseous or liquid, hydrocarbon fuel in a turbulent inhomogeneous mixture; and the simulation of NO_x emissions from hydrocarbon-air turbulent jet diffusion flames.

Finally, the objective of this project is also to establish a consortium of research institutions (PSC, SNL, UMD, UMI, UWI) that will bring together a critical mass of interdisciplinary skills, in order to tackle the increasing levels of complexity found in terascale technology. The proposed partnership will provide a suitable framework for ensuring the successful development and long-term support of the DNS code, as well as for maximizing its impact in the combustion research community.

Recent Progress

As explained above, the present developments for S3D include a complete software re-design, new numerical methods and new physical modeling capabilities. We present here a summary of progress made during the initial work period of this project extending from 09/01/01 to 03/31/02.

Software design developments:

- a new Fortran90 version of S3D has been developed and released by SNL (Scott Mason)
- GrACE has been ported on the PSC TCS computing system (TCS is a Compaq Alphaserver Cluster) and S3D is currently being adapted to the GrACE framework (PSC/Yang Wang, Roberto Gomez, Raghurama Reddy)

Numerical developments:

- an implicit/explicit (IMEX) additive Runge-Kutta (ARK) time integration scheme has been developed and implemented into S3D (SNL/Christopher Kennedy; PSC/Roberto Gomez, Raghurama Reddy)
- an acoustic reduction method has been developed [3] and is currently implemented into S3D (UMD/Arnaud Trouvé). This method allows for more efficient computations of slow flow problems while still using a fully compressible formulation.
- the immersed boundary method is currently implemented into S3D (UMD/Arnaud Trouvé). This method allows for solid wall representation using a body-forcing approach in a conventional Cartesian computational mesh.

Physical model developments:

- an optically-thin gas radiation model has been implemented into S3D (UMI/Hong Im). More advanced formulations for thermal radiation based on the radiative transfer equation are currently under development (UMI/Hong Im; UMD/Arnaud Trouvé)

- a phenomenological soot model based on transport equations for the soot volume fraction and particle number density is currently under development (UMD/Arnaud Trouvé)
- a Lagrangian particle model to describe dilute liquid sprays is currently under development (UWI/Christopher Rutland)

Future Plans

The main focus of the coming work period will be two-fold: (1) to release a GrACE-based version of S3D; (2) to initiate two pilot demonstration studies. The two pilot studies correspond to: the simulation of compression-ignition in a turbulent, gaseous, hydrogen-air mixture using IMEX ARK; and the simulation of hydrogen-air turbulent jet diffusion flames including detailed descriptions of NO_x, soot and radiation. In both studies, hydrogen has been selected as the fuel because of the relative simplicity of its oxidation chemistry. More complex hydrocarbon flames will be considered in a subsequent phase. The generation of these new DNS databases will also be associated with the development of adequate post-processing tools including tools for data visualization, flamelet-based analysis and statistical analysis.

References

- [1] Armstrong, R. C., *et al.* (2001) "Center for Component Technology for Terascale Simulation Software", SciDAC: Integrated Software Infrastructure Center.
- [2] Najm, H., *et al.* (2001) "A Computational Facility for Reacting Flow Science", SciDAC project.
- [3] Trouvé, A. (2002) "Artificial Removal of the Acoustic Penalty in Fully Compressible, Direct Numerical Simulation of Combustion", *presented at the 9th Intl. Conf. Num. Combustion*, Sorrento, Italy.

VARIATIONAL TRANSITION STATE THEORY

Principal investigator, mailing address, and electronic mail

Donald G. Truhlar
Department of Chemistry, University of Minnesota, 207 Pleasant Street SE,
Minneapolis, Minnesota 55455
truhlar@umn.edu

Program scope

This project involves the development of variational transition state theory (VTST) with multidimensional tunneling (MT) contributions and its application to gas-phase reactions. Our current work is focussed on developing and applying new methods for electronic structure theory and dynamics and for interfacing reaction-path and reaction-swath dynamics calculations with electronic structure theory. The work involves development of new theory, development and implementation of practical techniques for applying the theory to various classes of reactions and transition states, and applications to specific reactions, with special emphasis on combustion reactions and reactions that provide good test cases for methods needed to study combustion reactions. A theme that runs through our current work is the development of consistently and generally defined electronic structure methods with empirical elements, including molecular mechanics, density functionals, and scaled-electron-correlation components and the use of these methods in direct dynamics calculations of chemical reaction rates.

Recent progress

We have developed powerful new multi-coefficient correlation methods (MCCMs) that allow accurate evaluation of bond energies and reaction energies at relatively low cost compared to previously available methods. These methods are multi-level electronic structure methods in that the predicted energy surface results from extrapolating two or more electronic structure levels to the limit of infinite-order electron correlation (i.e., full CI) and a complete one-electron basis set. Four particularly promising methods of this type are the MP2-SAC, MCCM-CO-MP2, MC-QCISD and MCG3 methods. The full names of these methods are Moller-Plesset second-order perturbation theory with scaling all correlation energy, MCCM Colorado method based on MP2, multi-coefficient quadratic configuration interaction with single and double excitations, and multi-coefficient Gaussian-3 method. These methods are well suited for geometry optimization and direct dynamics calculations as well as energy calculations, and they have excellent performance-to-cost ratios, especially when compared to using single-level methods. We have also shown how even greater accuracy can be obtained by using parameters specifically optimized for combustion problems.

We developed a multi-configuration version of molecular mechanics (MCMM) that allows a convenient interface of high-level ab initio calculations with molecular mechanics force fields. Although, strictly speaking, the use of MCMM is not direct dynamics, it accomplishes much the same purpose because it does not require artfulness in surface fitting, and yet it yields a semiglobal potential energy surface that is valid in the whole reaction swath, not just along a one-dimensional path. It has the great advantage that it allows the use of high-level electronic methods at minimal cost. We have now developed a general strategy that demonstrates that one can obtain useful semiglobal fits to potential energy surfaces with on the order of only a dozen Hessians or less.

We have developed a new hybrid density functional method parameterized for kinetics, and we have tested this with several extended and polarized double zeta basis sets. The results have been tested against a 22-reaction database of barrier heights (that we developed specifically for this purpose), and the mean unsigned error in barrier heights is only 1.5 kcal/mol. The new methods have been shown to provide excellent quality for saddle point geometries.

A critical part of our work on both MCCMs and hybrid density functional theory has been the development of a new kinetics database containing best estimates of barrier heights and transition state geometries.

We recently improved the large-curvature tunneling (LCT) method so that it is more robust for anharmonic potential energy surfaces. The new method is called large-curvature tunneling, version 4.

We have now tested VTST with multidimensional tunneling against newly available accurate benchmark rate constants for $\text{CH}_4 + \text{H}$ on a given realistic potential energy surface. We agree with the benchmark results with an average deviation of only 13% over a factor of five in temperature.

We have made several applications of our methods to calculate rate constants for specific chemical reactions. Recent applications of this type include $\text{T} + \text{H}_2$, D_2 , and HD , $\text{Cl} + \text{CH}_4$, $\text{Cl} + \text{H}_2$ and D_2 , $\text{O}(^3\text{P}) + \text{HCl}$, $\text{CH}_3 + \text{H}_2$, $\text{Cl} + \text{HBr}$, $\text{CH}_4 + \text{O}(^3\text{P})$, $\text{OH} + \text{CH}_4$, $\text{NH}_2 + \text{CH}_4$, $\text{CH}_2\text{F} + \text{CH}_3\text{Cl}$, and $\text{OH} + \text{C}_3\text{H}_8$. We carried out parameterized direct dynamics calculations of the rate constants of the reaction $\text{CH}_4 + \text{H}$ from 250 K to 2400 K using several electronic structure methods, including MC-QCISD with specific reaction parameters and MCG3 with semiglobal reaction parameters optimized for combustion reactions. We obtained very good agreement with experimental results over the temperature range 348 K to 2400 K.

We have developed several software packages for applying variational transition state theory with optimized multidimensional tunneling coefficients to chemical reactions. The URL for our software distribution site is <http://comp.chem.umn.edu/Truhlar>. The number of license requests that we have fulfilled for selected software packages developed under DOE support since July 1, 1999 are as follows:

	<i>Total</i>	<i>academic</i>	<i>government</i>	<i>industry</i>
POLYRATE	164	142	13	9
GAUSSRATE	64	56	5	3
MORATE	28	23	2	3

Future plans

Our objective is to increase the applicability and reliability of variational transition state theory with semiclassical tunneling calculations for combustion reactions. An important part of how we plan to do this is further improvement of the interface with high-level electronic structure calculations. We will continue to develop single-level and dual-level direct dynamics methods as well as multi-configuration molecular mechanics methods for carrying out rate calculations with potential energy surfaces based on high-level electronic structure theory, and we will continue to develop new multi-level electronic structure methods for kinetics. In addition to developing the methods, we are putting them into user-friendly packages that will allow more researchers to carry out calculations conveniently by the new methods.

VTST is being applied to selected reactions of three types: (i) important test cases for the new methods, (ii) reactions of fundamental importance for further development of dynamical theory, and (iii) important combustion reactions, for example, reactions of hydroxyl radicals with unsaturated systems and reactions of hydrogen atoms with alcohols. We are also developing new methods for the calculation of substituent effects.

Publications, 2000-present

Journal articles

1. "Statistical Thermodynamics of Bond Torsion Modes," Y.-Y. Chuang and D. G. Truhlar, *Journal of Chemical Physics* **112**, 1221-1228 (2000).
2. "Multilevel Geometry Optimization," J. M. Rodgers, P. L. Fast, and D. G. Truhlar, *Journal of Chemical Physics* **112**, 3141-3147 (2000).
3. "Comment on Rate Constants for Reactions of Tritium Atoms with H₂, D₂, and HD," J. Srinivasan and D. G. Truhlar, *Journal of Physical Chemistry A* **104**, 1965-1967 (2000).
4. "How Should We Calculate Transition State Geometries for Radical Reactions? The Effect of Spin Contamination on the Prediction of Geometries for Open-Shell Saddle Points," Y.-Y. Chuang, E. L. Coitiño, and D. G. Truhlar, *Journal of Physical Chemistry A* **104**, 446-450 (2000).
5. "Potential Energy Surface, Thermal and State-Selected Rate Constants, and Kinetic Isotope Effects for Cl + CH₄ → HCl + CH₃" J. C. Corchado, D. G. Truhlar, and J. Espinosa-Garcia, *Journal of Chemical Physics* **112**, 9375-9389 (2000).
6. "Multiconfiguration Molecular Mechanics Algorithm for Potential Energy Surfaces of Chemical Reactions" Y. Kim, J. C. Corchado, J. Villà, J. Xing, and D. G. Truhlar, *Journal of Chemical Physics* **112**, 2718-2735 (2000).
7. "Dynamics of the Cl+H₂/D₂ Reaction: A Comparison of Crossed Molecular Beam Experiments with Quasiclassical Trajectory and Quantum Mechanical Calculations," M. Alagia, N. Balucani, L. Cartechini, P. Casavecchia, G. G. Volpi, F. J. Aoiz, L. Bañares, T. C. Allison, S. L. Mielke, and D. G. Truhlar, *Physical Chemistry Chemical Physics* **2**, 599-612 (2000).
8. "Thermochemical Analysis of Core Correlation and Scalar Relativistic Effects on Molecular Atomization Energies," J. M. L. Martin, A. Sundermann, P. L. Fast, and D. G. Truhlar, *Journal of Chemical Physics* **113**, 1348-1358 (2000).
9. "MC-QCISD: Multi-Coefficient Correlation Method Based on Quadratic Configuration Interaction with Single and Double Excitations," P. L. Fast and D. G. Truhlar, *Journal of Physical Chemistry A* **104**, 6111-6116 (2000).
10. "Adiabatic Connection for Kinetics," B. J. Lynch, P. L. Fast, M. Harris, and D. G. Truhlar, *Journal of Physical Chemistry A* **104**, 4811-4815 (2000).
11. "Improved Algorithm for Corner Cutting Calculations," A. Fernandez-Ramos and D. G. Truhlar, *Journal of Chemical Physics* **114**, 1491-1496 (2001).
12. "Thermal and State-Selected Rate Coefficients for the O(³P) + HCl Reaction and New Calculations of the Barrier Height and Width," S. Skokov, S. Zhou, J. M. Bowman, T. C. Allison, D. G. Truhlar, Y. Lin, B. Ramachandran, B. C. Garrett, and B. J. Lynch, *Journal of Physical Chemistry A* **105**, 2298-2307 (2001).
13. "How Well Can Hybrid Density Functional Methods Predict Transition State Geometries and Barrier Heights?" B. J. Lynch and D. G. Truhlar, *Journal of Physical Chemistry A* **105**, 2936-2941 (2001).

14. "Multi-Coefficient Correlation Method: Comparison of Specific-Range Reaction Parameters to General Reaction Parameters for $C_nH_xO_y$ Compounds," P. L. Fast, N. Schultz, and D. G. Truhlar, *Journal of Physical Chemistry A* **105**, 4143-4149 (2001).
15. "POTLIB 2001: A Potential Energy Surface Library for Chemical Systems," R. J. Duchovic, Y. L. Volobuev, G. C. Lynch, T. C. Allison, J. C. Corchado, D. G. Truhlar, A. F. Wagner, and B. C. Garrett, *Computer Physics Communications* **144**, 169-187 (2002).
16. "Molecular Mechanics for Chemical Reactions. A Standard Strategy for Using Multi-Configuration Molecular Mechanics for Variational Transition State Theory with Optimized Multidimensional Tunneling," T. Abu, J. C. Corchado, and D. G. Truhlar, *Journal of Physical Chemistry A* **105**, 8465-8487 (2001).
17. "Test of Variational Transition State Theory with Multidimensional Tunneling Contributions Against an Accurate Full-dimensional Rate Constant Calculation for a Six-Atom system," J. Pu, J. C. Corchado, and D. G. Truhlar, *Journal of Chemical Physics* **115**, 6266-6267 (2001).
18. "Parameterized Direct Dynamics Study of Rate Constants of H with CH_4 from 250 to 2400 K," J. Pu and D. G. Truhlar, *Journal of Chemical Physics* **116**, 1468-1478 (2002).
19. "What are the Best Affordable Multi-Coefficient Strategies for Calculating Transition State Geometries and Barrier Heights?" B. J. Lynch and D. G. Truhlar, *Journal of Physical Chemistry A* **106**, 842-846 (2002).
20. "Interpolated Algorithms for Large-Curvature Tunneling Calculations," A. Fernandez-Ramos, D. G. Truhlar, J. C. Corchado, and J. Espinosa-Garcia, *Journal of Physical Chemistry A*, in press.

Book chapters

1. "Vignette: Present-Day View of Transition State Theory," in *Physical Chemistry*, 2nd ed., edited by R. S. Berry, S. A. Rice, and J. Ross (Oxford University Press, New York, 2000), Section 30.6.
2. "Molecular Scale Modeling of Reactions and Solvation," D. G. Truhlar, in *Proceedings of FOMMS 2000: Foundations of Molecular Modeling and Simulation*, Keystone, Colorado, July 23-28, 2000, edited by P. T. Cummings, P. R. Westmoreland, and B. Carnahan (American Institute of Chemical Engineers Symposium Series Vol. 97, New York, 2001), pp. 71-83.

Computer programs

- "POLYRATE-version 8.7.2," J. C. Corchado, Y.-Y. Chuang, P. L. Fast, J. Villà, W.-P. Hu, Y.-P. Liu, G. C. Lynch, K. A. Nguyen, C. F. Jackels, V. S. Melissas, B. Lynch, I. Rossi, E. L. Coitiño, A. Fernandez-Ramos, J. Pu, R. Steckler, B. C. Garrett, A. D. Isaacson, and D. G. Truhlar, University of Minnesota, Minneapolis, Feb. 2002.
- "MORATE-version 8.5," Y.-Y. Chuang, P. L. Fast, W.-P. Hu, G. C. Lynch, Y.-P. Liu, and D. G. Truhlar, University of Minnesota, Minneapolis, Oct. 2000.
- "GAUSSRATE-version 8.7," J. C. Corchado, E. L. Coitiño, Y.-Y. Chuang, and Donald G. Truhlar, University of Minnesota, Minneapolis, Oct. 2001.
- "HONDO/S-version 4.0," H. Nakamura, J. Xidos, J. Thompson, G. D. Hawkins, J. Li, T. Zhu, B. J. Lynch, Y. Volobuev, D. Rinaldi, D. A. Liotard, C. J. Cramer, and D. G. Truhlar, University of Minnesota, Minneapolis, Apr. 2002.
- "MULTILEVEL-version 2.4," J. M. Rodgers, B. J. Lynch, P. L. Fast, Y.-Y. Chuang, J. Pu, and D. G. Truhlar, University of Minnesota, Minneapolis, Feb. 2002.
- "MC-TINKERATE-version 1.0," T. V. Abu, J. C. Corchado, Y. Kim, J. Villa, J. Xing, and D. G. Truhlar, University of Minnesota, Minneapolis, Mar. 2002.

Chemical Kinetic Data Base for Combustion Modeling

Wing Tsang
National Institute of Standards and Technology
Gaithersburg, MD 20899
wing.tsang@nist.gov

Program Scope or Definition: Modern developments in computer technology and scientific advances have made the simulation of complex technological processes a valuable tool for the conceptualization of new or the optimization of established processes. Key to the use of the technology is reliable input parameters. For the combustion of organic fuels a major problem is the scale of the chemical kinetic database required to describe the details of the process. This is not only due to the complexity of the combustion process itself, but the fact that long chained hydrocarbons are a major component. Thus it is difficult to apply computer simulations to real systems. Nevertheless there is now much quantitative understanding on the combustion of small organic fuels. There are also a number of models of soot formation of small unsaturates. The aim of this project is to begin the work that will extend the chemical kinetic database to cover real liquid fuels and gain insights into their PAH and soot formation propensity.

Recent Progress: All of the work in the current year has been concerned with multichannel unimolecular processes involving isomerization and decomposition of intermediate molecules and radicals. There are very little data on such processes. This is unfortunate for the extension of the database to realistic fuels and PAH formation. Indeed much of the experimental data used in the present analysis were generated in this laboratory several years ago.

Much of the current work is focussed on the $C_5 - C_7$ n-alkyl radicals. These are important intermediates from the decomposition of the n-alkanes. Their breakdown leads to the formation of smaller alkyl radicals and 1-olefins. This type of reaction reduces a large hydrocarbon radical to smaller fragments. These fragments can now be oxidized or oligomerized to form aromatic compounds leading to soot. The present work on hydrocarbon cracking thus seeks to define the boundary conditions to be used with existing combustion and (1) soot models (2).

The specific processes considered are the decomposition and isomerization of the pentyl, hexyl and heptyl radicals. These are formed from the decomposition of larger radicals or from radical attack on n-pentane, n-hexane and n-heptane. In a combustion situation the radicals can be attacked by oxygen molecule or thermally decompose. This is illustrative of the competitive nature of combustion processes and it is the relative importance of the various oxidation and pyrolysis reactions that determines the ultimate fate of the fuel.

The breakdown of long chained alkyl radicals is characterized not only by beta bond fission but also by isomerization (3). One must not only be concerned with a specific radical but also the other radicals formed as a result of the isomerization processes. The absence of ring strain in the six-membered transition state makes 1-5 hydrogen transfer important. The extra strain in the five membered transition state leads to smaller rate constants but it is known to be make contributions. There is almost no data on higher order hydrogen atom transfers.

Reactions	A-factor /s	Activation Energy cal/mol	Rate constant log (k, /s)
k1: C6H13-1----> C2H4 + nC4H9	1.69E+13	27994	8.334
k2: C6H13-2 ----> C3H6 + nC3H7	3.06E+13	28232	8.55
k3: C6H13-3 ----> 1-C4H8 + C2H5	3.27E+13	28363	8.5556
k4: C6H13-3 ----> 1-C5H10 + CH3	3.33E+13	30370	8.2126
k5: C6H13-2 <---> C6H13-1	1.63E+12	23010	8.1887
k6: C6H13-3 <---> C6H13-1	6.87E+12	28562	7.8434
k7: C6H13-1 <---> C6H13-2	1.14E+12	19626	8.6254
k8: C6H13-1 <---> C6H13-3	5.18E+12	25983	8.1715

Table 1: Rate expressions used in obtaining best fits to experimental observations 1250 K. Step size down in calculations is 500 cm⁻¹.

Our approach has been to review the literature on the decomposition of the smaller alkyl radicals (4) and to deduce from such data rate constants for beta bond fission. These results are then used to deduce rate constants for isomerization through a match with experimental observations on the decomposition of 1-alkyl radicals(5-7). The procedure is to begin with the simplest 1-alkyl radical where decomposition and isomerization can occur concurrently and then to go on to larger 1-alkyl radicals. The smallest such compound is 1-pentyl. Here, the main isomerization process involves a 1-4 hydrogen transfer. The next compound is 1-hexyl. Here the isomerization reactions involve 1-5 as well as 1-4 hydrogen transfer. The final molecule where data exists is 1-heptyl. Here one get 1-4,1-5 as well as 1-6 hydrogen transfer. In addition there is also the possibility of a 1-4 hydrogen transfer involving carbons in the 2 and the 5 position. The expectation is that it will be possible to obtain a set of rate expressions for isomerization that can be used for even larger alkyl radicals.

Aside from the identification of the reaction pathways energy transfer effects must be considered. The activation energies of these processes are small hence they are more likely to be subject to this effect. Furthermore, due to the contributions from the isomerization processes it will be necessary to employ the full master equation approach(8,9). We have pointed out some of the problems in earlier papers (10,11). This is exactly the type of problem for which the program that we have described in earlier reports is designed to treat. The process involves using the program first to derive high pressure rate expressions by fitting experimental results and then using it again to project the data to cover all relevant temperatures and pressures..

Typical results in term of rate constants as a function of time can be seen in Figure 1A. They are based on the high pressure rate expressions summarized in Table 1. The system under consideration is the decomposition of 1-hexyl. At very short times rate constants are very large. This is followed by a transient period before constant values are attained. For the 1-hexyl radical, the initial value is the high pressure thermal rate constant since the initial distribution is at the bath temperature. For the isomerization products initial rate constants are higher than the thermal value. Their initial distribution arises from molecules that have crossed the isomerization barrier. It corresponds to the chemically activated situation. The final constant rate constant is from the steady state distribution that is ultimately attained. Figure 1B contains a plot of the temporal behavior of the three isomers. Before the final steady state behavior is attained practically all the hexyl radicals have decomposed. Rate constants are changing with time.

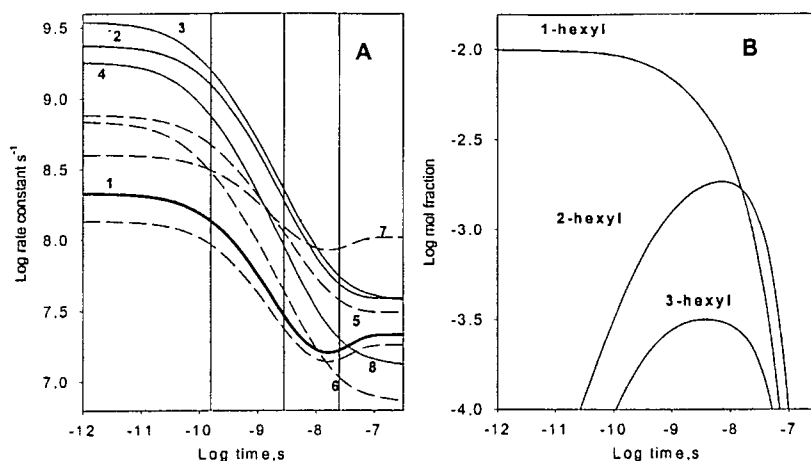


Figure 1 (A) Rate constant as a function of time for 1-hexyl decomposition at 1250 K and 2 bar. The lines are for 10%, 50% and 90% conversion of the 1-hexyl radical (B) Temporal behavior of the three hexyl radicals at 1250 K and 2 bar

Note the short lifetimes of the alkyl radicals. The competitive process is the reaction of the radical with oxygen molecules. This involves addition at the radical site with rate constants near $3 \times 10^{12} \text{ cm}^3 \text{ mol}^{-1} \text{ s}^{-1}$. At one bar and 1200 K the oxygen concentration is $2 \times 10^{-6} \text{ mol cm}^{-3}$. Since the reaction can be reversed and the existence of barriers to isomerization, a rate constant near 10^6 s^{-1} can be used as a boundary above which only the thermal reactions of hexyl radicals need be considered. From these calculation an appropriate temperature is near 900 K. Results in this context can be found in Figure 2. At the lower temperatures there is a small pressure dependence. With hexyl-2 (B) as the starting radical, the overwhelming channel is from its decomposition. This is due to the equilibrium constant favoring the secondary radical. With 3-hexyl the yields from its decomposition is even more predominating. Particularly interesting is the transferability of the isomerization rate constants for the radicals. PM-3(12) calculations show that 1-7 and higher hydrogen shifts will have considerably smaller rate constants. If this can be confirmed by experiments, it will be possible to predict the breakdown of all n-alkyl radicals.

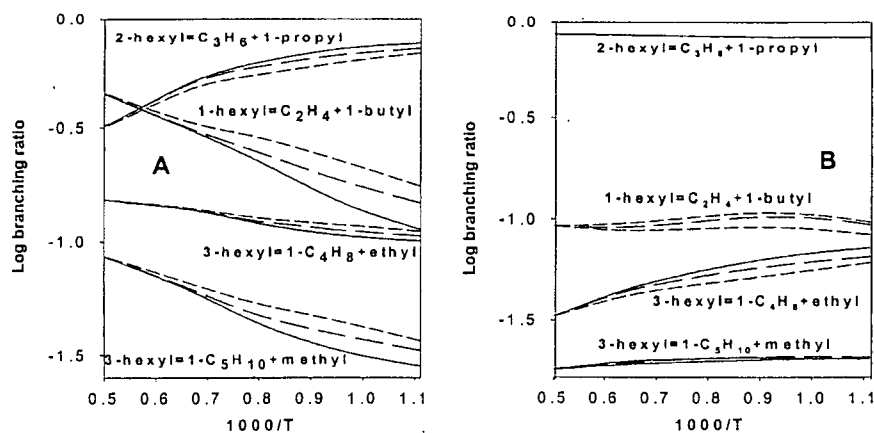


Figure 2: A: Branching ratios for the decomposition of hexyl radicals as a function of temperature as pressures of 0.2 (solid line), 2 (long dashed line), 20 (short dashed line) A: 1-heptyl starting reactant B: 2-heptyl starting reactant

Future Plans: We intend to extend this work to carry out similar calculations on the breakdown of the olefinic radicals. Chemically activated decompositions will also be considered. This will lead to the formation of the small unsaturates that can now be plugged into existing soot models. This will complete the work on the thermal cracking of normal alkane fuels with up to seven carbon atoms. The next phase of the work will involve reactions leading to aromatic and PAH formation.

Publications 2000-2002

1. Tsang, W. and Lifshitz, A., "Single Pulse Shock Tube" in Part III "Chemical Reactions in Shock Waves, in Handbook of Shock Waves", Academic Press, New York, 108, 2001
2. Tsang, W. and Mokrushin, V. Mechanism and Rate Constants for 1,3-butadiene Decomposition, P COMBUST INST 28: 1717-1723 Part 2 2000
3. Babushok V, Tsang W, and Noto T " Propargyl-type radicals as precursors for polychlorinated aromatic hydrocarbons during incineration" P COMBUST INST 28: 2691-2699 Part 2 2000
4. Knyazev, V. and Tsang, W. Chemically and Thermally Decomposition of Secondary Butyl Radical, J. Phys. Chem., A 104, 10747, 2000
5. Tsang, W., A Pre-processor for the Generation of Chemical Kinetic Data for Simulations AIAA Paper #20001-0359, Proc. 39th Aerospace Sciences Meeting, Reno, Nevada, 2001
6. Herzler, J., Manion, J. A., and Tsang, W. "1,2-Pentadiene Decomposition", Int. J. Chem. Kin., 33, 755, 2001
7. Tsang, W., "Important Factors in the Development of Combustion Mechanisms for Realistic Fuels", AIAA Paper #2002-1098, Proc. 40th Aerospace Sciences Meeting, Reno, Nevada, 2002

References

1. Curran, H.J., Gaffuri, P., Pitz, W.J., Westbrook, C.K. Combust.Flame, 114:149-177 (1998).
2. Richter H, and Howard J.B., Prog. Energ. Combust.: 4 565, 2000
3. Frey, H. M., Walsh, R., Chem. Rev., 69, 103, 1969
4. Tsang, W., J. Amer. Chem. Soc., 107, 2783, 1985
5. Tsang, W., Walker, J.A., and Manion, J.A., P COMBUST INST 28: 135-142 (1999).
6. Tsang, W., "Pathways for the Decomposition of 1-Hexyl Radicals"; Chemical and Physical Processes in Combustion", 1996 Fall Technical Meeting, Eastern States Section of the Combustion Institute, Hilton Head, SC., pg 515
7. Awan, I., Manion, J. A. and Tsang, W., in preparation
8. Tsang, W., "A Pre-processor for the Generation of Chemical Kinetics Data for Simulations" AIAA-2001-0359, 39th AIAA Aerospace Sciences Meeting and Exhibit, January 8-11, 2001 Reno. NV
9. Gilbert, R. S. and Smith S. C., "Theory of Unimolecular and Recombination Reactions", Blackwell Scientific, London, 1990
10. Tsang, W., Bedanov, V. and Zachariah, M. R., J. Phys. Chem., 1996, 100, 4011.
11. Tsang, W., Bedanov, V and Zachariah, M. R., Berichte der Busen-Gesellschaft fur Physikalische Chemie, 1997, 101, 491.
12. Allison, T. and Tsang, W., "Kinetics of Intramolecular Hydrogen Transfer in Alkyl Radicals from Ab initio Calculations" 2001 Technical Meeting of the US Combustion Institute, Oakland, CA

SINGLE-COLLISION STUDIES OF ENERGY TRANSFER AND CHEMICAL REACTION

James J. Valentini
Department of Chemistry
Columbia University
3000 Broadway, MC 3120
New York, NY 10027
jjv1@chem.columbia.edu

PROGRAM SCOPE

This research program aims to develop an understanding of the dynamics of reactions that are actually important in combustion media, those that are prototypes of such reactions, and those that illustrate fundamental dynamical principles that underlie combustion reactions. Study of reaction dynamics means asking many different questions. The one that we pose in our current work is how "many body" effects influence bimolecular reactions. By many-body effects we mean almost anything that results from having a reaction with a potential energy surface of more than three dimensions. These are polyatomic reactions, that is, reactions in which one or both the reactants and one or both of the products are triatomic or larger molecules. Our major current interest is in reactions for which the reactants offer multiple, identical reaction sites. Our aim is not to provide a complete description of any one molecular system, but rather to develop a general understanding of how the factors of energetics, kinematics, and reactant/product structure control the dynamics in a series of analogous systems. In a parallel, smaller, effort we are interested in many-body effects in simple reactions studied in molecular clusters.

Our experiments are measurements of quantum-state-resolved partial cross sections under single-collision conditions. We use pulsed uv lasers to produce reactive radical species and thereby initiate chemical reactions. The reaction products are detected and characterized by resonant multi-photon ionization (REMPI) and time-of-flight mass spectroscopy.

RECENT PROGRESS

We have explored an extensive series of homologous reactions, $H + RH \rightarrow H_2 + R$, where RH is an alkane, with many different alkanes, from methane to straight-chain to branched chain to cyclic. This year we completed analysis of results for the reactions of cyclobutane, cyclopentane, and cyclohexane, and finished experiments with the reactions of cyclopropane, isobutane, and neopentane. H atoms are prepared by laser photolysis; H_2 is state-selectively detected under single-collision conditions by pulsed-laser REMPI. The rovibrational state distributions of the H_2 product are measured. Doppler profiles of the REMPI transitions for each rovibrational state reveal the

translational energy disposal. All the reactions have the same light + light-heavy \rightarrow light-light + heavy kinematics. All have nearly the same thermochemistry. They are differentiated by their structure, specifically by the stereochemistry of neighboring C-H reaction sites and their moments of inertia.

Our results for the cyclic alkanes have led to further substantiation of a model of the H + RH reaction dynamics that we have developed. This local reaction model describes the structural and stereochemical features of reactions in which there are multiple, nearly identical reaction sites in a polyatomic molecule. The model is based on the idea of a local impact parameter, defined as the distance between the relative velocity vector and a line parallel to it that passes through a particular reactive atom in a polyatomic molecule. This local impact parameter replaces the ordinary impact parameter as the organizing principle of the reactive collision. Associated with this local impact parameter is a local opacity function and a local orbital angular momentum. In effect, the model portrays reaction in molecules with several different reaction sites as several separate reactions happening at the same time, and competing with one another.

The local reaction model posits two aspects of the structure of the RH reactant and R product as influencing the dynamics. The first is the proximity and stereochemistry of multiple, identical, competing C-H reaction sites in RH. The second is the small rotational constants of the alkyl radical. Multiple, competing reaction sites reduce the H₂ product rotational angular momentum through truncation of the local opacity function, which leads to a consequent reduction in local orbital angular momentum. The truncation of the opacity function comes from the overlap of opacity functions on adjacent C-H reaction sites. The small rotational constants of the alkyl radical product exert a counterbalancing effect, facilitating rotational excitation of the H₂ by relaxing the otherwise very strong coupling between conservation of total angular momentum and total energy. The rotational constants are small that enough that the energy "cost" of R rotational angular momentum is very small on the energy scale of these reactions.

Our model shows how these two opposing effects work differentially on H₂ in $v'=0$ and $v'=1$, leading to higher rotational excitation in $v'=1$ than in $v'=0$, the feature that is observed to be common to all H + RH reactions. It can also explain the differentiation of the reactions in terms of their energy disposal, accounting for the changes in energy disposal between classes and within classes of RH.

The analysis of the energy disposal in these H + RH reactions is done incorporating the kinematic constraint on product rovibrational energy that came from our kinematic model of reactions at suprathreshold collision energies, published last year. Our results for the H + RH reactions that we have studied this year show that the kinematic constraint expresses fully the consequences of conservation of total energy. By using the kinematically

constrained energy in the linear surprisal analysis of the H₂ product rovibrational state distributions, we separately extract the expression of angular momentum conservation. We find that in some of the H + RH reactions the H₂ rotational distribution shows a zero surprisal parameter, indicating that all rotational states that are energetically accessible are populated statistically. This outcome is expected from our local reaction model, and would be difficult to account for otherwise.

FUTURE PLANS

In the next year we expect to bring to a conclusion our studies of H + RH → H₂ + R reactions. Analysis of the results for the reactions of cyclopropane, isobutane, and neopentane will be done, and manuscripts reporting these results will be submitted for publication. These will further test the local reaction model. We expect to do similar experiments with substituted alkanes, specifically fluorocarbons. There are very many fluorine-substituted alkanes that are available commercially at low cost. These range from monosubstituted to completely fluorinated. These will allow us to explore the effects of reactant structure when there are non-reactive sites in the hydrocarbon at specific locations. (The reaction to produce HF is very endoergic and not appreciable even at the high collision energies of our experiments, so everywhere there is a C-F there is no reaction.) Also, through selective fluorination we can control the rotational constants of the fluoroalkyl radical product and thus control the angular momentum/energy decoupling that our model invokes.

PUBLICATIONS

1. H. Ni, J. Serafin, and J.J. Valentini, "Dynamics of the Vibrational Predissociation of HCl Dimer," *J. Chem. Phys.* **113**, 3055-3066 (2000).
2. C.A. Picconatto, A. Srivastava, and J.J. Valentini, "Reactions at Suprathreshold Energy: Evidence of a Kinematic Limit to the Internal Energy of the Products," *J. Chem. Phys.* **114**, 1663-1671 (2001).
3. C.A. Picconatto, A. Srivastava, and J.J. Valentini, "The H + n-C₅H₁₂/n-C₆H₁₄ → H₂(v', j') + C₅H₁₁/C₆H₁₃ Reactions: State-to-State Dynamics and Models of Energy Disposal," *J. Chem. Phys.* **114**, 4837-4845 (2001).
4. C.A. Picconatto, H. Ni, A. Srivastava, and J.J. Valentini, "Quantum State Distribution of HCl from the uv Photodissociation of HCl Dimer," *J. Chem. Phys.* **114**, 7073-7080 (2001).
5. C.A. Picconatto, A. Srivastava, and J.J. Valentini, "State-to-State Dynamics of the H + CD₃(CH₂)₄CD₃ → H₂ + CD₃((CH₂)₃CH)CD₃

Reaction: Dynamics of Abstraction of Secondary H in Linear Alkanes,"
Chem. Phys. Lett. 340 317-321 (2001).

6. J.J. Valentini, "State-to-State Chemical Reaction Dynamics in Polyatomic Systems: Case Studies," Ann. Rev. Phys. Chem. 52, 15-39 (2001).
7. A. Srivastava, C.A. Picconatto, and J.J. Valentini, "State-to-State Dynamics of the $H + c-C_6H_{12} \rightarrow H_2(v',j') + c-C_6H_{11}$ Reaction," J. Chem. Phys. 115, 2560-2565 (2001).
8. A. Srivastava, C.A. Picconatto, and J.J. Valentini, "State-to-State Dynamics of $H + c-RH \rightarrow H_2(v',j') + c-R$ Reactions: The Influence of Reactant Stereochemistry," Chem. Phys. Lett. 354, 25-30 (2002).
9. J.J. Valentini, " Mapping Reaction Dynamics via State-to-State Measurements: Rotations Tell the Tale," J. Phys. Chem. 106, xxxx (2002)

Theoretical Studies of the Dynamics of Chemical Reactions

Albert F. Wagner

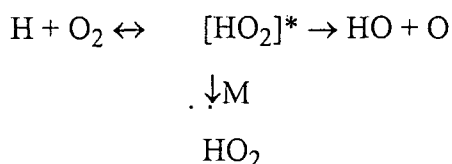
Gas Phase Chemical Dynamics Group, Chemistry Division
Argonne National Laboratory
Argonne, IL 60439
wagner@tcg.anl.gov

Program Scope

The goal of this program is to apply and extend dynamics and kinetics theories to elementary reactions of interest in combustion. Typically, the potential energy surfaces used in these applications are determined from ab initio electronic structure calculations, usually by other members of the group. Generally the calculated kinetics or dynamics is compared to experimental results, often generated by other members of the group.

Recent Progress

Electrostatic Effects in the Stabilization of HO_2^* : In collaboration with J. Michael in our group, we investigated the buffer gas dependence of the low pressure limit of the recombination of H with O_2 .



Recent experiments by Michael confirm the observations of others that when M is H_2O , the recombination rate constant to form HO_2 is an order of magnitude higher than when M is a rare gas or N_2 . The stabilization ability of M is controlled by two factors: the number of collisions between M and $[\text{HO}_2]^*$ and the average energy transfer that results from each collision. Traditional approaches to calculate the collision number when applied to this reaction require outrageous or unphysical values of the energy transfer between buffer gas and complex to agree with experiment. We have explored a new approach to determining the collision number by equating it to the thermal rate constant to recombine M and HO_2 as if they both were thermalized reactants colliding under the influence of long-range electrostatic forces. This is not to say that M- HO_2 form a collision complex that lasts long enough to influence chemistry but rather that the closeness of approach required by complex formation is a good measure of the kind of collisions that de-activate chemically activated molecules. This approach is easy to implement with even high order long-range electrostatic potentials. The central approximation is similar to the work of others (e.g., I. Smith at Birmingham) in estimating the high pressure limit of $\text{A}+\text{BC}$ by measuring the deactivation of $\text{A}+\text{BC}(v=1)$. The approach compares favorably with the closest available trajectory calculations (done by Miller and Brown (Combustion Research Facility) and Lendvey (Hungarian Academy of Science) and Schatz (Northwestern U.) on the collision number for the stabilization of the chemically activated triatomic molecule). In collaboration with L. Harding in our group, we have calculated the dipole and quadrupole moments of HO_2 and found them comparable to those of water. Along with other tabulated electrostatic information, we have used the code VariFlex to systematically study $\text{M}+\text{HO}_2$ "recombination" in the high pressure limit. For $\text{M}=\text{H}_2\text{O}$, this amounts to an electrostatic long range potential energy surface with R^{-3} , R^{-4} , R^{-5} , and R^{-6} terms. For $\text{M}=\text{Ar}$, only the R^{-6} induction term is present. The resulting collision numbers vary by about a factor of five between H_2O and Ar with H_2O

being higher. (Traditional estimates would have these collision numbers quite similar.) These collision numbers along with realistic average energy transfer parameters reproduce the kinetics measurements. This study suggests that electrostatics forces are an important component to energy transfer between polyatomics and many radicals. Further trajectory studies are needed to more carefully test the approximations in this approach.

Heat of Formation of OH: As discussed in greater detail in the abstract of B. Ruscic, our group initiated a multi-laboratory experimental/theoretical study of $\Delta H_{f0}^{\circ}(\text{OH})$. This study has definitively concluded that the consensus value in all standard thermochemical tabulations is incorrect by up to 0.5 kcal/mol (depending on the tabulation). Among the analyses carried out in this study was the Birge-Sponer extrapolation over only one missing vibrational level of the $A^2\Sigma^+$ of OH. This extrapolation is the origin of the error in the standard tabulations. Using a high quality ab initio curve for the same state by L. Harding and applying the same Birge-Sponer extrapolation method to all but the highest theoretical vibration level, the extrapolated dissociation energy falls well below the directly calculated one. Using the computed C_6 long-range constant and the experimental RKR curve, a Pade approximate extrapolation of the dissociation energy also indicates that the Birge-Sponer estimate was significantly low. The photoionization studies that underpin the ion-cycle value of $\Delta H_{f0}^{\circ}(\text{OH})$ are free of this extrapolation error and give a lower value that is corroborated by extremely high level electronic structure calculations on the ground state of OH by the Pacific Northwest National Laboratory members of our collaboration

Development and Implementation of Flexible Transition State Theory: In collaboration with D. Wardlaw (Queens U.) and S. Robertson (Accelrys Inc.), variable reaction coordinate FTST formalism has been significantly simplified at the energy and angular momentum resolved level. The inaugural treatment of FTST by Wardlaw and Marcus in the mid 1980s determined microcanonical and canonical rate constants by the minimization, along the center-of-mass separation coordinate, of a $2(n+1)$ nested set of phase space integrals over angular momenta and their conjugate angles where n is the number of transitional modes (modes that describe free rotation in the reactants but bound vibrations in the products). For bimolecular collisions, up to five transitional modes are possible resulting in tedious evaluations of up to 12-dimensional integrals. Since that time, especially over the last decade, our collaboration and others [S. Klippenstein (SNL), S. Smith (U. of Queensland)] have systematically discovered ways of formally doing many of the phase space integrals analytically, thereby reducing the residual number of integrals that must be done numerically and dramatically improving the computational efficiency of FTST. With our simplified formalism referred to above, the residual number of integrals has now been reduced to the minimum possible *without specification of the interaction potential*. For the energy-resolved microcanonical and for the canonical rate expressions, the dimension of the numerical phase space integral has been reduced to n . For energy- and angular momentum-resolved microcanonical rate expression, the dimension has been reduced to $n+1$ in general. However, the additional integration beyond n reduces to an elliptic integral expressible as an analytic series and, under certain circumstances, can be solved in closed form (i.e., can be done analytically). In all cases, the residual integrals are only over spatial coordinates and include the potential in the integrand. They have a physical interpretation as a steric factor. A Laplace transform relationship between canonical and microcanonical rate coefficients is exploited in the simplification of the formalism.

Future Plans

Reaction Kinetics of CN + OH: The experimental studies (see abstract of G. Macdonald) for both the overall rate and the branching ratio of the CN+OH will be compared to theoretical kinetics calculations. Mebel et al. has performed density functional electronic structure calculations on the ground triplet state potential energy surface. All the major stationary points

and transition states were characterized. With supplemental information on the barrierless reaction path for the initial CN+OH approach, a FTST/RRKM calculation will be performed with the VariFlex software to estimate the rate constant and branching ratios. The comparison between theory and experiment should help define the accuracy of the computed stationary points on the surface. The first excited triplet surface has recently been studied by Schaefer's group. They found that this surface interacts with the lowest triplet surface to produce conical intersections. The kinetic import of these conical intersections will be an issue in this study.

Cumulative Reaction Probability Code Development: With R. Shepard in our group and with M. Minkoff (ANL Math. and Comp. Sci. Division), we are developing a parallelized code for the direct calculation of the cumulative reaction probability (CRP) in a time independent manner using formalism originally developed by Miller et al. (Berkeley). Up to seven degree of freedom model problems have been examined on up to 128 processors at the NERSC SP with relatively good speed-up. The SPAM technique (see R. Shepard's abstract) may result in an effective preconditioner for this problem. This and other preconditioners will be explored.

Publications from DOE Sponsored Work from 2000 - Present.

Initiation in H₂/O₂: Rate Constants for H₂+O₂→H+HO₂ at High Temperature

J.V. Michael, J.W. Sutherland, L.B. Harding, and A.F. Wagner
28th Symposium (International) on Combustion 28,1471-1478 (2000)

Exploring the OH+CO Reaction Coordinate Via Infrared Spectroscopy of OH-CO Reactant Complexes

M. I. Lester, B. V. Pond, D. T. Anderson, L. B. Harding, A. F. Wagner
J. Chem. Phys. 113, 9889-9892 (2000)

Flexible Transition State Theory for a Variable Reaction Coordinate: Derivation of Canonical and Microcanonical Forms

S. H. Robertson, A. F. Wagner, D. M. Wardlaw
J. Chem. Phys. 113, 2648 (2000)

Evidence for a Lower Enthalpy of Formation of Hydroxyl Radical and a Lower Gas Phase Bond Dissociation Energy of Water

B. Ruscic, D. Feller, D. A. Dixon, K. A. Peterson, L. B. Harding, R. A. Asher, and A. F. Wagner
J. Phys. Chem. A 105, 1-4 (2001)

The Subspace Projected Approximate Matrix (SPAM) Modification of the Davidson Method

R. Shepard, A. F. Wagner, M. Minkoff, and J. L. Tilson
J. Comp. Phys. 172, 472-514 (2001)

Mapping the OH + CO → HOCO Reaction Pathway Through Infrared Spectroscopy of the OH-CO Reactant Complex

M. I. Lester, B. V. Pond, M. D. Marshall, D. T. Anderson, L. B. Harding, and A. F. Wagner
Faraday Discussions, 118, 373-385(2001)

Thermodynamic Functions for the Cyclopentadienyl Radical: the Effect of Jahn-Teller Distortion

J. H. Kiefer, R. S. Tranter, H. Wang, A. F. Wagner
Int. J. Chem. Kin. 33, 834-845 (2001)

POTLIB 2000: A Potential Energy Surface Library for Chemical Systems

R. J. Duchovic, Y. L. Volobuev, G. C. Lynch, T. C. Allison, D. G. Truhlar, A. F. Wagner, B. C. Garrett

Comp. Phys. Comm. 144, 169-187 (2002)

Ab initio Determination of Americium Ionization Potentials

J. L. Tilson, R. Shepard, C. Naleway, A. F. Wagner, W. C. Ermler
J. Chem. Phys. 112, 2292 (2000)

The Calculation of f-f Spectra of Lanthanide and Actinide Ions by the MCDF-CI Method

M. Seth, R. Shepard, A. F. Wagner, K. G. Dyall
J. Phys. B. 34, 2383-2406 (2001)

An Ab Initio Study of the f-f Spectroscopy of Americium+3

J. Tilson, M. Seth, C. Naleway, M. Seth, R. Shepard, A. F. Wagner, W. Ermler
J. Chem. Phys. 116, 5494 (2002)

An Ab Initio Study of the Ionization Potential and f-f Spectroscopy of Europium Atoms and Ions

C. Naleway, M. Seth, R. Shepard, A. F. Wagner, J. Tilson, W. C. Ermler, and S. R. Brozell
J. Chem. Phys. 116, 5481 (2002)

Flexible Transition State Theory for a Variable Reaction Coordinate: Analytic Expressions and an Application

S. Robertson, A. F. Wagner, and D. M. Wardlaw
J. Phys. Chem. A 106, 2598 (2002).

On the Enthalpy of Formation of Hydroxy Radical and Gas-Phase Bond Dissociation Energy of Water and Hydroxyl

B. Ruscic, A. F. Wagner, L. B. Harding, R. L. Asher, D. Feller, D. A. Dixon, K. A. Peterson, Y. Song, X. Qian, C.-Y. Ng, J. Liu and W. Chen
J. Phys. Chem. 106, 2727 (2002)

Rate Constants, 1100 $\leq T \leq$ 2000 K, for the Reaction, $H + NO_2 \rightleftharpoons OH + NO$, Using Two Shock Tube Techniques: Comparison of Theory to Experiment

M.-C. Su, S. S. Kumaran, K. P. Lim,
A. F. Wagner, L. B. Harding, and J. V. Michael
J. Phys. Chem. A (in press)

Rate Constants for $H + O_2 + M \rightleftharpoons HO_2 + M$ in Seven Bath Gases

J. V. Michael, M.-C. Su, J. W. Sutherland, J. J. Carroll, and A. F. Wagner
J. Phys. Chem. A, (in press)

Flexible Transition State Theory for a Variable Reaction Coordinate: Derivation of Canonical and Microcanonical Forms with Angular Momentum Conservation

S. H. Robertson, D. M. Wardlaw, A. F. Wagner
J. Chem. Phys. (in press)

Kinetic Modeling of Combustion Chemistry

Charles K. Westbrook and William J. Pitz
Lawrence Livermore National Laboratory
P. O. Box 808, Livermore, CA 94550

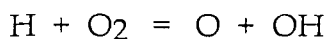
Program Scope

This program develops detailed chemical kinetic reaction mechanisms for combustion primarily of hydrocarbon fuels, and then uses those reaction mechanisms to study laboratory and applied combustion systems. The experimental and theoretical work of other program scientists is used to refine these reaction mechanisms, and the model applications are used to suggest reactions and other chemical details that merit further study.

Recent Progress

Advances have been made in each element of the kinetic modeling program, including development of new reaction mechanisms for hydrocarbon and other species of interest, as well as kinetic model applications.

New kinetic reaction mechanisms have been developed for all nine isomers of heptane (C₇H₁₆), providing an interesting range of chemical species to use in assessing the role that hydrocarbon fuel molecular structure plays in determining combustion properties. In a study [1] of ignition at high temperatures ($T \geq 1000\text{K}$), those isomers which produced the largest fraction of H atoms from the heptyl radicals possible for that isomer tended to react most rapidly, while those which produced large fractions of methyl radicals were generally slowest to ignite. These trends were interpreted in terms of the main high temperature chain branching reaction



which consumes one H atom radical species and produces two radicals, O and OH. In contrast, in the lower temperature regime, different heptane isomers ignited most rapidly [2], with the main chain branching sequences being initiated by addition of molecular oxygen to alkyl and hydroperoxyalkyl radicals. Also important in the lower temperature regime are alkylperoxy radical isomerization reactions, whose rates depend strongly on fuel molecular structure. These reaction mechanisms were selected in part to provide a testbed for computational algorithms which automatically derive reaction mechanisms from established principles or reduce reaction mechanisms to provide more economical computational models.

A combined experimental/kinetic modeling study was carried out [3] to refine current mechanisms for oxidation of toluene. Experimental data from shock tubes, flow reactors, and counter-flow nonpremixed flames were used to improve reaction rate estimates as well as reaction paths for toluene. Under shock tube conditions, toluene oxidation was most sensitive to reactions involving H atoms, such as toluene reaction with H atoms and toluene decomposition to benzyl radicals and H atoms. Under flow reactor and counterflow conditions, where the controlling temperatures are lower than in a shock tube, toluene oxidation was most sensitive to reactions of benzyl radicals with O₂, O and HO₂. This study produced some recommendations of future experimental work that is needed for additional model refinements.

One additional mechanism development project carried out in the past year has been the derivation of reaction mechanisms to describe the incineration of the chemical warfare (CW) nerve agent Sarin, as well as the related but much less toxic species dimethyl methyl phosphonate (DMMP), trimethyl phosphate (TMP), and di-isopropyl methyl phosphonate (DIMP). The three related species have each been used at times as credible approximations or surrogates for the combustion of Sarin. Note that Sarin is most similar to DIMP, with one of the isopropoxy radicals in DIMP replaced by a single F atom. It is also important to note that many CW agent molecules are largely made up of familiar hydrocarbon fragments, with only very minor alterations to incorporate a P=O group and an F or S atom. These reaction mechanisms required the development of large families of thermochemical data to provide bond energies, specific heats, and equilibrium constants for important species involving the F or S atoms and the P=O system that had not previously been required to describe purely hydrocarbon systems.

In the past, experiments and kinetic modeling studies were carried out using selected surrogate compounds rather than the highly toxic CW agent itself. Results of those experiments then were believed to provide the most realistic possible estimate of the reactivity of the real CW agent species. However, there was relatively little attention given to determining how likely the surrogate was to reproducing the actual CW agent reactivity. The logic of our new approach of using numerical kinetic models for CW chemicals in addition to models for the surrogates is that the kinetic models can be used to estimate how much and in what direction the reactivity of a surrogate might differ from the reactivity of the CW agent, then using that information to refine the experimental results for surrogate performance to arrive at a better estimate of the CW agent reaction. Using this approach, our studies [4,5] have successfully reproduced experimental results for many possible surrogate species, and they have shown that only DIMP ought to be used as a reliable surrogate for Sarin. The other possible

surrogates, especially DMMP and TMP are much less reactive than Sarin under conditions expected in incineration applications, so they are not likely to provide accurate Sarin predictions.

These new studies have also demonstrated that it is possible to use existing chemistry analysis tools such as bond additivity techniques to support kinetic studies of chemical systems not previously studied. This finding opens all sorts of future possibilities for analysis.

Kinetic model applications using hydrocarbon combustion mechanisms have focused on identifying fuel additives which reduce pollutant emissions from diesel engines. Recent kinetic studies we have carried out [6,7] have shown how oxygenated hydrocarbon species such as ethanol, dimethyl ether, and others reduce soot emissions from diesel engines. This was found to result primarily from the introduction of large numbers of C - O bonds which are very difficult to break during combustion. Since the major reaction paths to soot production involve unsaturated hydrocarbon fragments that include no oxygen atoms, the oxygenated additives work primarily by removing large fractions of the reactive C atoms from the pool of soot precursors available to lead to soot production. The effectiveness of oxygenates for soot reduction has been observed for many years, but the use of kinetic modeling established a coherent explanation for those trends for the first time, and this has led to identification of perhaps even more effective soot reduction additives. Additional modeling studies of diesel combustion have addressed problems of NO_x emissions [8].

Another area of practical application of kinetic combustion modeling involves studies of a novel engine concept called Homogeneous Charge, Compression Ignition (HCCI), which combines elements of spark ignition and diesel engine combustion. The concept provides exceedingly low NO_x emissions, but unburned hydrocarbon and CO emissions are often quite high. The combustion is sufficiently simple that purely kinetic modeling is capable of providing a great deal of valuable information [9]. Additional studies have focused on a general kinetic model of ignition [10], kinetics of isomers of pentane [11], and thermochemistry [12].

Future Plans

We expect to continue our development of hydrocarbon combustion kinetic reaction mechanisms and apply them to practical combustion problems of importance to DOE. Current applications areas of focus include diesel engines and HCCI engines, and recent DOE programs have also emphasized possible work on industrial burners and furnaces.

We hope to continue development and applications of mechanisms for organophosphorus compounds and additional CW agents. This work can provide a valuable link between counter-terrorist programs and BES Chemical Sciences fundamental science. Reaction mechanisms for CW agent species could be used in a wide range of applications to analyse various risks and strategies to defeat threats, but also to ensure safe destruction of aging and dangerous stockpile chemicals. This work requires very interesting extensions of theoretical tools for analysis of combustion kinetics and may provide new insights into the continued improvement of the same tools for combustion of hydrocarbon systems.

Publications

1. Westbrook, C.K., Pitz, W.J., Curran, H.J., Boercker, J., and Kunrath, E., "A Detailed Chemical Kinetic Modeling Study of the Shock Tube Ignition of Isomers of Heptane," *Int. J. Chem. Kinetics* **33**, 868-877 (2001).
2. Westbrook, C.K., Pitz, W.J., Boercker, J., Curran, H.J., Griffiths, J.F., Mohamed, C., and Ribaucour, M., "Detailed Chemical Kinetic Reaction Mechanisms for Autoignition of Isomers of Heptane Under Rapid Compression", *Proc. Combust. Inst.* **29**, in press (2002).
3. Pitz, W.J., Seiser, R., Bozzelli, J.W., Seshadri, K., Chen, C.-J., Da Costa, I., Fournet, R., Billaud, F., Battin-Leclerc, F., and Westbrook, C.K., submitted for publication (2002).
4. Glaude, P.-A., Curran, H.J., Pitz, W.J., and Westbrook, C.K., "Kinetic Study of the Combustion of Organophosphorus Compounds", *Proc. Combust. Inst.* **28**, 1749-1756 (2000).
5. Glaude, P.-A., Melius, C., Pitz, W.J., and Westbrook, C.K., "Detailed Chemical Kinetic Reaction Mechanisms for Incineration of Organophosphorus and Fluoro-organophosphorus Compounds", *Proc. Combust. Inst.* **29**, in press (2002).
6. Kaiser, E.W., Wallington, T.J., Hurley, M.D., Platz, J., Curran, H.J., Pitz, W.J., and Westbrook, C.K., "Experimental and Modeling Study of Premixed Atmospheric Pressure Dimethyl Ether-Air Flames", *J. Phys. Chem. A* **104**, No. 35, 8194-8206 (2000).
7. Fisher, E.M., Pitz, W.J., Curran, H.J., and Westbrook, C.K., "Detailed Chemical Kinetic Mechanisms for Combustion of Oxygenated Fuels", *Proc. Combust. Inst.* **28**, 1579-1586 (2000).

8. Flynn, P.F., Hunter, G.L., Farrell, L.A., Durrett, R.P., Akinyemi, O.C., zur Loye, A.O., Westbrook, C.K., and Pitz, W.J., "The Inevitability of Engine-Out NO_x Emissions from Spark-Ignition and Diesel Engines", *Proc. Combust. Inst.* **28**, 1211-1218 (2000).
9. Aceves, S.M., Flowers, D.L., Martinez-Frias, J., Smith, J.R., Westbrook, C.K., Pitz, W.J., Dibble, R., Wright, J.F., Akinyemi, W.C., and Hessel, R.P., "A Sequential Fluid-Mechanic Chemical Kinetic Model of Propane HCCI Combustion", Society of Automotive Engineers publication SAE-2001-01-1027 (2001).
10. Westbrook, C.K., "Chemical Kinetics of Hydrocarbon Ignition in Practical Combustion Systems", *Proc. Combust. Inst.* **28**, 1563-1577 (2000).
11. Ribaucour, M. Minetti, R., Sochet, L.R., Curran, H.J., Pitz, W.J., and Westbrook, C.K., "Ignition of Isomers of Pentane: an Experimental and Kinetic Modeling Study", *Proc. Combust. Inst.* **28**, 1671-1678 (2000).
12. Curran, H.J., Wu, C., Marinov, N.M., Pitz, W.J., Westbrook, C.K., and Burcat, A., "The Ideal Gas Thermodynamics of Diesel Fuel Ingredients: I. Naphthalene Derivatives and Their Radicals", *J. Phys. Chem. Ref. Data* **29**, 463-517 (2000).

PROBING FLAME CHEMISTRY WITH MBMS, THEORY, AND MODELING

Phillip R. Westmoreland

Department of Chemical Engineering
University of Massachusetts Amherst
159 Goessmann Laboratory, 686 N. Pleasant
Amherst, MA 01003-9303

Phone 413-545-1750
FAX 413-545-1647
westm@ecs.umass.edu

<http://www.ecs.umass.edu/che/westmoreland.html>

Program Scope

The objective is to establish kinetics of combustion and molecular-weight growth in hydrocarbon flames as part of an ongoing study of flame chemistry. Our approach combines molecular-beam mass spectrometry (MBMS) experiments on low-pressure flat flames; *ab initio* thermochemistry and transition-state structures; rate constants predicted by transition-state and chemical activation theories; and whole-flame modeling using mechanisms of elementary reactions. The MBMS technique is powerful because it can be used to measure a wide range of species, including radicals, quantitatively with high sensitivity and low probe perturbation. Ethylene and allene-doped ethylene flames are the present focus.

Recent Progress

In the past year, we have focused on three thrusts. First, we have probed new and previous ethylene-based flames in our MBMS experiments at UMass. Second, flame and reaction modeling has added to the resulting experimental insights into ethylene and allene flame chemistry, pointing to new kinetics and new flame models. Third, initial experiments have been carried out in a complementary MBMS at the LBNL Advanced Light Source, promising to answer questions about isomeric flame compositions that cannot be resolved otherwise.

Flame mapping. Flame chemistry of olefins is the key link between alkane combustion and formation of aromatic pollutants. Presently, two similar fuel-lean ethylene flames are being mapped, where one is doped with allene. These flames are similar to that of Bhargava and Westmoreland,¹ as shown in Table 1. One difference is that the earlier flame used a larger-diameter sintered-bronze burner (or "flameholder"; 9.91 cm vs. 6.03 cm), which makes measurements far from the burner less sensitive to experimental edge effects. However, we have changed to the smaller, standard McKenna burner in order that the burners in the UMass, ALS, and Sandia apparatus should all be the same.

The flame of Ref. 1 is also intriguing because of difficulties in modeling the undoped flame by our group and others, in contrast to more successful modeling of our fuel-rich ethylene flame.² The present data resolve questions about CO in the earlier, similar data set, while confirming that present lean ethylene mechanisms do not generate heat rapidly enough.

Table 1. Conditions of ethylene-based flames analyzed by MBMS.

Fuel-lean ethylene flame of Bhargava and Westmoreland (1998)	Current lean ethylene flame	Allene-doped lean ethylene flame
$\phi = 0.75$, $P = 30$ Torr, $v_o = 30.0$ cm/s (300 K, P) 8.6 mol% C_2H_4 , 34.5% O_2 , 56.9% Ar	$\phi = 0.70$, $P = 30$ Torr, $v_o = 30.6$ cm/s 8.3 % C_2H_4 , 35.3% O_2 , 56.4% Ar	$\phi = 0.69$, $P = 30$ Torr, $v_o = 30.6$ cm/s 7.9 % C_2H_4 , 0.20% C_3H_4 , 35.4% O_2 , 56.5% Ar

Thirty-five stable and radical species have been measured in both fuel-lean flames (Table 2). One valuable expansion is the result of the new mass spectrometer's heightened sensitivity and high mass-resolution capability within the 1 – 50 amu mass range, which makes it possible to resolve nearly isomeric species in the molecular beam. Thus, we now have mole fraction profiles

¹ A. Bhargava and P. R. Westmoreland, *Combustion and Flame* **115**, 456-467 (1998).

² A. Bhargava and P. R. Westmoreland, *Combustion and Flame* **113**, 333-347 (1998).

measured separately for O and CH₄ (mass 16), C₂H₄ and CO (mass 28), C₂H₅ and HCO (mass 29), C₂H₆ and H₂CO (mass 30), C₃H₄ and Ar (mass 40), C₃H₅ and HCCO (mass 41), C₃H₆ and CH₂CO (mass 42), and C₂H₄O and CO₂ (mass 44). The species at 28, 40, and 44 had been resolved before only by using ionization efficiency plots, subtracting the eV-extrapolated intensity of the lower-IP species from the total intensity, leaving the ionization efficiency and signal due to the higher-IP species. The new measurements do not rely on this linear extrapolation. Thus, they are more reliable and also provide a check on the validity of the extrapolation technique.

Table 2. Species with profiles measured in the present lean flames of ethylene and allene-doped ethylene, listed by molecular weight.

H	O	C ₂ H ₄	HO ₂	HCCO	C ₂ H ₄ O
H ₂	OH	HCO	H ₂ O ₂	C ₃ H ₅	C ₅ H ₅
CH	H ₂ O	C ₂ H ₅	C ₃ H ₂	CH ₂ CO	C ₅ H ₆
CH ₂	C ₂ H ₂	H ₂ CO	C ₃ H ₃	C ₃ H ₆	C ₆ H ₅
CH ₃	C ₂ H ₃	C ₂ H ₆	Ar	C ₂ H ₃ O	C ₆ H ₆
CH ₄	CO	O ₂	C ₃ H ₄	CO ₂	

The CO profiles were particularly interesting. Reference 1 reported that CO went to zero in the postflame gases, while whole-flame modeling and analyses of reaction equilibria indicated that low levels of CO should persist. The new measurements show that CO does in fact persist, even at the lean, high-temperature conditions.

Additional profiles are being measured, and net reaction rate is being calculated from the data for each species at each position. The latter is accomplished by numerically differentiating the mass flux, itself calculated as the sum of the convective flux and diffusive flux. We have used such rates with the measured concentrations to measure rate constants in flames for C₂H₄+H and C₂H₄+OH.²

Modeling combustion over a wide range of pressure and temperature. In collaboration with Fred Dryer's DOE-sponsored research at Princeton, we have developed a mechanism for use from 30 Torr to 10 atm in C₁ and C₂ hydrocarbon combustion [DOE Publ. 5]. The experimental systems are the Bhargava fuel-rich flat flame¹, operated at 20 Torr and a fuel-equivalence ratio of 1.9, and the Princeton Flow Reactor, operated at lower temperature (850-950 K) and higher pressure (5-10 atm). Ethylene combustion was modeled in each apparatus, showing differences that could be assigned to pressure, temperature, or combinations of the two.

Recent predictions with this mechanism point to crucial corrections needed for C₂H₃+O₂ kinetics. General behaviors of this set were described in last year's Contractors Meeting report and presented at the Joint Meeting of the US Sections of the Combustion Institute. In the low-pressure flame, C₂H₄ is mainly consumed by H abstraction making C₂H₃, while in the high-pressure system OH abstraction competes with addition of H, making C₂H₅. In both cases, C₂H₃+O₂ then proceeds to HCO and CH₂O and eventually to CO and CO₂. However, the model indicates that C₂H₃+O₂ → C₂H₃O+O should not be as important as several previous studies have proposed. A recent theoretical rate constant from Mebel et al.³ (corrected for a typographical error in the paper) indicated that C₂H₃+O₂ → C₂H₃O+O became dominant at higher temperatures. In the flame, this had little effect because of vinyl decomposition to C₂H₂. In the lower-temperature flow-reactor data, this rate constant was shown to be too high based on the poor predictions it would cause.

Developing a new flame modeling method. We have developed a solution method for solving the nonadiabatic energy equation in a flat flame [DOE Publ. 4]. This work was originally motivated when we found that the experimental maximum temperature in the lean ethylene flame was higher than the kinetically computed adiabatic flame temperature T_{adia} , while it must be lower than the true, thermodynamic T_{adia} . A similar problem is seen in modeling H₂/O₂ flame data. These examples illustrate how the energy balance can be violated by the conventional approach of using a measured temperature profile for flat-flame modeling.

³ A.M. Mebel, E.W.G. Diau, M.C. Lin, and K. Morokuma, *J. Am. Chem. Soc.* **118**, 9759 (1996).

We have developed modifications to the Chemkin II version of the Sandia Premix code that explicitly incorporate radiative losses and burner losses into the energy equation and boundary conditions. Initially we adapted NIST's RADCAL subroutine to model gas-phase radiation of CO_2 , H_2O , CH_4 , CO , O_2 , and N_2 in addition to the soot contribution, and we treated the flame as optically thin. Our subsequent work has incorporated analysis of potential reabsorption. Comparisons with the data are in progress.

Photoionization MBMS using the LBNL ALS. In collaboration with Terry Cool and Andy McIlroy, a flame-sampling MBMS apparatus using vacuum-ultraviolet photoionization has been constructed on the Chemical Dynamics Beamline at Lawrence Berkeley National Laboratory's Advanced Light Source (<http://www.chemicaldynamics.lbl.gov/es3/flamediagnostics.htm>). With the intense, finely tuned VUV photons, we should be able to discriminate many isomeric species by their photoionization thresholds. This is difficult with tunable laser photoionization because of intensity / resolution limits, and it is still more difficult with electron-impact ionization because of thermal spread in electron energies. Limited access time to the ALS photons precludes complete mapping of flames with this apparatus, but a McKenna burner has been chosen so the Sandia and UMass MBMS configurations match it, giving complementary measurement capabilities for identical flames.

In an opening campaign of equipment shakedown and testing in March 2002, the first flame was lit, photoionization mass spectrometry was successfully carried out with the time-of-flight mass spectrometer, and the beam was also analyzed by a residual gas analyzer using 25+ eV electron-impact ionization and a quadrupole. Stepping the photon energy at 1-eV intervals demonstrated that radicals could be distinguished with good sensitivity. During the next campaign beginning in June, we will seek to discriminate between the C_3H_4 isomers propadiene and propyne, as well as C_6H_6 isomers in the fuel-rich ethylene flame mapped previously.²

Future Plans

Upon completion of the ethylene flames, we plan to move the UMass MBMS experiments toward mapping cyclohexane flames. Cyclohexane has the advantage of having only secondary hydrogens to abstract, which will give us a clean measurement of these rate constants at high temperatures. The abstraction product cyclohexyl (C_6H_{11}) should mainly decompose, forming $2\text{C}_2\text{H}_4 + \text{C}_2\text{H}_3$ rather cleanly. Kinetics of the smaller amounts of 1-hexene and other heavy products should thus be easier to isolate.

Meanwhile, we will extract rate constants and improve overall kinetic mechanisms using the ethylene flame data. In that direction, we have begun a collaboration with other DOE contractors to improve theoretical rate constants for $\text{C}_2\text{H}_3 + \text{O}_2$, making use of a potential surface we have calculated for $\text{CH}_2\text{CHOO} \rightarrow \text{C}_2\text{H}_3\text{O} + \text{O}$. Also, the full nonadiabatic energy equation solutions will be used to probe causes of low heat release in the fuel-lean flame. Finally, we will begin to discriminate hydrocarbon isomers using the ALS MBMS, expanding the value of earlier MBMS data for development and testing of combustion kinetics.

Publications of DOE-sponsored Research, 1999-2002

1. P.-A. Bui, D.G. Vlachos, and P.R. Westmoreland, "On the local stability of multiple solutions and oscillatory dynamics of spatially distributed flames," *Combustion and Flame* **117**, 307-322 (1999).
2. T. Carrière and P.R. Westmoreland, "Improving Kinetic Models for Ethylene Flat Flames," *Chem. Phys. Prop. Combustion*, 125-128 (1999).
3. M. E. Law, T. Carrière, and P.R. Westmoreland, "New Insights into Fuel-Lean Ethylene Flames," *Chem. Phys. Prop. Combustion*, 194-197 (2001).
4. T. Carrière and P.R. Westmoreland, "Complete Solution of the Flat-Flame Equations in the Non-Adiabatic Case," *Chem. Phys. Prop. Combustion*, 241-244 (2001).
5. T. Carrière, P.R. Westmoreland, A. Kazakov, Y.S. Stein, and F.L. Dryer, "Modeling Ethylene Combustion from Low to High Pressure," *Proc. Combust. Inst.*, **29** (in press).

Photoinduced Molecular Dynamics in the Gas and Condensed Phases

M. G. White and R. J. Beuhler

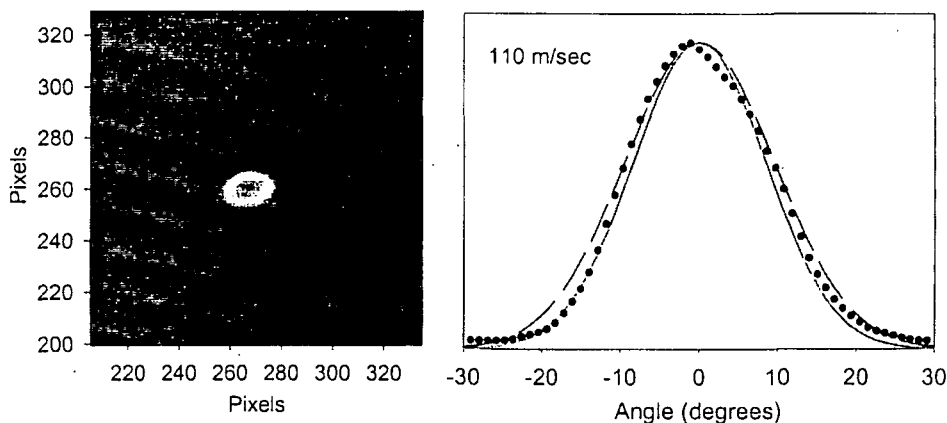
Chemistry Department, Brookhaven National Laboratory, Upton, NY 11973
(mgwhite@bnl.gov, beuhler@bnl.gov)

1. Project Scope

The goal of this program is to elucidate the dynamics of photoinduced and thermal reactions of molecules on surfaces through measurements of the state- and energy-distributions of the products. Particular emphasis is placed on systems that provide information on chemical intermediates or reactions that are important in combustion or energy-related catalysis. State- and energy-resolved measurements on the gas-phase products resulting from photodesorption, and photo-initiated and thermal reactions are used to infer the dynamics of product formation and desorption, *i.e.* the surface-bound transition state. Thermal oxidation and atom-atom recombination reactions important in energy-related catalysis are also being studied with the goal of obtaining microscopic description of the surface reaction dynamics.

2. Recent Progress

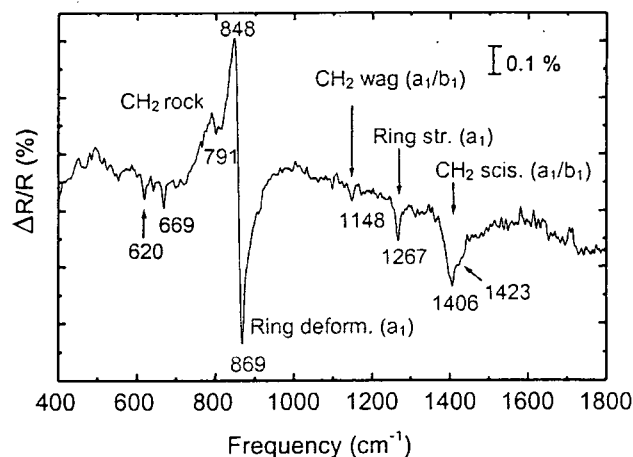
Spatial distributions of desorbed neutrals from ion imaging. We have recently designed and constructed a ion imaging system that will allow determination of the angular distribution of neutral molecules desorbed from a surface which have been previously state-selected by laser excitation and ionization. The angular distribution is sensitive to the scattering dynamics of the molecule just prior to desorption (molecule-surface potential), the desorption mechanism (thermal vs. electronic) and the corrugation of the surface and molecule adsorption site geometry. The detector makes use of a novel ion lens design based on velocity-focussing and is optimized for use with a line ionization source (VUV laser beam) and a relatively large source size (~2 cm). The latter is required for imaging products from a macroscopically large crystal surface (0.5–1cm diameter). Initial experiments imaging involve the state-resolved detection of CO and Kr resulting from IR-induced (1064 nm) desorption from Ag(111) at low temperatures (< 70 K). Earlier work in our laboratory has shown that the photodesorption process for weakly bound adsorbates (N₂, CO, Kr) on Ag(111) is not due to laser-induced thermal heating of the surface, but rather to a novel mechanism that involves the non-adiabatic coupling of IR-excited electron-hole pairs at the Ag surface with the center-of-mass motions of the adsorbate. Additional support for this non-thermal mechanism is provided by the spatial distributions obtained using the new ion-imaging detector, which were found to be strongly peaked along the surface normal. The latter could be characterized by $\cos^n\theta$ distributions with $25 \leq n \leq 30$ (see Figure 1). By contrast, IR-induced thermal desorption would result in a much broader angular distribution, typically $\cos^2\theta$. In addition, we did not observe any significant correlation of the angular distribution with internal rotational state (CO) or velocity



(CO, Kr). This latter observation suggests that the highly peaked angular distributions are intrinsic to the desorption process and indicative of strong repulsive forces normal to the surface.

State-resolved surface photochemistry: The spatial imaging capabilities of the ion imaging spectrometer discussed above are currently being focussed on the UV photochemistry of methyl nitrite adsorbed on Ag(111). For photolysis wavelengths below 350 nm, methyl nitrite dissociates to yield adsorbed methoxy and NO fragments which desorb into the gas-phase with a wide range of internal and kinetic energies. The dissociation dynamics of adsorbed methyl nitrite is unusual in that it is similar to that observed in the gas-phase, *i.e.*, an intramolecular process, in contrast to most adsorbate-metal photochemistry which involves the scattering of "hot" electrons generated at the metal surface (surface-mediated). Previous studies using electron impact mass spectrometry to detect desorbed NO following photoexcitation at 248 nm (J. M. White, Univ. Texas) indicate that NO fragments with high kinetic energies are ejected at angles greater than 20° relative to the surface normal. The latter is attributed to a prompt dissociation process in which NO dissociation is directed along the O-NO bond orientation of the intact adsorbed molecule (~45° with respect to surface normal). In this work, we have employed (1+1) REMPI detection via the $A^2\Sigma^+$ Rydberg state and surface ion imaging to probe the desorbed NO molecules resulting from the UV photolysis (266 nm) of methyl nitrite on Ag(111) at sub-monolayer coverages. State-resolved measurements for NO products in $v''=0$ and $v''=1$ show a strong correlation between internal energy and translational energy, with average kinetic energies as high as 0.7 eV for high rotational levels of $v''=1$ ($J''>20.5$). The latter is similar to the kinetic energy release observed for 266 nm dissociation of gas-phase methyl nitrite. Ion images for the prompt NO fragments at high kinetic energies, however, do not show the expected maxima at take-off angles greater than 20°, but exhibit spatial distributions which are peaked along the surface normal. We are currently investigating NO products with two quanta of vibrational excitation, in order to address the possibility that the off-normal ejection is associated with only the highest energy NO fragments. It is also possible that the low surface temperature used here (35 K) leads to adsorption overlayers (binding sites and packing) that are significantly different than that obtained in previous investigations at 90-100 K. Experiments at various surface temperatures up to 100 K will be performed to investigate the dependence of the dissociation dynamics on initial adsorption conditions.

Surface IR vibrational spectroscopy. We have recently begun an effort to use infrared surface vibrational spectroscopy (IRAS) as a probe for adsorbate binding and reaction on metal single-crystal and nanoparticle surfaces. These experiments are being performed on the U4IR beam line at the NSLS, whose low frequency capabilities (100 – 1000 cm^{-1}) are ideally suited for investigating vibrational modes that are strongly coupled to bonding to the surface. Initial experiments have focused on the chemisorption of ethylene oxide (EO) on Ag(111) which is related to the selective oxidation of ethylene to ethylene oxide on supported Ag catalysts. Of particular interest is the ring opening reaction of EO to form a Ag-O-CH₂-CH₂-Ag metallocycle which is thought to be the reaction intermediate whereby oxygen atoms are added to the ethylene double bond. Evidence for the EO metallocycle is based on very recent electron energy loss vibrational spectra (HREELS) obtained by Barteau and coworkers (Delaware) on Ag(111) and (110) surfaces. IRAS can provide new information on metallocycle formation though the observation of additional IR-allowed modes resulting from higher spectral resolution (1- 4 cm^{-1}) and low frequency capabilities ($\leq 1000 \text{ cm}^{-1}$). As the first step, we obtained the IR vibrational spectrum of EO/Ag(111) at monolayer and higher coverages. The most striking difference between the IRAS and HREELS spectra is the band centered around 860 cm^{-1} which exhibits a persistent "derivative" line shape as shown in Figure 2. This band is assigned to the C-O-C ring deformation mode and involves motion of the oxygen atom through which the molecule is bound to the Ag surface. Similar line shapes have been seen in IRAS for CO/Cu(100) and H/Mo(W)(100), and are attributed to a Fano-like interference between a sharp vibrational resonance and the background electron-hole pair excitation continuum of the metal surface. Such non-adiabatic couplings often play a key role in the dephasing of adsorbate vibrational



motions and may also lead to desorption via specific modes which are otherwise poorly matched to thermally excited phonons at the metal surface ($\leq 150 \text{ cm}^{-1}$ for Ag). Theoretical models predict variations in line shape with surface temperature and we are currently investigating this effect, as well as the influence of surface coverage and the density of surface defects.

3. Future

Near term efforts will continue to focus on the dynamics of oxidation reactions on Ag using spectroscopic probes of gas-phase products or surface intermediates. The interaction of oxygen with Ag surfaces is a subject of continued interest due to the unique abilities of Ag surfaces to catalyze selective oxidation reactions without promoting total combustion of hydrocarbon reactants. Adsorbed O-atoms are known to be the active surface species for these reactions, however, the incorporation of oxygen on Ag surfaces is quite complex with several chemically distinct O-atom species having been identified (surface, sub-surface, bulk). The overall reaction path leading to an oxygenated Ag surface involves the elementary steps of O_2 sticking, chemisorption, dissociation, O-atom sub-surface diffusion and Ag surface reconstruction, most of which remain poorly understood.

Our previous state-resolved study of the O-atom recombination reaction on a polycrystalline Ag surface demonstrated the utility of such measurements for extracting the state- and energy-dependence of O_2 adsorption (sticking). Future experiments will study the dynamics of the O-atom recombination reaction on well-defined Ag(111) and Ag(110) single crystal surfaces over a range of surface temperatures to explore the surface structure dependence and surface barrier heights. As in our earlier study, (2+1) REMPI via the $\text{C } ^3\Pi_u (3s\sigma)$ Rydberg state and time-of-flight mass spectrometry will be used to extract internal state (v'' , J'') and velocity distributions for desorbing O_2 molecules. Further development of the ion-imaging detector will also permit measurements of the spatial distribution of desorbing O_2 molecules. The latter can provide additional information on the O-atom recombination and O_2 desorption dynamics with respect to the corrugation of the (110) Ag surface and the anisotropy of the O_2 -Ag potential.

State-resolved methods will also be used in conjunction with a recently developed Ag membrane reactor to investigate the dynamics of elementary oxidation reactions on Ag surfaces. By supplying the oxygen to the surface via diffusion through the Ag membrane, surface reactions can be performed continuously at low pressures ($10^{-8} - 10^{-4}$ Torr) where the products can be sampled under collision-free conditions. In the case of ammonia oxidation, the reaction proceeds by complete dissociation of ammonia to N- and H-atoms on the Ag surface, which react with surface oxygen species to form NO via the $\text{N}_{(a)} + \text{O}_{(a)} \rightarrow \text{NO}_{(g)}$ association reaction (N_2 , H_2O , H_2 are also produced). Preliminary (1+1) REMPI measurements via the $\text{A } ^2\Sigma^+$ state have shown that the NO products can be readily observed, but their low kinetic energies have made it difficult to avoid interference with thermalized background NO. These experiments will be repeated on the new molecular beam apparatus, where differential pumping between the scattering chamber and the beam source should significantly reduce this thermal background and allow a complete spectroscopic analysis of the nascent NO products.

Current IRAS studies of surface intermediates in the oxidation of methanol and ethylene on clean Ag surfaces will be expanded to include pre-oxygen covered and polycrystalline surfaces to investigate how O-atoms (surface, sub-surface) modify binding and reaction. Future work will also include reactivity studies of Ag nanoparticles prepared by simple evaporation onto single-crystal metal oxide surfaces (e.g., $\text{TiO}_2(110)$). Here, we will be able to follow the binding and surface chemistry of adsorbates on Ag nanoparticles as a function of size (and morphology) and oxygen exposure.

4. Publications

R. J. Beuhler, R. M. Rao, J. Hrbek and M. G. White, *Study of the partial oxidation of Methanol to Formaldehyde on a Polycrystalline Ag Foil*, *J. Phys. Chem.* **105**, 5950 (2001).

D. A. Shea, L. Goodman and M. G. White, *Acetone, n-Radical Cation Internal Rotation Spectrum: the Torsional Potential Surface*, *J. Chem. Phys.* **112**, 2762 (2000).

Small Molecular Systems

Curt Wittig, Joelle Underwood, Delphine Chastaing, and Sun Lee
Department of Chemistry
University of Southern California
Los Angeles, CA 90089-0482
wittig@usc.edu

Program Scope

Our program deals with reactive and inelastic processes that are relevant to combustion. One goal has been to understand long-range interactions, which remains a frontier area for theory and experiment. For radical-radical and radical-molecule systems, long-range interactions contain contributions from several PES's that become degenerate at large separation. Another goal has been the development of diagnostics and experimental methods that can be adopted by the combustion community.

Some Recent Results

Ultraviolet absorption spectra of H_2O , H_2S , H_2Se , and H_2Te have broad features (Fig. 1) that are assigned as transitions to the lowest lying electronically excited state. H_2Te , however, differs in that it has a low energy tail extending to almost 400 nm. This feature has never been assigned, nor has it even been discussed. It is almost certainly responsible for the light sensitivity of H_2Te , because the feature that peaks ~ 250 nm lies well below the pyrex cutoff. This long wavelength feature prompted us to suggest, in a DOE proposal, that H_2Te might be a source of tunable, fairly-monoenergetic H atoms having modest translational energies. As discussed below, this in fact turns out to be the case.

Hydrogen telluride is the heaviest of the group VI hydrides that can be synthesized by using straightforward methods. Its preparation and handling, however, require careful attention. Reports of its sensitivities to light, impurities (especially water), surfaces, etc. are legion; indeed, we have found that it decomposes at 77 K in the dark, yielding tellurium films and enough H_2 to rupture the vacuum line. It is also extremely toxic, *e.g.*, much more so than H_2S . These obstacles probably account for the fact that H_2Te — which in principle is an attractive prototype for examining relativistic effects in a theoretically and experimentally tractable molecule — has received little attention.

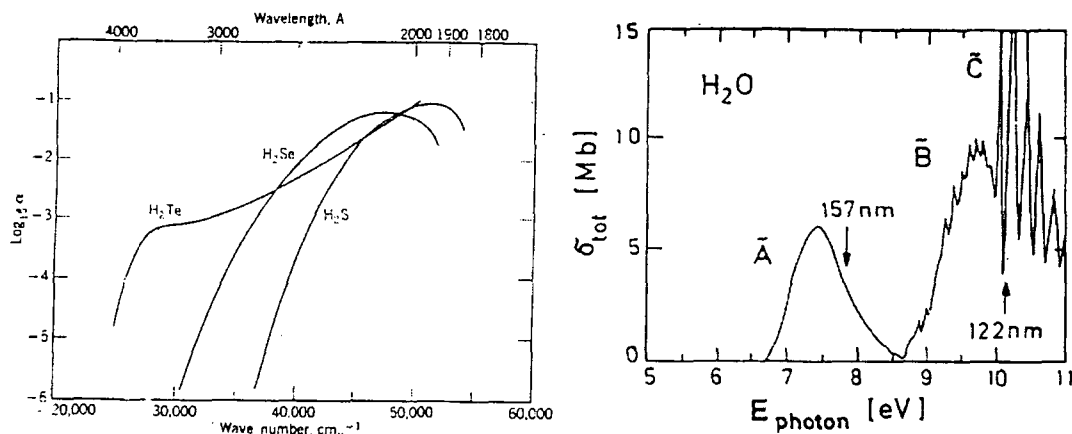


Figure 1. Low resolution UV spectra taken from Calvert and Pitts (left)¹ and Schinke (right).² At higher resolution (not shown), vibrational structure is evident. Note the long-wavelength tail for H_2Te .

Numerous photodissociation studies have been carried out in which parent molecules containing light atoms yield populations of product spin-orbit levels that can be rationalized in terms of the parent potential energy surfaces, including transitions between them.² Though the same is true when heavy atoms are involved, the energetics differ markedly. For example, the TeH $^2\Pi_{1/2}$ level lies 3815 cm^{-1} above the $^2\Pi_{3/2}$ ground state,³ and splittings of this order of magnitude are sufficiently large that it is reasonable to anticipate significant differences in the photochemistries of heavier molecules relative to their lighter counterparts. Namely, curve crossings at large H—TeH distances can influence reaction pathways much more than with the lighter systems, even changing qualitatively the photoexcitation and exit channel dynamics.

Sample Preparation

H_2Te samples were prepared in a collaborative effort between our group and that of an inorganic chemist in our department: Tom Flood and his students Paul Boothe and Patrick Vagner. Details will be published soon. The syntheses were usually carried out in the early evening and the H_2Te samples were transported to our building, where spectrophotometer traces were obtained and the HRTOF experiments (discussed below) were carried out. Samples decomposed rapidly, sometimes before the next morning. Clearly, H_2Te should be used shortly after its synthesis.

Ultraviolet Absorption Spectra

As mentioned above, freshly prepared samples were transported without delay to a Cary Series 50 spectrophotometer, where UV spectra were recorded. Figure 2(a) shows the main feature (peaked ~250 nm) as well as the long wavelength tail. In Fig. 2(b) the tail region is emphasized by using a higher concentration. This revealed — *to our great surprise* — what appears to be a low frequency (~300 cm^{-1}) vibrational progression at the end of the long wavelength tail. Note that this progression appears at energies that are close to that of the $^2\Pi_{1/2}$ excited spin-orbit level. This was our first clue that the $^2\Pi_{1/2}$ level might be important in the long wavelength photochemistry.

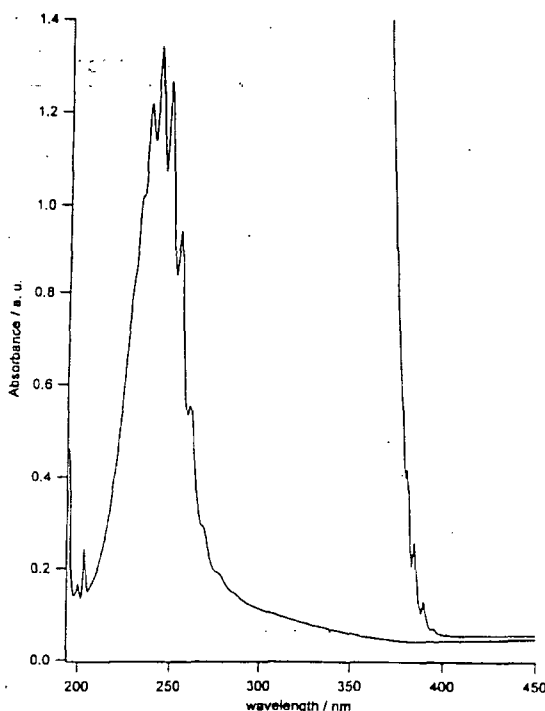


Figure 2. (left) Absorption spectrum showing the $^3A_2 \leftarrow ^1A_1$ vibrational progression. (right) A weak progression appears at the end of the long-wavelength tail.

Photodissociation Experiments

The photodissociation of H_2Te was studied by using high- n Rydberg time-of-flight (HRTOF) spectroscopy. With cold (*i.e.*, several K) parent molecules, the product c.m. translational energy distributions yield the corresponding TeH internal energy distributions. This method has been discussed in our previous papers. Currently, the sensitivity of the spectrometer is good and S/N has not been problematic. Figure 3 indicates the locations in the absorption spectra that are accessed by using 266 and 355 nm radiation. In each case, there is good S/N, because the low 355 nm absorption cross section is overcome easily by the high 355 nm fluence. The c.m. translational energy distribution for 355 nm is shown in Fig. 4; due to limited space, only the 355 nm result will be discussed here.

Both the distribution shown in Fig. 4 and the 266 nm result (not shown) yield a bond dissociation energy $D_0 = 22.800 \pm 100 \text{ cm}^{-1}$, which is, within the stated uncertainty, the same as the theoretical prediction of Balasubramanian and coworkers.⁴ The data also yield a ${}^2\Pi_{1/2} - {}^2\Pi_{3/2}$ separation of 3800 cm^{-1} , in agreement with the value of 3815 cm^{-1} obtained spectroscopically.³ All TeH rotational and vibrational excitations are easily fitted by using available spectroscopic constants. The high degree of spatial anisotropy is consistent with rapid dissociation. Many lumpy features in the spectrum are due to photolysis of the TeH photoproduct. The most remarkable effect seen in Fig. 4 is the high selectivity toward the ${}^2\Pi_{1/2}$ state. Only $\sim 10\%$ of the products are formed in the ${}^2\Pi_{3/2}$ ground state.

The translational energies of the H atoms, associated with the ${}^2\Pi_{1/2}$ channel are distributed as per the HTe $v=0$ rotational distribution. The $N=0$ level corresponds to $E_{\text{trans}} = 1560 \text{ cm}^{-1}$. The average rotational energy is $\sim 60 \text{ cm}^{-1}$, corresponding to $\langle E_{\text{trans}} \rangle \approx 1500 \text{ cm}^{-1}$. Because of the TeH rotations, this is not as monoenergetic as when H atoms are obtained by HX photolysis. The spread is, however, less than kT for room temperature samples. In molecular beam experiments, the large spatial anisotropy can be used to eliminate virtually all of the H atoms associated with the ${}^2\Pi_{3/2}$ channel.

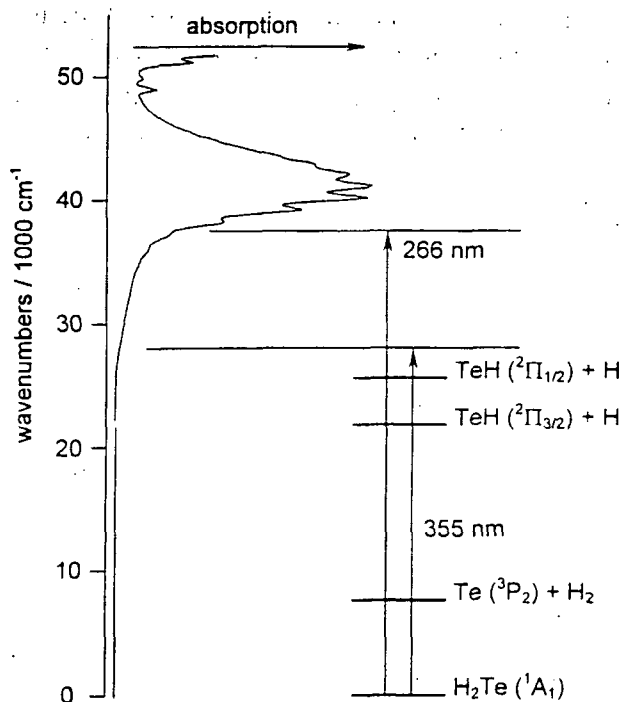


Figure 3. Diagram showing absorption spectrum and some product energy levels.

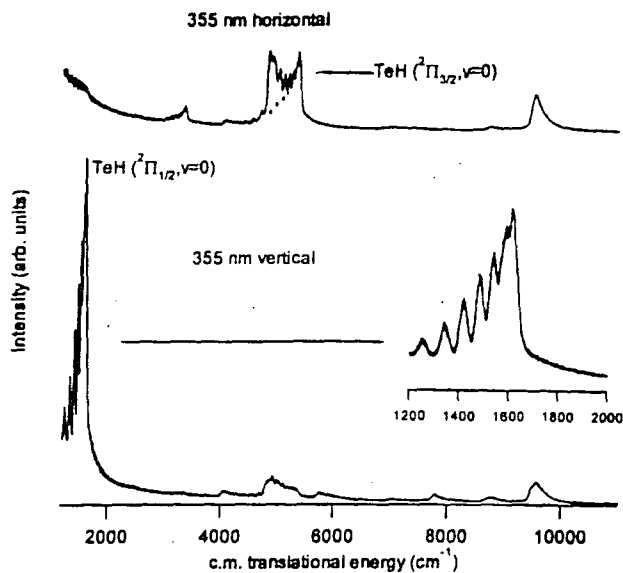


Figure 4. The labeled TeH features are from primary H_2Te photolysis.

This E_{trans} regime is important because it relates directly to combustion conditions, whereas numerous "hot H atom" reactions that have been studied to date have been carried out with significantly larger E_{trans} values. The E_{trans} values can, of course, be varied as per the photolysis wavelength. Note that high photolysis fluences can be used because the long wavelengths are benign toward most light reactant species. An interesting issue is the extent to which the trends observed at 355 nm can be extended to longer wavelengths. For example, at 365 nm, σ_{abs} is down by a factor of approximately 2, whereas the maximum E_{trans} value is 800 cm^{-1} . We predict that the $^2\Pi_{1/2}$ channel will be accessed at least as selectively as at 355 nm and the HTe rotational distribution will be narrower. If these predictions are borne out, H_2Te will be an excellent photolysis source for tunable energy H atoms from several hundred cm^{-1} to several thousand cm^{-1} , provided that adequate care is taken in its preparation and handling. This new H atom source will find applications in studies of combustion reactions.

We will examine these issues and continue to work on highly excited H_2O , including, above D_0 . The latter benefits from the arrival of a new excimer laser, after years of agony with an EMG 201.

References

1. J. Calvert and J. Pitts, *Photochemistry*, from C. Goodeve and N. Stein, *Trans. Far. Soc.* **1931**, 393.
2. R. Schinke, *Photodissociation Dynamics* (Cambridge University Press, 1993).
3. D. Gillett, J. P. Towle, M. Islam, J. M. Brown, *J. Mol. Spectrosc.* **163**, 459 (1994).
4. K. Sumathi and K. Balasubramanian, *J. Chem. Phys.* **92**, 6604 (1990).

DOE supported work

- Photoinitiated H_2CO unimolecular decomposition: accessing H + HCO products via S_0 and T_1 pathways, L.R. Valachovic, M.F. Tuchler, M. Dulligan, Th. Droz-Georget, M. Zyrianov, H. Reisler and C. Wittig. *J. Chem. Phys.* **112**, 2752 (2000).
- Intriguing near-ultraviolet photochemistry of H_2Te , J. Underwood, D. Chastaing, S. Lee, P. Boothe, P. Vagner, T. C. Flood, and C. Wittig, in preparation (2002).

Theoretical Studies of the Reactions and Spectroscopy of Radical Species Relevant to Combustion Reactions and Diagnostics

David R. Yarkony

Department of Chemistry, The Johns Hopkins University, Baltimore, MD 21218

yarkony@jhu.edu

Our research employs computational techniques to study spin-nonconserving and spin-conserving electronically nonadiabatic processes involving radical species that are relevant to combustion reactions and combustion diagnostics.

Conical Intersections and the spin-orbit interaction

Conical intersections play a key role in electronically nonadiabatic processes. For molecules with an odd number of electrons the spin-orbit interaction produces essential changes in the branching space and connectivity of points of conical intersection.¹ The dimension of the branching space, the space in which the conical topography is evinced, is η . In the nonrelativistic case, or when the molecule has an even number of electrons, η is 2. For molecules with an odd number of electrons the branching space is 5 dimensional ($\eta = 5$) in general, or 3 dimensional ($\eta = 3$) when C_s symmetry is present. As part of our DoE funded research we have used degenerate perturbation theory to extend a previous treatment of the $\eta = 3$ case² to the $\eta = 5$ case.³ Analytic representations of, the energy and of the derivative couplings, and a 'rigorous' diabatic basis near a conical intersection were obtained, providing valuable insights into the nature of this singular point.

As a result of this work the formalism for treating nonadiabatic processes involving the spin-orbit interaction in molecules with an odd number of electrons in terms of intersecting adiabatic potential energy surfaces (PESs) is now largely complete. This approach has proved enormously successful in the nonrelativistic case. Previously, in that case, guided by a perturbative analysis of their local topography, we used time dependent wave packets to analyze nuclear motion near conical intersections.⁴ The present results will enable us to extend this informative analysis to the $\eta = 5$ case. These capabilities together with our algorithm for locating $\eta = 3$ and 5 conical intersections⁵ will enable us to determine the prevalence, and significance for nuclear dynamics of, this class of conical intersections.

Photodissociation of CH₂OH

The hydroxymethyl radical (CH₂OH) and its geometrical isomer, the methoxy radical (CH₃O), both play important roles in atmospheric, combustion, CO/H₂ surface, and interstellar chemistry. Moreover, the hydroxymethyl radical is known to be a major link in the alkene photochemistry of polluted atmospheres. When the 3^2A state of D₂COH is excited broadened lines are observed and both D and H atoms are produced. When the 2^2A state is excited the spectrum is quite diffuse. These experimental observations in Hanna Reisler's laboratory at USC can be explained by $3^2A - 2^2A$ and $2^2A - 1^2A$ conical intersection seams.

In an article currently in press⁶ we showed that the $2^2A \leftarrow 1^2A$ excitation leads to rapid dissociation as a result of a seam of conical intersections connecting the 2^2A and 1^2A states. See Path2 below. The relevant region of the $2^2A - 1^2A$ seam of conical intersections occurs for R(O-

H) long and can lead to ground state $D_2CO + H$. Our calculations established the dissociative character of the 2^2A PES in the region where the wave function has 3s Rydberg character. This result is somewhat surprising in view of the fact that in this region the core of 3s Rydberg state is the bound cation H_2COH^+ .

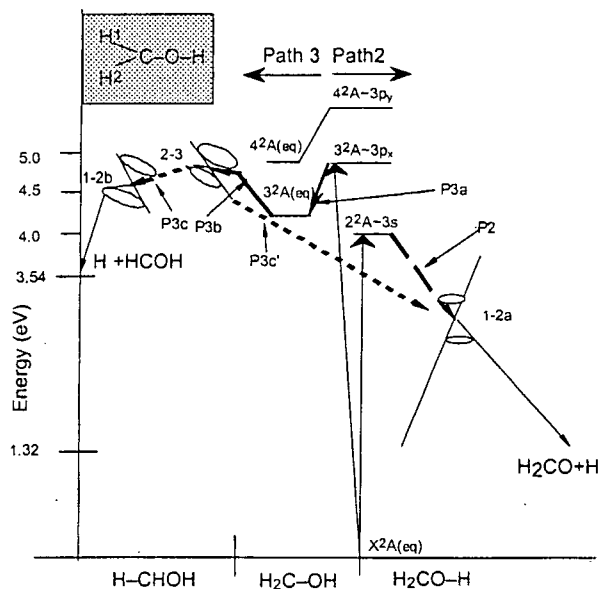


Figure 1 Pathways from $R_e(X^2A)$ on the 2^2A PES (Paths 2x) and, the 3^2A PES (Paths 3x) to the ground state

Decay pathways of the 3^2A state were also determined. Unlike the 2^2A state, the 3^2A state exhibits a local minimum which has $3p_x$ Rydberg character and a predicted adiabatic excitation energy of 4.16 eV. This state can decay radiationlessly to either $HCOH + H$ or $H_2CO + H$. The photo excited wave packet evolves on the 3^2A PES from $R^{eq,1}$ the ground state equilibrium geometry, via barrierless paths, to a portion of the $2^2A - 3^2A$ seam of conical intersection with large $R(H^2-C)$. See Paths 3a and 3b above. Conical intersections facilitate $3^2A - 2^2A$ radiationless decay. Once on the 2^2A PES paths exist to the region of the $1^2A - 2^2A$ seam of conical intersection noted above (Path 3C') and to a higher energy portion of the $1^2A - 2^2A$ seam of conical intersection (Path 3C) with large $R(H^2-C)$ leading to the ground state $HCOH + H$ channel.

Photodissociation of CH_2COH

The vinoxy radical (CH_2CHO), plays an important role in combustion chemistry, especially in reactions of oxygen atoms with olefins and has been studied experimentally in DoE supported laboratories.⁷ The X^2A'' ground state has C_s symmetry as do the two electronically excited states of interest the A^2A' state and the B^2A'' state ($T_e(B^2A'') = 27,786 \text{ cm}^{-1}$, See Fig. 2 below). Predissociation has been suggested to limit laser induced fluorescence from the B^2A'' state to less than $30,200 \text{ cm}^{-1}$ while the absorption spectrum extends to $35,700 \text{ cm}^{-1}$. Predissociation has also been suggested to limit the lifetime of the A^2A' state.

We have performed calculations at the multireference configuration interaction (MRCI) level in an effort determine the mechanism of the predissociations. A $1^2A - 2^2A$ seam of conical intersection is responsible for the A^2A' predissociation. A point, $R^{x,12}$, on that seam is pictured

below. This point of conical intersection has a coplanar structure quite similar to $R_c(A^2A')$, the equilibrium geometry of the A^2A' state (see Fig 2) and is only $\sim 2500\text{cm}^{-1}$ higher in energy.

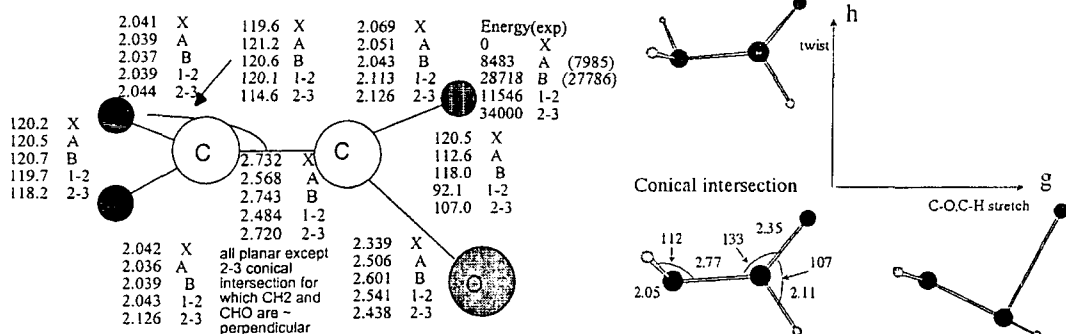


Figure 2: (Left) Geometry of points of conical intersection $R^{x,ij}$, $i,j=1-2, 3-4$ and $\sim R_c(j^2A')$, $j= X,A,B$
 Figure 3; (Right) Branching space for $R^{x,2,3}$

In this planar geometry the principal electron configuration, of the X^2A'' state is $\dots n^2 1\pi^2 2\pi$; of the A^2A' state is $\dots n 1\pi^2 2\pi^2$ (an $n \rightarrow 2\pi$ excitation); and of the B^2A'' state $\dots n^2 1\pi 2\pi^2$, (a $1\pi \rightarrow 2\pi$ excitation). Here n is a oxygen lone pair orbital, and $1\pi, 2\pi, 3\pi$ denote the delocalized molecular orbitals obtained from $2p_\pi$ orbitals on oxygen and the two carbons. It is relatively straightforward to characterize these electron configurations and hence the 1^2A-2^2A seam using MRCI wave functions.

The $2^2A - 3^2A$ seam of conical intersection is much more subtle. Its low energy portion occurs with the $\text{CH}_2 - \text{COH}$ dihedral angle near $\pi/2$. This twist destabilizes the π system. The electron configuration $\dots n 1\pi^2 2\pi 3\pi$ with its two (in this case nearly degenerate) spin-couplings becomes important and complicates determination of the 2^2A and 3^2A states near their intersection. To address this problem required a large MRCI expansion, 4783184 configuration state functions based on orbitals obtained from a flexible state-average MCSCF procedure in which as many as five states were averaged.

Fig. 2 gives a point, $R^{x,23}$ on the $2,3^2A$ seam of conical intersection. The $2,3^2A$ conical intersection does not produce ground state products. Rather the $2,3^2A$ conical intersection serves to orient the motion on the 2^2A PES reflecting the tendency of a conical intersection to route the molecule along the directions defining the branching space. These directions, \mathbf{g} and \mathbf{h} at $R^{x,2,3}$ are shown in Fig. 3. Our calculations demonstrate that molecules routed along \mathbf{h} can proceed downhill from $R^{x,23}$ to $R_c(2^2A)$. Starting from $R_c(2^2A)$ a nonadiabatic transition to the 1^2A state is possible through $R^{x,12}$ as discussed above. At $R^{x,23}$, which currently is only partially energy optimized, $E_{3^2A}(R_c(B^2A'')) - E_{3^2A}(R^{x,23}) \sim 0.7\text{eV}$ whereas the experimentally predicted onset of predissociation is $\sim 0.1\text{eV}$. We are currently investigating the implications of this result (see below).

The Future

In the absence of accessible conical intersections nonadiabatic transitions can occur through avoided intersections. To see if this is the case with the B state of the vinyoxy radical the energy of the minimum energy conical intersection must be reliably established. To this end the R -dependence of the energetics of the $2^2A - 3^2A$ seam of conical intersection is being considered.

If necessary the sensitivity of the energetics to the basis set and MRCI reference space will be considered. In the absence of low energy conical intersections we will locate avoided intersections and, using the corresponding derivative couplings, estimate their contribution to the predissociation.

The 1^2A-2^2A seam of conical intersection in CH_2OH is mechanistically significant in two distinct regions of nuclear coordinate space where the ground and first excited electronic states have $^2A''$ and $^2A'$ symmetry respectively. Thus as shown in our study of conical intersections in $HNCO$ ⁸ in these regions intersecting branches, or confluences, may exist. Portions of the 1^2A-2^2A and 2^2A-3^2A seams of conical intersection in the vinoxy radical may also exist exhibit confluences. The existence of confluences would have important consequences for nuclear dynamics.⁹ These issues will be considered in the upcoming grant period.

References

- 1 C. A. Mead, *J. Chem. Phys.* **70**, 2276 (1979).
- 2 S. Matsika and D. R. Yarkony, *J. Chem. Phys.* **116**, 2825 (2002).
- 3 S. Matsika and D. R. Yarkony, *J. Phys. Chem. A*, submitted (2002).
- 4 D. R. Yarkony, *J. Chem. Phys.* **114**, 2601 (2001).
- 5 S. Matsika and D. R. Yarkony, *J. Chem. Phys.* **115**, 2038 (2001).
- 6 B. C. Hoffman and D. R. Yarkony, *J. Chem. Phys.* to appear (2002).
- 7 D. L. Osborn, H. Choi, D. H. Mordant, R. T. Bise, D. M. Neumark, and C. M. Rohlfing, *J. Chem. Phys.* **106**, 3049 (1997); M. L. Morton, D. E. Szpunar, and L. J. Butler, *J. Chem. Phys.* **115**, 204 (2001).
- 8 D. R. Yarkony, *Molec. Phys.* **99**, 1463 (2001).
- 9 S. Matsika and D. R. Yarkony, *J. Phys. Chem. A* **106**, 2580 (2001).

PUBLICATIONS SUPPORTED BY DE-FG02-91ER14189: 2000 - present

- [1] *Vibronic Energies and the breakdown of the Born-Oppenheimer approximation in diatomic molecules: Adiabatic and Diabatic representations*
David R. Yarkony, in *Computational Molecular Spectroscopy*; Jensen, P.; Bunker, P., Eds.; J. Wiley, Chichester, 2000; p. 459-484.
- [2]^{††} The geometric phase effect. Perspective on: *Some Recent Developments in the Theory of Molecular Energy Levels*: by H. C. Longuet-Higgins [Adv. in Spec. 2, 429-472 (1961)].
David R. Yarkony, *Theoretical Chemistry Accts*, New century issue, **103**, 242-246 (2000).
- [3][†] *Conical intersections: The New Conventional Wisdom* – Feature Article,
D. R. Yarkony, *J. Phys. Chem. A* **105**, 6277-6293 (2001).
- [4] Conical Intersections and the Spin-Orbit Interaction, Spiridoula Matsika and David R. Yarkony, in *The Role of Degenerate States in Chemistry*, Advances in Chemical Physics, Michael Baer and Gert. D. Billing, eds, J. Wiley, New York, to appear.
- [5] *The Role of Conical Intersections in the Nonadiabatic Quenching of OH ($A^2\Sigma^+$) by Molecular Hydrogen*
Brian C. Hoffman and David R. Yarkony, *J. Chem. Phys.*, **113**, 10091 (2000)
- [6]^{††}. *Characterizing the Local Topology of Conical Intersections Using Orthogonality Constrained Parameters: Application to the internal conversion $S_1 \rightarrow S_0$*
David R. Yarkony, *J. Chem. Phys.* **114**, 2614 (2001)

- [7]^{††}. *Intersecting Conical Intersection Seams in Tetra atomic Molecules : The $S_1 - S_0$ Internal Conversion in HNCO*
David R. Yarkony, *Molec. Phys.* 99, 1463-1467 (2001).
- [8] *Photodissociation of the Hydroxymethyl Radical I. The Role of Conical Intersections in LineBroadening and Decomposition Pathways*
Brian C. Hoffman and David R. Yarkony, *J. Chem. Phys.* to appear.
- [9] *Spin-Orbit Coupling and Conical Intersection Seams in Molecules with an Odd Number of Electrons. IV: A perturbative determination of the electronic energies, derivative couplings and a rigorous diabatic representation near a conical intersection. The general case*
S. Matsika and D. R. Yarkony, *J. Phys. Chem A*, manuscript submitted (2002).

Laser Studies of the Chemistry and Spectroscopy Of Excited State Hydrocarbons

Timothy S. Zwier

Department of Chemistry, Purdue University, West Lafayette, IN 47907-1393
zwier@purdue.edu

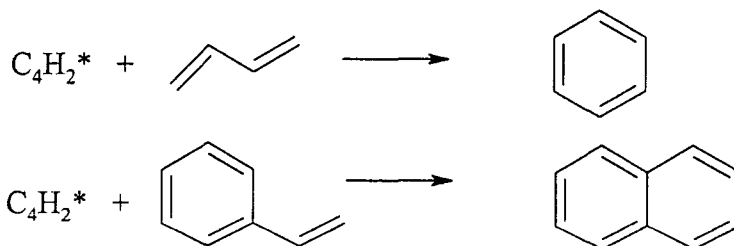
Program Definition/Scope

The objectives of this research program are to identify and spectroscopically characterize the primary products of reactions of electronically excited molecules with the hydrocarbons present in abundance in sooting flames. The molecules of current interest include diacetylene, vinylacetylene, butadiene, and various aromatic derivatives. The unusual soot-forming ability of these molecules when they are doped into flames suggests that they may contribute to the molecular chemistry important in moderate-temperature, sooting flames.¹ We seek to determine the structures, energies, and lifetimes of the triplet states of these molecules.^{2,3} Furthermore, the rich chemistry of the triplet states of diacetylene ($C_4H_2^*$) and vinylacetylene ($C_4H_4^*$) with other hydrocarbons also leads to products with unusual structures and unexplored spectroscopy, which we seek to characterize.⁴ Finally, we are interested in exploring the routes that lead to aromatics and aromatic derivatives in flames, employing isomer-specific excitation and detection.

Recent Progress

A. $C_4H_2^*$ chemistry and product spectroscopy

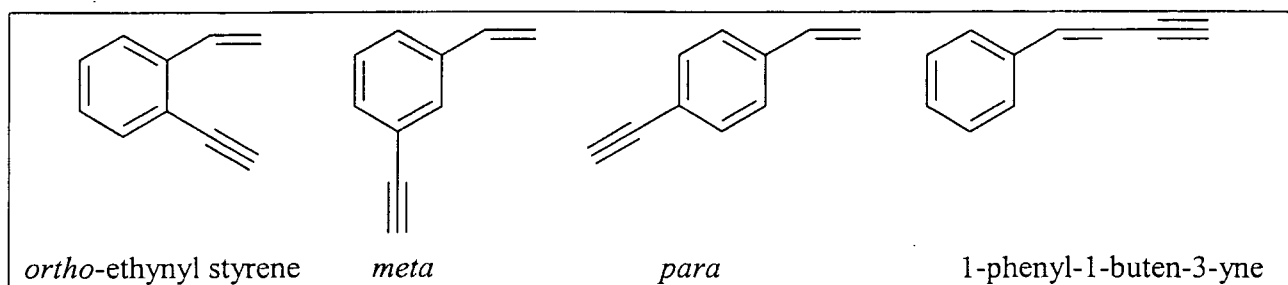
The reaction of metastable diacetylene with styrene has been studied in some detail because the structural similarity between styrene and 1,3-butadiene, highlighted below, suggested that naphthalene products might be formed.⁵



These studies of $C_4H_2^*$ chemistry utilize one tunable ultraviolet laser pulse to resonantly excite diacetylene to a singlet state from which intersystem crossing to the triplet manifold produces the metastable state responsible for the ultraviolet photochemistry. The high reactivity of $C_4H_2^*$ toward polymerization necessitates the use of a small reaction tube attached to our pulsed valve that limits reactive collisions to the first 20 microseconds following laser excitation. Reaction is initiated by the first UV laser pulse, but is quenched as the gas mixture expands from the tube into vacuum. VUV photoionization, resonant two-photon ionization (R2PI)/time-of-flight mass spectroscopy, and resonant ion-dip infrared spectroscopy (RIDIRS)⁶ are being used to detect, mass-analyze, and spectroscopically characterize the reaction products.

VUV photoionization studies showed that products with molecular formulae $C_{10}H_8$ and $C_{12}H_8$ were dominant products formed in the reaction. However, R2PI scans over the region of naphthalene's spectrum showed no detectable signs of naphthalene. Instead, R2PI scans in the 285-300 nm range showed well-resolved photoproduct transitions in the $C_{10}H_8$ mass channel.

UV-UV hole-burning was used to dissect the spectrum into two components, which were subsequently identified as *meta*-ethynyl styrene and 1-phenyl-1-buten-3-yne by comparison of the photochemical product spectrum with spectra of authentic samples.



The other ethynyl styrene isomers have not been unambiguously detected to date, but are anticipated to be present, based on earlier results from the $C_4H_2^* + \text{toluene}$ reaction.⁷ Their spectra are likely masked by transitions due to the other isomers. To test this, authentic samples of several $C_{10}H_6$ and $C_{10}H_8$ isomers have recently been synthesized, and we are presently recording R2PI spectra of these isomers in the ultraviolet and RIDIR spectra in the CH stretch region to obtain their spectral signatures under jet-cooled conditions.

B. Excited state spectroscopy

While the studies in the previous section had as their primary goal the determination of the major reaction pathways for $C_4H_2^*$ in its reactions with hydrocarbons, the present section describes experiments aimed at characterizing the excited states themselves. Our work has focused on the spectroscopy of the excited states of diacetylene and 1,3-butadiene.

1. Cavity ring-down spectroscopy of singlet-triplet transitions in C_4H_2 and 1,3-butadiene

Despite the growing body of knowledge about the chemistry of diacetylene triplet states, there is no experimental data on their structures, energies, vibrational frequencies, or lifetimes. As a first step in such characterization,² we recorded the first optical spectrum of the spin-forbidden $T_2 \leftarrow S_0$ transition in C_4H_2 using cavity ringdown spectroscopy in a meter-long, room temperature cell. Guided by the EELS spectrum of C_4H_2 from Michael Allan,⁸ we recorded a CRD spectrum in the lower-energy region of the $T_2 \leftarrow S_0$ transition. This spectrum has been published,² but is still largely unanalyzed, leaving open the important issue of the structure of the excited state. Motivated by the desire to analyze this spectrum in more detail, we have written and tested a program for calculating Franck-Condon factors for linear-bent transitions in polyatomics, using an algorithm recently developed by Prof. Kevin Lehmann of Princeton.⁹ Armed with the results of an extensive set of high-level PT2/ANO calculations on the structures and vibrational frequencies of the triplet excited states of C_4H_2 from Vila et al.,¹⁰ we have calculated Franck-Condon profiles for transitions to these states from the electronic ground state.⁹ The agreement with experiment is disappointing, suggesting the need either for higher level theory or (more likely) for a treatment of the bending levels that goes beyond the harmonic approximation. A manuscript detailing the analysis is being prepared.

We recently recorded and analyzed the analogous cavity ring-down spectrum of the $T_1 \leftarrow S_0$ transition in 1,3-butadiene, covering the 20,500 to 23,000 cm^{-1} region.³ 1,3-butadiene is the first member of the polyenes, which have interesting excited state structures and isomerization pathways. The $T_1 \leftarrow S_0$ spectrum, shown in **Figure 1**, is extremely weak (with a peak absorption cross section of only $2 \times 10^{-26} \text{ cm}^2/\text{molecule}$). Resolved vibrational structure and partially resolved rotational structure have been observed for the first time in the gas phase. The vibronic structure is well-fit by Franck-Condon calculations to a planar T_1 state, despite the fact that the highest level calculations show a barrier of only $\sim 100 \text{ cm}^{-1}$ separating it from a lower-energy twisted C_s minimum. We have modeled the two-dimensional torsional potential energy surface involving these minima, and find that a shallow minimum at the planar configuration with a barrier of only 100 cm^{-1} is sufficient to localize the first couple of torsional energy levels, giving the appearance of a harmonic Franck-Condon profile, despite the small barrier to twisting.

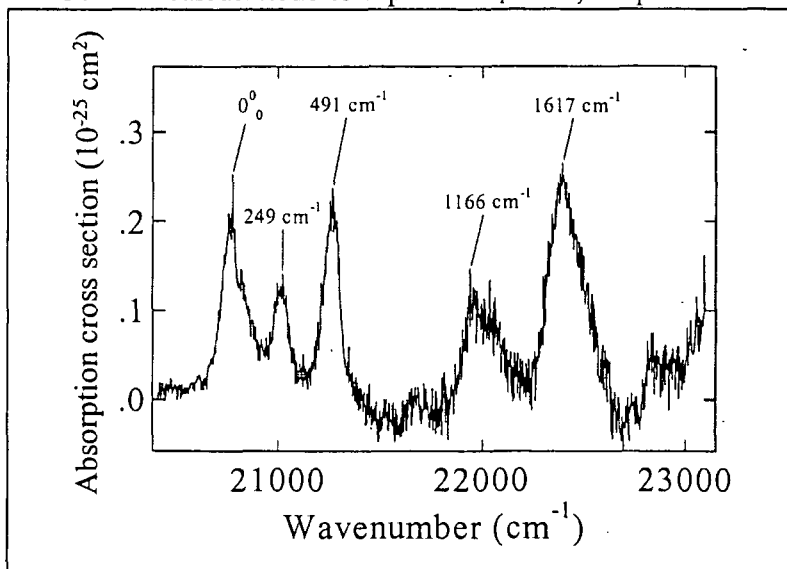


Figure 1: Cavity ring-down spectrum of the $T_1 \leftarrow S_0$ spectrum of 1,3-butadiene.

2. R2PI Photoelectron Spectroscopy of C_4H_2

The reactions of metastable diacetylene described in Section A are initiated by laser excitation of vibronic levels in the $^1\Delta_u$ state, followed by fast intersystem crossing to the triplet manifold. Unfortunately, despite considerable past effort, firm assignments are still not available for many of these bands, partly because the vibronic bands are inherently broad, and partly because the levels responsible for much of the vibronic activity are also Renner-Teller active, and thus show no regular progressions.¹¹ In an effort to improve this situation, we have collaborated with Dr. Stephen T. Pratt at Argonne to record photoelectron spectra following one-photon resonant, two-photon ionization of C_4H_2 via a number of intermediate vibronic levels of the $^1\Delta_u$ state.¹² Most of these photoelectron spectra show long progressions in what appear to be low frequency bending vibrations. At energies just above the ionization threshold, the observed progressions can be understood in terms of excitation of a single Renner-Teller active mode in the ion, with Renner-Teller parameters similar to those of the ν_4^+ trans-bending mode in the ground state acetylene cation.

Future Plans

Our primary focus over the past three years has been on the spectroscopy and chemistry of the excited states of diacetylene (C_4H_2). The photochemical results have particularly highlighted the need for and challenge associated with isomer-specific detection. The methods used in our studies have unusual power in this respect, and the continued utilization and development of such methods form a focus of the work proposed for the coming year. As a

result, we propose the application of these methods to a detailed, isomer-specific study of the C₆H₆ potential energy surface connecting two propargyl radicals to benzene. This will entail the synthesis of several of the C₆H₆ isomers that are isomers of benzene. Selective photoexcitation of these isomers under the 'limited collision' conditions of the reaction tube will be carried out, focusing on isomer-specific product detection. In addition, we will begin an analogous set of studies on a series of di-substituted benzenes that are interesting in their own right as likely intermediates on the way to naphthalene and its derivatives.

- 1) McEnally, C. S.; Pfefferle, L. D.; Robinson, A. G.; Zwier, T. S. *Combustion and Flame* **2000**, *123*, 344-357.
- 2) Hagemester, F. C.; Arrington, C. A.; Giles, B. J.; Quimpo, B.; Zhang, L.; Zwier, T. S. *Cavity Ringdown methods for studying intramolecular and intermolecular dynamics*; Busch, K. J. and Busch, M. A., Ed.; ACS Symposium Series 720, 1999, pp 210-232.
- 3) Robinson, A. G.; Winter, P. R.; Zwier, T. S. **in press**.
- 4) Arrington, C. A.; Ramos, C.; Robinson, A. D.; Zwier, T. S. *J. Phys. Chem. A* **1999**, *103*, 1294-1299.
- 5) Robinson, A. G.; Paul R, W.; Zwier, T. S. **submitted**.
- 6) Zwier, T. S. *J. Phys. Chem. A* **2001**, *105*, 8827-8839.
- 7) Robinson, A. G.; Winter, P. R.; Ramos, C.; Zwier, T. S. *J. Phys. Chem. A* **2000**, *104*, 10312-10320.
- 8) Allan, M. J. *J. Chem. Phys.* **1984**, *80*, 6020.
- 9) Winter, P. R.; Lehmann, K. K.; Zwier, T. S. **in preparation**.
- 10) Vila, F.; Borowski, P.; Jordan, K. D. *J. Phys. Chem. A* **2000**, *104*, 9009-9016.
- 11) Bandy, R. E.; Lakshminarayan, C.; Zwier, T. S. *J. Phys. Chem.* **1992**, *96*, 5337-5343.
- 12) Ramos, C.; Winter, P. R.; Zwier, T. S.; Pratt, S. T. *J. Chem. Phys.* **2002**, *116*, 4011.

Publications acknowledging DOE support, 2000-present:

Allison G. Robinson, Paul R. Winter, Christopher Ramos, and Timothy S. Zwier, "Ultraviolet Photochemistry of Diacetylene: Reactions with Benzene and Toluene", *J. Phys. Chem. A* **104**, 10312-10320 (2000).

Charles S. McEnally, Allison G. Robinson, Lisa D. Pfefferle, and Timothy S. Zwier, "Aromatic Hydrocarbon Formation in Nonpremixed Flames Doped with Diacetylene, Vinylacetylene, and Other Hydrocarbons: Evidence for Pathways Involving C₄ Species", *Combustion and Flame* **123**, 344-357 (2000).

C. Ramos, Paul R. Winter, Timothy S. Zwier, and Stephen T. Pratt, "Photoelectron Spectroscopy via the 1¹Δ_g state of Diacetylene", *J. Chem. Phys.* **116**, 4011 (2002).

Allison G. Robinson, Paul R. Winter, and Timothy S. Zwier, "The singlet-triplet spectroscopy of 1,3-butadiene using cavity ring-down spectroscopy", *J. Chem. Phys.* (in press). To appear in 08 May 2002 issue.

Allison G. Robinson, Paul R. Winter, and Timothy S. Zwier, "The Ultraviolet Photochemistry of Diacetylene with Styrene", *J. Phys. Chem. A* (submitted).

Participants

Dr. Musa Ahmed
Lawrence Berkeley Laboratory
One Cyclotron Road
Berkeley, CA 94720
mahmed@lbl.gov

Dr. Sarah W. Allendorf
Combustion Research Facility
Mail Stop 9055
Sandia National Laboratories
PO Box 969
Livermore, California 94551-0969
Phone: 925.294.3379
swallen@sandia.gov

Dr. William T. Ashurst
Combustion Research Facility
MS9051
Sandia National Laboratories
Livermore, California 94551-0969
Phone: 925.294.2274
ashurs@ca.sandia.gov

Prof. Tomas Baer
Department of Chemistry
University of North Carolina
Chapel Hill, North Carolina 27599-3290
Phone: 919.962.1580
baer@unc.edu

Prof. Richard Bersohn
Department of Chemistry
Columbia University
3000 Broadway
New York, New York 10027
Phone: (212)854-2192
rb18@columbia.edu

Prof. Joel M. Bowman
Department of Chemistry
Emory University
1515 Pierce Drive
Atlanta, Georgia 30322
Phone: (404)727-6590
bowman@euch4e.chem.emory.edu

Professor Kenneth Brezinsky
Chemical Engineering Dept.
810 S. Clinton
The University of Illinois at Chicago
Chicago, Illinois 60607-7022
Phone: (312)996-9430
kenbrez@uic.edu

Dr. Nancy Brown
Environmental Technologies
Division
Advanced Energy Technology
Lawrence Berkeley National
Laboratory MS 51-208
One Cyclotron Road
Berkeley, California 94720
Phone: (510)486-4241
njbrown@lbl.gov

Prof. Laurie J. Butler
The James Franck Institute
The University of Chicago
5640 S. Ellis Avenue
Chicago, Illinois 60637
Phone: 773.702.7206
ljb4@midway.uchicago.edu

Dr. Robert W. Carling
MS 9054
Combustion Research Facility
Sandia National Laboratories
Livermore, California 94551-0969
Phone: 925.294.2206
rwcari@sandia.gov

Prof. Barry K. Carpenter
Department of Chemistry &
Chemical Biology
Cornell University
Ithaca, NY 14853-1301
Phone: (607)255-3826
bkcl1@cornell.edu

Dr. David W. Chandler
Combustion Research Facility
MS 9054
Sandia National Laboratories
Livermore, California 94551-0969
Phone: 925.294.3132
chandler@ca.sandia.gov

Prof. Dr. Peter Chen
Laboratorium für Organische
Chemie
ETH-Honggerberg, HCI G 209
Universitätstrasse 16
CH-8093 Zürich SWITZERLAND
Phone: 41.1.632 4788
chen@org.chem.ethz.ch

Dr. Robert K. Cheng
Energy and Environment Division
University of California
Lawrence Berkeley National
Laboratory
One Cyclotron Road
Berkeley, California 94720
Phone: 510.486.5438
rkcheng@lbl.gov

Prof. Robert E. Continetti
Department of Chemistry and
Biochemistry, 0340
University of California, San Diego
9500 Gilman Drive
La Jolla, CA 92093-0340
Phone: 858.534.5559
rcontinetti@ucsd.edu

Prof. Terrill A. Cool
College of Engineering
School of Applied & Engineering
Physics
Cornell University
Ithaca, New York 14853-1301
Phone: 607.255.4191
tac13@cornell.edu

Prof. F. Fleming Crim
Department of Chemistry
University of Wisconsin
1101 University Avenue
Madison, Wisconsin 53706
Phone: (608)263-7364
fcrim@chem.wisc.edu

Prof. Robert F. Curl, Jr.
Department of Chemistry
Rice University
P.O. Box 1892
Houston, Texas 77005
Phone: (713)348-4816
rfcurl@rice.edu

Prof. Hai-Lung Dai
Department of Chemistry
University of Pennsylvania
Philadelphia, Pennsylvania 19104-6323
Phone: 215.898.5077
dai@sas.upenn.edu

Prof. H. Floyd Davis
Department of Chemistry &
Chemical Biology
Baker Laboratory
Cornell University
Ithaca, New York 14853-1301
Phone: 607-255-0014
hfd1@cornell.edu

Dr. Michael J. Davis
Chemistry Division
Argonne National Laboratory
9700 South Cass Avenue
Argonne, Illinois 60439
Phone: 630.252.4802
davis@tcg.anl.gov

Prof. Frederick L. Dryer
Department of Mechanical &
Aerospace Engineering
Princeton University
Princeton, New Jersey 08544
Phone: (609)258-5206
fldryer@princeton.edu

Prof. G. Barney Ellison
Department of Chemistry
University of Colorado
Boulder, Colorado 80309-0215
Phone: 303.492.8603
barney@jila.colorado.edu

Prof. Kent M. Ervin
Department of Chemistry/216
College of Arts and Sciences
University of Nevada, Reno
Reno, Nevada 89557-0020
Phone: 775.784.6676
ervin@chem.unr.edu

Prof. James M. Farrar
Department of Chemistry
University of Rochester
Rochester, New York 14627
Phone: 585.276.5834
farrar@chem.rochester.edu

Prof. Robert W. Field
Department of Chemistry
Room 6-219
Massachusetts Institute of
Technology
77 Massachusetts Ave.
Cambridge, Massachusetts 02139
Phone: 617.253.1489
rwfield@mit.edu

Prof. George Flynn
Department of Chemistry
Mail Stop 3109
Columbia University
3000 Broadway
New York, New York 10027
Phone: (212)854-4162
flynn@chem.columbia.edu

Dr. Christopher Fockenber
Chemistry Department
Building 555A
Brookhaven National Laboratory
Upton, NY 11973-5000
Phone: 631.344.4372
fknberg@bnl.gov

Prof. Michael Frenklach
Department of Mechanical
Engineering
Lawrence Berkeley National
Laboratory
University of California at Berkeley
Berkeley, California 94720-1740
Phone: (510)643-1676
myf@me.berkeley.edu

Prof. Graham P. Glass
Department of Chemistry
Rice University, MS 60
6100 Main St.
Houston, Texas 77251
Phone: 713.348.3285
gglass@rice.edu

Prof. Edward R. Grant
Department of Chemistry
Purdue University
West Lafayette, Indiana 47907
Phone: (765)494-9006
edgrant@purdue.edu

Dr. Stephen K. Gray
Chemistry Division
Argonne National Laboratory
9700 South Cass Ave.
Argonne, Illinois 60439
Phone: 630.252.3594
gray@tcg.anl.gov

Prof. William H. Green, Jr.
Department of Chemical
Engineering, 66-448
Massachusetts Institute of
Technology
77 Massachusetts Ave.
Cambridge, Massachusetts 02139
Phone: 617.253.4580
whgreen@mit.edu

Dr. Gregory E. Hall
Chemistry Department
Brookhaven National Laboratory
Upton, New York 11973
Phone: 631.344.4376
gehall@bnl.gov

Prof. Ronald K. Hanson
Department of Mechanical
Engineering
Stanford University
Stanford, California 94305
Phone: 650.723.4023
hanson@me.stanford.edu

Dr. Lawrence Harding
Chemistry Division
Argonne National Laboratory
9700 South Cass Avenue
Argonne, Illinois 60439
Phone: (630)252-3591
harding@anl.gov

Dr. Carl C. Hayden
Combustion Research Facility
MS 9055
Sandia National Laboratories
Livermore, California 94551-0969
Phone: 925.294.2298
cchayde@sandia.gov

Prof. Martin Head-Gordon
Department of Chemistry
University of California at Berkeley
Berkeley, California 94720
Phone: 510.642.5957
mhg@cchem.berkeley.edu

Prof. John Hershberger
Department of Chemistry
North Dakota State University
Fargo, ND 58105-5516
Phone: (701)231-8225
john.hershberger@ndsu.nodak.edu

Dr. Jan P. Hessler
Chemistry Division
Argonne National Laboratory
9700 South Cass Avenue
Argonne, Illinois 60439
Phone: (630)252-3717
hessler@anl.gov

Prof. Paul L. Houston
Department of Chemistry
122 Baker Laboratory
Cornell University
Ithaca, New York 14853-1301
Phone: 607.255.4303
plh2@cornell.edu

Prof. Jack B. Howard
Department of Chemical
Engineering
Massachusetts Institute of
Technology
Cambridge, Massachusetts 02139
Phone: (617)253-4574
jbhoward@mit.edu

Dr. Wen Hsu
Combustion Research Facility
MS9056
Sandia National Laboratories
Livermore, CA 94551
Phone: (925)294-2379

Prof. Philip M. Johnson
Department of Chemistry
State University of New York
at Stony Brook
Stony Brook, New York 11794
Phone: (631)632-7912
philip.johnson@sunysb.edu

Prof. Michael E. Kellman
Department of Chemistry
University of Oregon
Eugene, Oregon 97403
Phone: 541.346.4196
kellman@oregon.uoregon.edu

Prof. John Kiefer
Department of Chemical
Engineering
810 S. Clinton
University of Illinois at Chicago
Chicago, Illinois 60607
Phone: (312)996-5711
john.h.kiefer@uic.edu

Dr. William H. Kirchoff
Division of Chemical Sciences,
Geosciences and Biosciences SC-14
Office of Basic Energy Sciences
U.S. Department of Energy
19901 Germantown Road
Germantown MD 20874-1290
Phone: (301)903-5809
william.kirchoff@science.doe.gov

Dr. Stephen J. Klippenstein
Combustion Research Facility
MS 9055
Sandia National Laboratories
Livermore, California 94551-0969
Phone: (925)294-2289
SJKLIPP@sandia.gov

Dr. Allan H. Laufer
Division of Chemical Sciences,
Geosciences and Biosciences SC-14
Office of Basic Energy Sciences
U.S. Department of Energy
19901 Germantown Road
Germantown MD 20874-1290
Phone: 301.903.4417
allan.laufer@science.doc.gov

Prof. Stephen R. Leone
Department of Chemistry
University of Colorado
440 UCB
Boulder, Colorado 80309
Phone: 303.492.5128
srl@jila.colorado.edu

Prof. Marsha I. Lester
Department of Chemistry
University of Pennsylvania
231 South 34th Street
Philadelphia, Pennsylvania 19104-
6323
Phone: (215)898-4640
milester@sas.upenn.edu

Prof. William A. Lester, Jr.
Department of Chemistry
University of California at Berkeley
Berkeley, California 94720-1460
Phone: 510.643.9590
walester@cchem.berkeley.edu

Prof. John C. Light
The James Franck Institute
The University of Chicago
5640 S. Ellis Avenue
Chicago, Illinois 60637
Phone: 773.702.7197
j-light@uchicago.edu

Prof. Ming-Chang Lin
Department of Chemistry
Emory University
1515 Pierce Drive
Atlanta, Georgia 30322
Phone: (404)727-2825
chemmcl@emory.edu

Prof. Robert P. Lucht
Department of Mechanical
Engineering
323 Engineering/Physics Building
Texas A&M University
3123 TAMU
College Station, TX 77843-3123
Phone: 979.862.2623
rlucht@mengr.tamu.edu

Dr. R. Glen Macdonald
Chemistry Division
Argonne National Laboratory
9700 South Cass Avenue
Argonne, Illinois 60439
Phone: (630)252-7742
rgmacdonald@anl.gov

Dr. Andrew McIlroy
Combustion Research Facility
MS 9055
Sandia National Laboratories
Livermore, California 94551-0969
Phone: 925.294.3054
amcrlr@sandia.gov

Dr. William J. McLean
Combustion Research Facility
MS9054
Sandia National Laboratories
Livermore, California 94551-0969
Phone: (925)294-2687
wjmclea@sandia.gov

Dr. Joe V. Michael
Chemistry Division
Argonne National Laboratory
9700 South Cass Avenue
Argonne, Illinois 60439
Phone: (630)252-3171
michael@anlchm.chm.anl.gov

Dr. Hope A. Michelsen
Combustion Research Facility
M/S 9054
Sandia National Laboratories
Livermore, CA 94551
Phone: 925.294.2335
hamiche@sandia.gov

Dr. James A. Miller
Combustion Research Facility
MS-9055
Sandia National Laboratories
Livermore, California 94551-0969
Phone: 925.294.2759
jamille@ca.sandia.gov

Prof. Terry A. Miller
Department of Chemistry
Ohio State University
140 West 18th Avenue
Columbus, Ohio 43210
Phone: 614.292.2569
tamiller+@osu.edu

Prof. William H. Miller
Department of Chemistry
University of California at Berkeley
Berkeley, California 94720
Phone: (510)642-0653
miller@cchem.berkeley.edu

Dr. David Moncrieff
Supercomputer Comp. Res. Inst.
466 Science Center Library
Florida State University
Tallahassee, Florida 32306-4102
Phone: 850.644.4885
moncrieff@csit.fsu.edu

Prof. C. Bradley Moore
Office of Research
208 Bricker Hall
Ohio State University
190 N. Oval Mall
Columbus, Ohio 43210
Phone: 614.292.1582
moore.1@osu.edu

Dr. James Muckerman
Chemistry Department
Brookhaven National Laboratory
Upton, NY 11973
Phone: 631.344.4368
muckerma@bnl.gov

Dr. Habib N. Najm
Combustion Research Facility
MS9051
Sandia National Laboratories
Livermore, California 94551-0969
Phone: 925.294.2054
hnnajm@ca.sandia.gov

Prof. Daniel M. Neumark
Department of Chemistry
University of California at Berkeley
Berkeley, California 94720
Phone: 510.642.3502
neumark@cchem.berkeley.edu

Prof. Cheuk-Yiu Ng
Department of Chemistry
One Shields Avenue
University of California at Davis
Davis, CA 95616
Phone: (530)754-9645
cyng@chem.ucdavis.edu

Dr. David L. Osborn
Combustion Research Facility
MS 9055
Sandia National Laboratories
Livermore, California 94551-0969
Phone: 925-294-4622
dlosbor@sandia.gov

Prof. David S. Perry
Department of Chemistry
University of Akron
Akron, Ohio 44325
Phone: 330.972.6825
dperry@uakron.edu

Prof. Robert W. Pitz
Department of Mechanical
Engineering
Vanderbilt University
Box 1592, Station B
Nashville, Tennessee 37235
Phone: 615.322.0209
robert.w.pitz@vanderbilt.edu

Prof. Stephen B. Pope
Department of Mechanical and
Aerospace Engineering
Cornell University
106 Upson Hall
Ithaca, New York 14853
Phone: (607)255-4314
pope@mae.cornell.edu

Dr. Stephen Pratt
Chemistry Division
Argonne National Laboratory
9700 South Cass Avenue
Argonne, Illinois 60439
Phone: 630.252.4199
spratt@anl.gov

Dr. Jack M. Preses
Chemistry Department
Brookhaven National Laboratory
Upton, New York 11973
Phone: 631.344.4371
preses@bnl.gov

Prof. Herschel A. Rabitz
Department of Chemistry
Princeton University
Princeton, New Jersey 08544
Phone: (609)258-3917
hrabitz@princeton.edu

Dr. Larry A. Rahn
Combustion Research Facility
MS 9056
Sandia National Laboratories
Livermore, California 94551-0969
Phone: 925.294.2091
rahn@sandia.gov

Prof. Hanna Reisler
Department of Chemistry
University of Southern California
Los Angeles, California 90089-
0482
Phone: (213)740-7071
reisler@usc.edu

Dr. Branko Ruscic
Chemistry Division
Argonne National Laboratory
9700 South Cass Avenue
Argonne, Illinois 60439
Phone: 630.252.4079
ruscic@anl.gov

Prof. Henry Frederick Schaefer III
Department of Chemistry
University of Georgia
Athens, Georgia 30602
Phone: (706)542-2067
hfsiii@arches.uga.edu

Dr. Trevor Sears
Chemistry Department
Brookhaven National Laboratory
Upton, New York 11973
Phone: 631.344.4374
sears@bnl.gov

Dr. Thomas B. Settersten
Combustion Research Facility
MS 9056
Sandia National Laboratories
Livermore, California 94551-0969
Phone: 925.294.4701
tbsette@sandia.gov

Dr. Ron Shepard
Chemistry Division
Argonne National Laboratory
9700 South Cass Avenue
Argonne, Illinois 60439
Phone: 630.252.3584
shepard@tcg.anl.gov

Prof. Volker Sick
2202 G.G. Brown Building
Department of Mechanical
Engineering
University of Michigan
2350 Hayward Street
Ann Arbor, Michigan 48109-2125
Phone: 734.647.9607
vsick@umich.edu

Prof. Irene Slagle
Department of Chemistry
The Catholic University of America
Michigan Avenue at 7th Street, N.E.
Washington, D.C. 20064
Phone: (202)319-5384
slagle@cua.edu

Prof. Mitchell Smooke
Department of Mechanical
Engineering
Yale University
P.O. Box 208284
New Haven, Connecticut 06520-
8284
Phone: (203)432-4344
mitchell.smooke@yale.edu

Dr. Walter Stevens
Division of Chemical Sciences,
Geosciences and Biosciences SC-14
Office of Basic Energy Sciences
U.S. Department of Energy
19901 Germantown Road
Germantown MD 20874-1290
Phone: (301)903-2046
walter.stevens@science.doe.gov

Prof. Arthur G. Suits
Department of Chemistry
State University of New York
at Stony Brook
Stony Brook, NY 11794
Phone: 631.632.1702
arthur.suits@sunysb.edu

Dr. Craig Taatjes
Combustion Research Facility
MS 9055
Sandia National Laboratories
Livermore, California 94551-0969
Phone: 925.294.2764
cataatj@sandia.gov

Ms. Karen Talamini
Division of Chemical Sciences,
Geosciences and Biosciences SC-14
Office of Basic Energy Sciences
U.S. Department of Energy
19901 Germantown Road
Germantown MD 20874-1290
Phone: 301.903.4563
karen.talamini@science.doe.gov

Prof. Howard S. Taylor
Department of Chemistry
University of Southern California
Los Angeles, California
Phone: 213.740.4112
taylor@usc.edu

Prof. Donald G. Truhlar
Department of Chemistry
139 Smith Hall
University of Minnesota
207 Pleasant St. SE
Minneapolis, Minnesota 55455
Phone: (612)624-7555
truhlar@umn.edu

Dr. Wing Tsang
Chemical Kinetics Division
Center for Chemical Technology
A147 Chemistry Building
Natl. Inst. of Standards and
Technology
Gaithersburg, Maryland 20899
Phone: (301)975-2507
wing.tsang@nist.gov

Dr. Frank P. Tully
Division of Chemical Sciences,
Geosciences and Biosciences SC-14
Office of Basic Energy Sciences
U.S. Department of Energy
19901 Germantown Road
Germantown MD 20874-1290
Phone: (301)903-5998
frank.tully@science.doe.gov

Prof. James J. Valentini
Department of Chemistry
Columbia University
3000 Broadway, MC 3120
New York, New York 10027
Phone: (212)854-7590
jjv1@chem.columbia.edu

Dr. Albert F. Wagner
Chemistry Division
Argonne National Laboratory
9700 South Cass Avenue
Argonne, Illinois 60439
Phone: (630)252-3597
wagner@tcg.anl.gov

Dr. Charles K. Westbrook
Division of Computational Physics.
Lawrence Livermore National
Laboratory
P. O. Box 808, L-091
Livermore, California 94550
Phone: 925.422.4108
westbrook1@llnl.gov

Prof. Phillip R. Westmoreland
Department of Chemical Engineering
University of Massachusetts
Amherst, Massachusetts 01003
Phone: (413)545-1750
westm@ecs.umass.edu

Dr. Michael G. White
Department of Chemistry
Brookhaven National Laboratory
Upton, New York 11973
Phone: 631.344.4345
mgwhite@bnl.gov

Prof. Curt Wittig
Department of Chemistry
University of Southern California
Los Angeles, California 90089-0484
Phone: (213)740-7368
wittig@usc.edu

Prof. David R. Yarkony
Department of Chemistry
Johns Hopkins University
3400 N. Charles Street
Baltimore, Maryland 21218
Phone: 410.516.4663
yarkony@jhu.edu

Prof. Timothy S. Zwier
Department of Chemistry
Purdue University
West Lafayette, Indiana 47907
Phone: (765)494-5278
zwier@purdue.edu

Author Index

Ashurst, W.T.....1	Green, Jr., W.H.128	Osborn, D.L.253
Baer, T.....5	Hall, G.E.132	Perry, D.S.....257
Barlow, R.S.....9	Hanson, R.K.....136	Pitz, R.W.....261
Bersohn, R.....13	Harding, L.B.140	Pitz, W.J.....331
Beuhler, R.J.....339	Hayden, C.144	Pope, S.B.....265
Bowman, C.T.....136	Head-Gordon, M.....148	Pratt, S.T.269
Bowman, J.M.....17	Hershberger, J.F.....152	Preses, J.M.108
Brezinsky, K.21	Hessler, J.P.....156	Rabitz, H.273
Brown, N.J.25	Ho, T.S.273	Reddy, R.312
Butler, L.J.....29	Houston, P.L.160	Reisler, H.277
Carpenter, B.K.33	Howard, J.B.164	Richter, H.....164
Chandler, D.W.37	Im, H.G.312	Ruscic, B.281
Chastaing, D.....342	Johnson, P.M.....168	Rutland, C.J.....312
Chen, J.H.....312, 41	Kellman, M.E.....171	Sanielevici, S.....312
Cheng, R.K.....45	Kerstein, A.R.1	Schaefer III, H.F.285
Cioslowski, J.....49	Kiefer, J.H.....175	Sears, T.J.....132
Continetti, R.E.53	Klippenstein, S.J.179	Settersten, T.A.289
Cool, T.A.57	Lee, S.342	Shepard, R.....293
Crim, F.F.....61	Leone, S.R.....183	Sick, V.....261
Curl Jr., R.F.....64	Lester, M.I.....187	Silbey, R.J.....100
Dai, H.L.68	Lester, Jr., W.A.....191	Smooke, M.D.....297
Davis, H.F.....72	Light, J.C.....195	Slagle, I.R.....301
Davis, M.J.75	Lin, M.C.....199	Suits, A.G.....132
Drake, M.C.....261	Long, M.B.....297	Taatjes, C.A.305
Dryer, F.L.....79	Lucht, R.P.203	Talbot, L.....45
Echekki, T.41	Macdonald, R.G.....207	Taylor, H.S.....309
Ellison, G.B.....83	Mason, S.41	Tranter, R.S.....175
Ervin, K.M.88	McIlroy, A.....211	Trouve, A.312
Fansler, T.D.261	Michael, J.V.....215	Truhlar, D.G.....315
Farrar, J.M.....92	Michelsen, H.A.219	Tsang, W.319
Felker, P.M.....96	Miller, J.A.223	Howard, J.B.164
Field, R.W.....100	Miller, T.A.227	Underwood, J.342
Flynn, G.104	Miller, W.H.....231	Wagner, A.F.....327
Fockenberg, C.....108	Moncrieff, D.49	Westbrook, C.K.331
Frank, J.H.....112	Moore, C.B.....235	Westmoreland, P.R.336
Frenklach, M.....116	Muckerman, J.T.238	White, M.G.339
Glass, G.P.....64	Najm, H.N.....242	Wittig, C.....342
Grant, E.R.120	Neumark, D.M.246	Yarkony, D.R.346
Gray, S.K.124	Ng, C.Y.250	Zwier, T.S.351